



---

The Resilience of Marginal  
Populations of *Corallina officinalis*  
(Corallinales, Rhodophyta) to  
Climate Change

---

by

Regina Kolzenburg

School of Biological Sciences, Institute of Marine Sciences

The thesis is submitted in partial fulfilment of the requirements for the award of the  
degree of DOCTOR OF PHILOSOPHY of the University of Portsmouth

September 2019

# Abstract

With increasing severity of climatic implications on, for instance, socio-economy, health and ecosystems due to anthropogenically induced global climate change, the necessity to research the complex interactions and impacts of these changes on organisms is urgent. At present, the impacts of climatic changes on marine coastal ecosystems are poorly understood. Coralline algae were chosen for this study due to their wide global distribution and importance as habitat builders. As critical components of marine shallow water ecosystems and indicator species for climatic impacts, they are alarmingly affected. The species focussed on in this study and representing the traits of coralline algae, is *Corallina officinalis*. This study aimed at a combined approach of field and laboratory experiments to assess the impacts of climate change across the species distribution in the NE Atlantic ranging from the northern boundary in Iceland to the southern boundary in Spain. Physiological and structural measurements were performed in multiple experiments to determine thermal and chemistry-induced stress responses. These were compared between origins of populations and a distinct vulnerability of the southern marginal populations to increasing temperatures and changing carbonate chemistry were identified. However, northern marginal populations showed a great resilience and adaptation potential to future oceanic conditions. Based on these findings, the generally assumed Centre-to-Margin hypothesis regarding abundance as well as

adaptation and resilience potential is not observed in *C. officinalis* and has to be modified into a North-to-South gradient for this species. Overall, this thesis demonstrates that coralline algae (Rhodophyta, Corallinaceae) are vulnerable to ocean warming and ocean acidification. However, predicting the extent of their susceptibility to these changes is complex as it must be considered together with additional environmental and ecological factors. The studies presented herein highlight the importance of ecological interactions in determining species responses to environmental change.

**Keywords:** *Corallina officinalis*, climate change, NE Atlantic, marginal populations, physiology, structural integrity, uncoupling, North-to-South gradient

# Declaration

*Whilst registered as a candidate for the above degree, I have not been registered for any other research award. The results and conclusions embodied in this thesis are the work of the named candidate and have not been submitted for any other academic award.*

---

REGINA KOLZENBURG

Word count: 67,112



# Dedication

For my father, the realist, and  
my mother, the naturalist.

*For most of history, man has had to fight  
nature to survive; in this century he is  
beginning to realize that, in order to survive,  
he must protect it.*

Jacques Yves Cousteau



# Acknowledgements

My journey to the prestigious PhD started a very long time ago, without me even noticing. My parents took my siblings and me to Cornwall at least every other year and besides the screaming seagulls, the fish and chips restaurant near the harbour of Penzance and homemade sandwiches, there is one thing I remember the most – rock pooling.

We all got our own nets and shared a couple of buckets and off we went climbing around the rocks on various beaches, sitting by the pools waiting for anything to move. Back then I wasn't really interested in fish or crabs – they can pinch you. I was interested in everything else and all of us laid out what we could find in a rock pool. Long story short... I decided I wanted to become a marine biologist quite early on during my school time.

Graduating from the M.Sc. in Germany and deciding I wanted to do a PhD after working as a technician, my journey would lead me to Portsmouth. Thanks to you, Maria, I heard of this place for the first time, applied for the ideal PhD at the University here and I got it. So, in September 2015 I moved to Portsmouth. It turned out to be quite turbulent next few years with less weekends than expected but the curiosity outweighed the tiredness.

Fed, you always helped and were there when I needed any kind of support. Our sampling trips were great fun, including running from horses in Iceland, sampling in Spain being watched by dolphins and officials, warming your butt on the car heater at -3°C during field incubations or hanging out by the pool or beach whilst waiting for low tide to set in. I have learned so much from you and I hope I will still learn more. Thank you, I couldn't have asked for a better supervisor!

I would also like to thank my 2<sup>nd</sup> and 3<sup>rd</sup> supervisors, Professor Craig Storey and Professor Alex Ford. The discussion we had were super helpful and always lead to a much better outcome of any topic we discussed. Thank you both!

I would like to thank my collaborators around the world. Katy, Gerardo and Rita for their help during sampling, genetic analysis and stats discussions via Skype. Sophie, who was greatly involved in coming up with my PhD topic and who helped shuttling samples from the airport to the lab during busy sampling times and crazy stop overs between flights. Daniel Coaten, the University of Iceland, the Keilir Institute of Technology and the Fræðasetrið Nature Center in Sandgerði, Iceland for their help with field work and pointing me towards the right literature about the Island. I would also like to thank the University of Vigo, Dr. Pasantés and the whole team at ECIMAT for providing a valuable base for my field work and experiments, for welcoming me so warmly and helping me out with the organisation of permits and lab set-ups.

Conducting large long-term experiments needs a lot of manpower. I would like to thank each and everyone of the Undergraduate, ERASMUS, M.Sc., M.Res. and M.Phil students who helped me out over the last few years: Jessica, Abby, Michelle, Francesco D., Patricia, Aditya etc. Thank you all for your help without which, I would not have been possible to conduct these kinds of experiments.

I would also like to thank the technical staff at IMS, SEES and Engineering for their support throughout the project. It wasn't always easy, but we made it in the end. A huge thank you to Dr. Hugo Moreira! Even though you were busy with your own PhD, you found the time to sit with me, late and early to teach me how to use the laser etc. You spared a lot of time, which I really really appreciate, to teach a biology girl how to do geology... not an easy task 😊 I wish I had your patience and I am sure you are going to do some amazing research in the future.

Thank you, to all volunteers helping me out during my field trips: Rita, Fed, Maria, Laura, Ben, Shanelle, Rahmi, Aditya and Francesco D.

I would like to thank the University of Portsmouth for multiple funding opportunities. Most importantly, for funding my PhD and the RDF fund for Dr. Federica Ragazzola which helped me to build up a lab and to produce excellent science. I would also

like to thank the BPS, without which, I would not have been able to go to some of the best and most useful conferences I have been to.

The most important people in my life supported me throughout my whole journey.... my family. Mama und Papa, Ich kann gar nicht sagen wie dankbar ich bin eure Tochter zu sein und wie stolz ihr mich macht, Ich zu sein, denn das kommt ja alles von Euch! Tausend Dank für die Urlaube in Cornwall und die Unterstützung die ich während der Schulzeit und des Studiums immer und immer wieder von Euch bekommen habe. Ihr wart immer für mich da und habt geholfen, wannimmer es nötig war, entweder emotional oder in Person, beim Aufbau der Experimente. Ohne Euch und was Ihr mir in den letzten 32 Jahren beigebracht habt, hätte ich es nicht bis hierhin geschafft. DANKE!

Martin, Jarmila, Hannah und Kuno, Eure lockere Art hat mich immer gut abgelenkt und den Stress aus meinem Alltag genommen. Eure Positivität hat mir sehr geholfen die letzten Monate etwas lockerer zu sehen.

Stephan, Jazz and Kai. Thank you so much for your baby-video distractions which were greatly needed the whole office loves Kai 😊. And Stephan, especially to you for all the valuable feedback from someone who has finished a PhD and knows the struggles and me so well. You always know what to say to calm me down and help me through tricky times with diplomatic arguments.

Jose, the ONE! Thank you, a thousand times, for all your support and love. For cooking, while I am writing; for forcing me to go for coffee, while I am writing and for not stopping to believe in me when I thought it is almost too much for me to do. I know you took a lot upon you when commuting back and forth to Portsmouth and I really appreciate what you have done for me. With your constant positive outlook on life, you managed to cope with my emotional outbreaks and my grumpiness when I am stressed. I would not have been able to stay sane without you. Every weekend with you is like a mini holiday which I needed so much during the past months and years. You`re my rock and the way you taught me to look at things changed my life. You are the best thing that happened to me and I wouldn`t want to miss you in my life for a single second. I love you!

PhDs are a hard and long journey; on mine, I came across some of my best friends. Laura and Kira, you're such wonderful human beings and I'm glad I could share most of my time here with you. Your experience, wisdom and advises helped me so much during my PhD and beyond. I wouldn't want to miss any of our #GiKiLa adventures. I hope we will keep this friendship triangle up no matter where we will go, even if we are many km apart.

I want to thank "my girls" who were with me from the start of my PhD: Rahmi, Arianna and Kim, you all shared the stressful but also fun time of the life as a PhD. Thank you for all the distraction and fun we had, including running from Komodo dragons.

A big thanks also to the two, old and new, "Alpha males" in the office, Neil and Luke. You tried really hard to keep up your rank but with so many women around you, all we could do, is let you believe you're in charge 😊. Thank you for your terrible humour and 3 years of girls chat you didn't necessarily wanted to be involved in. Neil, I already miss our swimming, cooking and movie sessions. Luke, writing up side by side and having someone suffering with and next to me helped me a lot to not go insane the last few months. We might not seem normal to anyone else anymore, but we are, inside our own little office-bubble.

Last but not least, I would like to thank YOU for reading my thesis. I worked really hard on it. You're either my viva examiner, my supervisor, a new student that would like to continue my work or is looking for some kind of information or you are just a really interested or bored individual. Whichever of the above, thank you anyway.

Regina Kolzenburg

# Dissemination

## Publications

**Kolzenburg**, R. and Ragazzola, F., 2019. Geographic Distribution and Climate Change: the Challenges of Marginal Populations. (In submission).

Rendina, F., Bouchet, P.J., Appolloni, L., Russo, G.F., Sandulli, R., **Kolzenburg**, R., Putra, A. and Ragazzola, F., 2019. Physiological response of the coralline alga *Corallina officinalis* L. to both predicted long-term increases in temperature and short-term heatwave events. *Marine Environmental Research*, 150, p.104764.

**Kolzenburg**, R., Nicastro, K.R., McCoy, S.J., Ford, A.T., Zardi, G.I. and Ragazzola, F., 2019. Understanding the margin squeeze: Differentiation in fitness-related traits between central and trailing edge populations of *Corallina officinalis*. *Ecology and Evolution*, 9(10), pp.5787-5801.

Tavares, A.I., Nicastro, K.R., **Kolzenburg**, R., Ragazzola, F., Jacinto, R. and Zardi, G.I., 2018. Isolation and characterization of nine microsatellite markers for the red alga *Corallina officinalis*. *Molecular Biology Reports*, 45(6), pp.2791-2794.

Taucher, J., Stange, P., Algueró-Muñiz, M., Bach, L.T., Nauendorf, A., **Kolzenburg**, R., Büdenbender, J. and Riebesell, U., 2018. In situ camera observations reveal major role of zooplankton in modulating marine snow formation during an upwelling-induced plankton bloom. *Progress in Oceanography*, 164, pp.75-88.

Taucher, J., Bach, L.T., Boxhammer, T., Nauendorf, A., **KOSMOS Consortium**, Achterberg, E.P., Algueró-Muñiz, M., Arístegui, J., Czerny, J., Esposito, M., Guan, W. and Haunost, M., 2017. Influence of ocean acidification and deep water upwelling on oligotrophic plankton communities in the subtropical North Atlantic: insights from an in situ mesocosm study. *Frontiers in Marine Science*, 4, p.85.

---

## Conferences

### *Oral Presentations*

**Kolzenburg, R., Ragazzola, F. (2020)** The Effect of Climate Change on Coastlines – a Case Study of *Corallina officinalis*. British Phycological Society Winter Meeting 2020, Plymouth, conference talk

**Kolzenburg, R., Nicastro, K. R., McCoy, S., Ford, A., Zardi, G. I., Ragazzola, F. (2019)** Understanding the margin squeeze: differentiation in fitness-related traits between central and trailing edge populations of *Corallina officinalis*. British Phycological Society Winter Meeting 2019, Oban, conference talk

**Kolzenburg R., Ragazzola F. (2016)**, The resilience of marginal population to climate change, 13th Annual Marine Biological Association Postgraduate conference, Portsmouth, conference talk

### *Poster Presentations*

**Kolzenburg, R., Ragazzola, F. (2020)** Structural Integrity of *Corallina officinalis* (Corallinales, Rhodophyta) across its geographic distribution. British Phycological Society Winter Meeting 2020, Plymouth, conference poster

**Kolzenburg, R., Storey, C., Ford, A. T., Ragazzola, F. (2018)** Is *Corallina officinalis* (Corallinales, Rhodophyta) able to adapt to environmental conditions across its geographic distribution? Research and Innovation conference, Portsmouth, conference poster

**Kolzenburg, R., Storey, C., Ford, A. T., Ragazzola, F. (2018)** Is *Corallina officinalis* (Corallinales, Rhodophyta) able to adapt to environmental conditions across its geographic distribution? Institute of Biological and Biomedical Sciences conference, Portsmouth, conference poster

**Kolzenburg, R., Storey, C., Ford, A. T., Ragazzola, F. (2018)** Is *Corallina officinalis* (Corallinales, Rhodophyta) able to adapt to environmental conditions across its geographic distribution? 4th International Symposium of the Effects of Climate Change on the World's Oceans, Washington D.C., conference poster

**Kolzenburg R., Storey C., Ford A., Ragazzola F. (2017)**, Characterisation of *Corallina officinalis* (Corallinales, Rhodophyta) across its geographical



distribution, British Phycological Society Winter Meeting 2018, Southend-on-Sea, conference poster

**Kolzenburg R.**, Storey C., Ford A., Ragazzola F. (2016), The resilience of marginal populations of the benthic Macroalgae *Corallina officinalis* (Rhodophyta, Corallinales) to climate change, Science together Postgraduate conference, Portsmouth, conference poster, 2nd place best poster presentation

**Kolzenburg R.**, Voss M., Boersma M., Riebesell U. (2016), Ocean acidification and its impacts on nitrogen uptake by zooplankton communities during the KOSMOS study on Gran Canary 2014. 13th Annual Marine Biological Association Postgraduate conference, Portsmouth, conference poster presentation

#### Other Involvements

Royal Society of Biology Grant. PI: Dr. F. Ragazzola. Will coralline algae reef mitigate climate change effects on associated fauna? Experimental implementation including collaborators from Italy.

University of Portsmouth and ENEA (National Agency for new Technology, Energy and Sustainable Economy). PI: Dr. F. Ragazzola and Dr. C. Lombardi. The effect of temperature on a coralline algae. Sample and data analysis.

Binational Science Foundation, Research Grant. PI: Dr. S. Krueger-Hadfield, Dr. G. Rilov. Niche differentiation as a hypothesis underlying the maintenance of haplodiplontic life cycles. Sample and data analysis.

#### Courses and Training

NERC-funded NHM Course, 2017: Taxonomic principles and tools in botanical research at the Natural History Museum London, course leader: Prof. Juliet Brodie (macroalgae identification and sampling techniques)

NERC-funded NHM Course, 2017: Introduction to Computed Tomography – 3D Non-destructive Imaging for Taxonomy at the Natural History Museum London,

course leader: Dr. Farah Ahmed (state-of-the-art imagine techniques, data handling and 3D image reconstruction and analysis)

Pull-to-break, 2017: Structural integrity of materials at the University of Portsmouth, course leader: Colin Lupton (pull-to-break techniques in different conditions, structural analysis and data handling)

Zeiss Computed Tomography Course, 2017: Basic Training at the University of Portsmouth, course leader: Rachna Parwani (state-of-the-art imagine techniques and data handling)

Laser Ablation of Calcareous organisms at the University of Portsmouth, 2016: course leader: Prof. Craig Storey and Hugo Moreira (state-of-the-art laser ablation techniques, mass spectrometry and data handling for elemental composition determination)

Writing for the public: how and why. Workshop lead by The Conversation 2019

### Awards

**Grant in Aid of Research** of the Psychological Society of America, 2020: \$1500

**Awards and Training Award** of the British Psychological Society, 2019: £ 460

**Awards and Training Award** of the British Psychological Society, 2018: £ 477.60

**Awards and Training Award** of the British Psychological Society, 2018: £ 750

**Research Students Conference Bursary** of the University of Portsmouth, 2018: £ 450

**Awards and Training Award** of the British Psychological Society, 2017: £ 330

**Science Placement Award** of the University of Portsmouth, 2017: £ 1000

**Science Placement Award** of the University of Portsmouth, 2016: £ 1000

## Outreach

**Welcome Ambassador**, University of Portsmouth, United Kingdom: Helping first year undergraduate and postgraduate students with their start to University life.

**“See Bin Sea Change”** organising committee, United Kingdom: Plastic pollution awareness event to reduce plastic pollution in our seas.

**Pint of Science** organising committee, United Kingdom: Science talks for and interaction with the public

**STEM Ambassador**, United Kingdom: STEM outreach work with schools and University students

**Capturing our Coast (CoCoast)**, Portsmouth, United Kingdom: Institute introduction, volunteer supervision and training in species identification and ecological survey methods for a nationwide citizen science project

**University of Portsmouth**, Open Day Demonstrator, Portsmouth, United Kingdom: Different marine biological demonstrations for and communication with student candidates and parents

# Table of Contents

<b>ABSTRACT</b> .....	<b>I</b>
<b>DECLARATION</b> .....	<b>III</b>
<b>DEDICATION</b> .....	<b>IV</b>
<b>ACKNOWLEDGEMENTS</b> .....	<b>VI</b>
<b>DISSEMINATION</b> .....	<b>X</b>
<b>TABLE OF CONTENTS</b> .....	<b>XV</b>
<b>LIST OF FIGURES</b> .....	<b>XXI</b>
<b>LIST OF TABLES</b> .....	<b>XXXI</b>
<b>LIST OF ABBREVIATIONS</b> .....	<b>XXXIV</b>
<b>CHAPTER 1 - GENERAL INTRODUCTION</b> .....	<b>1</b>
1.1 SOURCES, EFFECTS AND FUTURE OF CLIMATE CHANGE .....	2
1.1.1 <i>What is Climate Change?</i> .....	2
1.1.2 <i>Sources and Cycling of Carbon Dioxide in the Environment</i> .....	4
1.1.3 <i>Key Factors of Climate Change in Our Oceans</i> .....	5
1.1.3.1 <i>Ocean Acidification and Carbonate Cycling in the Ocean</i> .....	5
1.1.3.2 <i>Sea Surface Temperature Increase</i> .....	9
1.1.4 <i>Effects of Climate Change on Marginal Marine and Intertidal     Populations</i> .....	10
1.2 CENTRE-MARGIN HYPOTHESIS .....	19
1.3 RHODOPHYTA, CORALLINALES: <i>CORALLINA OFFICINALIS</i> .....	20
1.4 THESIS OVERVIEW .....	24
1.5 RESEARCH AIMS AND OBJECTIVES .....	26
<b>CHAPTER 2 - MATERIALS AND METHODS</b> .....	<b>27</b>
2.1 STUDY SITES ALONG THE SPECIES DISTRIBUTION .....	28
2.1.1 <i>Northern Margin: Reykjanes, Iceland</i> .....	29

---

2.1.2	<i>Centre: England, United Kingdom</i> .....	30
2.1.3	<i>Southern Margin: Galicia, Spain</i> .....	31
2.2	SPECIMEN COLLECTION .....	32
2.3	SPECIMEN CULTURING .....	32
2.4	DATA LOGGER DEPLOYMENT .....	33
2.5	MONITORING THE BASIC PARAMETERS .....	34
2.6	MEASUREMENTS OF FUNDAMENTAL PHYSIOLOGICAL PROCESSES .....	35
2.6.1	<i>Oxygen and Calcification Evolution</i> .....	35
2.6.2	<i>Photosynthesis</i> .....	37
2.6.2.1	In situ .....	37
2.6.2.2	In the Laboratory.....	38
2.6.3	<i>Respiration</i> .....	38
2.6.3.1	In situ .....	38
2.6.3.2	In the Laboratory.....	38
2.6.4	<i>Calcification</i> .....	39
2.6.4.1	In situ .....	39
2.6.4.2	In the Laboratory.....	40
2.6.5	<i>Oxygen Chamber</i> .....	40
2.6.6	<i>Data Analysis</i> .....	41
2.6.7	<i>Linear Growth Rates</i> .....	43
2.6.7.1	Staining Procedure .....	43
2.6.7.2	Growth Rate Analysis .....	44
2.7	ALGAE TRANSPLANTS .....	45
2.8	STRUCTURAL INTEGRITY MEASUREMENTS .....	46
2.8.1	<i>Tensile Strength</i> .....	46
2.8.1.1	Sample Preparation .....	46
2.8.1.2	Analysis .....	47
2.8.2	<i>Laser Ablation Inductively Coupled Plasma Mass Spectrometry</i> .....	48
2.8.2.1	Sample Embedding.....	49
2.8.2.2	Sample Preparation .....	50
2.8.2.3	Analysis .....	50
2.8.3	<i>Scanning Electron Microscopy</i> .....	53
2.8.3.1	Sample Preparation .....	53
2.8.3.2	Analysis .....	53

2.9 EXPERIMENTAL DESIGNS.....	54
2.9.1 <i>Common Garden Experiment</i> .....	55
2.9.2 <i>Common Garden Experiment: Central and Southern Populations</i> .....	57
2.9.3 <i>Climate Change Experiment</i> .....	59
2.9.4 <i>Cross Experiment</i> .....	63
<b>CHAPTER 3 - CHARACTERISATION OF CORALLINA OFFICINALIS</b>	
<b>ACROSS ITS GEOGRAPHICAL DISTRIBUTION IN THE NE ATLANTIC .....</b>	<b>69</b>
3.1 COLLABORATION DISCLAIMER.....	70
3.2 INTRODUCTION .....	70
3.2.1 <i>Rhodophyta, Corallinales, Corallina officinalis</i> .....	70
3.2.1.1 Physiological Characteristics of <i>Corallina officinalis</i> .....	73
3.2.1.2 Structural and Elemental Properties, Skeletal Structure .....	75
3.2.1.3 Ecosystem Engineers and Functions.....	77
3.2.1.4 Distribution: Past, Present, Future .....	78
3.2.2 <i>Centre-to-Margin Hypothesis</i> .....	80
3.3 MATERIAL AND METHODS .....	82
3.3.1 <i>Specimens Collection</i> .....	82
3.3.2 <i>Measurements of Environmental Parameters</i> .....	83
3.3.3 <i>In situ Incubations – Photosynthesis, Respiration, Calcification</i> .....	84
3.3.4 <i>Laboratory incubations – Oxygen and Calcification Evolution</i> .....	85
3.3.5 <i>Laboratory structural analysis</i> .....	86
3.3.5.1 Tensile Strength.....	86
3.3.5.2 Trace Element Composition.....	87
3.3.5.1 Monthly Growth Rates .....	91
3.3.5.2 Cell Wall Thickness.....	91
3.3.6 <i>Data Analysis</i> .....	92
3.3.6.1 Physiological Parameters .....	92
3.3.6.1 Structural Parameters .....	92
3.4 RESULTS .....	94
3.4.1 <i>Field observations</i> .....	94
3.4.2 <i>In situ Physiological Responses along a Latitudinal Gradient</i> .....	101
3.4.2.1 Photosynthesis and Calcification Evolution.....	101
3.4.2.2 Primary Production and Respiration Rates .....	105

3.4.2.1	Calcification Rates .....	105
3.4.3	<i>In situ Structural Integrity Along a Latitudinal Gradient</i> .....	111
3.4.3.1	Linear Growth Rates: A Transplant Approach.....	111
3.4.3.2	Ultimate Tensile Strength.....	112
3.4.3.3	Elemental Composition of the Skeleton .....	115
3.4.3.1	Cell wall thickness and condition .....	121
3.5	DISCUSSION .....	124
3.5.1	<i>Northern Populations</i> .....	124
3.5.2	<i>Central Populations</i> .....	130
3.5.3	<i>Southern Populations</i> .....	134
3.5.4	<i>Comparison of Populations</i> .....	138
3.5.5	<i>Methodological Limitations</i> .....	147
3.6	CONCLUSION.....	148
 <b>CHAPTER 4 - ADAPTATION OF <i>CORALLINA OFFICINALIS</i> TO</b>		
<b>TEMPERATURE REGIMES ACROSS ITS GEOGRAPHICAL DISTRIBUTION IN</b>		
<b>THE NE ATLANTIC: A COMMON GARDEN APPROACH.....</b>		
<b>149</b>		
4.1	COLLABORATION DISCLAIMER .....	150
4.2	INTRODUCTION .....	150
4.3	MATERIAL AND METHODS .....	155
4.3.1	<i>Specimens Collection</i> .....	155
4.3.2	<i>Experimental Designs</i> .....	155
4.3.2.1	Common Garden Experiment of Northern Populations.....	156
4.3.2.2	Common Garden Experiment between Central and Southern Populations .....	157
4.3.3	<i>Monitoring of Water Parameters</i> .....	158
4.3.4	<i>Physiological Incubation Procedure and Measurements</i> .....	159
4.3.5	<i>Photosynthesis Recovery Rates</i> .....	161
4.3.6	<i>Laboratory Structural Analysis</i> .....	162
4.3.6.1	Trace Element Composition.....	162
4.3.6.2	Cell Wall Thickness.....	167
4.3.6.3	Monthly Growth Rates and Death rates .....	167
4.3.7	<i>Data Analysis</i> .....	168
4.3.7.1	Physiological Parameters .....	168

4.3.7.1	Structural Parameters .....	169
4.4	RESULTS .....	170
4.4.1	<i>Photosynthesis and Calcification Evolution</i> .....	171
4.4.2	<i>Oxygen Production Recovery</i> .....	174
4.4.3	<i>Primary Production and Respiration</i> .....	175
4.4.4	<i>Calcification Rates</i> .....	181
4.4.5	<i>Structural Integrity in Temperature Conditions along a Latitudinal Gradient</i> .....	185
4.4.5.1	Linear Growth Rates .....	185
4.4.5.2	Elemental Composition of the Skeleton .....	188
4.4.5.3	Cell wall thickness and condition .....	200
4.5	DISCUSSION .....	205
4.5.1	<i>Resilience to existing thermal conditions</i> .....	205
4.5.2	<i>Methodological Limitations</i> .....	216
4.6	CONCLUSION .....	218
 <b>CHAPTER 5 - ADAPTATION OF <i>CORALLINA OFFICINALIS</i> TO FUTURE CLIMATIC CHANGES ACROSS ITS GEOGRAPHICAL DISTRIBUTION IN THE NE ATLANTIC</b> .....		<b>219</b>
5.1	COLLABORATION DISCLAIMER .....	220
5.2	INTRODUCTION .....	220
5.3	MATERIAL AND METHODS .....	229
5.3.1	<i>Specimens Collection</i> .....	229
5.3.2	<i>Experimental Designs</i> .....	229
5.3.2.1	Climate Change Experiment .....	230
5.3.2.2	Cross Experiment .....	232
5.3.3	<i>Monitoring of Water Parameters</i> .....	235
5.3.4	<i>Physiological Incubation Procedure and Measurements</i> .....	236
5.3.5	<i>Laboratory Structural Analysis</i> .....	238
5.3.5.1	Trace Element Composition .....	238
5.3.5.2	Cell Wall Thickness .....	243
5.3.5.3	Monthly Growth Rates and Death rates .....	243
5.3.6	<i>Data Analysis</i> .....	244
5.3.6.1	Physiological Parameters .....	244



---

5.3.6.1 Structural Parameters .....	245
5.4 RESULTS .....	246
5.4.1 <i>Photosynthesis and Calcification Evolution</i> .....	247
5.4.2 <i>Primary Production and Respiration</i> .....	253
5.4.1 <i>Calcification Rates</i> .....	261
5.4.2 <i>Structural Integrity in Temperature and pCO<sub>2</sub> Elevated Conditions along a Latitudinal Gradient</i> .....	267
5.4.2.1 Linear Growth Rates .....	267
5.4.2.2 Elemental Composition of the Skeleton .....	274
5.4.2.3 Cell wall thickness and condition .....	301
5.5 DISCUSSION .....	311
5.5.1 <i>Resilience to future thermal conditions</i> .....	311
5.5.1 <i>Methodological Limitations</i> .....	319
5.6 CONCLUSION .....	321
<b>CHAPTER 6 - GENERAL DISCUSSION</b> .....	<b>323</b>
6.1 ARE LABORATORY CLIMATE CHANGE STUDIES APPLICABLE TO THE NATURAL ENVIRONMENT? .....	325
6.2 RAPID CHANGES IN TEMPERATURE AND CARBONATE CHEMISTRY IN THE OCEANS MAY SIGNIFICANTLY AFFECT THE PHYSIOLOGY OF <i>CORALLINA OFFICINALIS</i> .....	327
6.3 STRUCTURAL RESILIENCE AS A MECHANISM TO WITHSTAND CHANGES IN CARBONATE CHEMISTRY AND ELEVATED TEMPERATURES .....	330
6.4 HOW DOES THE CENTRE-TO-MARGIN HYPOTHESIS DEVELOP FOR <i>CORALLINA OFFICINALIS</i> IN FUTURE OCEANS? .....	334
6.5 FUTURE PERSPECTIVES, RECOMMENDATIONS & OPEN QUESTIONS .....	334
6.6 NOVELTIES AND CONCLUSIONS .....	336
<b>REFERENCES</b> .....	<b>338</b>
<b>APPENDIX A</b> .....	<b>373</b>
<b>APPENDIX B</b> .....	<b>376</b>
<b>APPENDIX C</b> .....	<b>387</b>
<b>APPENDIX D</b> .....	<b>408</b>

# List of Figures

- Figure 1.1:** Global carbon cycle. Carbon movements between the atmosphere, hydrosphere and geosphere. Purple arrows indicate fluxes in GtC/yr and values in black represent carbon (C) storage in GtC. Credit: NASA Earth Observatory ..... 4
- Figure 1.2:** Dissolution of CO<sub>2</sub> and the chemical equilibria of the CO<sub>2</sub> system in seawater. Left: natural conditions before industrialisation; right: anthropogenic increase of CO<sub>2</sub> concentrations in the atmosphere and the effect on the carbonate chemistry in the ocean. .... 6
- Figure 1.3:** Carbonate system: Bjerrum plot, taken from Zeebe and Wolf-Gladrow (2001). Circle and diamond show  $pK_1^* = 5.86$  and  $pK_2^* = 8.92$ , respectively, of carbonic acid. Note: Contrary to what this plot might suggest, in seawater, the pH is controlled by the relative proportions of CO<sub>2</sub>, HCO<sub>3</sub><sup>-</sup>, and CO<sub>3</sub><sup>2-</sup> and not *vice versa*. .... 7
- Figure 1.4:** Simplified life history cycle of *Corallina officinalis* ..... 21
- Figure 2.1:** The study sites across the distribution of *C. officinalis*. Top left: Reykjanes, Iceland. Bottom left: Galicia, Spain. Right: Kent, UK. Maps retrieved for free from: d-maps.com. .... 28
- Figure 2.2:** Top right: Map of Iceland with specification of sampling area magnification (pink square). Background: Sampling sites (red circles with labels) in South West Iceland near Keflavik. Maps adjusted from d-maps.com. .... 29
- Figure 2.3:** Top left: Map of the United Kingdom with specification of sampling area (pink square) and laboratory at the University of Portsmouth (green circle). Background: Sampling sites (red circles with labels) in South East England. Maps adjusted from d-maps.com. .... 30
- Figure 2.4:** Top right: Map of Spain with specification of sampling area (pink square). Background: Sampling sites (red circles with labels) in North West Spain. Maps adjusted from d-maps.com. .... 31

- Figure 2.5:** Specimens of *C. officinalis* used in the experimental design, fixed on a small flint rock with a net to mimic natural growth conditions. Each population was colour coded (red arrow) with coloured yarn for future identification. .... 33
- Figure 2.6:** Background: example of data logger deployed in the field. Foreground: close up of data logger mounting to the rock in the field including tag and coloured cable ties for easier rediscovery. .... 34
- Figure 2.7:** Schematic diagram of the oxygen chamber with electrode, similar to the model used in this study. Modified from Ragazzola (2008). .... 40
- Figure 2.8:** Overview of individual steps of linear growth rate analysis as explained in 2.6.7.2..... 43
- Figure 2.9:** Stained thalli of *C. officinalis* after the experimental phase. Structures below the stain grew prior to the experiment, in the field. Stained sections, in pink, grew during the 24 h staining period. Skeleton structure above the stain grew in the experimental condition in the laboratory. Red arrows: stained section. White dotted arrow: linear growth measurement example. .... 44
- Figure 2.10:** Example of *C. officinalis* transplant, recovered from the field..... 45
- Figure 2.11:** Completed dry tensile strength analysis of *C. officinalis*. Red arrow: breakpoint of this sample..... 47
- Figure 2.12:** Example of embedded *C. officinalis* in Epoxy resin..... 50
- Figure 2.13:** Individual cells of *C. officinalis* separated by intra- (horizontal to growth direction, blue line) and inter-cell walls (lateral to growth direction, pink line). .... 54
- Figure 2.14:** (A) Common Garden experimental design, close up. (B) Experimental design, overview including flow-through water supply. (C) Experimental design schematics. Blue lines indicate the individual water supply. Grey lines indicate individual air supply with regulators (grey squares). Squares with “P” illustrate a pump in each replicate. Letters and numbers display the country of origin (UK = United Kingdom, central population; SP = Spain, southern margin population; IC = Iceland, northern margin population) and the replicate number (1 - 4)..... 56
- Figure 2.15:** Detailed experimental design of the Common Garden Experiment with southern and central populations. Green and red coloured water baths represent central and southern temperature conditions, respectively. Central and Southern populations as well as conditions are abbreviated as UK and

SP, respectively. First abbreviation indicates the country of origin of the populations, second abbreviation indicates the temperature condition. Numbers 1-3 represent replicates of one treatment. ....	58
<b>Figure 2.16:</b> Climate change experiment design overview, with header tanks, individual water and air supply. ....	60
<b>Figure 2.17:</b> Detailed experimental design schematic of the Climate Change Experiment. The black background of the replicate experimental aquaria illustrates the insulation between aquaria.....	61
<b>Figure 2.18:</b> Schematic overview of experimental replication (n) of each treatment of the Climate Change Experiment.....	62
<b>Figure 2.19:</b> Detailed experimental design schematic of the Cross Experiment. .	64
<b>Figure 2.20:</b> Schematic overview of experimental replication (n) of each treatment of the Cross Experiment. ....	65
<b>Figure 3.1:</b> <i>Corallina officinalis</i> structure. White arrowheads represent calcified intergenicula segment. Black arrowheads represent genicula, a joint-like structure. Open arrowhead indicates a conceptacle.....	74
<b>Figure 3.2:</b> Accuracy of the reference material USGS MACS-3 for each measured and analysed trace element. Dark grey bars represent AV $\pm$ SD [ppm] of published data retrieved from the GeoReM database. Light grey bars represent AV $\pm$ SD [ppm] of trace elements in this study. ....	89
<b>Figure 3.3:</b> Accuracy of the reference material NIST SRM 612 for each measured and analysed trace element. Dark grey bars represent AV $\pm$ SD [ppm] of published data retrieved from the GeoReM database. Light grey bars represent AV $\pm$ SD [ppm] of trace elements in this study. ....	90
<b>Figure 3.4:</b> Data logger records of temperature ( $^{\circ}$ C) and light intensity ( $\mu$ mol photons $m^{-2} s^{-1}$ ) at northern sites of <i>Corallina officinalis</i> distribution in the NE Atlantic, Iceland, between July and October 2017. Light intensity is represented as the 150 moving average (black line) and temperature is represented as the <i>in situ</i> records (coloured line) and the 50 moving average (black dotted line). Temperatures above $20^{\circ}$ C and below $10^{\circ}$ C are coloured in red and blue, respectively.....	96
<b>Figure 3.5:</b> Data logger records of temperature ( $^{\circ}$ C) and light intensity ( $\mu$ mol photons $m^{-2} s^{-1}$ ) at central sites of <i>Corallina officinalis</i> distribution in the NE Atlantic, UK, between January 2017 and March 2018. Light intensity is	

represented as the 150 moving average (black line) and temperature is represented as the *in situ* records (coloured line) and the 50 moving average (black dotted line). Temperatures above 20°C and below 10°C are coloured in red and blue, respectively. Grey areas mark time periods not directly comparable to the other locations, but data loggers continued recording..... 97

**Figure 3.6:** Data logger records of temperature (°C) and light intensity ( $\mu\text{mol photons m}^{-2} \text{s}^{-1}$ ) at southern sites of *Corallina officinalis* distribution in the NE Atlantic, Spain, between February 2017 and July 2018. Light intensity is represented as the 150 moving average (black line) and temperature is represented as the *in situ* records (coloured line) and the 50 moving average (black dotted line). Temperatures above 20°C and below 10°C are coloured in red and blue, respectively. Grey areas mark time periods not directly comparable to the other locations, but data loggers continued recording..... 98

**Figure 3.7:** *In situ* temperature [°C] and light intensity [ $\mu\text{mol photons m}^{-2} \text{s}^{-1}$ ] before noon-incubations across sites ( $AV \pm SE$ ,  $n = 2$  per latitudinal region) of *C. officinalis* in the NE Atlantic. Chequered and solid bars represent temperature and light intensity, respectively. Coloured bars represent individual regions..... 99

**Figure 3.8:** Evolution curve characteristics for net production and calcification ( $AV \pm SE$ ,  $n = 5$ ) of central, southern and northern populations ( $n = 2$ ) in summer and winter. (A):  $P_{\text{max}}/C_{\text{max}}$  = maximum production, (B)  $\alpha$  = initial slope as indicator for photosynthetic efficiency, (C)  $I_K$  = saturating irradiance. For detailed graphs, Figure B1 (A) – (M). ..... 104

**Figure 3.9:** Net production, gross production and respiration rates [ $\mu\text{mol h}^{-1} \text{L}^{-1} \text{gDW}^{-1}$ ]  $AV \pm SE$  ( $n = 5$ ) of *C. officinalis* across its distribution in the NE Atlantic in summer and winter. .... 109

**Figure 3.10:** Net calcification, gross calcification and dark calcification rates [ $\mu\text{mol h}^{-1} \text{L}^{-1} \text{gDW}^{-1}$ ]  $AV \pm SE$  ( $n = 5$ ) of *C. officinalis* across its distribution in the NE Atlantic in summer and winter. .... 110

**Figure 3.11:** Monthly linear growth rates [mm] ( $AV \pm SE$ ) for northern ( $n = 289$ ) and central ( $n = 118$ ) populations of *C. officinalis* across its natural distribution in the NE Atlantic in summer conditions. Samplesizes vary in relation with staining success. .... 111

- Figure 3.12:** Ultimate tensile strength [N], displacement [mm] and normal strain  $AV \pm SE$  ( $n = 15$ ) of *C. officinalis* across its distribution in the NE Atlantic in summer and winter. .... 114
- Figure 3.13:** Element/Ca ratios for all elements in different parts of the branch. The lower, middle and upper 4 data points  $AV \pm SE$  ( $n = 9$ ) represent northern, central and southern regions, respectively. Within each region, populations ( $n = 2$ ) are represented above each other and are split into season. .... 119
- Figure 3.14:** PERMANOVA (A) and SIMPER (B) results for all populations across the geographic distribution of *C. officinalis* across the NE Atlantic. Blue triangles, green squares and red triangles represent northern, central and southern populations, respectively ..... 120
- Figure 3.15:** Inter- and intra-cell wall thickness of *C. officinalis* samples in the field. Black and grey bars represent inter- and intra-cell wall measurements [ $\mu\text{m}$ ], respectively. ( $AV \pm SE$ ,  $n = 15$ ). The left, middle and right section of the graph represent the northern, central and southern regions, respectively. Within each region, population ( $n = 2$ ) are compared during summer and winter conditions. .... 123
- Figure 4.1:** Accuracy of the reference material USGS MACS-3 for each measured and analysed trace element. Dark grey bars represent  $AV \pm SD$  [ppm] of published data retrieved from the GeoReM database. Light grey bars represent  $AV \pm SD$  [ppm] of trace elements in this study for session 1. White bars represent  $AV \pm SD$  [ppm] of trace elements in this study for session 2. .... 165
- Figure 4.2:** Accuracy of the reference material NIST SRM 612 for each measured and analysed trace element. Dark grey bars represent  $AV \pm SD$  [ppm] of published data retrieved from the GeoReM database. Light grey bars represent  $AV \pm SD$  [ppm] of trace elements in this study for session 1. White bars represent  $AV \pm SD$  [ppm] of trace elements in this study for session 2. .... 166
- Figure 4.3** Evolution curve characteristics for net production and calcification ( $AV \pm SD$ ,  $n = 3$ ) of the central (UK) and southern (SP) populations ( $n = 2$ ) under both southern (SP) and central (UK) conditions. (A):  $P_{\text{max}}/C_{\text{max}}$  = maximum production, (B)  $\alpha$  = initial slope as indicator for photosynthetic efficiency, (C)

- $I_k$  = saturating irradiance. Arrows indicate direction of change from original to altered conditions. .... 173
- Figure 4.4:** Maximum production rates  $P_{max}$  [ $\mu\text{mol O}_2 \text{ L}^{-1} \text{ h}^{-1}$ ] of northern populations of *C. officinalis*. Solid, dashed and dotted lines represent northern, central and southern temperature conditions, respectively ( $AV \pm SE$ ,  $n = 4$ ). The grey area indicates the change between identical patterns from northern and central populations to central and southern populations. .... 175
- Figure 4.5:** (A) Primary production and (B) respiration rates [ $\mu\text{mol O}_2/\text{CaCO}_3 \text{ h}^{-1} \text{ L}^{-1} \text{ gDW}^{-1}$ ]  $\pm SD$  ( $n = 3$ ) of *C. officinalis* before the Common Garden Experiment and after exposure to temperature of each geographic location. Southern populations (SP1 and SP2) are represented in grey, central populations (UK1 and UK2) are represented in black. Statistical differences are summarised in Table S1 of the supplementary document of Kolzenburg *et al.* (2019). .... 177
- Figure 4.6:** Oxygen production rates [ $\mu\text{mol h}^{-1} \text{ L}^{-1} \text{ gDW}^{-1}$ ]  $\pm SD$  ( $n = 4$ ) of *C. officinalis* before and after the Common Garden Experiment of northern populations in northern, central and southern temperature conditions. Light and dark grey bars represent primary production and respiration rates, respectively. .... 180
- Figure 4.7:** Calcification rates [ $\mu\text{Eq h}^{-1} \text{ L}^{-1} \text{ gDW}^{-1}$ ]  $\pm SD$  ( $n = 4$ ) of *C. officinalis* before and after the Common Garden Experiment of northern populations in northern, central and southern temperature conditions. Light and dark grey bars represent gross light and dark calcification rates, respectively. .... 183
- Figure 4.8:** (A) Calcification rates in the light and (B) dark [ $\mu\text{Eq h}^{-1} \text{ L}^{-1} \text{ gDW}^{-1}$ ]  $\pm SD$  of *C. officinalis* before and after the Common Garden Experiment of each population under each geographic treatment condition. Southern populations (SP1 and SP2) are represented in grey, central populations (UK1 and UK2) are represented in black. Statistical differences are summarised in Table S1 of the supplementary document of Kolzenburg *et al.* (2019). .... 184
- Figure 4.9:** Monthly linear growth rates [ $\text{mm month}^{-1}$ ] ( $AV \pm SD$ ) of *C. officinalis* for central ( $n = 79$  and  $85$ ) and southern ( $n = 70$  and  $73$ ) populations 1 and 2 under central conditions (black bars) and central ( $n = 83$  and  $88$ ) and southern ( $n = 84$  and  $79$ ) populations 1 and 2 under southern conditions (grey bars). Staining success is represented as circles ( $AV \pm SD$ ,  $n = 90$ ) in the respective colour. .... 186

- Figure 4.10:** Monthly linear growth rates [ $\text{mm month}^{-1}$ ] ( $AV \pm SD$ ) of northern population of *C. officinalis* under northern (light grey bar,  $n = 59$ ), central (black bar,  $n = 27$ ) and southern (dark grey bar,  $n = 26$ ) conditions. .... 187
- Figure 4.11:** Element/Ca ratios for all elements. Data points ( $AV \pm SE$ ,  $n = 15$ ) represent northern, central and southern, pre and post-experimental conditions, respectively, for northern populations of *C. officinalis*. .... 191
- Figure 4.12:** PERMANOVA (A) and SIMPER (B) results for the northern population of *C. officinalis* under current temperature conditions across its geographic range in the NE Atlantic. Blue triangles, green triangles and red squares represent northern (NC.), central (CC.) and southern (SC.) conditions, respectively. .... 192
- Figure 4.13:** Element/Ca ratios for all elements. Data points ( $AV \pm SE$ ,  $n = 15$ ) represent northern, central and southern, pre and post-experimental conditions, respectively, for central and southern populations of *C. officinalis*. .... 197
- Figure 4.14:** PERMANOVA (A) and SIMPER (B) results for central populations of *C. officinalis* under current temperature conditions in the centre and south across its geographic range in the NE Atlantic. Green triangles and red triangles represent central (CC.) and southern (SC.) conditions, respectively. .... 198
- Figure 4.15:** PERMANOVA (A) and SIMPER (B) results for southern populations of *C. officinalis* under current temperature conditions in the centre and south across its geographic range in the NE Atlantic. Green triangles and red triangles represent central (CC.) and southern (SC.) conditions, respectively. .... 199
- Figure 4.16:** Inter- (grey bars) and intra-cell wall thickness (black bars) [ $\mu\text{m}$ ] of *C. officinalis* across its geographical distribution in the NE Atlantic ( $AV \pm SE$ ,  $n = 15$ ) under central, southern and northern (for northern populations only) location conditions. Black line separates the two different experiments. .... 204
- Figure 5.1:** Accuracy of the reference material USGS MACS-3 for each measured and analysed trace element. Dark grey bars represent  $AV \pm SD$  [ppm] of published data retrieved from the GeoReM database. Light grey bars represent  $AV \pm SD$  [ppm] of trace elements in this study for the Climate



- Change Experiment (CCE). White bars represent AV  $\pm$ SD [ppm] of trace elements in this study for the Cross Experiment (CE). ..... 241
- Figure 5.2:** Accuracy of the reference material NIST SRM 612 for each measured and analysed trace element. Dark grey bars represent AV  $\pm$ SD [ppm] of published data retrieved from the GeoReM database. Light grey bars represent AV  $\pm$ SD [ppm] of trace elements in this study for the Climate Change Experiment (CCE). White bars represent AV  $\pm$ SD [ppm] of trace elements in this study for the Cross Experiment (CE). ..... 242
- Figure 5.3** Evolution curve characteristics for net production and calcification (AV  $\pm$ SD, n = 3) of the central (CP) and southern (SP) populations (n = 2) of the Cross Experiment. Each populations is divided into the experimental treatments (Control, T+3, CO<sub>2</sub>, CO<sub>2</sub>/T+3). (A): P<sub>max</sub>/C<sub>max</sub> = maximum production, (B):  $\alpha$  = photosynthetic efficiency, (C): I<sub>K</sub> = saturating irradiance. Arrows indicate direction of change: control to altered conditions. .... 252
- Figure 5.4:** Gross primary production and respiration rates [ $\mu$ mol h<sup>-1</sup> L<sup>-1</sup> gDW<sup>-1</sup>]  $\pm$ SE of *C. officinalis* after the Climate Change Experiment of each population under each treatment condition. Northern, central and southern populations are abbreviated as NP, CP and SP, respectively. .... 256
- Figure 5.5:** Primary production and respiration rates [ $\mu$ mol h<sup>-1</sup> L<sup>-1</sup> gDW<sup>-1</sup>]  $\pm$ SE of *C. officinalis* before (n = 4) and after (n = 3) the Cross Experiment of each population under each treatment condition. Central and southern populations are abbreviated as CP and SP, respectively. .... 260
- Figure 5.6:** Light calcification and dark calcification rates [ $\mu$ mol h<sup>-1</sup> L<sup>-1</sup> gDW<sup>-1</sup>]  $\pm$ SE of *C. officinalis* after the Climate Change Experiment of each population under each treatment condition. Northern, central and southern populations are abbreviated as NP, CP and SP, respectively. .... 263
- Figure 5.7:** Light calcification and dark calcification rates [ $\mu$ mol h<sup>-1</sup> L<sup>-1</sup> gDW<sup>-1</sup>]  $\pm$ SE of *C. officinalis* before and after the Cross Experiment of each population under each treatment condition. Central and southern populations are abbreviated as CP and SP, respectively. .... 266
- Figure 5.8:** Monthly linear growth rates [mm month<sup>-1</sup>] (AV  $\pm$ SE) of *C. officinalis* in the Climate Change Experiment for northern (n = 42, 48, 42 and 45 for Control, T+3, CO<sub>2</sub> and T+3/CO<sub>2</sub>, respectively), central (n = 65, 60, 44 and 46 for Control, T+3, CO<sub>2</sub> and T+3/CO<sub>2</sub>, respectively) and southern (n = 50, 55,

52 and 40 for Control, T+3, CO <sub>2</sub> and T+3/CO <sub>2</sub> , respectively) populations 1 and 2. Staining success is represented as closed circles (AV ±SE, n = see above). .....	270
<b>Figure 5.9:</b> Monthly linear growth rates [mm month <sup>-1</sup> ] (AV ±SE) of <i>C. officinalis</i> in the Cross Experiment for central (n = 193, 156, 175 and 145 for Control, T+3, CO <sub>2</sub> and T+3/CO <sub>2</sub> , respectively) and southern (n = 129, 121, 161 and 116 for Control, T+3, CO <sub>2</sub> and T+3/CO <sub>2</sub> , respectively) populations 1 and 2 under central and southern conditions, respectively. Staining success is represented as open circles (AV ±SE, n = see above). .....	273
<b>Figure 5.10:</b> Element/Ca ratios for all elements in the Climate Change Experiment. Data points (AV ±SE, n = 15) represent northern populations (NP1 and NP2) of <i>C. officinalis</i> , in pre and post-experimental conditions: Control, high pCO <sub>2</sub> (CO <sub>2</sub> ), high temperature (T+3) and high pCO <sub>2</sub> and high temperature (CO <sub>2</sub> /T+3). .....	283
<b>Figure 5.11:</b> Element/Ca ratios for all elements in the Climate Change Experiment. Data points (AV ±SE, n = 15) represent central populations (CP1 and CP2) of <i>C. officinalis</i> , in pre and post-experimental conditions: Control, high pCO <sub>2</sub> (CO <sub>2</sub> ), high temperature (T+3) and high pCO <sub>2</sub> and high temperature (CO <sub>2</sub> /T+3). .....	284
<b>Figure 5.12:</b> Element/Ca ratios for all elements in the Climate Change Experiment. Data points (AV ±SE, n = 15) represent southern populations (SP1 and SP2) of <i>C. officinalis</i> , in pre and post-experimental conditions: Control, high pCO <sub>2</sub> (CO <sub>2</sub> ), high temperature (T+3) and high pCO <sub>2</sub> and high temperature (CO <sub>2</sub> /T+3). .....	285
<b>Figure 5.13:</b> PERMANOVA (A-D) and SIMPER (E) results for northern populations of <i>C. officinalis</i> of the Climate Change Experiment. ....	286
<b>Figure 5.14:</b> PERMANOVA (A-D) and SIMPER (E) results for central populations of <i>C. officinalis</i> of the Climate Change Experiment. ....	287
<b>Figure 5.15:</b> PERMANOVA (A-D) and SIMPER (E) results for southern populations of <i>C. officinalis</i> of the Climate Change Experiment. ....	288
<b>Figure 5.16:</b> PERMANOVA (A-C) and SIMPER (D) results for all populations of <i>C. officinalis</i> of the Climate Change Experiment. ....	289
<b>Figure 5.17:</b> Element/Ca ratios for all elements in the Cross Experiment. Data points (AV ±SE, n = 15) represent central populations (CP1 and CP2) of <i>C.</i>	

	<i>officinalis</i> , in pre and post-experimental conditions: Control, high pCO <sub>2</sub> (CO <sub>2</sub> ), high temperature (T+3) and high pCO <sub>2</sub> and high temperature (CO <sub>2</sub> /T+3). .	296
<b>Figure 5.18:</b>	Element/Ca ratios for all elements in the Cross Experiment. Data points (AV ±SE, n = 15) represent southern populations (SP1 and SP2) of <i>C. officinalis</i> , in pre and post-experimental conditions: Control, high pCO <sub>2</sub> (CO <sub>2</sub> ), high temperature (T+3) and high pCO <sub>2</sub> and high temperature (CO <sub>2</sub> /T+3). .	297
<b>Figure 5.19:</b>	PERMANOVA (A-D) and SIMPER (E) results for central populations of <i>C. officinalis</i> of the Cross Experiment. ....	298
<b>Figure 5.20:</b>	PERMANOVA (A-D) and SIMPER (E) results for southern populations of <i>C. officinalis</i> of the Cross Experiment. ....	299
<b>Figure 5.21:</b>	PERMANOVA (A-C) and SIMPER (D) results for all populations of <i>C. officinalis</i> of the Cross Experiment. ....	300
<b>Figure 5.22:</b>	Inter- (grey bars) and intra-cell wall thickness (black bars) [μm] of <i>C. officinalis</i> in the Climate Change Experiment. Black and grey bars (AV ±SE, n = 45) represent northern populations (NP1 and NP2) pre and post-experimental, in each treatment, respectively. ....	307
<b>Figure 5.23:</b>	Inter- (grey bars) and intra-cell wall thickness (black bars) [μm] of <i>C. officinalis</i> in the Climate Change Experiment. Black and grey bars (AV ±SE, n = 45) represent central populations (CP1 and CP2) pre and post-experimental, in each treatment, respectively. ....	308
<b>Figure 5.24:</b>	Inter- (grey bars) and intra-cell wall thickness (black bars) [μm] of <i>C. officinalis</i> in the Climate Change Experiment. Black and grey bars (AV ±SE, n = 45) represent southern populations (SP1 and SP2) pre and post-experimental, in each treatment, respectively. ....	309
<b>Figure 5.25:</b>	Inter- (grey bars) and intra-cell wall thickness (black bars) [μm] of <i>C. officinalis</i> in the Cross Experiment. Black and grey bars (AV ±SE, n = 45) represent central and southern populations under central and southern conditions, pre and post-experimental, in each treatment, respectively. ....	310

# List of Tables

<b>Table 2.1:</b> Tensile strength operational parameters .....	48
<b>Table 2.2:</b> LA-ICP-MS operational parameters.....	52
<b>Table 3.1:</b> Reproducibility of Reference Materials USGS MACS-3, NIST SRM 610 and NIST SRM 612 (Total Mean $\pm 2SD$ ) for each element measured and analysed in this study. ....	89
<b>Table 3.2:</b> <i>In situ</i> sampling details, conditions and seawater analysis data (n = 1 measurement): carbonate chemistry, DO (dissolved oxygen) and pH, at all sites across <i>C. officinalis</i> distribution in the NE Atlantic. Abbreviations: AT: total alkalinity, DIC: dissolved inorganic carbon, $\Omega_{Ca}/\Omega_{Ar}$ : calcite and aragonite saturation state, $pCO_2$ : partial pressure of carbon dioxide.....	100
<b>Table 3.3:</b> (A) Mean $\pm SE$ (n = 5) for saturating photosynthesis ( $P_{max}$ ) and calcification ( $C_{max}$ ) levels, photosynthetic efficiency ( $\alpha$ ) and saturating light intensity ( $I_K$ ) of field populations (n = 2) of <i>C. officinalis</i> across its geographical distribution in the NE Atlantic. (B) Statistical comparison of $P_{max}$ and $C_{max}$ between populations within season and between seasons within populations. ....	103
<b>Table 3.4:</b> (A) Mean $\pm SE$ (n = 4) for gross and net production, respiration, gross and net calcification and dark calcification rates of field populations (n = 2) of <i>C. officinalis</i> across its geographical distribution in the NE Atlantic. (B) Statistical comparison between populations within season and between seasons within populations.....	108
<b>Table 3.5:</b> (A) Mean $\pm SE$ (n = 15) for displacement, force and strain of field populations (n = 2) of <i>C. officinalis</i> across its geographical distribution in the NE Atlantic. (B) Statistical comparison between populations within season and between seasons within populations. ....	113
<b>Table 3.6:</b> (A) Mean $\pm SE$ (n = 15) for inter- and intra-cell wall thickness (CWT) of field populations (n = 2) of <i>C. officinalis</i> across its geographical distribution in the NE Atlantic. (B) Statistical comparison between populations within season and between seasons within populations.....	122
<b>Table 4.1:</b> Reproducibility of Reference Materials USGS MACS-3, NIST SRM 610 and NIST SRM 612 (Total Mean $\pm 2SD$ ) for each element measured and analysed in this study. Top and bottom part of the table represent session 1, northern populations and session 2, central and southern populations, respectively. ....	164

<b>Table 4.2:</b> Carbonate system parameters of the central/southern (top) and northern (bottom) experiment during the culturing of <i>C. officinalis</i> . Values are mean values ( $n = 81 \pm \text{SD}$ and $n = 4 \pm \text{SD}$ , for top and bottom, respectively). Salinity, pH, temperature and total alkalinity ( $A_T$ ) were measured while other parameters were calculated. ....	170
<b>Table 4.3:</b> (A) Mean $\pm \text{SD}$ ( $n = 5$ ) for saturating photosynthesis ( $P_{\text{max}}$ ) and calcification ( $C_{\text{max}}$ ) levels, photosynthetic efficiency ( $\alpha$ ) and saturating light intensity ( $I_K$ ) of <i>C. officinalis</i> in the Common Garden Experiment of Central ( $n = 2$ ) and Southern ( $n = 2$ ) populations. (B) Statistical comparison of $P_{\text{max}}$ and $C_{\text{max}}$ between populations within temperature treatment and between temperature treatments within populations. ....	172
<b>Table 4.4:</b> (A) Mean $\pm \text{SD}$ for primary production, respiration, light and dark calcification of the northern margin population ( $n = 1$ ) of <i>C. officinalis</i> in the NE Atlantic. (B) Statistical comparison of parameters between time points (pre- and post-experimental exposure) within temperature conditions (northern, central and southern) across its geographic distribution in the NE Atlantic. ....	179
<b>Table 4.5:</b> (A) Mean $\pm \text{SE}$ ( $n = 15$ ) for monthly growth rates of <i>C. officinalis</i> across its geographical distribution in the NE Atlantic ( $n = 2$ and 1 populations in Central and Southern and northern locations, respectively) in the Common Garden Experiments. (B) Statistical comparison between populations within temperature treatment and between temperature treatments within populations. ....	187
<b>Table 4.6:</b> (A) Mean $\pm \text{SE}$ ( $n = 15$ ) for inter- and intra-cell wall thickness (CWT) of <i>C. officinalis</i> ( $n = 2$ populations for Central and Southern, respectively) within the Common Garden Experiment. (B) Statistical comparison between populations within temperature treatment and between temperature treatments within population, pre- and post-experimental. ....	203
<b>Table 5.1:</b> Reproducibility of Reference Materials USGS MACS-3, NIST SRM 610 and NIST SRM 612 (Total Mean $\pm 2\text{SD}$ ) for each element measured and analysed in this study. Top and bottom part of the table represent the Climate Change Experiment and Cross Experiment, respectively. ....	240
<b>Table 5.2:</b> Carbonate system parameters of the Climate Change (top) and Cross Experiment (bottom) design during the culturing of <i>C. officinalis</i> . All numbers are mean values ( $n = 62 \pm \text{SD}$ and $n = 71 \pm \text{SD}$ , for top and bottom, respectively). Salinity, pH (NBS and total scale, respectively), temperature and total alkalinity ( $A_T$ ) were measured while other parameters were calculated. ....	246
<b>Table 5.3:</b> (A) Mean $\pm \text{SD}$ ( $n = 5$ ) for saturating photosynthesis ( $P_{\text{max}}$ ) and calcification ( $C_{\text{max}}$ ) levels, photosynthetic efficiency ( $\alpha$ ) and saturating light intensity ( $I_K$ ) of <i>C. officinalis</i> in the Cross Experiment of Central ( $n = 2$ ) and Southern ( $n = 2$ ) populations. (B) Statistical comparison of $P_{\text{max}}$ and $C_{\text{max}}$ between populations within temperature treatment and between temperature treatments within populations. ....	251

<b>Table 5.4:</b> (A) Mean $\pm$ SE for primary production, respiration, light and dark calcification of the northern margin (n = 2), central (n = 2) and southern margin populations (n = 2) of <i>C. officinalis</i> in the NE Atlantic under Control (n = 3), elevated temperature (T+3, n = 3), elevated pCO <sub>2</sub> (n = 3) and Climate Change (T+3/CO <sub>2</sub> , n = 3) treatments in the Climate Change Experiment. (B) Statistical comparison between populations within treatments and treatments within populations. ....	255
<b>Table 5.5:</b> (A) Mean $\pm$ SE for primary production, respiration, light and dark calcification of central (n = 2) and southern margin populations (n = 2) of <i>C. officinalis</i> in the NE Atlantic under Control (n = 3), elevated temperature (T+3, n = 3), elevated pCO <sub>2</sub> (n = 3) and Climate Change (T+3/CO <sub>2</sub> , n = 3) treatments in the Cross Experiment. (B) Statistical comparison between populations within treatments and treatments within populations. ....	259
<b>Table 5.6:</b> (A) Mean $\pm$ SE for monthly linear growth rates of the northern margin (n = 2), central (n = 2) and southern margin populations (n = 2) of <i>C. officinalis</i> in the NE Atlantic under Control (n = 3), elevated temperature (T+3, n = 3), elevated pCO <sub>2</sub> (n = 3) and Climate Change (T+3/CO <sub>2</sub> , n = 3) treatments in the Climate Change Experiment. (B) Statistical comparison between populations within treatments and treatments within populations. ....	269
<b>Table 5.7:</b> (A) Mean $\pm$ SE for monthly linear growth rates of the central (n = 2) and southern margin populations (n = 2) of <i>C. officinalis</i> in the NE Atlantic under Control (n = 3), elevated temperature (T+3, n = 3), elevated pCO <sub>2</sub> (n = 3) and Climate Change (T+3/CO <sub>2</sub> , n = 3) treatments in the Cross Experiment. (B) Statistical comparison between populations within treatments and treatments within populations. ....	272
<b>Table 5.8:</b> (A) Mean $\pm$ SE (n = 15) for inter- and intra-cell wall thickness (CWT) of <i>C. officinalis</i> (n = 2 populations for Northern, Central and Southern origin) under Control (n = 3), elevated temperature (T+3, n = 3), elevated pCO <sub>2</sub> (n = 3) and Climate Change (T+3/CO <sub>2</sub> , n = 3) treatments in the Climate Change Experiment. (B) Pre- and post-experimental statistical differences in populations within treatment and between treatments within population. ...	303
<b>Table 5.9:</b> (A) Mean $\pm$ SE (n = 15) for inter- and intra-cell wall thickness (CWT) of <i>C. officinalis</i> (n = 2 populations for Central and Southern origin) under Control (n = 3), elevated temperature (T+3, n = 3), elevated pCO <sub>2</sub> (n = 3) and Climate Change (T+3/CO <sub>2</sub> , n = 3) treatments in the Cross Experiment. (B) Pre- and post-experimental statistical differences in populations within treatment and between treatments within population. ....	305
<b>Table 5.10:</b> Overview of cell wall thickness results divided into experiment: pre vs. post-experimental measurements (anomalies: red arrowheads, similarities: yellow background), comparison of treatments to the control (differences: blue arrowheads), ranking of the treatments from highest to lowest (similarities: pink) and a comparison between both populations in each treatment (anomalies: green). ....	306

# List of Abbreviations

<b>Abbreviation</b>	<b>Full term</b>
A <sub>T</sub>	Total alkalinity
ANOVA	Analysis of variance
Ba	Barium
Ba <sup>2+</sup>	Barium ions
BP	Before present
C	Treatment: Control
Ca <sup>2+</sup>	Calcium ions
CaCO <sub>3</sub>	Calcium carbonate
CC	Centre conditions
CCA	Crustose coralline algae
CCE	Climate Change Experiment
CCM	Carbon concentration mechanism
Cd	Cadmium
CE	Cross Experiment
CFCs	Chlorofluorocarbons
CH <sub>4</sub>	Methane
Chl a	Chlorophyll a
C-I curve	Calcification – Irradiance curve
C <sub>max</sub>	Maximum calcification rates
CO <sub>2</sub>	Carbon dioxide
CO <sub>2</sub>	Treatment: elevated CO <sub>2</sub>
CO <sub>2(aq)</sub>	CO <sub>2</sub> dissolved in water
CO <sub>2(g)</sub>	CO <sub>2</sub> in the atmosphere as gas
CO <sub>3</sub> <sup>2-</sup>	Carbonate ions
CP	Centre populations
Cr	Cromium
DO	Dissolved oxygen

---

DW	Dry weight
EHT	Electron high tension
Fe	Iron
$F_{tu}$	Ultimate tensile strength/ force
FW	Fresh weight
$G_D$	Dark calcification
$G_N$	Net calcification
GtC/yr	Giga tonnes carbon per year
$H^+$	Proton
$H_2CO_3$	Carbonic acid
$H_2O$	Water
HCl	Hydrochloric acid
$HCO_3^-$	Bicarbonate ions
Hg(II)Cl	Mercuric chloride
IC	Iceland
$I_k$	Saturating light intensity
IPCC	Intergovernmental Panel on Climate Change
$K^*_{sp}$	Specific solubility product
$L_0$	Initial length of sample
LA-ICP-MS	Laser ablation inductively coupled plasma mass
Mg	Magnesium
$N_2O$	Nitrous oxide
NASA	National Aeronautics and Space Administration
NC	Northern conditions
NE Atlantic	North East Atlantic
NP	Northern populations
NW	Northwest
OA	Ocean acidification
$pCO_2$	Partial pressure of carbon dioxide
PERMANOVA	Permutational analysis of variance
$P_G$	Gross primary production
P-I curve	Photosynthesis – Irradiance curve
$P_{max}$	Maximum photosynthetic rates
$P_N$	Net primary producton
ppmv	Parts per million volume



---

PS II	Photosystem II
R	Respiration
RO water	Reverse osmosis purified water
SC	Southern conditions
SEM	Scanning electron microscopy
SIMPER	Similarity percentages
SP	Spain / Southern populations
Sr	Strontium
SST	Sea surface temperature
SW	Southwest
T+3	Treatment: elevated temperature by 3°C
T+3/CO <sub>2</sub>	Treatment: elevated temperature and CO <sub>2</sub>
tX	Day X of the experiment
UK	United Kingdom
V	Vanadium
v	Volume
VP	Variable pressure
WD	Working distance
Zn	Zinc
$\alpha$	Light harvesting efficiency
$\varepsilon$	Strain
$\sigma_{\max}$	Maximum load
$\Omega$	Saturation state

# Chapter 1

## General Introduction

To be published in part as: Kolzenburg & Ragazzola (2019) (submitted)

## 1.1 Sources, Effects and Future of Climate Change

Environmental conditions fluctuated naturally within historically stable bounds for a minimum of the last 400.000 years. For instance, carbon dioxide (CO<sub>2</sub>) can range between 180 – 300 ppmv (Zhang *et al.*, 2013). However, since the beginning of the industrial era in the 18<sup>th</sup> century, a drastic increase of greenhouse gases (GHGs) in the atmosphere, exceeding natural fluctuations, is detectable, causing climatic changes accompanied by dramatic influences on our ocean, weather, food and health (IPCC, 2014a).

### 1.1.1 What is Climate Change?

The term ‘climate change’ refers to large-scale and long-term shifts within the global weather, temperatures and composition of the Earth’s atmosphere and ocean. Wide-spread industrialisation caused levels of GHGs - gases that absorb and emit radiant energy – to exceed natural increases, in a short amount of time (CO<sub>2</sub>, methane (CH<sub>4</sub>) and nitrous oxide (N<sub>2</sub>O) rose by 40%, 150% and 20%, respectively; IPCC, 2014a). While global climate can fluctuate naturally over long periods, high emission levels derived from human activity, especially CO<sub>2</sub>, have accelerated natural trends with average global temperatures rising at unprecedented rates. A “business as usual” GHG emission scenario (Representative Concentration Pathway of GHG concentrations, RCP8.5) modelled by the IPCC (2014a) predicted an increase of anthropogenic emissions up to 2- to 4-fold, depending on gas type, by the year 2100. This is posing significant risks to people, economies, societies and global ecosystems (IPCC, 2014b).

Climatic changes were not uncommon throughout the earth’s history. Paleo climatic changes, however, were mainly driven by orbital cycles and the amplification of temperature due to a lag of CO<sub>2</sub> (IPCC, 2013, Hain *et al.*, 2018). Similarly to recent

climatic changes, a greater impact on temperate and polar than on tropical seas was observed in the near-time past. The mid-Pliocene warm period (~3.3 – 3.0 million years (Ma)) and older warm intervals (global mean temperature ~3°C warmer than today) in the last 14 million years were accompanied by higher levels of ocean acidification than during recent pre-industrial times (IPCC, 2014b). Under the RCP8.5 emission scenario, comparable values are likely to be reached by the end of this century (Sosdian *et al.*, 2018). The future of organisms and their responses to climate stressors in a rapidly changing climate can be predicted from fossil records (Reddin *et al.*, 2020). Literature suggests a sharp decline in coral reef extend and species richness during previous climate change and ocean acidification (Kiessling and Simpson, 2011, Pandolfi *et al.*, 2011, Kiessling *et al.*, 2012, Pandolfi and Kiessling, 2014). Past climate change events had different causes, however they were mostly supported and further driven by massive increases of CO<sub>2</sub> and other GHGs. Migration, adaptation and extinction (up to 81% of marine fauna during the Permian period ~252 Ma ago, IPCC, 2014a, Stanley *et al.*, 2016) of organisms as well as the collapse of human societies were amongst the responses to these past climate change events. Marine fauna, especially in tropical regions, were at higher risk to face extinction than their terrestrial relatives. Additionally, terrestrial plants were less effects by extinction compared to terrestrial fauna, however, adjusting their range limits and reorganising vegetation types (Pinsky *et al.*, 2019, Lindström, 2016, Slater *et al.*, 2019). Overall, climatic changes throughout history, even when lower than RCP8.5, have always greatly influenced organisms, ecosystems and societies independent of magnitude. Therefore, future climatic changes are expected to affect organisms, ecosystems and societies in a similar way. Major and pronounced effects may be seen in organisms occupying special or rare habitats, have long life cycles, slow growth rates and low phenotypic plasticity.

### 1.1.2 Sources and Cycling of Carbon Dioxide in the Environment

When determining the sources of carbon and carbon dioxide in the environment, engaging with the carbon cycle is indispensable (Figure 1.1). Carbon and carbon dioxide are the main components of biological and organic chemical processes and, therefore, are essential for the functionality of life. CO<sub>2</sub> is produced and emitted by animals and plants. Simultaneously carbon is accumulated by plants when fixing CO<sub>2</sub> in photosynthetic reactions, producing new bioactive carbonate compounds. Deposits of organic oils, gases and coals deriving from ancient photosynthesis reactions store a large amount of carbon within the ground and are now exploited and burned as fossil fuels, releasing the carbon back into the atmosphere. An estimated 40% of CO<sub>2</sub> emissions produced in the last 45 years have remained in

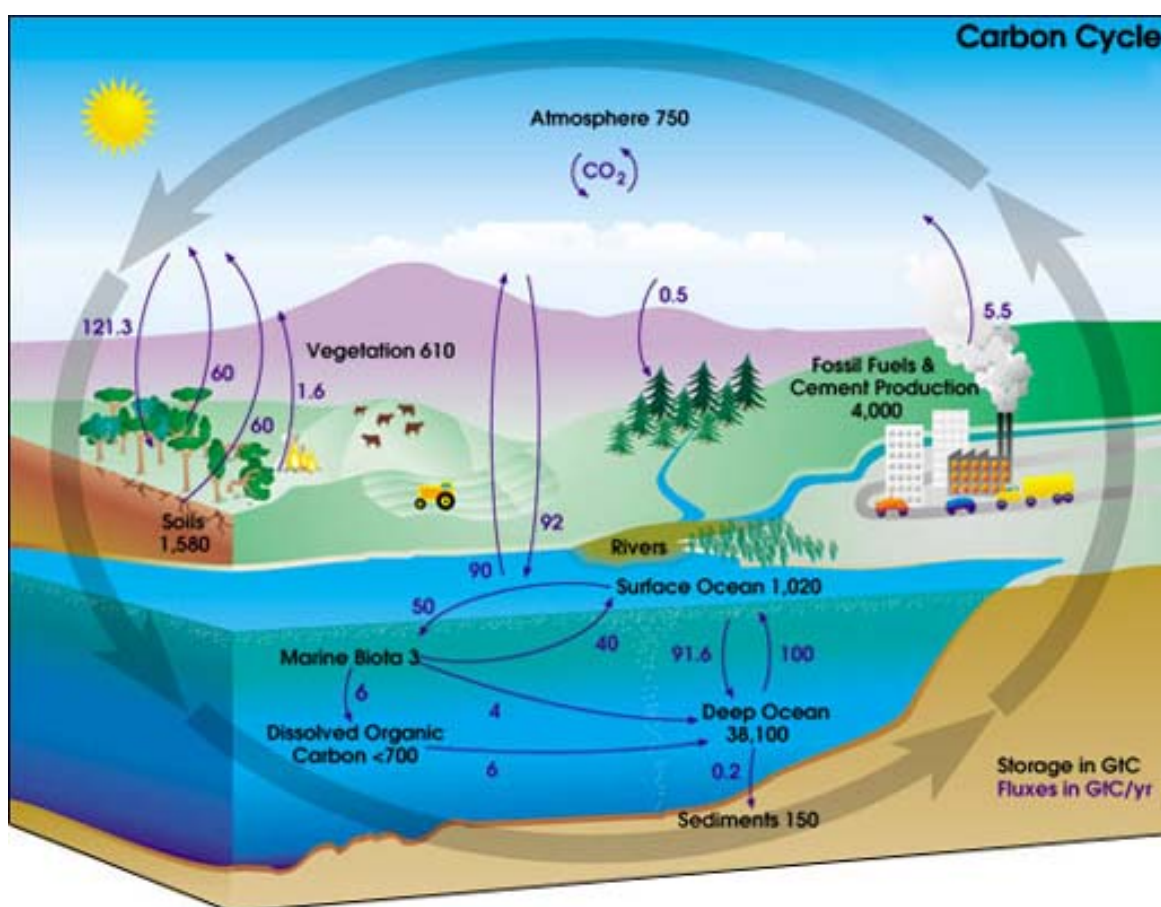


**Figure 1.1:** Global carbon cycle. Carbon movements between the atmosphere, hydrosphere and geosphere. Purple arrows indicate fluxes in GtC/yr and values in black represent carbon (C) storage in GtC. Credit: NASA Earth Observatory

the atmosphere. The remaining 60% was removed from the atmosphere and stored in biological carbon sinks such as biological material or soils (IPCC, 2014a). As atmospheric CO<sub>2</sub> is in equilibrium with dissolved CO<sub>2</sub> in the ocean, any increase in atmospheric CO<sub>2</sub> leads to an elevated dissolution in the ocean. According to the (IPCC, 2014a), 30% of anthropogenically emitted CO<sub>2</sub> was absorbed by the ocean causing changes in ocean chemistry (1.1.3.1; IPCC, 2014a). Due to the unprecedented increase of CO<sub>2</sub>, many marine organisms and ecosystems already show direct physical impacts which are likely to worsen in the next decades and century (Brierley and Kingsford, 2009) ultimately influencing the carbon cycle due to changes in biological carbon assimilation and emission.

### 1.1.3 Key Factors of Climate Change in Our Oceans

In the marine environment, there are two key factors of climate change influencing the ocean's chemistry, organisms and ultimately human societies: ocean acidification (OA) and rising sea surface temperatures (SSTs).

#### 1.1.3.1 Ocean Acidification and Carbonate Cycling in the Ocean

An increase in atmospheric pCO<sub>2</sub> (CO<sub>2(g)</sub>) due to anthropogenic input is strongly correlated with the elevated pCO<sub>2</sub> in the ocean (CO<sub>2(aq)</sub>) and negatively correlated with the oceans pH. A drop in ocean pH (~8.0 – 8.2) by ~0.1 since the Industrial Revolution is already detected and the pH is predicted to further drop by ~0.2 ± 0.1 (~pH 7.8) by the end of this century (Wolf-Gladrow *et al.*, 1999, IPCC, 2013). This stands for an approximate increase in hydrogen ion (H<sup>+</sup>) concentration levels of 150% and decrease in carbonate ion (CO<sub>3</sub><sup>2-</sup>) concentration levels of 150% (Orr *et al.*, 2005). Since the pH scale is a logarithmic scale, this implies a 10-fold change in H<sup>+</sup> concentrations. An increased amount of CO<sub>2(g)</sub> entails an increased amount of

$\text{CO}_{2(\text{aq})}$  and, therefore, increased concentrations of carbonic acid ( $\text{H}_2\text{CO}_3$ ) in the ocean due to the reaction of  $\text{CO}_{2(\text{aq})}$  with water ( $\text{H}_2\text{O}$ ) (Figure 1.2, equation (1), Figure 1.3). Consecutive acid dissociation reactions of  $\text{H}_2\text{CO}_3$  immediately take place after it is formed, splitting the molecule into bicarbonate ions ( $\text{HCO}_3^-$ ) and  $\text{H}^+$  (Figure 1.2, equation (2)), and in a further dissociation reaction, into  $\text{CO}_3^{2-}$  and  $\text{H}^+$  (Figure 1.2, equation (3)). Due to increased carbon dioxide emissions (Figure 1.2, right side, red  $\text{CO}_{2(\text{g})}$ ) and the dissociation of two  $\text{H}^+$  ions per dissolved  $\text{CO}_{2(\text{aq})}$  in the basic reactions of seawater carbonate chemistry, the  $\text{H}^+$  ions accumulate (Figure 1.2, right side, red  $\text{H}^+$ ) causing a decrease of pH ( $\text{pH} = -\log[\text{H}^+]$ , Figure 1.2) and, therefore, OA (Riebesell *et al.*, 2011, IPCC, 2013). On average, the carbonate system within seawater ( $\text{pH} 8.0 - 8.2$ ), consists mainly of carbonate ions in the following ratio: 90%  $\text{HCO}_3^-$ , 9%  $\text{CO}_3^{2-}$  and  $<1\%$   $\text{CO}_{2(\text{aq})}$  (Wolf-Gladrow *et al.*, 1999,

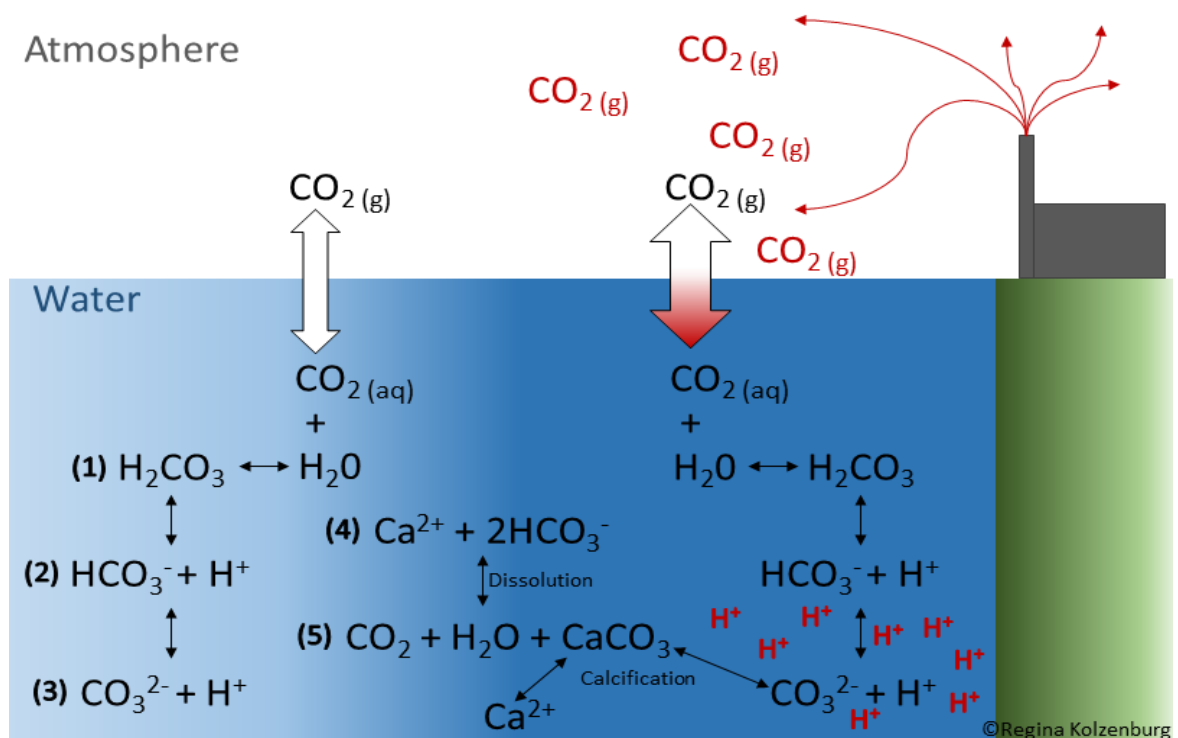


**Figure 1.2:** Dissolution of  $\text{CO}_2$  and the chemical equilibria of the  $\text{CO}_2$  system in seawater. Left: natural conditions before industrialisation; right: anthropogenic increase of  $\text{CO}_2$  concentrations in the atmosphere and the effect on the carbonate chemistry in the ocean.

Fabry *et al.*, 2008). The rate at which OA is progressing also depends on several environmental factors, including pressure and temperature. Both regulate the solubility of a gas and in this case the horizontal distribution of  $\text{CO}_{2(\text{aq})}$  depending on annual timescales (Zeebe and Wolf-Gladrow, 2001, 2009).

In addition, the carbonate chemistry and carbonate cycle are influenced by the dissolution and formation of calcium carbonate ( $\text{CaCO}_3$ ) in the water column and sediments (Figure 1.2, equation (4) + (5)). Calcium carbonate in the ocean is produced mainly by calcifying organisms like pteropods and other molluscs, corals, foraminifera, coccolithophorids and other calcifying algae, which precipitate and accumulate the molecule into their shells or skeletons (Kleypas *et al.*, 2006, Kuffner *et al.*, 2008). Carbonates descending in the water column, are either dissolved during their fall or deposited in sediments (Berelson *et al.*, 2007). Most  $\text{CO}_{2(\text{aq})}$  is

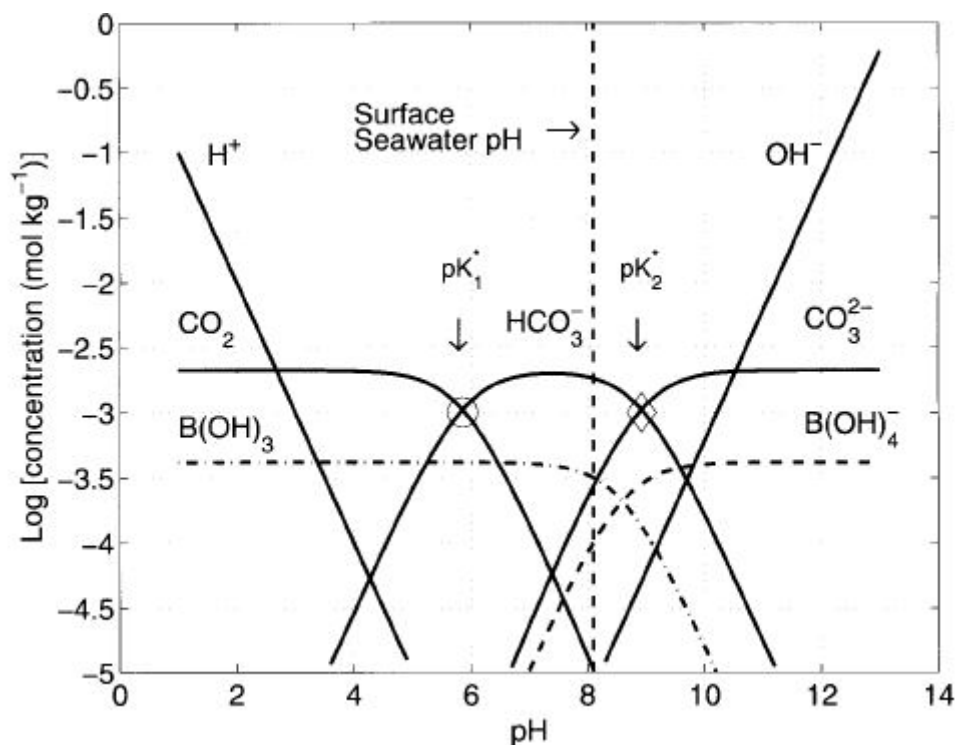


**Figure 1.3:** Carbonate system: Bjerrum plot, taken from Zeebe and Wolf-Gladrow (2001). Circle and diamond show  $\text{pK}_1^* = 5.86$  and  $\text{pK}_2^* = 8.92$ , respectively, of carbonic acid. Note: Contrary to what this plot might suggest, in seawater, the pH is controlled by the relative proportions of  $\text{CO}_2$ ,  $\text{HCO}_3^-$ , and  $\text{CO}_3^{2-}$  and not *vice versa*.



thought to be absorbed by the ocean (a process known as hypercapnia) in the reactions described above and illustrated in Figure 1.2. Ultimately, this  $\text{CO}_{2(\text{aq})}$  is neutralised by reactions with  $\text{CaCO}_3$  in marine sediments forming  $\text{HCO}_3^-$  and calcium ions ( $\text{Ca}^{2+}$ ) (Broecker and Takahashi, 1977, Zeebe and Wolf-Gladrow, 2001). Subsequently, this causes the dissolution of  $\text{CaCO}_3$ . Through all of these reactions (Figure 1.2), whether or not carbonate is stored or made available depends on external conditions such as temperature, salinity and pressure (Zeebe and Wolf-Gladrow, 2001). With increases in depth and, therefore, pressure, the solubility of  $\text{CaCO}_3$  and the disappearance in biogenic materials increases. The calcite specific solubility product,  $K_{sp}^*$ , increases and leads to a shift from calcite-rich ( $\Omega > 1$ ) to calcite-depleted ( $\Omega < 1$ ) environments and sediments with depth. This saturation state of calcite in seawater can be expressed as follows with  $[\text{Ca}^{2+}]$  and  $[\text{CO}_3^{2-}]$  representing the concentrations of the respective ions in seawater and  $K_{sp}^*$  is measured at *in situ* conditions of pressure, temperature and salinity:

$$\Omega = \frac{[\text{Ca}^{2+}]_{\text{sw}} \times [\text{CO}_3^{2-}]_{\text{sw}}}{K_{sp}^*} \quad (1.1)$$

For aragonite and calcite, a  $K_{sp}^*$  of  $10^{-6.19}$  and  $10^{-6.37} \text{ mol}^2 \text{ kg}^{-2}$  respectively, are reported in literature (Zeebe and Wolf-Gladrow, 2001, 2009). The production of  $\text{CaCO}_3$  in the ocean's surface is profoundly affected by the increase in OA due to a decreased availability of  $\text{CO}_3^{2-}$  ions, lowering biogenic calcification rates in marine organisms and altering carbon ion concentrations (Wolf-Gladrow *et al.*, 1999, Zeebe and Wolf-Gladrow, 2001).

### 1.1.3.2 Sea Surface Temperature Increase

Gasses in the atmosphere such as water vapour, CO<sub>2</sub>, N<sub>2</sub>O, CH<sub>4</sub> and Chlorofluorocarbons (CFCs) allow sunlight and solar radiation to pass but prevent some of the reflected heat to escape again, eventually leading to the retention and accumulation of heat in the atmosphere (IPCC, 2013). The more gases that accumulate, e.g. since the industrial era (Figure 1.2), the more heat is retained and stored in the Earth's atmosphere. The immense amount of 93% of additional anthropogenically-derived heat produced since the 1970s, is due to this greenhouse effect and other human activities (IPCC, 2013).

This overproduction of heat was buffered and absorbed by the ocean, affecting even the deep sea (Broecker and Takahashi, 1977, IPCC, 2013). It started with the warming of the upper 75 meters of the ocean's surface waters by an average of 0.11°C per decade from 1950 to 2010, eventually transmitting heat further down into greater depths (Levitus *et al.*, 2009, IPCC, 2014). Due to the high density of seawater, a specific volume is able to take up and store more than 4000 times as much heat as the same volume of air (Reid and Hill, 2016). This heat, however, is not sealed off in the ocean but can be accumulated, together with the stored CO<sub>2</sub>, and released back into the atmosphere if the SST is abnormally warm. According to the review of Laffoley and Baxter (2016), there will be an increase of 1-4°C of the mean global ocean temperature by 2100, with the greatest warming occurring in the Southern Hemisphere with a predicted temperature increase of up to +8°C (Hampe and Jump, 2011). Elevated SSTs will reduce the capability of the ocean to store gasses like CO<sub>2(g)</sub>, resulting in a negative feedback in the ocean carbon sinks and, therefore, increasing atmospheric CO<sub>2</sub> concentrations (Zeebe and Wolf-Gladrow, 2009, Reid and Hill, 2016). By acting together, potentially also with local changes

like pollution or eutrophication, these two global drivers can lead to multi-layered, interactive and intensified effects on species and ecosystems (IPCC, 2014b). Further, more frequent and severe heatwaves may occur and have supplementary effects on species and humanity (Kerr, 2011, IPCC 2014a). All these drivers and consequences of recent climate change can directly or indirectly influence organisms, e.g. through changing metabolic processes such as consumption rates, biotic interactions such as stronger top-down effects (O'Connor, 2009, Hampe and Jump, 2011), or through the alteration of ocean circulations (IPCC, 2014b).

#### 1.1.4 Effects of Climate Change on Marginal Marine and Intertidal Populations

Abiotic and biotic environments change continuously. This is accompanied by a constant challenge to maintain homeostasis forcing individuals, populations and species to acclimatise to and evolve around these local and global changes, and adapt physiologically and structurally along their geographic range of distribution.

Within their distribution, there are naturally occurring central and marginal populations throughout the species range. Comparing central to marginal populations of species provides an understanding of determinants of species ranges and an understanding of how spatial variation in fitness translates to population-level differences in abundance (Sexton *et al.* 2009, Araújo *et al.*, 2014, Guo, 2014). Thus, range limits can aid as testing grounds to understand the conditions by which populations can adapt — or fail to adapt — to new conditions (Sexton *et al.*, 2009). Marginal populations are, often but not necessarily, living on the edge of their favourable conditions and tolerance and suitable environments and are mostly isolated from central and continuous populations (Bertocci *et al.*, 2011, Bridle and Vines, 2007). They will exhibit greater temporal variability when environmental fluctuations exceed the species' tolerance in some years; this is a pattern more

strongly supported by a literature survey carried out by Sexton *et al.* (2009). Marginal populations, therefore, represent an important source for speciation events in the future, triggered by e.g. climatic changes, subsequently developing unique eco-physiological local adaptations and genetic structures (Sexton *et al.*, 2009, Araújo *et al.*, 2009). As such, the study and conservation of marginal populations is thought to be beneficial for the protection of these evolutionary processes, producing future evolutionary diversity of a species (Lesica and Allendorf, 1995).

Hampe and Petit (2005) summarised that work on current impacts of global change indicates greater stability of low-latitude than of high-latitude range margins: two visions of the future of rear edge populations currently coexist, ranging between predictions of complete disappearance (Hampe and Jump, 2011) based on modelling, and more optimistic expectations based on past persistence. Northern peripheral populations may exhibit limited evolutionary responses to climate change, which could see northerly populations experience environmental changes more typical of southern sites (Etterson and Shaw, 2001).

Intertidal species inhabit the shores along coastlines where frequent increases and decreases of water levels due to tidal influence prevail. Therefore, as part of the daily cycle, these organisms are exposed to additional abiotic and biotic stress such as exposure to air, direct sunlight, elevated temperatures, elevated salinity, strongly fluctuating pH and oxygen levels, wind forces, wave action and a number of different predators, e.g. birds (Hampe and Petit, 2005, Egilsdottir *et al.*, 2013, Williamson *et al.*, 2014). Due to the additional stress, microclimatic variations in the intertidal zone are vast and, in addition with predicted climatic changes, this may influence intertidal organisms in their physiology, structure and distribution (Helmuth *et al.*, 2002).

Rock pools represent another extraordinary habitat within intertidal environments. Environmental parameters within rock pools are shown to be highly variable and extreme. Experiencing these conditions might make rock pool organisms more resilient to abiotic changes due to a greater capacity for adaptation and acclimatisation (Brodie et al., 2013). The coastal shores, therefore, entail highly climatically affected, exposed and influenced ecosystems, especially for marginal populations. A review by Eckert *et al.* (2008) on the genetic variation across species geographical ranges found that only 9% of the studies conducted for this topic were marine, highlighting an immense lack of studies at species distribution range. This lack of understanding makes the prediction of climatic impacts on marine marginal populations more difficult and establishing effective conservation methods incorporating local adaptations becomes a greater challenge (Bennett *et al.*, 2015).

Within all marine and intertidal studies conducted, negative impacts were among the most dominant findings. Sagarin *et al.* (2006) found that populations near the range margins might show both relatively low abundance and depressed organismal conditions reflecting negative growth, stress resilience and reproduction success. They concluded that the species distribution appeared to be more complicated than previously assumed. Negative effects on marine and intertidal fauna were observed in a number of studies, positive effects of climatic changes on intertidal and marine fauna, however, are scarce. For a detailed review of effects on marginal populations, see Kolzenburg and Ragazzola (submitted, 2019).

An exceptional large amount of negative impacts are found in algae. Influences of climatic changes as well as anthropogenic impacts, such as trampling, on *Ascophyllum nodosum* were found to be detrimental in the southern distribution range. *Ascophyllum nodosum* was unable to re-cover at the locations studied and

return to the pre-disturbed state (Araújo *et al.*, 2009). A different study by Araújo *et al.* (2015) revealed that edge populations of *A. nodosum* showed increased investment in reproduction compared to relatively higher investments in defence in central populations, signifying that reproduction and defence have different fitness values for this species. Changing conditions may force these fitness values to change resulting in species investing in traits that are unfavourable for keeping their fitness status quo, leaving marginal populations with an increased investment in defence causing negative long-term consequences (Araújo *et al.*, 2015). Bertocci *et al.* (2011) highlighted the need for protection and management measures regarding *A. nodosum* that would allow for preservation of marginal populations and an important component of the biodiversity of European rocky shores. In the southern populations of *Fucus serratus*, *Fucus vesiculosus* and *Fucus spiralis*, a maladaptation to desiccation and heat stress caused the southern edge populations to be less resilient compared to central populations. Marginal populations of these species also showed a reduced capacity to recover to pre-stress levels of Fv/Fm, a chlorophyll fluorescence measuring parameter used to test stress and effects on the photosystem II (PSII). This may be either due to damage during the stress or less efficient or impaired PSII repair (Kim *et al.*, 1993, Pearson *et al.*, 2009, Ferreira *et al.*, 2014). These results suggest that ongoing climate change and the stress it forces on *Fucus* marginal populations may threaten small, fragmented marginal populations due to reduced fitness and lower adaptive capacity compared to central populations (Pearson *et al.*, 2009). For *F. vesiculosus*, a climate-correlated diversity loss was revealed by Nicastro *et al.* (2013), predicting a southern range contraction in the marine realm. Such an elimination of *F. vesiculosus* is likely to cause other immediate ecological effects. Thus, its large-scale disappearance may modify and

decrease ecosystem complexity, reducing diversity and abundance of associated species with potential effects on all trophic levels (Nicastro *et al.*, 2013).

A comparison between southern and northern edge populations of *F. vesiculosus* and *Zostera marina* by Mota *et al.* (2018) showed higher thermal resistance and recovery in southern populations of *F. vesiculosus* and an opposing finding for northern and southern populations of *Z. marina*. This confirms that differentiation of thermal stress responses can arise between peripheral populations.

Due to climate change, intertidal benthic algal communities are predicted to change and disappear in the southern part of the northern hemisphere by 2200 (Kuffner *et al.*, 2008, Juterbock *et al.*, 2014). The resulting habitat loss could be extenuated if algae are able to physiologically acclimatize to elevated temperatures. Responses of intertidal organisms can be considered as an early warning (Pearson *et al.*, 2009) due to species already living at their maximum thermal tolerance and, therefore, low potential in responding to increased climatic stressors over the next century (Somero, 2010, Tomanek, 2010). An intertidal macroalgae and indicator species is *F. serratus*. While it has created some adaptive responses to climatic changes, the reproduction capacity at the southern edge of its species distribution was severely diminished compared to central populations, likely due to unfavourable abiotic conditions linked to either climate change or short-term extreme environmental fluctuations (Viejo *et al.*, 2011).

Compared to northern edge populations, populations on the southern range edge like the ones above of *F. serratus* have only recently gained the interest of the research community (Hampe and Petit, 2005, Araújo *et al.*, 2011, Lepais *et al.*, 2013, Ferreira *et al.*, 2014, Zardi *et al.*, 2015). In the brown algae *Hormosira banksii*, specimens from warm edge populations showed increased thermal sensitivity

indicated by decreased photosynthetic yields of the PSII and delays in recovery after desiccation stress, contrasting studies of Ferreira *et al.* (2014) or Saada *et al.* (2016) (Clark *et al.*, 2018). Marginal populations of *A. nodosum* showed a higher reproductive output at their southern distribution limit compared to a more central location in another study conducted by Araújo *et al.* (2011). However, both populations showed similar mortality at all life stages. However, within the latter study, specimens were smaller and populations denser due to increased energy costs channelled into reproduction or defence. In the same study *F. serratus* showed a distribution into narrower vertical habitat ranges. For both species at their southern edge of their distribution in the Northeast (NE) Atlantic, they found different patterns of potential adaptations to environmental changes (Araújo *et al.*, 2011).

High irradiances of photosynthetic active radiation (PAR) and ultraviolet radiation (UVR) during low tide can cause photoinhibition and are relatively common in macroalgae in intertidal zones (Martínez *et al.*, 2012). The negative effect also showed an increasing trend under elevated temperatures in intertidal fucoids (Altamirano *et al.*, 2003). This is shown for central populations; and the study by Martínez *et al.* (2012) suggests that the three additive stressors (air and ocean temperatures and solar radiation) are highly relevant to predict range shifts of *F. serratus*. Thus far, only one study, published as part of this PhD study, researched the resilience of marginal populations of calcifying macroalgae to existing temperature conditions across its geographical distribution, reporting a decoupling of photosynthetic and calcification processes in marginal populations as a result of stress (Kolzenburg *et al.*, 2019).

In addition to elevated temperatures, OA affects calcareous organisms across their distribution range due to the lowering of the calcium carbonate saturation state



(equation 1.1) in the seawater (Orr *et al.*, 2005, Doney *et al.*, 2009). This translates into a decrease in the magnesium (Mg) content of calcite hard parts in most marine environments. Additionally, the proportion of calcifiers depositing low-Mg calcite will increase and the average Mg content of organic carbonate sediments is decreasing due to dissolution (Andersson *et al.*, 2008). A study looking at natural CO<sub>2</sub> seeps and acidified seawater in today's oceans revealed that calcifying macroalgae such as coralline algae will be severely impacted and are the first calcifying organism to disappear in these areas (Kleypas *et al.*, 2006, Hall-Spencer *et al.*, 2008). Other studies on crustose coralline algae have shown that a combination of elevated pCO<sub>2</sub> and temperature can affect dissolution, calcification and survival and should be considered in combination when predicting potential future climate impacts (Martin and Gattuso, 2009, Williamson *et al.*, 2014). Due to all these changes and challenges, coralline algae are considered to be especially susceptible to OA showing a dissolution of their high-Mg calcite skeletons, subsequently reducing recruitment, growth and survival rates (Kroeker *et al.*, 2013a).

Early life stages of *Corallina vancouveriensis*, for example, were more resilient to the direct effects of future acidification levels than adult individuals (Padilla-Gamino *et al.*, 2016). It is possible that coralline algae are able to shift their energy budget from growth to maintaining structural integrity, which gets weakened in acidified conditions (Ragazzola *et al.*, 2013). In other calcifying algae photosynthesis is stimulating calcification and an increase in photosynthesis could lead to an initiation of CaCO<sub>3</sub> dissolution in response to decreased pH in the surrounding (Borowitzka, 1982, Gattuso *et al.*, 1999, Hoffman *et al.*, 2012a; Johnson *et al.*, 2012).

The photosynthetic efficiency ( $\alpha$ ) is also negatively influenced by carbonate chemistry changes in the seawater. This was shown for one centre population of the

articulated coralline algae *Corallina officinalis*, which consequently showed less competitiveness under future scenario ocean chemistry conditions when combined with decreased physiological traits (Hofmann *et al.*, 2012b). In order to withstand these negative impacts, long-term experiments have shown that coralline algae increase calcification rates in order to survive prolonged exposure to low pH treatments, related dissolution and structural weaknesses (Kamenos *et al.*, 2013). The physiological response to OA, especially regarding calcification, is very variable amongst species (Ries *et al.*, 2009). OA is proven to cause even more severe effects on whole benthic community structures, especially in shallow warm-water carbonate ecosystems such as the tropics and subtropics (Kuffner *et al.*, 2008). Antarctic and tropical macroalgae in coastal waters appear to be the most vulnerable to warming, (Pörtner *et al.*, 2014, IPCC, 2014a and references therein) resulting in a negative change in the total oceanic production, of which coastal macrophytes coverage supplies 2-5%. Species able to tolerate high fluctuations in pCO<sub>2</sub> levels might, therefore, be resilient to OA (Egilsdottir *et al.*, 2013). An increase of 3°C in SST is likely to cause an increase in Mg content in *C. officinalis* and *Corallina caespitosa* around 1.1 mol% Mg-calcite. This increase corresponds to ~32% of the seasonal variability of Mg content found in NE Atlantic species (Williamson *et al.*, 2014), increasing susceptibility to OA. For instance, an average reduction of 0.013 mol% Mg/Ca in new structures formed under OA conditions was discovered for another species of articulated coralline algae, *Ellisolandia elongata* (Egilsdottir *et al.*, 2013). In contrast to the observed negative changes, unlike other marine organisms, algae have the exceptional capability of absorbing CO<sub>2</sub> from seawater (Gattuso *et al.*, 1999). Both, CO<sub>2</sub> and bicarbonate can be used as a substrate for photosynthesis, reducing the effects of OA (Raven and Beardall, 2003, Galbraith *et al.*, 2016).

Additional studies have shown how a doubling in pCO<sub>2</sub> concentration in seawater can have a positive effect on red, temperate, non-calcifying algae (Kübler *et al.*, 1999) and other species (Gao *et al.*, 1993). Primary producers relying exclusively on CO<sub>2</sub> are expected to enhance photosynthesis rates with elevated CO<sub>2</sub> availability (Kübler *et al.*, 1999) and may outcompete algae that cannot down-regulate their carbon concentration mechanisms (Hepburn *et al.*, 2011, Cornwall *et al.*, 2012, Raven *et al.*, 2012). Studies focusing on CO<sub>2</sub> vents in the Mediterranean, even though not focussing on marginal populations, show that for calcifying algae and other organisms, the tissue and external organic layers provide a vast amount of protection of their shells and skeletons (Rodolfo-Metalpa *et al.*, 2011). When comparing two *Fucus* species, *F. vesiculosus* and *Fucus radicans*, in the Baltic Sea, which includes their distribution northern edge and limit of salinity tolerance, prevention of receptacle formation was exhibited in both *Fucus* species under climate change scenarios, signifying that *Fucus* failed to reproduce sexually, whereas photosynthesis and growth was not affected. This suggests, that these marginal populations may be resilient to future conditions but only if they are able to reproduce asexually (Rothäusler *et al.*, 2018). Another study on *F. vesiculosus* found that southern range populations may be more resilient to heat stress than their northern counterparts, as growth rates in this study did not change significantly in either population (Saada *et al.*, 2016).

The little understanding of how stressors interact and what influence it might have on organisms is limiting the capacity of scientists to predict the effects of climate change (Martínez *et al.*, 2012), supporting a need for more physiological studies.

## 1.2 Centre-Margin Hypothesis

The “centre-periphery” hypothesis is described by Mayr (1963). Here, the adaptive ability of marginal populations could be limited due to genetically less diverse populations compared to central populations. It is suggested that the geographic centre of a species distribution holds the most favourable conditions and, therefore, holds the highest population density (Whittaker, 1956, Brussard, 1984). In the centre, a species is reaching the highest abundance and declines toward the range edges; this is also called the “abundant-centre” hypothesis (Brown, 1984, Sagarin and Gaines, 2002). When moving away from the centre towards the margins of the distribution, environmental variables are thought to become less favourable due to greater abiotic stress and increased interspecific competition (Aitken *et al.*, 2008), initiating a decrease in population densities and lower relative fertility (Case and Taper, 2000, but see Sexton *et al.*, 2009).

With increasing research knowledge, exemptions were found for these hypotheses. The decreased genetic diversity in edge populations appears to be the case for most species but not for all. In addition, genetic diversity does not always follow the centre-margin hypothesis but instead, may have been influenced by many other factors (e.g. latitude, ecological environmental gradients, phylogeographic history etc., Yang *et al.*, 2016). Other studies also showed a complex pattern, in which peaks of abundances are shifted towards one end of the species range edge or show no pattern (Sagarin and Gaines, 2006, Sagarin *et al.*, 2006). In future climatic conditions, marginal populations are thought to be more vulnerable to changes and extreme conditions than central populations (Walther *et al.*, 2002).

### 1.3 Rhodophyta, Corallinales: *Corallina officinalis*

Rhodophyta (red algae) are one of the oldest phyla of eukaryotic marine algae. Within the phylum Rhodophyta, the order Corallinales was formed incorporating families, *inter alia*, of crustose coralline algae (CCA, e.g. Lithothamniaceae) and articulated (or geniculated) coralline algae, e.g. Corallinaceae (Guiry, 2019). All forms of the genera *Corallina* located within the family of Corallinaceae belong to the benthic macroalgae inhabiting the photic zone, the part of the ocean floor where light penetrates and enables photosynthesis. Apart from *Pneophyllum cetinaensis*, the first described freshwater species (Žuljević *et al.*, 2016), all species within the order of Corallinales are inhabiting marine environments. Species assigned to this order developed a carbonate concentration mechanism (CCM) enabling them to transform  $\text{HCO}_3^-$  into  $\text{CO}_2$  and, therefore, are not carbon limited. They crystallise and accumulate high-Mg calcite in their cell walls to enhance stability, protection and mechanical resistance (Padilla-Gamino *et al.*, 2016). These high-Mg calcites (>3 - 4 mol%  $\text{MgCO}_3$ ) were found to surpass the solubility of aragonite around 12 mol%  $\text{MgCO}_3$  (Chave, 1954a) and consequently present the most soluble form of carbonate in the ocean. Therefore, Mg-calcites were identified to be the first material in the ocean to respond to decreasing pH associated with a declining saturation state. It is also known that species with a wide geographical range, such as coralline algae, are in general very plastic and able to acclimatise to a variety of habitats through morphological and functional responses (Brody, 2004, Ragazzola *et al.*, 2013). To maintain their abundance in temperate, shallow, intertidal ecosystems around the globe, coralline algae are suggested to have a good ability to adapt to a wide and fast changing range of external influences such as solar irradiance, temperature, mechanical stress and carbonate chemistry. Geniculated coralline algae form turfs covering large areas of hard substratum in intertidal ecosystems.

One of these turf forming species is *C. officinalis*. It is commonly found in low, sheltered intertidal zones, where it predominantly inhabits the lower part of rock pools and channels that remain damp or filled during extreme tides or conditions, and at the edge of the intertidal to subtidal zones (Digby, 1977, Egilsdottir *et al.*, 2013, Williamson *et al.*, 2014). It forms, like all articulated algae in this order, branches that consist of calcified segments (intergenicula), which are produced through the precipitation of high-Mg calcite in the cell walls, and non-calcified segments (genicula), with clear visible annual growth banding. This structure provides flexibility and elasticity for every individual branch (Martone and Denny, 2008). The turf beds are highly variable in frond length and density at small spatial scales with coralline algae potentially being able to shift their energy budget from growth extension to the maintenance of structural integrity (Ragazzola *et al.*, 2013). Coralline algae reproduce by forming tetraspores (or bispores), spermatia, carpogonia, and carpospores within conceptacles. Life histories in this family are generally diplobiontic with isomorphic gametophytic and tetrasporophytic stages (**Figure 1.1**Figure 1.4, Johansen, 1981, Woelkerling, 1988).

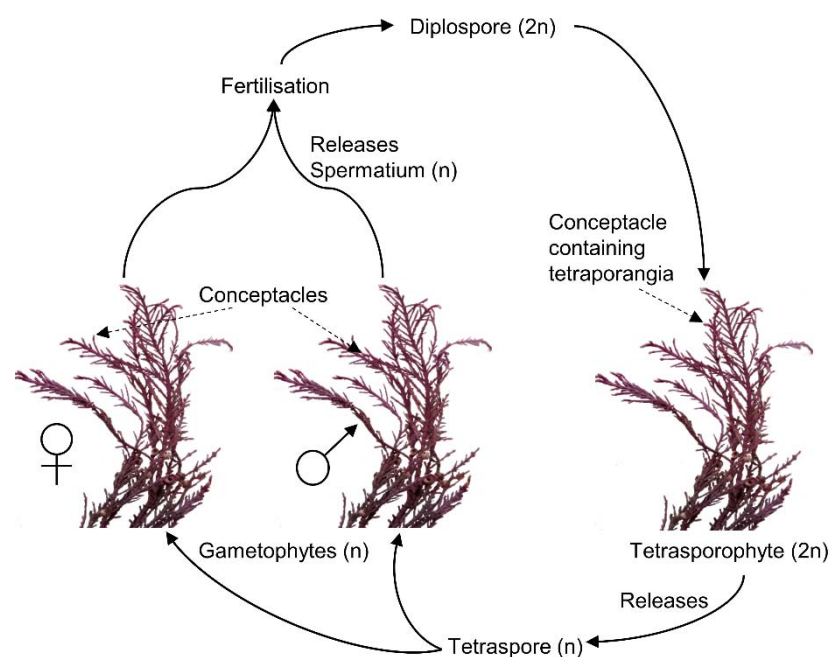


**Figure 1.4:** Simplified life history cycle of *Corallina officinalis*

*Corallina officinalis* (Rhodophyta, Corallinales, Corallinaceae) is a common species around the North Atlantic and North Pacific (Hind *et al.*, 2014, Magill *et al.*, 2019). It grows on hard substratum in the lower intertidal zone, and sometimes inhabits the upper most subtidal zones. *C. officinalis* is commonly found in damp channels and rock pools (Guiry and Guiry, 2019 and references therein). It is a geniculated, calcareous branching alga that forms fronds up to 12 cm in length but it is often much shorter and coarse to the touch (Guiry and Guiry, 2019 and references therein). The fronds grow upright from a calcareous crustose disk-shaped holdfast which can reach up to 70 mm in diameter (Guiry and Guiry, 2019 and references therein). Side branches grow out of the main branch opposite from each other, also called pinnate growth. *C. officinalis* is epilithic on hard substrata under macroalgal canopies and tidal action may influence branch length due to mechanical influences of tidal action (Guiry and Guiry, 2019 and references therein). Specimens display a variety of colours ranging from purple to pink and red or yellowish, with white tips and joints. The colour, a result of changes in ratios and/or degradation of pigments, can also be induced by light damage, such as the yellow or orange colour after intensive light exposure and close to death. Reproductive cells, conceptacles, are drop-shaped and can be found either at the tip of a branch or laterally on an intergenicula (Brodie *et al.*, 2013, Johansen, 1975). Branches can drastically differ in their physiology between zones on the same rocky shore. Irvine and Chamberlain (1994) found 1-2 cm long fronds in the lower littoral compared to 10-17 cm long fronds in rock pools. Growth rates were established by Colhart and Johansen (1973) and show an average growth of 2.2 mm/month at 12°C and 18°C, and slowed down to 0.2 mm/month at 6°C and no growth was observed at 25°C.

The species focussed on in this study, *C. officinalis*, is an important part of intertidal ecosystems and is functioning as ecosystem engineer. Ecosystem engineers are organisms that play a crucial role in creation, modification and maintenance of habitats (Jones *et al.*, 1994). Without it, up to 80% of other organisms would not be able to survive in this habitat, and shores would be drastically depleted in diversity (Kelaher *et al.*, 2001, 2003, Liuzzi and Gappa, 2008). Coralline algae, therefore, function as vital ecosystem engineers and play a crucial role as an essential structural element in the majority of rocky coastal zones provide rigid substrate for organisms to settle (Chisholm, 2000, Benedetti-Cecchi, 2006, Dayton, 1972, van der Heijden & Kamenos, 2015, Johansen, 1981, Jones *et al.*, 1994; Kelaher *et al.*, 2001, Nelson, 2009, Noël *et al.*, 2009). By creating these habitats, they are providing a hard substrate with a complex structure and thereby increasing the biodiversity of ecosystems (Foster, 2001, Steller *et al.*, 2003, Ragazzola *et al.*, 2013, Daume *et al.*, 1999, Ritson-Williams *et al.*, 2009, Gherardi and Bosence, 1999). They often form complex, extremely dense and highly branched turfs, which are considered the extreme end of algal structural complexity (Coull and Wells, 1983, Davenport *et al.*, 1999) and contribute to reef accretion (Adey, 1998, Chisholm, 2000).

These complex structures are able to accommodate abundant and diverse macrofaunal assemblages with up to 250,000 individuals per m<sup>2</sup> (Kelaher *et al.*, 2001). Coralline algae are also able to influence microclimate on a local scale by changing the water chemistry around them through metabolic processes like photosynthesis and calcification, releasing or absorbing oxygen as well as various forms of carbonate ions into the surrounding waters. Subsequently, they contribute approximately 25% to the CaCO<sub>3</sub> production within coastal regions (Morris and Taylor, 1983, Amado-Filho *et al.*, 2012, Williamson *et al.*, 2014; Williamson *et al.*,



2017) representing a significant component of the global carbon system (Mackenzie *et al.*, 2004, Martin *et al.*, 2007, Ragazzola *et al.*, 2013).

#### 1.4 Thesis Overview

Despite numerous international research studies and a recent focus on the effects of climate change on geographical, marginal populations, significant knowledge gaps remain. For example, the majority of the studies are only focussed on one edge of a species distribution. Most of the studies have focussed on the southern edge of species distribution but have not looked at potential impacts of ocean acidification or freshwater influences in higher latitude ecosystems which can force a species to shift southern ward. This lack of sampling across the whole species distribution can be observed throughout all territories, terrestrial, freshwater and marine as well as animals and plants/algae within these sectors (Kolzenburg & Ragazzola, 2019 (submitted)). Another major limitation is the discrepancy between the available data obtained in the laboratory and data collected in the field, which frequently fails to match the same magnitude. This underpins the need for combined laboratory and field studies of biota to understand the applicability of controlled exposures to natural populations. This study has disclosed the lack of environmentally relevant data regarding the effect of climate change on marginal populations across the species geographic distribution.

This study is an investigation into the physiology, structural integrity and ecology of coralline algae in the NE Atlantic, where *C. officinalis* was found living at the margins most predisposed to climate change: temperate as well as the sub-polar regions. There are two types of marginality, ecological marginality and geographical marginality and this thesis focuses on the geographical marginality. Since important for understanding regional and global species responses to climate change, broader

scales are also referred to in this thesis when necessary. The focus of this research is the coralline algal *C. officinalis* across its geographical distribution in the NE Atlantic, yet the concepts and effects on marginal populations of this species can also be applied to other calcifying organisms. Additionally, margins of species distribution were not researched to the same extent, but the focus is usually only set on one margin. Therefore, in this study both north and south population margins, as well as the central, were sampled and exposed to various treatments.

This thesis comprises a comprehensive look at the physiology and structural integrity of a species living in a harsh and demanding environment. A multidisciplinary and multi-technique approach was implemented to create a complete view of potential adaptation and the relationship between physiology, structure, adaptation and resilience in terms of energetic costs and relocation within the organism. Consequently, this study aimed to adopt a combined field and laboratory approach to assess the context of resilience. The factors studied in this thesis are physiological traits such as photosynthesis, respiration, light calcification, dark calcification, photosynthesis-irradiance (P-I) and calcification-irradiance (C-I) curves; and structural differences such as tensile strength, strain, elasticity, skeletal trace elemental composition, growth rates and cell wall thickness.

With the continuous increase of climatic changes such as SST warming and OA in natural marine environments, there is a growing risk of extinction (~15 – 37%) for all species (Thomas *et al.*, 2004, IPCC, 2014a). Species compositions are changing and ecosystem structures are threatened to extraordinary levels beyond that which humanity has faced before. Therefore, it is indispensable to understand how these long-term climatic changes force species to change their physiology and ecology and become resilient. This understanding will allow for better predictions of future

species distributions, effects on them and the fate of the ecosystems they are inhabiting today, to form conservation strategies.

### 1.5 Research Aims and Objectives

This thesis seeks to improve the understanding of the resilience of marginal populations of the coralline algae *C. officinalis* to future climatic changes. The first of the four aims of this study was to identify, through analysis of physiology and structural integrity (Chapter 2), the differences between populations across their geographical distribution, comparing central to peripheral populations (Chapter 3).

A second aim of this study was to elucidate the likelihood of adaptation of populations to predominant conditions across the geographic range of *C. officinalis*, and to determine whether each chosen existing population, with a focus on edge populations, would be able to survive in all of these conditions (Chapter 4).

With a constantly changing climate and the predictions for vast increases in SST and OA, calcareous organisms such as *C. officinalis* are thought to be at the forefront of negatively affected species. This study will, as a third aim, establish how the effects of ocean acidification and sea surface water warming would influence the biology and structure of these important and potentially vulnerable calcareous macroalgae (Chapter 5).

The research will look at differentiations in physiological and structural traits between trailing and leading edge as well as central populations and the means by which they can potentially adapt and develop resilience to future climatic changes. Further, and as last aim of this research, the applicability and relevance of laboratory climate change studies with respect to their natural environment will be assessed (Chapter 6).

# Chapter 2

## Materials and Methods

## 2.1 Study Sites along the Species Distribution

Multiple study sites were chosen along the latitudinal distribution range of *Corallina officinalis* in the North East (NE) Atlantic (Figure 2.1). Sites were selected on the basis of genetic evidence from specimens sampled around the same locations prior to the start of this study (Walker *et al.*, 2009, Yesson *et al.*, 2018). Moreover, confirmation of species was obtained for specimens subsampled from *Corallina* specimens collected for this research (Tavares *et al.*, 2018). Specimens of two populations per country were chosen with a minimum distance of 1.5 km shoreline between each other and sampled over a course of 2 years from 2015 – 2017, in summer and in winter. This representation of populations enabled the comparison of physiological and structural responses to climatic changes in the species *C. officinalis*, as well as helping to predict climate change induced effects.

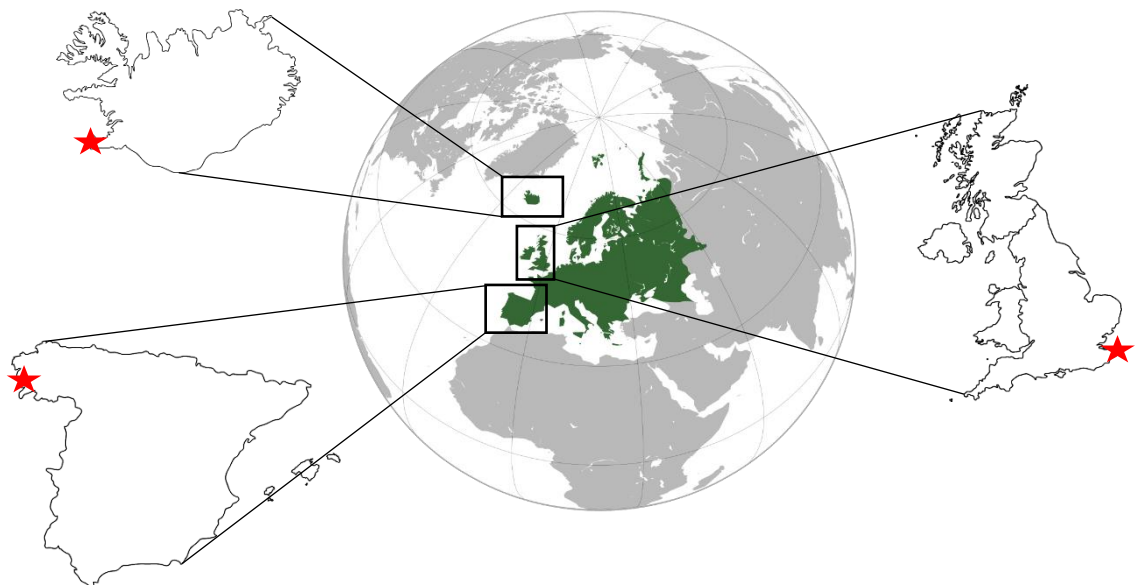


**Figure 2.1:** The study sites across the distribution of *C. officinalis*. Top left: Reykjanes, Iceland. Bottom left: Galicia, Spain. Right: Kent, UK. Maps retrieved for free from: d-maps.com.

### 2.1.1 Northern Margin: Reykjanes, Iceland

The northern margin was represented by specimens collected from populations south ( $63^{\circ}58'06.4''$  N,  $22^{\circ}45'03.1''$  W) and north ( $63^{\circ}58'27.8''$  N,  $22^{\circ}45'13.0''$  W) of Stafnes, Reykjanes in South West Iceland (Figure 2.2). Distance between populations: 1.59 km shoreline. Field incubations were conducted at the 03.11.2017 and 04.11.2017 and 22.07.2017 and 23.07.2017, for winter and summer incubations, respectively.

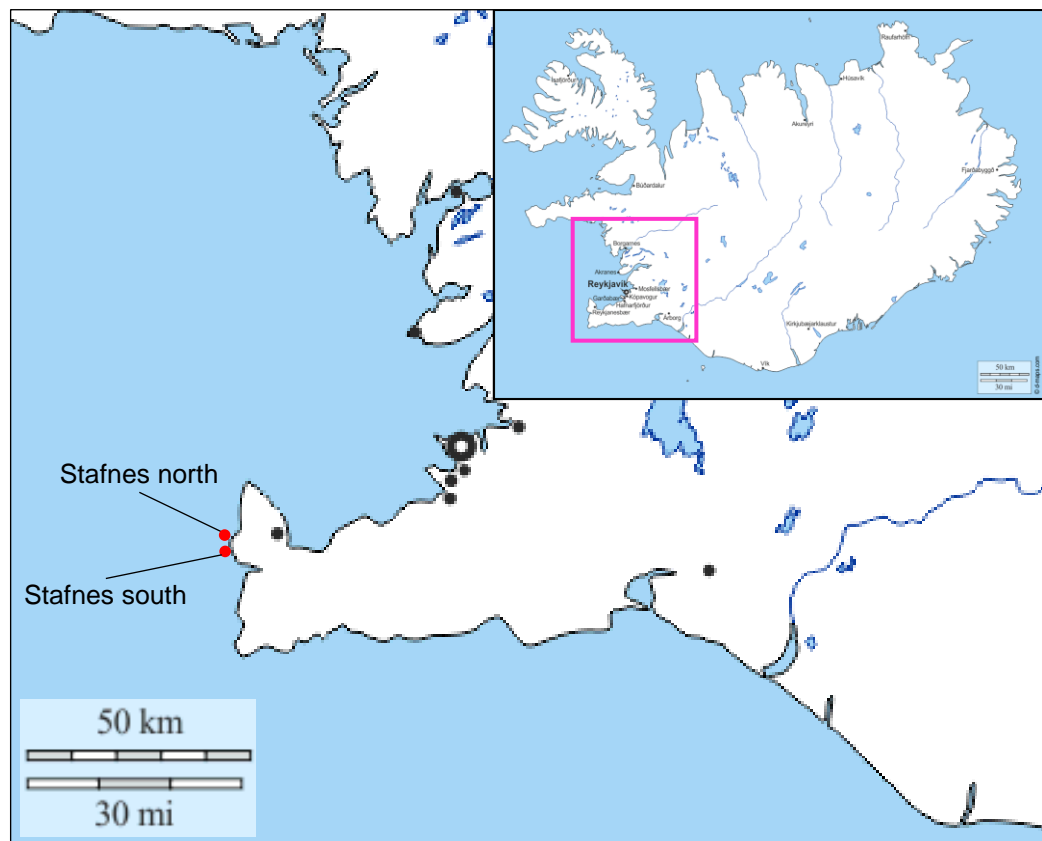


**Figure 2.2:** Top right: Map of Iceland with specification of sampling area magnification (pink square). Background: Sampling sites (red circles with labels) in South West Iceland near Keflavik. Maps adjusted from d-maps.com.

### 2.1.2 Centre: England, United Kingdom

The centre of the species distribution in the NE Atlantic is the United Kingdom. Here specimens from Westbrook Bay, Margate, Kent ( $51^{\circ}23'19.8''$  N,  $1^{\circ}22'01.8''$  E) and St. Margaret's Bay, Kent ( $51^{\circ}08'52.9''$  N,  $1^{\circ}23'06.9''$  E) in South East England were collected to represent the centre populations (Figure 2.3). Distance between populations: 40.87 km shoreline. Field incubations were conducted at the 29.01.2017 and 30.01.2017 and 10.07.2017 and 11.07.2017, for winter and summer incubations, respectively.



**Figure 2.3:** Top left: Map of the United Kingdom with specification of sampling area (pink square) and laboratory at the University of Portsmouth (green circle). Background: Sampling sites (red circles with labels) in South East England. Maps adjusted from d-maps.com.

### 2.1.3 Southern Margin: Galicia, Spain

The southern margin was represented using specimens collected at A Illa de Arousa, Pontevedra, Galicia, Spain ( $42^{\circ}34'07.7''$  N,  $8^{\circ}53'29.5''$  W) and Tragove, Pontevedra, Galicia, Spain ( $42^{\circ}31'28.0''$  N,  $8^{\circ}49'39.2''$  W; Figure 2.4). Distance between populations: 21.12 km shoreline. Field incubations were conducted at the 11.02.2017 and 12.02.2017 and 14.07.2018 and 15.07.2018, for winter and summer incubations, respectively.



**Figure 2.4:** Top right: Map of Spain with specification of sampling area (pink square). Background: Sampling sites (red circles with labels) in North West Spain. Maps adjusted from d-maps.com.



## 2.2 Specimen Collection

Specimens of *C. officinalis* populations were collected during low tide at the lowest water mark at all sampling times. Specimens were still submerged and found in cracks and ridges with flowing water, not rock pools, at a depth of  $26 \pm 4$  cm from the water surface at all sites at the afore named coordinates. In this way a minimum of stress was imposed on the specimens. Collections took place in summer and winter conditions to allow for comparisons between seasons. A hammer and chisel were used to ensure complete removal of specimens including the encrusting base and to cause as little damage to the fronds as possible. Specimens were chosen through visual determination of exterior integrity and cleaned from epiphytes using forceps prior to transport. A total of 30 - 40g of *C. officinalis* were collected at each site. Specimens were transported into the temperature controlled laboratory at the Institute of Marine Sciences of the University of Portsmouth, UK, using 24 hours temperature-conserving and temperature-insulating containers (Laken Classic Thermo, Laken Bottles Corporation, USA). Only healthy specimens, cleaned of epiphytes and without indication of bleaching or damage, were selected for the studies.

## 2.3 Specimen Culturing

In the temperature controlled laboratory at the Institute of Marine Sciences of the University of Portsmouth, specimens were carefully placed upright onto a small flint rock through a net of 2 mm mesh size to hold specimens in place and simulate natural growing conditions (Figure 2.5). In each experiment, populations were coded using coloured yarn, for future identification. Rocks with specimens attached in this way ( $n =$  depending on experiment) were placed into each replicate aquarium of the

treatment and cultured for the designated time of the experiment (Chapter 2.9 for detailed descriptions of the experiments).



**Figure 2.5:** Specimens of *C. officinalis* used in the experimental design, fixed on a small flint rock with a net to mimic natural growth conditions. Each population was colour coded (red arrow) with coloured yarn for future identification.

#### 2.4 Data Logger Deployment

In 2017, for every sampling site, a minimum of one data logger (HOBO UA-002-64 Pendant Temp/Light, Tempcon Instrumentation Ltd., Arundel, UK; accuracy: 0.47°C, resolution: 0.1°C, Figure 2.6) was deployed *in situ* to collate environmental light and temperature measurements throughout one year. Each data logger was deployed at low tide in a channel or rock pool within the sampling area of the specimens collected for the experiments. They were fixed to a rock with marine stainless steel screws and cable ties as well as tagged with contact information and warning sign in order to minimise loss or theft.

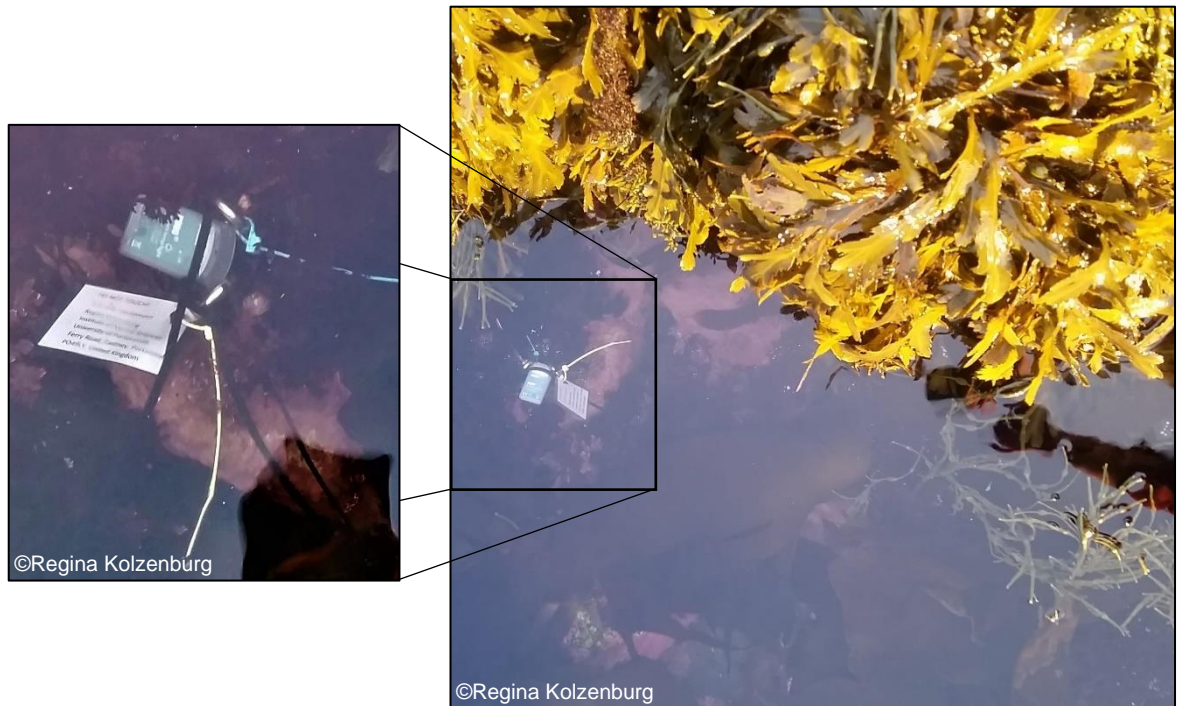


**Figure 2.6:** Background: example of data logger deployed in the field. Foreground: close up of data logger mounting to the rock in the field including tag and coloured cable ties for easier rediscovery.

## 2.5 Monitoring the Basic Parameters

In all laboratory experiments, temperature, salinity, dissolved oxygen (DO), pH and total alkalinity ( $A_T$ ) were monitored daily. Temperature and salinity were measured with a VWR CO310-1 portable salinity and temperature probe (VWR, Leuven, Belgium; accuracy: 0.2% for salinity,  $\pm 0.2^\circ\text{C}$  for temperature; resolution: 0.1 for salinity,  $0.1^\circ\text{C}$  for temperature). DO and pH were measured with a HACH HQ30d portable multi-parameter meter (Hach Lange GmbH, Duesseldorf, Germany) and a luminescent dissolved oxygen (LDO101; accuracy:  $\pm 0.1$  mg/L) and pH probe (PHC301, accuracy:  $\pm 0.02$ , calibrated on the National Bureau of Standards (NBS) scale and converted into total scale values using Tris/HCl and 2-aminopyridine/HCl buffer solutions after Dickson *et al.* (2007). Irradiance was measured once a month to monitor a potential reduction in light intensity using a HOBO UA-002-64 Pendant

Temp/Light data logger (Tempcon Instrumentation Ltd., Arundel, UK; accuracy: 0.47°C, resolution: 0.1°C).  $A_T$  was monitored in a randomly chosen replicate out of all replicates of a treatment, alternating daily, using the alkalinity anomaly technique after Smith and Key (1975), Chisholm and Gattuso (1991) and Dickson *et al.* (2007).  $A_T$  titrations were carried out with an automatic titrator (TitroLine 7000, Schott SI Analytics, Farnborough, UK; measurement accuracy: 0.002  $\pm$ 1 digit, dosing accuracy: 0.15%, dosing precision: 0.05-0.07%) to ensure minimal variation. As titrant a 0.1N hydrochloric acid (HCl; Sigma-Aldrich Company Ltd., Gillingham, UK) was freshly prepared and validated against Certified Reference Material provided by Andrew G. Dickson (Batch #154, Scripps Institution of Oceanography). During measurements in the field, identical instruments were used and measurements were taken three times at one site to create an average result.

## 2.6 Measurements of Fundamental Physiological Processes

The mass of algal fronds used in the incubations was transformed from fresh weight (FW) to dry weight (DW) by multiplying FW measurements with the factor 0.62286. This factor was determined from FW and DW measurements of thirty 1 g frond bundles from all populations before and after algae were left to dry for 48 h in an oven (Universal Fan Oven, Memmert, Schwabach, Germany) at 60°C (Egilsdottir *et al.*, 2013). This factor was then used to calculate the DW of algae used in the incubations described below.

### 2.6.1 Oxygen and Calcification Evolution

To determine saturating light levels of *C. officinalis* populations before the experiment as well as after the exposure to various treatments, oxygen production

evolution (P-I curves) and calcification evolution (C-I curves) under increasing light conditions were measured. For this purpose, algae were transferred into a clear, closed cell incubation chamber and incubated successively for 1 h at light intensities of 0 (darkness), 20, 80 and 160  $\mu\text{mol photons m}^{-2} \text{s}^{-1}$  and further, for 30 minutes at 320, 500 and 700  $\mu\text{mol photons m}^{-2} \text{s}^{-1}$  (AQUARAY Nature Perfect, Tropic Marine Centre, London), starting from the lowest to the highest to minimise stress. Incubation times were reduced in higher light intensities to avoid damage to the photosynthetic apparatus and to avoid oversaturation of oxygen in the water. A set of incubation chambers ( $n = 3$ ) per light intensity were incubated simultaneously and bubble-free in 58 ml incubation chambers. Mean FW of the incubated algae was  $0.97 \pm 0.07$  g and was obtained by tap drying the algae carefully with paper towel prior to weighing. Aluminium foil, covering each incubation chamber, was used to determine calcification and respiration rates in the dark. To account and correct for metabolism effects by other organisms, reference incubations without algae were performed alongside the above-described incubations for all light intensities. Irradiance was measured with a Hansatech Quantitherm PAR/Temperature Sensor with a QTP1 probe (resolution: 1  $\mu\text{mol photons m}^{-2} \text{s}^{-1}$ , 0.02°C, respectively).

Differences in oxygen concentration, pH and  $A_T$  were determined in order to calculate photosynthesis, respiration and calcification rates by measuring oxygen, pH and  $A_T$ , respectively, before and after the incubations (Chapter 2.6.6, equations 2.3 - 2.5). Prior to  $A_T$  measurements, seawater samples were filtered through a syringe filter (Fisherbrand, hydrophilic 25 mm, 0.2  $\mu\text{m}$  PTFE) into sterile 50 ml tubes (Fisherbrand, Plastic Centrifuge Tubes). Immediately after, potentiometric titrations were performed using an automatic titrator (TitroLine 7000, Schott SI Analytics, details: see above) calibrated on the NBS scale. Results were calculated based on

a Gran function after Dickson *et al.*, (2007). The carbonate system of the seawater was calculated from pH,  $A_T$ , salinity and temperature using the Excel (Microsoft office, USA) Macro CO2Sys (Version 2.1, Lewis and Wallace, 1998) with K1 and K2 according to Mehrbach *et al.*, (1973) and refit by Dickson and Millero (1987). Calculations to determine the following P-I curve and C-I curve variables: maximum photosynthetic/ calcification rates ( $P_{max}/ C_{max}$ ), the light harvesting efficiency ( $\alpha$ ) and the saturating light intensity ( $I_K$ ) as well as photosynthetic, respiration and calcification rates in the light and in the dark were performed using the methodology as described in Chapter 2.6.6.

## 2.6.2 Photosynthesis

### 2.6.2.1 *In situ*

To determine photosynthetic rates most likely to be found in the field, incubations ( $n = 5$ ) of all populations at ambient light conditions ( $72 \pm 21.21 \mu\text{mol photons m}^{-2} \text{s}^{-1}$  and  $410 \pm 63.64 \mu\text{mol photons m}^{-2} \text{s}^{-1}$  for UK populations in winter and summer, respectively;  $207 \pm 32.53 \mu\text{mol photons m}^{-2} \text{s}^{-1}$  and  $953 \pm 127.99 \mu\text{mol photons m}^{-2} \text{s}^{-1}$  for Spanish populations in winter and summer, respectively;  $63 \pm 13.44 \mu\text{mol photons m}^{-2} \text{s}^{-1}$  and  $334 \pm 195.16 \mu\text{mol photons m}^{-2} \text{s}^{-1}$  for Icelandic populations in winter and summer, respectively) were performed *in situ* following the protocol above (Chapter 2.6.1) before the transport and the experiment. Incubations were carried out in the same area in which specimens were collected. Incubation times were set to 1 h in order to be able to compare results later on with laboratory incubations. Calculations determining primary production in the field were performed following the methodology as described in section 2.6.6.

### 2.6.2.2 *In the Laboratory*

Immediately before the start of the experiment, incubations (Chapter 2.6.1) were performed to identify photosynthetic activity prior to the exposure to various treatments. The incubations took place in the 11 L replicate aquaria under *in situ* light and temperature conditions set in the experiment after associated field measurements. These incubations were repeated once a month throughout the experiment and final incubations were conducted in each treatment and replicate to determine the ultimate change between the start and the end of the experiment. Calculations determining primary production rates were performed following the methodology as described in section 2.6.6.

## 2.6.3 Respiration

### 2.6.3.1 *In situ*

To determine respiration rates most likely to be found in the field, incubations ( $n = 5$ ) of all populations were performed in the dark ( $0 \mu\text{mol photons m}^{-2} \text{s}^{-1}$ ) under *in situ* conditions following the protocol above (Chapter 2.6.1), before the transport and the experiment. Incubations were carried out in the same area in which specimens were collected. Incubation times were set to 1 h in order to be able to compare results later on with laboratory incubations. Calculations to determine respiration rates of field populations were performed following the methodology as described in section 2.6.6.

### 2.6.3.2 *In the Laboratory*

Alongside photosynthetic incubations, immediately before the start of the experiment, incubations were performed to identify respiration rates (Chapter 2.6.1) prior to the exposure to various treatments. 11 L aquaria served as replicates for all conditions as well as containers for incubations in the dark and under temperature

conditions set in the experiment after associated *in situ* field measurements. These incubations were repeated once per month until the end of the experiment and final incubations in each treatment and replicate to determine the final change between the start and the end of the experiment. Calculations to determine respiration rates were performed following the methodology as described in section 2.6.6.

## 2.6.4 Calcification

### 2.6.4.1 *In situ*

To determine calcification rates in the light and in the dark most likely to be found in the field, water samples from all replicates ( $n = 5$ ) of the photosynthesis and respirations incubations, as explained in 2.6.2 and 2.6.3, of all populations at ambient light conditions ( $72 \pm 21.21 \mu\text{mol photons m}^{-2} \text{s}^{-1}$  and  $410 \pm 63.64 \mu\text{mol photons m}^{-2} \text{s}^{-1}$  for UK populations in winter and summer, respectively;  $207 \pm 32.53 \mu\text{mol photons m}^{-2} \text{s}^{-1}$  and  $953 \pm 127.99 \mu\text{mol photons m}^{-2} \text{s}^{-1}$  for Spanish populations in winter and summer, respectively;  $63 \pm 13.44 \mu\text{mol photons m}^{-2} \text{s}^{-1}$  and  $334 \pm 195.16 \mu\text{mol photons m}^{-2} \text{s}^{-1}$  for Icelandic populations in winter and summer, respectively) and in the dark were performed *in situ* following the protocol above (Chapter 2.6.1) before the transport and the experiment. Incubations were carried out in the same area in which specimens were collected. Incubation times were set to 1 h in order to be able to compare results later on with laboratory incubations. After sterile filtration of water samples ( $0.2 \mu\text{m}$  pore size), they were stored and transported in a sterile container in a cold and dark place until further analysis in the laboratories at the University of Portsmouth (Chapter 2.6.1) immediately after arrival. Calculations to determine calcification rates in the field were performed following the methodology as described in Chapter 2.6.6.



### 2.6.4.2 In the Laboratory

To obtain data for calcification rates in the light and in the dark, water samples of photosynthesis and respiration incubations (Chapter 2.6.2 and 2.6.3) were 0.2  $\mu\text{m}$  sterile filtrated and immediately titrated (Chapter 2.6.1) to determine  $A_T$  values. Calculations to determine  $A_T$  and calcification rates were performed following the methodology as described in Chapter 2.6.6.

### 2.6.5 Oxygen Chamber

As an alternative method to determine photosynthesis and respiration an oxygen chamber (DW3 Electrode Chamber, Oxy-Lab, software: O2view 2.05, Hansatech Instruments, Norfolk, UK, Figure 2.7) was used to continuously measure oxygen production or consumption rates in the first Common Garden Experiment (Chapter 2.9.1). The chamber was effectively temperature controlled at a set temperature, depending on the treatment of the specimen, by a constant water flow through the water jacket which was attached to a recirculating water bath (LTC2 water bath, TC120 heating circulator, R2 refrigeration unit, Grant Instruments, Cambridge, UK).

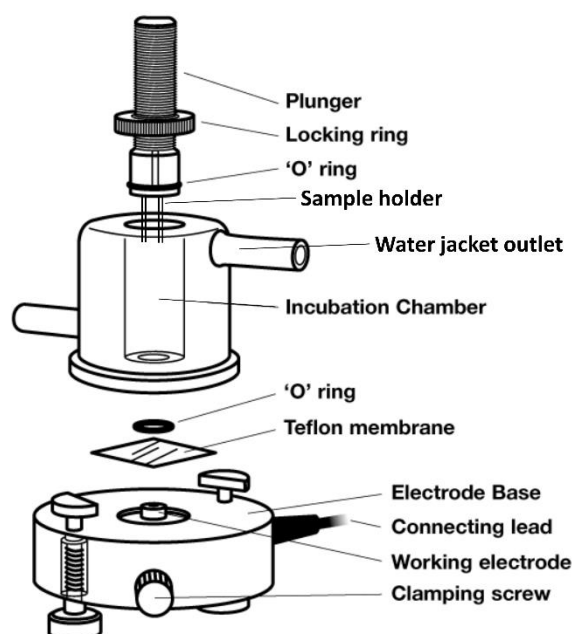


**Figure 2.7:** Schematic diagram of the oxygen chamber with electrode, similar to the model used in this study. Modified from Ragazzola (2008).

One branch of *C. officinalis* was attached to the holder on the lid and submerged into the oxygen chamber. The specimen was kept in the dark for 2 minutes to allow for acclimatisation to the chamber, then, the specimen was exposed to saturating light intensity of an average of  $1330 \pm 93 \mu\text{mol photons m}^{-2} \text{ s}^{-1}$ , for 5 minutes to determine oxygen production rates and absolute oxygen values in the waterbody. Following the light exposure, the specimen was kept in the dark for 5 minutes in order to recover from the light exposure, followed by additional 5 minutes in the dark to determine oxygen consumption rates. A light, recovery and dark incubation time of 5 minute was chosen to ensure correct measurements of the specimens' metabolic response to light or dark exposure.

#### 2.6.6 Data Analysis

The maximum potential photosynthetic rate and calcification rate per individual ( $P_{\text{max}}$  [ $\text{mg O}_2 \text{ gFW}^{-1} \text{ h}^{-1}$ ] and  $C_{\text{max}}$  [ $\text{meq CaCO}_3 \text{ gFW}^{-1} \text{ h}^{-1}$ ], respectively) as well as the slope of the light-limited region of the P-I curve and C-I curve showing the efficiency of the algae to harvest light ( $\alpha$ ), were directly determined from the P-I curves and C-I curves using Excel (Microsoft office, USA). The irradiance at which photosynthesis and calcification is saturated ( $I_k$  [ $\mu\text{mol photons m}^{-2} \text{ s}^{-1}$ ]) was calculated using the following relationship

$$I_k = \frac{P_{\text{max}}}{\alpha} \quad (2.1)$$

Primary production was measured by oxygen fluxes such as photosynthesis ( $P_N$  [ $\text{mg O}_2 \text{ gFW}^{-1} \text{ h}^{-1}$ ]) and respiration ( $R$  [ $\text{mg O}_2 \text{ gFW}^{-1} \text{ h}^{-1}$ ]) and were calculated as follows:

$$P_N \text{ or } R (\text{O}_2) = \left( \frac{\Delta\text{O}_2 \times V}{\Delta t \times \text{FW}} \right) \quad (2.2)$$

with  $\Delta O_2$  as the change in dissolved oxygen concentration [mg/L],  $V$  as the volume of the incubation chamber [L],  $\Delta t$  as the incubation time [h] and FW as the fresh weight of the algae [g].

Total alkalinity  $A_T$  was calculated using potentiometric titration data (Chisholm and Gattuso, 1991). A known volume of seawater sample is titrated with a strong acid (0.01 M HCl) until reaching the endpoint corresponding to the formation of carbonic acid from bicarbonate (Dickson, 1981). The volume of acid used is proportional to the total amount of hydrogen ions that is required to neutralise the negative charges in the sample. Gran (1952) created a procedure in which only a few steps of the pH development between pH 4.4 and pH 3.7 are recorded. These steps of acid titrant volume and corresponding pH in the given range, pH 4.3 to pH 3.5 adapted for this study, are used to calculate  $F_2$ , a Gran function, as followed:

$$F_2 = [\text{antilog}(5 - pH)] \times (V_s \times v) \quad (2.3)$$

with  $V_s$  as the sample volume [ml] and  $v$  as the titrant volume [ml]. As a result of this function, a linear plot can be created against the volume of titrant  $v$ . A point of intersection with the horizontal axis,  $v_2$ , can be determined via extrapolation of this graph, marking the alkalinity equivalence end-point. With these parameters,  $A_T$  [meq/L] can be calculated as followed:

$$A_T = v_2 \times \left(\frac{1000}{V_s}\right) \times n \quad (2.4)$$

with  $n$  as the concentration of the titrant.

Calcification rates can be determined from changes in  $A_T$  due to the chemical reaction of formation and dissolution of  $CaCO_3$  and the concomitant change in ions and charges in seawater. Calcification ( $G$  [meq  $CaCO_3$  gFW<sup>-1</sup> h<sup>-1</sup>]) rates in the light and in the dark were estimated using the following equation:

$$G (\text{CaCO}_3) = - \left( \frac{\Delta A_T \times V}{2 \times \Delta t \times \text{FW}} \right) \quad (2.5)$$

with  $\Delta A_T$  as the change in total alkalinity [meq/L].

Data for Oxygen Chamber incubations were analysed using Excel and plotting total oxygen concentrations and oxygen production and consumption rates against time.

### 2.6.7 Linear Growth Rates

The effects of various environmental changes on linear growth rates were measured to determine the impact of this exposure to the condition of the algae. Determining linear growth rates comprises multiple analytical steps (Figure 2.8).

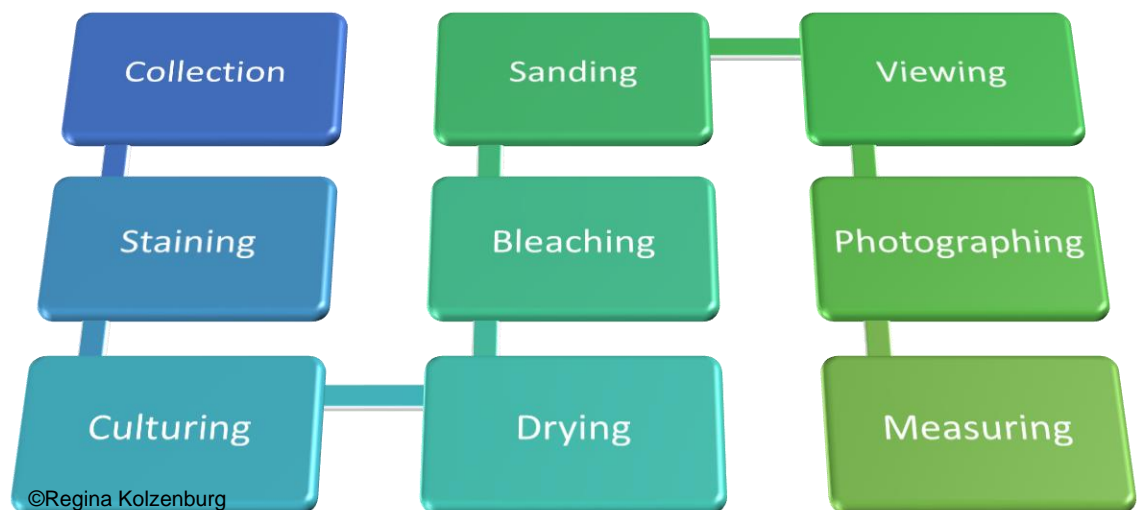


**Figure 2.8:** Overview of individual steps of linear growth rate analysis as explained in 2.6.7.2

#### 2.6.7.1 Staining Procedure

Before the start of the experiment and after the acclimatisation phase, all specimens ( $n =$  depending on experiment) of each population were stained with a solution of  $0.5 \text{ g L}^{-1}$  of the vital stain Alizarin Red S (Fluks, Sigma-Aldrich, Steinheim, Germany), following Andrade and Johansen (1980) and Ragazzola *et al.*, (2012). Algae were submerged in the solution for 24 h under a light intensity of 1990 lux

(equals  $\sim 35 \mu\text{mol photons m}^{-2} \text{ s}^{-1}$ ) to ensure the incorporation of the stain in the skeleton without exposing the specimens to unnecessary irradiation stress. After staining, algae were carefully and thoroughly rinsed with filtered seawater in order to remove the residual staining solution and placed back into the aquaria.

#### 2.6.7.2 Growth Rate Analysis

After the experiment, algae were carefully dried at room temperature for a minimum of 3 days. Longitudinal thallus sections of dried replicates of each treatment ( $n = 20$ ) were prepared using sand paper of two different grit sizes consecutively (Granulation: 180 and 1200, Silicon carbide sanding sheet waterproof T489, NORTON Abrasives, Stafford, UK). Prior to sanding the thalli very carefully and with a constant light pressure, thalli were exposed to a 5% diluted solution of household bleach for 3 minutes (Domestos Pink Bleach, Unilever UK Ltd, Leatherhead, UK)

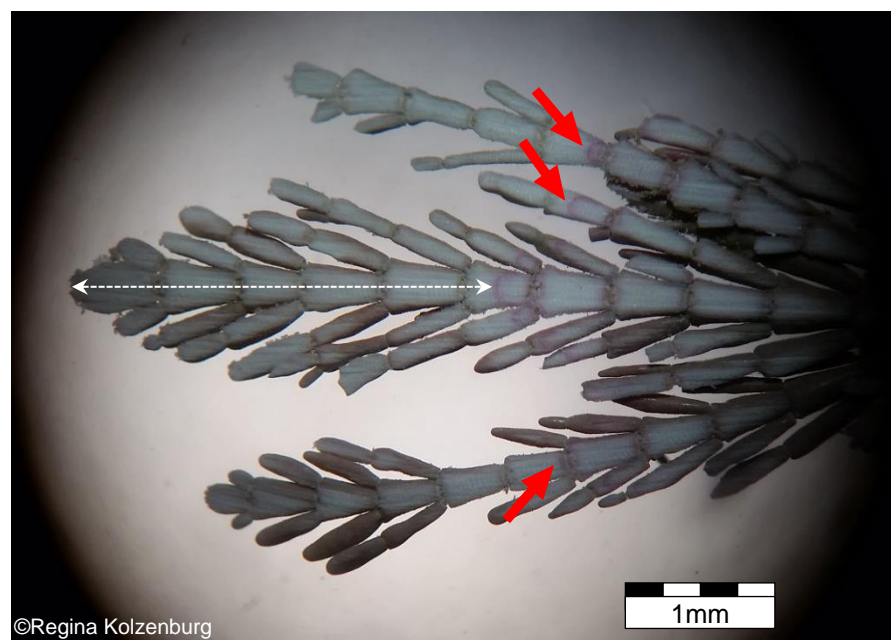


**Figure 2.9:** Stained thalli of *C. officinalis* after the experimental phase. Structures below the stain grew prior to the experiment, in the field. Stained sections, in pink, grew during the 24 h staining period. Skeleton structure above the stain grew in the experimental condition in the laboratory. Red arrows: stained section. White dotted arrow: linear growth measurement example.

and rinsed with RO (Reverse osmosis purified water) to reduce a potential impact of the bleach on the skeleton (Loxton *et al.*, 2017). Following the bleaching and sanding, thalli were viewed and photographed under a stereo microscope (S8 APO, Leica Microsystems, Milton Keynes, UK) with an attached microscope camera (MC120 HD, Leica Microsystems, Milton Keynes, UK) under the magnification 1. Where stain was visible (Figure 2.9), growth was measured from the stain to the tip of the main branch using the software ImageJ (Rasband, 2016) with the scale bar set to 1 mm/193 pixels, which was determined using scale paper under the same magnification.

## 2.7 Algae Transplants

In order to obtain growth rates in the field, transplants of *C. officinalis* were conducted at one sampling site in Iceland and one in the UK. For this, specimens



**Figure 2.10:** Example of *C. officinalis* transplant, recovered from the field.

were carefully removed from the field following the procedure described in 2.2 and stained over night as described in 2.6.7.1. The following day specimens were placed back at the point of collection and were fixed with epoxy resin (Splash Zone A-788, KOP-COAT, Inc., NJ, USA) and left for 3 and 5 months in Iceland and UK, respectively. After re-collection of the transplants (Figure 2.10), specimens were carefully dried and growth rates were determined following the protocol in 2.6.7.2.

## 2.8 Structural Integrity Measurements

Structural integrity of all samples was determined by a combination of multiple measurements, such as pull-to-break, scanning electron microscopy (SEM) and laser ablation coupled to a plasma mass spectrometer (LA-ICP-MS).

### 2.8.1 Tensile Strength

In order to determine the ultimate tensile strength ( $F_{tu}$ ), which is the materials capacity to withstand loads elongating a specimen, and, therefore, to determine whether there are differences in strength and the resistance of tension of the high-Mg calcite skeleton between treatments, pull-to-break measurements were conducted.

#### 2.8.1.1 *Sample Preparation*

Dry samples of each replicate or treatment were fixed to a 2 cm long piece of flat wooden surface, using instant adhesive (Figure 2.11). For consistency and comparability, only the top and the bottom 3 calcified intergenicula segments of all specimens were fixed to the wood and a  $1.00 \pm 0.13$  cm sample length was adjusted. It was ensured the tested sample length was not contaminated with adhesive in order to make sure no structural properties would be changed.

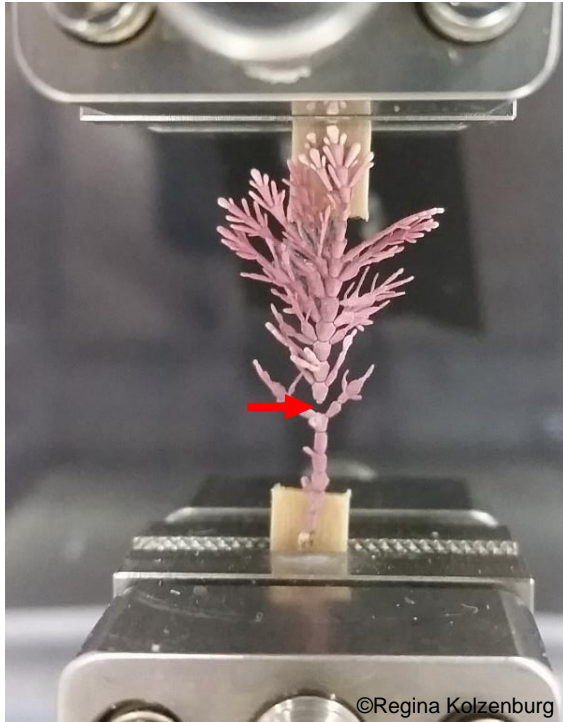


**Figure 2.11:** Completed dry tensile strength analysis of *C. officinalis*. Red arrow: breakpoint of this sample.

### 2.8.1.2 Analysis

Dry analyses were conducted using an ElectroForce fatigue test instrument (Model 3220 Series II, Bose Corporation, Eden Prairie, MN, USA) attached to a computer with the analysing software WinTest 7 (Bose Corporation, Eden Prairie, MN, USA). The wooden stick with a prepared sample was clamped between the holder (bottom) and the mover (top) on its endings. The mover is the part of the device that can apply the test conditions to the specimen. Detailed parameters for the chosen settings can be found in Table 2.1. Data were plotted and analysed using Excel (Microsoft office, USA) plotting Load against displacement indicating the breaking point of each sample, the tension needed to break each sample and the strain, representing the elongation of each sample. Normal strain was calculated using the following equation

$$\varepsilon = \frac{\Delta L}{L_0} \quad (2.6)$$



where  $\Delta L$  represents the change in length of the sample [mm] and  $L_0$  represents the initial length of the sample [mm].

Due to the length of sample to be mounted for this test, tensile strength of field samples could be performed; unfortunately, specimens of experimental conditions were not suitable for these analyses as growth was not sufficient enough.

**Table 2.1:** Tensile strength operational parameters

<b>Tensile strength parameters</b>	
Waveform	Ramp
Mover type	Absolute
Control channel	Displacement
Rate	0.00835 mm sec <sup>-1</sup>
Scan type	Standard
Maximum displacement	±6.5 cm
Maximum load	±225 N
Scan info	Time: 5 Points: 250 Number of scans: 50

### 2.8.2 Laser Ablation Inductively Coupled Plasma Mass Spectrometry

*Corallina officinalis* accumulates Mg within its calcareous cell walls to build a high-Mg calcite skeleton (Stanley *et al.*, 2002, Andersson *et al.*, 2008). In order to determine the Mg/Ca ratio of this calcite and its fate in various conditions, laser

ablation inductively coupled plasma mass spectrometry (LA-ICP-MS) was performed. This method enables the measurement of predetermined trace elements, which ultimately leads to the specimens' elemental composition.

### 2.8.2.1 *Sample Embedding*

Specimens, which were initially used for growth rate analysis, were fixed to a reversed, customary packaging tape on a microscope glass slide. After samples were positioned in the middle of the embedding mounts (25 mm diameter, cylindrical mounting cup, batch no: 8127-2242, SeriForm, Struers ApS, Ballerup, Denmark), mount cups were thinly coated with silicone oil (Batch no: 8128-01, Struers ApS, Ballerup, Denmark). Epoxy resin (EpoFix Kit, batch no: 8134-01, Struers ApS, Ballerup, Denmark) was prepared by mixing the hardener (EpoFix Hardener, batch no: 8075-01, Struers ApS, Ballerup, Denmark) with the resin (EpoFix Resin, batch no: 8106-01, Struers ApS, Ballerup, Denmark) in a ratio of 3 – 4 g hardener with 25 g resin followed by careful mixing with a wooden stick to ensure no bubbles are created during this process. The resin was gently poured into the mounting cup with the specimens, ensuring no bubbles were created by the filling process. Mounts were kept under vacuum (-0.8 bar) for initial hardening before the resin was set to cure overnight under a vacuum of -2.6 bar in a pressure chamber. Thereafter, the tape was removed and the mount was loosened and detached from the mounting cup. Afterwards, the mount was polished with a polishing machine (MetaServ 3000 or VibroMet 2, Buehler, Esslingen, Germany) using gentle side to side vibration. A self-adhesive pad with a thick tufted fabric pile was used in conjunction with an aluminium oxide solution (aluminium oxide powder (Micropolish Alumina, Buehler, Esslingen, Germany) and distilled water) of 0.05 µm grain size. The machine polished for 7 minutes until specimens were exposed and polished enough for

subsequent LA-ICP-MS analysis (Figure 2.12). Mounts were then cleaned under running water and gently dried with paper tissue.

### 2.8.2.2 Sample Preparation

All mounts were cleaned with Isopropanol and pressure nitrogen gas prior to LA-ICP-MS analysis. Depending on the size of the samples, an ablation cell (Laurin Technic S155, Australian Scientific Instruments, Fyshwick, Australia) with either a combination holder for 30 mm and 40 mm round mounts or a universal holder for individually fixable, irregular objects was used to fix the sample mounts.

### 2.8.2.3 Analysis

Trace element analyses were conducted in multiple sessions at the School of Earth and Environmental Sciences, University of Portsmouth, United Kingdom. The first analytical session was carried out using an Agilent 7500cs (quadrupole) ICP-MS coupled with a Nd:YAG 213 nm New Wave solid-state Laser ablation system. Laser ablation parameters were as follow: 55  $\mu\text{m}$  spot size for NIST glasses and MACS-3 carbonate references (NIST SRM 610 and 612, US National Institute of Standard and Technology Standard Reference Material; MACS-3, the United States Geological Survey) and 80  $\mu\text{m}$  for unknowns, approximately 55% laser energy and 10 Hz. Each analysis consisted of 25 seconds of background, 10 seconds of laser



©Regina Kolzenburg

**Figure 2.12:** Example of embedded *C. officinalis* in Epoxy resin

warming up (starting at 15 seconds of background), 35 seconds of acquisition and 15 seconds of washing out (75 seconds in total). The following sessions used a RESOLUTION 193 nm ArF excimer Laser with a Laurin Technic S155 Ablation cell coupled to an Analytic Jena Plasma Quant MS Elite ICP-MS. Analyses consisted of 55  $\mu\text{m}$  spot size, laser fluency was 3.0 J/cm<sup>2</sup> and its repetition rate was 5 Hz. Background measurements took 20 seconds, followed by 30 seconds of ablation and 15 seconds of washout for each analysis (65 seconds in total). Detailed operating conditions for both instruments are listed in Table 2.2.

Background and signal counts were integrated, time-drift corrected and reduced to concentrations using the SILLS (Guillong *et al.*, 2008) and Lolite 3.4 software packages (Paton *et al.*, 2011), respectively for first and following sessions. Synthetic silicate glass reference material NIST SRM 610 as well as NIST SRM 612 were used for instrumental calibration and as primary and secondary standards. Synthetic calcium carbonate USGS MACS-3 was also used as secondary standard and analysed in the same conditions as the unknowns. Each run consisted of at least six external standard analyses (NIST 610) and four secondary standards NIST 612 and MACS-3 ( $n = 8$ ). Detection limits (99% confidence) for the spot measurements of the NIST glasses were: Mg = ~3 ppm for session 1 and ~28 ppm for following sessions; Ca = ~30 ppm for session 1 and ~100 ppm for following sessions. Internal standard element used for normalization of the data was <sup>43</sup>Ca, which was obtained from the GeoReM data base and own measurements. All reference materials were ablated prior, in the middle and after sample ablation. Following every 6th sample analysis one analysis of NIST SRM 610 was added to correct for time-dependent drift of mass discrimination and instrument sensitivity. Final elemental composition ratios in this study were calculated as a 'mean count rate' including standard error

of  $n = 5 - 9$ , depending on experiment, drift and background corrected single ablation spot analysis for each of the three replicates. This method is commonly used for LA-ICP-MS data reduction (Longerich *et al.*, 1996). Values obtained in the course of this study are reproducible within 10% for Mg, of the GeoReM recommended values and were compared with this data base to determine accuracy as well as internal and external reproducibility (Jochum *et al.*, 2005).

**Table 2.2:** LA-ICP-MS operational parameters

LASER PARAMETERS		
	Session 1	Following sessions
Wavelength	213 nm	193 nm
Fluence	3.5 – 4.0 J cm <sup>-2</sup>	Ø 3.0 J cm <sup>-2</sup>
Laser Energy	55%	3.6 mJ
Carrier gas	Helium (He)	Helium (He) + Argon (Ar)
Ablation style	Static	Static
Ablation spot size	55 µm for glasses, 80 µm for unknowns	55µm
Repetition rate	10 Hz	5 Hz
ICP-MS PARAMETERS		
	Session 1	Following sessions
RF power	1450 W	1300 W
Plasma gas	16 L/min	10 L/min
Auxiliary gas	1.0 L/min	1.65 L/min
Nebulizer flow	0 L/min	0.87 L/min
Sampling depth	~5.0 mm	~8.5 mm
Detector	Single collector	Single collector
Dwell time per mass	10 ms	10 ms

### 2.8.3 Scanning Electron Microscopy

Cell wall thickness is a key parameter completing the picture when determining the fate of the calcareous skeleton of coralline algae in changing environments. With this measurement, using SEM, the modification of the cell wall structure and therefore, a potential change in growth or metabolic processes can be connected. Measurements were taken from the combined cell walls between two cells due to the difficulty of separation of cells in the SEM images.

#### 2.8.3.1 *Sample Preparation*

The same sample mounts prepared in 2.8.2.1 for LA-ICP-MS analysis, were used for SEM analysis. An SEM, suitable to analyse uncoated samples, was used (EVO MA10 with a W filament electron source, Zeiss, Oberkochen, Germany), to be able to utilise the same mounts in both machines without any interference of sample coating. This allows for direct comparison of the SEM pictures and the LA-ICP-MS data. Sample mounts were fixed on stabs with double coated carbon conductive tabs and cleaned using Isopropanol, prior to loading the SEM and applying a variable pressure (VP) vacuum of 28 Pa.

#### 2.8.3.2 *Analysis*

Images were taken at 20 kV electron high tension (EHT), representing the accelerating voltage used for each sample. A working distance (WD) of 7 - 9 mm was set. Pictures were taken with a probe of 300 pA, a scan speed of 20.5 s, a magnification of 3 K and a line average noise reduction in the Backscatter (HDBSD) mode. After all images were produced, the software ImageJ (Rasband, 2016) was used to determine the average intra- (lateral to growth direction) and inter-cell wall (horizontal to growth direction) thickness of specimens (n = 15, Figure 2.13).

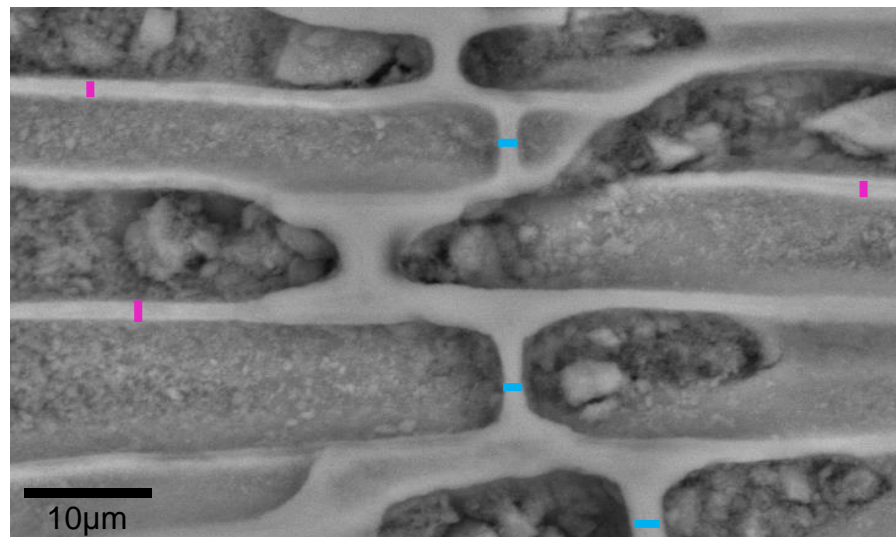


**Figure 2.13:** Individual cells of *C. officinalis* separated by intra- (horizontal to growth direction, blue line) and inter-cell walls (lateral to growth direction, pink line).

## 2.9 Experimental Designs

The effects of existing and future environmental conditions were investigated through different long-term experiments. Common Garden Experiments were performed to investigate how populations of *C. officinalis* were affected by currently existing temperature and light conditions across their geographic distribution. For this, populations of different countries, representing the centre or the margin of this species distribution in the NE Atlantic, were collected, acclimatised to each other's field conditions and cultured in the laboratories of the Institute of Marine Sciences, University of Portsmouth. To further investigate if and how future predicted environmental changes (IPCC, 2014a) affects the same populations, additional long-term experiments were conducted exposing populations across the geographic range of *C. officinalis* to future predicted pH decrease and temperature increase for the respective country. All experiments were conducted in temperature controlled (15°C) laboratory facilities at the Institute of Marine Sciences, University of

Portsmouth and were supplied with natural, filtered surface seawater from outside the institute through a twin-pump filter system with attached settlement tank, sand filter and storage tank. Weekly cleaning of all aquaria was performed to ensure optimal growth conditions. When necessary, algae were gently and carefully cleaned with a soft brush in order to prevent coverage of epibionts or silt and to provide optimum conditions. All aquaria in all experimental designs were covered with a plastic lid to minimise evaporation.

### 2.9.1 Common Garden Experiment

Four 11.1 L aquaria for each of the three countries, Iceland (representing the northern margin), UK (representing the central population) and Spain (representing the southern margin) and temperature conditions were randomly distributed and set up in a flow-through seawater system in the laboratories of the Institute of Marine Sciences of the University of Portsmouth (Figure 2.14). Each aquarium was equipped with individual water supply from multiple header tanks, each water source was kept at constant *in situ* temperatures measured in the field by TECO TK-2000 chillers (cooling capacity of 870 W, 800L/h), a water pump (TMC, V<sup>2</sup>PowerPump 800, Flow rate: 700 L/h) and a 35 cm long air diffuser to imitate tidal water movements and ensure oxygen supply with ambient air. The discarded seawater was treated with UV light (Tropic Marine Centre (TMC) P2-110W Commercial UV Steriliser, max. flow rate: 65 L/min) prior to disposal to ensure no non-native organism was released into the surrounding waters of the institute. Specimens (total rocks with specimens per population and treatment replicate:  $n = 4$ ) were kept at their *in situ* temperatures measured during sampling (northern margin conditions: temperature: 7.9°C, light: 228  $\mu\text{mol photons m}^{-2} \text{s}^{-1}$ ; central conditions: temperature: 12.0°C, light: 159  $\mu\text{mol photons m}^{-2} \text{s}^{-1}$ ; southern margin conditions: temperature:



16.0°C, light: 690  $\mu\text{mol photons m}^{-2} \text{s}^{-1}$ ). Temperature conditions were kept constant using TECO TK-2000 chillers (cooling capacity of 870 W, 800 L/h). All aquaria had a light/dark cycle of 9.5/14.5 h (as an average of natural light lengths) produced and controlled by TMC AQUABEAM 600 Ulima Reef White lights with cloud function. Additionally, sunset and sunrise were mimicked through a slow increase and decrease of light intensities over a period of 1 h. All specimens were kept in their corresponding conditions for a minimum of 1 week to acclimate to aquaria conditions. Following the initial acclimatisation, half of the northern/centre/southern populations were gradually acclimatised (increase/decrease of 1.5°C/week and 40  $\mu\text{mol photons m}^{-2} \text{s}^{-1}$ /week, respectively) to the northern/central/southern temperature and the average light conditions ( $\sim 300 \mu\text{mol photons m}^{-2} \text{s}^{-1}$ ) over a

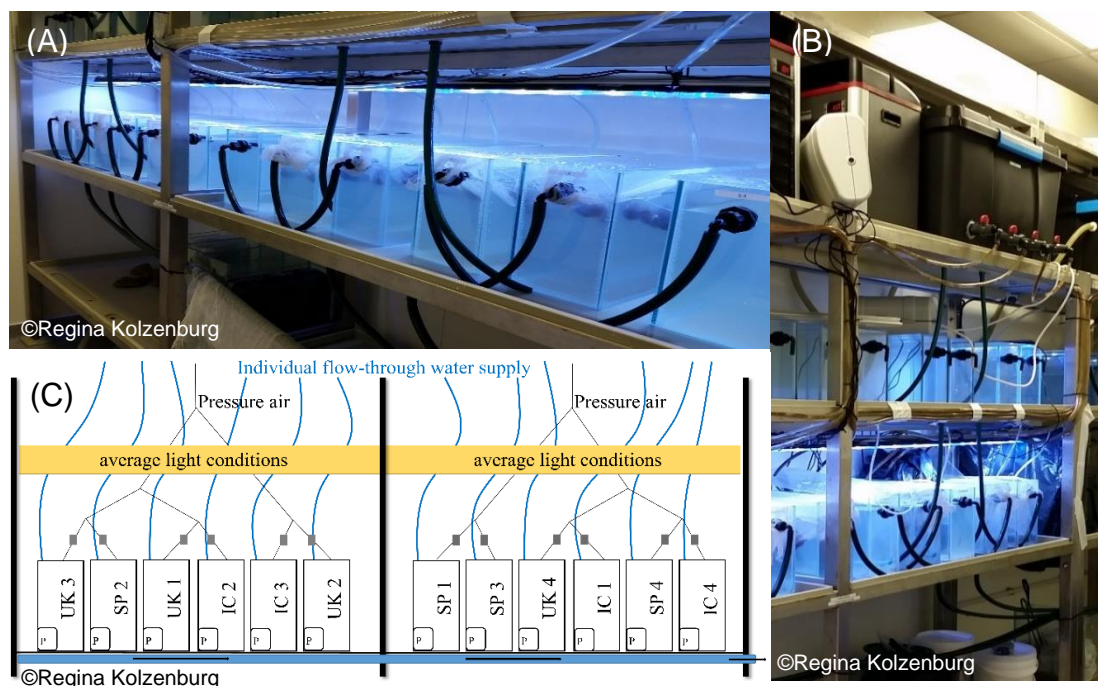


**Figure 2.14:** (A) Common Garden experimental design, close up. (B) Experimental design, overview including flow-through water supply. (C) Experimental design schematics. Blue lines indicate the individual water supply. Grey lines indicate individual air supply with regulators (grey squares). Squares with “P” illustrate a pump in each replicate. Letters and numbers display the country of origin (UK = United Kingdom, central population; SP = Spain, southern margin population; IC = Iceland, northern margin population) and the replicate number (1 - 4).

period of five weeks. After acclimatisation and colour coding in order to identify each population (Figure 2.5), specimens were randomly and equally distributed within the corresponding replicate aquaria and cultured for 10 weeks. Following the protocol 2.6.5, photosynthesis and respiration were measured once per week, calcification was determined once per month, pH and  $A_T$  were measured twice per month and growth rates were determined at the end of the experiment. LA-ICP-MS, SEM as well as tensile strength analysis were conducted after the experiment according to the protocol described in 2.8.1 – 2.8.3.

### 2.9.2 Common Garden Experiment: Central and Southern Populations

Three 11.1 L aquaria for each of the two central and southern margin populations ( $n = 4$ ) and corresponding temperature conditions were set up in a water bath (Figure 2.15) with water pumps (TMC, V<sup>2</sup>PowerPump 800, Flow rate: 700 L/h) to circulate and mix the containing water to obtain an even tempering. 75% of the water in the replicate aquaria was changed every second day and treated with UV light (Tropic Marine Centre (TMC) P2-110W Commercial UV Steriliser, max. flow rate: 65 L/min) prior to disposal. Each aquarium was equipped with a water pump and air stone to imitate tidal water movements and ensure oxygen supply with ambient air. Specimens (total rocks with specimens per population and treatment replicate:  $n = 10$ ) were kept at their *in situ* temperatures measured during sampling (central conditions: temperature: 5.7°C, light: 57  $\mu\text{mol photons m}^{-2} \text{s}^{-1}$ ; southern margin conditions: temperature: 11.3°C, light: 184  $\mu\text{mol photons m}^{-2} \text{s}^{-1}$ ). Temperature conditions were kept constant using TECO TK-2000 chillers (cooling capacity of 870 W, 800L/h) for each water bath. Both treatments had a light/dark cycle of 10/14 h (as an average of 9/15 h for central and 10.5/13.5 h for southern environmental conditions) produced and controlled by TMC AQUABEAM 600 Ulima Reef White

lights with cloud function. Additionally, sunset and sunrise were mimicked through a slow increase and decrease of light intensities over a period of 1 h. Two populations of each geographic location were used for this study. All populations were colour coded with coloured yarn prior to the start of the acclimatisation. All specimens were kept in their corresponding conditions for a minimum of 1 week to acclimate to aquaria conditions. Following the initial acclimatisation, half of the central/southern populations were gradually acclimatised (increase/decrease of  $1.5^{\circ}\text{C}/\text{week}$  and  $40 \mu\text{mol photons m}^{-2} \text{s}^{-1}/\text{week}$ , respectively) to the southern/central temperatures and light conditions over a period of 3.5 weeks. After acclimatisation specimens were randomly and equally distributed within the corresponding replicate aquaria and cultured for three months. Monitoring parameters: pH, temperature, salinity and DO were measured daily in each replicate,  $A_T$  was measured daily in one randomly chosen replicate of each treatment. Photosynthesis, respiration and calcification incubations were performed prior and after the experiment, according to the protocol

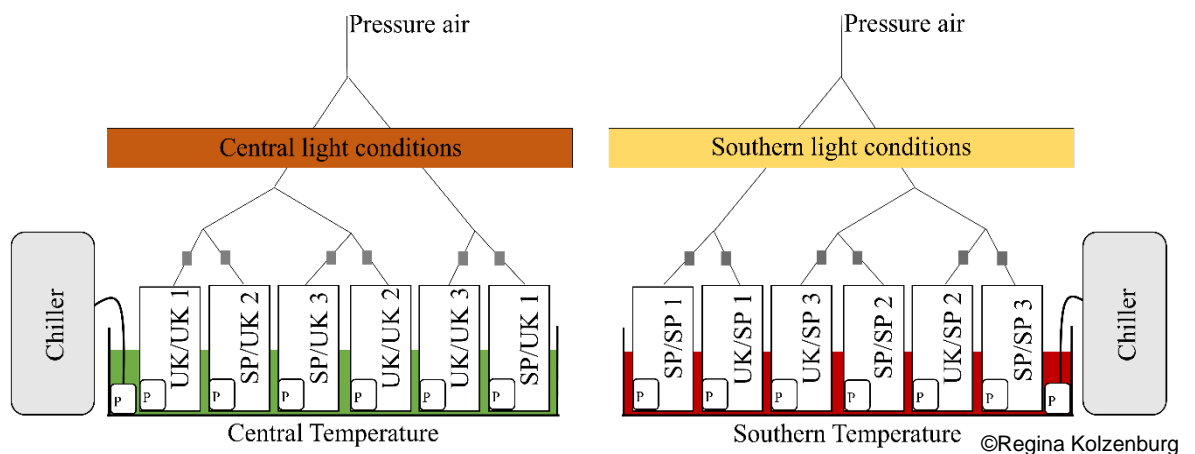


**Figure 2.15:** Detailed experimental design of the Common Garden Experiment with southern and central populations. Green and red coloured water baths represent central and southern temperature conditions, respectively. Central and Southern populations as well as conditions are abbreviated as UK and SP, respectively. First abbreviation indicates the country of origin of the populations, second abbreviation indicates the temperature condition. Numbers 1-3 represent replicates of one treatment.

described in 2.6.2 – 2.6.4. P-I curves and C-I curves of each population in each treatment were conducted before and after the experiment following the protocol in 2.6.1. Structural integrity analyses were conducted after the experiment as described in 2.8.

### 2.9.3 Climate Change Experiment

For this study, two populations of three geographic locations ( $n = 6$ ) across the species distribution were sampled (Iceland = northern margin populations; UK = central populations; Spain = southern margin populations) and exposed to four treatments: (1) Control (ambient temperature, ambient  $p\text{CO}_2$  (pH 8.1 – 8.2/ 380 – 400 ppm  $p\text{CO}_2$ , IPCC, 2014a)), (2) high temperature (high temperature ( $T+3$ ; IPCC, 2014), ambient  $p\text{CO}_2$ ), (3) high  $p\text{CO}_2$  (ambient temperature, high  $p\text{CO}_2$  (pH 7.75 - 7.80/ ~1000 ppm  $p\text{CO}_2$ ; RCP 8.5, IPCC, 2014a), (4) climate change (high temperature, high  $p\text{CO}_2$ ) and cultured for four months. All populations were colour coded with coloured yarn prior to the start of the acclimatisation for easier recognition throughout the experiment. Fifty 11.1 L aquaria were set up in a flow-through, open seawater system (Figure 2.16 and Figure 2.17). Each was supplied with an individual water supply (turn-over of aquarium volume: minimum 5 x/day = ~40 ml/min flow rate), a water pump (TMC, V<sup>2</sup>PowerPump 800, Flow rate: 700 L/h) and an adjustable air diffuser, to circulate and mix the containing water to obtain an even tempering as well as imitating movement and air saturation most likely experienced in the natural environment. Aquaria were insulated with Styrofoam between each other in order to minimise temperature loss and exchange with the environment and between replicates of different treatments. Waste water of the replicate aquaria was treated with UV light (Tropic Marine Centre (TMC) P2-110W Commercial UV Steriliser, max. flow rate: 65 L/min) prior to disposal.

Each of the four water source header tanks (74 L) was also equipped with a water pump for mixing purposes and had twelve individually controllable outlets attached. The header tanks were temperature controlled by up to 3 chillers (TK-2000 chillers, cooling capacity: 870 W, 800 L/h, TECO) to maintain the desired temperature. Tubes for individual water supply to the replicate aquaria were individually insulated using foam pipe insulation and radiator heat reflector roll to ensure a minimised temperature loss and exchange with the environment from the water source tanks to the aquarium. Carbon dioxide treatments were supplied with CO<sub>2</sub> enriched pressure air in the identical way the ambient pCO<sub>2</sub> treatments were supplied with pressure air. The CO<sub>2</sub> enriched air was constantly produced by mixing pure CO<sub>2</sub> (VK cylinder, BOC, Portsmouth, UK) with pressure air in a mixing flask (5 L) prior to distribution to the treatments. The mixture was consistently monitored with a gas analyser (LI-820, LI-COR Environmental, NB, USA) and a preconnected flowmeter (Rotameter 1.2 L/min, Caché Instrumentation, Wakefield, UK) throughout the time of the experiment, to ensure the correct concentration of pCO<sub>2</sub> was supplied to the experimental aquaria. The quantity of CO<sub>2</sub> enriched air reaching the experimental

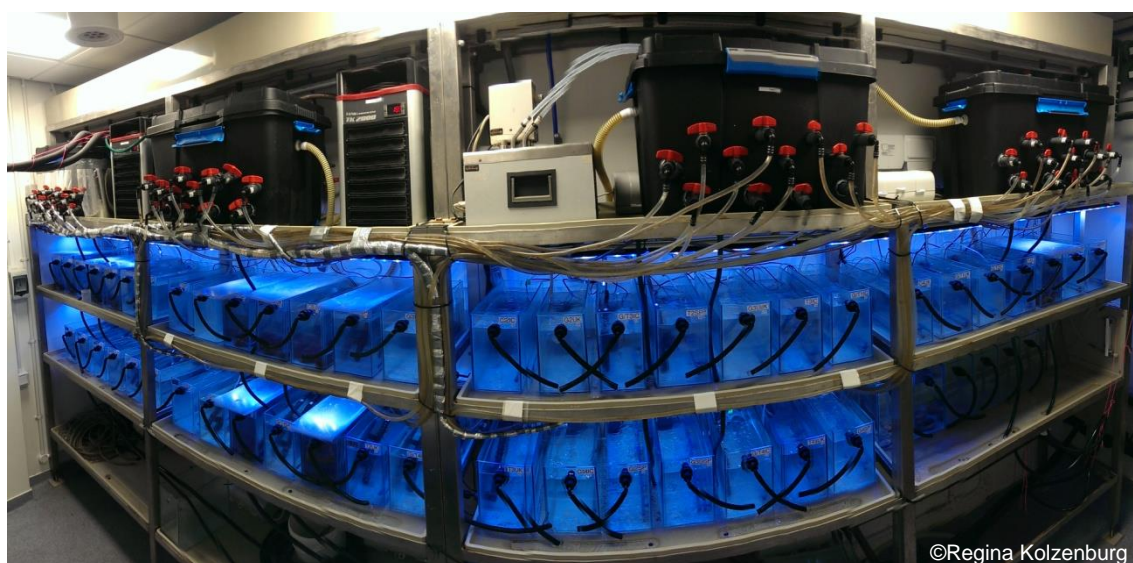


**Figure 2.16:** Climate change experiment design overview, with header tanks, individual water and air supply.

aquaria was monitored and adjusted using flowmeter (LPM Air 5 ml and 0.5 ml for ambient air and CO<sub>2</sub>, respectively, Cole-Parmer Instrument Co., IL, USA) which allowed for 0.5 bar of enriched air to pass. The Fifty aquaria were randomly assigned to a treatment (Cornwall and Hurd, 2015) and were subdivided into treatments as follows (Figure 2.18): 24 aquaria were designated to ambient pCO<sub>2</sub> treatments, 24 aquaria were designated to elevated pCO<sub>2</sub> treatments. Out of these two batches of 24 aquaria, 12 aquaria per batch were equipped with digital heaters (V<sup>2</sup>Therm 100, Tropical Marine Centre, London, UK) in order to reach elevated temperatures for each treatment. These four batches of 12 aquaria consisted of 4 replicates for each of the three regions of origin (northern margin, central and southern margin). Two additional aquaria solely with flint stones, which were used to fix the specimens on, were set up alongside the experiment, one with ambient air supply, one with CO<sub>2</sub>

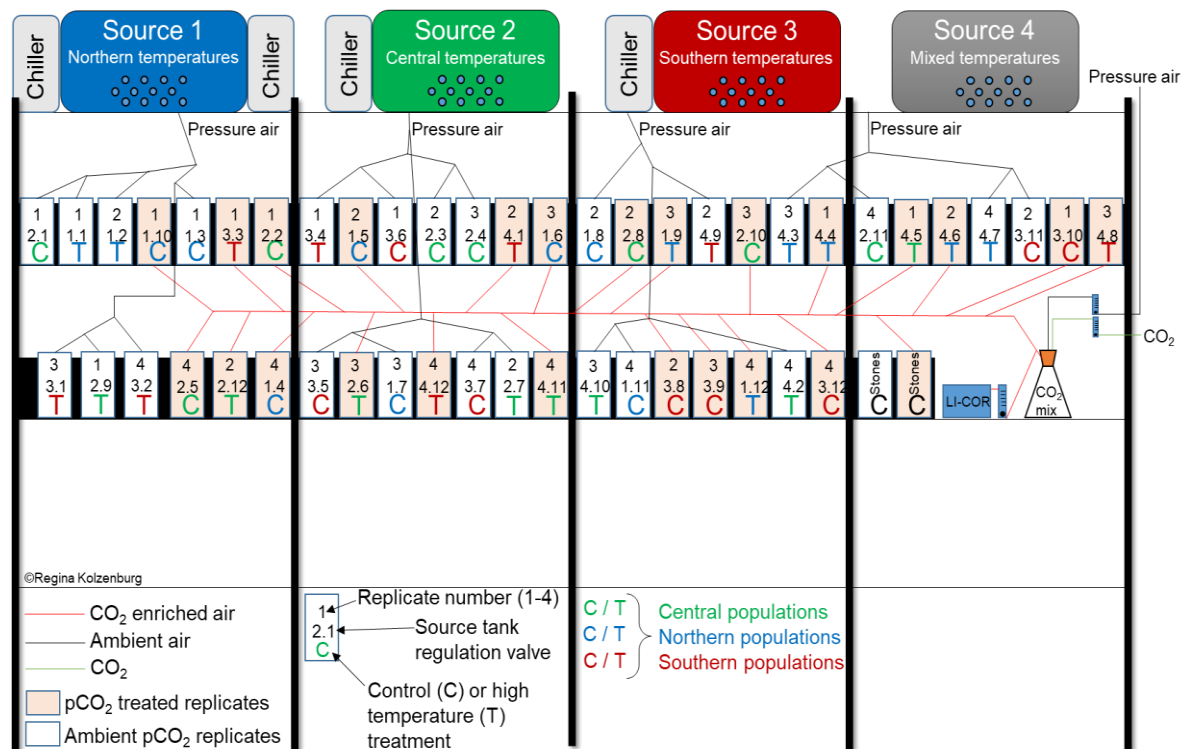


**Figure 2.17:** Detailed experimental design schematic of the Climate Change Experiment. The black background of the replicate experimental aquaria illustrates the insulation between aquaria.



enriched air supply. These were added in order to monitor potential influences of the flint stones to the seawater chemistry and were treated like the other aquaria.

At the inception, specimens (total rocks with specimens per population and treatment replicate:  $n = 4$ ) were kept at their *in situ* temperatures measured during sampling (northern margin temperature: 11.0°C; central temperature: 16.0°C; southern margin temperature: 18.5°C). The system was set to a light/dark cycle of 9/15 h and an intensity of 230  $\mu\text{mol photons m}^{-2} \text{s}^{-1}$  (taken from the average of natural conditions of northern, centre and southern locations) produced and controlled by TMC AQUABEAM 600 Ulma Reef White lights with cloud function. Additionally, sunset and sunrise were mimicked through a slow increase and decrease of light intensities over a period of 1 h. All specimens were kept in their corresponding conditions for a minimum of 1 week to acclimate to aquaria conditions. Following the initial acclimatisation, over the next 3 weeks,  $\frac{1}{4}$  of all, the northern, central and southern populations, were gradually acclimatised (increase

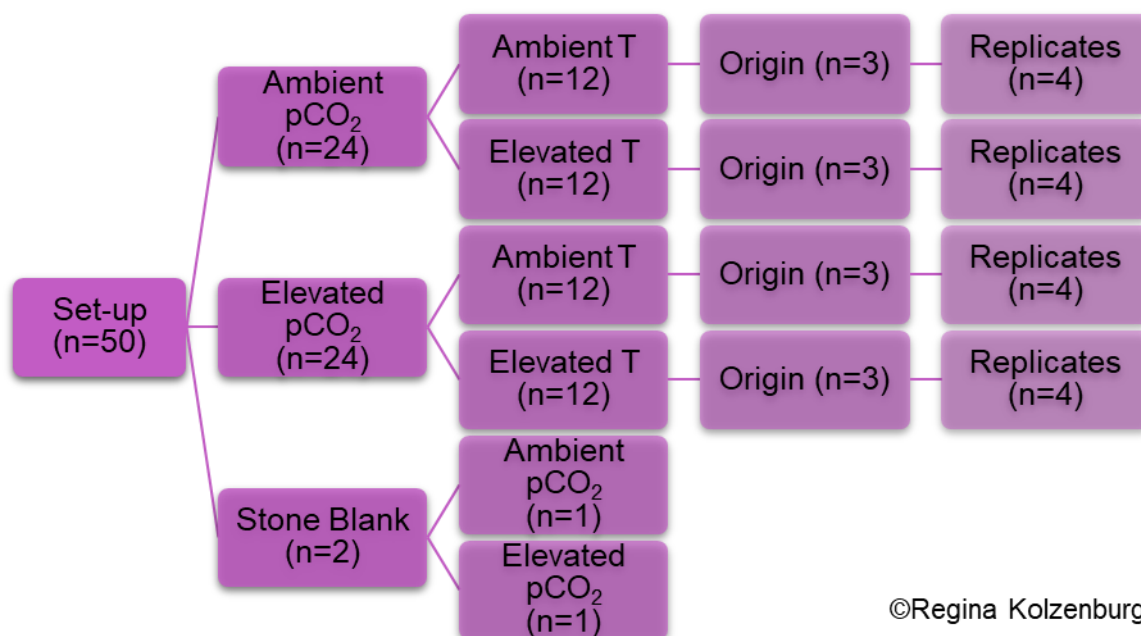


**Figure 2.18:** Schematic overview of experimental replication ( $n$ ) of each treatment of the Climate Change Experiment.

of 1.0°C/week and increase or decrease of 50  $\mu\text{mol photons m}^{-2} \text{ s}^{-1}$ /week, respectively) to elevated temperatures, a further  $\frac{1}{4}$  of all populations was gradually acclimatised to elevated pCO<sub>2</sub> (increase of 200 ppm pCO<sub>2</sub>/week which is equivalent to a decrease in pH of  $\sim 0.1$ ) and light conditions. A further  $\frac{1}{4}$  of all populations was gradually acclimatised to the combination of elevated temperature and pCO<sub>2</sub> as described above and the last  $\frac{1}{4}$  of all populations was retained in their initial, control conditions. After acclimatisation specimens were randomly and equally distributed within the corresponding replicate aquaria. Monitoring parameters: pH, temperature and salinity were measured daily in each replicate, A<sub>T</sub> was measured daily in one randomly chosen replicate of each treatment. Photosynthesis, respiration and calcification incubations were performed prior, once per month during, and after the experiment, according to the protocol described in 2.6.2 – 2.6.4. Due to the high number of samples, each water samples was sterile filtered and subsequently poisoned with 25  $\mu\text{l}$  of a saturated Hg(II)Cl solution (Mercuric chloride 99.5%, ACROS Organics, Thermo Fisher Scientific, Geel, Belgium) prior to the titrations for A<sub>T</sub> determination. Samples were stored in a cool and dry place pending processing. P-I curves and C-I curves of each population in each treatment were conducted before and after the experiment following the protocol in 2.6.1. Structural integrity analyses were conducted after the experiment as described in 2.8.

#### 2.9.4 Cross Experiment

For this study, two populations of two geographic locations ( $n = 4$ ) across the species distribution (UK = central populations; Spain = southern margin populations) were sampled and exposed to six treatments: (1) Control Common Garden Conditions (corresponding *in situ* temperature and light conditions, ambient pCO<sub>2</sub> (pH 8.1 – 8.2/ 380 – 400 ppm pCO<sub>2</sub>, IPCC, 2014)), (2) Common Garden Conditions



(*in situ* temperature and light conditions of the other geographic location), (3) Control Climate Change Conditions (corresponding *in situ* temperature and light conditions, ambient pCO<sub>2</sub>), (4) high pCO<sub>2</sub> (corresponding *in situ* temperature and light conditions, high pCO<sub>2</sub> (pH 7.75 - 7.80/ ~1000 ppm pCO<sub>2</sub>; RCP 8.5, IPCC, 2014a), (5) high temperature (T+3 (*in situ* temperature elevated by 3°C (IPCC, 2014a)) and *in situ* light conditions, ambient pCO<sub>2</sub>) and (6) T+3/high pCO<sub>2</sub> (T+3 and *in situ* light conditions in combination with elevated pCO<sub>2</sub>). All populations were colour coded with coloured yarn prior to the start of the acclimatisation for easier recognition throughout the experiment. Thirty-six 11.1 L aquaria were set up in a water bath, closed system (Figure 2.19 and Figure 2.20) each was supplied with a water pump (TMC, V<sup>2</sup>PowerPump 800, Flow rate: 700 L/h) and an air diffuser, to circulate and mix the containing water to obtain an even tempering as well as imitating movement and air saturation most likely experienced in the natural environment. The water baths containing the experimental aquaria were endowed with two of the same

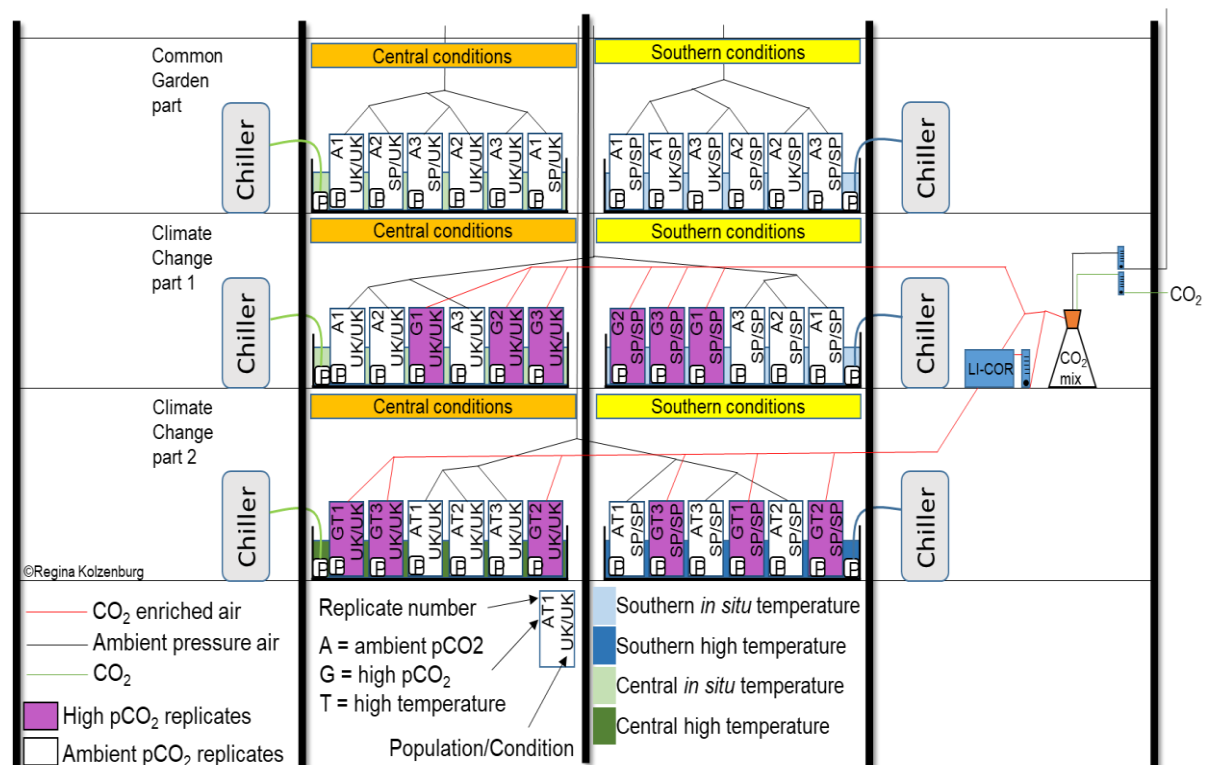


**Figure 2.19:** Detailed experimental design schematic of the Cross Experiment.

pumps, one on either side to ensure even commingling of the containing water. Seventy-five percent of the water in the replicate aquaria was changed every second day and wastewater of the replicate aquaria was treated with UV light (Tropic Marine Centre (TMC) P2-110W Commercial UV Steriliser, max. flow rate: 65 L/min) prior to disposal. Each of the water baths was temperature controlled by a chiller (TK-2000 chillers, cooling capacity: 870 W, 800L/h, TECO) to maintain the desired

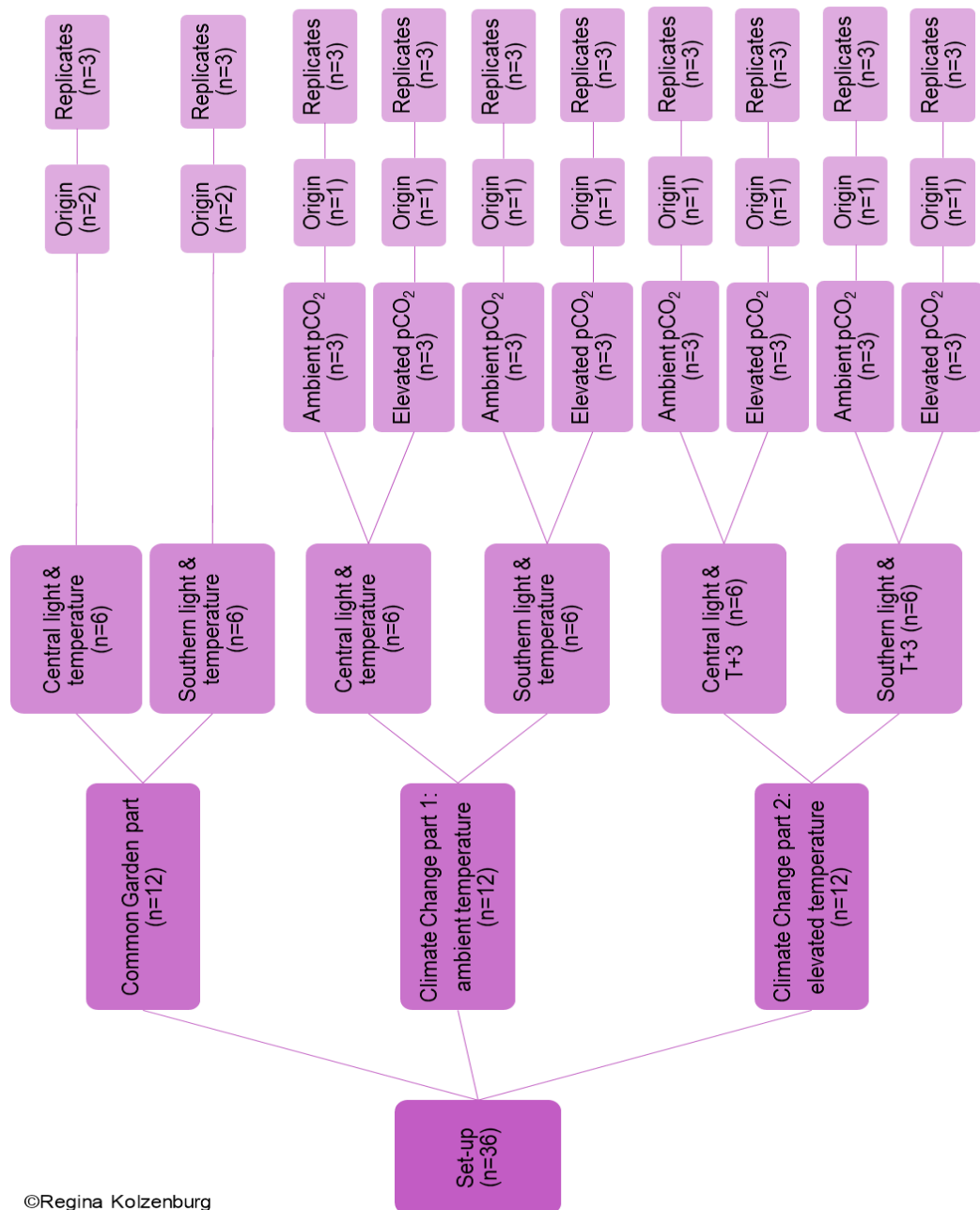


**Figure 2.20:** Schematic overview of experimental replication (n) of each treatment of the Cross Experiment.

temperature. Carbon dioxide treatments were supplied with CO<sub>2</sub> enriched pressure air in the identical way the ambient pCO<sub>2</sub> treatments were supplied with pressure air. The CO<sub>2</sub> enriched air was constantly produced by mixing pure CO<sub>2</sub> (VK cylinder, BOC, Portsmouth, UK) with pressure air in a mixing flask (5 L) prior to distribution to the treatments. The mixture was consistently monitored with a gas analyser (LI-820, LI-COR Environmental, NB, USA) and a preconnected flowmeter (Rotameter 1.2 L/min, Caché Instrumentation, Wakefield, UK) throughout the time of the experiment, to ensure the correct concentration of pCO<sub>2</sub> was supplied to the experimental aquaria. The quantity of CO<sub>2</sub> enriched air reaching the experimental aquaria was monitored and adjusted using flowmeter (LPM Air 5 ml and 0.5 ml for ambient air and CO<sub>2</sub>, respectively, Cole-Parmer Instrument Co., IL, USA) which allowed for 0.5 bar of enriched air to pass.

The 36 aquaria were split into three experimental subunits with three replicates for each condition (central and southern *in situ* temperature and light): the Common Garden Experiment part (treatment (1) and (2), n = 12) and the Climate Change Experiment part 1 (treatment (3) and (4), n = 12) and the Climate Change part 2 (treatment (5) and (6), n = 12). Each subunit was divided into southern and central environmental conditions on one side of the experiment, respectively. Aquaria were randomly assigned to a treatment (Cornwall and Hurd, 2015) and were subdivided into treatments. Out of the 36 aquaria, 12 were chosen for an additional Common Garden experiment which is explained in detail in a separate section (Chapter 2.9.2). Further 12 aquaria were assigned to central temperature (6.0°C) and light intensities (57 μmol photons m<sup>-2</sup> s<sup>-1</sup>) and southern temperature (11.5°C) and light intensities (184 μmol photons m<sup>-2</sup> s<sup>-1</sup>), respectively, within these 12 aquaria, 6, 3 for each region of origin, were treated with ambient pCO<sub>2</sub> and other 6, 3 for each origin,

were treated with elevated pCO<sub>2</sub> air (~1000ppm pCO<sub>2</sub> or pH 7.75 - 7.80). As a last subunit of the experiment, the exact same assignments and conditions as just explained were chosen in further 12 aquaria, with the distinction, that temperatures of each treatment were elevated by 3.0°C according to predictions for future sea surface temperatures (IPCC, 2014a). At the inception, specimens (total rocks with specimens per population and treatment replicate: n = 4) were kept at their *in situ* temperatures measured during sampling. The system was set to a light/dark cycle of 10/14 h (taken from the average of natural conditions of centre (9/15 h) and southern (10.5/13.5 h) locations) produced and controlled by TMC AQUABEAM 600 Ulima Reef White lights with cloud function. Additionally, sunset and sunrise were mimicked through a slow increase and decrease of light intensities over a period of 1 h. All specimens were kept in their corresponding conditions for a minimum of 1 week to acclimate to aquaria conditions. Following the initial acclimatisation, in the Common Garden Experiment part, specimens were acclimatised as describes in 2.9.2. In the remaining two subunits of the experiment, the Climate Change Experiment part 1 and part 2, over the next 3 weeks, the remaining specimens of all populations were either kept constant (treatment (3)) or gradually acclimatised (increase/decrease of 1.5°C/week and increase/decrease of 40 μmol photons m<sup>-2</sup> s<sup>-1</sup>/week and increase of ~200 pm (decrease in pH of ~0.1), respectively) to elevated temperatures and decreased pH levels, depending on their allocated treatment. After acclimatisation specimens were randomly and equally distributed within the corresponding replicate aquaria.

Monitoring parameters: pH, temperature, salinity and DO were measured daily in each replicate, A<sub>T</sub> was measured daily in one randomly chosen replicate of each treatment. Photosynthesis, respiration and calcification incubations were performed

prior and after the experimental culturing, according to the protocols described in 2.6.2 – 2.6.4. Due to the high number of samples, each water sample was sterile filtered and subsequently poisoned with 25  $\mu$ l of a saturated Hg(II)Cl solution (Mercuric chloride 99.5%, ACROS Organics, Thermo Fisher Scientific, Geel, Belgium) prior to the titrations for  $A_T$  determination. Samples were stored in a cool and dry place pending processing. P-I curves and C-I curves of each population in each treatment were conducted before and after the experiment following the protocol in 2.6.1. Structural integrity analyses were conducted after the experiment as described in 2.8.

# Chapter 3

Characterisation of *Corallina officinalis*  
across its geographical distribution in  
the NE Atlantic

### 3.1 Collaboration Disclaimer

The data describing the *in situ* physiological and structural properties of the populations of *Corallina officinalis* used in this thesis and in this chapter were gathered with the help of several volunteers. Some of the data collected during this thesis is also used by MPhil and MSc students at the University of Portsmouth Aditya Putra and Francesco D'Amore. Accreditation of the Icelandic sampling site as “certified organic” was initiated, pursued and kindly provided by Daniel Coaten from the University of Iceland (Appendix B, Figure B2 (A) – (C)).

### 3.2 Introduction

To determine responses of coralline algae to climatic changes, a characterisation of physiological properties and structural integrity of in target species is needed. Here, such a characterisation of *C. officinalis* is outlined. The results found were critically compared between marginal and central populations to highlight phenotypic plasticity across distribution range. The data from this chapter, were used to put laboratory experiments in Chapter 4 and 5 in perspective.

#### 3.2.1 Rhodophyta, Corallinales, *Corallina officinalis*

Rhodophyta (red algae) are one of the oldest groups of eukaryotic marine algae. Within the phylum Rhodophyta, the order Corallinales was formed incorporating families, *inter alia*, of crustose coralline algae (CCA, e.g. Lithothamniaceae) and articulated (or geniculated) coralline algae, e.g. Corallinaceae (Guiry and Guiry, 2019). All forms of the genera *Corallina* located within the family of Corallinaceae belong to the benthic macroalgae inhabiting the benthic photic zone, the part of the ocean floor where light penetrates and enables photosynthesis. Apart from

*Pneophyllum cetinaensis*, the first described freshwater species (Žuljević *et al.*, 2016), Corallinales inhabit marine environments.

Depending on location, coralline algae are exposed to various abiotic (e.g. solar irradiance, turbidity, pH, depth, temperature, salinity, water oxygen content or nutrient availability) and biotic factors (e.g. inter-species and intra-species interactions, predation, epibionts) and variations within these. It is known that all these factors can influence the physiology and morphology of organisms and the shallow-water ecosystem they dominate. However, it is also known that species with a wide geographical range, such as coralline algae, are in general very plastic and able to acclimatise to a variety of habitats through morphological and functional responses (Brody, 2004, Ragazzola *et al.*, 2013). To maintain their abundance in temperate, shallow, intertidal ecosystems around the globe coralline algae are suggested to have a good ability to adapt to a wide and fast changing range of external influences such as solar irradiance, temperature, mechanical stress and carbonate chemistry.

Amongst others, they developed a carbonate concentration mechanism (CCM) enabling it to transform  $\text{HCO}_3^-$  into  $\text{CO}_2$  and, therefore, are not carbon limited in low  $\text{CO}_2$  environments. Species with CCMs not only enhance photosynthesis in this way but also crystallise and accumulate high-Magnesium (high-Mg) calcite in their cell walls enhancing stability, protection, and mechanical resistance (Padilla-Gamino *et al.*, 2016). Calcification is thought to be directly related to photosynthesis (Pentecost, 1978) and inorganic carbon concentrations (Smith and Roth, 1979, Gao *et al.*, 1993). Two functional associations between photosynthesis and calcification were described:



a) “cis” calcification, stimulated by photosynthetically absorbed carbon and controlled by the carbonate equilibrium. Carbon removal for photosynthetic processes produces a  $\text{CaCO}_3$  super-saturated environment, enhancing carbonate precipitation in the cell walls;

b) “trans” calcification, initiated through active transport mechanisms. A  $\text{Ca}^{2+}$  efflux, driven by the chemical adenosine triphosphate (ATP) and a simultaneous uptake of 2  $\text{H}^+$  is creating a  $\text{Ca}^{2+}$  rich, alkaline environment leading to an absorption of  $\text{CO}_2$  from the cells and a precipitation of  $\text{CaCO}_3$  (McConnaughey and Falk, 1991, McConnaughey *et al.*, 1994). The active uptake of  $\text{H}^+$  during the trans-calcification, leads to the conversion of  $\text{HCO}_3^-$  to molecular  $\text{CO}_2$ , allowing a more efficient carbon uptake from mildly alkaline high-calcium waters, compared to cis-calcification (McConnaughey *et al.*, 1994).

At small spatial scale, within habitat locations, differences in Mg contents in individuals may be related to the location of the individual on the shore. The higher the specimen was collected on the shore, the more influence of extreme fluctuations of abiotic factors it would have been exposed to; the lower it grew on the shore, the more stable the conditions would have been and the Mg incorporation would have been influenced more by the actual SST rather than air temperature and stress (Williamson *et al.*, 2014). Mg-calcites (>3-4 mol%  $\text{MgCO}_3$ ) - identified as first calcite polymorph in the ocean to respond to decreasing pH associated with a declining saturation state - were found to surpass the solubility of aragonite around 12 mol%  $\text{MgCO}_3$  (Chave, 1954a) and consequently present the most soluble form of carbonate in the ocean.

Coralline algae contribute to  $\text{CaCO}_3$  assimilation (Amado-Filho *et al.*, 2012), therefore reef growth (Adey, 1998; Chisholm, 2000) and provide substrate and

habitat for other organisms to settle and live (Daume *et al.*, 1999, Ritson-Williams *et al.*, 2009, Gherardi and Bosence, 1999, Chenelot *et al.*, 2011).

A turf forming species with CCM is *C. officinalis*. It is commonly found in low, sheltered intertidal zones, where it predominantly inhabits the lower part of rock pools and channels that remain damp or filled during extreme tides or conditions, and at the edge of the intertidal to subtidal zones (Digby, 1977, Egilsdottir *et al.*, 2013, Williamson *et al.*, 2014). It forms, like all articulated algae in this order, branches that consist of calcified segments (intergenicula, Figure 3.1), which are produced through the precipitation of high-Mg calcite in the cell walls, and non-calcified segments (genicula, Figure 3.1). This structure provides flexibility and elasticity for every individual branch (Martone and Denny, 2008). The turf beds are highly variable in frond length and density at small spatial scales with coralline algae potentially being able to shift their energy budget from growth extension to the maintenance of structural integrity (Ragazzola *et al.*, 2013). Coralline algae reproduce by forming tetraspores (or bispores), spermatia, carpogonia, and carpospores within conceptacles. Life histories in this family are generally diplobiontic with isomorphic gametophytic and tetrasporophytic stages (Johansen, 1981, Woelkerling, 1988, Figure 1.4).

*Corallina officinalis* Linnaeus, 1758 (Rhodophyta, Corallinales, Corallinaceae) is a common species around the temperate regions on our planet. It grows on hard substratum in the lower intertidal zone, and sometimes also inhabiting the upper most subtidal zones. *C. officinalis* is commonly found in damp channels and rock pools (Brodie *et al.*, 2013, Guiry and Guiry, 2019).

#### 3.2.1.1 Physiological Characteristics of *Corallina officinalis*

*Corallina officinalis* forms fronds up to 12 cm length but often much shorter and coarse to the touch. The fronds grow upright from a calcareous crustose disk-shaped holdfast which can reach up to 70 mm in diameter (Brodie *et al.*, 2013). Side branches grow out of the main branch opposite from each other, also called pinnate growth. This species grows epilithic on hard substratum under macroalgal canopies and tidal action may influence branch length due to mechanical influences of tidal action. Specimens display a variety of colours ranging from purple to pink and red or yellowish, with white tips and joints. The colour, a result of changes in ratios and/or degradation of pigments, can be induced by light damage, such as the yellow or orange colour after intensive light exposure. Reproductive cells, conceptacles, are drop-shaped and can be found either at the tip of a branch or laterally on an intergenicula (Brodie *et al.*, 2013, Johansen, 1975, Figure 3.1). Reproductive cells of both, haploid and diploid life cycle stages look alike and cannot be visually distinguished. Branches can drastically differ in their morphology between zones on the same rocky shore. Irvine and Chamberlain



**Figure 3.1:** *Corallina officinalis* structure. White arrowheads represent calcified intergenicula segment. Black arrowheads represent genicula, a joint-like structure. Open arrowhead indicates a conceptacle.

(1994) found 1 - 2 cm long fronds in the lower littoral compared to 10 - 17 cm long fronds in rock pools. Growth rates were established by Colhart and Johanssen (1973) and showed an average growth of 2.2 mm month<sup>-1</sup> at 12°C and 18°C and slowed down to 0.2 mm month<sup>-1</sup> at 6°C and no growth was observed at 25°C. To date, an extensive elemental composition for *C. officinalis* skeletons beyond magnesium (Williamson *et al.*, 2014), is not available. This chapter will characterise the elemental compositions of six populations of which two are located at the centre, the northern margin and the southern margin of the species distribution, respectively, across the NE Atlantic.

#### 3.2.1.2 Structural and Elemental Properties, Skeletal Structure

In addition to the description in 1.3, a branch of *C. officinalis* and other articulate coralline algae, consists of multiple intergenicula arising from another and connect by a geniculum (**Figure 3.1**). A frond consists of a system of branches growing from one initial point on the holdfast disc. The intergenicula size and shape is characteristic for certain genera or species but can be influenced by external factors such as abiotic or biotic stressors (Johansen, 1981 and references therein). The single intergenicula in most geniculated coralline algae is broader distally than proximally and flattened. In *C. officinalis* it is known that this shape can vary when grown in the laboratory or deep water environments, where it will produce a more barrel-shaped phenotype (Johansen, 1981 and references therein). Each intergeniculum is built out of tiers of intergenicula cells in which the primary pit-connections form arching lines, looking like growth rings. At intervals of 14 tiers, *C. officinalis* produced a layer of genicular cells of an average length of 80 µm (Johansen, 1981 and references therein). Genicular form the joints of each branch of geniculate coralline algae and are uncalcified cells separating

intergenicula resulting in high flexibility. It is a single cell layer with thick cell walls and an unknown elemental composition. Cells are up to 0.5 mm long and very thin (6 - 10  $\mu\text{m}$ ) and elongate as they age. Due to constant growth, these cells stain intensely with numerous stains. Each geniculum in *C. officinalis* is restricted in its flexibility by claw-shaped calcified excrescences growing at each end of the adjoining intergenicula (Johansen, 1981 and references therein).

The cell wall of *C. officinalis* is composed of high Mg-calcite and Mg concentrations can vary and be directly or indirectly influenced by growth rates, light, physiological cycles and temperature (Chave and Wheeler, 1965, Moberly, 1968). This calcite incorporates not only Mg cations but also iron (Fe), Manganese (Mn), Sodium (Na), Strontium (Sr), Potassium (K) and Barium (Ba) cations (Milliman *et al.*, 1971, Johansen, 1981 and references therein). In aragonite, generally, ions with large radii are incorporated, in contrast to calcite which incorporates mainly small radii. This suggests that strontium values are usually reported alongside aragonite values and magnesium and iron values are reported to be higher in calcite crystals. In the calcite lattice  $\text{Mg}^{2+}$  ions increasingly substitute  $\text{Ca}^{2+}$  ions with increasing temperatures, a positive correlation between Mg content as well as Mg/Ca ratios with temperature (Oomori *et al.*, 2006). Studies have shown exponential temperature dependency of Mg uptake into calcite of 1 – 3 mol% per  $1^\circ\text{C}$  increase depending on species (Henrich *et al.*, 1996, Rosenthal *et al.*, 1997, Kamenos *et al.*, 2008). Coralline algae, amongst others, can contain between 7.7 – 28.8 mol% Mg-calcite (Vinogradov, 1953, Chave, 1954a,b, Henrich *et al.*, 1996, Halfar *et al.*, 2000, Kamenos *et al.*, 2008). A concentration of around 8 mol% would translate to approximately 2% of Mg in

relation to the total weight, making coralline algae the main producer of high-Mg calcite in the ocean.

Due to the nature of its habitat in the rocky shore intertidal zones across the NE Atlantic, *C. officinalis* is extruded to tremendous wave action and powerful velocities ( $>20 \text{ m s}^{-1}$ ) (Denny, 1988). Genuculated coralline algae have evolved to adapt to these harsh environments with high tensile strength resistance and elasticity as a result of their segmented and jointed structure. This structure is determining their location and survival on the rocky shores (Martone and Denny, 2008a) and can withstand high forces. Physical and ecological stress may cause damage to the organisms *via* cuts, scars or even holes of the frond (De Bettignies *et al.*, 2012). The limit of flexibility before breakage is the maximum load or stress ( $\sigma_{\max}$ ) that can affect the joints in an alga, for clusters of fronts it can go as high as  $\sigma_{\max} = 5.4 \pm 0.5 \text{ MPa}$  in *E. elongata* (Ragazzola *et al.*, 2017). Besides this study by Ragazzola *et al.* (2012), very few studies have determined tensile strength, stress and elasticity which articulated coralline algae are exposed to and are able to withstand, none of which looking at marginal populations (Martone, 2007, Martone and Denny 2008a,b, Ragazzola *et al.*, 2012, Melbourne *et al.*, 2015, Denny and King 2016a,b).

### 3.2.1.3 Ecosystem Engineers and Functions

Ecosystem engineers are organisms that play a crucial role in creation, modification and maintenance of habitats (Jones *et al.*, 1994). The focussed species in this study, *C. officinalis*, is an important part of intertidal ecosystems. Up to 80% of other organisms would not be able to survive in this habitat without it, and shores would be drastically depleted in diversity (Grahame and Hanna, 1989). Coralline algae, therefore, function as vital ecosystem engineers playing a crucial

role as an essential structural element in the majority of rocky coastal zones providing rigid substrate for organisms to settle (Chisholm, 2000, Benedetti-Cecchi, 2006, Dayton, 1972, van der Heijden and Kamenos, 2015, Johansen, 1981, Jones *et al.*, 1994, Kelaher *et al.*, 2001, Nelson, 2009, Noël *et al.*, 2009).

By creating these habitats, they are providing a hard substrate with a complex structure and thus increasing the biodiversity of ecosystems (Foster, 2001, Steller *et al.*, 2003, Ragazzola *et al.*, 2013, Daume *et al.*, 1999; Ritson-Williams *et al.*, 2009; Gherardi and Bosence, 1999). They often form complex, extremely dense and highly branched turfs, which are considered the extreme end of algal structural complexity (Coull and Wells, 1983, Davenport *et al.*, 1999) and contribute to reef accretion (Adey, 1998, Chisholm, 2000). These complex structures are able to accommodate abundant and diverse macrofaunal assemblages with up to 250,000 individuals per m<sup>2</sup> (Kelaher *et al.*, 2001). Coralline algae are also able to influence microclimate on a local scale by changing the water chemistry around them through photosynthesis and calcification metabolic processes. They release or absorb oxygen as well as various forms of carbonate ions into the surrounding waters and subsequently contributing approximately 25% to the CaCO<sub>3</sub> production within coastal regions (Morris and Taylor, 1983, Amado-Filho *et al.*, 2012, Williamson *et al.*, 2014; Williamson *et al.*, 2017) representing a significant component of the global carbon system (Mackenzie *et al.*, 2004; Martin *et al.*, 2007, Ragazzola *et al.*, 2013).

#### 3.2.1.4 Distribution: Past, Present, Future

*Corallina officinalis* was first described in 1758 in “Oceano Europaeo” by Linnaeus (Linnaeus, 1758) and sightings, relying on visual, not genetic identification, expanded around the world on temperate, intertidal, rocky shore coasts. Records

show a slow increase of visually identified occurrences around the world after the first description, the second discovery was in 1800 in South Wales, UK. Up to 1850, the next sightings based on visual identification were recorded in: Southeast (SE) Australia, North Island New Zealand, Germany, Ireland and Northeast (NE) of the USA. In the following 25 years records of *C. officinalis* was thought to become even more global with sightings in the Mediterranean, Scandinavia, multiple around the UK, the Northwest (NW) and Southwest (SW) coast of the USA and in Argentina. In the following 25 years up to 1900, new records from Iceland, Italy, Brazil and additional records from SE Canada and NE of the USA were added to the collection. After 1900 a great number of visually identified records were added up until 2019, including sub-polar regions as well as sub-tropical regions: Alaska, Peru, South Africa, Tasmania, Chile, Uruguay, Mexico, Denmark, Russia, Spain, UK overseas territories, Galapagos, in the Caribbean, Columbia, Venezuela, Costa Rica, Japan, Canaries, Tunisia, North Norway, South Island of New Zealand and Israel. Occurring to a greater or lesser extent in this order (GBIF Secretariat).

However these were all descriptions based on visual identification, which can be very challenging in the field. Greatly important, modern technological, genetic confirmations of *C. officinalis* were only described in the North Atlantic and the North East Pacific (Brodie *et al.*, 2013, Pardo *et al.*, 2015, Williamson *et al.*, 2017, Tavares *et al.*, 2018, Yesson *et al.*, 2018, Magill *et al.*, 2019).

In the future, due to climatic changes, *C. officinalis* might not be able to inhabit the same ecosystems they are found in today. As well as other species, *C. officinalis* may experience a shift in distribution and therefore range margins (Parmesan *et al.*, 1999, Parmesan and Yohe, 2003, Eckert *et al.*, 2008, Nicastro *et al.*, 2013). According to models by Cerasuolo *et al.* (unpublished data) *C. officinalis* will



retract its southern, trailing edge and inhabit more suitable ecosystems further north in the NE Atlantic. Whereas northern leading edge populations are thought to be affected by changes in the oceans carbonate chemistry and relocate in more southern habitats, resulting in a thinning of the species distribution belt in the northern hemisphere.

### 3.2.2 Centre-to-Margin Hypothesis

A hypothesis described by Mayr (1963) is called the “centre-periphery” hypothesis. Here, the adaptive ability of marginal populations could be limited due to genetically less diverse populations compared to central populations. It is suggested that the geographic centre of a species distribution holds the most favourable conditions and therefore holds the highest population density (Brussard, 1984, Whittaker, 1956). In the centre a species is reaching the highest abundance and declines toward the range edges; this is also called the “abundant-centre” hypothesis (Brown, 1984, Sagarin and Gaines, 2002). When moving away from the centre towards the margins of the distribution, environmental variables are thought to become less favourable due to greater abiotic stress and increased interspecific competition (Aitken *et al.*, 2008), initiating a decrease in population densities and lower relative fertility (Case and Taper, 2000, but see Sexton *et al.*, 2009). Further, Watkinson and Sutherland (1995) described a higher mortality than recruitment rate for local marginal populations, also called sink populations, whose survival depends on influx of zygotes or spores from source populations.

Adults from the Northern populations are already experiencing high pCO<sub>2</sub> and, as predicted, were more tolerant to these levels (Padilla-Gamino *et al.*, 2016). It was also shown for multiple organisms that gene flow is reduced towards the periphery of the species distribution (Hampe and Petit, 2005) and that marginal populations

are lower in genetic diversity compared to central populations (Abeli *et al.*, 2014). However, marginal populations engender exceptional genetic variations, enabling species to adapt to new environments and environmental conditions and abiotic and biotic stressors (Mayr, 1963, Levin, 1970, Guo *et al.*, 2005, Abeli *et al.*, 2014).

With increasing research knowledge, exceptions are found for these hypotheses. The decreased genetic diversity in edge populations is accurate for most species but not for all. For the shrub *Liriodendron chinense*, Yang *et al.* (2016) proved that its genetic diversity does not follow the centre-margin hypothesis but instead, may have been influenced by many other factors (e.g. latitude, ecological environmental gradients, phylogeographic history etc.). Other studies have analysed the demographical pattern between central and edge populations questioning the “abundant-centre” hypothesis. They showed a complex pattern in which peaks of abundances are shifted towards one end of the species range edge or show no pattern (Sagarin and Gaines, 2006, Sagarin *et al.*, 2006). In future climatic conditions, marginal populations are thought to be more vulnerable to changes and extreme conditions than central populations (Walther *et al.*, 2002).

The aim of this chapter was to identify, through analysis of physiology and structural integrity, the differences between populations across their geographical distribution, comparing central to peripheral populations.

### 3.3 Material and Methods

Detailed descriptions of the Material and Methods including experimental designs are specified in Chapter 2.

#### 3.3.1 Specimens Collection

Individuals of *C. officinalis* were chosen and studied from the centre ( $n = 2$  populations) as well as the northern ( $n = 2$  populations) and southern ( $n = 2$  populations) edge of the species latitudinal distribution across the NE Atlantic. Study sites of the northern and southern margin as well as central populations are specified in Chapter 2 section 2.1 (Figures 2.1 – 2.4). All specimens were collected intertidally, during low tide and at a depth of  $26 \pm 4$  cm from the water surface during winter as well as summer seasons. During sampling, environmental parameters were measured and water samples and specimens were collected. A total amount of 11g of *C. officinalis* specimens ( $n = 11 \times 1g$ ) were cleaned from visually identifiable epiphytes using forceps and kept aside in separate insulated containers for *in situ* incubations at each site, performed after sampling procedures and measurements. Remaining algae were cleaned the same way and transported to the laboratories of the collaborating Universities (University of Portsmouth, University of Vigo and University of Iceland) of the respective countries in temperature-insulating containers. In the laboratory facilities, specimens were immediately placed into an ambient, flow-through holding tank for acclimatisation, prior to further incubations. Only healthy individuals without epiphytes and indication of bleaching or damage were selected for further studies.

### 3.3.2 Measurements of Environmental Parameters

During field sampling, data loggers (HOBO UA-002-64 Pendant Temp/Light, Tempcon Instrumentation Ltd., Arundel, UK; accuracy: 0.47°C, resolution: 0.1°C, Figure 2.6) were deployed submerged at lower low tide lines of each site to record the annual temperature and light regime every 30 minutes (Figure 3.4 – Figure 3.6). Data logger measurements at northern sites were not recorded throughout the period of one year due to environmental conditions as well as time and financial limitations. However, both incubation seasons, summer and winter, were covered in the available records and are similar to recordings of the Associated Icelandic Ports (Faxaflóahafnir sf., 2019) for the respective years and months. Temperature measurements for midday incubations resembled those for each season.

Temperature, salinity, dissolved oxygen (DO), pH, irradiance and total alkalinity ( $A_T$ ) were measured during sample collection. Temperature and salinity were measured with a CO310-1 portable salinity and temperature probe (accuracy: 0.2% for salinity,  $\pm 0.2^\circ\text{C}$  for temperature; resolution: 0.1 for salinity,  $0.1^\circ\text{C}$  for temperature. VWR, Leicestershire, UK). Dissolved oxygen and pH were measured with an HQ30d portable multi-parameter meter and a luminescent DO (LDO101, accuracy:  $\pm 0.1$  mg/L. HACH, Manchester, UK) and pH probe (PHC301, accuracy:  $\pm 0.02$  pH, HACH, Manchester, UK. Calibrated on the National Bureau of Standards (NBS) scale and converted into total scale values using Tris/HCl and 2-aminopyridine/HCl buffer solutions after Dickson *et al.*, (2007). Irradiance was measured with a Hansatech Quantitherm PAR/Temperature Sensor with a QTP1 probe (resolution:  $1 \mu\text{mol photons m}^{-2} \text{s}^{-1}$ ,  $0.02^\circ\text{C}$ , respectively).

Prior to transportation and immediately after collection, water samples for  $A_T$  determination were sterile filtrated through a syringe filter (Fisherbrand, hydrophilic 25 mm, 0.2  $\mu\text{m}$  PTFE) into sterile 50 ml tubes (Fisherbrand, Plastic Centrifuge Tubes). Using the alkalinity technique after Smith and Key (1975), Chisholm and Gattuso (1991) and Dickson *et al.* (2007),  $A_T$  was determined in the laboratory at the University of Portsmouth promptly upon arrival via potentiometric titrations using an automatic titrator (TitroLine 7000, Schott SI Analytics, Farnborough, UK; measurement accuracy:  $0.002 \pm 1$  digit, dosing accuracy: 0.15%, dosing precision: 0.05 - 0.07%) calibrated on the NBS scale, to ensure minimal variation. As titrant 0.1 N hydrochloric acid (HCl) was used and validated against Certified Reference Material provided by Andrew G. Dickson (Batch 154, Scripps Institution of Oceanography). The carbonate system of the seawater was calculated from pH,  $A_T$ , salinity and temperature using the Excel (Microsoft office, USA) Macro CO2Sys (Version 2.1, Lewis and Wallace, 1998) with K1 and K2 according to Mehrbach *et al.*, (1973) and refit by Dickson and Millero (1987).

### 3.3.3 *In situ* Incubations – Photosynthesis, Respiration, Calcification

Incubations to determine *in situ* photosynthesis, respiration, light calcification and calcification in the dark were performed with a mean of  $0.53 \pm 0.11$  g,  $0.59 \pm 0.20$  g and  $0.79 \pm 0.25$  g dry weight (DW) of *C. officinalis*, for central (CP), southern (SP) and northern populations (NP), respectively. At 12:00 noon, in ambient light conditions, replicates ( $n = 3$ ) were incubated bubble-free, in clear, closed cell 58 ml incubation chambers (Fisherbrand, Plastic Centrifuge Tubes), *in situ* for 60 minutes. Dissolved oxygen concentrations, pH and  $A_T$  were determined before and after the incubations, in order to calculate photosynthesis, respiration and calcification rates in the light and in the dark (detailed description in Chapter 2). To

account and correct for metabolism effects by microscopic organisms in the water column, reference incubations with just seawater were performed alongside the above-described incubations. Aluminium foil, covering each incubation chamber, was used to determine calcification and respiration rates in the dark. Calculations determining primary production, respiration, calcification and dissolution rates in the field were performed following the methodology as described in section 2.6.6.

### 3.3.4 Laboratory incubations – Oxygen and Calcification Evolution

In the respective University laboratory, incubations to determine oxygen (P-I curve) and calcification evolution (C-I curve) of the investigated populations were conducted. Specimens of *C. officinalis* were incubated at increasing light intensities (0, 20, 80, 160, 320, 500 and 700  $\mu\text{mol photons m}^{-2} \text{s}^{-1}$ ) (AQUARAY Nature Perfect, Tropic Marine Centre, London), under *in situ* temperatures and seawater compositions. For each light intensity a set of 5 clear incubation chambers were filled with  $0.62 \pm 0.03$  gDW,  $0.59 \pm 0.03$  gDW and  $0.63 \pm 0.04$  gDW, for CP, SP and NP, respectively, of *C. officinalis* and closed bubble-free. To account and correct for metabolism effects by other organisms, reference incubations without algae were performed alongside the above-described incubations. Aluminium foil, covering each incubation chamber, was used to determine calcification and respiration rates in the dark. Irradiance was measured with a Hansatech Quantitherm PAR/Temperature Sensor with a QTP1 probe (resolution: 1  $\mu\text{mol photons m}^{-2} \text{s}^{-1}$ , 0.02°C, respectively). At the end of the incubation, DO, pH and temperature measurements were taken. Water samples for later  $A_T$  analyses were sterile filtrated and treated alike the field samples, as described in 3.3.2. Calculations to determine the following P-I curve and C-I curve variables: maximum photosynthetic/ calcification rates ( $P_{\text{max}}$ /  $C_{\text{max}}$ ), the light

harvesting efficiency ( $\alpha$ ) and the saturating light intensity ( $I_K$ ) as well as photosynthetic, respiration and calcification rates in the light and in the dark were performed using the methodology as described in 2.6.6.

### 3.3.5 Laboratory structural analysis

To determine the structural integrity of the different populations across the species distribution, tensile strength, trace element composition, cell wall thickness as well as growth rates were determined.

#### 3.3.5.1 Tensile Strength

Ultimate tensile strength, the materials capacity to withstand loads elongating the specimen and subsequently determine the strength and resistance to tension was analysed. Dried samples were fixed to a 2 cm, flat wooden surface, using instant adhesive (Figure 2.11). A  $1.00 \pm 0.13$  cm sample length was adjusted. It was ensured the tested sample length was not contaminated with adhesive in order to prevent altering of structural properties.

Dry analyses were conducted using an ElectroForce fatigue test instrument (Model 3220 Series II, Bose Corporation, Eden Prairie, MN, USA) attached to a computer with the analysing software WinTest 7 (Bose Corporation, Eden Prairie, MN, USA). Detailed parameters for the analytic settings can be found in Table 2.1. Data was plotted and analysed using Excel (Microsoft office, USA) plotting load against displacement indicating the breaking point of each sample, the tension needed to break each sample and the strain, representing the elongation of each sample. Normal strain was calculated following the procedure in 2.8.1.2.

### 3.3.5.2 Trace Element Composition

Mg/Ca ratios within the calcite and the differentiation of it within various conditions were determined by laser ablation inductively coupled plasma mass spectrometry (LA-ICP-MS). This measured predetermined trace elements (Mg, V, Cr, Fe, Zn, Sr, Cd, Ba) ultimately leading to the specimens' elemental composition.

Replicates ( $n = 3$ ) of each population were embedded into epoxy resin (EpoFix Kit, batch no: 8134-01, Struers ApS, Ballerup, Denmark) and polished with a polishing machine (MetaServ 3000 or VibroMet 2, Buehler, Esslingen, Germany) and an aluminium oxide solution (aluminium oxide powder (Micropolish Alumina, Buehler, Esslingen, Germany) and distilled water) of 0.05  $\mu\text{m}$  grain size (Chapter 2.8.2.1). Trace element analysis were conducted at the School of Earth and Environmental Sciences, University of Portsmouth, United Kingdom, using a RESOLUTION 193 nm ArF excimer Laser with a Laurin Technic S155 Ablation cell coupled to an Analytic Jena Plasma Quant MS Elite ICP-MS. Analyses consisted of 55  $\mu\text{m}$  spot size, laser fluency was 3.0  $\text{J}/\text{cm}^2$  and its repetition rate was 5 Hz. Background measurements were taken for 20 seconds, followed by 30 seconds of ablation and 15 seconds of washout for each analysis (65 seconds in total). Detailed operating conditions for both instruments are listed in Table 2.2. Background and signal counts were integrated, time-drift corrected and reduced to concentrations using Iolite 3.4 software packages (Paton *et al.*, 2011). Synthetic silicate glass reference material NIST SRM 610 as well as NIST SRM 612 were used for instrumental calibration and as primary and secondary standards. Synthetic calcium carbonate USGS MACS-3 was also used as secondary standard and analysed in the same conditions as the unknowns (= samples). Each run consisted of at least six external standard analyses (NIST 610) and four secondary standards NIST 612



and MACS-3 (n = 8). Detection limits (99% confidence) for the spot measurements of the NIST glasses were: Mg = ~28 ppm and Ca = ~100 ppm.

Internal standard element used for normalization of the data was  $^{43}\text{Ca}$ , which was obtained from the GeoReM database and own measurements. All reference materials were ablated prior, in the middle and after sample ablation. Following every sixth sample analysis one analysis of NIST SRM 610 was added to correct for time-dependent drift of mass discrimination and instrument sensitivity. Final elemental composition ratios in this study were calculated as a 'mean count rate' including standard error of 9 drift and background corrected single ablation spot analysis for each of the three replicates. Spots (n = 3) were ablated at lower, middle and upper regions, respectively, of the selected branch. This method is commonly used for LA-ICP-MS data reduction (Longerich *et al.*, 1996). Values obtained are reproducible within 10% for Mg, of the GeoReM recommended values (Jochum *et al.*, 2005) and were compared with the GeoReM data base to determine accuracy (Figure 3.2 + Figure 3.3) as well as internal (NIST 610) and external reproducibility (MACS-3 and NIST 612; Table 3.1).

**Table 3.1:** Reproducibility of Reference Materials USGS MACS-3, NIST SRM 610 and NIST SRM 612 (Total Mean  $\pm 2\text{SD}$ ) for each element measured and analysed in this study.

	Mg [ppm]	Ca [ppm]	V [ppm]	Cr [ppm]	Fe [ppm]	Zn [ppm]	Sr [ppm]	Cd [ppm]	Ba [ppm]
MACS-3	1841.67 $\pm 71.86$	394416.66 $\pm 43703.26$	47.46 $\pm 2.85$	121.88 $\pm 8.97$	12258.33 $\pm 2060.27$	128.22 $\pm 12.00$	7675 $\pm 2541.05$	48.41 $\pm 5.73$	61.25 $\pm 2.54$
NIST 610	464.99 $\pm 4.38$	82157.79 $\pm 375.31$	442.01 $\pm 2.66$	405.00 $\pm 1.86$	455.31 $\pm 28.76$	456.07 $\pm 2.25$	515.85 $\pm 7.18$	259.01 $\pm 2.04$	435.03 $\pm 2.35$
NIST 612	56.10 $\pm 5.35$	85075.00 $\pm 678.09$	38.02 $\pm 0.29$	36.43 $\pm 0.97$	31.00 $\pm 19.80$	37.47 $\pm 1.66$	76.20 $\pm 9.75$	27.70 $\pm 1.14$	38.07 $\pm 0.73$

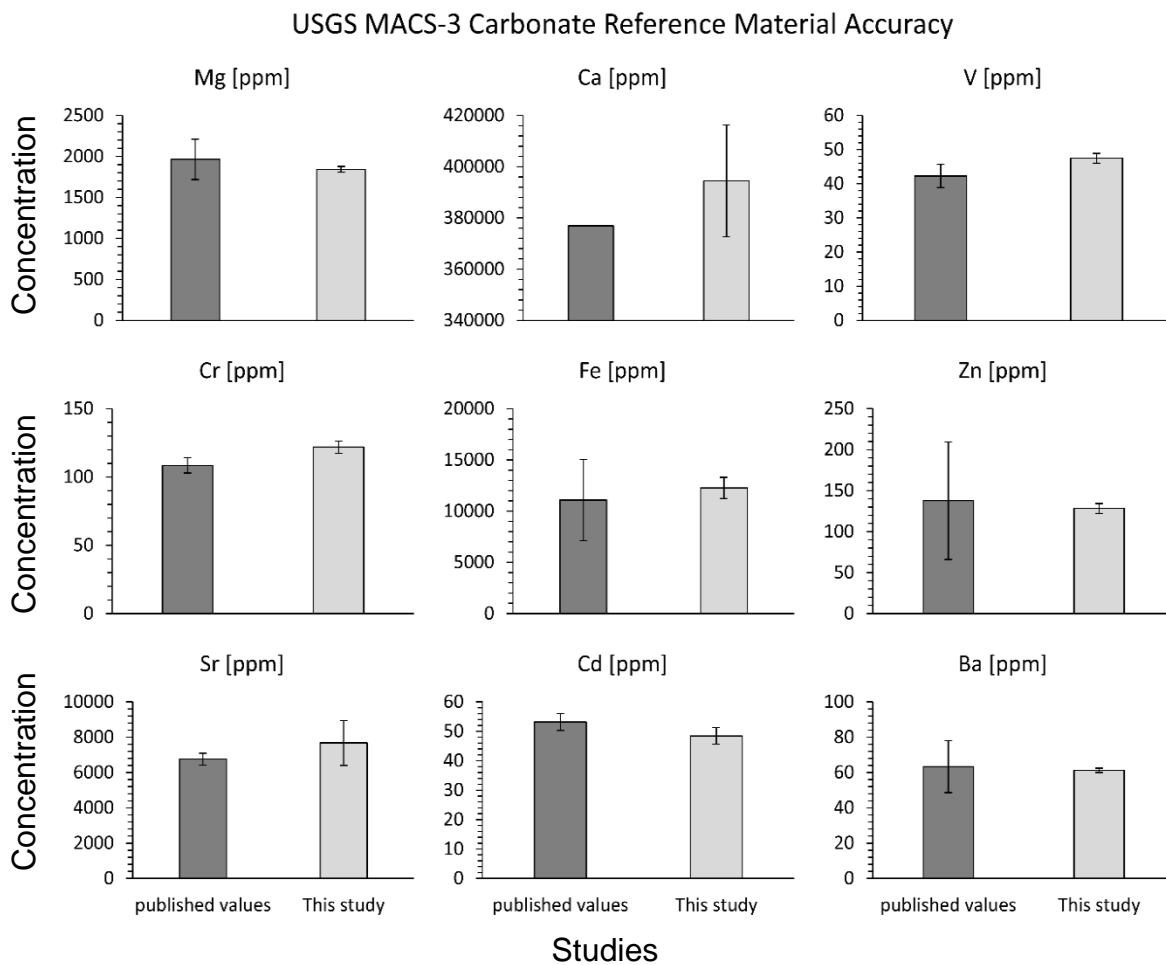


**Figure 3.2:** Accuracy of the reference material USGS MACS-3 for each measured and analysed trace element. Dark grey bars represent AV  $\pm$ SD [ppm] of published data retrieved from the GeoReM database. Light grey bars represent AV  $\pm$ SD [ppm] of trace elements in this study.

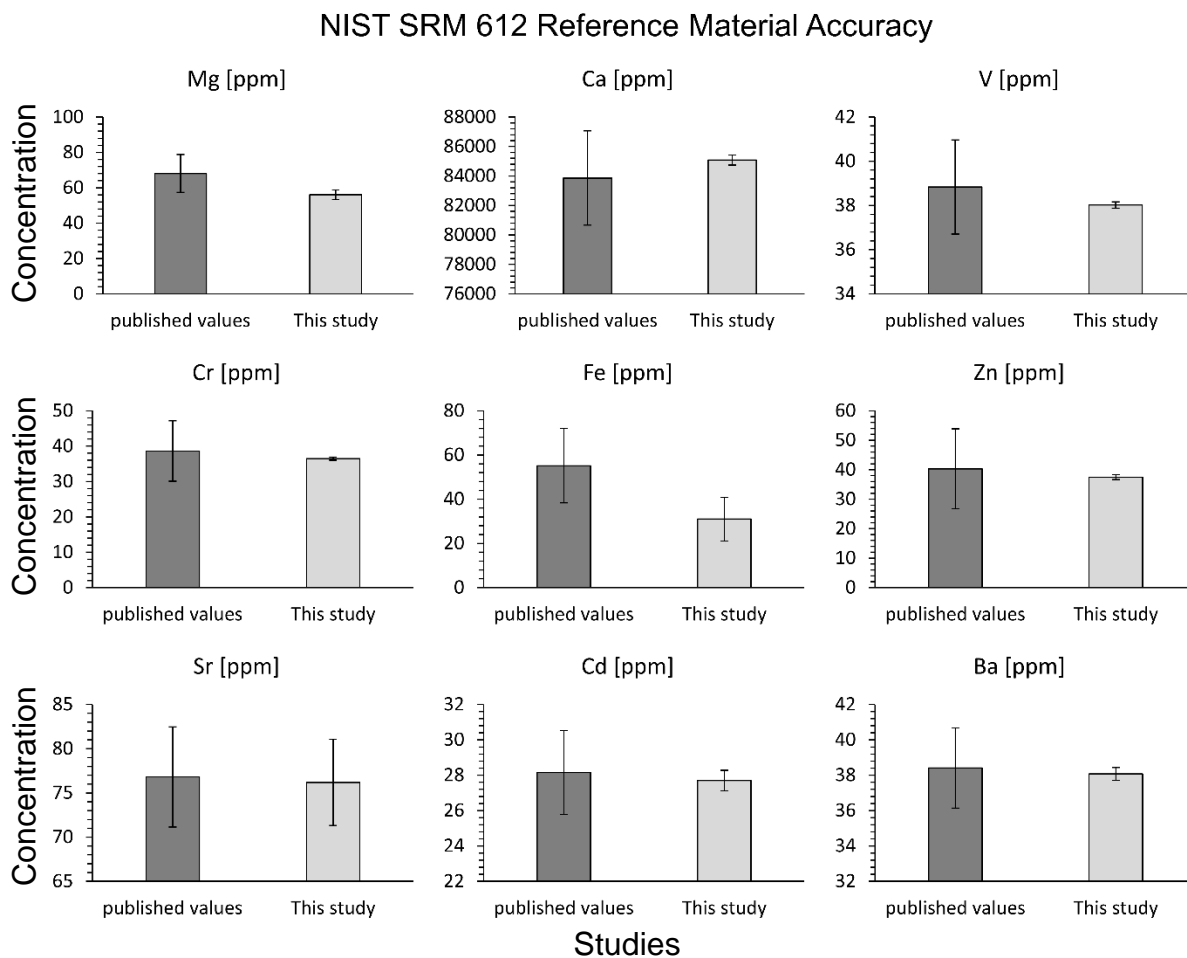


**Figure 3.3:** Accuracy of the reference material NIST SRM 612 for each measured and analysed trace element. Dark grey bars represent AV  $\pm$ SD [ppm] of published data retrieved from the GeoReM database. Light grey bars represent AV  $\pm$ SD [ppm] of trace elements in this study.

### 3.3.5.1 Monthly Growth Rates

In order to obtain growth rates in the field, transplants of *C. officinalis* were conducted at one sampling site in Iceland and in the UK. Specimens were carefully removed from the field following the procedure described in 2.2 and stained over night as described in 2.6.7.1. The following day, specimens were placed back at the point of collection, using epoxy resin (Splash Zone A-788, KOP-COAT, Inc., NJ, USA) to attach the holdfast. Transplants were collected after 3 months in Iceland and 5 months in the UK (Figure 2.9), and specimens were carefully dried and growth rates were determined following the protocol in 2.6.7.2. Analysis consisted of 298 Icelandic and 118 UK replicates for NP and CP, respectively. No transplant was deployed in Spain, southern populations, due to official restrictions.

### 3.3.5.2 Cell Wall Thickness

Using scanning electron microscopy (SEM) the natural state, modification of the cell wall structure and potential change in growth or metabolic processes in experimental individuals were measured.

The same samples mounts prepared in 2.8.2.1 for LA-ICP-MS analysis, were used for SEM analysis. A SEM suitable to take pictures of uncoated samples was used (EVO MA10 with a W filament electron source, Zeiss, Oberkochen, Germany) to be able to use the same mounts in both machines without any interference of sample coating. Sample mounts were fixed on stabs with double coated carbon conductive tabs and cleaned using Isopropanol. Samples were placed into the SEM and a variable pressure (VP) vacuum of 28 Pa was applied.

Images were taken at 20 kV electron high tension (EHT), representing the accelerating voltage used for each sample. A working distance (WD) of 7 - 9 mm

was set. Pictures were taken with a probe of 300 pA, a scan speed of 20.5 s, a magnification of 3 K and a line average noise reduction in the Backscatter (HDBSD) mode. After all images were produced, the software ImageJ (Rasband, 2016) was used to determine the average intra- (lateral to growth direction) and inter-cell wall (horizontal to growth direction) thickness of specimens ( $n = 15$ ).

### 3.3.6 Data Analysis

#### 3.3.6.1 Physiological Parameters

Data were analysed as described in Chapter 2. For statistical analysis, SPSS Statistics 25 (IBM Corp, 2016) was used and data were tested for normality (Shapiro-Wilk Test) and homogeneity of variance (Levene's Test) prior to analyses. Data for net production ( $n = 4$ ), respiration ( $n = 4$ ), light calcification ( $n = 4$ ), dark calcification ( $n = 4$ ),  $P_{\max}$  ( $n = 5$ ) and  $C_{\max}$  ( $n = 5$ ) displayed normality and homogeneity of variance. These data sets were analysed using two-way analyses of variance (ANOVAs) for replicates ( $n = 4$  or 5, respectively) from each population (north ( $n = 2$ ), central ( $n = 2$ ) and south ( $n = 2$ )) within seasons ( $n = 2$ ; summer and winter) as the fixed factors. Where significant effects were found, data was further explored by post hoc Tukey HSD tests.

#### 3.3.6.1 Structural Parameters

Not normally distributed and homogenic data were analysed using independent-sample Kruskal-Wallis H tests with pairwise comparison. In this way, tensile strength parameters displacement, force and strain (all  $n = 20$ ) as well as intra- and inter-cell wall thickness (all  $n = 45$ ) and monthly linear growth rates of NP and CP (all  $n = 118$ ) were analysed.

Trace element data was analysed using PRIMER 6.1 (Anderson *et al.*, 2009), after data normalisation by fourth root transformation due to extreme high variability of elemental concentrations, a permutational analysis of variance (PERMANOVA) with country, population and seasons as factors and populations nested into country and 9999 permutations was performed. Additional similarity of percentage (SIMPER) analysis were performed to determine the major influential trace elements for each group. Due to higher accuracy, only lower branch sections were analysed in this way.

## 3.4 Results

### 3.4.1 Field observations

Temperatures at the northernmost sampling site of the distribution of *C. officinalis*, Stafnes North (NP2) (Figure 3.4, Figure 2.2) did not exceed 20°C during the recording period and dropped to below than 10°C end of September 2017. In comparison to Stafnes North, Stafnes South (NP1) showed higher temperature variations exceeding 20°C and occasionally 25°C. Extreme high or low temperatures can be linked to tidal influence and the exposure of the data logger to air temperatures. The moving average (150 per mov. avg.) light intensities at Stafnes North (Figure 3.4) showed a natural fluctuation not exceeding 50  $\mu\text{mol photons m}^{-2} \text{s}^{-1}$ . The 3-times higher rates measured *in situ* were likely to be caused by direct exposure to sunlight during desiccation at low tide.

Much higher variations in temperature as well as light intensity were measured in CP sampling sites (Figure 3.5, Figure 2.3), where temperature reached up to 18 – 20°C during summer and 5 – 7°C during winter at both sites. Temperature variations were higher at Margate (CP2) than at St. Margaret's at Cliffe (CP1, **Figure 3.5**: Data logger records of temperature (°C) and light intensity ( $\mu\text{mol photons m}^{-2} \text{s}^{-1}$ ) at central sites of *Corallina officinalis* distribution in the NE Atlantic, UK, between January 2017 and March 2018. Light intensity is represented as the 150 moving average (black line) and temperature is represented as the *in situ* records (coloured line) and the 50 moving average (black dotted line). Temperatures above 20°C and below 10°C are coloured in red and blue, respectively. Grey areas mark time periods not directly comparable to the other locations, but data loggers continued recording. Figure 3.5). Light intensity was much lower at St. Margaret's at Cliffe than at Margate with levels

reaching  $\sim 120 \mu\text{mol photons m}^{-2} \text{ s}^{-1}$  and  $\sim 300 \mu\text{mol photons m}^{-2} \text{ s}^{-1}$ , respectively. A trend towards higher variation in temperature as well as light intensity in summer months compared to winter months was clearly visible at both sampling sites. Overly high or low pronounced values were due to the data logger being exposed to air and environmental conditions during low tide.

Similar variations than in the central sites were found at one of the southern sites, where Tragove (SP2) showed higher variations in temperature but similar variations in light intensity compared to Arousa (SP2; Figure 3.6, Figure 2.4). Temperatures exceeded  $20^\circ\text{C}$  during summer on a regular basis at Tragove, but not at Arousa. Colder temperatures were also found to be more variable at Tragove compared to Arousa with values not measured below  $5^\circ\text{C}$  at both sites. As for the other geographic sites, overly high or low pronounced values were due to the data logger being exposed to air and environmental conditions during low tide. Additionally, a trend towards higher variation in temperature as well as light intensity in summer months compared to winter months was noticeable but not as distinct as at CP sampling sites.



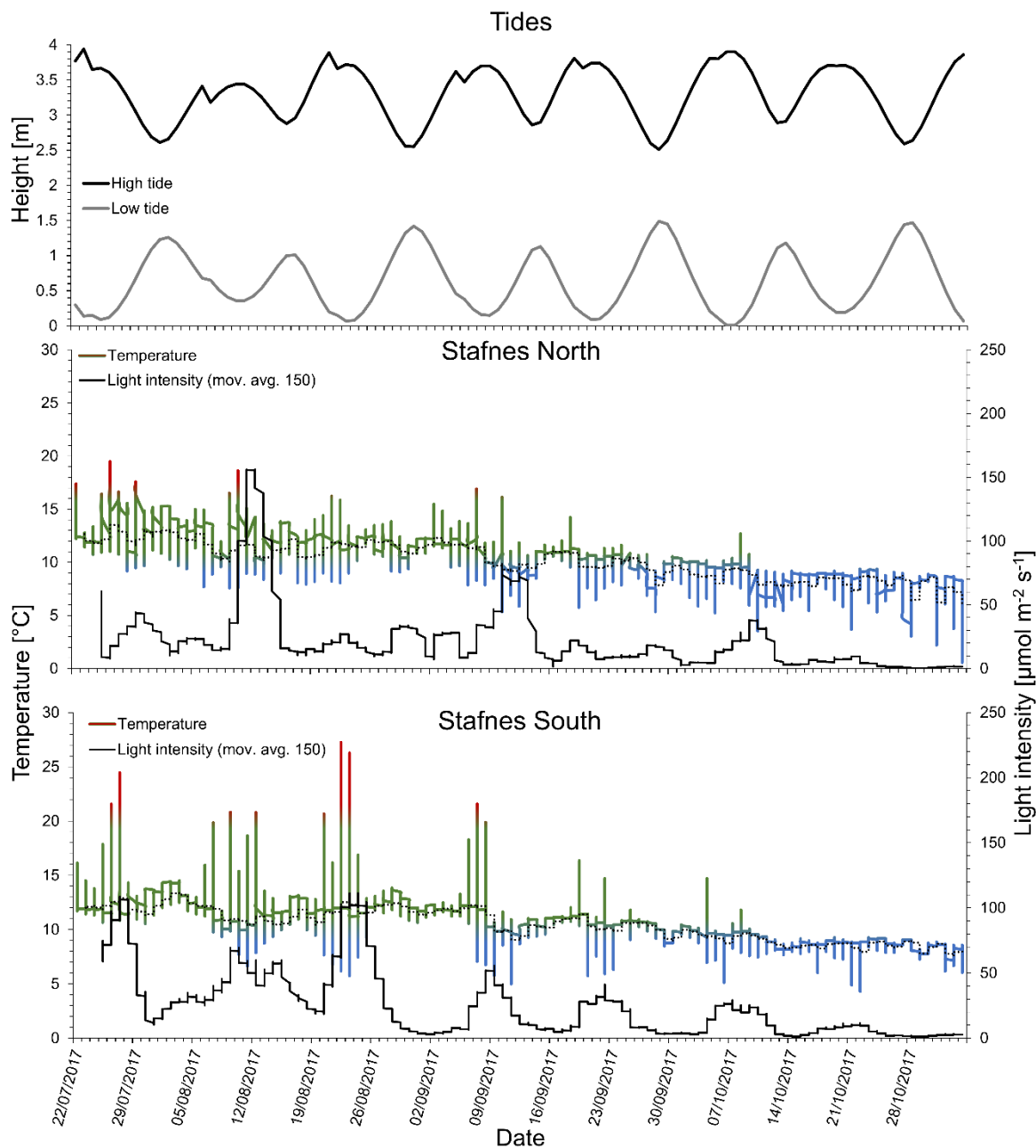


**Figure 3.4:** Data logger records of temperature ( $^{\circ}\text{C}$ ) and light intensity ( $\mu\text{mol photons m}^{-2} \text{s}^{-1}$ ) at northern sites of *Corallina officinalis* distribution in the NE Atlantic, Iceland, between July and October 2017. Light intensity is represented as the 150 moving average (black line) and temperature is represented as the *in situ* records (coloured line) and the 50 moving average (black dotted line). Temperatures above  $20^{\circ}\text{C}$  and below  $10^{\circ}\text{C}$  are coloured in red and blue, respectively.

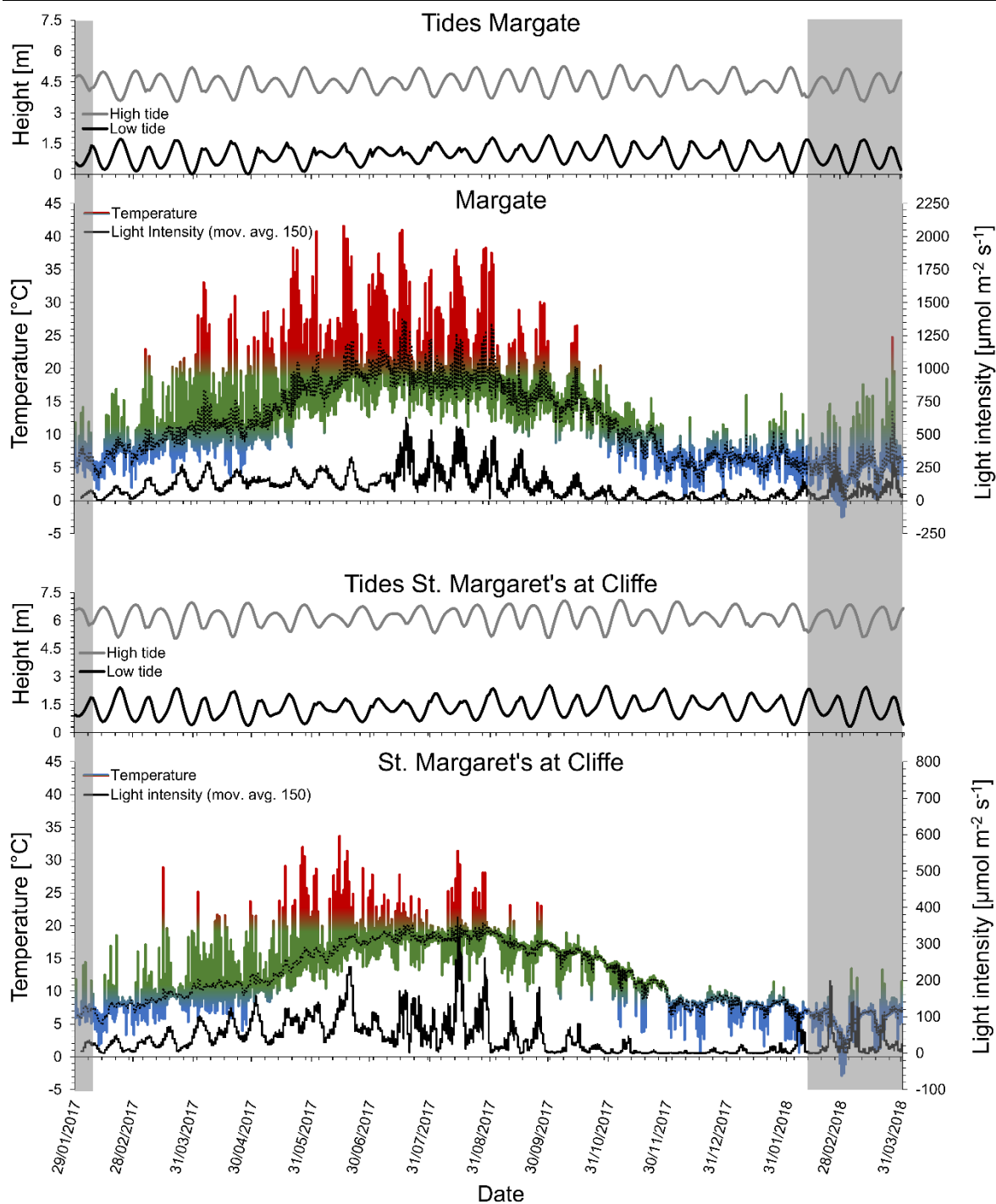


**Figure 3.5:** Data logger records of temperature ( $^\circ\text{C}$ ) and light intensity ( $\mu\text{mol photons m}^{-2} \text{s}^{-1}$ ) at central sites of *Corallina officinalis* distribution in the NE Atlantic, UK, between January 2017 and March 2018. Light intensity is represented as the 150 moving average (black line) and temperature is represented as the *in situ* records (coloured line) and the 50 moving average (black dotted line). Temperatures above  $20^\circ\text{C}$  and below  $10^\circ\text{C}$  are coloured in red and blue, respectively. Grey areas mark time periods not directly comparable to the other locations, but data loggers continued recording.

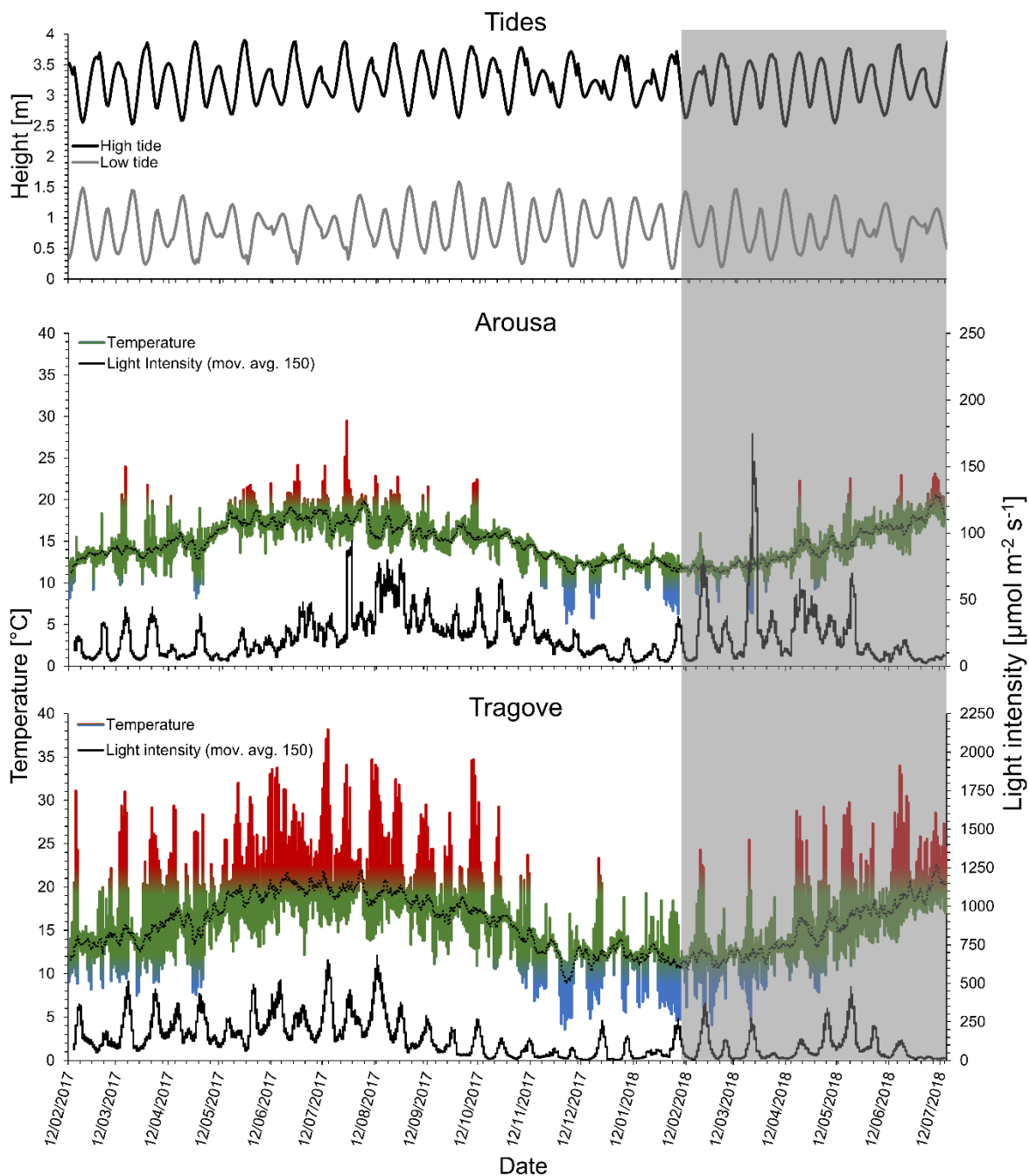


**Figure 3.6:** Data logger records of temperature ( $^{\circ}\text{C}$ ) and light intensity ( $\mu\text{mol photons m}^{-2} \text{s}^{-1}$ ) at southern sites of *Corallina officinalis* distribution in the NE Atlantic, Spain, between February 2017 and July 2018. Light intensity is represented as the 150 moving average (black line) and temperature is represented as the *in situ* records (coloured line) and the 50 moving average (black dotted line). Temperatures above  $20^{\circ}\text{C}$  and below  $10^{\circ}\text{C}$  are coloured in red and blue, respectively. Grey areas mark time periods not directly comparable to the other locations, but data loggers continued recording.

Temperature and light readings prior to noon-incubations are shown in Figure 3.7. At all sampling sites, light intensities showed a 5.35 (for NP), 5.69 (for CP) and 4.60 (for SP) fold increase from winter to summer. *In situ* temperatures showed a 1.50 (for NP), 3.25 (for CP) and 1.68 (for SP) fold increase from summer to winter. The carbonate system was calculated using incubation conditions (Table 3.2).

Light intensities during winter were lowest at northern (62.5  $\mu\text{mol photons m}^{-2} \text{s}^{-1}$ ) and central (72.0  $\mu\text{mol photons m}^{-2} \text{s}^{-1}$ ) sites and 2.87 and 3.31 fold higher at southern sites (207.0  $\mu\text{mol photons m}^{-2} \text{s}^{-1}$ , Figure 3.7). The same pattern was detected in summer light irradiance measurements. Temperatures in the winter were warmest in southern sites (11.6°C), followed by northern sites (7.9°C), showing the lowest values at central sites (5.8°C). Temperatures in the summer were lowest at northern sites (11.8°C) and showed similar values at central (18.7°C) and southern sites (19.5°C).

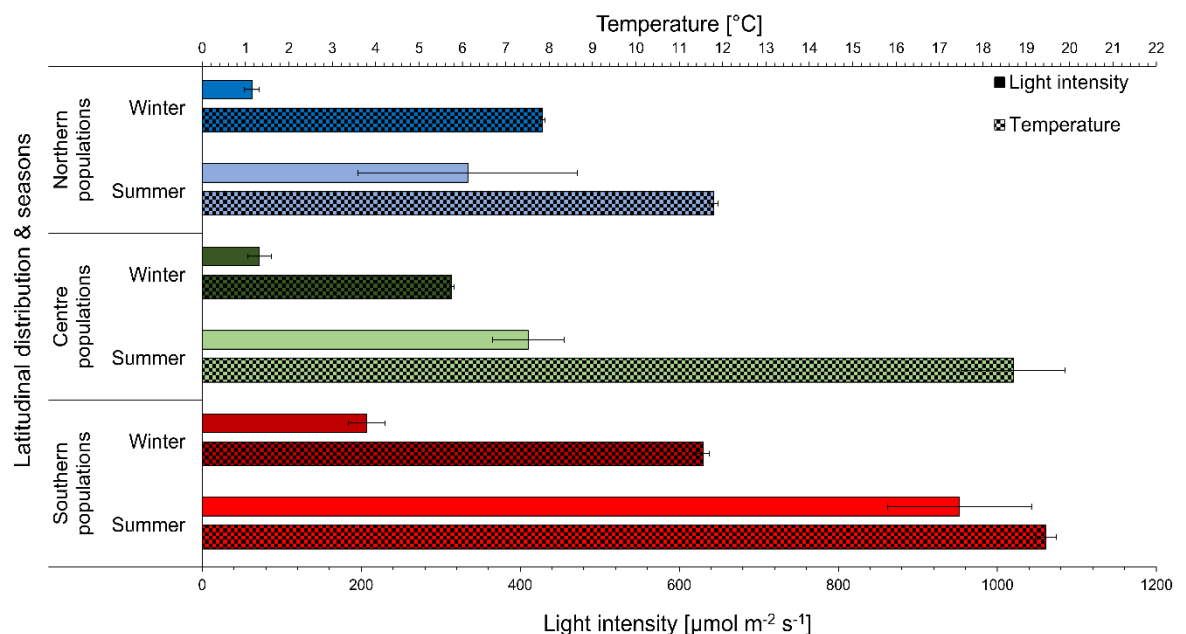


**Figure 3.7:** *In situ* temperature [ $^{\circ}\text{C}$ ] and light intensity [ $\mu\text{mol photons m}^{-2} \text{s}^{-1}$ ] before noon-incubations across sites (AV  $\pm$ SE, n = 2 per latitudinal region) of *C. officinalis* in the NE Atlantic. Chequered and solid bars represent temperature and light intensity, respectively. Coloured bars represent individual regions.

**Table 3.2:** *In situ* sampling details, conditions and seawater analysis data ( $n = 1$  measurement): carbonate chemistry, DO (dissolved oxygen) and pH, at all sites across *C. officinalis* distribution in the NE Atlantic. Abbreviations: A<sub>T</sub>: total alkalinity, DIC: dissolved inorganic carbon,  $\Omega_{Ca}/\Omega_{Ar}$ : calcite and aragonite saturation state, pCO<sub>2</sub>: partial pressure of carbon dioxide.

Latitudinal distribution/site	Season	Sampling date	pH (total scale)	Pressure [hPa]	DO [mg L <sup>-1</sup> ]	Salinity	Temperature [°C]	A <sub>T</sub> [μmol kg <sup>-1</sup> ]	DIC [μmol kg <sup>-1</sup> ]	HCO <sub>3</sub> <sup>-</sup> [μmol kg <sup>-1</sup> ]	$\Omega_{Ca}$	$\Omega_{Ar}$	pCO <sub>2</sub> [μatm]	Radiation [μmol m <sup>-2</sup> s <sup>-1</sup> ]	Weather conditions
North / population 1	Summer	22.7.17	8.03	1006	8.84	32.6	11.6	2233.0	2090.79	1959.95	2.66	1.69	494.51	196	windy, cloudy
	Winter	3.11.17	7.94	919	9.79	32.9	7.8	2330.7	2227.66	2110.36	2.14	1.35	596.28	8	rain, cold
North / population 2	Summer	23.7.17	8.16	1019	10.73	31.7	11.9	2320.6	2132.58	1975.47	3.42	2.17	390.99	326	windy, cloudy
	Winter	4.11.17	7.99	1003	11.06	33.7	7.9	2299.9	2168.29	2041.48	2.49	1.58	488.60	40	high waves, sunny, sporadic clouds
Centre / population 1	Summer	11.7.17	7.94	1012	8.88	34.1	17.5	2624.9	2289.84	2032.09	5.92	3.82	320.14	30	cloudy, warm, windy
	Winter	29.1.17	8.04	1020	11.97	32.3	5.8	2452.3	2365.24	2249.09	2.00	1.26	652.44	1	cloudy, later rain
Centre / population 2	Summer	10.7.17	8.48	1008	14.95	33.6	19.9	2513.9	2023.40	1667.70	8.46	5.48	167.05	278	sunny, later cloudy
	Winter	30.1.17	8.04	1014	11.14	30.3	5.7	2499.2	2423.90	2309.66	1.91	1.19	696.60	0	cloudy, foggy
South / population 1	Summer	14.7.18	8.22	1017	10.98	32.7	19.7	2281.5	1984.95	1763.53	5.14	3.32	301.11	862	sunny, warm
	Winter	11.2.17	8.14	1004	10.05	35.3	11.1	2205.7	2064.22	1935.28	2.55	1.63	510.25	230	sunny, sporadic clouds
South / population 2	Summer	15.7.18	8.15	1018	9.58	33.0	19.2	2433.3	2159.12	1944.98	4.89	3.16	378.37	595	sunny, warm
	Winter	12.2.17	8.21	1001	9.71	36.1	11.4	2051.4	1887.72	1755.58	2.73	1.74	402.71	184	cloudy, heavy rain

### 3.4.2 *In situ* Physiological Responses along a Latitudinal Gradient

#### 3.4.2.1 Photosynthesis and Calcification Evolution

The mean  $\pm$ SE saturating production rates ( $P_{\max}$ ) for CP1 declined significantly in winter compared to summer (Figure 3.8 (A); Figure B1 (E) - (H), Table 3.3).  $P_{\max}$  of CP in the summer were significantly higher than those of SP and showed similar or higher values in SP in winter. Compared to CP, both SP showed a significant increase of  $P_{\max}$  from summer to winter conditions. All NP showed a significant lower  $P_{\max}$  in summer as well as winter compared to CP and SP. In comparison with declining summer to winter trends in CP and increasing summer to winter trends in SP, NP showed both, a decrease and increase of  $P_{\max}$  for NP1 and NP2, respectively. Only NP2 showed significant differences between seasons, for NP1 no significant difference was found between seasons (Table 3.3).

The photosynthetic efficiency ( $\alpha$ ) in P-I curves of CP and SP showed opposing trends with a decrease from summer to winter efficiency in CP1 and SP1 and an increase from summer to winter efficiency in CP2 and SP2 (Figure 3.8 (B); Figure B1 (E) – (M), Table 3.3). Southern population 1 showed no drastic change in  $\alpha$  between seasons whereas SP2 displayed a steep, decrease of  $\alpha$  in winter. Northern populations presented a decline in  $\alpha$  in winter compared to summer. Therefore, NP were the only ones with a trend towards a lower  $\alpha$  in winter compared to summer (Table 3.3).

The saturating light intensity ( $I_k$ ) of P-I curves decreased in CP but increased in all other populations from winter to summer (Figure 3.8 (C); Figure B1 (E) – (H), Table 3.3). Mean values for  $I_k$  were highest in CP, decreased in SP and further decrease in NP, with greatest differences between CP and NP (Table 3.3).

The mean saturating calcification levels ( $C_{\max}$ ) of all populations were higher in summer than winter conditions except for CP1 where it was higher in winter. (Figure 3.8 (A); Figure B1 (E) – (H)). All CP and SP showed a significant change between seasons in  $C_{\max}$  (Table 3.3), NP were not significantly different. As the only data point, SP1 showed great error bars in winter.  $C_{\max}$  showed significantly lower values in all NP compared to CP and SP in winter and summer (Table 3.3), except for NP1 with SP2 that showed no statistically significant difference in winter. However, when data for seasons was pooled, NP1 and SP2 show significant differences (Tukey HSD  $P < 0.01$ , 2-way ANOVA). Southern population 1 showed higher values than the SP2 as well as both CP.

In C-I curves  $\alpha$  of CP increased 1.48-times in winter relative to summer measurements (Figure 3.8 (B); Figure B1 (E) – (H), Table 3.3). The same patterns were observed in SP (1.33-times). Northern populations showed different tendencies, with a decrease in  $\alpha$  in NP1 (0.56-times) and no significant change (0.95-times) in NP2 between summer and winter season. Of the three geographical regions, the SP showed the highest  $\alpha$  values.

$I_k$  of C-I curves were higher in CPs compared to both marginal populations (Figure 3.8 (C); Figure B1 (E) – (H), Table 3.3). Southern and NPs showed similar values. All populations showed a decrease in  $I_k$  of C-I curves in winter compared to summer conditions, except for NP1, which showed an increase of the same magnitude as the other populations decrease.

Photoinhibition of photosynthesis rates was not observed in any population (max. light intensity:  $700 \mu\text{mol photons m}^{-2} \text{s}^{-1}$ );  $P_{\max}$  was reached in all populations and treatments. Calcification inhibition was observed in summer for CP1 and NP1 and

in winter for CP2 and SP2. P-I and C-I curves for each population and season can be found in Appendix B, Figure B1.

**Table 3.3:** (A) Mean  $\pm$ SE ( $n = 5$ ) for saturating photosynthesis ( $P_{\max}$ ) and calcification ( $C_{\max}$ ) levels, photosynthetic efficiency ( $\alpha$ ) and saturating light intensity ( $I_k$ ) of field populations ( $n = 2$ ) of *C. officinalis* across its geographical distribution in the NE Atlantic. (B) Statistical comparison of  $P_{\max}$  and  $C_{\max}$  between populations within season and between seasons within populations.

(A)

Region	Population	Season	Net Production Rates [ $\mu\text{mol h}^{-1} \text{gDW}^{-1}$ ]				Net Calcification Rate [ $\mu\text{mol h}^{-1} \text{gDW}^{-1}$ ]			
			$P_{\max}$	$\pm$ SE	$\alpha$ Oxygen evolution	$I_k$ Oxygen evolution	$C_{\max}$	$\pm$ SE	$\alpha$ Calcification evolution	$I_k$ Calcification evolution
North	1	Summer	567.30	31.41	11.44	41.44	151.94	8.25	5.42	27.11
		Winter	471.39	39.20	9.85	43.59	141.51	8.30	3.05	48.11
	2	Summer	488.62	31.74	13.23	30.10	130.21	16.86	4.38	29.26
		Winter	565.24	15.51	12.22	43.65	120.05	6.19	4.59	25.25
Central	1	Summer	1017.64	40.00	16.02	60.90	186.79	7.09	2.84	68.08
		Winter	692.78	22.24	13.25	49.16	217.33	14.00	4.21	53.44
	2	Summer	890.17	43.10	8.63	96.72	212.14	7.31	2.30	92.47
		Winter	776.20	16.25	11.45	65.03	175.98	12.26	3.76	47.12
South	1	Summer	628.45	27.10	12.34	45.49	279.54	14.76	7.26	36.35
		Winter	744.22	44.75	12.56	56.93	270.85	72.00	9.64	23.19
	2	Summer	817.29	24.86	18.39	40.19	220.97	9.67	5.59	41.68
		Winter	876.26	31.28	14.40	60.01	168.80	4.96	6.22	27.44

(B)

$P_{\max}$ Significances		North				Central				South			
$C_{\max}$ Significances		1		2		1		2		1		2	
2-way ANOVA		Summer	Winter	Summer	Winter	Summer	Winter	Summer	Winter	Summer	Winter	Summer	Winter
North	1	Summer	NS	NS		***		***		NS		***	
		Winter	NS		*		***		***		***		***
	2	Summer	NS		**		***		***		***		***
		Winter		*	NS			*		***		***	
Central	1	Summer	***		***		***	*		***		***	
		Winter		***		***	*		*		NS		***
	2	Summer	***		***		NS		NS		***		*
		Winter		*		***		***	*			NS	
South	1	Summer	***		***		***		***		***		***
		Winter		***		***		NS		***		**	
	2	Summer	***		***		**		NS		*		**
		Winter		NS		***		***		NS		***	

Significance levels: NS = not significant \* =  $P < 0.05$  \*\* =  $P < 0.01$  \*\*\* =  $P < 0.005$



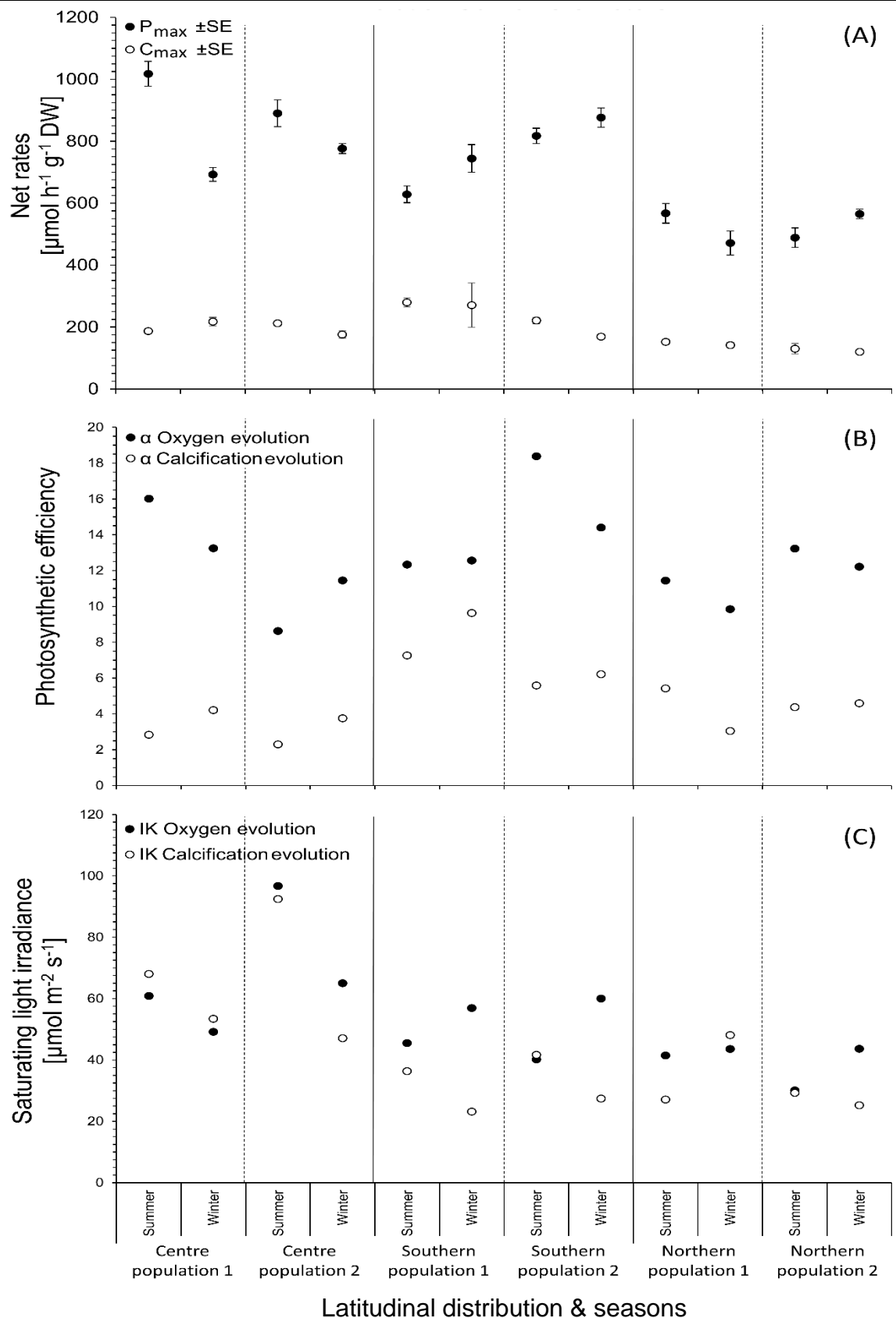


**Figure 3.8:** Evolution curve characteristics for net production and calcification ( $AV \pm \text{SE}$ ,  $n = 5$ ) of central, southern and northern populations ( $n = 2$ ) in summer and winter. (A):  $P_{\text{max}}/C_{\text{max}}$  = maximum production, (B)  $\alpha$  = initial slope as indicator for photosynthetic efficiency, (C)  $I_K$  = saturating irradiance. For detailed graphs, Figure B1 (A) – (M).

### 3.4.2.2 Primary Production and Respiration Rates

Net production rates ( $P_N$ ) and gross production rates ( $P_G$ ) were significantly lower in winter compared to summer in NP1 but not NP2 and both CP. However, no significant change in SP was found (Table 3.4, Figure 3.9). Both production rates in summer were significantly higher in CP than in all other populations. Rates of  $P_N$  and  $P_G$  of NP in winter were the lowest of all populations. CP were not significantly different from any marginal population, however, NP1 was significantly different to SP1 and SP2, NP2 was significantly different to SP1 (Table 3.4(B)). Central population 1 showed a significant higher production rate than CP2 in winter, but not in summer.

Respiration rates ( $R$ ; Figure 3.9) were lower in winter compared to summer in all populations, with CP1 showing production instead of respiration rates (Figure 3.9, Table 3.4(A)). A significant difference between seasons was found for CP and SP but not for NP (Table 3.4(B)). The lowest values were measured in NP; highest values were measured in CP. Respiration rates of SP2 in both seasons were significantly higher than those of NP and those of SP1 were significantly higher than those of NP2 but not NP1 (Table 3.4(B)). Rates of NP and SP show consistent values, CP showed very high variability within R rates and therefore showed variable significances within season to other populations. For instance, CP1 was only significantly different to CP2 and SP2 in summer, but significantly different to both SP and NP1 in winter. Additionally, CP2 was significantly different to all other populations in summer but only to SP2 in winter (Table 3.4(B)).

### 3.4.2.1 Calcification Rates

Calcification rates in the dark ( $G_D$ ; Figure 3.10) were not significantly higher in summer than winter in CP with CP2 showing calcification instead of dissolution in

dark conditions during summer (Figure 3.10, Table 3.4). In relation to CP, NP showed lower dissolution rates in winter and similar rates in summer with the exception of NP1 that displayed calcification instead of dissolution in the summer in dark incubations (Table 3.4(A)). Populations inhabiting the southern margin of the species distribution showed dominant calcification instead of dissolution in dark conditions with calcification rates being higher in the winter than in the summer in dark conditions (Table 3.4(A)). This reports the highest dissolution rates for CP and the lowest dissolution rates for NP. Between seasons, only SP showed significant differences (Table 3.4(B)). In summer, out of all populations, only NP2 showed a significant difference with SP1 all other results were not significant (Table 3.4(B)). In winter, SP were significantly different to NP and CP but not with each other. NP and CP were not significantly different (Table 3.4(B)).

Net calcification ( $G_N$ ; Figure 3.10) in light conditions showed similar values in all seasons in CP. Only CP2 displayed a significantly higher calcification rate in summer compared to winter (Table 3.4(B); Figure 3.10). Standard errors in CP1 in winter conditions were higher than in the other measurements for CP. Higher  $G_N$  rates were measured in summer compared to winter for both NP (Table 3.4(A)), however, only NP1 showed significance (Table 3.4(B)). The rates for  $G_N$  in NP compared to CP were drastically lower, both in winter and in summer. Net calcification rates for SP showed 1.91 and 3.65-times significantly higher values for SP1 and SP2, respectively, in winter compared to summer. In summer, both SP showed significantly higher values than CP but only SP1 showed significant different values to NP (Table 3.4(B)). In winter SP were not significantly different from each other but from all other populations. Rates in SP in summer were equal or less than rates for CP in summer and winter and were not extensively higher

than rates for NP. Northern populations were significantly lower from the other regions' populations in both seasons (Table 3.4(B)), except for SP2 in summer.

Gross calcification rates ( $G_G$ ) followed  $G_N$ , except in SP where  $G_N$  exceeds  $G_G$  due to calcification instead of dissolution rates in the dark (Figure 3.10).

**Table 3.4:** (A) Mean  $\pm$ SE (n = 4) for gross and net production, respiration, gross and net calcification and dark calcification rates of field populations (n = 2) of *C. officinalis* across its geographical distribution in the NE Atlantic. (B) Statistical comparison between populations within season and between seasons within populations.

(A)

Region	Population	Season	Gross Production Rates		Net Production Rates		Respiration Rate		Gross Calcification Rates		Net Calcification Rates		Dark Calcification Rates	
			[ $\mu\text{mol O}_2 \text{ h}^{-1} \text{ gDW}^{-1}$ ]						[ $\mu\text{mol CaCO}_3 \text{ h}^{-1} \text{ gDW}^{-1}$ ]					
				$\pm$ SE		$\pm$ SE		$\pm$ SE		$\pm$ SE		$\pm$ SE		$\pm$ SE
North	1	Summer	299.83	27.99	240.43	37.93	-59.40	11.85	108.87	11.29	<b>6.93</b>	3.83	115.80	13.57
		Winter	137.05	14.97	101.48	14.57	-35.57	2.17	26.92	15.87	<b>-9.84</b>	2.86	17.08	15.56
	2	Summer	430.56	25.64	382.01	28.22	-48.56	3.52	57.42	20.89	-24.09	11.16	33.32	19.45
		Winter	191.83	7.75	171.05	8.46	-20.78	6.12	35.99	2.21	-8.17	1.04	27.82	2.95
Central	1	Summer	1267.34	160.11	1194.54	169.00	-72.79	16.63	231.22	15.29	-19.30	5.43	211.92	14.17
		Winter	389.83	74.22	406.36	60.91	16.53	17.57	222.47	62.02	-10.89	3.35	211.58	59.88
	2	Summer	593.89	47.42	327.08	39.16	-266.81	32.09	357.52	15.90	7.39	20.88	364.90	35.57
		Winter	158.00	50.97	155.85	63.51	-2.16	20.43	235.54	20.03	-25.12	11.99	210.42	20.41
South	1	Summer	453.01	33.79	347.93	30.04	-105.08	5.85	210.07	18.78	12.99	4.34	223.06	22.85
		Winter	425.23	73.34	375.31	60.61	-49.92	19.61	356.09	15.98	69.34	20.55	425.43	17.36
	2	Summer	416.08	11.03	263.84	8.64	-152.24	10.31	97.28	6.14	-6.04	8.85	91.24	8.67
		Winter	318.75	145.05	223.34	148.61	-95.41	25.29	294.01	18.44	39.40	18.66	333.41	5.69

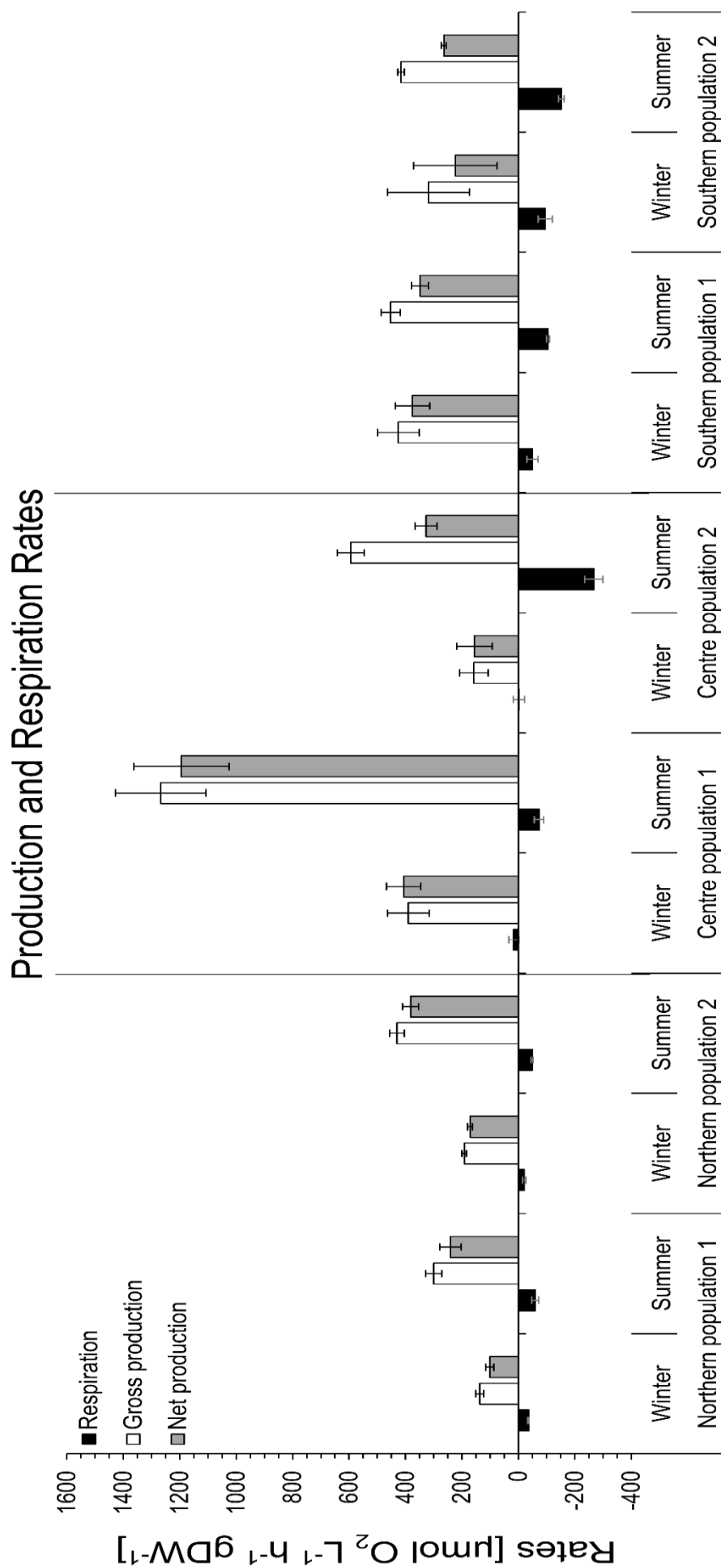
(B)

Net & Gross Production Significances			North				Central				South			
Respiration Significances			1		2		1		2		1		2	
2-way ANOVA			Summer	Winter	Summer	Winter	Summer	Winter	Summer	Winter	Summer	Winter	Summer	Winter
North	1	Summer		NS	NS	NS	***		***		NS	NS	NS	
		Winter	NS			NS		NS		NS		**		*
	2	Summer	NS			*	***		***		NS		NS	
		Winter		NS	NS			NS		NS		*		NS
Central	1	Summer	NS		NS		***		***		***		***	
		Winter		*		NS	***			NS		NS		NS
	2	Summer	***		***		***		***		**		*	
		Winter		NS	NS			NS	***		**		*	
South	1	Summer	NS		*		NS		***			NS	NS	
		Winter		NS		NS		**		NS		*		NS
	2	Summer	***		***		***		***		NS		NS	
		Winter		*		***	***		***		NS		NS	*
Net & Gross Calcification Significances			North				Central				South			
Dark Calcification Significances			1		2		1		2		1		2	
2-way ANOVA			Summer	Winter	Summer	Winter	Summer	Winter	Summer	Winter	Summer	Winter	Summer	Winter
North	1	Summer		NS	NS	NS	***		***		***		NS	
		Winter	NS			NS		***		***		***		***
	2	Summer	NS			NS	***		***		***		NS	
		Winter		NS	NS			***		***		***		***
Central	1	Summer	NS		NS		NS		***		NS		***	
		Winter		NS	NS	NS	NS			NS		***		*
	2	Summer	NS		NS		NS		***		***		***	
		Winter		NS	NS	NS		NS	NS			***		NS
South	1	Summer	NS		*		NS		NS		***		***	
		Winter		***		***		***		***		***		NS
	2	Summer	NS		NS		NS		NS		NS		NS	
		Winter		**		**		***		***		NS		***

Significance levels:

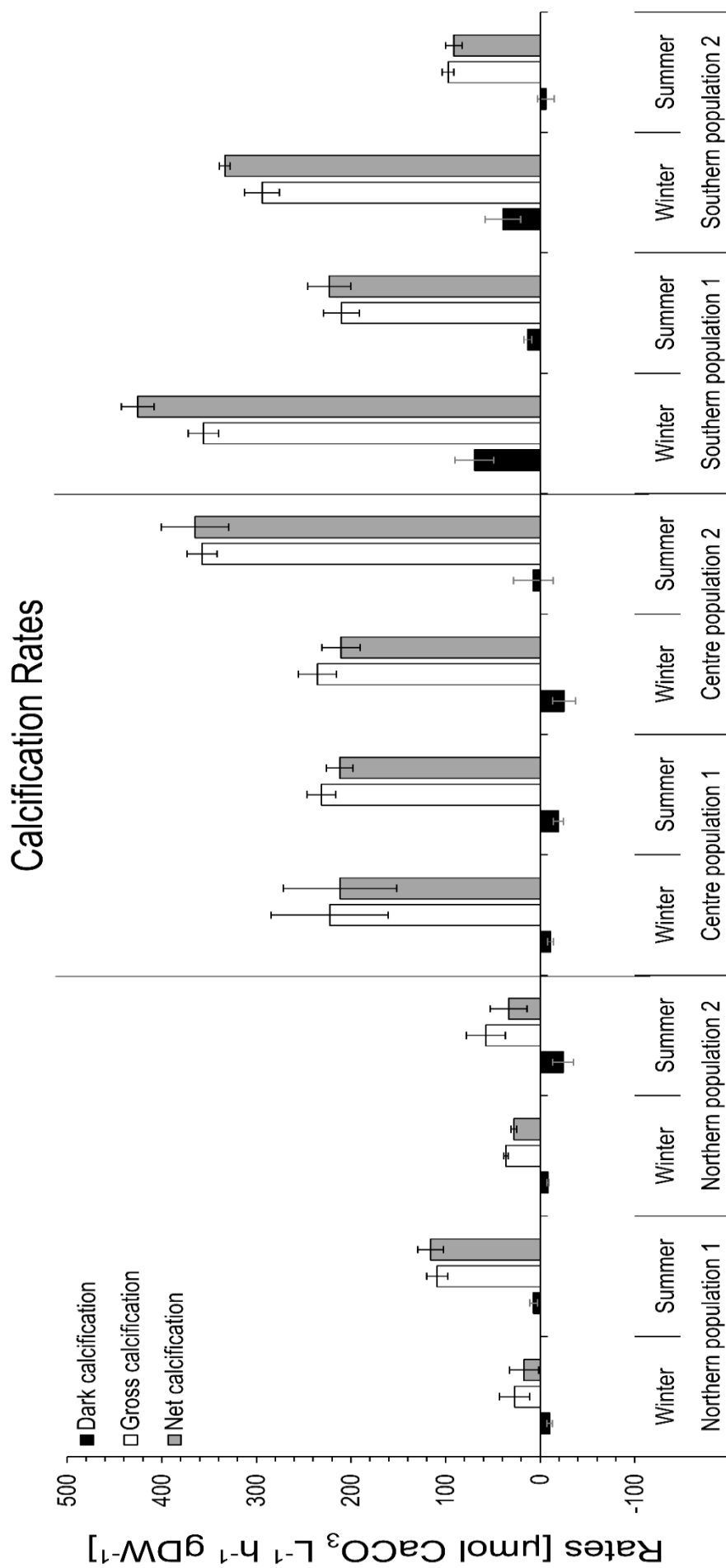
NS = not significant

\* =  $P < 0.05$ \*\* =  $P < 0.01$ \*\*\* =  $P < 0.005$



### Latitudinal distribution & seasons

**Figure 3.9:** Net production, gross production and respiration rates [ $\mu\text{mol h}^{-1} \text{L}^{-1} \text{gDW}^{-1}$ ] AV  $\pm$ SE (n = 5) of *C. officinalis* across its distribution in the NE Atlantic in summer and winter.



### Latitudinal distribution & seasons

**Figure 3.10:** Net calcification, gross calcification and dark calcification rates [ $\mu\text{mol h}^{-1} \text{L}^{-1} \text{gDW}^{-1}$ ] AV  $\pm$ SE (n = 5) of *C. officinalis* across its distribution in the NE Atlantic in summer and winter.

### 3.4.3 *In situ* Structural Integrity Along a Latitudinal Gradient

#### 3.4.3.1 Linear Growth Rates: A Transplant Approach

Monthly linear growth rates in the field were measured for NP and CP but not for SP due to official restrictions (Figure 3.11). Growth rates found for NP were  $2.08 \pm 0.03$  mm month<sup>-1</sup> and those found for CP were significantly lower at  $0.25 \pm 0.03$  mm/month (Kruskal-Wallis  $H = 171.278$ ,  $P < 0.001$  with a mean rank growth score of 176.66 and 60.34 for NP and CP, respectively). Staining success totals ~57% and ~70% for CP and NP, respectively.

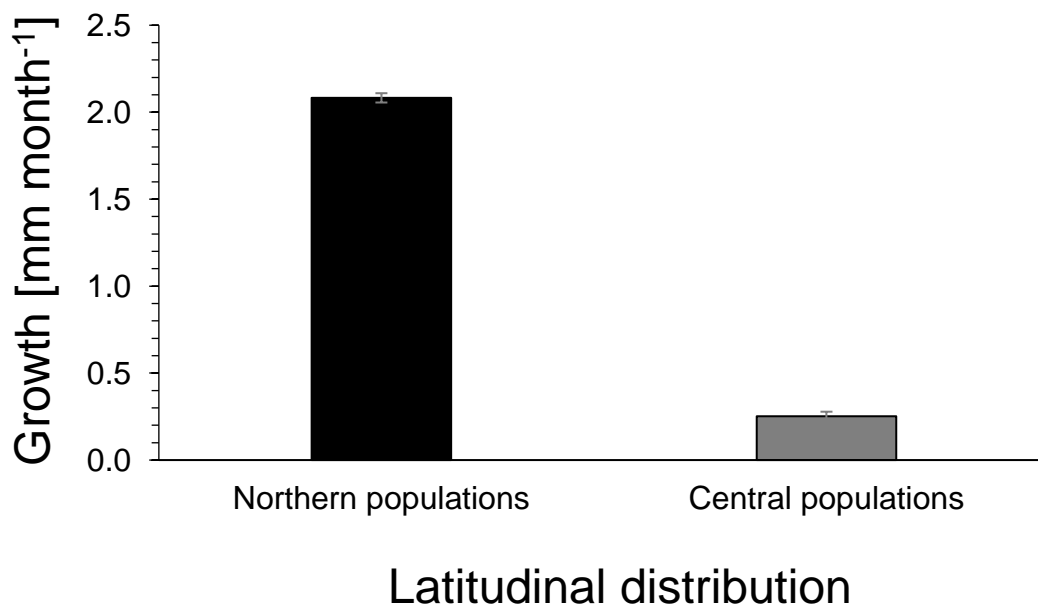


**Figure 3.11:** Monthly linear growth rates [mm] ( $AV \pm SE$ ) for northern ( $n = 289$ ) and central ( $n = 118$ ) populations of *C. officinalis* across its natural distribution in the NE Atlantic in summer conditions. Samplesizes vary in relation with staining success.



### 3.4.3.2 Ultimate Tensile Strength

The ultimate tensile strength (UTS or  $F_{tu}$ ) did not significantly decrease in both NP from summer to winter conditions (0.99-times and 0.90-times for NP1 and NP2, respectively; Table 3.5, Figure 3.12). Values for  $F_{tu}$  were higher in NP compared to CP and SP (Table 3.5(A)). In CP,  $F_{tu}$  decreased from summer to winter in CP1 and increased from summer to winter in CP2, showing opposite trends within this region of the species distribution. Both maximum values in CP were lower than those of NP. In SP,  $F_{tu}$  decreased in both populations from summer to winter conditions. Values of  $F_{tu}$  in winter conditions of SP were similar to values for CP in both seasons. Values of SP in summer were higher than those of CP and comparable to those of NP. Relevant significant differences in  $F_{tu}$  were found between CP1 vs. NP2 in summer, SP1 vs. NP2 in summer and CP2 vs. NP2 in summer (Table 3.5(B)).

Normal strain,  $\epsilon$  also referred to as elongation, did not decrease significantly in NP from summer to winter (Table 3.5, Figure 3.12). Central populations had similar values to NP, but showed a decrease in  $\epsilon$  from summer to winter in CP1 (0.77-times) but an increase in CP2 (1.25-times). In SP  $\epsilon$  showed no change in SP1 (1.00-times) and a decrease in SP2 (0.79-times), leaving only CP2 to increase in strain from summer to winter conditions. Relevant statistical differences in  $\epsilon$  were not found (Table 3.5(B)). However, NP1 in winter vs. NP2 in summer and SP2 in winter vs. NP2 in summer showed significant differences (Table 3.5(B)).

The displacement, also referred to as elongation, of the specimens before rupture followed the same pattern as the normal strain  $\epsilon$  (Figure 3.12).

**Table 3.5:** (A) Mean  $\pm$ SE (n = 15) for displacement, force and strain of field populations (n = 2) of *C. officinalis* across its geographical distribution in the NE Atlantic. (B) Statistical comparison between populations within season and between seasons within populations.

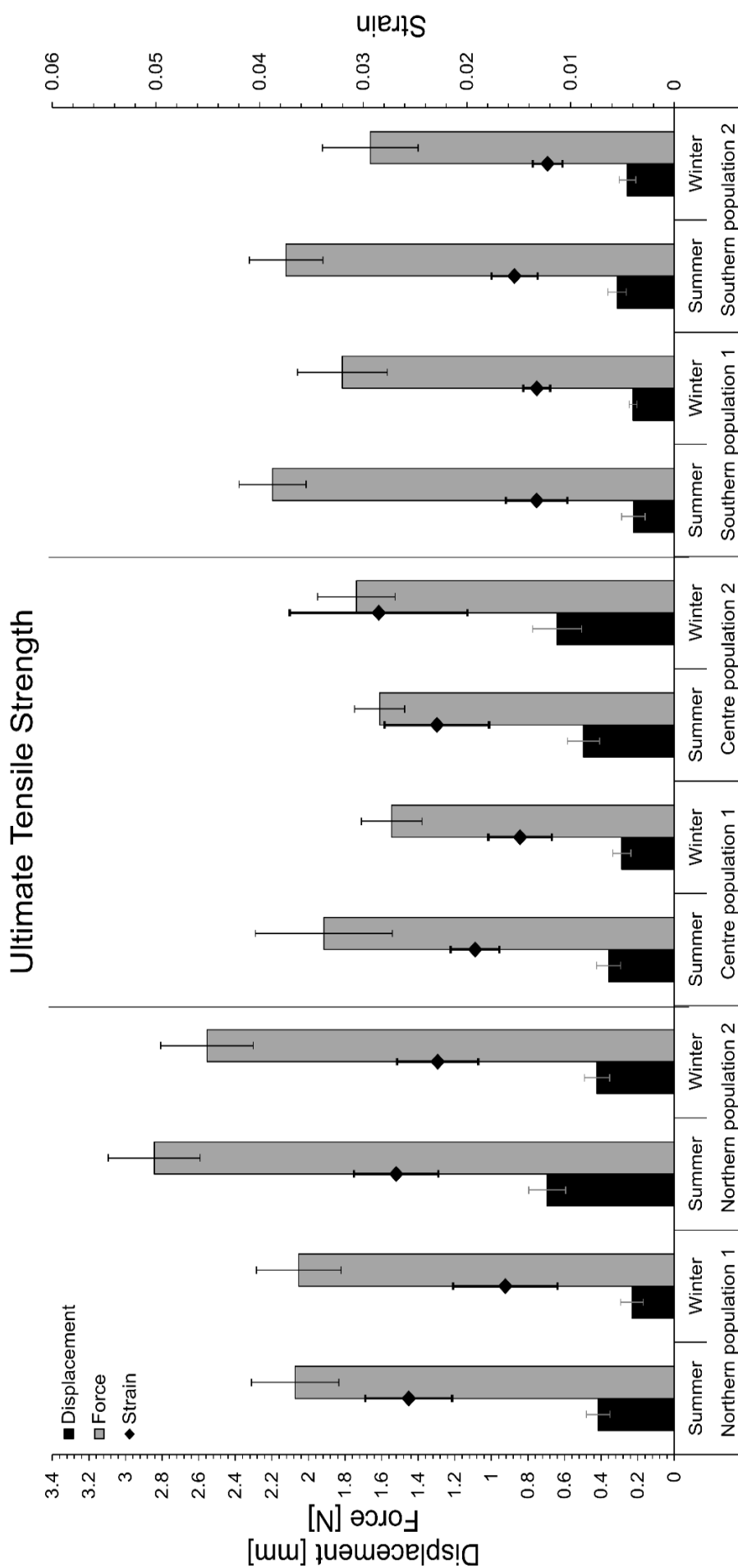
(A)

Region	Populatio c	Season	Displacement		Force		Strain	
			[mm]		[N]			
			Mean	$\pm$ SE	Mean	$\pm$ SE	Mean	$\pm$ SE
North	1	Summer	0.42	0.06	2.07	0.24	0.026	0.004
		Winter	0.23	0.06	2.05	0.23	0.016	0.005
	2	Summer	0.69	0.10	2.84	0.25	0.027	0.004
		Winter	0.42	0.07	2.55	0.25	0.023	0.004
Central	1	Summer	0.36	0.07	1.92	0.37	0.019	0.002
		Winter	0.29	0.05	1.55	0.17	0.015	0.003
	2	Summer	0.50	0.09	1.61	0.14	0.023	0.005
		Winter	0.64	0.13	1.74	0.21	0.029	0.009
South	1	Summer	0.22	0.06	2.20	0.18	0.013	0.003
		Winter	0.23	0.02	1.82	0.25	0.013	0.001
	2	Summer	0.31	0.05	2.12	0.20	0.015	0.002
		Winter	0.26	0.05	1.66	0.26	0.012	0.001

(B)

Displacement Significance			North				Central				South			
Force Significances			1		2		1		2		1		2	
Kruskal-Wallis Test			Summer	Winter	Summer	Winter	Summer	Winter	Summer	Winter	Summer	Winter	Summer	Winter
North	1	Summer		*	***		NS		NS		NS		NS	
		Winter	NS			***		***		*		NS		NS
	2	Summer	*			*	NS		***		***		***	
		Winter		NS	NS			NS		NS		*		*
Central	1	Summer	NS		***			NS		NS		*		NS
		Winter		NS		NS	NS			NS		***		***
	2	Summer	***		***		NS			NS		NS		NS
		Winter		*		***		NS	NS			NS		NS
South	1	Summer	***		***		NS		NS			NS		NS
		Winter		NS		NS	NS		NS	NS				NS
	2	Summer	NS		*		NS		***		***			NS
		Winter		*		***		NS		NS		NS		***
Strain Significances			North				Central				South			
Kruskal-Wallis Test			1		2		1		2		1		2	
Kruskal-Wallis Test			Summer	Winter	Summer	Winter	Summer	Winter	Summer	Winter	Summer	Winter	Summer	Winter
North	1	Summer		NS		NS		NS		NS		NS		NS
		Winter				*		**		NS		NS		NS
	2	Summer				NS	NS		NS		**		*	
		Winter						NS		NS		*		*
Central	1	Summer						NS		NS		NS		NS
		Winter								NS		*		***
	2	Summer								NS		NS		NS
		Winter										NS		NS
South	1	Summer										NS		NS
		Winter												NS
	2	Summer												NS
		Winter												NS

Significance levels: NS = not significant \* =  $P < 0.05$  \*\* =  $P < 0.01$  \*\*\* =  $P < 0.005$



Latitudinal distribution & seasons

**Figure 3.12:** Ultimate tensile strength [N], displacement [mm] and normal strain  $AV \pm SE$  ( $n = 15$ ) of *C. officinalis* across its distribution in the NE Atlantic in summer and winter.

### 3.4.3.3 Elemental Composition of the Skeleton

For detailed values, trace element raw data is stored in an online repository, for link, see Appendix B.

Magnesium/Calcium (Mg/Ca) ratios in NP were lower in summer than winter. In all other populations, winter ratios were lower than summer ratios (Figure 3.13). The upper part of the analysed branch section in all populations and seasons had lower Mg/Ca ratios compared to the lower part of the branch section, except for NP2 where values were constant. Northern populations showed a lower variation in Mg/Ca ratios compared to CP and SP. Central populations have higher values, and CP and SP show a clear decrease from summer to winter.

Vanadium/Calcium (V/Ca) ratios showed no significant differences between summer and winter in NP, however, in CP and SP, V/Ca ratios were higher in summer compared to winter (Figure 3.13). No clear pattern was found between lower, middle and upper part of the analysed branch section. Values found in SP were higher compared to CP and NP in all seasons and regions of the branch.

Chromium/Calcium (Cr/Ca) ratios showed no significant changes between summer and winter analyses (Figure 3.13). Lower branch sections presented a different Cr/Ca ratio compared to upper branch sections in CP and NP. Across the latitudinal distribution, NP showed the lowest values with the lowest variability; CP and SP demonstrate the highest values with SP presenting the highest variability.

Iron/Calcium (Fe/Ca) ratios showed an increase from the lower to the upper region of the branch section (Figure 3.13). Average Fe/Ca ratios in winter in NP were lower, showed mixed variations for CP and presented higher values in SP compared to summer. Southern populations showed higher Fe/Ca ratios than NP.

Fe/Ca showed a high variability in all populations, seasons and regions of the branch section.

Zinc/Calcium (Zn/Ca) ratios showed significantly higher values in winter than in summer in all populations, except for NP2 where the same trend was visible but not significant (Figure 3.13). No significant increase or decrease was found between lower, middle or upper region of the analysed branch sections in any of the examined populations. However, a trend towards lower values in the upper compared to the lower part of the branch was visible. Between latitudinal regions, lowest ratios were found in NP, the highest in SP and intermediate values in CP.

Strontium/Calcium (Sr/Ca) ratios showed no significant difference within the branch regions for any of the populations (Figure 3.13). Higher Sr/Ca ratios were found in summer compared to winter conditions in all populations. No significant difference between values measured for CP and SP was found, however, NP showed lower values compared to CP and SP.

Cadmium/Calcium (Cd/Ca) ratios showed a decrease from lower to upper branch section in NP and constant values for CP and SP (Figure 3.13). Summer ratios for NP were lower compared to winter ratios and show the opposite trend for CP. For SP, both, an increase and decrease of ratios between summer and winter can be observed in the different populations. Central populations showed the most stable and lowest values and SP showed the most variable values. Northern populations showed higher ratios compared to CP and SP.

Barium/Calcium (Ba/Ca) ratios in lower, middle and upper regions of the analysed branch section showed no significant difference between each other in any of the populations of latitudinal regions (Figure 3.13). Additionally, only marginal

differences were found between seasons in each population. However, NP showed lower Ba/Ca ratios compared to CP and SP across branch and seasons. Central populations showed the highest values of Ba/Ca ratios but not significantly different to SP.

V/Ca, Cr/Ca, Zn/Ca and Ba/Ca ratios demonstrated an increase in value from the northern margin of the species distribution towards the southern margin of the species distribution, contrary to Cd/Ca ratios, which decline from the northern to southern margin.

PERMANOVA and SIMPER analysis indicated that chemical composition of *C. officinalis* cell walls was not significantly different between country and seasons ( $P > 0.05$ , PERMANOVA), indicating the chemical composition of ambient environment has no effect on the cell wall trace elemental composition. However, it showed a significant difference between populations nested in the country ( $P < 0.001$ , PERMANOVA) and 'populations nested in the country' and season ( $P < 0.001$ , PERMANOVA). A clear separation between NP and SP was determined (Figure 3.14 (A)). Additionally, SIMPER analysis presented the main composition of elements for each country's elemental signature. Overall, 92.47%, 93.12% and 92.25% of the data were represented in SIMPER for NP, CP and SP, respectively. For NP, CP and SP 86.43%, 85.52% and 84.03%, respectively, of the data were channelled in Ca, Mg and Sr, in this order. The remaining major contributing elements were Zn and Cr. However, Zn and Cr contributions in this particular order were reversed in NP compared to CP and SP. No significant influence of Ca, Sr, Ba and Zn within and between the populations was found (Figure 3.14 (B), 2D stress: 0.17). However, it was discovered that Cd was the dominating element in the NP, Cr and Mg were determining the CP and SP. When comparing these

findings with geological data, elevated concentrations of Cr and Mg, as found in SP, may be attributed to local substrate compositions which in NW Spain typical consists of Mg and Cr rich ophiolites (Prof. C. Storey, personal communication).

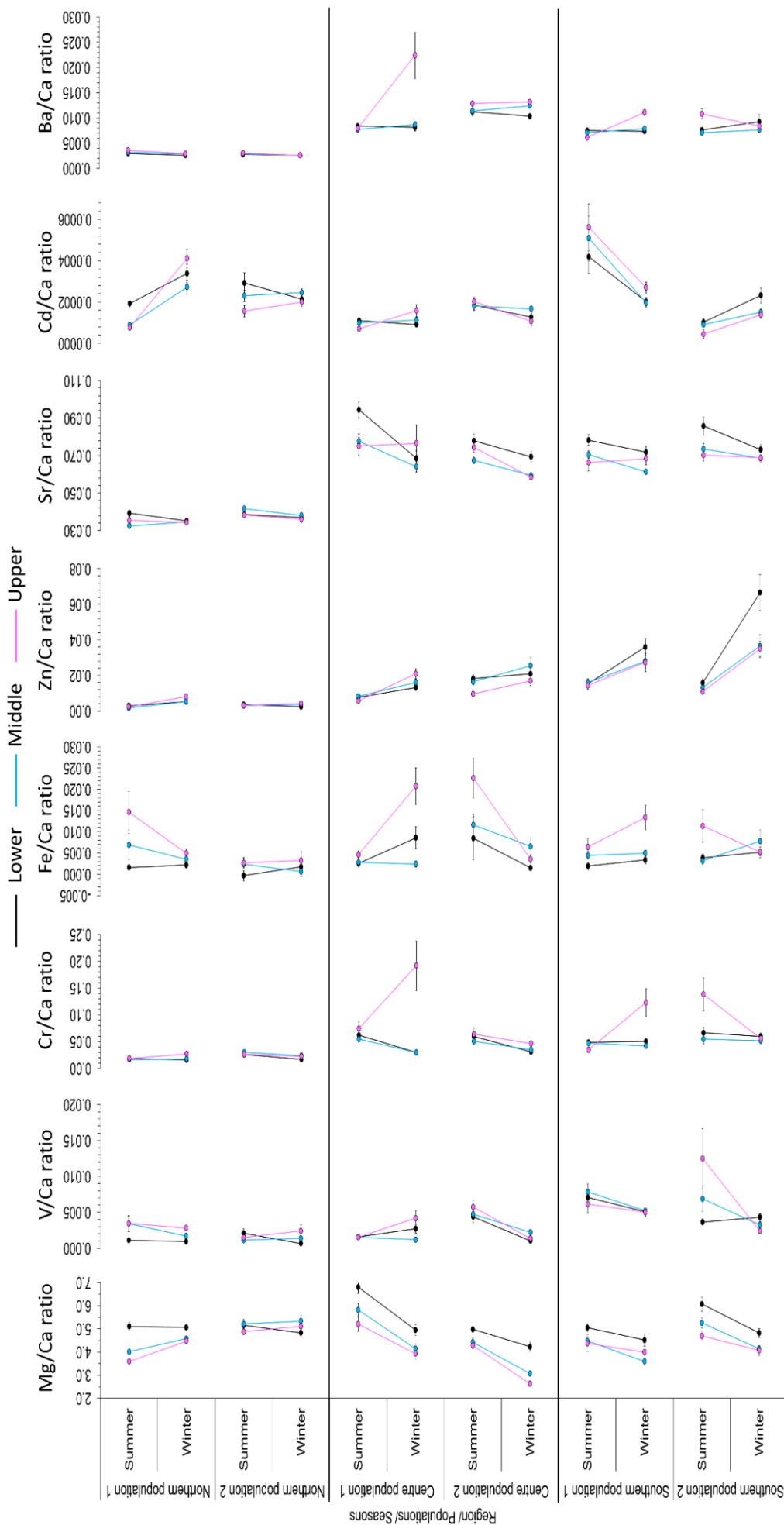


**Figure 3.13:** Element/Ca ratios for all elements in different parts of the branch. The lower, middle and upper 4 data points  $\pm$ SE ( $n = 9$ ) represent northern, central and southern regions, respectively. Within each region, populations ( $n = 2$ ) are represented above each other and are split into season.



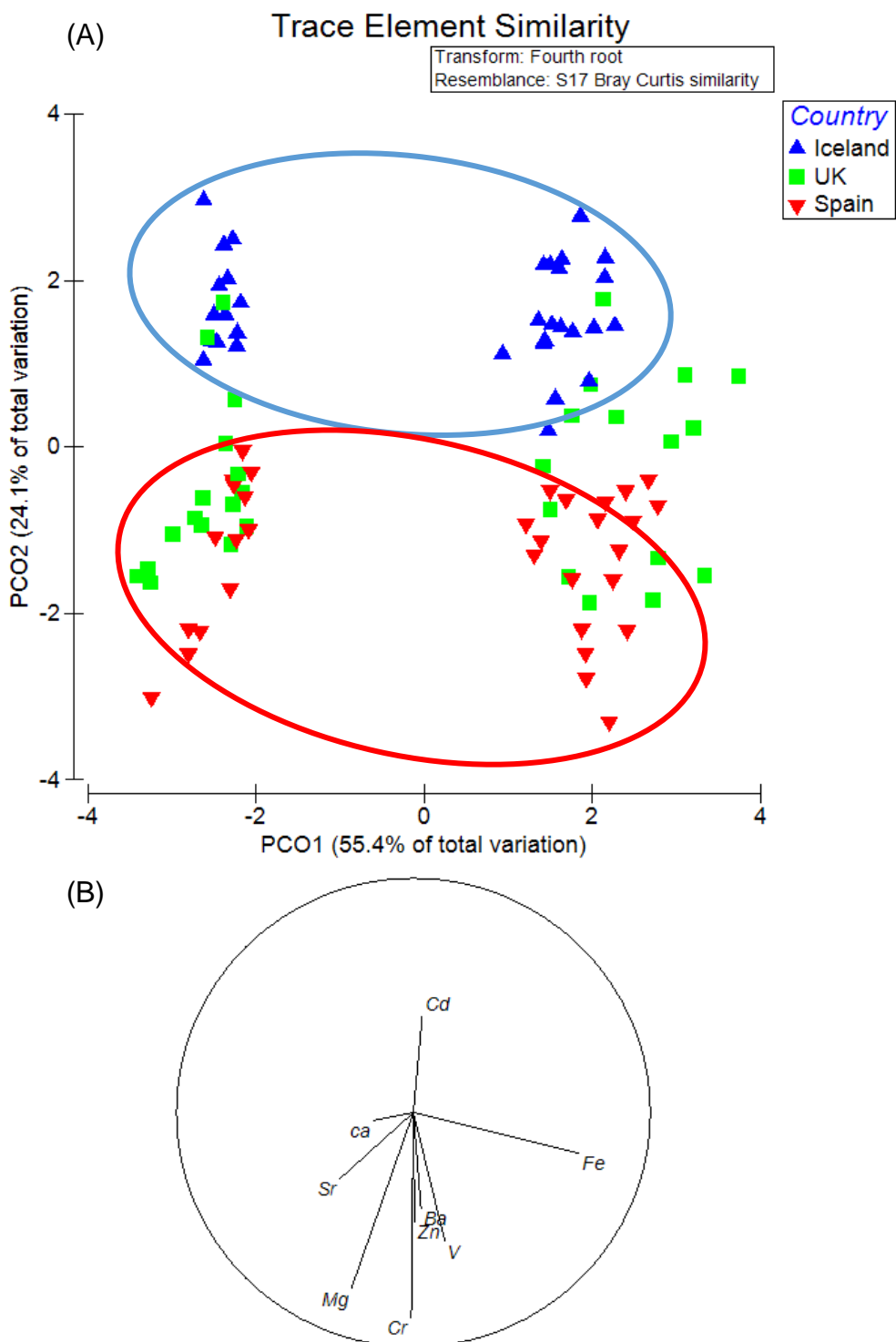


**Figure 3.14:** PERMANOVA (A) and SIMPER (B) results for all populations across the geographic distribution of *C. officinalis* across the NE Atlantic. Blue triangles, green squares and red triangles represent northern, central and southern populations, respectively

### 3.4.3.1 Cell wall thickness and condition

Cell wall thickness was measured for inter- (lateral to growth direction) and intra-cell walls (horizontal to growth direction, Figure 2.13, Table 3.6(A)). Inter-cell wall thickness (Figure 3.15) was significantly higher in NP compared to CP and SP in both seasons (Table 3.6(B)). Significant differences between CP and SP were found in summer for CP2 vs. SP2 and in winter for SP1 vs. CP1 (Table 3.6(B)). The SP showed higher variability within their measurements. Inter cell walls in the winter were marginally thicker than in the summer in NP and CP. In SP a significant difference between seasons between both populations was found ( $P < 0.001$ , Kruskal-Wallis H test in both cases).

Intra-cell wall thickness was more variable than inter-cell wall thickness (Figure 3.15, Table 3.6(A)). Northern populations showed significantly higher intra-cell wall thickness compared to CP and SP in one of the seasons (Table 3.6(B)). Central population 2 showed significant differences in summer with CP1 and SP1 (Table 3.6(B)). In winter CP showed significant differences with SP1, and SP1 with SP2. Summer values were significantly lower than winter values in all populations (Table 3.6(B)), except for NP2 and SP1 which showed increasing values.

**Table 3.6:** (A) Mean  $\pm$ SE (n = 15) for inter- and intra-cell wall thickness (CWT) of field populations (n = 2) of *C. officinalis* across its geographical distribution in the NE Atlantic. (B) Statistical comparison between populations within season and between seasons within populations.

(A) Region	Population	Season	Inter-cell wall thickness		Intra-cell wall thickness	
			[ $\mu$ m]		[ $\mu$ m]	
			Mean	$\pm$ SE	Mean	$\pm$ SE
North	1	Summer	1.80	0.06	1.49	0.06
		Winter	1.86	0.06	2.08	0.05
	2	Summer	1.85	0.06	1.90	0.04
		Winter	1.89	0.05	1.83	0.06
Central	1	Summer	1.47	0.05	1.57	0.06
		Winter	1.48	0.04	1.67	0.06
	2	Summer	1.33	0.05	1.31	0.04
		Winter	1.35	0.04	1.67	0.05
South	1	Summer	1.32	0.06	1.70	0.05
		Winter	1.05	0.04	1.30	0.05
	2	Summer	1.70	0.05	1.54	0.04
		Winter	1.47	0.06	1.65	0.06

(B)

Inter-CWT Significances		North				Central				South			
Intra-CWT Significances		1		2		1		2		1		2	
Kruskal-Wallis Test		Summer	Winter	Summer	Winter	Summer	Winter	Summer	Winter	Summer	Winter	Summer	Winter
North	1	Summer		NS	NS	***		***		***		NS	
		Winter	NS			NS		***		***		***	
	2	Summer	NS			NS		***		NS		***	
		Winter		*	***			***		***		***	
Central	1	Summer	***		NS		NS		NS		NS		**
		Winter		*		***	NS			NS		***	
	2	Summer	***		**		***			NS		NS	
		Winter		NS		***		NS	***			***	
South	1	Summer	*		*		NS		***		***		Ns
		Winter		***		***		***		***		***	
	2	Summer	***		NS		NS		***		*		**
		Winter		*		***		NS		NS		***	

Significance levels: NS = not significant \* =  $P < 0.05$  \*\* =  $P < 0.01$  \*\*\* =  $P < 0.005$

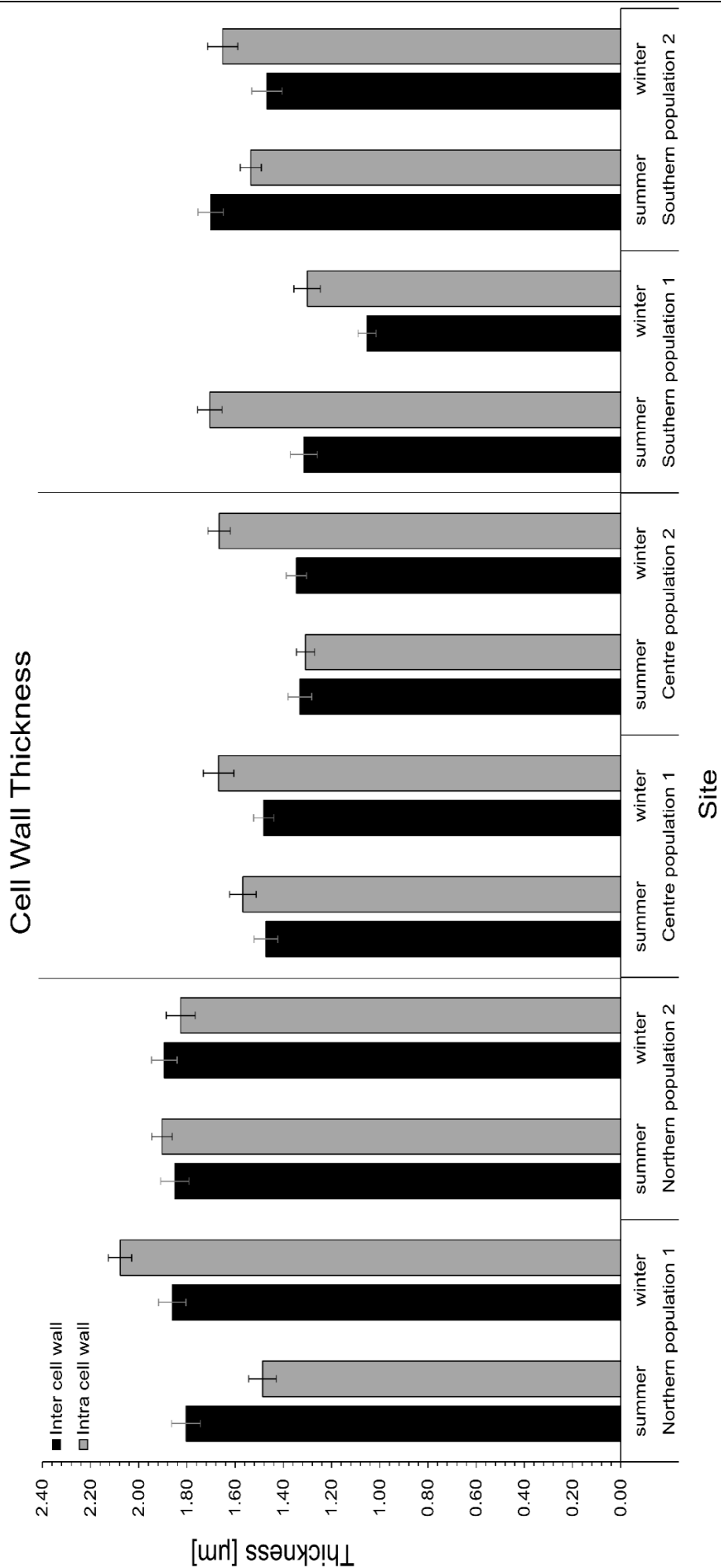


**Figure 3.15:** Inter- and intra-cell wall thickness of *C. officinalis* samples in the field. Black and grey bars represent inter- and intra-cell wall measurements [µm], respectively. (AV ±SE, n = 15). The left, middle and right section of the graph represent the northern, central and southern regions, respectively. Within each region, population (n = 2) are compared during summer and winter conditions.

### 3.5 Discussion

In this study, physiological and structural traits of *C. officinalis* across its geographical distribution in the NE Atlantic were investigated. Various natural physiological and structural parameters were defined and are discussed in the following sections. Due to the exposure to a wide range of abiotic and biotic factors, *C. officinalis* showed different, local and seasonal, adaptations to regions.

#### 3.5.1 Northern Populations

Light intensity measurements for midday incubations were higher than those recorded by the data logger for the respective season; however, they were still within the acceptable range (Williamson *et al.*, 2018). It can therefore be concluded that incubation results are representative for the responses of *C. officinalis* in the environment.

Both NP show an opposing response to each other, within the interaction of  $P_{\max}$  and  $C_{\max}$ , NP2 shows a decoupling of primary production and calcification as defined by Johansen (1981), contrary to NP1,  $P_{\max}$  was expected to show lower values in winter compared to summer conditions due to light constraints and a lower efficiency owing to temperature effects on the metabolism. All these aspects are found in P-I curves of NP, except for NP2 where  $P_{\max}$  values are higher in winter compared to summer, likely due to local adaptation. Lower light intensities in winter, including periods of very low light due to the geographic high latitudinal location, are expected to result in low  $P_N$  rates. However, this was not the case for NP2 showing higher rates in winter compared to summer, reinforcing the finding of local adaptation in this population, enabling these specimens to flourish at low light conditions as well as simultaneously being hidden under canopy algae. The light harvesting efficiency  $\alpha$  of P-I curves was expected to increase since the organism

would try to compensate low light availability with increased efficiency. In both NP, a decrease in efficiency from summer to winter may be caused by the effect of low temperatures on the metabolism, which might conceal the organisms' effort to increase the light harvesting efficiency in colder and darker conditions. Together with  $\alpha$ ,  $I_K$  mirrors the interrelation between these parameters and  $P_{max}$ , where a high  $\alpha$  results in a low  $I_K$ , which in turn means that  $P_{max}$  would be reached faster, and *vice versa*. This means that with no prominent change in  $I_K$  of P-I curves in NP1 between seasons, but yet a decrease in  $\alpha$ ,  $P_{max}$  shows the expected, lower values in winter compared to summer. In contrast, NP2 decreased in  $\alpha$  and increased in  $I_K$  of P-I curves from summer to winter resulting in a slower reach of a lower  $P_{max}$ . However, this was not the case for NP2, which implies that other, not yet defined, interfering mechanisms are dominant that ensure the algal survival of dark periods.

Rates of  $P_N$  and  $R$  in the summer are expectedly higher and lower, respectively, than in winter with both populations showing similar results which coincides with literature findings of high latitude populations and their seasonal photoacclimation to changing irradiances (Williamson *et al.*, 2018). The maximum photosynthetic rate of P-I curves of NP1 in winter was reflected in a less distinct decrease of  $P_N$  values of this population, compared to a steeper decrease in rates for NP2, resulting in higher  $P_N$  due to higher  $P_{max}$  values for NP2. In winter, NP2 shows higher  $P_{max}$  values compared to NP1, leading to higher  $P_N$  values in NP2 than NP1. It was expected for both NP to show the pattern observed in NP2; this highlights the importance of including multiple populations into test and experimental designs, in order to account for random effects on or responses of tested populations.

Similar responses in terms of  $C_{\max}$  rates are observed in both NP, with only a marginal decrease from summer to winter conditions. Specimens of NP may try to build and conserve the calcareous, protective skeleton during winter. In this case, more energy may be spent for calcification and  $P_N$  rates may reduce over prioritised protection of cells and stability of the specimen. The light harvesting efficiency of C-I curves either declined (NP1) or showed no change, which can also be explained by the negative effect of low temperatures of the organisms' metabolic processes. Rather stable  $C_{\max}$  values of both NP are a result of different physiological background processes; NP1 shows a decrease in  $\alpha$  and an increase in  $I_K$ , conversely, NP2 shows a marginal increase in  $\alpha$  and a marginal decrease in  $I_K$ , resulting in the same effect on  $C_{\max}$ .

Net calcification was expectedly higher in the summer than in winter in NP1. For NP2 however,  $G_N$  was not different between summer and winter. This may be due to high  $G_D$  rates and constant  $C_{\max}$  observed for NP2 in summer conditions. Calcification in winter was not enhanced and relatively low in summer conditions with high dissolution rates in the dark, leaving NP2 more vulnerable to environmental factors compared to NP1. The slower reaching of  $C_{\max}$  of NP2 due to higher  $I_K$  in accordance with lower  $\alpha$  in the summer may be a protection mechanism against photodamage, since NP are better adapted to low-light than high-light conditions. Due to the time needed to reach  $C_{\max}$  as well as the low temperatures, NP1 calcifies less in winter compared to summer, which was represented by the results of  $G_N$  data.

Trace element data show low Ba/Ca ratios in winter compared to summer in both NP. Barium is an indicator element for freshwater discharge (Gillikin *et al.*, 2006) and is directly inverse proportionally between Ba/Ca in the skeleton and salinity,

consequently low Ba resembles high salinity values in the winter. This may be due to absent freshwater input at the beginning of the winter since freshwater may still be accumulated as snow or ice. The water body around the northern sites in Iceland is substantially low in nutrients, coinciding with low phytoplankton abundances (Stefánsson and Ólafsson, 1991) and low element/Ca ratios in the skeleton of *C. officinalis*. Cd/Ca ratios are lower in summer than winter. Cadmium concentrations increase due to anthropogenic input into the environment and may be introduced to intertidal ecosystems in the North Atlantic through rain, snow, ice melting and washouts. Cadmium can be used as proxy for pollution and has negative effects on plant growth and nutrient uptake capability (Kangwe *et al.*, 2001, Vymazal, 1987 and references therein, Nazar *et al.*, 2012); however, it does not play an essential role in living cells and is associated with Zn concentrations. No clear pattern could be detected for Cd/Ca rates in NP. Sr/Ca rates feature a proxy for salinity with higher rates of Sr/Ca with higher salinity. This rate for NP was higher in summer than in winter due to freshwater input into the intertidal ecosystem by e.g. rain in autumn.

Zinc is an essential macronutrient in cells and is required in photosynthetic reactions as well as CO<sub>2</sub>-assimilation (Kitano and Hood, 1962, Rout and Das, 2003, Raven *et al.*, 1999). Zn/Ca ratios are lower in summer compared to winter, implying an enhanced support for photosynthesis and CO<sub>2</sub>-assimilation in winter months due to low light and cold temperatures. This was also supported by higher Fe/Ca ratios in winter than summer. Iron assists electron transportation in photosynthetic reactions and therefore, enhanced photosynthetic as well as respiration rates (Raven *et al.*, 1999 and references therein). Increased Zn/Ca and



Fe/Ca ratios may also be the explanation for increased  $P_{\max}$  values in winter. Toxicity levels are found to be low around NP sites.

The low levels of Cr as an element that, for instance, modifies DNA and inhibits growth and primary production (Sari and Tuzen, 2008), reflects the status of these sites as organically certified. Cr/Ca levels were found to be lower in winter compared to summer due to anthropogenic input of pollutants during summer months. Elevated V/Ca ratios in summer compared to winter imply a higher production rate in summer due to its support in chlorophyll a production and its function as catalyst for amino acid production (Wilhelm and Wild, 1984a,b, Meisch *et al.*, 1978). However, ratios do not differ exceptionally between seasons, resulting in rather constant rates throughout the year. Mg/Ca ratios are temperature dependant, high Mg content relates to higher temperatures in the surrounding environment (Milliman *et al.*, 1971, Kolesar, 1978). Ratios are slightly higher in summer compared to winter revealing the expected warmer temperatures. The negligible difference between summer and winter may be due to little change in average temperatures in summer (13 - 15 °C) and winter (5 - 8°C). The direct correlation of Mg/Ca ratios to temperature and the use of coralline algae to reconstruct historic seawater temperatures may enable scientists to predict future growth rates with the help of Mg/Ca ratios. The concentration of Mg in the algal skeleton is also known to have an influence on hardness and elasticity (Ragazzola *et al.*, 2016). The higher the Mg content within the carbonate, the harder the skeleton and the lower is the elasticity of intergenicula. In addition to the Mg content, cell wall thickness has a similar effect on hardness and elasticity.

The inter-cell walls (vertical to growth direction) are thinner than intra-cell walls (horizontal to growth direction) in NP, this may imply that these cells may be less

important in absorbing mechanical impacts and may playing a minor role in buffering seawater chemistry, inflicting changes on the skeleton. Cell wall thickness was marginally higher in winter compared to summer even though calcification rates of NP in the winter are lower compared to summer. In addition to low calcification rates, Mg/Ca ratios are also lower in winter than in summer making the branches softer and more elastic and keeping the same cell wall thickness at the same time, presumably to be able to withstand mechanical forces imposed by winter storms and harsh environmental conditions and temperatures. Additional analysis by nanoindentation to measure hardness and elasticity modulus may help interpret these data and are suggested for future work.

Tensile strength of NP, the force northern specimens are able to withstand before rupture and the level of enduring such deformation is expressed through normal force and strain. This force can partly be determined by the interaction of trace element ratios and cell wall thickness. In NP, cell walls were thinner in summer than winter and Mg/Ca ratios were relatively stable in both seasons, leading to the ability to withstand higher (NP2) or equal (NP1) forces prior to rupture in summer months. This may be due to warmer temperatures counteracting brittleness and softening the algae tissue, making it more pliable and elastic. Underpinning this finding, are results obtained for strain  $\epsilon$ , which are equivalent to those of CP. They imply an excess ability to withstand deformation. Therefore, NP seem have found multiple adaptations to maintain resistance to both, summer and winter conditions.

### 3.5.2 Central Populations

Temperatures in CP midday incubations align with those of the environmental data recorded by the data logger, therefore, the result gained by these incubations represents the behaviour of *C. officinalis* in the environment to the tested conditions. Expectedly, Temperature and light conditions are lower in winter compared to summer and both parameters follow tidal cycles. Due to slightly lower values of light intensity than recorded by data logger, results gained in midday incubations might be underestimated.

The high variability between populations and seasons can be explained by differences in the efficiency to reach  $P_{max}$  and a potential adaptation to low light conditions and short light periods experienced during winter. This potential adaptation to winter conditions was also reflected in lower  $P_N$  and  $R$  rates in both CP. The unusual difference in  $P_N$  rates in the summer between CP is likely due to the higher  $\alpha$  and  $P_{max}$  for CP1.

Comparing both CP,  $P_N$  and  $R$  show high variability in between population and season, this can equally be found and explained in P-I curve parameters. A decoupling of photosynthetic and calcification processes is found for CP1 but not CP2, showing again the very variable responses of CP highlighting the urge to include multiple populations in experimental designs. The decoupling between photosynthesis and calcification in CP1 is expressed as high  $P_N$  rates in summer and stable  $G_N$  rates between seasons including a decrease of photosynthetic efficiency and an increase of calcification efficiency. An additional reason for the difference between CP may be differences between the origin of specimens of both CP. Even though CP2 shows high  $R$  rates in summer,  $G_D$  rates are positive leading to calcification instead of an expected dissolution in the dark. A reason for

this decoupling could be a slower adaptation to colder than warmer conditions. Additionally, both CP show low production rates in winter, which may be due to local adaptation and no or little exposure to stressful environmental conditions such as very low or high temperatures and light conditions compared to what marginal populations might experience. Another reason for decoupling processes or moderate contrary to expected reactions is the exposure of the specimens to abiotic and biotic environmental factors such as mechanical, light, anthropogenic induced stress (e.g. trampling, climatic changes, pollutants) and positioning within the intertidal zone as well as impacts from grazing and epibionts.

With similar responses measured for  $\alpha$  and  $I_k$  of C-I curves, a similar response in  $C_{max}$  of both CP was expected but did not arise. Instead, opposing trends in  $C_{max}$  were found. This may be unusual behaviour in CP2 and was not confirmed by increasing  $G_N$  and  $G_D$  rates obtained during midday calcification. Due to higher  $C_{max}$  values of CP1 in winter compared to summer it is expected for the  $G_N$  values to be elevated. However,  $G_N$  rates are similar between seasons and to those of CP1 in winter implying that other mechanisms have to be in place to limit calcification of CP1 in summer, confirming the decoupling of photosynthetic and calcification processes. High  $G_N$  and  $G_D$  rates in CP2 may be due to local adaptation to exposed locations and the attempt to sustain skeletal properties against mechanical stress. Similar findings are reported for *C. officinalis* and *E. elongata* which demonstrated both long-term (seasonal) and short-term (hourly) acclimation to their environment (Williamson *et al.*, 2014).

Trace element composition show a high variability between analysed regions of the branch section. In order to interpret the elemental composition reliably, the focus on this discussion lays mainly on the lower part of the branch. Ba/Ca ratios

are higher in summer compared to winter suggesting more freshwater influx in spring and summer months (Gillikin *et al.*, 2006) due to a negative correlation with salinity (Caragnano *et al.*, 2014, Hanor and Chan, 1977, Nelson *et al.*, 2018, McCoy and Kamenos 2015 and references therein). However, Sr/Ca values, a second and more reliable proxy for salinity in seawater (Schöne *et al.*, 2010, de Villiers, 1999), suggests a higher salinity in summer compared to winter months, representing a more trustworthy result. Cd/Ca ratios indicating pollution through anthropogenic input and therefore inhibiting plant growth (Kangwe *et al.*, 2001, Vymazal, 1987 and references therein) are lower in winter compared to summer; this could be inflicted by increased washouts of human habitation, increased boat and ferry traffic or a combination of these factors close to the locations. Elevated concentration of Zn increase protein and enzyme formation and are essential for photosynthetic and CO<sub>2</sub>-assimilation processes (Kitano and Hood, 1962, Rout and Das, 2003, Raven *et al.*, 1999). Ratios are higher in winter compared to summer reflecting the need of compensation for lower light and temperature conditions to sustain the minimum rate for survival. Fe/Ca ratios show a high variability and no clear pattern between seasons. Iron was expected to be higher in summer compared to winter due to the thermodynamically controlled uptake of this element into cells and skeletons (Raven *et al.*, 1999 and references therein). However, Fe/Ca ratios measured in the tip may be outstandingly high as articulate coralline algae form new cells at the tip of their branch, incorporating trace elements from their surrounding environment into their skeleton. High Fe/Ca rates could therefore be beneficial in increased P<sub>N</sub> and G<sub>N</sub> to build new cell walls for protection faster. Levels of Cr/Ca ratios indicating toxicity levels are higher in summer compared to winter in accordance with Cr/Ca ratios representing pollution, again confirm pollutant influx into the intertidal environment in these locations (Sari and Tuzen,

2008). With an extraordinary high  $P_N$  in summer in CP1, V/Ca levels would have expected to increase simultaneously. Vanadium concentration, however, do not resemble production rates in CP1, even though, within the cell, it has an essential function as catalyst for amino acid production and chlorophyll a formation (Wilhelm, 1984a,b, Meisch and Benzschawel, 1978). Magnesium concentrations in the skeleton are positively correlated with temperature (Milliman *et al.*, 1971, Kolesar, 1978), which is confirmed by higher Mg/Ca values in summer compared to winter in both CP.

Inter-cell walls are thinner compared to intra-cell walls and marginally thicker in winter compared to summer, possibly to account for enhanced protection during autumn and winter storms in addition to increased brittleness of the skeleton due to lower temperatures. Intra-cell wall structures might therefore play a major role in supporting the resistance against external forces, as already described for NP. Cell wall thickness is not mirrored by  $G_N$ .

Ultimate tensile strength ( $F_{tu}$ ) showed different responses in both populations. With a decrease in CP1 and an increase in CP2. The grade of deformation before rupture, strain  $\epsilon$ , and the maximum stretch follow the same pattern. Despite  $\epsilon$  following the same pattern, it is greatly enhanced in CP2 than in CP1 due to increased exposure to abiotic stress in its flat and exposed location atop of rocks, compared to a rocky and more sheltered location at CP2 where specimens mostly grow in cracks and channels. Net calcification follows the pattern of  $F_{tu}$  and  $\epsilon$  and even though cell walls are thicker in winter in both CP, strain is only increased in CP2 and  $F_{tu}$  is only higher in CP2, not CP1, strengthening confidence in the theory above.

### 3.5.3 Southern Populations

Temperature and light of midday incubations are nested within recordings of data logger within each season, therefore data obtained in this study mirror the behaviour populations of *C. officinalis* in the environment at the south of their distribution in the NE Atlantic. Light as well as temperature are lower in winter compared to summer and follow the tidal cycle.

Higher  $P_{\max}$  in winter compared to summer were found in both populations, possibly due to light and temperature inhibition of photosynthetic processes during summer that is more pronounced in SP2 than SP1. This finding suggests that winter conditions, lower light and temperature regimes, are more favourable for SP and further enhanced temperatures or seawater chemistry changes due to future climatic changes may have a damaging effect on the survival of SP. Both SP show a decoupling of photosynthetic and calcification processes, as already shown for NP. Light harvesting efficiency of SP2 decreases unexpectedly in winter compared to summer, showing an effort to increase photosynthetic rates in the summer, the opposite effect than in CP and NP. In SP1, a high  $I_k$  and a marginally increasing  $\alpha$  lead to the expected increase of  $P_{\max}$  in winter conditions. Increased  $I_k$  and decreased  $\alpha$  will result  $P_{\max}$  to be reached slower as it is the case for SP2, however,  $P_{\max}$  did not decrease as expected, this could be due to inhibition during the summer and therefore distorted results. Stable results for  $P_N$  in both populations across seasons support this finding.

The maximum calcification rate  $C_{\max}$  decreases from summer to winter, even though SP1 shows a high  $\pm$ SE in winter, leading to the assumption that there is minimal change in  $C_{\max}$  of SP1. The high error bar could be an artefact of incubation due to a broken or insufficiently cover of foil.  $C_{\max}$  of SP2 decreases

from summer to winter and highlights again the decoupling when comparing  $P_{\max}$  and  $C_{\max}$ . The saturating light intensity  $I_k$  and  $\alpha$  are both developing as expected with an increase in  $\alpha$  in winter months to enhance calcification processes and counteract limited supply of light and nutrients, however  $C_{\max}$  is decreasing for all SP. The higher  $\alpha$  in both SP in winter conditions is mirrored in calcification rates  $G_D$ ,  $G_G$  and  $G_N$ . All calcification measurement show positive results, including  $G_D$  for SP1 and SP2 in winter. With higher positive  $G_D$  rates in winter,  $G_N$  increases accordingly and reveals the urge of the organisms to counteract negative summer conditions, for instance heat stress and damage including elevated dissolution rates, by disproportional high calcification rates in the winter. Comparable values of  $P_N$  of both SP across seasons as well as the highest V/Ca ratios of all populations, responsible for chlorophyll a and amino acid formation, confirm this finding. Kim *et al.*, (2013) already showed that photosynthetic pigment content decreased significantly with increasing light intensity. Exceptionally more energy is spend on calcification processes, skeletal reconstruction and maintenance than on primary production in SP resulting in low adaptation potential to future changing environmental conditions.

Trace element ratios for Ba/Ca did not show a seasonal pattern in SP and intermediate values for SP even though direct measurements revealed highest values for salinity in SP. Subsequently, it did not reflect environmental parameters correctly, and is unlikely to constitute as an appropriate proxy for salinity in articulated coralline algae (Gillikin *et al.*, 2006). However, Sr/Ca ratios that are positively correlated to salinity reflect environmental salinity with higher values in summer compared to winter indicating freshwater influx from outside, for instance by rain or rivers. This finding is already shown (Schöne *et al.*, 2010, de Villiers,



1999) and are here confirmed for *C. officinalis*. Elevated Cd/Ca ratios are indicating pollution through anthropogenic sources (Kangwe *et al.*, 2001, Vymazal, 1987 and references therein) and are found to be enhanced in winter compared to summer conditions in SP2 and *vice versa*. Cd/Ca ratios of SP2 in summer are unusually high, potentially due to the influence of upstream fish farms, boat traffic to and from these farms or a combination of these factors. Similar to Cd, the origin of Zn is mostly anthropogenic, however, less toxic (Kitano and Hood, 1962, Rout and Das, 2003, Raven *et al.*, 1999). Zn/Ca and Fe/Ca values are lower in summer what may be due to its function in photosynthetic processes and CO<sub>2</sub>-assimilation and mirrors the inhibiting of photosynthetic processes already shown by P-I and C-I curves as well as P<sub>N</sub> and G<sub>N</sub>. Higher G<sub>N</sub>, G<sub>D</sub> and Zn/Ca values in the winter reflects elevated calcification and the efforts to sustain sturdiness. Zn/Ca ratios might therefore be used as calcification proxies in articulated coralline algae.

In addition to the temperature and light induced inhibition of physiological processes, Cr could reinforce the inhibition. The carcinogenic, metal-based trace element is known to modify DNA and gene transcriptions, inhibit growth and photosynthesis and its toxicity is positively correlated with salinity and temperature (Sari and Tuzen, 2008). High salinity and temperature as well as elevated Cr/Ca ratios in SP locations in summer support that finding. Elevated V/Ca ratios in SP compared to both other geographic locations reflects G<sub>N</sub>, but not P<sub>N</sub>. A clear decrease between summer and winter values can be found in Mg/Ca ratios. As temperature indicator (Milliman *et al.*, 1971, Kolesar, 1978), these findings support the higher temperature measurements in the summer. An increase in Mg assimilation within the skeleton leads to an increase in hardness; therefore,

branches are softer in winter compared to summer and are able to withstand higher mechanical forces.

Enhanced calcification rates are also mirrored in the thickness of inter- and intra-cell walls of SP. Thinner cell walls in winter compared to summer contrary to high  $G_N$  rates in winter lead to the assumption that cell walls dissolve during summer which is confirmed by low  $G_D$  and dissolution rates. Subsequently, SP have to build up and maintain their cell wall thickness during winter to recover from dissolution and inhibition of physiological processes, including calcification, during summer. As for all other populations, intra-cell walls are thicker than inter-cell walls, which stresses the assumption that these are more important and may be able to absorb and distribute mechanical shocks better compared to inter-cell walls. Cell walls of SP are most influenced due to lowest thickness and are therefore more prone to breakages.

Thinner cell walls result in less resistivity to elongation and deformation; SP show the lowest values for  $\epsilon$  compared to all other locations and values are higher in summer compared to winter due to temperature-induced flexibility. However, the  $F_{tu}$  that SP are able to withstand is higher than those for NP and are only marginally smaller than for CP.

The data for SP in this study suggest that decoupling of photosynthetic and calcification processes (Johansen, 1981) in all SP represent an “emergency stress response” of the organisms to overpowering abiotic stress, induced by predominantly temperature and light conditions. Considerably more energy is spent on calcification and sustaining the cell wall than on  $P_N$  or R, which are similar but more pronounced findings as for the other, NP. Elevated stress levels of SP in summer forces the populations to exist and survive rather than flourish.

This negative trend can also be seen visually on site. In personal observations, a decline in population size and increase in bleaching was documented over 4 years of investigation. Associated with a low adaptation potential, SP might be severely impacted by future temperature, pollution or carbonate chemistry changes or a combination of these factors.

#### 3.5.4 Comparison of Populations

Temperature and light intensities across the geographical distribution of *C. officinalis* in the NE Atlantic are highly variable. For instance, readings for NP in summer report similar values than SP in winter. Light intensities in northern locations in summer reflect those in central locations in winter, and temperature measurements in CP in winter those of NP in winter. Both parameters in southern locations in the summer are similar to central locations in summer. The measurements of all midday incubations reflect measurements of data logger during the observed seasons. Therefore, all data represent the environment and physiologically response of the populations correctly.

Temperatures measured in this study are in line with literature measurements determined in rock pools, however, ambient irradiance levels are approximately half as much (Williamson *et al.*, 2018). The differences in temperature and light intensity are highest out of all comparisons between the two marginal populations, SP and NP. As a result of only single incubations during seasons, which are greatly dependant on weather and environmental conditions, values of parameters may therefore be under or overestimated, depending on temperature as well as light intensities. This could explain potentially high differences within populations in

midday incubations and can be subject to change in future experiments. In order to form correct conclusions from this data, P-I and C-I curves were performed for every population and season and can correct for potential misleading comparisons of light intensities. Light intensities of midday incubations are much lower in all populations compared to the experimentally determined  $P_{\max}$ , leaving potential for further increased values. Measurements for  $I_K$  in this study (min. 30 – max. 95  $\mu\text{mol photons m}^{-2} \text{s}^{-1}$ ) are considerably decremented compared to what was found by Hofmann *et al.* (2012b) where values from 240 – 327  $\mu\text{mol photons m}^{-2} \text{s}^{-1}$  were reported for a CP of *C. officinalis*. The same reference reported values of 11.6 – 20.8  $\text{mmol O}_2 \text{ mg chl a}^{-1} \text{s}^{-1}$  for  $P_{\max}$  which is also substantially higher than what was found in this study across the whole geographic distribution. A study on a closely related species of *C. officinalis*, *Ellisolandia elongata*, in France revealed 10 - 20-times lower  $P_{\max}$  and  $C_{\max}$  values in both, summer and winter (Egilsdottir *et al.*, 2016). This demonstrates the importance of light regimes in the *in situ* environment for not only *E. elongata*, but all algae, including *C. officinalis*. Additionally, together with the finding of uncoupled photosynthetic and calcification processes, this highlights the dynamic interactions between these processes and reveals rather complex relationships instead of direct dependencies.

Measurements for  $P_N$  and  $R$  show a higher variability in CP compared to both marginal populations with constant values within season. Highest values are not found in SP as expected due to increased light and temperature, but in CP, followed by SP, followed by NP, with marginal locations showing relatively similar results due to temperature inhibition in SP and comparably low temperatures in NP. Lowest  $P_N$  rates in NP compared to both other latitudinal regions may be due to lower temperature in northern regions or maintenance of structure to withstand

winter and autumn storms, against which cell walls are build and reinforced, channelling most of the physiological energy into these processes. This may also cause the relatively constant  $G_N$  between summer and winter seasons in NP, compared to a higher decrease of  $G_N$  in winter in the other geographical locations. Respiration rates of SP in winter are highest of all populations showing stress and lack of adaptation. The same populations showed comparable or higher rates in summer than CP or NP, respectively. NP show the lowest R rates, implying least stress as well as temperature-induced deceleration of photosynthetic processes. Production and R rates determined in this study were found to be marginally lower compared to literature values which report rates of  $\sim 1900 \mu\text{mol O}_2 \text{ L}^{-1} \text{ h}^{-1} \text{ gDW}^{-1}$  for production rates and  $\sim -215 \mu\text{mol O}_2 \text{ L}^{-1} \text{ h}^{-1} \text{ gDW}^{-1}$  for respiration rates (El Haïkali *et al.*, 2004). Additional studies on *E. elongata* in France, however, reported drastically lower values of  $14.14 \pm 0.91$  and  $-3.80 \pm 0.29 \mu\text{mol O}_2 \text{ L}^{-1} \text{ h}^{-1} \text{ gDW}^{-1}$  for net production and respiration, respectively (Egilsdottir *et al.*, 2013). A strong seasonality was found between  $P_N$  and R in NP and CP in this study, however, not in SP which show a clear decoupling of photosynthesis and calcification (Johansen, 1981) and confirms literature findings (Williamson *et al.*, 2017).

Significantly higher  $G_N$ ,  $G_G$  and  $G_D$  rates in SP compared to CP and NP are potentially caused by continuous calcification and the lack of dissolution, except for low  $G_D$  rates of CP2 in summer. Marginal populations show highest (SP) and lowest (NP) as well as more constant calcification rates but lower  $P_N$  and R rates compared to CP. One hundred-times and 10-times lower rates of  $2.14 \pm 0.16$  and  $-0.73 \pm 0.17 \mu\text{mol CaCO}_3 \text{ L}^{-1} \text{ h}^{-1} \text{ gDW}^{-1}$  for  $G_N$  and  $G_D$ , respectively, were reported for *E. elongata* (Egilsdottir *et al.*, 2013). This shows the high variability even within

the same family of coralline algae and underlines the importance of investigation not only of indicator species but a broad spectrum of representatives of macroalgae in the intertidal across the globe.

Ba/Ca ratios, indicating freshwater discharge (Gillikin *et al.*, 2006) and a negative correlation with salinity (Caragnano *et al.*, 2014, Hanor and Chan, 1977, Nelson *et al.*, 2018, McCoy and Kamenos, 2015 and references therein), are lowest in northern and highest in central locations when compared across geographic distribution. This does not reflect the environmental salinity levels measured at the locations, where southern locations show the highest salinities, therefore, Ba/Ca ratios might not be suitable as environmental proxy for freshwater input in articulated algae. A better proxy for salinity is shown to be Sr (Schöne *et al.*, 2010, de Villiers, 1999) in water as well as in reconstructions in organisms. Values of Sr/Ca ratios are lowest in NP and higher in CP, which are comparable with SP. This reprints the decrease of salinity with increasing latitude due to increasing freshwater input along this gradient. Zinc values were lowest in NP, followed by CP, which are comparable with SP. With Zn/Ca ratios indicating elevated enzyme and protein build-up as well as reduced viability of cell walls, DNA damage and inhibit calcite precipitation (Kitano and Hood, 1962, Rout and Das, 2003, Raven *et al.*, 1999), CP and SP are heavily affected, which is reflected in reduced cell wall thickness. In comparison, NP would show less cell damage but also slower growth. Cd/Ca ratios are lower in CP than in marginal populations, indicating higher pollution rates, lower productivity in marginal populations and prevention of calcite precipitation and photosynthetic activities (Kangwe *et al.*, 2001, Vymazal, 1987 and references therein). This was not only shown for algae but also for terrestrial plants urging the potential detrimental effect on all organisms (Nazar *et*

*al.*, 2012). Cd/Ca rates are confirmed by  $P_N$   $P_G$  and R data when comparing central and marginal populations. A negative correlation between Cd/Ca and Ba/Ca, Zn/Ca V/Ca, Fe/Ca, Sr/Ca and Cr/Ca ratios in all locations and seasons is found.

An increased Zn concentration in the skeleton from summer to winter shows the effort of the organism to increase  $P_N$  and therefore  $CO_2$ -assimilation under winter conditions. SP show the highest ratios, followed by CP, followed by NP. With temperature and light inhibition in the summer, SP are trying to increase the  $P_N$  rates in winter, supported by the macronutrient zinc. Increased Fe/Ca ratios indicate increased electron transportation during photosynthetic processes (Raven *et al.*, 1999 and references therein). While the limiting step during Fe incorporation is controlled thermodynamically, a higher Fe/Ca rate is expected in SP. However, highest rates were found in CP, followed by NP, which are comparable to SP, causing the high difference between CP and NP / SP locations. A possible explanation for relatively low Fe rates in SP is the increased concentration of Cd, which is known to inhibit nutrient uptake. Values for Fe/Ca ratios found in CP are not only highest, but they also show the highest variability, this is correlated with the high variability in  $P_N$  and R data. Both marginal populations encounter low variability; possibly due to the necessity of efficiency as these populations already inhabit the edges of their favourable environmental conditions.

Cr/Ca ratios are lowest in NP, followed by CP, which are comparable with SP, mirroring the same pattern as Sr/Ca. Chromium is reported to have a carcinogenic effect and has a potential to modify DNA transcription and is efficiently and actively taken up by marine macroalgae (Sari and Tuzen, 2008). Concentrations of Cr within the skeleton are lower in winter compared to summer in all populations,

leading to enhanced photosynthetic and growth inhibition. This is emphasized by greater growth rates in NP compared to CP. Vanadium, representing a catalyst for amino acid as well as Chl a production (Wilhelm and Wild, 1984a,b, Meisch and Benzschawel, 1978) is lowest in NP, followed by CP, followed by SP. Ratios are higher in NP in summer and showed opposite trends within seasons for each population in CP and SP, respectively. These ratios demonstrate that NP are locally adapted to low light temperature conditions and are not in the need of building up and store high chlorophyll a contents, contrary to SP.

As Mg/Ca is directly correlated with temperature (Milliman *et al.*, 1971, Kolesar, 1978), Mg/Ca ratios in NP do not differ greatly between summer and winter due to low temperature difference between seasons. Additionally, upper regions of the analysed branch section showed lower Mg incorporation, followed by the middle region, followed by the lower region, which was already found for calcification measures (Johansen, 1981, Egilsdottir *et al.*, 2013). In CP and SP, differences in Mg/Ca ratios between seasons are higher following higher temperature differences between seasons. Magnesium concentrations are comparable in CP and SP, due to similar temperatures in the summer as well as winter, and are marginally higher in NP. This data shows only a weak relationship between latitude and Mg content in *C. officinalis*, similar to literature findings (Smith *et al.*, 2012). Overall, all populations show lower values in winter compared to summer and present a suitable proxy for temperature changes as well as reconstruction in coralline algae (e.g. Kamenos *et al.*, 2008). It was already suggested by Yildiz *et al.* (2013) that changes in the organisms' skeletal content might affect the ability of *C. officinalis* to absorb light and increased exposure to ultra violet radiation may change growth



and photosynthetic performance. This suggestion was confirmed in this present study.

As already pointed out by Melbourne *et al.* (2015), little research was conducted on changes in structural integrity of coralline algae. Until today, it was understood that hardness and elasticity is positively correlated with Mg/Ca ratios and temperature. Therefore, branches are softer in all populations in winter due to lower Mg/Ca ratios and temperatures, however, no clear trend between seasonal cell wall thicknesses across the geographic distribution is found. In order to determine elasticity of these populations in-depth, it is recommended to conduct nanoindentation analysis in the future. Comparing locations, NP build thicker cell walls than SP and CP, which are comparable. Therefore, NP are in need of lower Mg concentrations within their skeleton in order to soften and withstand autumn and winter storms. This coincides with temperature and Mg/Ca measurements, which are lowest in NP. The thickness of cell walls might also be an explanation why staining success during growth rate determination is higher in NP compared to CP. Additional reasons for reduced staining success may be the lack of uptake or loss due to abrasion which was described for *C. officinalis* (Andrake and Johansen, 1980). In addition to this study, other studies have also found Alizarin Red to be a suitable stain for *C. officinalis* and report similar growth rates of approximately 2 mm/month at various depths (Colthart and Johansen 1973, Andrake and Johansen 1980, Blake and Maggs, 2003). In conditions with exceeding optimal temperatures, biochemical components are becoming less efficient or even damaged (Kordas *et al.*, 2011, Eggert, 2012), resulting in an expected decline in growth rates and calcification. Therefore, growth rates of SP would be expected to be similar or lower than those of NP due to summer

inhibition as well as an increased concentration of the growth-inhibiting element Cd. All these parameters, most probably in combination, may lead to a reduction of coralline algae cover in tropical and subtropical ecosystems (Doney *et al.*, 2009).

Intra-cell walls (horizontal to growth direction) are thicker in all populations, indicating their function for structural stabilisation as well as protection of the cell interior. Due to their shorter and thicker design compared to inter-cell walls (vertical to growth direction), intra-cell walls are able to absorb, buffer and channel exogenous mechanical impacts through spreading. Thinner cell walls in CP and SP compared to NP can be explained by shorter exposure to autumn, winter and potentially spring storms, thereby less exposure to potential mechanical damage. This may also explain the greater difference between inter-and intra-cell wall thickness in SP, followed by CP, followed by NP, and therefore firmer branches in NP. The average cell wall thickness of all populations determined in this study independent from orientation lays within the reported literature values of  $1.8 \pm 0.71 \mu\text{m}$  (Walsh *et al.*, 2008).

Even though calcification rates in CP are higher, cell walls are thinner which may be due to simultaneously increasing dissolution rates. As a result,  $G_N$  is increased to compensate for dissolution. Lowest calcification rates in NP contrast the fact that these populations build the thickest cell walls. Therefore, low  $P_N$  may be a result of focussing energy expenditure on cell wall formation.

Confirmation for the fact that cell wall thickness may make up an essential part of the stability and resilience of this algae is found in the ability of NP to withstand highest forces ( $F_{tu}$ ) as well as highest strain ( $\epsilon$ ) before rupture and building the thickest well walls compared to all other locations. This confirms local adaptation

to harsh environmental conditions in subarctic environments. Strain and  $F_{tu}$  are only measured as a combined value between genicula and intergenicula. All branches tested, ruptured in the genicular, the joints which allow for flexible and rapid adjustments of branch shapes and are primary responsible for bending in moving waters (Aguirre *et al.*, 2010). Previous studies on coralline species investigating  $F_{tu}$  resistance focussed on rupture of genicula in a single branch as experienced in this study and found a mean force to break the tenth genicular to be around 22.7 N in *Calliarthron cheilosporioides* (Martone and Denny 2008a,b). A study investigating the strength of branch bundles found that *Ellisolandia elongata* in the Mediterranean is able to withstand a maximum stress of  $2.1 \pm 0.4$  up to  $5.4 \pm 0.5$  N mm<sup>-2</sup> (mean  $\pm$ SEM) (Ragazzola *et al.*, 2017). Values found by Martone and Denny (2008a,b) are considerably higher compared to this study which could be due to the initial location of the specimens or a difference in species. However, values for *E. elongata* are relatively similar which could lead back to the closer relationship between the species used in the latter and this study.

Populations in the centre of the distribution are able to withstand the comparatively lowest force, however, SP show the highest deficit in deformation resistance. Such structural properties as displayed by NP are not only beneficial for the organisms itself, it has also found attention in biomedical research in enhancing bone and dental replacement or filling materials (Clarke *et al.*, 2011 and references therein).

In the physiology and structural properties of the populations across the geographic distributions, NP are different to CP and SP, however, CP are not always different to SP. From this, it can be deduced that the Centre-to-Margin Hypothesis (Sagarin and Gaines, 2002), has to be adjusted and transformed into a North-to-South gradient regarding the physiology and structural integrity of *C.*

*officinalis*. A similar finding was reported by Yesson *et al.*, (2018); the authors found significant genetic differences between populations across the species distribution, and close to the sampling locations used in this study, in the NE Atlantic. Its characterisation across the NE Atlantic validated the adaptation of *C. officinalis*, predominantly to low light and temperatures conditions.

### 3.5.5 Methodological Limitations

Due to some limitations in preparation of samples or implementation of analysis, some aspects were carefully considered. It was made sure that none of the limited sample sections were analysed, however, during cell wall thickness measurements it was noticed that some parts were not polished horizontally but at an angle due to the nature of the branch and the embedding process. Therefore, when discussing these data, potential uncertainties were taken into consideration.

Additionally, a high variability in trace elemental data sets can be observed, especially in the upper region of the analysed branch section. This may be due to the positioning of the ablation spot on the branch, which may not represent the exact same spot during growth in the investigated season in all replicates.

The efficacy of the light data logger recordings in the field may have been influenced by the growth of epibionts on sensor windows. For instance, the data logger recovered at a southern site (SP1) showed growth of epiphytes on the light sensor; the data logger at both northern sites showed barnacle and epiphyte growth, however, not on the sensor windows.

### 3.6 Conclusion

This study characterised sample populations of *C. officinalis* across its geographic distribution in the NE Atlantic. It clarified significant differences between latitudes and presented an unequivocal North-to-South gradient in their physiology as well as their structural integrity. Further nanoindentation measurements would prove beneficial to confirm hardness and elasticity for each population and to complete the set of the most important analyses of structural integrity. Northern populations proved to be more robust and locally adapted to their current environment compared to CP or SP. Southern populations showed a lack of local adaptation culminating in survival rather than thriving within their current environment. This implies that SP are located at the fringe of this species favourable conditions, compared to NP, which show adaptation potential to a wider range of the parameters. In the future, this could lead to a permanent decline and disappearance of *C. officinalis* in the southern locations in the NE Atlantic, which may be accelerated by predicted future climatic changes. The severe effects on *C. officinalis* could also lead to changes within the respective ecosystem due to missing important functions these algae would no longer perform.

# Chapter 4

## *Adaptation of *Corallina officinalis* to temperature regimes across its geographical distribution in the NE Atlantic: A Common Garden Approach*

Published in part as: Kolzenburg *et al.*, (2019) *Ecol. Evol.*, 9(10), 5787 - 5801 (Appendix C)

#### 4.1 Collaboration Disclaimer

The data describing the physiological and structural properties of the populations of *Corallina officinalis* used in this thesis and in this chapter were gathered with the help of several volunteers. Some of the data collected during this thesis is also used by MSc and Erasmus student in 2017, Francesco D'Amore.

#### 4.2 Introduction

Anthropogenic input of carbon dioxide in the atmosphere resulted in a changing climate over the past decades and might further fuel global climate change in future centuries (IPCC, 2014a). Key components of climate change in the ocean are ocean acidification (OA; decreasing pH and  $\Omega\text{CO}_3^{2-}$ ) and rising sea surface temperatures. Living organisms already experience effects of climatic changes and will continue to be critically affected by these changes (Lesica and McCune, 2004, Sanford et al., 2006, Bentz et al., 2010). Investigating and monitoring organism physiology provides important information to predict their acclimatisation and resilience to future environmental conditions and potential changes in their distribution (Kelly and Hofmann, 2013).

It is suggested that the geographic centre of a species distribution holds the most favourable conditions and therefore holds the highest population density (Whittaker, 1956; Brussard, 1984). When moving away from the centre towards the margins of the distribution, environmental variables are thought to become less favourable due to greater abiotic stress and increased interspecific competition (Aitken *et al.*, 2008), initiating a decrease in population densities and lower relative fertility (Case and Taper, 2000). Further, Watkinson and Sutherland (1995) described a higher mortality than recruitment rate for local marginal populations, also called sink

populations, whose survival depends on influx of zygotes or spores from source populations.

Species react differently to environmental changes. In terrestrial studies, for instance, Franco *et al.* (2006) showed that three out of four butterfly species that were investigated were reported extinct or showed drastic distributional changes due to climate change along with habitat degradation and loss at their low-latitude range boundary. Another study by Lesica and McCune (2004) showed that the southern margin of arctic-alpine indicator plants species declined in their abundance within 13 years which was caused by increasing average summer temperatures. Previous research has also found that different populations of the same species respond differently to altered environmental conditions (Gaston, 2009, Bozinovic *et al.*, 2011; Calosi *et al.*, 2017). In the marine environment, a number of studies across several taxonomic groups, e.g. fish, molluscs, zooplankton or seaweed, have focused on the diversification of populations along a thermal-latitudinal gradient (Morley *et al.*, 2009, Dam, 2013; Bennett *et al.*, 2015, Lucassen *et al.*, 2006).

Calcifying organisms are at the forefront of those affected by climatic changes and can therefore act as indicator species for induced impacts on marine organisms. One of the major groups effected by climate change are calcifying benthic macroalgae (Kroeker *et al.*, 2013b). Amongst those are coralline red algae (Corallinales, Rhodophyta), which are critical components of marine shallow water ecosystems from polar regions to the tropics (Adey and MacInyre, 1973, Steneck, 1986). They function as important ecosystem engineers and play a crucial role as an essential structural element in the majority of rocky coastal zones (Johansen, 1981, Jones *et al.*, 1994, Nelson, 2009, van der Heijden and Kamenos, 2015, Dayton, 1972, Kelaher *et al.*, 2001, Benedetti-Cecchi, 2006, Noël *et al.*, 2009). They



often form complex, extremely dense and highly branched turfs which are considered the extreme end of algal structural complexity (Coull and Wells 1983, Davenport *et al.*, 1999). Branches consist of calcified segments (intergenicula) which are produced through high-magnesium (Mg) calcite precipitation in the cell walls, and non-calcified segments (genicula); this structure provides flexibility and elasticity for every individual branch (Martone and Denny, 2008a,b). Coralline turf is highly variable, with frond length and density differing at small spatial scales, they can host abundant and diverse macrofaunal assemblages with up to 250,000 individuals per m<sup>2</sup> (Kelaher *et al.*, 2001). In addition, macroalgal physiological processes such as photosynthesis and respiration alter CO<sub>2</sub> and HCO<sub>3</sub><sup>-</sup> in the water in the intertidal environment. This causes changes in pH across diurnal as well as spatial scales related to species distributions (Morris and Taylor, 1983, Williamson *et al.*, 2014, 2017). Depending on the extent of these changes in the carbonate chemistry and especially in combination with the climatic changes named above, calcification of coralline algae can be severely affected.

Geniculate coralline algae (also known as articulated coralline algae), like *C. officinalis*, form turfs across large areas on hard substratum in the intertidal ecosystems of the Northeast Atlantic. *C. officinalis* is commonly found in sheltered, low intertidal zones, where it primarily inhabits the lower part of rock pools and channels that remain damp or filled during extreme tides or conditions, and at the edge of the intertidal to subtidal zones (Digby, 1977, Egilisdottir *et al.*, 2013, Williamson *et al.*, 2014). In order to maintain their abundance in temperate intertidal ecosystems, coralline algae are suggested to have a good ability to adapt to great and fast changes in environmental conditions, such as solar irradiance, physical stress, water temperature or carbonate chemistry (e.g. large pH variations) which

fluctuate tidally, diurnal, monthly and seasonally (Martone *et al.*, 2010; Egilsdottir *et al.*, 2013; Hofmann *et al.*, 2014; Williamson *et al.*, 2014).

In particular, temperature is one of the main factors governing the small-scale vertical distribution of macroalgae on a shore (Lüning, 1990) and the large-scale geographical distribution of macroalgal species (Ganning, 1971). At the organism level, temperature regulates major chemical reactions, which in turn affect metabolic pathways (Lobban and Harrison, 1994). For example, carbonic anhydrase is affected by temperature altering the carbon fixation pathways in photosynthesis (Lobban and Harrison, 1994). Water temperature affects recruitment, survival, growth as well as reproduction of macroalgae and thus drives the species' distribution (Breemann, 1988; Lüning, 1990). Most importantly, current increase in global temperature and therefore a possible exceeding of the species' temperature threshold, is causing species-level responses in macroalgae, such as species range shifts (reviewed by Helmuth *et al.*, 2006 and Parmesan, 2006, Wernberg *et al.*, 2011, Nicastro *et al.*, 2013; Smale and Wernberg, 2013). This ongoing temperature increase, and what is predicted for future scenarios, is causing a chronic, due to gradual warming, or an acute stress, due to extreme temperature events (Brodie *et al.*, 2014). Adaptations will need to include facilitation of all metabolic processes at elevated temperatures, especially those for photosynthesis, respiration, calcification and therefore growth.

Hofmann *et al.* (2012a,b), Egilsdottir *et al.* (2013) and Noisette *et al.* (2013) found that with ongoing climate change, and therefore declining pH and rising water temperatures, interactions between coralline algal physiology and variable environmental parameters are likely to be significantly negatively affected.

It remains unclear how and whether the wider distributed, turf-forming algae *C. officinalis* will be able to withstand such changes. It is likely that the species as a whole will show some resilience when exposed to predicted climate change conditions. However, it is uncertain which areas or portions of the species distribution will be affected the most by the changes. At present, there are very few studies regarding the physiological responses of intertidal benthic organisms to current climate conditions across its distribution (reviewed by Helmuth *et al.*, 2006; Díez *et al.*, 2012). This gap in knowledge complicates the establishment of detailed predictions for this species future (Nelson, 2009, Brodie *et al.*, 2014; Williamson *et al.*, 2017).

In this study, physiological responses (photosynthesis, respiration, calcification, Photosynthesis-Irradiance curves and Calcification-Irradiance curves) and structural parameters (cell wall thickness, growth rates and skeletal trace element composition) of *C. officinalis* across its natural distribution in the NE Atlantic were investigated using the approach of Common Garden Experiments. England was chosen as central population for this study, referring to confirmed genetic data by Brodie *et al.* (2013). Spain was studied representing the southern margin of the species distribution (Williamson *et al.*, 2015). Iceland was chosen to represent the northern margin of the species distribution.

It was hypothesised that central populations are more robust to elevated temperatures and therefore are able to adapt to the temperature conditions already experienced by southern and northern populations. In contrast, it was predicted that southern and northern populations will be able to adapt to the most favourable central conditions.

### 4.3 Material and Methods

Detailed descriptions of the Material and Methods are specified in Chapter 2.

#### 4.3.1 Specimens Collection

*Corallina officinalis* populations ( $n = 2$ ) were collected intertidally ( $n = 36$  per population, total  $n = 72$ ), during low tide in an average depth of 0.31 m from the water surface at sites in the South East coast of the UK (CP; central population 1: St Margarets Bay: N 51.148056, E 1.385056; central population 2: Westbrook Bay: N 51.388840, E 1.367170; beeline distance between populations: 26.85 km), the North West coast of Spain (SP; southern margin population 1: Illa del Arousa: N 42.56870, W 8.89171; southern population 2: Tragove: N 42.52444, W 8.82772; beeline distance between populations: 7.19 km) and the South West coast of Iceland (NP; northern margin population: Stafnes: N 63.968444, W 22.750861) in February 2017 (CP and SP) and October 2015 (NP). Specimens were transported into the lab at the Institute of Marine Sciences of the University of Portsmouth, UK using temperature-insulating containers. Only healthy specimens without epiphytes and indication of bleaching or damage were selected for this study.

#### 4.3.2 Experimental Designs

The two experimental designs described below were build. The second design described in 4.3.2.2 was a direct development from the first, described in 4.3.2.1. Improvements included the change from a flow through open system, which was vulnerable to high changes in temperature, to a water bath closed system. For this reason, the results in the next part of this chapter will be split and presented separately from each other. The second experiment was performed due to the decease of SP and most CP in the first Common Garden Experiment. To

compensate for the lack of data an additional experiment was performed focussing only on CP and SP.

#### 4.3.2.1 Common Garden Experiment of Northern Populations

Four 11.1 L aquaria for each of the three temperature conditions, Iceland (representing the northern margin), UK (representing the centre) and Spain (representing the southern margin) were set up in a flow-through seawater system in the laboratories of the Institute of Marine Sciences of the University of Portsmouth. Each aquaria was equipped with individual water supply from multiple header tanks, each water source was kept at constant respective *in situ* temperatures measured in the field by TECO TK-2000 chillers (cooling capacity of 870 W, 800L/h), a water pump (TMC, V<sup>2</sup>PowerPump 800, Flow rate: 700 L h<sup>-1</sup>) and a 35 cm long air diffuser to imitate tidal water movements and ensure oxygen supply with ambient air. The discarded seawater was treated with UV light (Tropic Marine Centre (TMC) P2-110W Commercial UV Steriliser, max. flow rate: 65 L min<sup>-1</sup>) prior to disposal to ensure non-native organism were not released into the surrounding waters of the institute. Specimen (total rocks with specimens per population and treatment replicate: n = 10) of the NP were kept at their *in situ* temperatures measured during sampling (northern margin conditions: temperature: 7.9°C, light: 228  $\mu\text{mol photons m}^{-2} \text{s}^{-1}$ ). The additional aquaria were set to the conditions of the two remaining locations: central conditions: temperature: 12.0°C, light: 159  $\mu\text{mol photons m}^{-2} \text{s}^{-1}$ ; southern margin conditions: temperature: 16.0°C, light: 690  $\mu\text{mol photons m}^{-2} \text{s}^{-1}$ . Temperature conditions were kept constant using TECO TK-2000 chillers (cooling capacity of 870 W, 800 L h<sup>-1</sup>). All aquaria had a light/dark cycle of 9.5/14.5 h (as an average of natural light lengths) produced and controlled by TMC AQUABEAM 600 Ulima Reef White lights with cloud function. Additionally, sunset

and sunrise were mimicked through a slow increase and decrease of light intensities over a period of 1 h. All specimens were kept in their corresponding conditions for a minimum of 1 week to acclimate to aquaria conditions. Following the initial acclimatisation,  $\frac{1}{3}$  of the NP were gradually acclimatised (increase/decrease of  $1.5^{\circ}\text{C week}^{-1}$  and  $40 \mu\text{mol photons m}^{-2} \text{s}^{-1} \text{ week}^{-1}$ , respectively) to the northern/central/southern temperature and the average light conditions ( $\sim 300 \mu\text{mol photons m}^{-2} \text{s}^{-1}$ ) over five weeks. After acclimatisation and colour coding, specimens were randomly and equally distributed within the corresponding replicate aquaria and cultured for 10 weeks.

#### 4.3.2.2 Common Garden Experiment between Central and Southern Populations

In the laboratory, specimens were carefully placed upright onto a rock in the water, held in place with a net (2 mm mesh size) in order to simulate natural conditions and each population was colour coded for future identification. Aquaria of 11.1 L ( $n = 3$ ) for each of the two countries and temperature conditions (total  $n = 12$ ) were set up in a water bath. 75% of the water in the replicate aquaria was changed every second day and treated with UV light (P2-110W Commercial UV Steriliser, max. flow rate:  $65 \text{ L min}^{-1}$ . Tropic Marine Centre (TMC), London, UK) prior to disposal. Temperature conditions were kept constant using TK-2000 chillers (cooling capacity of 870 W,  $800 \text{ L h}^{-1}$ . TECO, Ravenna, Italy). Each aquarium was equipped with a water pump (V<sup>2</sup>PowerPump 800, Flow rate:  $700 \text{ L h}^{-1}$ . TMC, London, UK) and an air stone to simulate tidal water movements and ensure oxygen supply with ambient air. Specimens (total rocks with specimens per population and treatment replicate:  $n = 10$ ) were kept at their respective local *in situ* temperatures measured during sampling (central conditions: temperature:  $5.7^{\circ}\text{C}$ , light:  $57 \mu\text{mol photons m}^{-2} \text{s}^{-1}$ ;

southern conditions: temperature: 11.3°C, light: 184  $\mu\text{mol photons m}^{-2} \text{s}^{-1}$ ). Both treatments were subject to a light:dark cycle of 10:14 h (taken from the average of natural conditions of central and southern locations) produced and controlled by AQUABEAM 600 Ultima Reef White lights with cloud function (TMC, London, UK). Additionally, sunset and sunrise were mimicked through a slow increase and decrease of light intensities over a period of 1 h. All specimens were kept in their corresponding conditions for a minimum of one week to acclimate to aquaria conditions. Following the initial acclimatisation, half of the CP and SP were gradually acclimatised (increase/decrease of 1.5°C week<sup>-1</sup> and 40  $\mu\text{mol photons m}^{-2} \text{s}^{-1}$  week<sup>-1</sup>, respectively) to the opposite temperature and light conditions over a period of 3.5 weeks. After acclimatisation, specimens were randomly and equally distributed within the corresponding replicate aquaria and kept for three months.

#### 4.3.3 Monitoring of Water Parameters

In the central/southern Common Garden Experiment, temperature, salinity, dissolved oxygen, pH and total alkalinity ( $A_T$ ) were monitored daily. Irradiance was measured once a month to monitor the decrease in light intensity using a HOBO UA-002-64 Pendant Temp/Light data logger (accuracy: 0.47°C, resolution: 0.1°C. Tempcon, Arundel, UK). Temperature and salinity were measured with a CO310-1 portable salinity and temperature probe (accuracy: 0.2% for salinity,  $\pm 0.2^\circ\text{C}$  for temperature; resolution: 0.1 for salinity, 0.1°C for temperature. VWR, Leicestershire, UK). Dissolved oxygen and pH were measured with an HQ30d portable multi-parameter meter and a luminescent dissolved oxygen (LDO101, accuracy:  $\pm 0.1$  mg/L. HACH, Manchester, UK) and pH probe (PHC301, accuracy:  $\pm 0.02$  pH, HACH, Manchester, UK), Calibrated on the National Bureau of Standards (NBS) scale and converted into total scale values using Tris/HCl and 2-aminopyridine/HCl

buffer solutions after Dickson *et al.* (2007).  $A_T$  was monitored daily in one randomly chosen replicate for each treatment, using the alkalinity anomaly technique after Smith and Key (1975), Chisholm and Gattuso (1991) and Dickeson *et al.* (2007, SOP 3b).  $A_T$  titrations were carried out with an automatic titrator TitroLine 7000 (measurement accuracy:  $0.002 \pm 1$  digit, dosing accuracy: 0.15%, dosing precision: 0.05 - 0.07%. Schott SI Analytics, Mainz, Germany) to ensure minimal variation. As titrant 0.1 N hydrochloric acid (HCl) was used and validated against certified reference material provided by Andrew G. Dickson (Batch 154, Scripps Institution of Oceanography).

In the northern Common Garden Experiment, following the protocol in Chapter 2, photosynthesis and respiration were measured once per week, calcification and photosynthesis recovery periods were determined once per month, pH and  $A_T$  were measured twice per month and growth rates were determined at the end of the experiment. LA-ICP-MS and SEM analysis were conducted after the experiment according to the protocol described in Chapter 2. The equipment used was identical to these used in the central/southern Common Garden Experiment described above, except for the titrations, which were performed by hand instead of an automatic titrator using the same method.

#### 4.3.4 Physiological Incubation Procedure and Measurements

To determine saturating light levels of *C. officinalis* populations before and after the central/southern experiment, the oxygen production (P-I curve) and calcification (C-I curve) evolution under increasing light conditions were measured. For this,  $0.97 \pm 0.07$  g fresh weight of algal fronds were transferred into a clear closed cell 58 ml incubation chamber and incubated successively for 1 h at each of the seven different light intensities (0, 20, 80, 160, 320, 500 and 700  $\mu\text{mol photons m}^{-2} \text{s}^{-1}$ ; AQUARAY



Nature Perfect, TMC, London, UK), starting from the lowest to the highest to minimise stress. Three replicates per light intensity were incubated simultaneously and bubble-free. To account and correct for metabolism effects by other organisms, reference incubations without algae were performed alongside the above-described incubations for all light intensities. Aluminium foil was used to coat the chambers to determine calcification and respiration rates in the dark. Irradiance was measured with a Quantitherm PAR/Temperature Sensor with a QTP1 probe (resolution: 1  $\mu\text{mol photons m}^{-2} \text{s}^{-1}$ , 0.02°C, respectively. Hansatech, Norfolk, UK).

Differences in oxygen concentration, pH and  $A_T$  were determined in order to calculate photosynthesis, respiration and calcification rates by measuring oxygen, pH and  $A_T$ , respectively, before and after the incubations. Prior to  $A_T$  measurements, seawater samples were filtered through a syringe filter (hydrophilic 25 mm, 0.2  $\mu\text{m}$  PTFE. Fisherbrand, Loughborough, UK) into sterile 50 ml tubes (Plastic Centrifuge Tubes. Fisherbrand, Loughborough, UK). Immediately after, potentiometric titrations were performed using an automatic titrator (details: see above) calibrated on the NBS scale. Results were calculated based on a Gran function after Dickson *et al.*, (2007). The carbonate system of the seawater was calculated from pH,  $A_T$ , salinity and temperature using the Excel Macro CO2Sys (Version 2.1, Lewis and Wallace, 1998) with  $K_1$  and  $K_2$  according to Mehrbach *et al.* (1973) and refit by Dickson and Millero (1987) (Table 2). Measurement ranges of pH values represent *in situ* values and are highly dependent on temperature.

To determine changes in photosynthesis, respiration and calcification rates most likely to be found in the field, additional incubations ( $n = 3$ ) of all treatments at ambient light conditions (57  $\mu\text{mol photons m}^{-2} \text{s}^{-1}$  for CP and 184  $\mu\text{mol photons m}^{-2}$

s<sup>-1</sup> for SP) were performed before and after the study following the protocol above. Calculations were performed following the methodology described above. The weight of algal fronds used in the incubations was transformed from FW into dry weight (DW) by multiplying FW measurements with the factor 0.62286. This factor was determined from FW and DW weight measurements of thirty 1g frond bundles from all populations before and after algae were left to dry for 48 h in an oven at 60°C (Egilsdottir *et al.*, 2013).

P-I and C-I curves were not determined for the northern populations.

#### 4.3.5 Photosynthesis Recovery Rates

Instead of P-I and C-I curves of NP, photosynthesis recovery rates were performed in order to determine the potential and the speed of the NP to recover photosynthetic rates in a range of temperatures. Specimens (n = 1 for each incubation, weight 0.147 ±0.07 g (AV ±SD), total n = 4 per temperature) were acclimatised to the oxygen chamber (DW3 Electrode Chamber, Oxy-Lab, software: O2view 2.05, Hansatech Instruments, Norfolk, UK, with a Hansatech Quantitherm PAR/Temperature Sensor with a QTP1 probe (resolution: 1 μmol photons m<sup>-2</sup> s<sup>-1</sup>, 0.02°C, respectively)) which was temperature controlled using an attached, recirculating water bath (LTC2 water bath, TC120 heating circulator, R2 refrigeration unit, Grant Instruments, Cambridge, UK) and set to the respective temperature of the experiment. One branch of *C. officinalis* was attached to the holder on the lid and submerged into the oxygen chamber. The specimen was kept in the dark for 2 minutes to allow for acclimatisation to the chamber, then, the specimen was exposed to over its saturating light intensity to an average of 1330 ±93 μmol photons m<sup>-2</sup> s<sup>-1</sup>, for 5 minutes to determine oxygen production rates and absolute oxygen values in the waterbody. Times for exposure were determined during pre-experiments. Following

the light exposure, the specimen was kept in the dark for 5 minutes in order to recover from the light exposure, followed by additional 5 minutes in the dark to determine oxygen consumption rates.

#### 4.3.6 Laboratory Structural Analysis

To determine the structural integrity of the different populations across the species distribution trace element compositions, cell wall thickness and growth rates were determined.

##### 4.3.6.1 Trace Element Composition

In order to determine the Mg/Ca ratios within the calcite and the differentiation of it within various conditions, laser ablation inductively coupled plasma mass spectrometry (LA-ICP-MS) was performed. This method enables the measurement of predetermined trace elements, which ultimately leads to the specimens' elemental composition. For detailed description Chapter 2.8.2.3.

Replicates ( $n = 3$  and  $n = 3 - 4$  for central/southern and northern experiment, respectively) were embedded into epoxy resin (EpoFix Kit, batch no: 8134-01, Struers ApS, Ballerup, Denmark) and polished with a polishing machine (MetaServ 3000 or VibroMet 2, Buehler, Esslingen, Germany) and an aluminium oxide solution (aluminium oxide powder (Micropolish Alumina, Buehler, Esslingen, Germany) and distilled water) of  $0.05 \mu\text{m}$  grain size (Chapter 2.8.2.1). Trace element analysis were conducted at the School of Earth and Environmental Sciences, University of Portsmouth, United Kingdom. Synthetic silicate glass reference material NIST SRM 610 as well as NIST SRM 612 were used for instrumental calibration and as primary and secondary standards. Synthetic calcium carbonate USGS MACS-3 was also used as secondary standard and analysed in the same conditions as the unknowns

(NIST SRM 610 and 612, US National Institute of Standard and Technology Standard Reference Material; MACS-3, the United States Geological Survey).

The first analytical session (NP) was carried out using an Agilent 7500cs (quadrupole) ICP-MS coupled with a Nd:YAG 213 nm New Wave solid-state Laser ablation system. Laser ablation parameters were as follow: 55  $\mu\text{m}$  for NIST glasses and MACS-3 carbonate references and 80  $\mu\text{m}$  for unknowns, approximately 55% laser energy and 10 Hz. Each analysis consisted of 25 seconds of background, 10 seconds of laser warming up (starting at 15 seconds of background), 35 seconds of acquisition and 15 seconds of washing out (75 seconds in total, Table 2.2).

Samples of the central/southern Common Garden Experiment were analysed using a RESOLUTION 193 nm ArF excimer Laser with a Laurin Technic S155 Ablation cell coupled to an Analytic Jena Plasma Quant MS Elite ICP-MS. Analyses consisted of 55  $\mu\text{m}$  spot size, laser fluency was 3.0 J/cm<sup>2</sup> and its repetition rate was 5 Hz. Background measurements took 20 seconds, followed by 30 seconds of ablation and 15 seconds of washout for each analysis (65 seconds in total). Detailed operating conditions for both instruments are listed in Table 2.2.

Background and signal counts were integrated, time-drift corrected and reduced to concentrations using the SILLS (Guillong *et al.*, 2008) and lolite 3.4 software packages (Paton *et al.*, 2011), respectively for first and following sessions. Each run consisted of at least six external standard analyses (NIST 610) and four secondary standards NIST 612 and MACS-3 ( $n = 8$ ). Detection limits (99% confidence) for the spot measurements of the NIST glasses were: Mg = ~28 ppm and Ca = ~100 ppm.

Internal standard element used for normalization of the data was <sup>43</sup>Ca, which was obtained from the GeoReM certificate and own measurements. All reference

materials were ablated prior, in the middle and after sample ablation. Following every 6th sample analysis one analysis of NIST SRM 610 was added to correct for time-dependent drift of mass discrimination and instrument sensitivity. Final elemental composition ratios in this study were calculated as a 'mean count rate' including standard error of drift and background corrected single ablation spot analysis for each of the three replicates. Spots ( $n = 5$ ) were ablated below and above the stain line of the selected branch section. This method is commonly used for LA-ICP-MS data reduction (Longerich *et al.*, 1996). Values obtained in the course of this study were reproducible within 10% for Mg, of the GeoReM recommended values (Jochum *et al.*, 2005) and were compared with the GeoReM data base to determine accuracy (Figure 4.1 – Figure 4.2) as well as internal (NIST 610) and external reproducibility (MACS-3 and NIST 612; Table 4.1).

**Table 4.1:** Reproducibility of Reference Materials USGS MACS-3, NIST SRM 610 and NIST SRM 612 (Total Mean  $\pm 2SD$ ) for each element measured and analysed in this study. Top and bottom part of the table represent session 1, northern populations and session 2, central and southern populations, respectively.

		Mg [ppm]	Ca [ppm]	V [ppm]	Cr [ppm]	Fe [ppm]	Zn [ppm]	Sr [ppm]	Cd [ppm]	Ba [ppm]
CGE northern population	MACS-3	1603.54 $\pm 455.50$	302944 $\pm 75907.06$	37.59 $\pm 19.51$	96.76 $\pm 46.00$	8725.96 $\pm 4871.83$	82.85 $\pm 29.20$	5707.56 $\pm 1730.82$	34.14 $\pm 13.36$	51.37 $\pm 16.11$
	NIST 610	1.00 $\pm 0.00$	0.02 $\pm 0.01$	14.49 $\pm 13.81$	10.72 $\pm 10.38$	0.37 $\pm 0.62$	3.85 $\pm 5.23$	42.61 $\pm 43.84$	6.64 $\pm 8.63$	9.20 $\pm 9.33$
	NIST 612	64.77 $\pm 10.14$	85002 $\pm 0.00$	43.13 $\pm 6.54$	41.10 $\pm 8.03$	82.81 $\pm 89.29$	40.75 $\pm 10.65$	74.85 $\pm 16.56$	30.93 $\pm 8.01$	38.64 $\pm 8.77$
CGE centre/southern populations	MACS-3	1855.63 $\pm 126.29$	400900.00 $\pm 11947.98$	52.61 $\pm 6.15$	132.13 $\pm 11.94$	13937.50 $\pm 1909.04$	139.58 $\pm 19.36$	6881.75 $\pm 520.29$	51.23 $\pm 3.28$	64.06 $\pm 6.83$
	NIST 610	465.02 $\pm 2.85$	82146.97 $\pm 326.07$	442.00 $\pm 1.07$	405.02 $\pm 1.97$	453.11 $\pm 52.33$	456.02 $\pm 52.33$	515.37 $\pm 5.11$	259.00 $\pm 1.87$	435.00 $\pm 1.45$
	NIST 612	56.41 $\pm 7.53$	84430.00 $\pm 783.25$	38.30 $\pm 0.23$	37.28 $\pm 0.69$		37.50 $\pm 2.70$	83.84 $\pm 4.80$	27.68 $\pm 1.72$	37.89 $\pm 0.52$

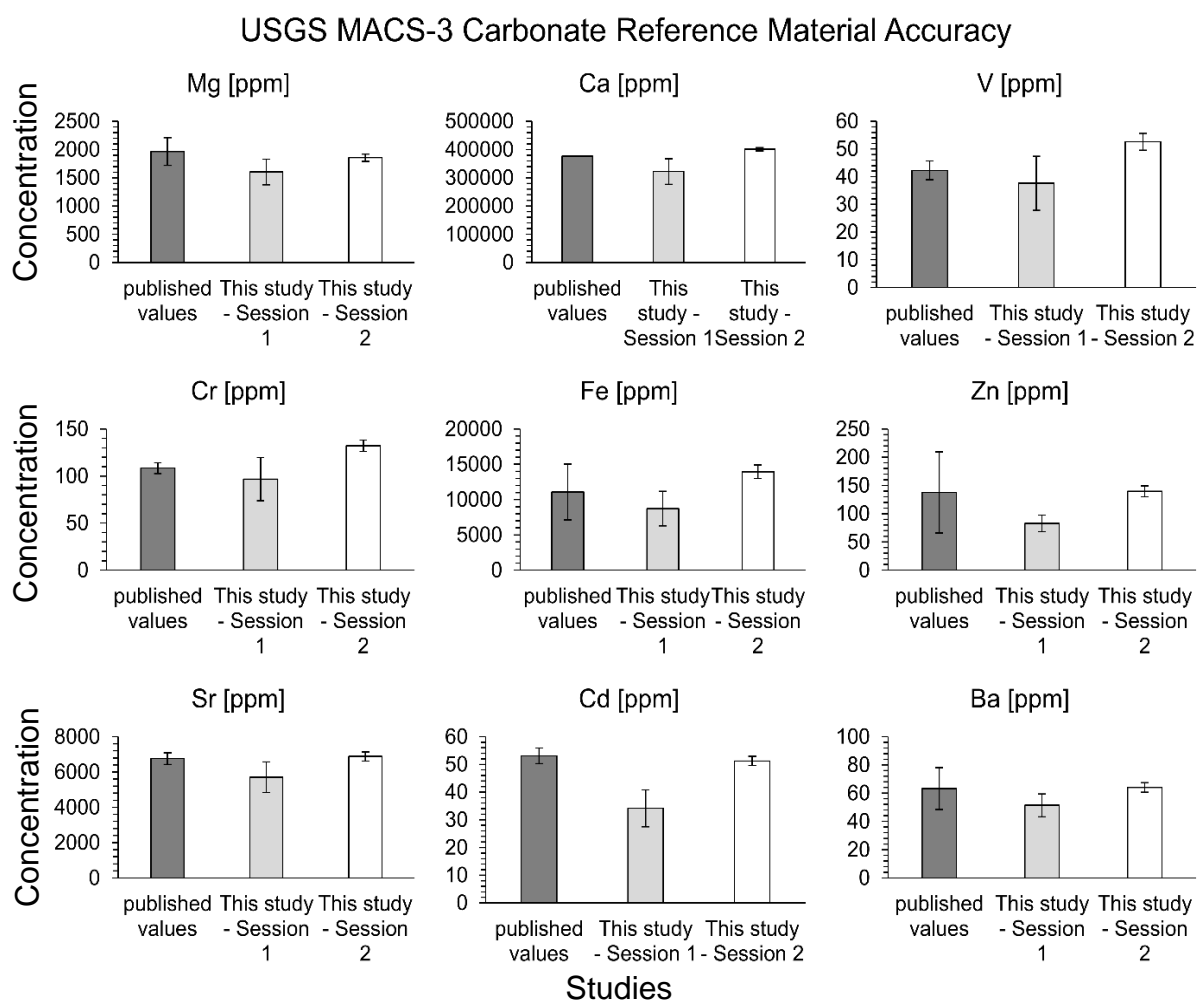
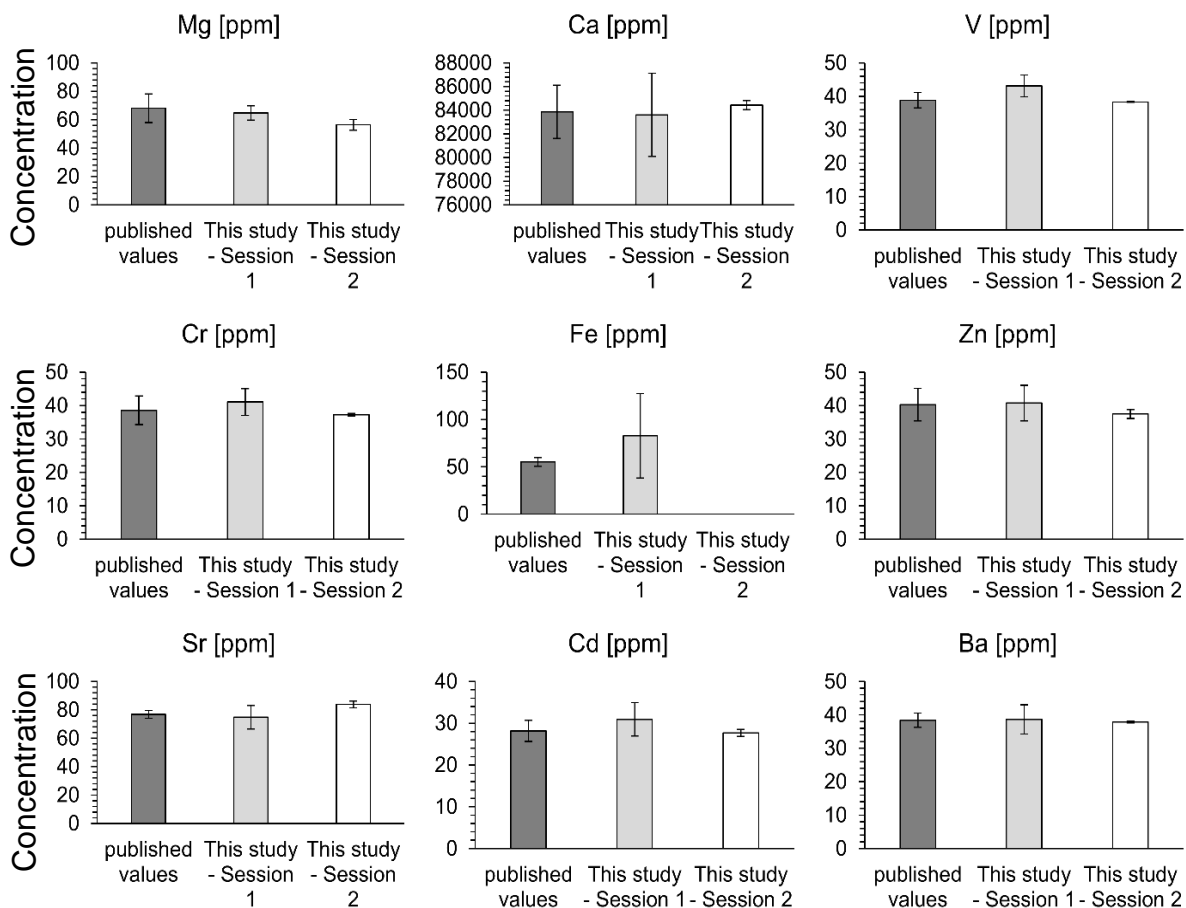


**Figure 4.1:** Accuracy of the reference material USGS MACS-3 for each measured and analysed trace element. Dark grey bars represent  $AV \pm SD$  [ppm] of published data retrieved from the GeoReM database. Light grey bars represent  $AV \pm SD$  [ppm] of trace elements in this study for session 1. White bars represent  $AV \pm SD$  [ppm] of trace elements in this study for session 2.

## NIST SRM 612 Reference Material Accuracy



## Studies

**Figure 4.2:** Accuracy of the reference material NIST SRM 612 for each measured and analysed trace element. Dark grey bars represent  $AV \pm SD$  [ppm] of published data retrieved from the GeoReM database. Light grey bars represent  $AV \pm SD$  [ppm] of trace elements in this study for session 1. White bars represent  $AV \pm SD$  [ppm] of trace elements in this study for session 2.

#### 4.3.6.2 Cell Wall Thickness

With this measurement, using scanning electron microscopy (SEM), the modification of the cell wall structure and therefore, a potential change in growth or metabolic processes can be connected.

The same samples mounts prepared in 2.8.2.1 for LA-ICP-MS analysis, were used for SEM analysis. A SEM suitable to take pictures of uncoated samples was used (EVO MA10 with a W filament electron source, Zeiss, Oberkochen, Germany), to be able to use the same mounts in both machines without any interference of sample coating. Sample mounts were fixed on stabs with double coated carbon conductive tabs and cleaned using Isopropanol, prior to loading the SEM and applying a variable pressure (VP) vacuum of 28 Pa.

Images were taken at 20 kV electron high tension (EHT), representing the accelerating voltage used for each sample. A working distance (WD) of 7 - 9 mm was set. Pictures were taken with a probe of 300 pA, a scan speed of 20.5 s, a magnification of 3 K and a line average noise reduction in the Backscatter (HDBSD) mode. After all images were produced, the software ImageJ (Rasband, 2016) was used to determine the average intra- (lateral to growth direction) and inter-cell wall (horizontal to growth direction) thickness of specimens (total n = 90 per condition; n = 45 below stain, n = 45 above stain; n = 15 per replicate; replicate: n = 3).

#### 4.3.6.3 Monthly Growth Rates and Death rates

In order to obtain growth rates in the laboratory, specimens were carefully removed following the procedure described in 2.2 and stained over night as described in 2.6.7.1. The following day specimens were placed back into their respective aquaria.



After the experiments, specimens of each temperature condition were carefully dried and growth rates were determined following the protocol in 2.6.7.2. Growth rate analysis for the central/southern Common Garden Experiment incorporated replicate measurements of CP in central conditions ( $n = 164$ ), CP in southern conditions ( $n = 171$ ), SP in southern conditions ( $n = 163$ ) and SP in central conditions ( $n = 143$ ). Analysis of the NP consisted of  $n = 59$ , 27 and 26 replicates for northern, central and southern temperature conditions, respectively. During daily checks of the Common Garden Experiment with the NP, dead specimens were collected, labelled, dried and saved throughout the experiment in order to determine death rates at the end of the experiment.

#### 4.3.7 Data Analysis

##### 4.3.7.1 Physiological Parameters

Data were analysed as described in Chapter 2.6.6. Analyses were carried out in SPSS Statistics 24 and 25 (IBM Corp, 2016 and 2018, respectively). Normality and homogeneity were determined prior analyses (Shapiro-Wilk and Levene's Test).

In the central/southern Common Garden Experiment, data for net production ( $n = 3$ ) was not normally distributed, resulting in statistical analysis using the non-parametric Kruskal-Wallis H test. Data for respiration ( $n = 3$ ) as well as dark calcification ( $n = 3$ ) measurements showed a significant Levene's test with raw as well as transformed data due to high variance. Therefore, data were analysed using multiple single comparisons of one-way analysis of variance (ANOVA). Normally distributed data of the dependant variable light calcification ( $n = 3$ ) was analysed using two-way ANOVAs for individuals from each country of origin (UK (centre) or SP (southern margin)) with treatment (3 levels: pre-experiment, central conditions and southern conditions) as the fixed factor. When significant effects were found,

data were further explored by running a post hoc Tukey HSD test. Tests were performed for CP and SP under each temperature condition comparing measurements before and after the experiment.

Additional two-way ANOVAs and Tukey HSD post hoc tests of CP and SP were performed to identify significant differences in their maximum oxygen production and calcification level of all populations in all temperature treatments.

In the Common Garden Experiment with NP, maximum oxygen production rates of the NP ( $n = 4$ , for each time point) was analysed using 2-way ANOVAs and Tukey HSD post hoc tests with condition and condition\*“day of experiment” as fixed factors. Light calcification ( $n = 3$ ) and dark calcification ( $n = 3$ ) showed no normal distribution and no homogeneity of variance, subsequently Kruskal-Wallis H tests for these parameters were performed. Respiration ( $n = 3$ ) and primary production ( $n = 3$ ) showed normal distribution and homogeneous variances, data was analysed with 2-way ANOVAs and Tukey HSD post hoc tests.

#### 4.3.7.1 Structural Parameters

Not normally distributed and homogeneous data were analysed using independent-sample Kruskal-Wallis H tests with pairwise comparison. In this way, growth rates (all  $n = 26$ ), intra-and inter-cell wall thickness (all  $n = 45$ ) were analysed.

Trace element data were analysed for both Common Garden Experiments separately using PRIMER 6.1 (Anderson *et al.*, 2009), after data normalisation by fourth root transformation due to extreme high variability of elemental concentrations, a permutational analysis of variance (PERMANOVA) with condition, population and time-point as factors and condition nested into population and 9999 permutations was performed. Additional similarity of percentage (SIMPER) analysis were performed to determine the major influential trace elements for each group.

## 4.4 Results

The experimental design allowed for very stable parameters under all conditions and was not influential towards physiological behaviour of specimens (Table 4.2). Saturation states for calcite and aragonite and pH were highest in southern conditions.

**Table 4.2:** Carbonate system parameters of the central/southern (top) and northern (bottom) experiment during the culturing of *C. officinalis*. Values are mean values ( $n = 81 \pm \text{SD}$  and  $n = 4 \pm \text{SD}$ , for top and bottom, respectively). Salinity, pH, temperature and total alkalinity ( $A_T$ ) were measured while other parameters were calculated.

Treatment	pH (total scale)	Salinity	Temperature [°C]	$A_T$ [ $\mu\text{mol kg}^{-1}$ ]	DIC [ $\mu\text{mol kg}^{-1}$ ]	$\text{HCO}_3^-$ [ $\mu\text{mol kg}^{-1}$ ]	$\Omega_{\text{Ca}}$	$\Omega_{\text{Ar}}$	$\text{pCO}_2$ [ $\mu\text{atm}$ ]
Centre	8.19 $\pm 0.07$	32.9 $\pm 0.6$	5.70 $\pm 0.73$	2344 $\pm 43$	2185.9 $\pm 46.6$	2049.1 $\pm 50.6$	2.32 $\pm 0.27$	1.48 $\pm 0.17$	377 $\pm 61$
South	8.22 $\pm 0.08$	33.2 $\pm 0.5$	11.33 $\pm 0.39$	2326 $\pm 37$	2100.0 $\pm 46.4$	1925.6 $\pm 54.3$	3.23 $\pm 0.30$	2.08 $\pm 0.19$	319 $\pm 45$
Populations/ Treatment	pH (NBS scale)	Salinity	Temperature [°C]	$A_T$ [ $\mu\text{mol kg}^{-1}$ ]	DIC [ $\mu\text{mol kg}^{-1}$ ]	$\text{HCO}_3^-$ [ $\mu\text{mol kg}^{-1}$ ]	$\Omega_{\text{Ca}}$	$\Omega_{\text{Ar}}$	$\text{pCO}_2$ [ $\mu\text{atm}$ ]
Northern/ Northern	8.42 $\pm 0.03$	34.6 $\pm 0.1$	9.08 $\pm 0.13$	1927 $\pm 39$	1712.0 $\pm 25.5$	1565.0 $\pm 19.1$	3.31 $\pm 0.26$	2.08 $\pm 0.17$	149 $\pm 11$
Northern/ Centre	8.41 $\pm 0.03$	34.6 $\pm 0.1$	12.58 $\pm 0.41$	1794 $\pm 170$	1592.8 $\pm 152.3$	1459.1 $\pm 136.3$	3.00 $\pm 0.42$	1.88 $\pm 0.27$	143 $\pm 14$
Northern/ South	8.54 $\pm 0.09$	34.7 $\pm 0.1$	16.48 $\pm 1.14$	1965 $\pm 24$	1691.0 $\pm 36.7$	1510.0 $\pm 62.1$	4.17 $\pm 0.71$	2.62 $\pm 0.45$	114 $\pm 28$

#### 4.4.1 Photosynthesis and Calcification Evolution

The mean saturating light levels ( $P_{\max}$ ) for all populations of one country did not differ between central or southern temperature conditions after 3 months of culturing (Figure 4.3; Figures C1-C8).  $P_{\max}$  of CP were  $\sim 1.8$  and  $\sim 1.2$ -times higher than of SP under southern and central conditions, respectively (Table 4.3(A)). CP1 showed a significant difference vs. SP under central conditions (Table 4.3(B)). SP1 showed a significant difference vs. CP under southern conditions (Table 4.3(B)). The photosynthetic efficiency,  $\alpha$ , of CP did not differ in both treatments (Table 4.3(A)). However, all SP under central conditions showed up to 50% less light harvesting efficiency than under southern conditions. The saturating light intensity  $I_k$  of all populations was higher in CP than in SP, under southern conditions, but very similar under central conditions (Table 4.3(A)). Southern populations developed a  $\sim 50\%$  higher saturating light intensity in central than under southern conditions (Table 4.3(A)).

All populations showed significantly higher mean saturating calcification levels ( $C_{\max}$ ) under central than southern conditions (Figure 4.3; Figures C1-C8, Table 4.3(B)). The calcification efficiency  $\alpha$  was higher under central than under southern conditions (Table 4.3(A)). Central populations needed more light harvesting for saturation than southern populations regardless of central or southern temperatures (Figure 4.3, Table 4.3(A)). Central populations decreased in efficiency under southern conditions compared to central conditions by 1.6 times. Southern populations were more efficient at light harvesting under central conditions. The saturating light intensity  $I_k$  did not change drastically in SP under southern or central conditions. In CP, however,  $I_k$  increased by 132.5% under southern conditions (Table 4.3(A)).

Photoinhibition of photosynthesis rates was not observed in any of the populations;  $P_{\max}$  was reached in all populations and treatments. Inhibition of calcification was observed in all populations under southern conditions.

For detailed graphs, see Figures C1-C8. Statistical differences are summarised in Kolzenburg *et al.* (2019).

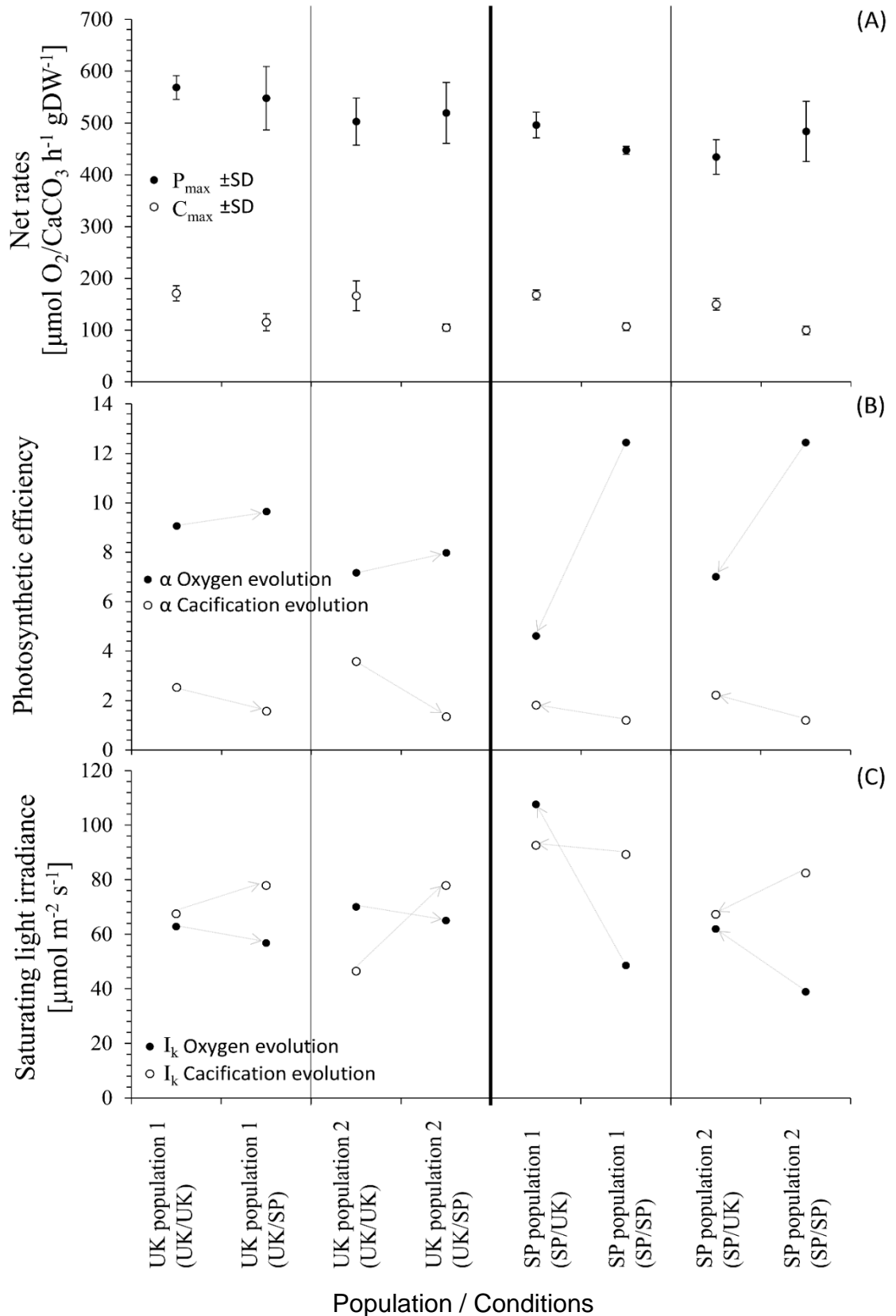
**Table 4.3:** (A) Mean  $\pm$ SD ( $n = 5$ ) for saturating photosynthesis ( $P_{\max}$ ) and calcification ( $C_{\max}$ ) levels, photosynthetic efficiency ( $\alpha$ ) and saturating light intensity ( $I_K$ ) of *C. officinalis* in the Common Garden Experiment of Central ( $n = 2$ ) and Southern ( $n = 2$ ) populations. (B) Statistical comparison of  $P_{\max}$  and  $C_{\max}$  between populations within temperature treatment and between temperature treatments within populations.

(A)			Net Production Rates [ $\mu\text{mol h}^{-1} \text{gDW}^{-1}$ ]				Net Calcification Rate [ $\mu\text{mol h}^{-1} \text{gDW}^{-1}$ ]			
Region	Population	Treatment	$P_{\max}$	$\pm$ SD	$\alpha$ Oxygen evolution	$I_K$ Oxygen evolution	$C_{\max}$	$\pm$ SD	$\alpha$ Calcification evolution	$I_K$ Calcification evolution
Central	1	Central	568.55	22.97	9.06	62.79	170.98	14.58	2.53	67.53
		South	548.00	61.13	9.65	56.77	114.83	16.30	1.57	73.15
	2	Central	502.67	45.57	7.17	70.07	166.24	28.73	3.58	46.46
		South	519.15	58.96	7.98	65.05	104.77	6.75	1.35	77.88
South	1	Central	495.94	24.93	4.61	107.59	167.71	9.57	1.81	92.60
		South	447.57	7.60	9.22	48.53	106.73	7.61	1.20	89.30
	2	Central	434.23	33.13	7.01	61.95	149.54	11.20	2.22	67.27
		South	483.63	57.75	12.44	38.88	99.27	8.28	1.20	82.47

(B) $P_{\max}$ Significances		Central				South			
$C_{\max}$ Significances		1		2		1		2	
2-way ANOVA		Central	South	Central	South	Central	South	Central	South
Central	1	Central		NS	NS	*		***	
		South	***			NS	*		NS
	2	Central	NS			NS	NS		NS
		South		*	*		*		NS
South	1	Central	NS		NS		NS	NS	
		South		NS		NS	***		NS
	2	Central	NS		NS		NS		NS
		South		NS		NS	NS	***	

Significance levels: NS = not significant \* =  $P < 0.05$  \*\* =  $P < 0.01$  \*\*\* =  $P < 0.005$



**Figure 4.3** Evolution curve characteristics for net production and calcification (AV  $\pm$ SD,  $n = 3$ ) of the central (UK) and southern (SP) populations ( $n = 2$ ) under both southern (SP) and central (UK) conditions. (A):  $P_{\text{max}}/C_{\text{max}}$  = maximum production, (B)  $\alpha$  = initial slope as indicator for photosynthetic efficiency, (C)  $I_k$  = saturating irradiance. Arrows indicate direction of change from original to altered conditions.

#### 4.4.2 Oxygen Production Recovery

Oxygen production rates of northern specimens were measured at super-optimum light irradiances, therefore, maximum rates [ $\mu\text{mol O}_2 \text{ L}^{-1} \text{ h}^{-1}$ ] measured during the light represent  $P_{\text{max}}$  of NP in respective temperature conditions (Figure 4.4). Under northern and central conditions,  $P_{\text{max}}$  of NP showed the same course of pattern at the beginning of the experiment with a steeper increase under central conditions. Towards the end of the experiment, NP declined drastically under central conditions but increased under native environmental conditions. Under southern conditions,  $P_{\text{max}}$  showed relatively stable values throughout and followed the pattern of central conditions from t23 onwards.

All populations showed a drop in  $P_{\text{max}}$  from day 13 (t13) to 23 (t23) of the experiment and recovered again in the next 10 days of the experiment. A change in pattern was observed on t23. Prior to that time point, NP and CP showed the same trend, whereas after that time point, CP and SP showed identical patterns.

Significant differences for the NP were found under central conditions between t13 and the start (t9) and end (t41) of the experiment ( $P < 0.05$ , Tukey HSD  $P < 0.05$ , 2-way ANOVA in both cases, Figure 4.4). Significant differences of the oxygen production under central conditions were found between the start day (t0) and all other days, except t9 and t41 ( $P < 0.05$  in all cases, Tukey HSD  $P < 0.05$ , 2-way ANOVA for t23 and Tukey HSD  $P < 0.001$ , 2-way ANOVA in all other cases (t13, t27, t34)).

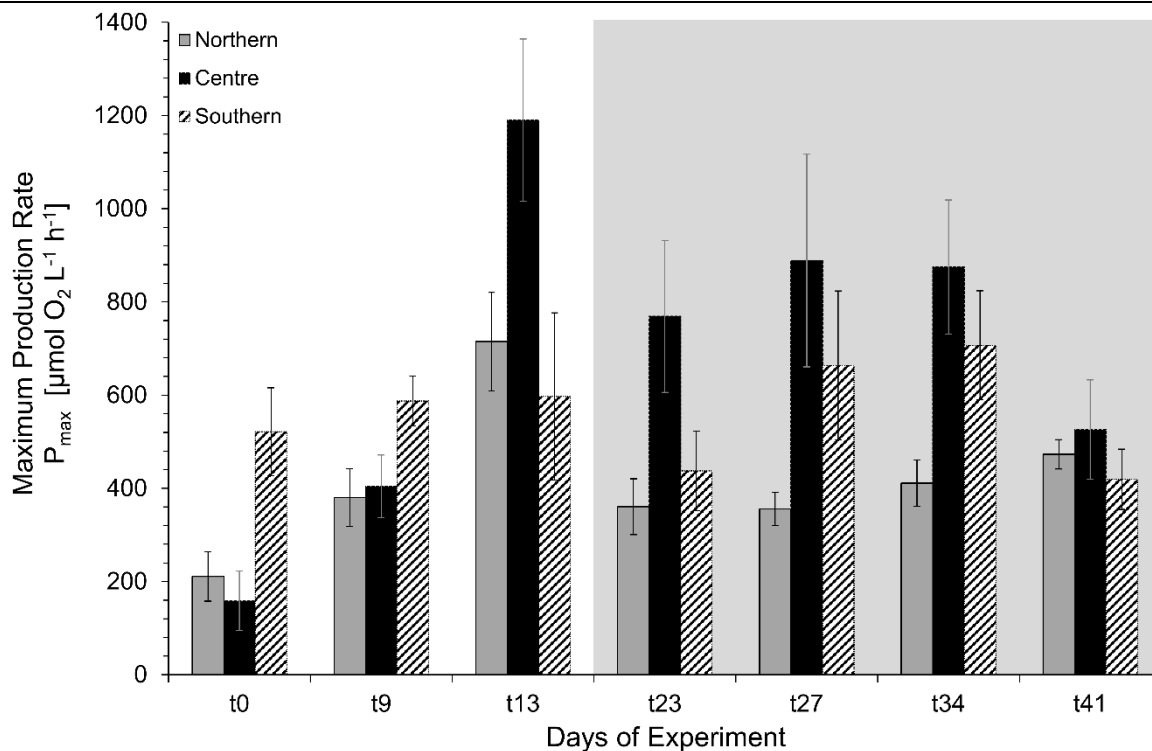


**Figure 4.4:** Maximum production rates  $P_{max}$  [ $\mu\text{mol O}_2 \text{ L}^{-1} \text{ h}^{-1}$ ] of northern populations of *C. officinalis*. Solid, dashed and dotted lines represent northern, central and southern temperature conditions, respectively ( $AV \pm SE$ ,  $n = 4$ ). The grey area indicates the change between identical patterns from northern and central populations to central and southern populations.

#### 4.4.3 Primary Production and Respiration

In the central/southern Common Garden Experiment net production rates of CP (Figure 4.5) did not change significantly over the course of the experiment under the different conditions. Central populations were significantly different from SP1 prior to the experiment ( $P < 0.05$ , Kruskal-Wallis H test). After the experiment, CP2 showed significantly lower primary production rates under southern conditions than under central conditions ( $P < 0.05$ , Kruskal-Wallis H test). Southern populations under southern conditions showed similar oxygen production rates before and after the experiment. Central populations under southern conditions showed lower



oxygen production rates but higher rates under central conditions compared to pre-experiment measurements (Figure 4.5). Only SP2 showed a significant decline in production rates, resulting in respiration rates under central experimental conditions ( $P < 0.05$ , Kruskal-Wallis H test). When comparing populations within regions, none of the CP or SP were significantly different within each other before the experiment. Respiration rates of CP (Figure 4.5) did not change significantly throughout the experiment despite a positive trend under central conditions and were stable under southern conditions. Respiration rates of SP were stable under southern conditions whereas they increased significantly under central compared to southern conditions ( $F_{1,5} = 25.346$  and  $F_{1,5} = 21.848$  for SP1 and SP2, respectively,  $P < 0.01$ , 1-way ANOVA for both SP). Central populations showed a significant difference between each other after the experiment under both temperature treatments ( $F_{1,5} = 36.975$  and  $F_{1,5} = 26.769$  for CP1 and CP2, respectively,  $P < 0.01$ , 1-way ANOVA in both cases). Comparing populations, none of the populations within a region were significantly different from each other before the experiment. Under central as well as southern conditions, all CP were significantly different from all SP (Under central conditions:  $F_{1,5} = 19.119$  for UK1 vs. SP1,  $F_{1,5} = 18.837$  for UK1 vs SP2,  $F_{1,5} = 16.455$  for UK2 vs. SP1,  $F_{1,5} = 16.431$  for UK2 vs. SP2,  $P < 0.05$ , 1-way ANOVA for all cases; under southern conditions:  $F_{1,5} = 130.367$  for UK1 vs. SP1,  $F_{1,5} = 125.643$  for UK1 vs SP2,  $F_{1,5} = 61.485$  for UK2 vs. SP1,  $F_{1,5} = 60.270$  for UK2 vs. SP2,  $P < 0.01$ , 1-way ANOVA for all cases) but not significantly different from each other.

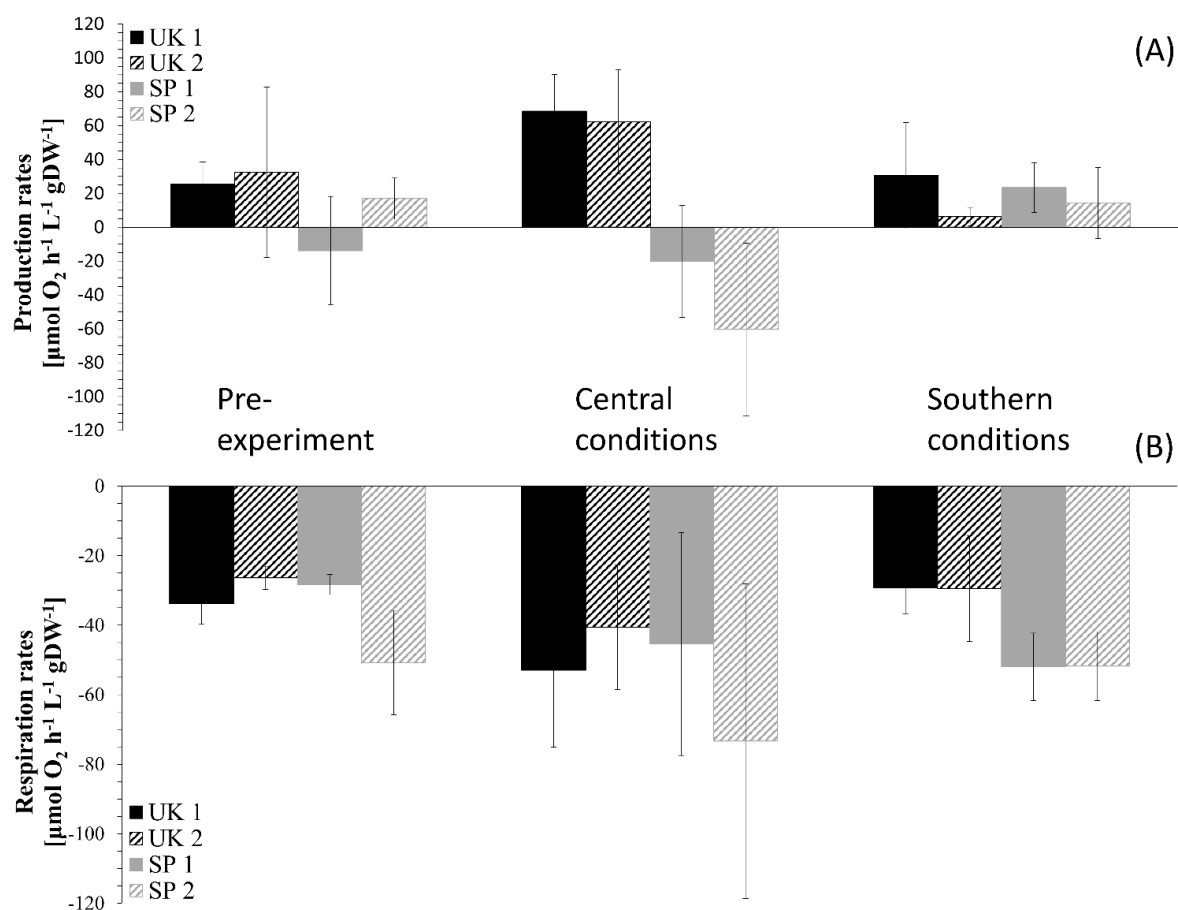


**Figure 4.5:** (A) Primary production and (B) respiration rates [ $\mu\text{mol O}_2/\text{CaCO}_3 \text{ h}^{-1} \text{ L}^{-1} \text{ gDW}^{-1}$ ]  $\pm$ SD ( $n = 3$ ) of *C. officinalis* before the Common Garden Experiment and after exposure to temperature of each geographic location. Southern populations (SP1 and SP2) are represented in grey, central populations (UK1 and UK2) are represented in black. Statistical differences are summarised in Table S1 of the supplementary document of Kolzenburg *et al.* (2019).

Northern populations showed no significant difference between production rates in pre-experimental and post-experimental, northern and central conditions (Table 4.4, Figure 4.6). A significant difference was found between pre-experimental and post-experimental production rates under southern conditions (Table 4.4(B)). A significant difference was also found between central and northern conditions prior to the experiment as well as between central and southern and northern and southern conditions after the experiment (Table 4.4(B)). Primary production rates showed a decline under northern conditions, stable rates under central conditions and increasing rates under southern conditions (Table 4.4(A)).

Respiration rates (Figure 4.6) of the NP showed no significant differences between pre and post-experimental measurements under all conditions (Table 4.4(B)). However, a trend towards higher respiration rates was observed under all conditions (Table 4.4(A)). Respiration rates were not significantly different between the three temperature conditions (Table 4.4(B)).

**Table 4.4:** (A) Mean  $\pm$ SD for primary production, respiration, light and dark calcification of the northern margin population ( $n = 1$ ) of *C. officinalis* in the NE Atlantic. (B) Statistical comparison of parameters between time points (pre- and post-experimental exposure) within temperature conditions (northern, central and southern) across its geographic distribution in the NE Atlantic.

(A)

Time Point	Temperature Treatment	Primary Production		Respiration		Light Calcification		Dark Calcification	
		[ $\mu\text{mol O}_2 \text{ h}^{-1} \text{ L}^{-1} \text{ gDW}^{-1}$ ]		[ $\mu\text{mol O}_2 \text{ h}^{-1} \text{ L}^{-1} \text{ gDW}^{-1}$ ]		[ $\mu\text{mol O}_2 \text{ h}^{-1} \text{ L}^{-1} \text{ gDW}^{-1}$ ]		[ $\mu\text{mol O}_2 \text{ h}^{-1} \text{ L}^{-1} \text{ gDW}^{-1}$ ]	
		Mean	$\pm$ SD	Mean	$\pm$ SD	Mean	$\pm$ SD	Mean	$\pm$ SD
Pre-experimental	Northern	83.26	20.75	-2.93	21.77	689.53	226.09	507.43	469.61
	Central	46.27	6.29	-18.53	11.53	585.49	154.91	1177.23	342.48
	Southern	60.51	1.89	-0.29	6.52	851.99	472.78	512.29	518.00
Post-experimental	Northern	60.36	33.94	-23.77	19.09	-83.91	72.96	34.20	37.92
	Central	45.93	17.34	-11.52	8.61	28.11	58.29	-16.05	49.72
	Southern	92.93	8.31	-11.40	23.05	-14.51	71.95	57.97	110.80

(B)

Primary Production Significances		Pre-experimental			Post-experimental		
Respiration Significances		[ $\mu\text{mol O}_2 \text{ h}^{-1} \text{ L}^{-1} \text{ gDW}^{-1}$ ]					
2-way ANOVA		Northern	Central	Southern	Northern	Central	Southern
Pre-experimental	Northern		*	NS	NS		
	Central	NS		NS		NS	
	Southern	NS	NS				*
Post-experimental	Northern	NS				NS	*
	Central		NS		NS		**
	Southern			NS	NS	NS	
Light Calcification Significances		Pre-experimental			Post-experimental		
Dark Calcification Significances		[ $\mu\text{Eq CaCO}_3 \text{ h}^{-1} \text{ L}^{-1} \text{ gDW}^{-1}$ ]					
Kruskal-Wallis Test		Northern	Central	Southern	Northern	Central	Southern
Pre-experimental	Northern		NS	NS	***		
	Central	*		NS		**	
	Southern	NS	*				***
Post-experimental	Northern	NS				NS	NS
	Central		***		NS		NS
	Southern			NS	NS	NS	

Significance levels: NS = not significant \* =  $P < 0.05$  \*\* =  $P < 0.01$  \*\*\* =  $P < 0.005$

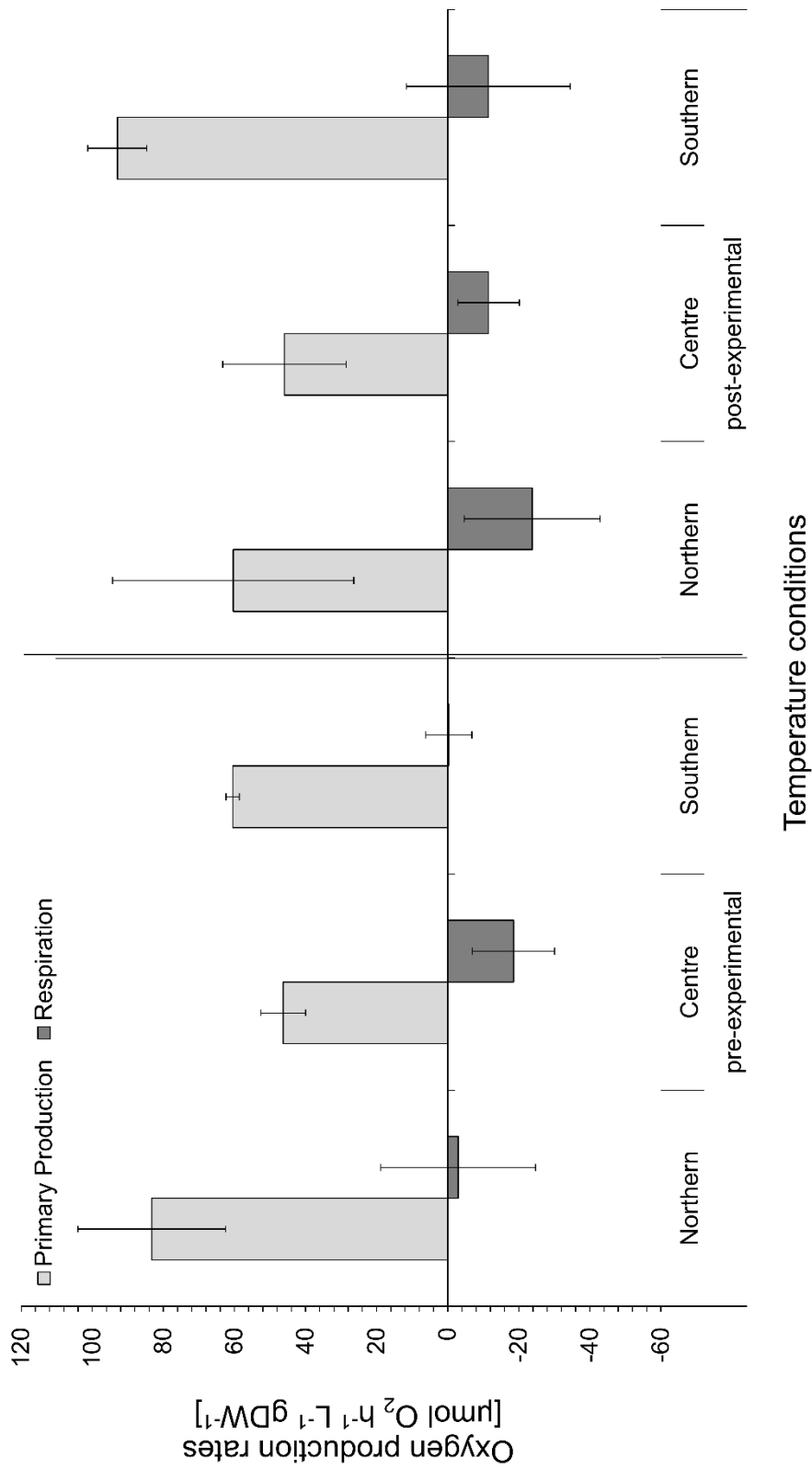


**Figure 4.6:** Oxygen production rates [ $\mu\text{mol h}^{-1} \text{ L}^{-1} \text{ gDW}^{-1}$ ]  $\pm\text{SD}$  (n = 4) of *C. officinalis* before and after the Common Garden Experiment of northern populations in northern, central and southern temperature conditions. Light and dark grey bars represent primary production and respiration rates, respectively.

#### 4.4.4 Calcification Rates

Calcification rates of the NP in the light (Figure 4.7) were significantly higher under northern conditions before the experiment compared to post-experimental measurements (Table 4.4(B)). Additionally, light calcification rates under southern conditions were significantly lower in pre-experimental compared to post-experimental measurements (Table 4.4). Under central conditions a significant difference was found comparing pre- and post-experimental measurements.

No significant difference was found within temperature treatments, however a trend towards increased dissolution under northern conditions was observed.

Significantly higher calcification rates of the NP in the dark (Figure 4.7) were only found under central conditions before the experiment compared to those after the experiment (Table 4.4). No significant difference was found within the other two temperature treatments before or after the experiment as well as between conditions. However a trend towards a greater decrease of calcification rates under central conditions compared to the decrease in both marginal location conditions was observed. Dissolution of the skeleton of the NP in the dark was only observed for central but not margin location temperatures.

Calcification rates of CP and SP in light (Figure 4.8) were significantly different before and after the experiment under southern conditions for SP1 ( $P < 0.05$ , Tukey HSD  $P < 0.05$ , 2-way ANOVA), but not for SP2. Under central conditions, SP showed a non-significant decrease of calcification rates. In contrast to CP2, CP1 showed a significant increase in calcification rates in the light under central conditions ( $P < 0.05$ , Tukey HSD  $P < 0.01$ , 2-way ANOVA) and both showed a highly significant lower rate under southern conditions ( $P < 0.01$ , Tukey HSD  $P < 0.01$ , 2-way ANOVA in both cases) compared to pre-experiment as well as the central

conditions ( $P < 0.05$ , Tukey HSD  $P < 0.05$ , 2-way ANOVA in both cases). In contrast to the second population, SP1 is significantly different to both CP under central conditions ( $P < 0.05$ , Tukey HSD  $P < 0.05$ , 2-way ANOVA in both cases). Calcification rates for populations within a region were not significantly different from each other throughout the experiment.

Calcification rates in the dark of CP and SP (Figure 4.8) increased under central conditions but decreased under southern conditions for CP. The development of dark calcification rates for SP showed a significant increase for SP1 under southern conditions compared to the beginning of the experiment ( $F_{2,6} = 5.013$ ,  $P < 0.05$ , Tukey HSD  $P < 0.05$ , 2-way ANOVA) but no significant change for SP2. Under central conditions, SP showed an increasing trend. Comparing populations within a region, only the SP were significantly different from each other before the experiment ( $F_{1,4} = 11.016$ ,  $P < 0.05$ , 1-way ANOVA).

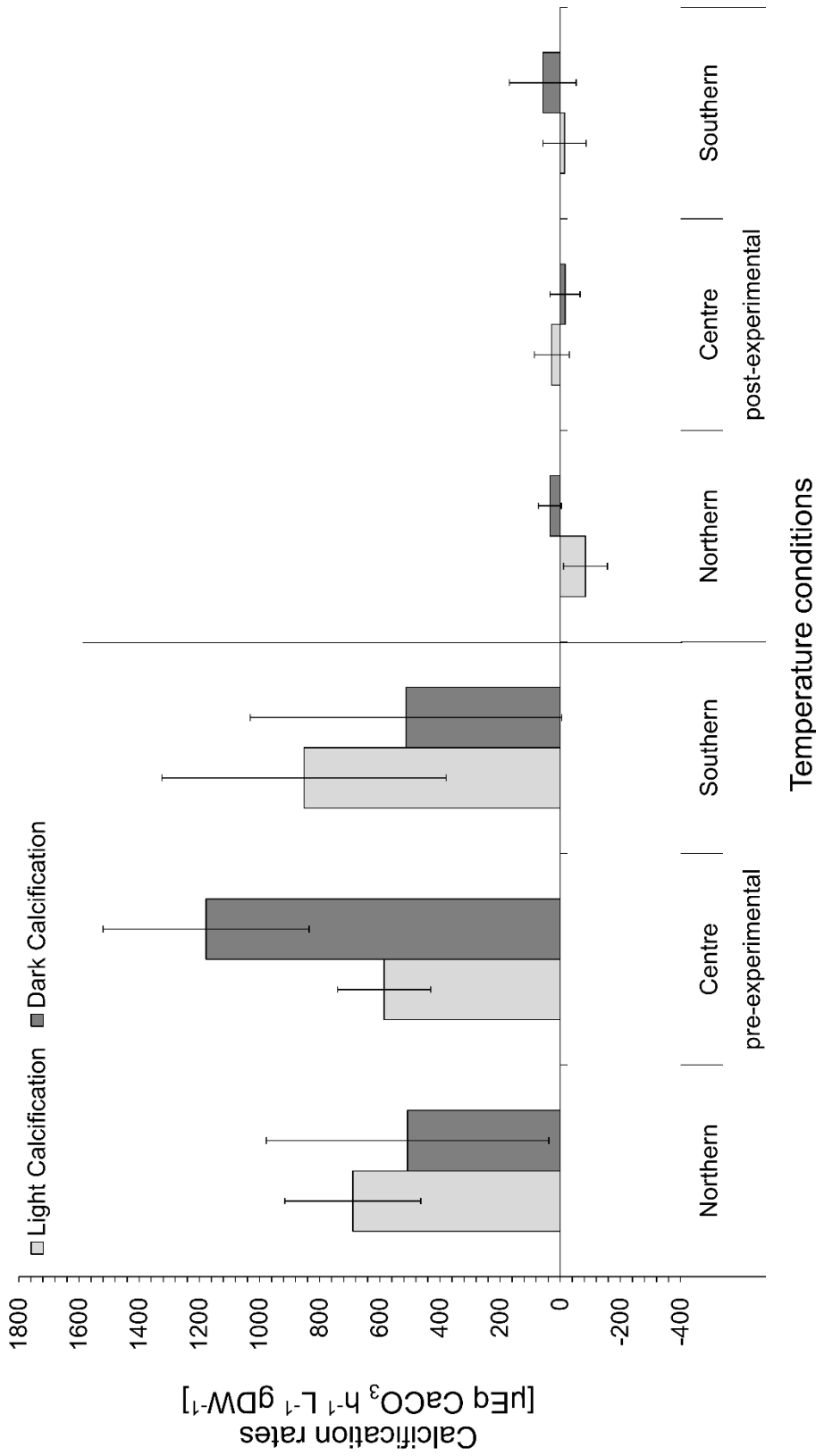


**Figure 4.7:** Calcification rates [ $\mu\text{Eq h}^{-1} \text{ L}^{-1} \text{ gDW}^{-1}$ ]  $\pm\text{SD}$  ( $n = 4$ ) of *C. officinalis* before and after the Common Garden Experiment of northern populations in northern, central and southern temperature conditions. Light and dark grey bars represent gross light and dark calcification rates, respectively.



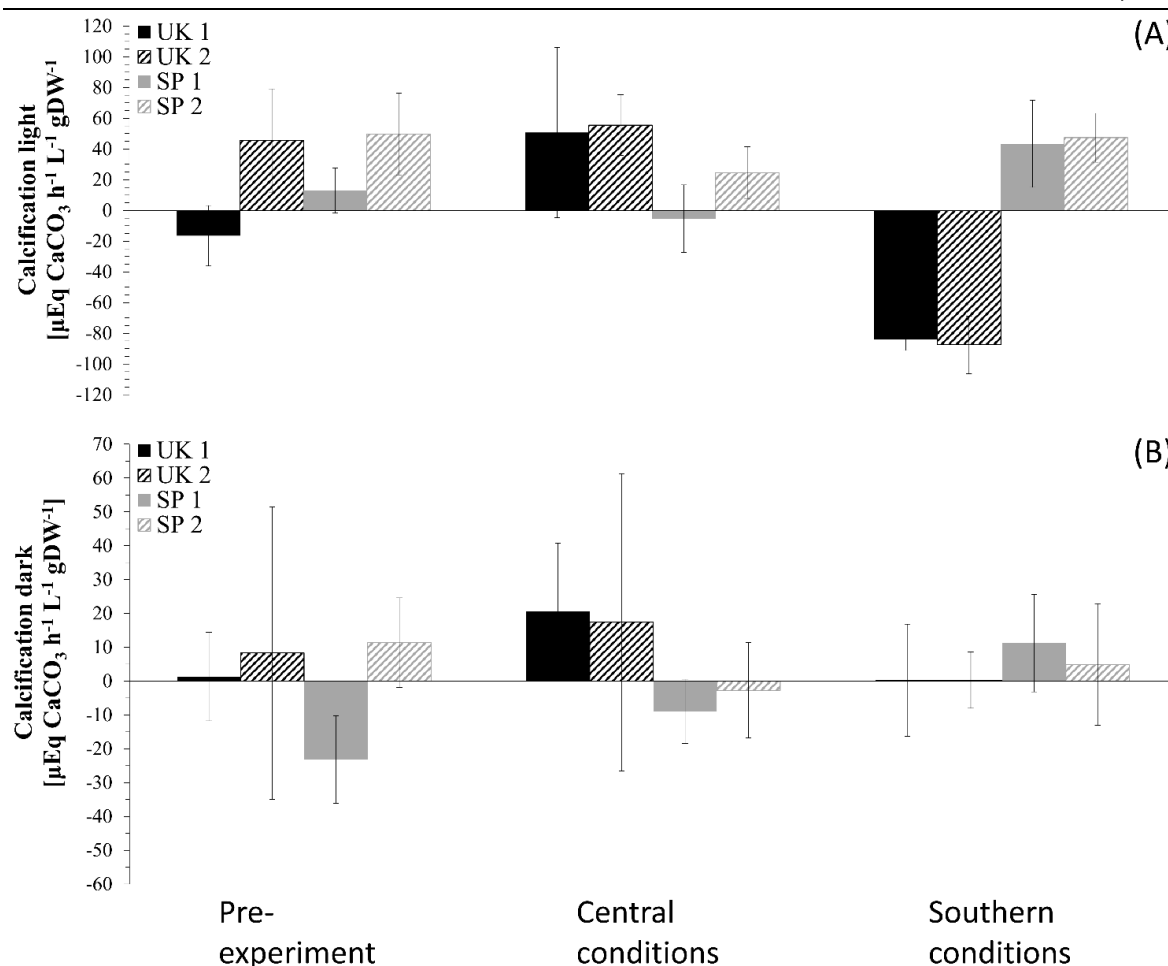


**Figure 4.8:** (A) Calcification rates in the light and (B) dark [ $\mu\text{Eq h}^{-1} \text{ L}^{-1} \text{ gDW}^{-1}$ ]  $\pm$ SD of *C. officinalis* before and after the Common Garden Experiment of each population under each geographic treatment condition. Southern populations (SP1 and SP2) are represented in grey, central populations (UK1 and UK2) are represented in black. Statistical differences are summarised in Table S1 of the supplementary document of Kolzenburg *et al.* (2019).

#### 4.4.5 Structural Integrity in Temperature Conditions along a Latitudinal Gradient

##### 4.4.5.1 Linear Growth Rates

Monthly linear growth rates (Figure 4.9, Table 4.5) of CP1 and CP2 under central conditions were not significantly different from each other. However, they were significantly different from each other under southern conditions (Table 4.5(B)). The NP (Figure 4.10) showed significantly higher growth compared to one of each CP and SP (CP2 and SP2 ( $0.38 \pm 0.12$  mm)) under central conditions (Table 4.5(B)). However, NP did not differ significantly between temperature conditions. Nevertheless, a trend toward increased growth in southern conditions was observed. The least growth occurred under central conditions. Both SP showed a significant lower growth under central conditions compared to both CP (Table 4.5(B)). Under Spanish conditions, CP1 showed a significantly higher growth compared to all other populations (Table 4.5(B)). Both SP showed significantly higher growth rates under southern compared to central conditions (Table 4.5(B)), but not between populations.

Staining success (Figure 4.9) did not fall below  $76.9 \pm 11.6\%$  throughout the experiment and were not significantly different between populations. However, a trend towards less staining success in SP was noticed.

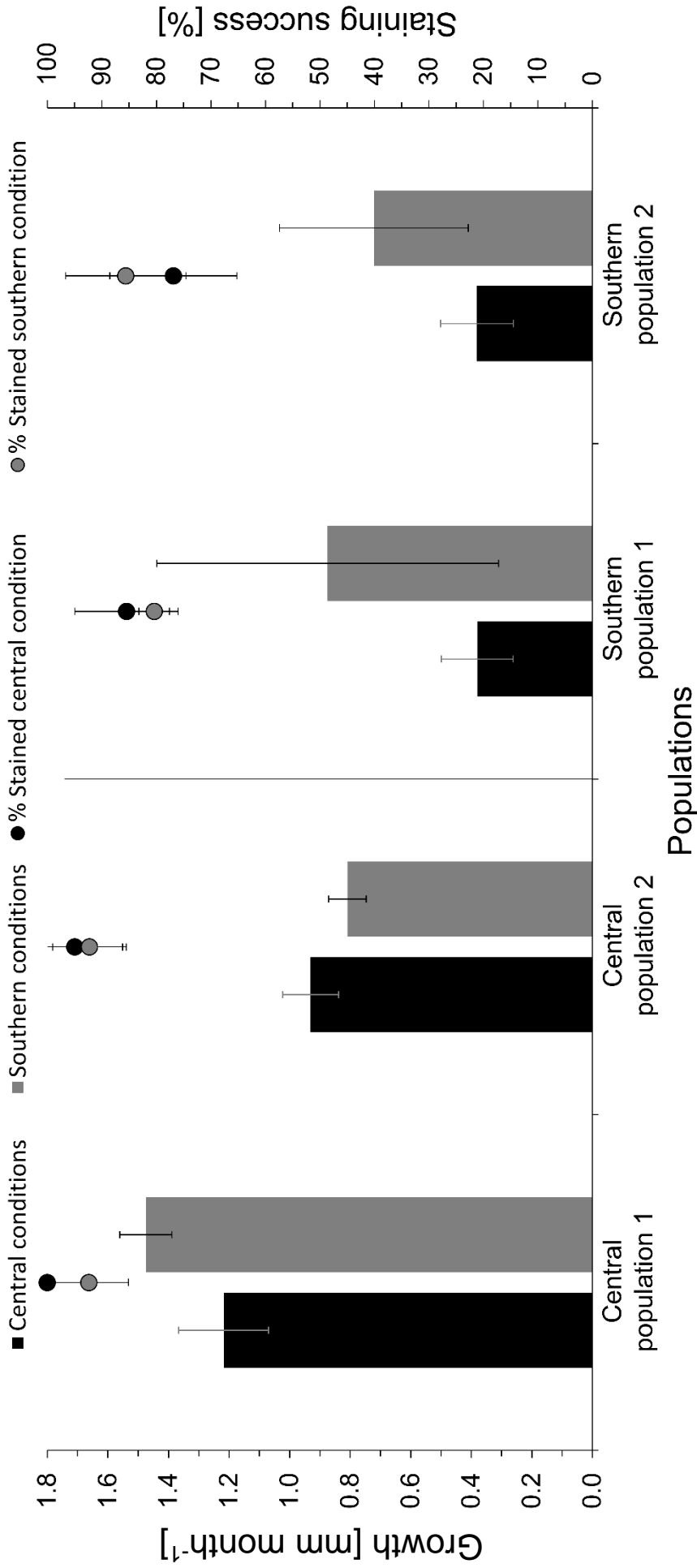


**Figure 4.9:** Monthly linear growth rates [mm month<sup>-1</sup>] (AV ±SD) of *C. officinalis* for central (n = 79 and 85) and southern (n = 70 and 73) populations 1 and 2 under central conditions (black bars) and central (n = 83 and 88) and southern (n = 84 and 79) populations 1 and 2 under southern conditions (grey bars). Staining success is represented as circles (AV ±SD, n = 90) in the respective colour.

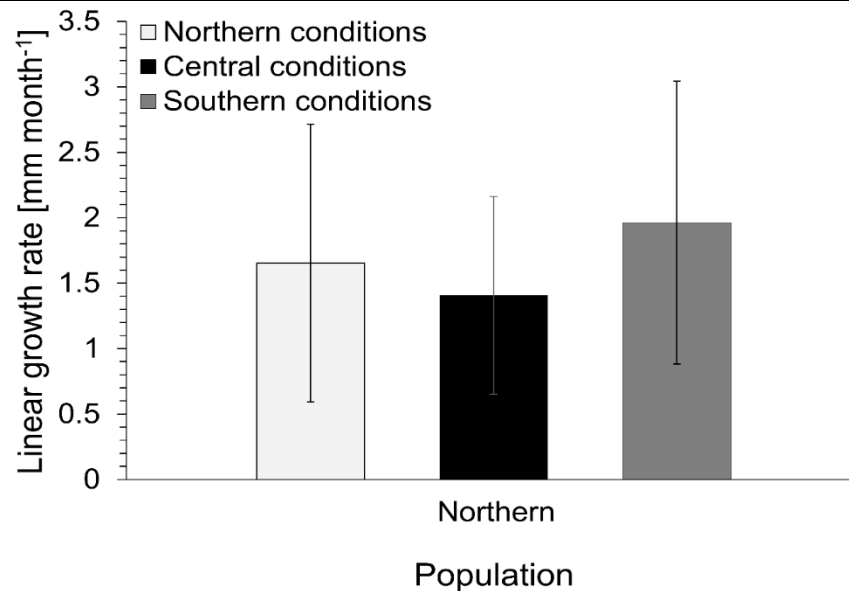


**Figure 4.10:** Monthly linear growth rates [mm month<sup>-1</sup>] (AV  $\pm$ SD) of northern population of *C. officinalis* under northern (light grey bar, n = 59), central (black bar, n = 27) and southern (dark grey bar, n = 26) conditions.

Region	Population	Treatment	Growth rates [mm month <sup>-1</sup> ]	
			Mean	$\pm$ SD
North	1	North	1.65	1.06
		Central	1.41	0.75
		South	1.96	1.08
Central	1	Central	1.22	0.15
		South	1.47	0.09
	2	Central	0.93	0.09
		South	0.81	0.06
South	1	Central	0.38	0.12
		South	0.72	0.31
	2	Central	0.38	0.12
		South	0.87	0.56

**Table 4.5:** (A) Mean  $\pm$ SE (n = 15) for monthly growth rates of *C. officinalis* across its geographical distribution in the NE Atlantic (n = 2 and 1 populations in Central and Southern and northern locations, respectively) in the Common Garden Experiments. (B) Statistical comparison between populations within temperature treatment and between temperature treatments within populations.

Growth rate Significances		North			Central				South			
		1			1		2		1		2	
Kruskal-Wallis H test		North	Central	South	Central	South	Central	South	Central	South	Central	South
North	1	North	NS	NS		NS		NS		NS		NS
		Central			NS	***		***		NS		*
		South					***		NS		NS	
Central	1	Central				NS	NS		***		***	
		South						***		***		***
	2	Central						NS	***		***	
		South								NS		NS
South	1	Central							***	NS		
		South										NS
	2	Central										***
		South										

Significance levels: NS = not significant \* = P < 0.05 \*\* = P < 0.01 \*\*\* = P < 0.005

#### 4.4.5.2 Elemental Composition of the Skeleton

For trace element raw data, a link to the online repository is given in Appendix C.

Magnesium/Calcium (Mg/Ca) ratios of NP were higher in pre than post-experimental conditions under all treatments (Figure 4.11). Under central conditions ratios declined drastically compared to under both marginal location conditions. Pre-experimental values of NP under both marginal location conditions were comparable, those under central conditions were much higher.

Vanadium/Calcium (V/Ca) ratios of NP decreased from pre to post-experimental conditions under northern and central condition but an increase under southern conditions (Figure 4.11). The steepest change was observed under southern conditions. Values of NP under northern conditions were noticeable lower than those under central and southern conditions. Pre-experimental values of NP under both marginal location conditions were comparable, whereas those under central conditions were much higher.

Chromium/Calcium (Cr/Ca) ratios of NP showed no drastic changes between the beginning and the end of the experiment (Figure 4.11). Values of NP under central conditions were noticeably higher than those under northern and southern conditions. Cr/Ca ratios of NP showed the highest and lowest variability under southern and northern conditions, respectively. Pre-experimental values were comparable under both marginal location conditions.

Iron/Calcium (Fe/Ca) ratios of NP showed no change under northern conditions between pre and post-experimental measurements (Figure 4.11). However ratios increased under central and decreased under southern conditions, respectively.

Zinc/Calcium (Zn/Ca) ratios of NP showed comparable values under both marginal location conditions (Figure 4.11). Under central conditions, only post-experimental values of NP showed a similar value than under both marginal population conditions. Pre-experimental ratios of NP under central conditions showed a noticeable higher ratio, however, also a high variation. Pre-experimental values under northern conditions were lowest.

Strontium/Calcium (Sr/Ca) ratios of NP showed a decline from pre to post-experimental values under northern and central conditions (Figure 4.11). However, under southern conditions no drastic change was observed and values were similar to those of post-experimental measurements of NP under the other conditions. Pre-experimental values under northern and central conditions were comparable and higher than those under southern conditions.

Cadmium/Calcium (Cd/Ca) ratios of NP showed no drastic change between before and after the experiment under northern and southern conditions (Figure 4.11). However, a steep decrease of Cd/Ca ration was observed under central conditions from pre to post-experimental measurements. Post-experimental values of NP under central conditions were comparable to those of pre and post-experimental values under northern and southern conditions, following the same pattern as Zn/Ca ratios. Pre-experimental values under both marginal location conditions were comparable but lower than those under central conditions.

Barium/Calcium (Ba/Ca) ratios of NP showed an increase from pre to post-experimental conditions under both marginal location conditions (Figure 4.11). A decrease of ratios from the beginning to the end of the experiment was observed under central conditions. The slopes of the increase or decrease under the different temperature conditions were comparable. Under both marginal location conditions

lower pre-experimental and similar post-experimental values of NP were observed compared to under central conditions.

Pre-experimental values of NP for all element ratios, except for Fe/Ca and Sr/Ca, were comparable between both marginal location conditions. Additionally, values under both marginal location conditions of these ratios were much lower compared to pre-experiment values measured under central conditions. All ratios of NP under northern and southern temperature conditions were relatively stable and did not show drastic changes, except for Ba/Ca, Sr/Ca and Mg/Ca and V/Ca under southern conditions (Figure 4.11).

PERMANOVA and SIMPER analysis (Figure 4.12), investigating if NP of *C. officinalis* is taking up the chemical signature of the experimental conditions (e.g. elevated temperature), showed no significant difference between temperature conditions across the geographical gradient in the NE Atlantic ( $P > 0.05$  in all cases, PERMANOVA main test and pairwise comparisons). Additionally, SIMPER analysis presented the main composition of elements for the NP in each locations' thermal condition. Overall, 90.39%, 90.13% and 90.76% of the data were represented in the SIMPER analysis for northern, central and southern conditions (NC, CC and SC), respectively by five major trace elements: Mg, Sr, Zn, Fe and Ba, in that order. For NC, CC and SC 77.76%, 77.20% and 77.88%, respectively, of the data were channelled only in Mg, Sr and Zn in this order. Under all conditions the NP showed the identical order of major contributing elements under all conditions. It was discovered, that Fe, Ba, V and Cr were the elements determining the outliers within CC and SC. However, this is likely to be caused by variations during analysis. The elements describing the NP the most were Mg and Sr. No significant influence of Cd and Zn within and between the conditions was found (Figure 4.12 (B)).

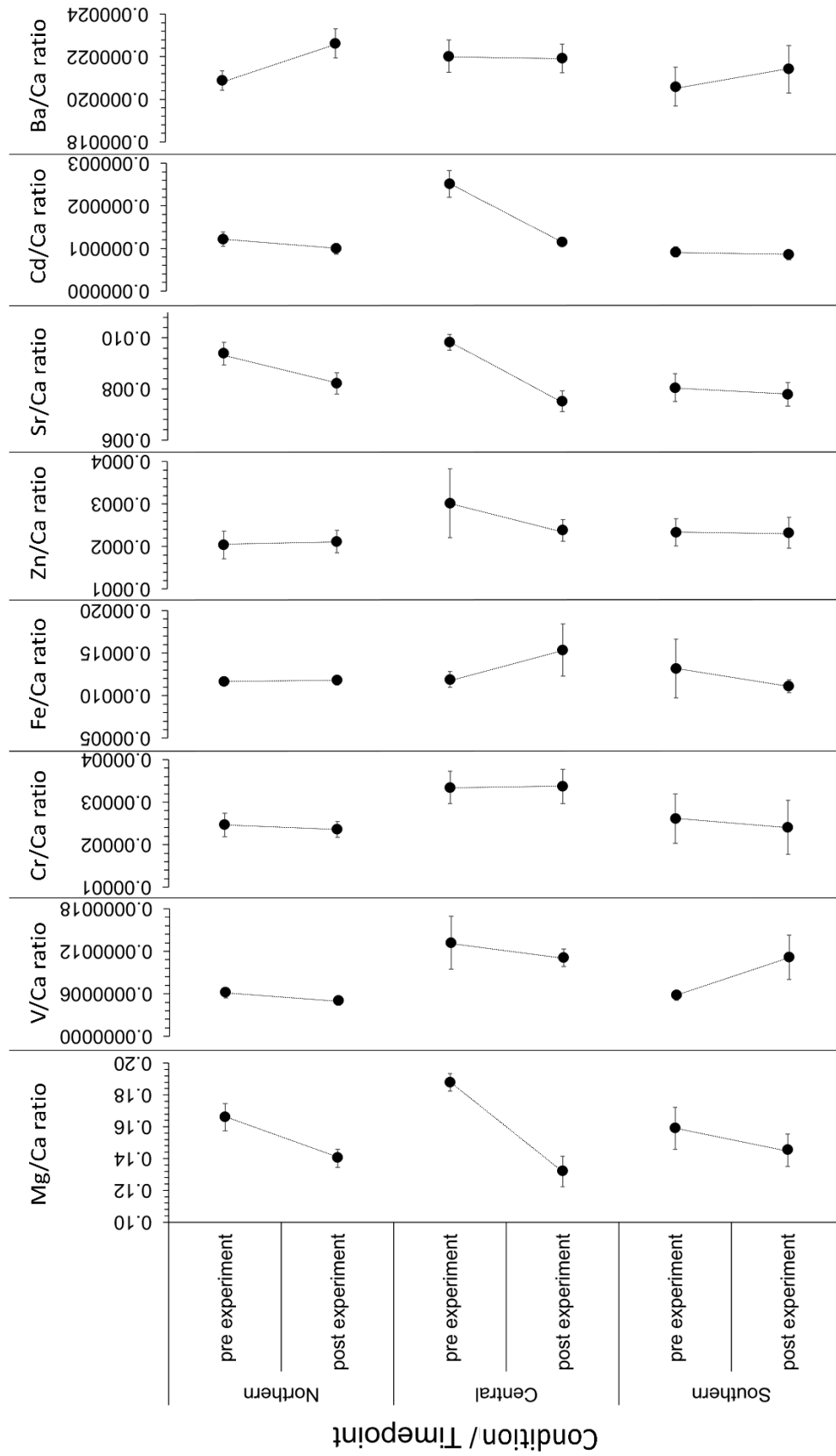


**Figure 4.11:** Element/Ca ratios for all elements. Data points (AV  $\pm$ SE, n = 15) represent northern, central and southern, pre and post-experimental conditions, respectively, for northern populations of *C. officinalis*.



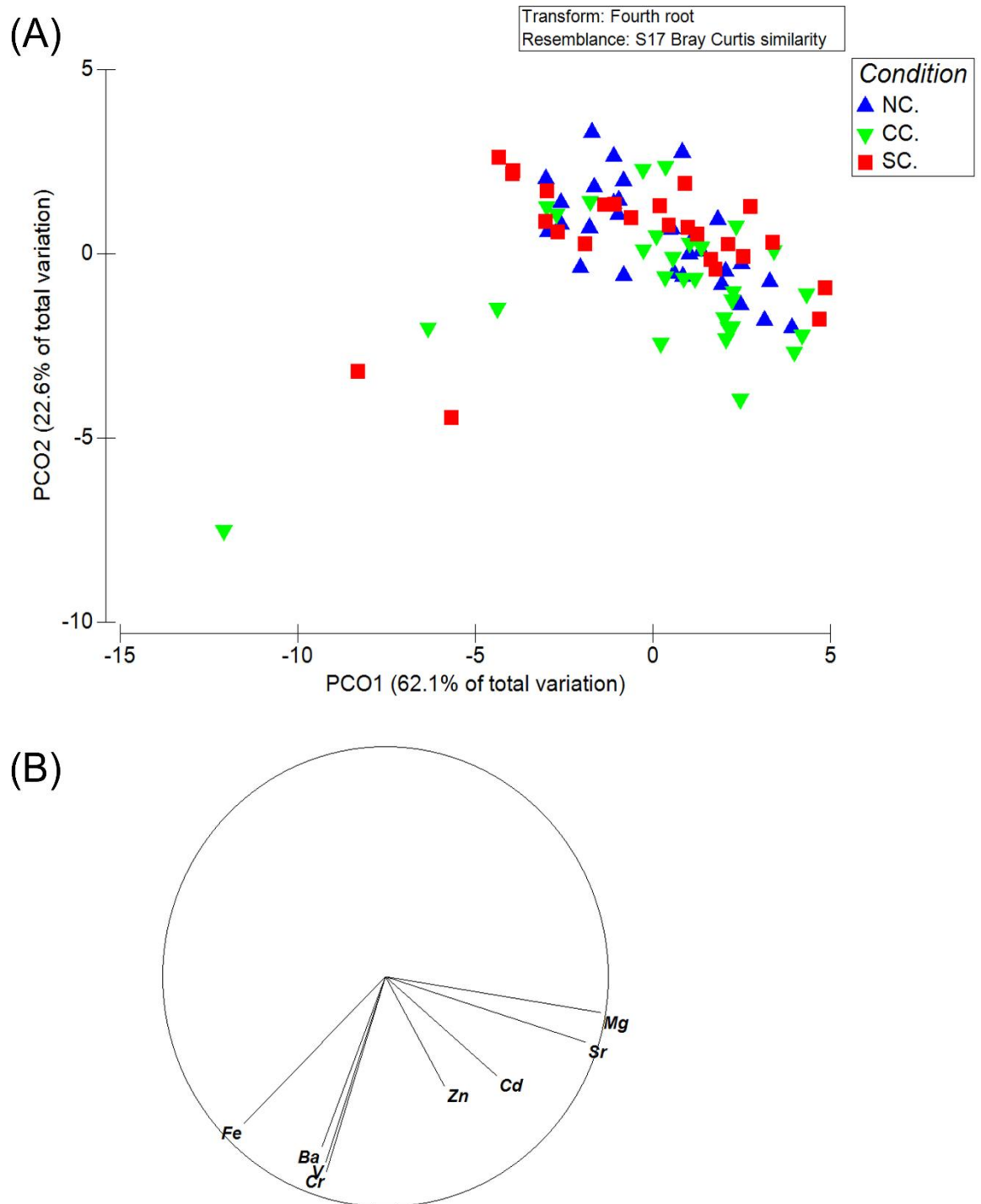


**Figure 4.12:** PERMANOVA (A) and SIMPER (B) results for the northern population of *C. officinalis* under current temperature conditions across its geographic range in the NE Atlantic. Blue triangles, green triangles and red squares represent northern (NC.), central (CC.) and southern (SC.) conditions, respectively.

In the central/southern Common Garden Experiment, magnesium/calcium (Mg/Ca) ratios of all populations (Figure 4.13) under all conditions decreased from before to after the experiment, except for CP1 under southern conditions, which increased. All values were within a comparable range, however, those of both SP under central conditions decreased more and steeper compared to all other. No difference was found between CP under both treatments, for pre and post-experimental measurements, respectively. No difference was found in pre-experimental measurements within SP under each condition. However, a larger decrease of Mg/Ca ratios were observed for post-experimental measurements for both SP under central conditions compared to southern conditions.

Vanadium/Calcium (V/Ca) ratios in SP showed higher values in both, pre and post-experimental measurements as well as under both conditions (Figure 4.13). Ratios for SP were higher under southern conditions compared to those under central conditions. In CP, ratios were marginally higher under southern conditions compared to central conditions. Except for both SP under southern conditions and SP2 in central conditions, no noticeable change was observed between measurements before and after the experiment. Central populations showed no difference between conditions.

Chromium/Calcium (Cr/Ca) ratios showed an increase in all populations under all conditions, except for SP1 under southern conditions and SP2 under central conditions (Figure 4.13). Under southern conditions, no difference between populations ratios range was observed. Under central conditions higher ratio ranges were observed compared to those under southern condition, with steepest increases within CP from pre compared to post-experimental measurements. Cr/Ca ratios of SP were not different between conditions. Those of CP, however were

comparable between pre-experimental conditions but increased more under central conditions compared to under southern conditions.

Iron/Calcium (Fe/Ca) ratios showed a great increase in both SP under both conditions from pre to post-experimental measurements (Figure 4.13). Central populations did not show a noticeable change but variable responses from before to the end of the experiment under both conditions. All pre-experimental values of all populations under all conditions were within a comparable range.

Zinc/Calcium (Zn/Ca) ratios showed only a marginal increase from before until after the experiment for CP under both conditions (Figure 4.13). For SP, all populations showed a steep decrease in Zn/Ca ratio from before until after the experiment under all conditions, except for SP1 that showed an unnoticeable increase in central conditions. Central populations showed comparable values under both conditions before and after the experiment, respectively. Southern populations showed comparable values for pre and post-experimental measurements, respectively. However, ratios for SP were much higher than those for CP under both conditions as well as for pre and post-experimental measurements.

Strontium/Calcium (Sr/Ca) ratios showed a similar range for all populations between pre and post-experimental measurements (Figure 4.13). Ratios for CP increase from before until the end of that experiment under all conditions. However, those of SP decrease around the same amount from before until the end of the experiment under all conditions, presenting an opposing trend between geographic location populations. Pre-experimental ratios were always higher in SP compared to CP, under both conditions, except for CP2 under southern conditions.

Cadmium/Calcium (Cd/Ca) ratios showed a decrease in CP under both conditions, except for CP1 under central conditions (Figure 4.13). No change in Cd/Ca ratios was observed for SP under central conditions before and after the experiment. However, a drastic decrease of these ratios from before to the end of the experiment was noticed in SP under southern conditions. These were the only drastic changes within these ratio measurements. Within each condition, CP showed marginally lower values in pre as well as post-experimental values compared SP.

Barium/Calcium (Ba/Ca) ratios showed an increase from pre to post-experimental measurements in all populations under all treatments (Figure 4.13). Under central conditions, SP increased much more compared to CP. Under central conditions and in SP pre-experimental values were much lower and post-experimental values were much higher compared to the respective values for CP. Under southern conditions SP increased only marginally more from the beginning to the end of the experiment, compared to CP. Pre-experimental values for all populations under southern conditions were comparable whereas post-experimental values of SP were noticeably but not much higher than those of CP.

Changes in all elemental ratios (Figure 4.13) showed little changes and variability in CP independent of temperature conditions. Southern populations showed steeper increases and decreases of elemental ratios under all conditions compared to CP.

PERMANOVA and SIMPER analysis (Figure 4.14 and Figure 4.15 for CP and SP, respectively), investigating if *C. officinalis* is taking up the chemical signature of the experimental treatments (e.g. elevated or decreased temperatures), showed no significant difference between treatments for each populations ( $n = 4$ ) ( $P > 0.05$ , PERMANOVA main test and pairwise comparisons of conditions nested within population). However, it showed a significant difference between the beginning and

the end of the experimental exposure for all populations ( $P < 0.001$ , PERMANOVA pairwise comparison in all 4 cases). A significant difference was found in each condition between locations ( $P < 0.001$ , PERMANOVA main test,  $P < 0.05$ , PERMANOVA pairwise comparison of CP1 and CP2 with SP1 and SP2, but not between populations within one location (CP1 with CP2 and SP1 with SP2, respectively).

Additionally, SIMPER analysis presented the main composition of elements for each country's elemental signature. In CP, 93.17% and 93.23% of the data were represented in SIMPER for CP1 and CP2, respectively. For CP1 and CP2 87.94% and 87.91%, respectively, of the data were channelled in Mg, Sr, Zn and Cr, in this order. The remaining major contributing element is Ba. The same elemental pattern was found for combined CP between the two tested conditions central condition (93.94% described data) and southern condition (92.42% described data). For SP1 and SP2 91.11% and 91.60%, respectively, were represented in the SIMPER analysis and 86.05% and 86.53% for SP1 and SP2, respectively were accumulated by the following elements: Mg, Sr, Zn and Cr, in this order. The remaining major contributing element is Ba. The same elemental pattern was found for combined SP between the two tested conditions CC (91.12% described data) and SC (91.55% described data). It was discovered, that Mg and Sr as well as Fe were the trace elements determining CP under both conditions. The elements Cd, Zn, Cr, V and Ba were of no significant influence (Figure 4.14(B)). In SP under both conditions, the determining trace elements were Mg, Sr, Zn and Fe, with limited influence of Cd, Cr, V and Ba (Figure 4.15).

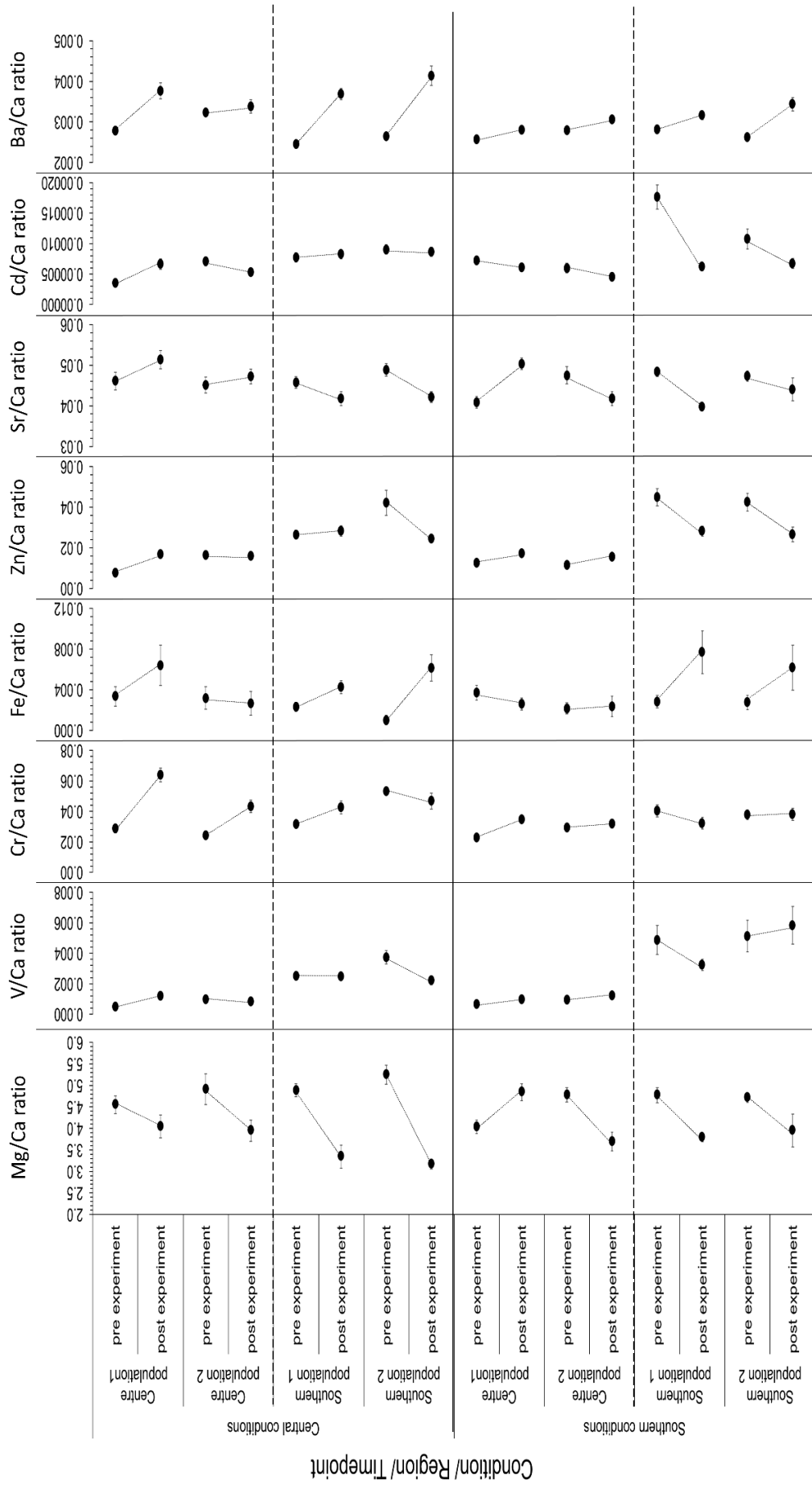


**Figure 4.13:** Element/Ca ratios for all elements. Data points (AV ±SE, n = 15) represent northern, central and southern, pre and post-experimental conditions, respectively, for central and southern populations of *C. officinalis*.

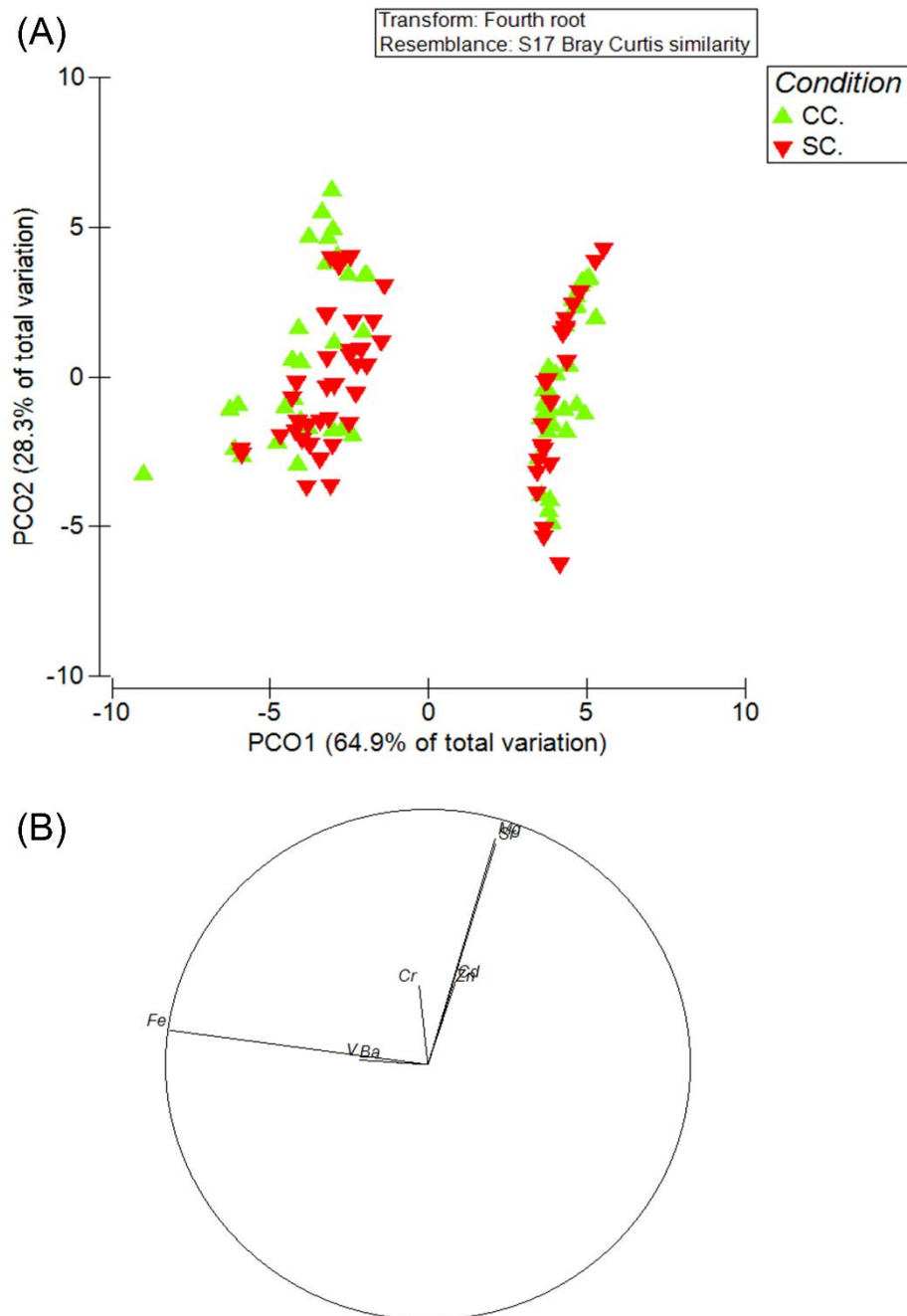


**Figure 4.14:** PERMANOVA (A) and SIMPER (B) results for central populations of *C. officinalis* under current temperature conditions in the centre and south across its geographic range in the NE Atlantic. Green triangles and red triangles represent central (CC.) and southern (SC.) conditions, respectively.

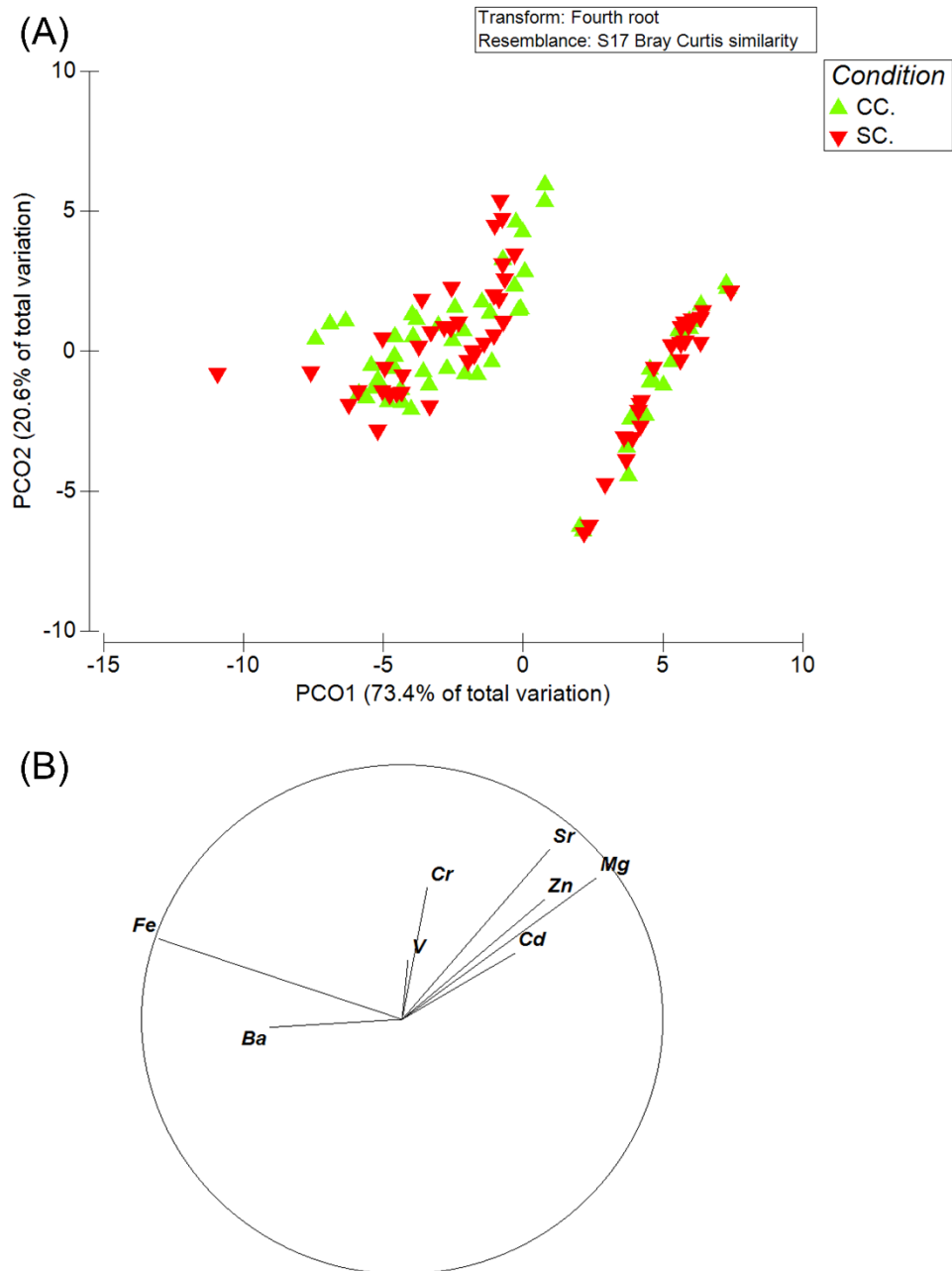


**Figure 4.15:** PERMANOVA (A) and SIMPER (B) results for southern populations of *C. officinalis* under current temperature conditions in the centre and south across its geographic range in the NE Atlantic. Green triangles and red triangles represent central (CC.) and southern (SC.) conditions, respectively.



#### 4.4.5.3 Cell wall thickness and condition

Cell wall thickness was measured for inter- (lateral to growth direction) and intra-cell walls (horizontal to growth direction, Figure 2.13). Due to difficulties in separating cell walls of individual cells, the combined cell wall of two neighbouring cells was measured. Inter-cell walls were thicker than intra-cell walls in all populations under all conditions, prior and after the experiment. Except for SP2 under southern conditions, all pre-experimental measurements were higher compared to post-experimental measurements for all populations under all conditions (Figure 4.16).

The NP of the separate Common Garden Experiment showed similar cell wall thickness than CP. It showed no drastic change from pre to post-experimental measurements under northern conditions. Under central and southern conditions cell wall thickness decreased throughout the experiment but not significantly. Thickness decreased equally in inter- and intra-cell walls. After the experiment, the NP showed significant differences in intra- as well as inter-cell wall thickness with SP1 and CP1 under central conditions ( $P < 0.01$ , Kruskal-Wallis H test in all cases) as well as with CP2 under southern conditions ( $P < 0.01$ , Kruskal-Wallis H test in all cases). Within inter-cell wall thickness, the NP showed a significant difference before and after the experiment under northern conditions. Additionally, a significant increase in inter-cell wall thickness was found after the experiment between northern and southern conditions ( $P < 0.01$ , Kruskal-Wallis H test).

Central population 1 showed a significant decrease in inter- and intra-cell wall thickness between pre and post-experimental measurements under central conditions ( $P < 0.01$ , Kruskal-Wallis H test in both cases). The difference in thickness between intra- and inter-cell walls was greater prior compared to after the experiment in both CP under all conditions. Under central conditions a significant

difference in intra-cell wall thickness was found before the experiment between SP and CP ( $P < 0.01$ , Kruskal-Wallis H test in all cases). Under southern conditions a significant difference before the experiment in intra-cell walls were found between SP2 and SP1 and both CP ( $P < 0.01$ , Kruskal-Wallis H test in all cases). Additionally, intra-cell wall thickness of SP was significantly different after the experiment compared to CP2 under southern conditions and between SP2 and CP2 to SP1 and CP1 under central conditions ( $P < 0.05$ , Kruskal-Wallis H test in all cases). Both CP showed significant differences in intra-cell wall thickness after the experiment, between central and southern condition. Inter-cell wall thickness of CP showed a significant difference between each other after the experiment under central conditions ( $P < 0.01$ , Kruskal-Wallis H test). Additionally, a significant decrease in thickness was found under southern conditions for CP2 from before to the end of the experiment ( $P < 0.01$ , Kruskal-Wallis H test). After the experiment, CP1 showed a significant difference between central and southern conditions ( $P < 0.01$ , Kruskal-Wallis H test) and CP1 is significantly lower compared to SP1 under central conditions after the experiment.

Southern populations showed a moderate decrease in pre and post-experimental measurements under any condition compared to central and NP. A greater difference between intra- and inter-cell wall thickness was found for SP under central conditions compared to southern conditions. In intra-cell wall thickness, a significant difference was found in SP1 between central and southern conditions after the experiment ( $P < 0.01$ , Kruskal-Wallis H test) and for SP2 before the experiment ( $P < 0.01$ , Kruskal-Wallis H test). Additionally, within inter-cell wall thickness, a significant difference was found after the experiment for SP2 between central and southern conditions ( $P < 0.01$ , Kruskal-Wallis H test). When comparing

pre and post-experimental inter-cell wall thickness, a significant decrease was found in SP under central conditions ( $P < 0.01$ , Kruskal-Wallis H test in both cases).

Whereas marginal populations showed higher variations in their response to changed temperature conditions, CP exhibited more stable patterns within their changing cell wall thickness due to temperature increase.

**Table 4.6:** (A) Mean  $\pm$ SE (n = 15) for inter- and intra-cell wall thickness (CWT) of *C. officinalis* (n = 2 populations for Central and Southern, respectively) within the Common Garden Experiment. (B) Statistical comparison between populations within temperature treatment and between temperature treatments within population, pre- and post-experimental.

(A)						(B)																																	
Region	Population	Treatment	Experiment time point	Inter-cell wall thickness [mm month <sup>-1</sup> ]		Intra-cell wall thickness [mm month <sup>-1</sup> ]		Significance levels: NS = not significant * = P < 0.05 ** = P < 0.01 *** = P < 0.005																															
				Mean	$\pm$ SE	Mean	$\pm$ SE	Northern population				Central population				Southern population				Northern population				Central population				Southern population											
								1				2				1				2				1				2											
								pre				post				pre				post				pre				post				pre				post			
North	1	North	pre	1.47	0.041	1.16	0.045	NS				NS				NS				NS				NS				NS											
			post	1.30	0.047	1.13	0.046	NS				NS				NS				NS				NS				NS											
		post	1.41	0.048	1.37	0.047	NS				NS				NS				NS				NS																
	post	1.70	0.066	1.35	0.038	NS				NS				NS				NS				NS																	
	Central	1	Central	pre	1.76	0.064	1.42	0.064	NS				NS				NS				NS				NS														
				post	1.08	0.041	0.92	0.028	NS				NS				NS				NS				NS														
post			1.31	0.055	1.11	0.041	NS				NS				NS				NS				NS																
post		1.31	0.043	1.24	0.047	NS				NS				NS				NS				NS																	
post		1.26	0.040	1.04	0.039	NS				NS				NS				NS				NS																	
South		1	Central	pre	1.62	0.045	1.07	0.041	NS				NS				NS				NS				NS														
	post			1.31	0.030	1.00	0.028	NS				NS				NS				NS				NS															
	post		1.41	0.039	1.18	0.038	NS				NS				NS				NS				NS																
	post	1.18	0.048	1.14	0.037	NS				NS				NS				NS				NS																	
	post	1.41	0.052	1.18	0.040	NS				NS				NS				NS				NS																	

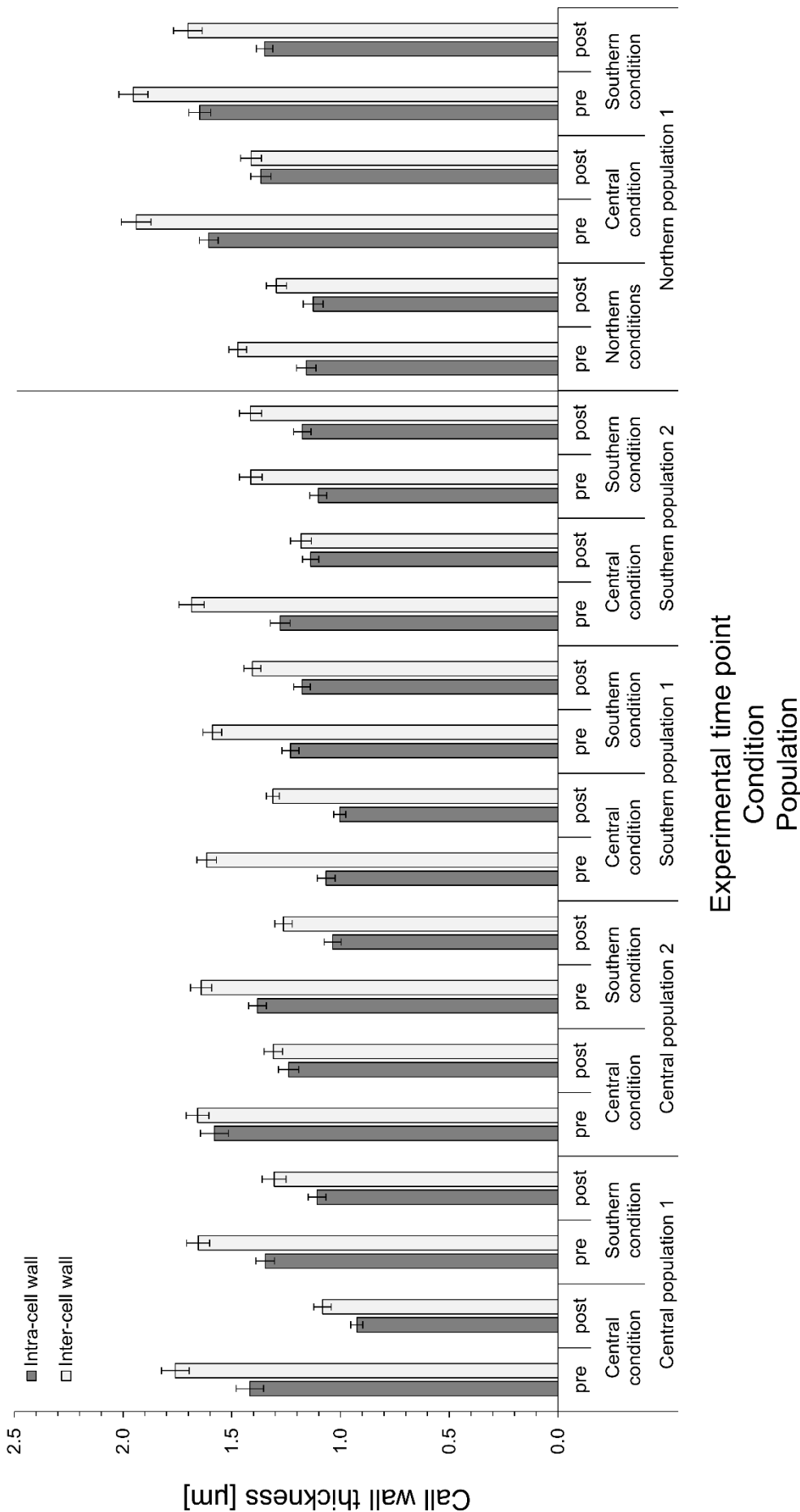


**Figure 4.16:** Inter- (grey bars) and intra-cell wall thickness (black bars) of *C. officinalis* across its geographical distribution in the NE Atlantic ( $AV \pm SE$ ,  $n = 15$ ) under central, southern and northern (for northern populations only) location conditions. Black line separates the two different experiments.

## 4.5 Discussion

In this study, it is investigated, how physiological and structural traits of *C. officinalis* differs when exposed to temperatures across its geographical distribution in the NE Atlantic. For this, various physiological and structural parameters were determined and discussed in the following paragraphs. Due to the exposure to a wide range of temperatures, *C. officinalis* shows different, including local and seasonal, adaptation depending on their location.

### 4.5.1 Resilience to existing thermal conditions

Understanding the physiology of *C. officinalis* and its interactions with the environment is crucial to be able to predict how different portions of the species distribution may be affected by current and future warming rates. Here, evidence for distinct vulnerability to thermal stress of central and peripheral populations of *C. officinalis*, a key marine ecosystem engineer (Kelaher *et al.*, 2003, Daleo *et al.*, 2006) is presented.

During the experiments, southern conditions presented highest pH and saturation states. This finding is caused by the interplay of parameters, such as temperature, salinity, carbonate chemistry, gas solubility in seawater etc., and organisms in the experimental aquaria. Such differences in natural environments are very likely to cause species specific local adaptation.

Oxygen evolution curves (P-I curves) and calcification evolution curves (C-I curves) show clear regional responses. This suggests that data obtained in this study could be interpreted as representative for most populations of these and surrounding regions (Egilsdottir *et al.*, 2016; Williamson *et al.*, 2017), excluding those in extreme environments. However, there is added complexity when considering the maximum

level of oxygen produced ( $P_{\max}$ ), indicating its dependency on and potential adaptations to the initial environment of the population, due to genetic differences between populations (Yesson *et al.*, 2018). No photoinhibition was detected during this study, which could be due to physiological mechanisms leading to the ability to cope with higher light conditions and/or possible shore adaptation.

Central and northern populations may become more stressed under higher temperature conditions, as already published for central crustose coralline algae (Diaz-Pulido *et al.*, 2012). Central populations seemingly experience their temperature optimum. Northern populations may be locally adapted and additionally, show a capability to thrive in warmer conditions, hereafter have not reached their temperature optimum in their current geographic location. Northern populations may be able to adapt to warmer conditions, which is also reflected by stable primary production rates. However, southern temperature conditions induced a decrease in  $P_{\max}$ , leading to the assumption, that all populations, including SP, were temperature inhibited in southern conditions. Southern populations may be temperature inhibited although exposed to their local temperature condition due to the fact that at the current southern margin, populations are already impacted by increasing sea surface temperatures.  $P_{\max}$  of the NP increases in temperature elevated central conditions, however primary production and respiration rates stay stable and calcification rates decline which may lead to shorter individuals. Declining calcification rates, however, may also be caused by the decreased  $T_A$  in the experimental design that was noticeable lower in the first compared to the second Common Garden Experiment, even though a constant water supply was assured. A decrease of  $P_{\max}$  of the NP under southern conditions in combination with increased primary production and respiration rates but decreasing calcification rates

implies that in NP energy might be primarily used for photosynthetic processes instead of maintaining calcification rates and growth. Giving primary production a priority amongst their metabolic processes could be explained by the fact that these populations have the thickest cell walls and therefore may not need to spend as much energy on maintaining these compared to the other geographic location populations. This finding could mean that NP were compensating for the lack of production during low light winter periods by increased production when light is available.

$C_{max}$  confirms that central conditions were more favourable than southern conditions for all four populations. In P-I curves, SP show a steeper  $\alpha$  than CP, demonstrating a more efficient light harvesting capability. The steeply decreasing  $\alpha$  in oxygen evolution curves of SP under central conditions can be explained by either increased physiological stress and a lower capacity for photosynthesis or by a geographic effect causing different responses depending on latitudinal origin of populations (Williamson *et al.*, 2018). For the same populations and conditions however,  $\alpha$  of the calcification evolution curves increase slightly which indicates an opposite trend compared to  $\alpha$  of oxygen evolution curves described above. This coincides with the observed, significant reduction of net production but not calcification rates for SP. A minimal increase of  $\alpha$  in oxygen evolution curves of CP under southern conditions correlates with Williamson *et al.* (2018), who also found that CP do not differ significantly in winter and summer conditions, which were similar to populations exposed to southern conditions in this study. In warmer temperatures, the tested populations also show an increase in their saturating light irradiance ( $I_k$ ) for C-I curves. However, even higher  $I_k$  values for calcification evolution were reported in France and the UK (Egilsdottir *et al.*, 2016; Williamson *et al.*, 2017). This indicates



that *C. officinalis* might be able to withstand future central conditions regarding  $I_K$  for its calcification, up to a certain extent.  $I_K$  values for P-I curves were lower under southern compared to central conditions for all populations in this study. This indicates that all specimens maintained under southern conditions reach their maximum photosynthetic level at lower irradiance and could therefore experience damage of photosynthetic systems sooner compared to same populations living under central conditions. Similar findings were reported in Williamson *et al.* (2018), who found a photoacclimation to changing irradiances at seasonal timescale as well as a protection of photosystems during high-light conditions. Those high-light conditions could be resembled by southern light conditions for central and northern populations during the experiments in this study. Additionally, maximum photosynthetic levels at low irradiance together with the lower light harvesting efficiency may result in exhaustion of photosynthetic systems due to very fast reactions within the metabolic pathways and the energy consumption for photon harvesting. Southern temperature conditions, therefore, present a less favourable environment for all populations.

This study highlights a significant change in primary production of southern margin and CP when subjected to temperature conditions of the opposite distributional region. Central populations show reduced respiration rates under southern conditions. Similar behaviour was found by Davison (1991) for the brown alga *Saccharina latissima*. Central populations show reduced net production under southern conditions indicating stress. However, they were still able to withstand warmer temperatures, in contrast to SP which may not be able to survive changing conditions over prolonged periods in their current habitat and may experience a southern range contraction (Lima *et al.*, 2007). Net production rates of SP drop

drastically under central conditions, resulting in oxygen uptake instead of production. These rates were similar to rates found under southern conditions, indicating these populations were unable or may take a longer time to adapt to central conditions. It was shown that photosynthesis can stimulate calcification and that its increase could offset the  $\text{CaCO}_3$  dissolution in different calcifying algae in response to increased  $\text{CO}_2$  (Borowitzka, 1982, Gattuso *et al.* 1999, Hofmann *et al.* 2012a,b, Johnson and Carpenter, 2012, McCoy *et al.*, 2016). Therefore, it can be expected, and findings indicate, that CP downregulate calcification before photosynthesis and respiration in warmer temperature conditions. The NP showed drastically higher calcification rates prior to and comparable rates with CP and SP after the experiment. This leads to the assumption, that these rates may be responsible for highest cell wall thickness that is found for NP independent of temperature conditions. Contrary to central conditions, the NP did not show temperature inhibition under southern conditions. This could be another reason for the increased adaptability of NP contrary to these at lower latitudes across the species distribution.

The recovery rate of all locations showed high variability in NP and CP, with highest and lowest rates of all, and were reflected in the respective primary production rates. The change in pattern observed at t23, where NP discontinue to and SP start to show the identical pattern to CP, may imply that NP were more resilient to changing conditions which can be interpreted by the increase in recovery contrary to a decrease in CP and SP towards the end of the experiment. Another interpretation of this change focusses on the acclimatisation time needed. T23 demonstrates to be the time point when high variation between measurements reduces and a more constant response is measured. Therefore the behaviour of populations regarding

recovery time needed is mostly reflected in the second half of the experiment. This is reflected in the end results for primary production and respiration which also decreased. This pattern is reflected by personal observations during the first Common Garden Experiment in which a 100% survival rate was observed for NP, however, CP and in particular SP were dramatically affected by changed conditions. Southern populations did not survive under all conditions and CP did not survive under southern conditions.

Pre-experimental values of primary production during recovery measurements show the same pattern in CP and NP but not SP. Southern populations showed a lower primary production rate and therefore, may be better adapted to fast changing light conditions (from dark or low to high light intensities), whereas NP and CP show local adaptation to lower light levels and shorter light periods through adaptation over time rather than a relatively constant level as observed in SP. At the same time, SP may be at the limit of their adaptation potential since no increase in rates was observed under any exposure.

Calcification in the light and in the dark showed drastic negative changes for CP under southern conditions, confirming the uncoupling of photosynthesis and calcification. Central populations were shutting down light calcification metabolism resulting in dissolution which coincides with the respective growth rate and cell wall thicknesses, losing  $\text{CaCO}_3$  in intra-cell walls. Central and southern populations have similar light calcification before and after the experiment under central control conditions demonstrating that there was no tank/experiment effect on the populations. Light and dark calcification found in the literature were lower than these found in this study (El Haïkali *et al.*, 2004, Egilsdottir *et al.*, 2013; Williamson *et al.*, 2017). This coincides with the elevated photosynthesis and respiration rates.

Southern populations reduce light calcification only by a small amount under central conditions (McCoy *et al.*, 2016) but show increased respiration and decreased net production, suggesting down regulation of photosynthetic activity before calcification mechanisms. This is also supported by  $C_{max}$  values obtained in this study which were higher under central conditions than under the control southern conditions.

Additionally, SP under central conditions showed a reduced growth but an increased cell wall thickness. It can therefore be concluded that the little calcification that is observed is helping to maintain the inter-cell wall thickness instead of supporting growth. High variability in dark calcification was observed in all populations in all treatment, reflecting findings of McCoy *et al.* (2016), and indicating that the already small amount of dark calcification is easily influenced by environmental parameters such as temperature. Dark calcification rates of CP decreased to close to zero under southern conditions, confirming downregulation of dark calcification. This, in addition to the decline in light calcification rates, results in a higher dissolution rate of CP under southern conditions than under control conditions. A decrease of dark calcification of SP under central conditions indicated slow or no ability of SP to adapt to colder temperature regimes. At the same time CP show similar behaviour in warmer temperatures. All of this shows that the two processes of calcification and photosynthesis are not as tightly coupled as previously assumed.

While oxygen evolution and calcification evolution data perfectly mirror the net production and respiration, calcification results could resemble the high *in situ* variability between CP which may be due to environmental adaptations rather than genetic adaptations. This is supported by the very similar calcification rates in the light after the incubation of CP in southern conditions compared to the pre-experimental measurements. This also means that it was not possible to determine

the timing of when CP kept under southern conditions began to reduce light calcification rates.

A high variability in both  $\alpha$  and  $I_k$  of P-I and C-I curves, also found by Egilisdottir *et al.* (2016), in SP shows that adaptation ability can strongly depend on region of origin and the stress already experienced in their natural environment. Combining the knowledge gained from this study, CP seem to be more robust, resilient and adaptable to future climatic changes as predicted by the IPCC (2013) than SP. According to Williamson *et al.* (2017), *C. officinalis* populations in Southern England are adapted to variability in environmental stressors both, in short (tidal) and long (seasonal) timescales. This is consistent with the findings of primary production, respiration as well as light and dark calcification, leaving the CP better adapted to changes than SP in this study and others. This supports the centre-to-margin hypothesis (Guo *et al.*, 2005) for *C. officinalis*. Additionally, this study also demonstrates that *C. officinalis* needs a minimum amount of 4 weeks, but preferably longer, to fully acclimatise to altered conditions such as changes in temperature or pCO<sub>2</sub>.

Even though relatively static conditions were kept in this experiment and no tidal movement was simulated due to facility restrictions, parameters were chosen to be at the predominant existing light and temperature conditions of the season in which the algae were sampled in and which they would experience when submerged during inter-tidal periods. This ensured the measurement of the optimum and most realistic physiological responses of *C. officinalis* to the opposite populations conditions by being in their predominant state of being submerged and not stressed by abiotic factors during low tide conditions.

The speed in which climatic changes are observed today may be too rapid for this species to be able to adapt fully to them. This may result in loss of genetic diversity in *C. officinalis* and species ranges may shift and become confined. This was previously also found by Collevatti *et al.* (2011) in a Common Garden Experiment with the neotropical tree species *Caryocar brasiliense*, which experiences a climate change-induced restriction of ideal habitat for their southern margin populations. According to the authors, this leads to a drastic decrease of genetic diversity and numbers of alleles due to the survival and reproduction success of only the most adapted genotypes under future climatic conditions. Additionally, it leads to the reduction in individual fitness and therefore population evolutionary potential. Another study performed a Common Garden Experiment on multiple species of ants and found an elevated temperature induced decrease in survival and brood production (Pelini *et al.*, 2012). The authors of this study indicate that the decline in these two factors will lead to a loss of genetic diversity. A potential change in genetic diversity and percentage cover due to a potential decrease in growth rates of *C. officinalis* in rocky shore intertidal ecosystems was suggested to lead to loss of diversity of this macroalgal genus as well as associated flora and fauna. It is unclear, however, how flora and fauna would adapt to gradual changes in hosts.

As already pointed out by Melbourne *et al.* (2015), little research was conducted on changes in structural integrity of coralline algae. Structural components such as cell wall thickness are reflecting growth rates as well as calcification rates and show highest values in NP and comparable values between CP and SP. Growth of SP were lower under central than southern conditions and showed much greater error bars, which could be caused by the growth of reproductive cells which were overly present in SP compared to both other population locations. This production of

conceptacles may be the reason for constant calcification rates and decreased primary production rates in SP contrary to the expected decrease in calcification under temperature elevated conditions. Southern populations, therefore, may try to increase their chance of survival in unfavourable conditions by focussing on increasing reproduction instead of growth and calcification which is underlined by stable primary production rates to produce the energy needed to grow conceptacles but now linearly. The highest growth rates and cell wall thickness were measured in the NP, this coincides with ~10-times higher calcification rates prior to the experiment, which declined to comparable values (with CP and SP) after the experiment under all temperature conditions. Therefore, elevated growth rates and cell wall thicknesses were expected and observed.

Staining success above  $76.9 \pm 11.6\%$  throughout the study confirms practicability of the chosen stain as already found by other studies (Colthart and Johansen 1973, Andrade and Johansen, 1980, Blake and Maggs, 2003). It can be safely assumed that other factors had no major external influence on staining, such as e.g. loss of stain due to abrasion as it was described for *C. officinalis* (Andrade and Johansen, 1980). Staining success using the same stain and method revealed staining success of ~30% in other studies on coralline algae (Ragazzola *et al.*, 2013, Blake and Maggs, 2003).

Trace element/Calcium ratios were considerably lower in the NP compared to CP and SP. Additionally, all elements were most variable in increase or decrease under southern conditions and/or in SP which may be due to a highly variable metabolism caused by stress. Until today, it was understood, that hardness and elasticity is positively correlated with Mg/Ca ratios and temperature. Mg/Ca ratios had declined in all populations by the end of the experiment causing branches to become softer.

Due to the design of the study, it can be ruled out that the decline in ratio values was introduced by external factors, such as light availability, which are known to alter Mg/Ca content indirectly through altered growth (Caragnano *et al.*, 2017, Andersson *et al.*, 2008). Mg/Ca ratios represent a temperature indicator for environmental temperatures (Milliman *et al.*, 1971, Kolesar, 1978) which is expressed as steepness of decreasing ratio values in this study e.g. due to colder temperatures that SP were exposed to. Comparable findings were described by Caragnano *et al.* (2014), here the authors found higher mol% MgCO<sub>3</sub> within the genus in specimens exposed to higher temperatures. Elevated V/Ca ratios under warmer conditions in all populations mirror greater growth rates as V represents an indicator function for chlorophyll a production, as well as increased growth (Wilhelm, 1984a,b, Meisch and Benzschawel, 1978). Cr/Ca ratios shows no greater impact on any of the populations across the latitudinal gradient. However, a greater increase from pre to post-experimental conditions was observed under colder central compared to southern conditions. No decrease in photosynthetic activity and growth was observed that may be due to increased Cr concentrations causing a decrease in productivity (Sari and Tuzen, 2008). Fe/Ca ratios were less variable and showed less increase or decrease in colder conditions. This leads to the assumption that due to its function to enhance electron transport in photosynthetic reactions and subsequently the enhancement of primary production rates (Raven *et al.*, 1999 and references therein), a greater amount of Fe is necessary to influence metabolic processes than it is observed in this study. The assimilation of CO<sub>2</sub> as well as elevated protein and amino acid build-up is associated with Zn/Ca ratios (Kitano and Hood, 1962, Rout and Das, 2003, Raven *et al.*, 1999). It is found to be higher in SP, however it is temperature independent due to its increase under all temperature conditions. An increase Zn concentration in the skeleton may lead to higher primary



production rates as well as calcification rates. However, NP show the lowest Zn concentration within their skeleton but the highest calcification and comparable primary production and respiration rates. Ratios of Sr/Ca and Ba/Ca are known to represent an indicator for salinity that the specimens were exposed to (Schöne *et al.*, 2010, de Villiers 1999). Even though Sr/Ca ratios did not show a clear correlation with salinity, the steepness of the increase or decrease under central conditions is higher compared to under northern or southern conditions. This may confirm the central conditions to be the most favourable conditions whereas marginal location conditions are considered to be less favourable and therefore changes in skeletal elemental compositions might be harder to identify.

Ba/Ca ratios, indicating freshwater discharge into the marine environment (Gillikin *et al.*, 2006) and a negative correlation with salinity (Caragnano *et al.*, 2014, Hanor and Chan, 1977, Nelson *et al.*, 2018, McCoy and Kamenos 2015 and references therein), do not show a clear indicator ability within *C. officinalis* and is also shown for other genera, to present very little changes (Caragnano *et al.*, 2014). Indicating pollution and therefore reduced productivity and growth in algae and higher plants (Kangwe *et al.*, 2001, Vymazal, 1987 and references therein, Nazar *et al.*, 2012), Cd/Ca ratios were higher under warmer temperature conditions and in SP mirroring their origin from sites close to fish farms and shellfish factory outflows as well as anthropogenic pollution. Throughout the experiment, values decreased which may be caused by the exposure to cleaner water condition in the culturing facilities compared to the origin.

#### 4.5.2 Methodological Limitations

Due to some limitations in preparation of samples or implementation of analysis, some aspects were carefully considered. It was made sure that none of the limited

sample sections were analysed, however, during cell wall thickness measurements it was noticed, that some parts were not polished horizontally but at an angle due to the nature of the branch and the positioning during the embedding process. Therefore, when discussing this data, it has to be taken into consideration that high errors might emerge.

Additionally, a relatively high variability in trace elemental data sets can be observed. This may be due to the positioning of the ablation spot on the branch, which may not include the same amount of material in the top of the branch compared to lower parts of the branch due to age of the cell walls and the associated lower amount of material with younger age as cell walls are still under construction. Both Common Garden Experiments were conducted as winter experiments, however, the first Common Garden Experiment with the NP was set up in a flow-through aquaria system with constant water supply, whereas the second Common Garden Experiment was conducted as a closed system with aquaria being placed in water baths to keep the temperature constant. The two different experimental designs urge for caution when comparing northern ( $n = 1$ ) to CP or SP ( $n = 2$  for central and southern, respectively).

Different magnitude of ratios in most trace elements may be due to the usage of two different laser set-ups during analysis with the second laser being more accurate and reliable than the first. An additional reason could be the data reduction after collection using two different software, which is supported by the observation of much lower count in the NIST 610 Standard in session 1 compared to session 2. A justification of this magnitude of increase between both experiments cannot be justified by the increase of temperature which is associated with an increase of mol% Mg/Ca (Williamson *et al.*, 2014).

## 4.6 Conclusion

To conclude, central and northern populations may be able to adapt to warmer temperature conditions in future oceans but at the same time central populations may experience a loss in percentage cover in intertidal, rocky, coastal zones. Central populations' calcification and cell wall thickness is negatively impacted by elevated sea surface temperatures, potentially resulting in reduced resilience. Southern populations' most negatively affected physiological process in central conditions was production rates, implying a reduced resilience in these populations as well. With sea surface temperatures warming up in northern regions of the species distribution, southern populations may be able to shift their distribution northern wards and therefore potentially disappear entirely in their original environment due to even warmer conditions in future ocean environments. This study showed adaptation potentials of sample populations of *C. officinalis* to various existing temperatures across its geographic distribution in the NE Atlantic. It clarified significant differences between populations of different countries and presented an unequivocal North-to-South gradient in their physiology as well as their structural integrity and the ability to adapt to changing temperature. Northern populations were proven to be more adaptable to changing temperatures compared to central or southern populations. The severe effects on *C. officinalis* caused by changing temperatures could also lead to changes within the respective ecosystem due to missing important functions these algae would no longer perform.

# Chapter 5

*Adaptation of Corallina officinalis to  
future climatic changes across its  
geographical distribution in the NE  
Atlantic*

## 5.1 Collaboration Disclaimer

The data describing the physiological and structural properties of the populations of *Corallina officinalis* used in this thesis and in this chapter were gathered with the help of several volunteers. Some of the monitoring data collected during this thesis was also used by MPhil Aditya Putra (Putra, A.D., 2019).

## 5.2 Introduction

Anthropogenic input of carbon dioxide in the atmosphere has resulted in a changing climate over the past 17 decades and might further fuel global climate change in future centuries (IPCC, 2014a). Key components of climate change in the ocean are ocean acidification (OA; decreasing pH and carbonate ion concentration [ $\text{CO}_3^{2-}$ ]) and rising sea surface temperatures. Living organisms already experience effects of climatic changes and will continue to be critically affected by these changes (Lesica and McCune, 2004, Sanford *et al.*, 2006, Bentz *et al.*, 2010). Investigating and monitoring organism physiology and structure provides important information to predict their acclimatisation and resilience to future environmental conditions and potential changes in their distribution (Kelly and Hofmann, 2013).

Climatic changes are engendered and enhanced by increasing greenhouse gas levels in the atmosphere since industrialisation around 1750. Greenhouse gas emissions are expected to double by the year 2100 (IPCC, 2014c, Feely *et al.*, 2004), therefore, these climatic changes pose risks for people, economies, societies and global ecosystems (IPCC, 2014c). Sources and sinks of carbon and carbon dioxide in the environment are the emission of  $\text{CO}_2$  by animals and plants through respiration as well as the accumulation of carbon by plants through photosynthetic reactions and binding it in biomaterial. According to the IPCC, until today, 30% of the total anthropogenically emitted  $\text{CO}_2$  were absorbed by the ocean causing

changes in ocean chemistry (Figure 1.1; IPCC, 2014c) and therefore changes in organisms and ecosystems. CO<sub>2</sub> absorbed in the ocean also causes a drop in pH within the ocean which was observed to already have changed by ~0.1 since the industrialisation and is predicted to drop a further ~0.2 until the end of the century (Wolf-Gladrow *et al.*, 1999, IPCC, 2013). This drop of pH is accompanied by increased concentrations of carbonic acid (H<sub>2</sub>CO<sub>3</sub>) in the ocean due to the reaction of CO<sub>2(aq)</sub> with water (H<sub>2</sub>O). Lower pH is mainly caused by decreasing CO<sub>3</sub><sup>2-</sup> concentrations and increasing HCO<sub>3</sub><sup>-</sup> concentrations (Zeebe and Wolf-Gladrow, 2001). This change in ocean carbonate chemistry also has an effect on the dissolution and formation of calcium carbonates (CaCO<sub>3</sub>) which subsequently affects calcifiers, which precipitate and accumulate CaCO<sub>3</sub> in their shells and skeletons. Changing saturation states of calcite and aragonite, the two main building blocks for shells and skeletons in the marine environment, and decreased availability of CO<sub>3</sub><sup>2-</sup> ions have a profound negative effect on the ability of calcifiers to build their structures.

Additional pressure is imposed on marine organisms by warming sea surface temperatures (~0.11°C per decade), induced by climatic changes (Broecker and Takahashi, 1977, Levitus *et al.*, 2009, IPCC, 2013, 2014a). More frequent and severe heatwaves may occur and have supplementary effects on species and humanity (Kerr, 2011, IPCC, 2014a). All these different drivers and consequences of recent climate change can directly or indirectly influence organisms, e.g. through changing metabolic processes like consumption rates or biotic interactions like stronger top-down effects (O'Connor, 2009, Hampe and Jump, 2011) or even through alteration of ocean circulations (IPCC, 2014b).

It is suggested that the geographic centre of a species distribution holds the most favourable conditions and therefore holds the highest population density (Whittaker, 1956, Brussard, 1984). When moving away from the centre towards the margins of the distribution, environmental variables are thought to become less favourable due to greater abiotic stress and increased interspecific competition (Aitken *et al.*, 2008), initiating a decrease in population densities and lower relative fertility (Case and Taper, 2000). Further, Watkinson and Sutherland (1995) described a higher mortality than recruitment rate for local marginal populations, also called sink populations, whose survival depend on influx of zygotes or spores from source populations.

Species in different ecosystems react differently to environmental changes. In terrestrial studies Franco *et al.* (2006) showed that three out of four butterfly species were reported extinct or showed drastic distributional changes due to climate change along with habitat degradation and loss. Another study by Lesica and McCune (2004) showed that the southern margin of arctic-alpine indicator plant species declined in their abundance within 13 years which is caused by increasing average summer temperatures. Previous research has also found that different populations of the same species respond differently to altered environmental conditions (Gaston, 2009, Bozinovic *et al.*, 2011, Calosi *et al.*, 2017). In the marine environment, a number of studies across several taxonomic groups, *e.g.* fish, molluscs, zooplankton or seaweed, have focused on the diversification of populations along a thermal-latitudinal gradient (Morley *et al.*, 2009, Dam, 2013, Bennett *et al.*, 2015, Teske *et al.*, 2019).

Comparing central to marginal populations of species provides an understanding of determinants of species ranges and an understanding of how spatial variation in

fitness translates to population-level differences in abundance (Sexton *et al.*, 2009, Araújo *et al.*, 2014, Guo, 2014). Thus, range limits can aid as testing grounds to understand the conditions by which populations can adapt — or fail to adapt — to novel conditions (Sexton *et al.*, 2009). Marginal populations therefore represent an important source for speciation events in the future, triggered by e.g. climatic changes, subsequently developing unique eco-physiological local adaptations and genetic structure (Sexton *et al.*, 2009, Araújo *et al.*, 2009).

Intertidal species inhabit the shores along coastlines where frequent increases and decreases of water levels due to tidal influence prevail. Therefore, as part of the daily cycle, these organisms are exposed to additional abiotic and biotic stress, such as exposure to air, direct sunlight, elevated temperatures, elevated salinity, strongly fluctuating pH and oxygen levels, wind forces, wave action and a number of different predators, e.g. birds (Hampe and Petit, 2005).

Calcifying organisms are at the forefront of those affected by climatic changes and can therefore act as indicator species for induced impacts on marine organisms. One of the major groups effected by climate change are calcifying benthic macroalgae (Kroeker *et al.*, 2013b). Amongst those are coralline red algae (Corallinales, Rhodophyta) which are critical components of marine shallow water ecosystems from polar regions to the tropics (Adey and MacLnyre, 1973, Steneck, 1986). They function as important ecosystem engineers and play a crucial role as an essential structural element in the majority of rocky coastal zones (Johansen, 1981, Jones *et al.*, 1994, Nelson, 2009, van der Heijden and Kamenos, 2015, Dayton, 1972, Kelaher *et al.*, 2001, Benedetti-Cecchi, 2006, Noël *et al.*, 2009). They often form complex, extremely dense and highly branched turfs which are considered the extreme end of algal structural complexity (Coull and Wells, 1983,



Davenport *et al.*, 1999). Branches consist of calcified segments (intergenicula) which are produced through high-magnesium (Mg) calcite precipitation in the cell walls, and non-calcified segments (genicula); this structure provides flexibility and elasticity for every individual branch (Martone and Denny, 2008a). Coralline turf is highly variable, with frond length and density differing at small spatial scales, they can host abundant and diverse macrofaunal assemblages with up to 250,000 individuals per m<sup>2</sup> (Kelaher *et al.*, 2001). In addition, macroalgal physiological processes such as photosynthesis and respiration alter CO<sub>2</sub> and HCO<sub>3</sub><sup>-</sup> in the water in the intertidal environment. This causes changes in pH across diurnal as well as spatial scales related to species distributions (Morris and Taylor, 1983, Williamson *et al.*, 2014, 2017). Depending on the extent of these changes in the carbonate chemistry and especially in combination with the climatic changes named above, calcification of coralline algae can be severely affected.

Geniculate coralline algae (also known as articulated coralline algae), like *C. officinalis*, form turfs across large areas on hard substratum in the intertidal ecosystems of the NE Atlantic. *C. officinalis* is commonly found in sheltered, low intertidal zones, where it primarily inhabits the lower part of rock pools and channels that remain damp or filled during extreme tides or conditions, and at the edge of the intertidal to subtidal zones (Digby, 1977, Egilsdottir *et al.*, 2013, Williamson *et al.*, 2014). In order to maintain their abundance in temperate intertidal ecosystems, coralline algae are suggested to have a good ability to adapt to great and fast changes in environmental conditions, such as solar irradiance, physical stress, water temperature or carbonate chemistry (e.g. large pH variations) which fluctuate tidally, diurnal, monthly and seasonally (Martone *et al.*, 2010, Egilsdottir *et al.*, 2013, Hofmann *et al.*, 2014, Williamson *et al.*, 2014).

Temperature is one of the main factors governing the small-scale vertical distribution of macroalgae on a shore (Lüning, 1990) and the large-scale geographical distribution of macroalgal species (Ganning, 1971). At the organism level, temperature regulates major chemical reactions, which in turn affect metabolic pathways (Lobban and Harrison, 1994). For example, carbonic anhydrase is affected by temperature altering the carbon fixation pathways in photosynthesis (Lobban and Harrison, 1994). Water temperature affects recruitment, survival, growth as well as reproduction of macroalgae and thus drives the species' distribution (Breemann, 1988, Lüning, 1990). Most importantly, current increase in global temperature and therefore a possible exceeding of the species' temperature threshold, is causing species-level responses in macroalgae, such as range shifts (reviewed by Helmuth *et al.*, 2006 and Parmesan, 2006, Wernberg *et al.*, 2011, Nicastro *et al.*, 2013, Smale and Wernberg, 2013). This ongoing temperature increase, and what is predicted for future scenarios, is causing a chronic, due to gradual warming, or an acute stress, due to extreme temperature events (Brodie *et al.*, 2014). Adaptations will need to include facilitation of all metabolic processes at elevated temperatures, especially those for photosynthesis, respiration, calcification and therefore growth. Colthart and Johansen (1973), Hofmann *et al.* (2012a,b), Egilisdottir *et al.* (2013) and Noisette *et al.*, (2013) found that with ongoing climate change, and therefore worsening OA and rising water temperatures, interactions between coralline algal physiology and variable environmental parameters are likely to be significantly negatively affected.

The second main factor responsible for change is ocean acidification (OA) which effects calcareous organisms across their distribution range due to the lowering of the calcium carbonate saturation state (equation 1.1) in the seawater (Orr *et al.*,

2005, Doney *et al.*, 2009). This translates into a decrease in the Mg content of calcite hard parts in most marine environments. Additionally, the proportion of calcifiers depositing low-Mg calcite will increase and the average Mg content of organic carbonate sediments is decreasing due to dissolution (Andersson *et al.*, 2008). Studies have shown that coralline algae are amongst the first calcareous organisms to disappear due to acidified seawater (Kleypas *et al.*, 2006, Hall-Spencer *et al.* 2008). Other studies on crustose coralline algae have shown that a combination of elevated pCO<sub>2</sub> and temperature can affect dissolution, calcification and survival and should be considered in combination when predicting potential future climate impacts (Martin and Gattuso, 2009, Williamson *et al.*, 2014). Due to all these changes and challenges, coralline algae are considered to be especially susceptible to OA showing a dissolution of their high-Mg calcite skeletons, subsequently reducing recruitment, growth and survival rates (Kroeker *et al.*, 2013b). Additionally, it is possible that coralline algae are able to shift their energy budget from growth extension to maintaining structural integrity, which is weakened in acidified conditions (Ragazzola *et al.*, 2013). It was shown for different calcifying algae, that photosynthesis is stimulating calcification and that an increase in photosynthesis could lead to an initiation of CaCO<sub>3</sub> dissolution in response to decreased pH in the surrounding water (Borowitzka, 1982, Gattuso *et al.*, 1999, Hofmann *et al.*, 2012a, Johnson and Carpenter, 2012).

Coralline algae species have already shown an influence of warming and mainly of acidification on structural parameters. For instance, cell wall thickness and cell elongation were already negatively influenced at low gains in pCO<sub>2</sub> concentrations resulting in a decrease in cell density (Ragazzola *et al.*, 2012). In another study, a thinning particularly in inter-filament cell walls was found. Authors of this study

concluded that for different species, different mechanisms for a reduction of CaCO<sub>3</sub> production are in place, caused by energetic trade-offs due to building and maintenance of their skeleton in decreasing pH environments (McCoy and Ragazzola, 2014). However, in the same study it was found that even though cell walls were thinning, growth rates were maintained.

To the authors knowledge only few studies (Kangwe *et al.*, 2001, Couto *et al.*, 2010) were performed with the focus on investigating trace elemental compositions of articulated coralline algae, except for the commonly used Mg/Ca, Sr/Ca and Ba/ Ca ratios.

It remains unclear how and whether the wider distributed, turf-forming algae *C. officinalis* will be able to withstand future changes. It is likely that the species as a whole will show some resilience when exposed to predicted climate change conditions. However, it is uncertain which areas or portions of the species distribution will be affected the most by the changes. At present, there are very few studies regarding the physiological and structural responses of intertidal benthic organisms to current climate conditions across its distribution (reviewed by Helmuth *et al.*, 2006; Díez *et al.*, 2012). This gap in knowledge complicates the establishment of detailed predictions for this species future (Nelson, 2009, Brodie *et al.*, 2014, Williamson *et al.*, 2017). In this study, physiological responses (photosynthesis, respiration, calcification, Photosynthesis-Irradiance curves and Calcification-Irradiance curves) and structural parameters (cell wall thickness, growth rates and skeletal trace element composition) of *C. officinalis* across its natural distribution in the eastern North Atlantic to future climatic changes were investigated. England was chosen as central population for this study, referring to confirmed genetic data by Brodie *et al.* (2013). Spain was studied representing the southern margin of the

species distribution (Williamson *et al.*, 2015). Iceland was chosen to represent the northern margin of the species distribution.

We hypothesised that central populations are more robust to lower pH levels and elevated temperatures and therefore are able to adapt to the predicted level of acidification and temperature increase. In contrast, we predicted that southern populations are likely to be negatively influenced under higher temperatures and northern populations might be most influenced by lower pH levels due to the increased solubility of CO<sub>2</sub> in colder waters. All populations are predicted to be negatively influenced by the treatment combining lower pH and elevated temperatures.

### 5.3 Material and Methods

Detailed descriptions of the Material and Methods are specified in Chapter 2.

#### 5.3.1 Specimens Collection

*Corallina officinalis* populations ( $n = 2$ ) were collected intertidally ( $n = 36$  per population, total  $n = 72$ ), during low tide in an average depth of 0.31 m from the water surface at sites in the South East coast of the UK (CP; central population 1: St Margarets Bay: N 51.148056, E 1.385056; central population 2: Westbrook Bay: N 51.388840, E 1.367170; beeline distance between populations: 26.85 km), the North West coast of Spain (SP; southern margin population 1: Illa del Arousa: N 42.56870, W 8.89171; southern margin population 2: Tragove: N 42.52444, W 8.82772; beeline distance between populations: 7.19 km) and the South West coast of Iceland (NP; northern margin population 1: Stafnes South: N 63.968444, W 22.750861; northern margin population 2: Stafnes North: N 63.974380, W 22.753610, beeline distance between populations: 1.59 km) in January 2017 (CP and SP) and February 2017 (NP). Specimens were transported into the lab at the Institute of Marine Sciences of the University of Portsmouth, UK using temperature-insulating containers. Only healthy specimens without epiphytes and indication of bleaching or damage were selected for this study.

#### 5.3.2 Experimental Designs

Two experimental designs as described below were used. The second experiment was performed with the aim to check for repeatability of results of the first experiment. Improvements included the change from a flow through open system, which was vulnerable to high changes in temperature, to a water bath closed

system. For this reason, the results in the next part of this chapter will be split and presented separately from each other.

### 5.3.2.1 Climate Change Experiment

After initial acclimatisation to laboratory/aquarium conditions, the collected populations ( $n = 6$ ) were colour coded and exposed to four treatments: (1) Control (ambient temperature, ambient  $p\text{CO}_2$  (pH 8.1 – 8.2/ 380 – 400 ppm  $p\text{CO}_2$ , IPCC, 2014a)), (2) high temperature (high temperature (T+3; IPCC, 2014a), ambient  $p\text{CO}_2$ ), (3) high  $p\text{CO}_2$  (ambient temperature, high  $p\text{CO}_2$  (pH 7.75 - 7.80/ ~1000ppm  $p\text{CO}_2$ ; RCP 8.5, IPCC, 2014a), (4) climate change (high temperature, high  $p\text{CO}_2$ ) and cultured for four months. Fifty 11.1 L aquaria were set up in a flow-through, open seawater system. Each was supplied with an individual water supply, a water pump and an adjustable air diffuser, to circulate and mix the containing water to obtain an even tempering as well as imitating movement and air saturation most likely experienced in the natural environment. Aquaria were insulated with Styrofoam between each other in order to minimise temperature loss and exchange with the environment and between replicates of different treatments. Waste water of the replicate aquaria was treated with UV light (Tropic Marine Centre (TMC) P2-110W Commercial UV Steriliser, max. flow rate: 65 L/min) prior to disposal. Each of the four water source tanks (74 L) was also equipped with a water pump for mixing purposes and had twelve individually controllable outlets attached. The header tanks were temperature controlled by up to 3 chillers (TK-2000 chillers, cooling capacity: 870 W, 800 L/h, TECO) to maintain the desired temperature. Tubes for individual water supply to the replicate aquaria were individually insulated using foam pipe insulation and radiator heat reflector roll to ensure a minimised temperature loss and exchange with the environment from the water source tanks

to the aquarium. Carbon dioxide treatments were supplied with CO<sub>2</sub> enriched pressure air in the identical way the ambient pCO<sub>2</sub> treatments were supplied with pressure air. The CO<sub>2</sub> enriched air was constantly produced by mixing pure CO<sub>2</sub> (VK cylinder, BOC, Portsmouth, UK) with pressure air in a mixing flask (5 L) prior to distribution to the treatments. The mixture was consistently monitored with a gas analyser (LI-820, LI-COR Environmental, NB, USA) and a preconnected flowmeter (Rotameter 1.2 L/min, Caché Instrumentation, Wakefield, UK) throughout the time of the experiment, to ensure the correct concentration of pCO<sub>2</sub> was supplied to the experimental aquaria. The quantity of CO<sub>2</sub> enriched air reaching the experimental aquaria was monitored and adjusted using flowmeter (LPM Air 5 ml and 0.5 ml for ambient air and CO<sub>2</sub>, respectively, Cole-Parmer Instrument Co., IL, USA) which allowed for 0.5 bar of enriched air to pass. The Fifty aquaria were randomly assigned to a treatment (Cornwall and Hurd, 2015) and were subdivided into treatments as described in 2.9.3 and Figure 2.17. Two additional aquaria solely with flint stones, which were used to fix the specimens on, were set up alongside the experiment, one with ambient air supply, one with CO<sub>2</sub> enriched air supply. These were added in order to monitor potential influences of the flint stones to the seawater chemistry and were treated like the other aquaria.

At the inception, specimens (total rocks with specimens per population and treatment replicate:  $n = 4$ ) were kept at their *in situ* temperatures measured during sampling (northern margin temperature: 11.0°C; central temperature: 16.0°C; southern margin temperature: 18.5°C). The system was set to a light/dark cycle of 9/15 h and an intensity of 230  $\mu\text{mol photons m}^{-2} \text{s}^{-1}$  (taken from the average of natural conditions of northern, central and southern locations) produced and controlled by TMC AQUABEAM 600 Ulima Reef White lights with cloud function.



Additionally, sunset and sunrise were mimicked through a slow increase and decrease of light intensities over a period of 1 h. All specimens were kept in their corresponding conditions for a minimum of 1 week to acclimate to aquaria conditions. Following the initial acclimatisation, over the next 3 weeks,  $\frac{1}{4}$  of all, the northern, CP and SP, were gradually acclimatised (increase of  $1.0^{\circ}\text{C}/\text{week}$  and increase or decrease of  $50 \mu\text{mol photons m}^{-2} \text{s}^{-1}/\text{week}$ , respectively) to elevated temperatures, a further  $\frac{1}{4}$  of all populations was gradually acclimatised to elevated  $\text{pCO}_2$  (increase of  $200 \text{ ppm pCO}_2/\text{week}$  which is equivalent to a decrease in pH of  $\sim 0.1$ ) and light conditions. A further  $\frac{1}{4}$  of all populations was gradually acclimatised to the combination of elevated temperature and  $\text{pCO}_2$  as described above and the remaining 25% of all populations was retained in their initial, control conditions. After acclimatisation specimen were randomly and equally distributed within the corresponding replicate aquaria.

#### 5.3.2.2 Cross Experiment

For this study, two populations of two geographic locations ( $n = 4$ ) across the species distribution (UK = central populations; Spain = southern margin populations) were sampled and exposed to six treatments:

- (1) Control Common Garden Conditions (corresponding *in situ* temperature and light conditions, ambient  $\text{pCO}_2$  (pH 8.1 – 8.2/ 380 – 400 ppm  $\text{pCO}_2$ , IPCC, 2014a)),
- (2) Common Garden Conditions (*in situ* temperature and light conditions of the other geographic location),
- (3) Control Climate Change Conditions (corresponding *in situ* temperature and light conditions, ambient  $\text{pCO}_2$ ),

(4) High pCO<sub>2</sub> (corresponding *in situ* temperature and light conditions, high pCO<sub>2</sub> (pH 7.75 - 7.80/ ~1000 ppm pCO<sub>2</sub>; RCP 8.5, IPCC, 2014a),

(5) High temperature (T+3 (*in situ* temperature elevated by 3°C (IPCC, 2014a)) and *in situ* light conditions, ambient pCO<sub>2</sub>) and

(6) T+3/high pCO<sub>2</sub> (T+3 and *in situ* light conditions in combination with elevated pCO<sub>2</sub>).

All populations were colour coded prior to acclimatisation. Thirty-six 11.1 L aquaria were set up in a 6 water baths, closed system, six aquaria per water bath. Each was supplied with a water pump (TMC, V<sup>2</sup>PowerPump 800, Flow rate: 700 L/h) and air diffuser, to circulate and mix the containing water to obtain an even tempering as well as imitating movement and air saturation most likely experienced in the natural environment. The water baths containing the experimental aquaria were endowed with two of the same pumps, one on either side to ensure even commingling of the containing water. Seventy-five percent of the water in the replicate aquaria was changed every second day and waste water of the replicate aquaria was treated with UV light (Tropic Marine Centre (TMC) P2-110W Commercial UV Steriliser, max. flow rate: 65 L/min) prior to disposal. Each of the water baths was temperature controlled by a chiller (TK-2000 chillers, cooling capacity: 870 W, 800 L/h, TECO) to maintain the desired temperature. Carbon dioxide treatments were supplied with CO<sub>2</sub> enriched pressure air in the identical way the ambient pCO<sub>2</sub> treatments were supplied with pressure air. The CO<sub>2</sub> enriched air was constantly produced by mixing pure CO<sub>2</sub> (VK cylinder, BOC, Portsmouth, UK) with pressure air in a mixing flask (5 L) prior to distribution to the treatments. The mixture was consistently monitored with a gas analyser (LI-820, LI-COR Environmental, NB, USA) and a preconnected flowmeter (Rotameter 1.2 L/min, Caché Instrumentation, Wakefield, UK) throughout

the time of the experiment, to ensure the correct concentration of pCO<sub>2</sub> was supplied to the experimental aquaria. The quantity of CO<sub>2</sub> enriched air reaching the experimental aquaria was monitored and adjusted using flowmeter (LPM Air 5 ml and 0.5 ml for ambient air and CO<sub>2</sub>, respectively, Cole-Parmer Instrument Co., IL, USA) which allowed for 0.5 bar of enriched air to pass. The 36 aquaria were split into three experimental subunits with three replicates for each condition (central and southern *in situ* temperature and light): the Common Garden Experiment part (treatment (1) and (2), n = 12) and the Climate Change Experiment part 1 (treatment (3) and (4), n = 12) and the Climate Change part 2 (treatment (5) and (6), n = 12). Each subunit was divided into southern and central environmental conditions on one side of the shelf, respectively. Aquaria were randomly assigned into treatments (Cornwall and Hurd, 2015). Out of the 36 aquaria, 12 were chosen for an additional Common Garden Experiment which is separately discussed in detail in Chapter 4. Further 12 aquaria were assigned to central temperature (6.0°C) and light intensities (57 μmol photons m<sup>-2</sup> s<sup>-1</sup>) and southern temperature (11.5°C) and light intensities (184 μmol photons m<sup>-2</sup> s<sup>-1</sup>), respectively, within these 12 aquaria, six, three for each region of origin, were treated with ambient pCO<sub>2</sub> and other six, three for each origin, were treated with elevated pCO<sub>2</sub> air (~1000 ppm pCO<sub>2</sub> or pH 7.75 - 7.80). As a last subunit of the experiment, the same assignments and conditions as just explained were chosen in further 12 aquaria, with the distinction that temperatures of each treatment were elevated by 3.0°C according to predictions for future sea surface temperatures (IPCC, 2014a). At the inception, specimens were kept at their *in situ* temperatures measured during sampling. The system was set to a light/dark cycle of 10/14 h (taken from the average of natural conditions of central (9/15 h) and southern (10.5/13.5 h) locations) produced and controlled by TMC AQUABEAM 600 Ulma Reef White lights with cloud function. Additionally, sunset and sunrise were

mimicked through a slow increase and decrease of light intensities over a period of one h. All specimens were kept in their corresponding conditions for a minimum of one week to acclimate to aquaria conditions. Following the initial acclimatisation, over the next three weeks, the remaining specimens of all populations were either kept constant (treatment (3)) or gradually acclimatised (increase/decrease of  $1.5^{\circ}\text{C}/\text{week}$  and increase/decrease of  $40 \mu\text{mol photons m}^{-2} \text{s}^{-1}/\text{week}$  and increase of  $\sim 200 \text{ ppm}$  (decrease in pH of  $\sim 0.1$ ), respectively) to elevated temperatures and decreased pH levels, depending on their allocated treatment ((4)-(6)). After acclimatisation specimens were randomly and equally distributed within the corresponding replicate aquaria.

### 5.3.3 Monitoring of Water Parameters

In the Climate Change as well as Cross Experiment, pH, temperature, salinity, dissolved oxygen (DO, only for Cross Experiment) were measured daily in each replicate,  $A_T$  was measured daily in one randomly chosen replicate of each treatment. Irradiance was measured once a month to monitor the decrease in light intensity using a HOBO UA-002-64 Pendant Temp/Light data logger (accuracy:  $0.47^{\circ}\text{C}$ , resolution:  $0.1^{\circ}\text{C}$ . Tempcon, Arundel, UK). Temperature and salinity were measured with a CO310-1 portable salinity and temperature probe (accuracy: 0.2% for salinity,  $\pm 0.2^{\circ}\text{C}$  for temperature; resolution: 0.1 for salinity,  $0.1^{\circ}\text{C}$  for temperature. VWR, Leicestershire, UK). Dissolved oxygen and pH were measured with an HQ30d portable multi-parameter meter and a luminescent dissolved oxygen (LDO101, accuracy:  $\pm 0.1 \text{ mg/L}$ . HACH, Manchester, UK) and pH probe (PHC301, accuracy:  $\pm 0.02 \text{ pH}$ , HACH, Manchester, UK. Calibrated on the National Bureau of Standards (NBS) scale and converted into total scale values using Tris/HCl and 2-aminopyridine/HCl buffer solutions after Dickson *et al.*, (2007). Total alkalinity ( $A_T$ )

was monitored daily in one randomly chosen replicate for each treatment, using the alkalinity anomaly technique after Smith and Key (1975), Chisholm and Gattuso (1991) and Dickson *et al.* (2007, SOP 3b). Total alkalinity titrations were carried out with an automatic titrator TitroLine 7000 (measurement accuracy:  $0.002 \pm 1$  digit, dosing accuracy: 0.15%, dosing precision: 0.05 - 0.07%. Schott SI Analytics, Mainz, Germany) to ensure minimal variation. As titrant 0.1 N hydrochloric acid (HCl) was used and validated against Certified Reference Material provided by Andrew G. Dickson (Batch 154, Scripps Institution of Oceanography).

Due to the high number of samples, each water sample was sterile filtered and subsequently poisoned with 25  $\mu$ l of a saturated Hg(II)Cl solution (Mercuric chloride 99.5%, ACROS Organics, Thermo Fisher Scientific, Geel, Belgium) prior to the titrations for  $A_T$  determination. Samples were stored in a cool and dry place pending processing.

#### 5.3.4 Physiological Incubation Procedure and Measurements

To determine saturating light levels of *C. officinalis* populations in the Cross Experiment before and after the experiments, the oxygen production (P-I curve) and calcification (C-I curve) evolution under increasing light conditions were measured (Chapter 2.6.1). P-I and C-I curves were only performed in the Cross Experiment with CP and SP under control (C), elevated temperature (T+3), elevated  $pCO_2$  ( $CO_2$ ) and climate change (T+3/ $CO_2$ ) treatments (Figure 5.3). Due to time and personnel restrictions, P-I and C-I incubations could not be performed in the Climate Change Experiment.

Algal fronds with a fresh weight of  $1.04 \pm 0.28$  g were transferred into a clear closed cell 58 ml incubation chamber and incubated successively for one h at lower light

intensities (0, 20, 80, 160  $\mu\text{mol photons m}^{-2} \text{s}^{-1}$ ) and for 30 minutes at higher light intensities (320, 500 and 700  $\mu\text{mol photons m}^{-2} \text{s}^{-1}$ ; AQUARAY Nature Perfect, TMC, London, UK), starting from the lowest to the highest to minimise stress and reducing incubation time in higher light levels to avoid oversaturation. Five replicates per light intensity were incubated simultaneously and bubble-free. To account and correct for metabolism effects by other organisms, reference incubations without algae were performed alongside the above-described incubations for all light intensities. Aluminium foil was used to coat the chambers to determine calcification and respiration rates in the dark. Irradiance was measured with a Quantitherm PAR/Temperature Sensor with a QTP1 probe (resolution: 1  $\mu\text{mol photons m}^{-2} \text{s}^{-1}$ , 0.02°C, respectively. Hansatech, Norfolk, UK).

Differences in oxygen concentration, pH and  $A_T$  were determined in order to calculate photosynthesis, respiration and calcification rates by measuring oxygen, pH and  $A_T$ , respectively, before and after the incubations. Prior to  $A_T$  measurements, seawater samples were filtered through a syringe filter (hydrophilic 25 mm, 0.2  $\mu\text{m}$  PTFE. Fisherbrand, Loughborough, UK) into sterile 50 ml tubes (Plastic Centrifuge Tubes. Fisherbrand, Loughborough, UK). Immediately after, potentiometric titrations were performed using an automatic titrator (Chapter 5.3.3) calibrated on the NBS scale. Results were calculated based on a Gran function after Dickson *et al.* (2007). The carbonate system of the seawater was calculated from pH,  $A_T$ , salinity and temperature using the Excel Macro CO2Sys (Version 2.1, Lewis and Wallace, 1998) with  $K_1$  and  $K_2$  according to Mehrbach *et al.* (1973) and refit by Dickson and Millero (1987) (Table 5.2). Measurement ranges of pH values represent *in situ* values and are highly dependent on temperature. P-I and C-I curve incubations could not be completed within the remit and time availability of the climate change experiment.

To determine changes in photosynthesis, respiration and calcification rates most likely to be found in the field, additional incubations ( $n = 4$  and  $n = 3$ , for Cross and Climate Change Experiment, respectively) of all treatments at ambient light conditions ( $57 \mu\text{mol photons m}^{-2} \text{s}^{-1}$  for central and  $184 \mu\text{mol photons m}^{-2} \text{s}^{-1}$  for SP in the Cross Experiment and  $230 \mu\text{mol photons m}^{-2} \text{s}^{-1}$  for all treatments in the Climate Change Experiment as an average of all sites) were performed before and after the study and calculated following the protocol above and in 2.6.2 – 2.6.4. Calculations were performed following the methodology described in 2.6.6.

The weight of algal fronds used in the incubations was transformed from FW into dry weight (DW) by multiplying FW measurements with the factor 0.62286. This factor was determined from FW and DW weight measurements of thirty 1 g frond bundles from all populations before and after algae were left to dry for 48 h in an oven at  $60^{\circ}\text{C}$  (Egilsdottir *et al.*, 2013).

### 5.3.5 Laboratory Structural Analysis

To determine the structural integrity of the different populations across the species distribution trace element compositions, cell wall thickness and growth rates were determined as detailed in 2.6.7.2, 2.8.2 and 2.8.3.

#### 5.3.5.1 Trace Element Composition

In order to determine the Mg/Ca ratios within the calcite and the differentiation of it within various conditions, laser ablation inductively coupled plasma mass spectrometry (LA-ICP-MS) was performed. This method enables the measurement of predetermined trace elements, which ultimately leads to the specimens' elemental composition. For detailed description Chapter 2.8.2.3.

Replicates ( $n = 3$ ) were embedded into epoxy resin (EpoFix Kit, batch no: 8134-01, Struers ApS, Ballerup, Denmark) and polished with a polishing machine (MetaServ 3000 or VibroMet 2, Buehler, Esslingen, Germany) and an aluminium oxide solution (aluminium oxide powder (Micropolish Alumina, Buehler, Esslingen, Germany) and distilled water) of  $0.05 \mu\text{m}$  grain size (Chapter 2.8.2.1). Trace element analysis were conducted at the School of Earth and Environmental Sciences, University of Portsmouth, United Kingdom. Synthetic silicate glass reference material NIST SRM 610 as well as NIST SRM 612 were used for instrumental calibration and as primary and secondary standards, respectively. Synthetic calcium carbonate USGS MACS-3 was also used as secondary standard and analysed in the same conditions as the unknowns (NIST SRM 610 and 612, US National Institute of Standard and Technology Standard Reference Material; MACS-3, the United States Geological Survey).

Samples of both experiments were analysed using a RESOLUTION 193 nm ArF excimer Laser with a Laurin Technic S155 Ablation cell coupled to an Analytic Jena Plasma Quant MS Elite ICP-MS. Analyses consisted of  $55 \mu\text{m}$  spot size, laser fluency was  $3.0 \text{ J/cm}^2$  and its repetition rate was 5 Hz. Background measurements took 20 seconds, followed by 30 seconds of ablation and 15 seconds of washout for each analysis (total: 65 seconds). Detailed operating conditions for both instruments are listed in Table 2.2.

Background and signal counts were integrated, time-drift corrected and reduced to concentrations using the Lolite 3.4 software (Paton *et al.*, 2011). Each run consisted of at least six external standard analyses (NIST 610) and four secondary standards NIST 612 and MACS-3 (total  $n = 14$ ). Detection limits (99% confidence) for the spot measurements of the NIST glasses were: Mg =  $\sim 28$  ppm and Ca =  $\sim 100$  ppm.



Internal standard element used for normalization of the data was  $^{43}\text{Ca}$ , which was obtained from the GeoReM certificate and own measurements. All reference materials were ablated prior, in the middle and after sample ablation. Following every sixth sample analysis one analysis of NIST SRM 610 was added to correct for time-dependent drift of mass discrimination and instrument sensitivity. Final elemental composition ratios in this study were calculated as a 'mean count rate' including standard error of drift and background corrected single ablation spot analysis for each of the three replicates. Spots ( $n = 5$ ) were ablated below and above the stain line of the selected branch section. This method is commonly used for LA-ICP-MS data reduction (Longerich *et al.*, 1996). Values obtained in the course of this study are reproducible within 10% for Mg, of the GeoReM recommended values (Jochum *et al.*, 2005) and were compared with the GeoReM data base to determine accuracy (Figure 5.1 and Figure 5.2) as well as internal (NIST 610) and external reproducibility (MACS-3 and NIST 612; Table 5.1).

**Table 5.1:** Reproducibility of Reference Materials USGS MACS-3, NIST SRM 610 and NIST SRM 612 (Total Mean  $\pm 2\text{SD}$ ) for each element measured and analysed in this study. Top and bottom part of the table represent the Climate Change Experiment and Cross Experiment, respectively.

		Mg [ppm]	Ca [ppm]	V [ppm]	Cr [ppm]	Fe [ppm]	Zn [ppm]	Sr [ppm]	Cd [ppm]	Ba [ppm]
Climate Change Experiment	MACS-3	1824.67 $\pm 121.48$	38635.00 $\pm 5835.98$	47.45 $\pm 2.99$	121.97 $\pm 5.87$	13480.00 $\pm 2214.68$	139.47 $\pm 50.34$	7259.67 $\pm 793.80$	49.16 $\pm 3.24$	60.54 $\pm 2.67$
	NIST 610	464.98 $\pm 2.06$	82147.50 $\pm 335.30$	442.02 $\pm 1.50$	405.00 $\pm 0.97$	453.69 $\pm 48.31$	456.05 $\pm 2.85$	515.59 $\pm 3.92$	259.01 $\pm 2.26$	435.01 $\pm 0.62$
	NIST 612	56.03 $\pm 6.25$	84635.00 $\pm 572.26$	38.16 $\pm 0.13$	37.15 $\pm 0.46$		37.79 $\pm 0.63$	77.13 $\pm 3.14$	28.11 $\pm 0.57$	38.03 $\pm 0.67$
Cross Experiment	MACS-3	1855.63 $\pm 126.29$	400900.00 $\pm 11947.98$	52.61 $\pm 6.15$	132.13 $\pm 11.94$	13937.50 $\pm 1909.04$	139.58 $\pm 19.36$	6881.75 $\pm 520.29$	51.23 $\pm 3.28$	64.06 $\pm 6.83$
	NIST 610	465.02 $\pm 2.85$	82146.97 $\pm 326.07$	442.00 $\pm 1.07$	405.02 $\pm 1.97$	453.11 $\pm 52.33$	456.02 $\pm 52.33$	515.37 $\pm 5.11$	259.00 $\pm 1.87$	435.00 $\pm 1.45$
	NIST 612	56.41 $\pm 7.53$	84430.00 $\pm 783.25$	38.30 $\pm 0.23$	37.28 $\pm 0.69$		37.50 $\pm 2.70$	83.84 $\pm 4.80$	27.68 $\pm 1.72$	37.89 $\pm 0.52$

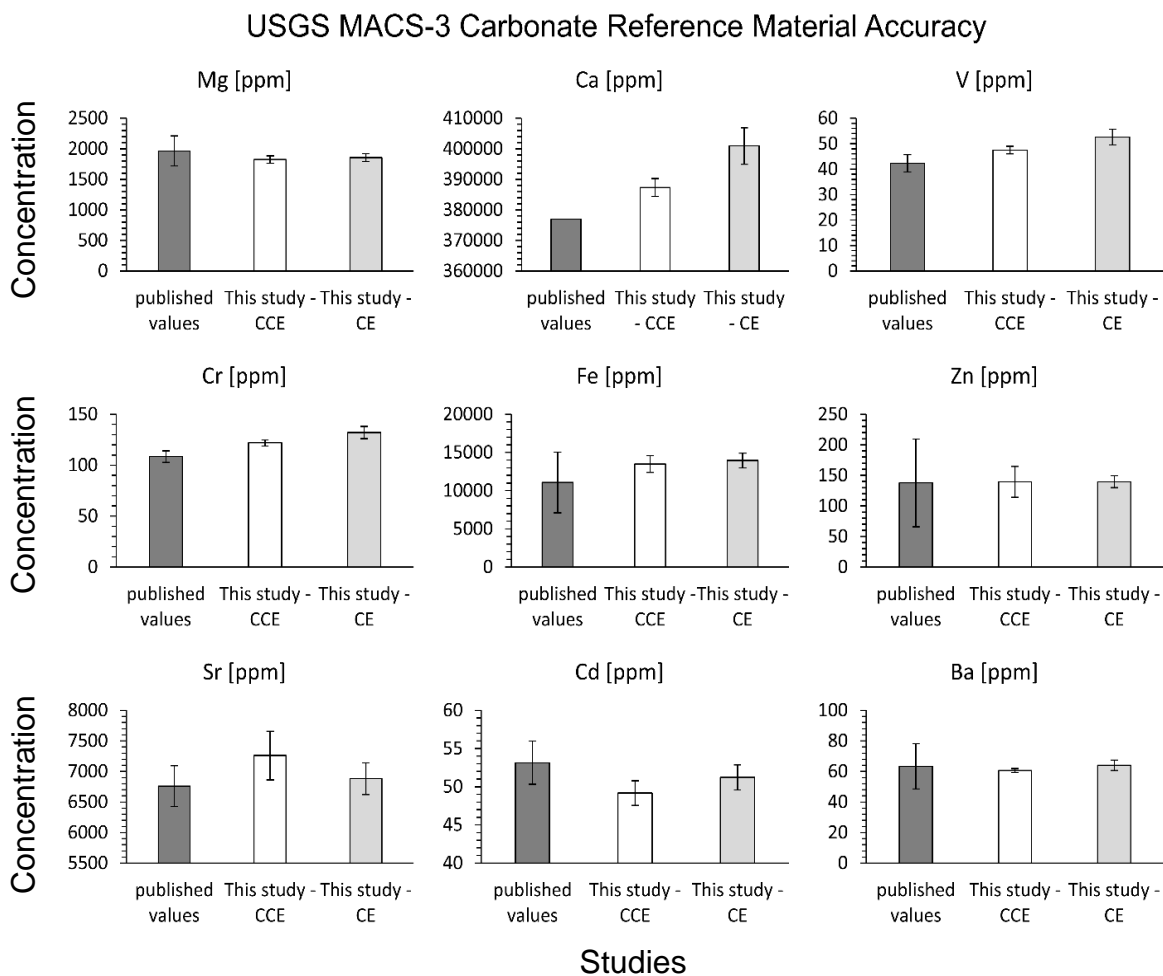


**Figure 5.1:** Accuracy of the reference material USGS MACS-3 for each measured and analysed trace element. Dark grey bars represent  $AV \pm SD$  [ppm] of published data retrieved from the GeoReM database. Light grey bars represent  $AV \pm SD$  [ppm] of trace elements in this study for the Climate Change Experiment (CCE). White bars represent  $AV \pm SD$  [ppm] of trace elements in this study for the Cross Experiment (CE).

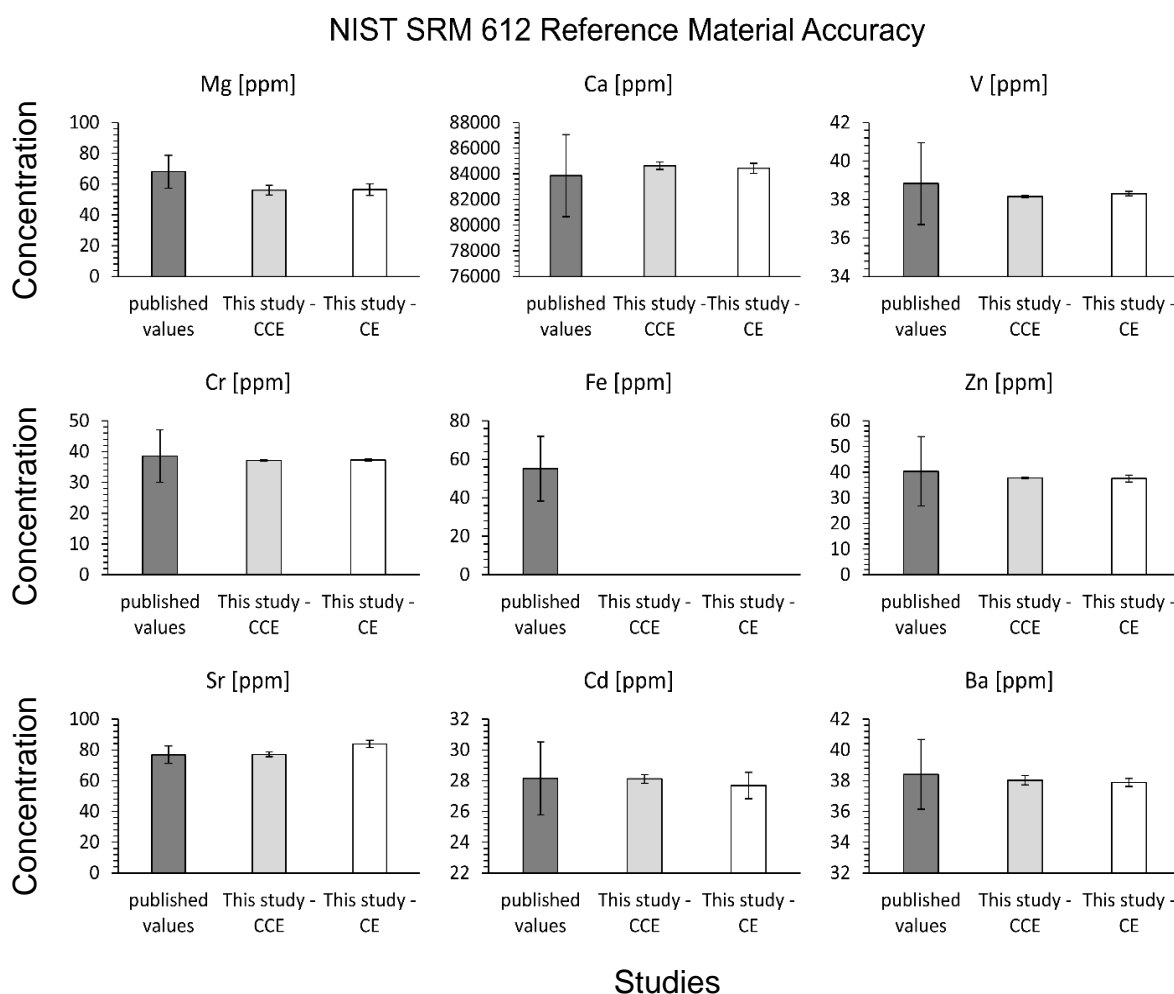


**Figure 5.2:** Accuracy of the reference material NIST SRM 612 for each measured and analysed trace element. Dark grey bars represent  $AV \pm SD$  [ppm] of published data retrieved from the GeoReM database. Light grey bars represent  $AV \pm SD$  [ppm] of trace elements in this study for the Climate Change Experiment (CCE). White bars represent  $AV \pm SD$  [ppm] of trace elements in this study for the Cross Experiment (CE).

### 5.3.5.2 Cell Wall Thickness

Using scanning electron microscopy (SEM), the modification of the cell wall structure and thus, changes in growth or metabolic processes can be connected.

The same samples mounts prepared in 2.8.2.1 for LA-ICP-MS analysis, were used for SEM analysis. An SEM was used that was suitable to take pictures of uncoated samples (EVO MA10 with a W filament electron source, Zeiss, Oberkochen, Germany), to be able to use the same mounts in both machines without any interference of sample coating. Sample mounts were fixed on stabs with double coated carbon conductive tabs, cleaned using Isopropanol and loaded into the SEM applying a variable pressure (VP) vacuum of 28 Pascal.

Images were taken at 20 kV electron high tension (EHT), representing the accelerating voltage used for each sample. A working distance (WD) of 7 - 10 mm was set, depending on the sample. Pictures were taken with a probe of 300 pA, a scan speed of 20.5 s, a magnification of 3 K and a line average noise reduction in the Backscatter (HDBSD) mode. After all images were produced, the software ImageJ (Rasband, 2016) was used to determine the average intra- (lateral to growth direction) and inter-cell wall thickness (horizontal to growth direction, Figure 2.13) of specimens (total  $n = 90$  per condition;  $n = 45$  below stain,  $n = 45$  above stain;  $n = 15$  per replicate; replicate:  $n = 3$ ). Measurements below stain represent material grown in the field, measurements above stain represent material grown in experimental conditions.

### 5.3.5.3 Monthly Growth Rates and Death rates

To obtain growth rates in the laboratory, specimens were carefully removed following the procedure described in 2.2 and stained over night as described in 2.6.7.1. The following day specimens were placed back into their respective aquaria.

After the experiments, specimens of each temperature condition were carefully dried and growth rates were determined following the protocol in 2.6.7.2. Growth rate analysis of Cross Experiment samples incorporated measurements of CP in central conditions (n = 369), CP in central conditions under elevated pCO<sub>2</sub> (n = 301), SP in southern conditions (n = 290) and SP in southern conditions under elevated pCO<sub>2</sub> (n = 237) as well as the same treatments, including elevated temperatures for all. Analysis of the Climate Change Experiment growth rates consisted of replicate specimens for northern, CP and SP, respectively, under control (n = 42, 50 and 65), elevated temperatures (n = 42, 52 and 44), pCO<sub>2</sub> (n = 45, 40 and 46) and temperature/pCO<sub>2</sub> (n = 48, 55 and 60).

### 5.3.6 Data Analysis

#### 5.3.6.1 Physiological Parameters

Data were analysed as described in Chapter 2.6.6. All analyses were run in SPSS Statistics 24 and 25 (IBM Corp, 2016 and 2018, respectively) and data were tested for normality and homogeneity prior analyses (Shapiro-Wilk and Levene Test).

In the Climate Change Experiment, data for net production, respiration, light calcification and dark calcification (n = 3 for all) was normally distributed and showed homogeneity of variance. This resulted in statistical analysis using the parametric two-way analysis of variance (ANOVAs) for individuals from each country of origin (NP, CP and SP (n = 2 each)) with treatment (4 levels: Control, T+3, CO<sub>2</sub>, T+3/CO<sub>2</sub> conditions) as the fixed factor. When significant effects were found, data was further explored by running a post hoc Tukey HSD test. Tests were performed for central and southern populations under each temperature and pCO<sub>2</sub> condition comparing measurements after exposure to treatments and control.

In the Cross Experiment with six populations from across the geographic distribution in the NE Atlantic, primary production, respiration, light calcification and dark calcification ( $n = 3$  for each) showed normal distribution and homogeneous variances, data was analysed with two-way ANOVAs and Tukey HSD post hoc tests. Additional two-way ANOVAs and Tukey HSD post hoc tests of CP and SP were performed to identify significant differences in their maximum oxygen production level ( $n = 5$ ) of all populations in all temperature and  $p\text{CO}_2$  treatments. For maximum calcification levels ( $n = 5$ ) observed during C-I curves, non-parametric Kruskal Wallis H tests were performed due to the lack of homogeneity of variances in the data.

#### 5.3.6.1 Structural Parameters

Not normally distributed and homogeneous data was analysed using independent-sample Kruskal-Wallis H tests with pairwise comparison. In this way, growth rates ( $n = 12$  and  $39$ , for Climate Change and Cross Experiment, respectively), intra- and inter- cell wall thickness (all  $n = 45$  for pre and post-experimental measurements of the Climate Change and Cross Experiment, respectively) were analysed.

Trace element data for both experiments were analysed using PRIMER 6.1 (Anderson *et al.*, 2009), after data normalisation by fourth root transformation due to extreme high variability of elemental concentrations, permutational analyses of variance (PERMANOVA) were performed. The following factors combinations were chosen: (1) population, treatment and time point, (2) country, population and treatment with both: (a) treatments nested into population and (b) populations nested within treatments and 9999 permutations. Additional similarity of percentage (SIMPER) analysis were performed determining the major influential trace elements for each group.

## 5.4 Results

The experimental design allowed for very stable parameters under all conditions and was not influential towards physiological behaviour of specimens (Table 5.2). Saturation states and pH for calcite and aragonite were highest in warmer conditions. In the Climate Change Experiment, pH was measured on the NBS scale

**Table 5.2:** Carbonate system parameters of the Climate Change (top) and Cross Experiment (bottom) design during the culturing of *C. officinalis*. All numbers are mean values ( $n = 62 \pm SD$  and  $n = 71 \pm SD$ , for top and bottom, respectively). Salinity, pH (NBS and total scale, respectively), temperature and total alkalinity ( $A_T$ ) were measured while other parameters were calculated.

Population	Treatment	pH (NBS scale)	Salinity	Temperature [°C]	$A_T$ [ $\mu\text{mol kg}^{-1}$ ]	$D_C$ [ $\mu\text{mol kg}^{-1}$ ]	$D_A$ [ $\mu\text{mol kg}^{-1}$ ]	$D_{CO_3}$ [ $\mu\text{mol kg}^{-1}$ ]	$D_{CO_2}$ [ $\mu\text{mol kg}^{-1}$ ]	$\alpha_{CO_2}$ [atm]	Dissolved Oxygen [mg/L]
Northern	Control	8.17 $\pm$ 0.01	35.5 $\pm$ 0.29	10.38 $\pm$ 0.81	2174 $\pm$ 25	1983.9 $\pm$ 23.2	1840.0 $\pm$ 21.71	3.11 $\pm$ 0.08	1.95 $\pm$ 0.05	222.2 $\pm$ 5.9	
	T+3	8.16 $\pm$ 0.01	35.6 $\pm$ 0.14	13.42 $\pm$ 1.86	2156 $\pm$ 70	1953.4 $\pm$ 67.1	1804.1 $\pm$ 63.80	3.26 $\pm$ 0.22	2.05 $\pm$ 0.14	204.7 $\pm$ 18.0	
	CO <sub>2</sub>	7.82 $\pm$ 0.06	35.6 $\pm$ 0.03	11.32 $\pm$ 1.42	2308 $\pm$ 318	2236.8 $\pm$ 305.8	2132.1 $\pm$ 289.62	1.65 $\pm$ 0.37	1.04 $\pm$ 0.23	570.4 $\pm$ 85.8	
	CO <sub>2</sub> /T+3	7.78 $\pm$ 0.08	35.7 $\pm$ 0.21	13.93 $\pm$ 1.42	2357 $\pm$ 194	2290.2 $\pm$ 193.6	2183.1 $\pm$ 186.03	1.64 $\pm$ 0.34	1.03 $\pm$ 0.21	619.4 $\pm$ 156.9	
Central	Control	8.17 $\pm$ 0.01	35.7 $\pm$ 0.24	15.33 $\pm$ 1.44	2182 $\pm$ 30	1960.3 $\pm$ 26.4	1800.4 $\pm$ 29.97	3.54 $\pm$ 0.13	2.23 $\pm$ 0.08	187.4 $\pm$ 6.8	
	T+3	8.15 $\pm$ 0.01	35.8 $\pm$ 0.22	18.95 $\pm$ 1.39	2197 $\pm$ 21	1961.4 $\pm$ 14.1	1793.1 $\pm$ 15.36	3.75 $\pm$ 0.22	2.36 $\pm$ 0.14	175.9 $\pm$ 12.4	
	CO <sub>2</sub>	7.82 $\pm$ 0.09	35.7 $\pm$ 0.30	15.88 $\pm$ 1.53	2191 $\pm$ 32	2105.6 $\pm$ 22.0	2001.2 $\pm$ 26.49	1.77 $\pm$ 0.42	1.11 $\pm$ 0.26	489.9 $\pm$ 134.2	
	CO <sub>2</sub> /T+3	7.78 $\pm$ 0.03	35.8 $\pm$ 0.33	19.53 $\pm$ 1.38	2198 $\pm$ 32	2110.8 $\pm$ 26.5	2007.4 $\pm$ 24.99	1.77 $\pm$ 0.17	1.11 $\pm$ 0.11	470.6 $\pm$ 48.9	
Southern	Control	8.16 $\pm$ 0.01	35.8 $\pm$ 0.27	18.70 $\pm$ 1.19	2194 $\pm$ 94	1955.3 $\pm$ 78.5	1785.4 $\pm$ 65.78	3.80 $\pm$ 0.31	2.39 $\pm$ 0.20	172.0 $\pm$ 2.6	
	T+3	8.15 $\pm$ 0.01	35.9 $\pm$ 0.31	20.85 $\pm$ 0.45	2195 $\pm$ 73	1944.2 $\pm$ 66.0	1767.5 $\pm$ 59.05	3.97 $\pm$ 0.19	2.50 $\pm$ 0.12	161.4 $\pm$ 5.2	
	CO <sub>2</sub>	7.77 $\pm$ 0.06	35.8 $\pm$ 0.30	18.77 $\pm$ 1.21	2152 $\pm$ 54	2069.9 $\pm$ 36.0	1968.9 $\pm$ 31.15	1.69 $\pm$ 0.31	1.07 $\pm$ 0.19	483.1 $\pm$ 95.9	
	CO <sub>2</sub> /T+3	7.72 $\pm$ 0.08	35.9 $\pm$ 0.32	20.92 $\pm$ 0.41	2193 $\pm$ 84	2121.3 $\pm$ 83.2	2020.5 $\pm$ 81.65	1.60 $\pm$ 0.35	1.01 $\pm$ 0.22	541.5 $\pm$ 106.4	
Northern	Control	8.20 $\pm$ 0.08	33.4 $\pm$ 0.26	6.42 $\pm$ 2.12	2317 $\pm$ 48	2079.4 $\pm$ 49.8	1901.8 $\pm$ 60.3	3.27 $\pm$ 0.46	2.09 $\pm$ 0.3	243.3 $\pm$ 47.1	11.92 $\pm$ 0.52
	T+3	8.21 $\pm$ 0.08	33.4 $\pm$ 0.26	9.03 $\pm$ 0.49	2306 $\pm$ 42	2041.5 $\pm$ 50.7	1847.1 $\pm$ 67.5	3.66 $\pm$ 0.54	2.34 $\pm$ 0.34	235.8 $\pm$ 47.6	11.19 $\pm$ 0.18
	CO <sub>2</sub>	7.85 $\pm$ 0.11	33.3 $\pm$ 0.27	6.04 $\pm$ 2.35	2425 $\pm$ 53	2329.4 $\pm$ 64.5	2211.2 $\pm$ 69.6	1.70 $\pm$ 0.37	1.08 $\pm$ 0.24	643.2 $\pm$ 187.5	12.00 $\pm$ 0.59
	CO <sub>2</sub> /T+3	7.81 $\pm$ 0.13	33.4 $\pm$ 0.28	9.05 $\pm$ 0.49	2452 $\pm$ 64	2352.9 $\pm$ 88.7	2229.1 $\pm$ 94.4	1.80 $\pm$ 0.44	1.15 $\pm$ 0.28	738.9 $\pm$ 260.1	11.18 $\pm$ 0.18
Southern	Control	8.21 $\pm$ 0.08	33.5 $\pm$ 0.22	11.54 $\pm$ 0.39	2336 $\pm$ 37	2043.2 $\pm$ 53.4	1829.7 $\pm$ 74.1	4.08 $\pm$ 0.57	2.63 $\pm$ 0.37	235.4 $\pm$ 48.3	10.54 $\pm$ 0.16
	T+3	8.22 $\pm$ 0.07	33.5 $\pm$ 0.24	15.18 $\pm$ 1.6	2357 $\pm$ 41	2027.9 $\pm$ 59.8	1788.6 $\pm$ 82.2	4.68 $\pm$ 0.64	3.03 $\pm$ 0.42	235.1 $\pm$ 47	9.82 $\pm$ 0.29
	CO <sub>2</sub>	7.78 $\pm$ 0.12	33.5 $\pm$ 0.23	11.45 $\pm$ 0.41	2500 $\pm$ 73	2396.6 $\pm$ 77.9	2267.7 $\pm$ 82	1.9 $\pm$ 0.49	1.22 $\pm$ 0.32	808.3 $\pm$ 241.7	10.55 $\pm$ 0.14
	CO <sub>2</sub> /T+3	7.80 $\pm$ 0.11	33.5 $\pm$ 0.25	15.21 $\pm$ 1.61	2508 $\pm$ 86	2375.8 $\pm$ 96	2234.3 $\pm$ 101.2	2.28 $\pm$ 0.53	1.48 $\pm$ 0.34	785.4 $\pm$ 238.9	9.80 $\pm$ 0.30

instead of performing conversions to the total scale due to high error caused by manual titration and temperature increase during titration processes which falsified the conversion into the pH on total scale.

#### 5.4.1 Photosynthesis and Calcification Evolution

The average saturating light levels ( $P_{max}$ ) of CP under central conditions showed comparable control values between both populations (Figure 5.3 (A), Table 5.3). Both CP showed a significant increase under elevated temperatures (Table 5.3(B)). Under elevated  $pCO_2$  conditions, CP1 and CP2 showed a non-significant decrease and increase of  $P_{max}$ , respectively. Under climate change treatment with elevated temperature and  $pCO_2$ , CP1 showed a significant decrease and CP2 showed no change of  $P_{max}$  (Figure 5.3 (A), Table 5.3(A)). Additional significant differences were found for CP1 between T+3 and  $CO_2$  and T+3/ $CO_2$ , respectively (Table 5.3(B)) as well as for CP2 between T+3 and T+3/ $CO_2$  (Table 5.3(B)).

The photosynthetic efficiency,  $\alpha$ , of CP1 under central conditions decreased in all treatments, with the steepest decrease in the T+3 and T+3/ $CO_2$  treatment (Figure 5.3 (B), Table 5.3(A)). In CP2,  $\alpha$  increased in all except the T+3/ $CO_2$  treatment compared to control conditions (Table 5.3(A)).

The saturating light intensity  $I_k$  for net oxygen production of CP under central conditions is expected to react oppositely to the light harvesting efficiency (Figure 5.3 (C), Table 5.3(A)). This is the case for treatment T+3 and  $CO_2$  in CP1 and  $CO_2$  in CP2. However, a steep decline in  $\alpha$  as well as  $I_k$  was observed in treatment T+3/ $CO_2$  in CP1 and relatively constant values of all three parameters were observed in the same treatment in CP2. CP2 increased in all parameters in treatment T+3 (Table 5.3(A)).



The average saturating calcification levels ( $C_{max}$ ) of CP under central conditions changed non-significantly in CP1, nevertheless, all showed positive trends (Figure 5.3 (A), Table 5.3(A)). CP2 showed higher rates in all treatments compared to the control (Table 5.3(A)), with no significant changes between treatments, however, T+3/CO<sub>2</sub> showed significantly higher rates compared to the control (Table 5.3(B)).

The calcification efficiency,  $\alpha$ , of CP under central conditions increased in all CO<sub>2</sub> included treatments (Figure 5.3 (B), Table 5.3(A)). In treatments with elevated temperature, however, only CP2 showed an increase, when CP1 showed a clear decrease in efficiency (Table 5.3(A)).

The saturating light intensity  $I_k$  for calcification of CP under central conditions was expected to show opposing trends to  $\alpha$ . However, in CP1,  $I_k$  of T+3 and CO<sub>2</sub> increased and no change was observed in T+3/CO<sub>2</sub> compared to the control treatment (Figure 5.3 (C), Table 5.3). Therefore, for  $I_k$ , CP1 showed no anticipated reactions to the CO<sub>2</sub>-included treatments. In all treatments including elevated temperatures, CP2 showed an opposing trend than expected. In the CO<sub>2</sub> treatment, CP2 showed the expected opposing trend to  $\alpha$  with a decline in  $I_k$ .

The mean saturating light levels ( $P_{max}$ ) of SP under southern conditions declined significantly in T+3/CO<sub>2</sub> treatments compared to control treatments, with steeper declines in SP1 compared to SP2 (Figure 5.3 (A), Table 5.3). No significant change between experimental treatments in both populations was found. However, a significant decline was observed for SP1 from the Control to the T+3 and CO<sub>2</sub> treatments (Table 5.3(B)).

The photosynthetic efficiency,  $\alpha$ , of SP under southern conditions decreased drastically in all treatments compared to control treatments, in both populations

(Figure 5.3 (B)). With the exception of SP2 in the elevated CO<sub>2</sub> treatment, which was the sole treatment to increase in efficiency.

The saturating light intensity  $I_k$  for net oxygen production of SP under southern conditions declined in all CO<sub>2</sub>-included treatments in both populations, acting opposite to expectations formed by a decline in  $\alpha$  (Figure 5.3 (C), Table 5.3). Only in the treatment T+3  $I_k$  increased, in both populations similarly.

The average saturating calcification levels ( $C_{max}$ ) of SP under southern conditions showed a decrease in the T+3 compared to the control treatment (Figure 5.3 (A), Table 5.3(A)). In both populations,  $C_{max}$  in T+3/CO<sub>2</sub> treatments increased, however, not significantly. In SP1 in the CO<sub>2</sub> treatment  $C_{max}$  increased non-significantly. It also increased in SP2 when not combined with elevated temperature. A significant difference was found in SP2 between T+3 and CO<sub>2</sub> treatments (Table 5.3(B)).

The calcification efficiency,  $\alpha$ , of SP under southern conditions showed a decline in all treatments, except for SP2 in elevated pCO<sub>2</sub>, which was the sole treatment to show an increase in light harvesting efficiency compared to the control, equivalent to  $\alpha$  of P-I curves (Table 5.3(A)). The steepest decline compared to the control treatment was observed for SP1 in the T+3 treatment (Figure 5.3 (B), Table 5.3(A)).

The saturating light intensity  $I_k$  for calcification of SP under southern conditions increased in all populations in all treatments, except for the treatment T+3 in SP2 where it decreased compared to the control treatment (Table 5.3(A)). All treatments in SP2 showed a steeper increase or decrease compared to SP1 (Figure 5.3 (C)).

When comparing  $P_{max}$  of CP and SP within the same treatment, it was observed that significant differences were found between both CP and both SP in the T+3 treatment (Figure 5.3 (A), Table 5.3(B)). Additionally, marginally significant

differences in the control treatment were observed between SP1 and SP2 (Table 5.3(B)). Further, significant differences were found in CO<sub>2</sub> treatments between CP1 and SP1 as well as CP2 and both CP (Table 5.3(B)). Significant differences in the T+3/CO<sub>2</sub> treatment were found between both CP and both SP (Table 5.3(B)).

When comparing  $C_{max}$  of CP and SP within the same treatment, it was observed that significant differences were found in the T+3 treatment between both CP and both SP (Figure 5.3 (A), Table 5.3(B)). Additionally in the T+3/CO<sub>2</sub> treatment, both CP were significantly different to SP2, but not SP1 (Table 5.3(B)).

Synoptically, the climate change treatment had a negative effect on all populations under all conditions in all oxygen production curve parameters ( $P_{max}$ ,  $\alpha$  P-I and  $I_K$  P-I, Figure 5.3, Table 5.3). Regarding the influence of this treatment on calcification curve parameters, it caused an increase in  $C_{max}$  and  $I_K$  for all populations under respective conditions and an increase in light harvesting efficiency  $\alpha$  in CP, but a decrease in SP under the respective conditions.

Detailed graphs of P-I and C-I curves can be found in Appendix D, Figures D1-D16.

(A)

Temperature condition	Population	Treatment	Gross Production Rates [ $\mu\text{mol h}^{-1} \text{gDW}^{-1}$ ]				Net Calcification Rate [ $\mu\text{mol h}^{-1} \text{gDW}^{-1}$ ]				
			Pmax	$\pm\text{SD}$	$\alpha$ Oxygen evolution	I <sub>K</sub> Oxygen evolution	Cmax	$\pm\text{SD}$	$\alpha$ Calcification evolution	I <sub>K</sub> Calcification evolution	
Central	Central 1	Control	511.87	81.24	3.56	143.70	144.65	23.68	1.26	115.21	
		T+3	657.28	51.88	2.89	227.09	196.93	57.95	0.90	219.42	
		CO <sub>2</sub>	487.39	23.23	3.37	144.66	179.45	31.93	1.44	124.23	
	Central 2	T+3/CO <sub>2</sub>	188.71	65.40	2.89	65.37	186.05	9.08	1.59	116.99	
		Control	496.29	103.88	2.94	169.00	142.00	26.05	1.15	123.93	
		T+3	668.53	102.57	3.51	190.73	234.19	32.77	1.69	138.39	
South	Southern 1	CO <sub>2</sub>	568.71	75.51	3.85	147.54	225.14	13.35	2.01	112.15	
		T+3/CO <sub>2</sub>	504.18	57.98	2.90	173.87	260.02	39.67	1.79	145.20	
		Control	566.78	53.76	3.63	156.25	153.70	18.44	1.57	97.88	
	Southern 2	T+3	355.39	36.09	1.87	190.20	93.80	8.80	0.58	160.76	
		CO <sub>2</sub>	330.12	124.22	2.58	127.73	179.65	41.93	1.50	119.85	
		T+3/CO <sub>2</sub>	350.62	13.76	2.83	123.93	163.60	6.26	1.46	111.93	
	Southern 1	Southern 1	Control	448.15	71.38	3.07	146.19	86.49	19.13	0.79	109.53
			T+3	368.14	72.57	2.14	171.89	56.87	8.54	0.71	80.46
			CO <sub>2</sub>	396.16	26.93	3.33	118.94	169.78	52.90	1.15	147.47
		Southern 2	T+3/CO <sub>2</sub>	329.98	60.51	2.35	140.43	114.58	22.77	0.63	181.99

(B)

P <sub>max</sub> (2-way ANOVA) C <sub>max</sub> (Kruskal-Wallis H Test)	Central condition						Southern condition					
	Central population 1			Central population 2			Southern population 1			Southern population 2		
	Control	T+3	CO <sub>2</sub>	T+3/CO <sub>2</sub>	Control	T+3	CO <sub>2</sub>	T+3/CO <sub>2</sub>	Control	T+3	CO <sub>2</sub>	T+3/CO <sub>2</sub>
Central condition	NS	*	NS	**	NS	NS	NS	NS	NS	***	NS	NS
Central population 1	NS	NS	NS	NS	NS	NS	NS	NS	NS	NS	NS	NS
Central population 2	NS	NS	NS	NS	NS	NS	NS	NS	NS	NS	NS	NS
Southern condition	NS	NS	NS	NS	NS	NS	NS	NS	NS	NS	NS	NS
Southern population 1	NS	NS	NS	NS	NS	NS	NS	NS	NS	NS	NS	NS
Southern population 2	NS	NS	NS	NS	NS	NS	NS	NS	NS	NS	NS	NS

Significance levels: NS = not significant \* = P < 0.05 \*\* = P < 0.01 \*\*\* = P < 0.005

**Table 5.3:** (A) Mean  $\pm\text{SD}$  (n = 5) for saturating photosynthesis (P<sub>max</sub>) and calcification (C<sub>max</sub>) levels, photosynthetic efficiency ( $\alpha$ ) and saturating light intensity (I<sub>K</sub>) of *C. officinalis* in the Cross Experiment of Central (n = 2) and Southern (n = 2) populations. (B) Statistical comparison of P<sub>max</sub> and C<sub>max</sub> between populations within temperature treatment and between temperature treatments within populations.

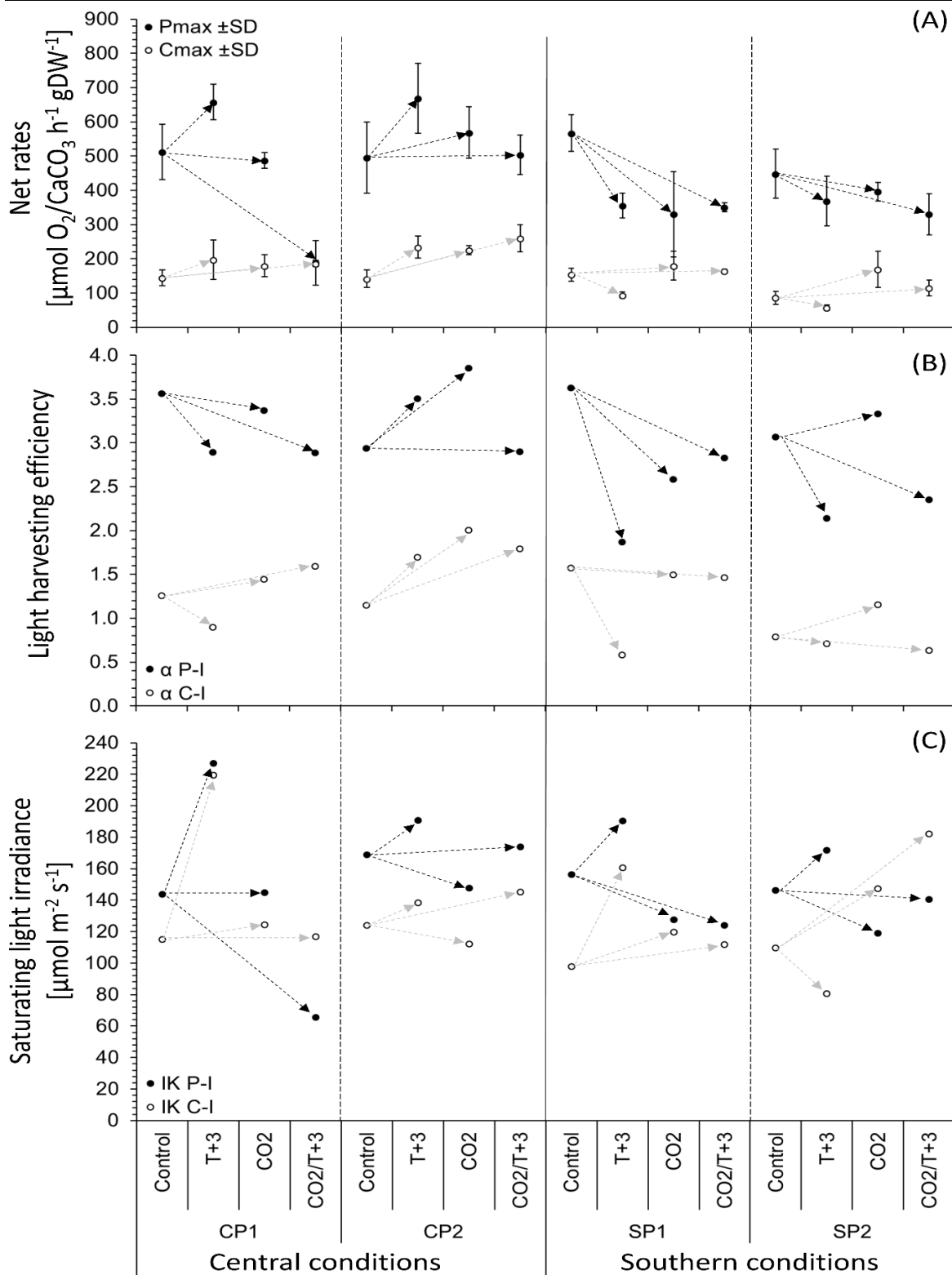


**Figure 5.3** Evolution curve characteristics for net production and calcification ( $AV \pm \text{SD}$ ,  $n = 3$ ) of the central (CP) and southern (SP) populations ( $n = 2$ ) of the Cross Experiment. Each populations is divided into the experimental treatments (Control, T+3, CO<sub>2</sub>, CO<sub>2</sub>/T+3). (A):  $P_{\text{max}}/C_{\text{max}}$  = maximum production, (B):  $\alpha$  = photosynthetic efficiency, (C):  $I_K$  = saturating irradiance. Arrows indicate direction of change: control to altered conditions.

### 5.4.2 Primary Production and Respiration

In the Climate Change Experiment, photosynthetic rates were highly variable throughout the regions of origin (Figure 5.4, Table 5.4).

Northern populations (NP), NP1 showed higher rates in T+3-included treatments compared to the other two treatments (Figure 5.4, Table 5.4(A)). However, under CO<sub>2</sub>-included treatments rates of NP1 declined marginally significant compared to the T+3 treatment (Table 5.4(B)). In control, T+3 and T+3/CO<sub>2</sub> treatments, NP2 showed stable rates. Only in the CO<sub>2</sub> treatment, NP2 showed a decline in photosynthetic rates in accordance with NP1 (Table 5.4(A)).

Central populations (CP), like NP, showed higher photosynthetic rates in elevated temperature treatments compared to their respective control treatment (Table 5.4(A)), except for CP2, which showed lower rates in T+3 compared to the control (Figure 5.4, Table 5.4(A)). All CO<sub>2</sub>-elevated treatments showed a decrease in photosynthetic rates compared to their respective control. Except for CP2 which showed lower rates in the CO<sub>2</sub> compared to the T+3/CO<sub>2</sub> treatment, but also higher error bars. A significant difference was found in CP1 T+3 vs. CO<sub>2</sub> (Table 5.4(B)).

Due to the lack of material of SP2, only SP1 was incubated for physiological measurements. Control and T+3 treatments are higher in SP1 compared to both CO<sub>2</sub>-included treatments (Figure 5.4, Table 5.4(A)). Under treatment T+3/CO<sub>2</sub>, SP1 showed the lowest values of all populations in all treatments. In treatment T+3, SP1 showed highest rates within all treatments. A significant difference was therefore found for SP1 between control and T+3 with the T+3/CO<sub>2</sub> treatment (Table 5.4(B)).

Respiration rates (Figure 5.4) were lowest in NP compared to all other regions of origin, CP and SP showed comparable rates (Table 5.4(A)). Both NP showed the

lowest respiration values in T+3 treatments, whereas all CP and SP showed lowest values in control treatments, followed by T+3 treatments. All populations showed highest respiration rates in the CO<sub>2</sub>-included treatments, with only SP1 showing the highest rates in T+3/CO<sub>2</sub> and all others in the CO<sub>2</sub> treatments (Table 5.4(A)). Significant differences were found in: T+3: NP1 vs. both CP; CO<sub>2</sub>: both NP vs. both CP, SP1 vs. CP2; T+3/CO<sub>2</sub>: both NP vs. CP2 and SP1, NP2 vs. CP1 (Table 5.4(B)).

In NP1, rates were highest in the control and CO<sub>2</sub> treatments (Table 5.4(A)) and lowest in the temperature-included treatments, with T+3 showing the lowest values (Figure 5.4, Table 5.4(A)). Treatments including elevated temperatures were lower compared to their respective control treatment. In NP2, less pronounced changes were observed, however, highest rates were shown in CO<sub>2</sub>-included treatments, with highest rates in the CO<sub>2</sub> treatment and lowest values were observed in the T+3 treatment (Figure 5.4, Table 5.4(A)). Both NP showed a less defined but similar response scheme and a different response scheme compared to CP and SP.

In CP, both populations showed the same pattern with highest respiration rates found in the CO<sub>2</sub> treatment, followed by the T+3/CO<sub>2</sub> treatment, followed by the T+3 treatment and the lowest rates shown in control treatments (Figure 5.4, Table 5.4(A)). Significant differences were found in CP1 Control vs. CO<sub>2</sub> and in CP2 CO<sub>2</sub> vs. Control, T+3, T+3/CO<sub>2</sub> (Table 5.4(B)).

Southern population 1 was the only population where highest respiration rates were observed in the climate change treatment (Figure 5.4, Table 5.4(A)). All other treatments follow the same pattern of CP, with higher rates in the CO<sub>2</sub> treatment, followed by the T+3 treatment, and followed by the control treatment. Significant differences were found in T+3/CO<sub>2</sub> vs. Control and T+3 (Table 5.4).

(A)	Region	Population	Treatment	Primary production		Respiration		Light Calcification		Dark Calcification	
				[ $\mu\text{mol O}_2 \text{ L}^{-1} \text{ h}^{-1} \text{ gDW}^{-1}$ ]		[ $\mu\text{mol O}_2 \text{ L}^{-1} \text{ h}^{-1} \text{ gDW}^{-1}$ ]		[ $\mu\text{mol CaCO}_3 \text{ L}^{-1} \text{ h}^{-1} \text{ gDW}^{-1}$ ]		[ $\mu\text{mol CaCO}_3 \text{ L}^{-1} \text{ h}^{-1} \text{ gDW}^{-1}$ ]	
				Mean	$\pm\text{SE}$	Mean	$\pm\text{SE}$	Mean	$\pm\text{SE}$	Mean	$\pm\text{SE}$
North	1	Control	14.24	6.50	-29.91	8.07	-25.82	4.11	-10.16	5.07	
		T+3	49.42	18.61	-15.33	2.27	-23.82	19.03	18.78	9.76	
		CO <sub>2</sub>	6.52	0.54	-29.84	5.30	-4.74	8.50	-29.98	11.44	
	2	T+3/CO <sub>2</sub>	20.23	19.19	-25.96	1.82	22.53	14.86	-2.18	18.82	
		Control	28.54	10.99	-17.68	6.32	-13.11	14.25	-7.89	0.98	
		T+3	28.80	9.41	-16.67	0.64	-70.92	62.45	7.46	8.79	
Central	1	CO <sub>2</sub>	14.39	5.04	-27.55	2.77	2.38	7.68	-26.38	11.90	
		T+3/CO <sub>2</sub>	30.64	17.09	-22.47	5.34	7.26	21.87	-4.29	9.98	
		Control	22.25	12.86	-34.95	4.91	11.92	7.38	-1.00	16.31	
	2	T+3	53.33	10.70	-43.96	4.76	-37.44	19.09	-59.17	20.82	
		CO <sub>2</sub>	8.88	14.20	-64.53	7.50	35.24	8.86	-11.87	7.62	
		T+3/CO <sub>2</sub>	37.17	21.84	-47.93	15.36	-5.50	7.56	10.29	9.91	
South	1	Control	33.64	14.96	-30.26	1.65	6.59	8.23	3.26	21.02	
		T+3	24.05	11.01	-40.30	5.12	-29.85	12.91	-47.79	14.37	
		CO <sub>2</sub>	15.88	26.37	-80.62	10.75	42.95	11.84	-26.77	6.06	
	2	T+3/CO <sub>2</sub>	32.47	6.37	-52.91	11.33	-3.54	1.73	9.45	1.98	
		Control	45.96	16.28	-28.34	5.77	-85.83	29.58	-160.32	58.32	
		T+3	52.67	19.09	-28.92	13.37	84.05	16.20	16.82	5.75	
1	CO <sub>2</sub>	10.25	22.73	-50.06	6.22	75.05	30.78	159.90	127.32		
	T+3/CO <sub>2</sub>	3.08	5.19	-66.21	19.92	-81.76	9.42	-94.80	47.16		

(B)	Primary production	Respiration	Light Calcification	Dark Calcification	North						Central						South					
					1		2		1		2		1		2		1		2			
					Control	T+3	Control	T+3	Control	T+3	Control	T+3	Control	T+3	Control	T+3	Control	T+3	Control	T+3		
North	1	Control	NS	NS	NS	NS	NS	NS	NS	NS	NS	NS	NS	NS	NS	NS	NS					
		T+3	NS	NS	NS	NS	NS	NS	NS	NS	NS	NS	NS	NS	NS	NS	NS					
		CO <sub>2</sub>	NS	NS	NS	NS	NS	NS	NS	NS	NS	NS	NS	NS	NS	NS	NS	NS				
	2	Control	NS	NS	NS	NS	NS	NS	NS	NS	NS	NS	NS	NS	NS	NS	NS	NS				
		T+3	NS	NS	NS	NS	NS	NS	NS	NS	NS	NS	NS	NS	NS	NS	NS	NS				
		CO <sub>2</sub>	NS	NS	NS	NS	NS	NS	NS	NS	NS	NS	NS	NS	NS	NS	NS	NS				
Central	1	Control	NS	NS	NS	NS	NS	NS	NS	NS	NS	NS	NS	NS	NS	NS	NS					
		T+3	NS	NS	NS	NS	NS	NS	NS	NS	NS	NS	NS	NS	NS	NS	NS					
		CO <sub>2</sub>	NS	NS	NS	NS	NS	NS	NS	NS	NS	NS	NS	NS	NS	NS	NS	NS				
	2	Control	NS	NS	NS	NS	NS	NS	NS	NS	NS	NS	NS	NS	NS	NS	NS	NS				
		T+3	NS	NS	NS	NS	NS	NS	NS	NS	NS	NS	NS	NS	NS	NS	NS	NS				
		CO <sub>2</sub>	NS	NS	NS	NS	NS	NS	NS	NS	NS	NS	NS	NS	NS	NS	NS	NS				
South	1	Control	NS	NS	NS	NS	NS	NS	NS	NS	NS	NS	NS	NS	NS	NS	NS					
		T+3	NS	NS	NS	NS	NS	NS	NS	NS	NS	NS	NS	NS	NS	NS	NS					
		CO <sub>2</sub>	NS	NS	NS	NS	NS	NS	NS	NS	NS	NS	NS	NS	NS	NS	NS	NS				
	2	Control	NS	NS	NS	NS	NS	NS	NS	NS	NS	NS	NS	NS	NS	NS	NS	NS				
		T+3	NS	NS	NS	NS	NS	NS	NS	NS	NS	NS	NS	NS	NS	NS	NS	NS				
		CO <sub>2</sub>	NS	NS	NS	NS	NS	NS	NS	NS	NS	NS	NS	NS	NS	NS	NS	NS				

**Table 5.4:** (A) Mean  $\pm$ SE for primary production, respiration, light and dark calcification of the northern margin (n = 2), central (n = 2) and southern margin populations (n = 2) of *C. officinalis* in the NE Atlantic under Control (n = 3), elevated temperature (T+3, n = 3), elevated pCO<sub>2</sub> (n = 3) and Climate Change (T+3/CO<sub>2</sub>, n = 3) treatments in the Climate Change Experiment. (B) Statistical comparison between populations within treatments and treatments within populations.

Significance levels: NS = not significant \* = P < 0.05 \*\* = P < 0.01 \*\*\* = P < 0.005



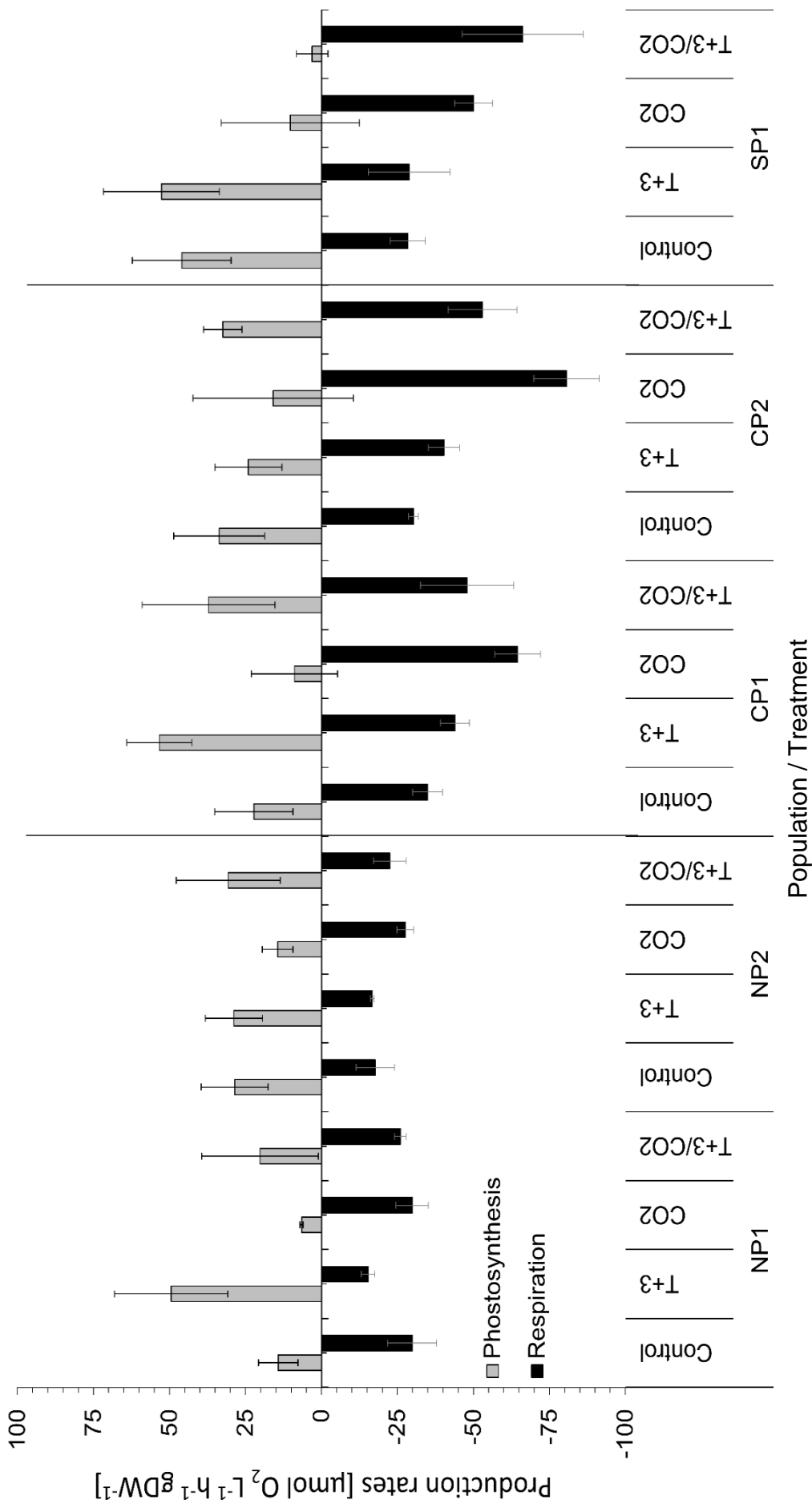


**Figure 5.4:** Gross primary production and respiration rates [ $\mu\text{mol h}^{-1} \text{ L}^{-1} \text{ gDW}^{-1}$ ]  $\pm$ SE of *C. officinalis* after the Climate Change Experiment of each population under each treatment condition. Northern, central and southern populations are abbreviated as NP, CP and SP, respectively.

In the Cross Experiment, highly variable responses in primary production and respiration rates of all populations were observed in all treatments. The Cross Experiment was run under conditions that would be experienced during winter months, explaining the occasionally low primary production and respiration caused by slow metabolic rates (Figure 5.5, Table 5.5).

When comparing pre- and post-experimental control incubations of primary production rates, all rates increased significantly in CP1 (Figure 5.5, Table 5.5(B)). CP2 increased significantly from prior to the post CO<sub>2</sub> treatment (Table 5.5(B)). Within treatments the following significances were found (Table 5.5(B)): Control: CP1 vs. CP2 and SP1; T+3: CP1 vs. CP2, both SP; CO<sub>2</sub>: SP1 vs. both CP, SP2; T+3/CO<sub>2</sub>: CP2 vs. CP1, SP2.

Compared to control conditions after the exposure to experimental conditions, CP1 showed an increase in primary production rates in the T+3 treatment (Table 5.5), however a decrease of rates was observed in both CO<sub>2</sub>-included treatments (Figure 5.5, Table 5.5(A)). The second CP showed stable or marginally changing rates in both elevated temperature treatments compared to the Control and the only increase in primary production rates was observed in the pCO<sub>2</sub> elevated treatment (CO<sub>2</sub> > T+3 ≈ Control > T+3/CO<sub>2</sub>). When comparing both populations of one country, CP1 showed higher rates in Control, T+3 and T+3/CO<sub>2</sub> and equal rates in the CO<sub>2</sub> treatment compared to CP2. Significant differences were found in CP1 T+3 vs. CO<sub>2</sub>, T+3/CO<sub>2</sub> (Table 5.5(B)) and in CP2 CO<sub>2</sub> vs. Control, T+3, T+3/CO<sub>2</sub> (Table 5.5(B))

In SP1, all treatments declined in primary production rates compared to the Control, except for the climate change treatment (T+3/CO<sub>2</sub>) that showed an increase (T+3/CO<sub>2</sub> > Control > CO<sub>2</sub> > T+3, Figure 5.5, Table 5.5(A)). In SP2, rates increased in all treatments compared to the Control and elevated temperature-included

treatments were higher than their respective control treatment ( $T+3/CO_2 > CO_2 > T+3 > Control$ , Table 5.5(B)). When comparing both populations of one country, SP1 showed lower rates in all treatments compared to SP2.

Respiration was higher in SP than CP in all treatments and less variable than primary production (Figure 5.5, Table 5.5(A)). Populations within treatment showed significant differences in (Table 5.5(B)): Before: SP2 vs. both CP, SP1; Control: both CP vs. both SP;  $CO_2$ : both CP vs. SP1;  $T+3/CO_2$ : both CP vs. both SP.

In both CP, rates in the Control are significantly higher after compared to prior to the experiment (Table 5.5(A)) and presented primary production instead of respiration (Figure 5.5, Table 5.5(B)). In CP1, significant changes were observed in respiration rates between control and other treatments (Table 5.5(B);  $CO_2 \approx T+3 \approx T+3/CO_2 > Control$ ). Unusually, post-experimentally, the Control showed primary production instead of respiration rates. In CP2, compared to the Control, all treatments increased and showed significant difference between Control and the other treatments (Table 5.5(A);  $T+3 \approx CO_2 > T+3/CO_2 > Control$ ; Table 5.5(B), Figure 5.5). Comparing both populations of one country, CP1 showed higher rates in Control and  $T+3/CO_2$  and equal rates in the  $T+3$  and  $CO_2$  treatment compared to CP2.

In SP1, pre-experimental respiration rates were significantly lower compared to post-experimental respiration rates under  $CO_2$  and  $T+2/CO_2$  treatments (Table 5.5, Figure 5.5). When comparing both populations of one country, SP1 showed higher rates in  $CO_2$  and  $T+3/CO_2$ , lower rates in the Control and equal rates in the  $T+3$  treatment, compared to SP2 (Table 5.5(B)). In  $CO_2$ -included treatments, SP1 showed increased respiration rates, whereas in treatment  $T+3$ , no significant change was found ( $CO_2 > T+3/CO_2 > T+3 \approx Control$ ). Compared to the Control, SP2 showed reduced respiration rates in all treatments ( $Control > T+3/CO_2 > T+3 > CO_2$ ).

SP1 showed significantly different rates in CO<sub>2</sub> compared to the control and T+3 treatments (Table 5.5(B)).

**Table 5.5:** (A) Mean  $\pm$ SE for primary production, respiration, light and dark calcification of central (n = 2) and southern margin populations (n = 2) of *C. officinalis* in the NE Atlantic under Control (n = 3), elevated temperature (T+3, n = 3), elevated pCO<sub>2</sub> (n = 3) and Climate Change (T+3/CO<sub>2</sub>, n = 3) treatments in the Cross Experiment. (B) Statistical comparison between populations within treatments and treatments within populations.

(A)

Temperature condition	Population	Treatment	Gross production rates		Respiration rates		Gross calcification rates		Dark calcification rates	
			[ $\mu\text{mol O}_2 \text{ h}^{-1} \text{ L}^{-1} \text{ gDW}^{-1}$ ]		[ $\mu\text{mol O}_2 \text{ h}^{-1} \text{ L}^{-1} \text{ gDW}^{-1}$ ]		[ $\mu\text{mol CaCO}_3 \text{ h}^{-1} \text{ L}^{-1} \text{ gDW}^{-1}$ ]		[ $\mu\text{mol CaCO}_3 \text{ h}^{-1} \text{ L}^{-1} \text{ gDW}^{-1}$ ]	
			Mean	$\pm$ SE	Mean	$\pm$ SE	Mean	$\pm$ SE	Mean	$\pm$ SE
Central	Central 1	Control	66.74	8.60	16.85	7.47	32.20	1.03	8.69	4.97
		T+3	103.12	30.18	-26.64	2.47	39.02	5.12	-17.00	3.44
		CO <sub>2</sub>	55.95	12.82	-27.85	1.60	60.66	7.41	6.14	8.60
		T+3/CO <sub>2</sub>	55.48	2.72	-26.59	1.29	15.64	9.48	17.54	3.12
	Central 2	Control	2.11	0.48	35.23	6.19	14.55	2.25	18.21	13.12
		T+3	2.42	0.25	-31.21	5.89	26.55	6.05	-19.31	5.21
		CO <sub>2</sub>	49.73	15.99	-29.86	4.24	39.85	9.07	1.66	2.23
		T+3/CO <sub>2</sub>	1.59	0.21	-26.52	12.28	22.64	4.94	9.30	0.25
South	Southern 1	Control	6.10	12.84	-41.44	10.23	17.32	4.95	8.97	9.11
		T+3	1.82	0.43	-41.99	5.02	39.86	6.14	-17.60	4.42
		CO <sub>2</sub>	4.17	10.21	-62.27	14.88	-6.76	19.28	56.86	26.24
		T+3/CO <sub>2</sub>	30.67	18.45	-51.74	8.31	49.73	14.86	-5.20	3.44
	Southern 2	Control	32.82	17.03	-52.02	10.40	20.89	4.64	-4.63	6.13
		T+3	35.32	14.73	-42.10	4.42	23.77	3.96	-30.63	16.21
		CO <sub>2</sub>	48.15	8.05	-35.49	0.70	-16.43	4.21	29.63	7.60
		T+3/CO <sub>2</sub>	54.59	16.02	-47.73	2.73	69.23	11.82	9.30	11.74

(B)

Gross production		Central condition								Southern condition									
Respiration		Central population 1				Central population 2				Southern population 1				Southern population 2					
2-way ANOVA		Control	T+3	CO <sub>2</sub>	T+3/CO <sub>2</sub>	Control	T+3	CO <sub>2</sub>	T+3/CO <sub>2</sub>	Control	T+3	CO <sub>2</sub>	T+3/CO <sub>2</sub>	Control	T+3	CO <sub>2</sub>	T+3/CO <sub>2</sub>		
Central condition	Central population 1	Control	***	NS	*	*	***	***			***	***			NS	***			
		T+3	***	NS		NS			NS				***				NS		
		CO <sub>2</sub>	***	NS	NS	NS				NS				***				NS	
		T+3/CO <sub>2</sub>	***	NS	NS					**				NS					NS
	Central population 2	Control	NS	NS			***	NS	*	NS	NS	NS			NS	NS			
		T+3		NS			***	NS	*	NS	NS	NS			NS	NS			
		CO <sub>2</sub>			NS		***	NS	*				*				NS		
		T+3/CO <sub>2</sub>				NS	***	NS	NS					NS					**
Southern condition	Southern population 1	Control	***	NS			***			NS	NS	NS	NS	NS	NS				
		T+3		NS			NS			NS	NS	NS	NS	NS	NS				
		CO <sub>2</sub>			***				***	*	*	*	NS				*		
		T+3/CO <sub>2</sub>				*			*	NS	NS	NS	NS						NS
	Southern population 2	Control	***	NS			***			NS	NS	NS	NS	NS	NS	NS			
		T+3		NS			NS			NS	NS	NS	NS	NS	NS	NS			
		CO <sub>2</sub>			NS				NS	*	NS	NS	NS	NS	NS	NS	NS	NS	NS
		T+3/CO <sub>2</sub>				*			*				NS	NS	NS	NS	NS	NS	NS
Gross calcification		Central condition								Southern condition									
Dark calcification		Central population 1				Central population 2				Southern population 1				Southern population 2					
2-way ANOVA		Control	T+3	CO <sub>2</sub>	T+3/CO <sub>2</sub>	Control	T+3	CO <sub>2</sub>	T+3/CO <sub>2</sub>	Control	T+3	CO <sub>2</sub>	T+3/CO <sub>2</sub>	Control	T+3	CO <sub>2</sub>	T+3/CO <sub>2</sub>		
Central condition	Central population 1	Control	NS	NS	*	NS	NS			NS	NS			NS	NS				
		T+3	NS	NS	NS	NS			NS			***			NS	NS		***	
		CO <sub>2</sub>	NS	NS	*	***				NS			***	*				***	***
		T+3/CO <sub>2</sub>	NS	*	NS					NS				*					***
	Central population 2	Control	NS	NS			*		NS	NS	NS	NS			NS	NS			
		T+3		NS			*		NS	NS	NS	NS			NS	NS			
		CO <sub>2</sub>			NS		NS	NS	NS	NS			***				***		***
		T+3/CO <sub>2</sub>				NS	NS	*	NS					*					***
Southern condition	Southern population 1	Control	NS	NS			NS			NS	NS	NS	*	NS	NS				
		T+3		NS			NS			NS	NS	NS	***	NS	NS				
		CO <sub>2</sub>			***				***	*	***	***	***					NS	
		T+3/CO <sub>2</sub>				NS			NS	NS	NS	NS	***						NS
	Southern population 2	Control	NS	NS			NS			NS	NS	NS			NS	NS			
		T+3		NS			NS			NS	NS	NS			NS	NS			
		CO <sub>2</sub>			NS				NS				NS		*	***		***	***
		T+3/CO <sub>2</sub>				NS			NS				NS	NS	**	NS			***

Significance levels: NS = not significant \* = P < 0.05 \*\* = P < 0.01 \*\*\* = P < 0.005

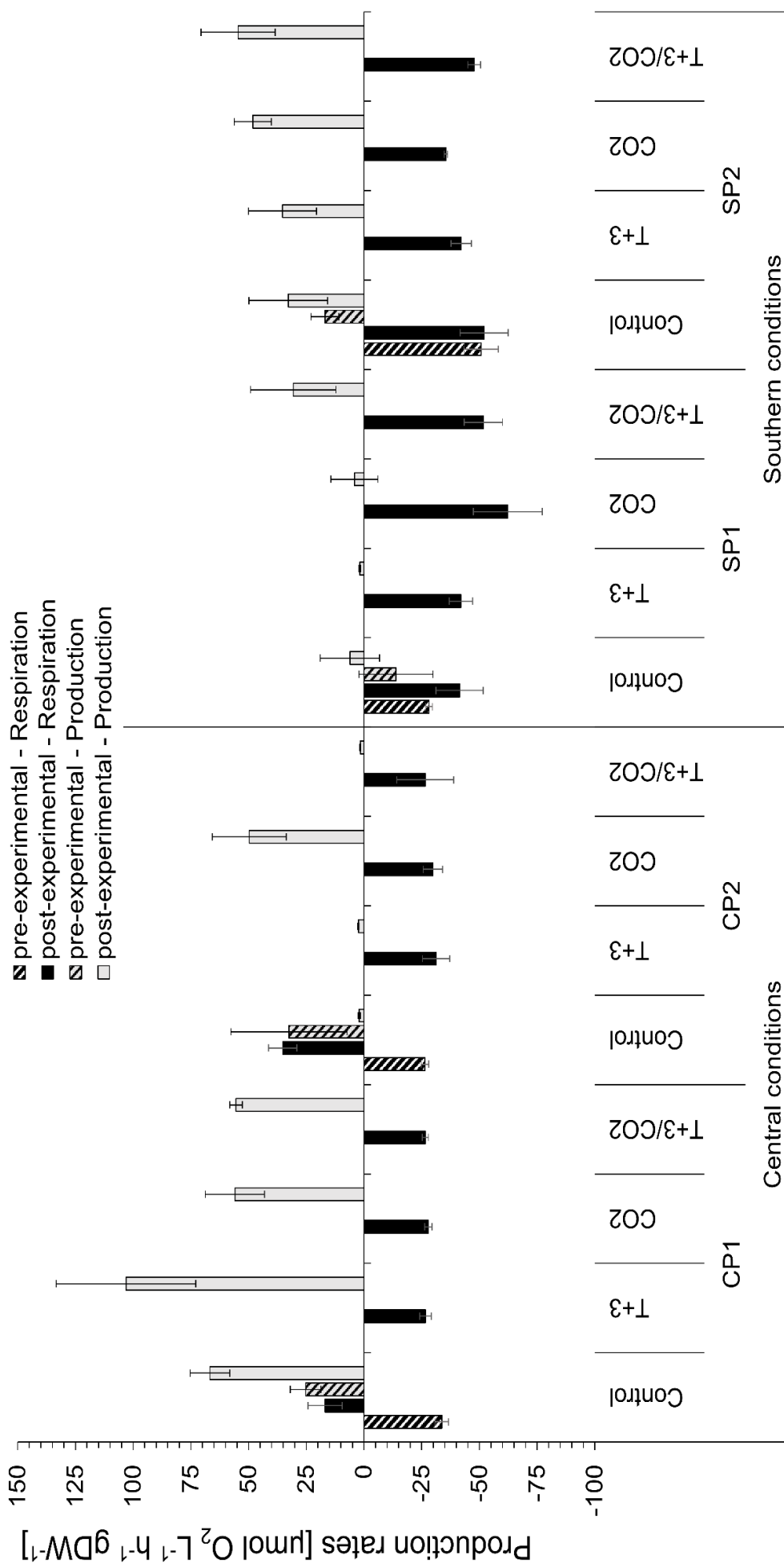


**Figure 5.5:** Primary production and respiration rates [ $\mu\text{mol h}^{-1} \text{L}^{-1} \text{gDW}^{-1}$ ]  $\pm$ SE of *C. officinalis* before ( $n = 4$ ) and after ( $n = 3$ ) the Cross Experiment of each population under each treatment condition. Central and southern populations are abbreviated as CP and SP, respectively.

### 5.4.1 Calcification Rates

Within the Climate Change Experiment, calcification rates showed a great variability. Light calcification rates were low in all populations and in most treatments, with some populations showing dissolution (Table 5.4(A)). Comparing populations within a treatment, SP1 was significantly different to both NP in all treatments (Table 5.4(B)) and to both CP in all but the CO<sub>2</sub> treatments (Table 5.4(B)).

In NP2, calcification rates in the light (Figure 5.6, Table 5.4(A)) were significantly higher under the T+3 treatment compared to control measurements (Table 5.4(B)). Additionally, light calcification rates in the T+3 treatment were significantly higher in NP2 compared to the CO<sub>2</sub> and T+3/CO<sub>2</sub> treatment (Table 5.4) and more negative compared to the Control (T+3/CO<sub>2</sub> > CO<sub>2</sub> > T+3 > Control and T+3/CO<sub>2</sub> > CO<sub>2</sub> > Control > T+3 for NP1 and NP2, respectively). All CO<sub>2</sub>-including treatments showed higher rates than the respective control treatment. Comparison between populations showed lower rates of light calcification in NP1 than NP2 in treatments T+3, CO<sub>2</sub>, T+3/CO<sub>2</sub> and higher rates in NP1 compared to NP2 in the control treatment.

In CP, both populations showed the same order of elevated rates in treatments with the highest light calcification rates under CO<sub>2</sub> (Table 5.4(A)) and the lowest rates under T+3 treatments (Table 5.4(A); CO<sub>2</sub> > Control > T+3/CO<sub>2</sub> > T+3) (Table 5.4(B), Figure 5.6). All CO<sub>2</sub>-including treatments showed higher rates than the respective control treatment (Table 5.4(A)). Comparison between populations showed higher rates of light calcification in CP1 than CP2 in treatments Control, T+3, T+3/CO<sub>2</sub> and lower rates in CP1 compared to CP2 in the CO<sub>2</sub> treatment.

Southern population 1 showed higher and the most pronounced rates of all populations in all treatments (Figure 5.6, Table 5.4(A)), except dark calcification NP1 vs. SP1. In the control and the climate change treatment, light calcification rates

were negative and not significantly different (Table 5.4). Rates in T+3 and CO<sub>2</sub> treatments were significantly higher and positive, no significant difference was found (Table 5.4(A)). However, a significant difference between the groups Control and T+3/CO<sub>2</sub> and T+3 and CO<sub>2</sub> was found (Table 5.4(B)).

Calcification rates in the dark (Figure 5.6, Table 5.4) showed a similar variability than calcification rates in the light. Northern populations showed the same trend of differences between treatments with only the CO<sub>2</sub>-treatment showing higher rates than the Control (Table 5.4(A); CO<sub>2</sub> > Control > T+3/CO<sub>2</sub> > T+3). Comparison between populations showed higher rates of dark calcification in NP1 than NP2 in treatments Control, T+3, CO<sub>2</sub> and lower rates in NP1 than NP2 in T+3/CO<sub>2</sub>.

In CP, as in NP, an identical trend of differences between treatments was observed with significantly lowest, negative dark calcification rates in the T+3 and highest, positive rates in the T+3/CO<sub>2</sub> treatment (Table 5.4(A); T+3/CO<sub>2</sub> > Control > CO<sub>2</sub> > T+3, Figure 5.6). Comparison between populations showed lower rates of dark calcification in CP1 than CP2 in treatments Control, CO<sub>2</sub>, higher rates in the T+3 treatment and similar rates in the T+3/CO<sub>2</sub> treatment.

In SP1, lowest, negative rates were found in the control treatment, followed by higher, negative rates in the T+3/CO<sub>2</sub> treatment; higher, positive rates in the T+3 treatment and the highest, positive rates in the CO<sub>2</sub> treatment (Table 5.4(A); CO<sub>2</sub> > T+3 > T+3/CO<sub>2</sub> > Control, Figure 5.6). Significant differences were found in SP1 T+3 vs. Control, CO<sub>2</sub>, T+3/CO<sub>2</sub> and CO<sub>2</sub> vs. Control, T+3/CO<sub>2</sub> (Table 5.4(B)). Additional significant differences between SP1 and other populations were found within treatments: Control: SP1 vs. both NP, both CP; CO<sub>2</sub>: SP1 vs. both NP, both CP; T+3/CO<sub>2</sub>: SP1 vs. both CP (Table 5.4(B)).

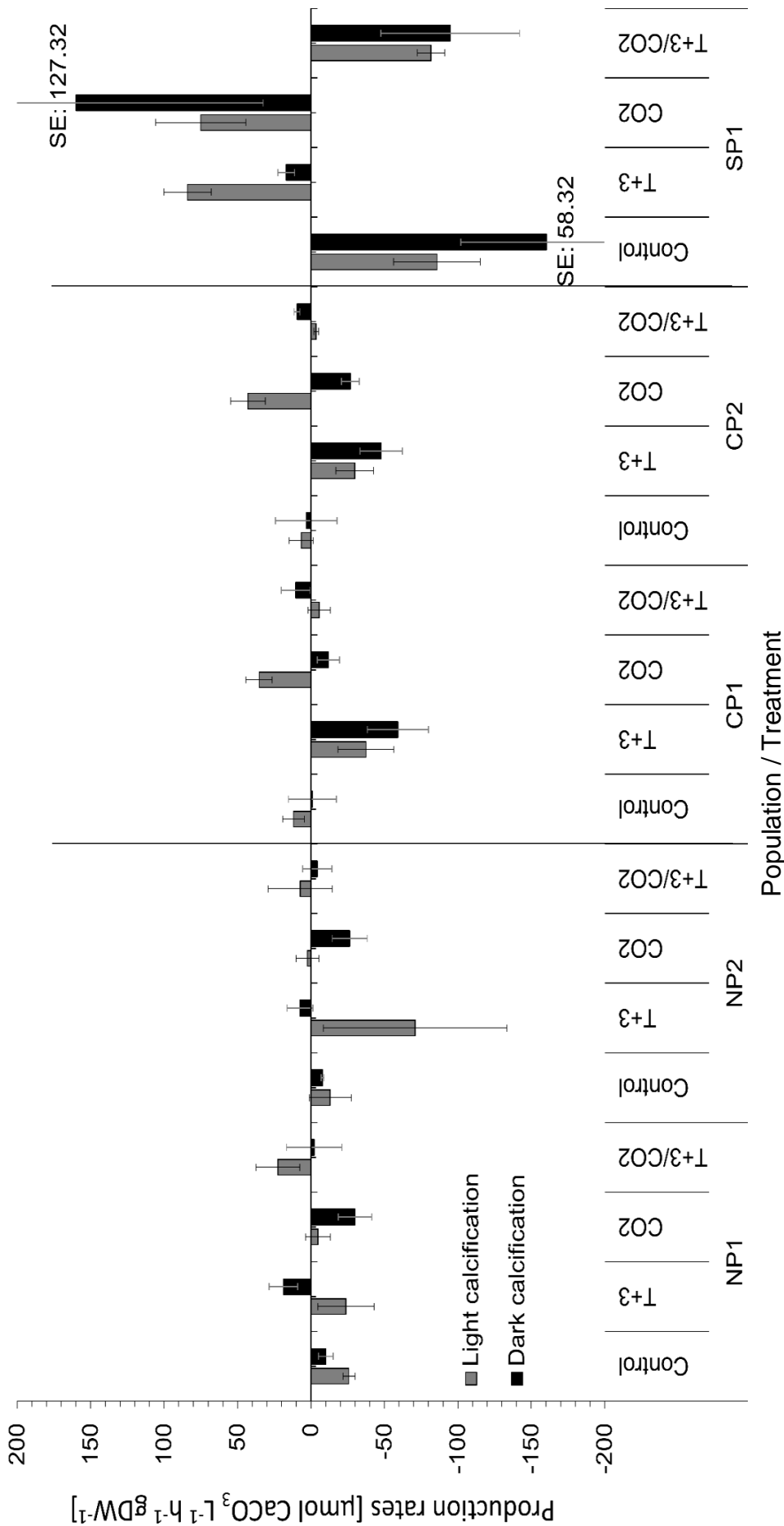


**Figure 5.6:** Light calcification and dark calcification rates [ $\mu\text{mol h}^{-1} \text{L}^{-1} \text{gDW}^{-1}$ ]  $\pm$ SE of *C. officinalis* after the Climate Change Experiment of each population under each treatment condition. Northern, central and southern populations are abbreviated as NP, CP and SP, respectively.



In the Cross Experiment (Figure 5.7, Table 5.5), all populations showed an increase from control to high temperature treatments in light calcification. However, only SP showed an increase from CO<sub>2</sub> to T+3/CO<sub>2</sub> treatments, whereas CP showed a decrease from CO<sub>2</sub> to T+3/CO<sub>2</sub> treatments (Table 5.5(A)). In dark calcification rates, all populations showed positive or near positive calcification rates. In all populations the rates decreased from positive into negative, hence dissolution, rates from control to T+3 treatments. A similar but opposite pattern to the light calcification was observed in dark calcification, a decline in rates from CO<sub>2</sub> to T+3/CO<sub>2</sub> treatments was found in SP, however, an increase in dark calcification rates was found in CP from CO<sub>2</sub> to T+3/CO<sub>2</sub> treatments. Significant differences were found between populations: Before CP1 vs. CP2, CP1 vs. SP2, SP1 vs. CP2, SP2; CO<sub>2</sub>: both CP vs. both SP; T+3/CO<sub>2</sub>: both CP vs. both SP (Table 5.5(B)).

In CP, highest light calcification rates were observed in CO<sub>2</sub> treatments (Figure 5.7, Table 5.5(A)) and lowest rates were observed in the T+3/CO<sub>2</sub> and control treatment, for CP1 and CP2, respectively (Table 5.5(A); CP1: CO<sub>2</sub> > T+3 > Control > T+3/CO<sub>2</sub>; CP2: CO<sub>2</sub> > T+3 > T+3/CO<sub>2</sub> > Control). Comparison between populations showed higher rates of light calcification in CP1 than CP2 in all treatments. Both CP showed a significant change Before vs. Control, T+3 (Table 5.5(B)). Additionally, in CP1 the CO<sub>2</sub> treatment was significantly different to the Before, Control, T+3/CO<sub>2</sub> treatment (Table 5.5(B)). CP2 was significantly different to T+3/CO<sub>2</sub> (Table 5.5(B)).

In both SP, highest light calcification rates were found in T+3/CO<sub>2</sub> treatments and lowest, negative rates, were found in CO<sub>2</sub> treatments (Table 5.5(A); T+3/CO<sub>2</sub> > T+3 > C > CO<sub>2</sub>; Figure 5.7, Table 5.5(B)). A comparison between both SP revealed lower light calcification rates in SP1 than SP2 in the control and T+3/CO<sub>2</sub> treatment, higher rates in SP1 than SP2 in the T+3 treatment and more negative rates in SP2 than

SP1 in the CO<sub>2</sub> treatment. Significant differences were also found in the following comparisons: SP1 T+3/CO<sub>2</sub> vs. Before, Control, SP1 T+3 vs. CO<sub>2</sub>; SP2: Before vs. Control, T+3, CO<sub>2</sub>, CO<sub>2</sub> vs. Control, T+3, T+3/CO<sub>2</sub> vs. Control, T+3 (Table 5.5(B)).

Dark calcification rates in CP were highest in T+3/CO<sub>2</sub> and the control treatment, for CP1 and CP2, respectively (Figure 5.7, Table 5.5(A)). Lowest rates were found in the T+3 treatment in both CP (Table 5.5(A); CP1: T+3/CO<sub>2</sub> > Control > CO<sub>2</sub> > T+3; CP2: Control > T+3/CO<sub>2</sub> > CO<sub>2</sub> > T+3). Comparison between populations showed higher rates of dark calcification in CP1 than CP2 in the CO<sub>2</sub>-included treatments and lower rates in CP1 than CP2 in the control and T+3 treatments. Significant differences were found in the CO<sub>2</sub> treatment between SP1 and both CP (Table 5.5(B)). Significant differences were found within treatment of one population: CP1 T+3 vs. T+3/CO<sub>2</sub>; CP2 T+3 vs. Control, T+3/CO<sub>2</sub>; both SP CO<sub>2</sub> vs. T+3, Control; both SP Before vs. CO<sub>2</sub>, T+3; both SP T+3/CO<sub>2</sub> vs. CO<sub>2</sub>, T+3 (Table 5.5(B)).

Dark calcification rates in both SP were highest in the CO<sub>2</sub> treatment and lowest in the T+3 treatment (Table 5.5(A); SP1: CO<sub>2</sub> > Control > T+3/CO<sub>2</sub> > T+3; SP2: CO<sub>2</sub> > T+3/CO<sub>2</sub> > Control > T+3, Figure 5.7). A comparison between both populations revealed lower dark calcification rates in SP1 than SP2 in the T+3/CO<sub>2</sub> treatment, higher rates in SP1 than SP2 in the Control and CO<sub>2</sub> treatments and more negative rates in SP2 than SP1 in the T+3 treatment.

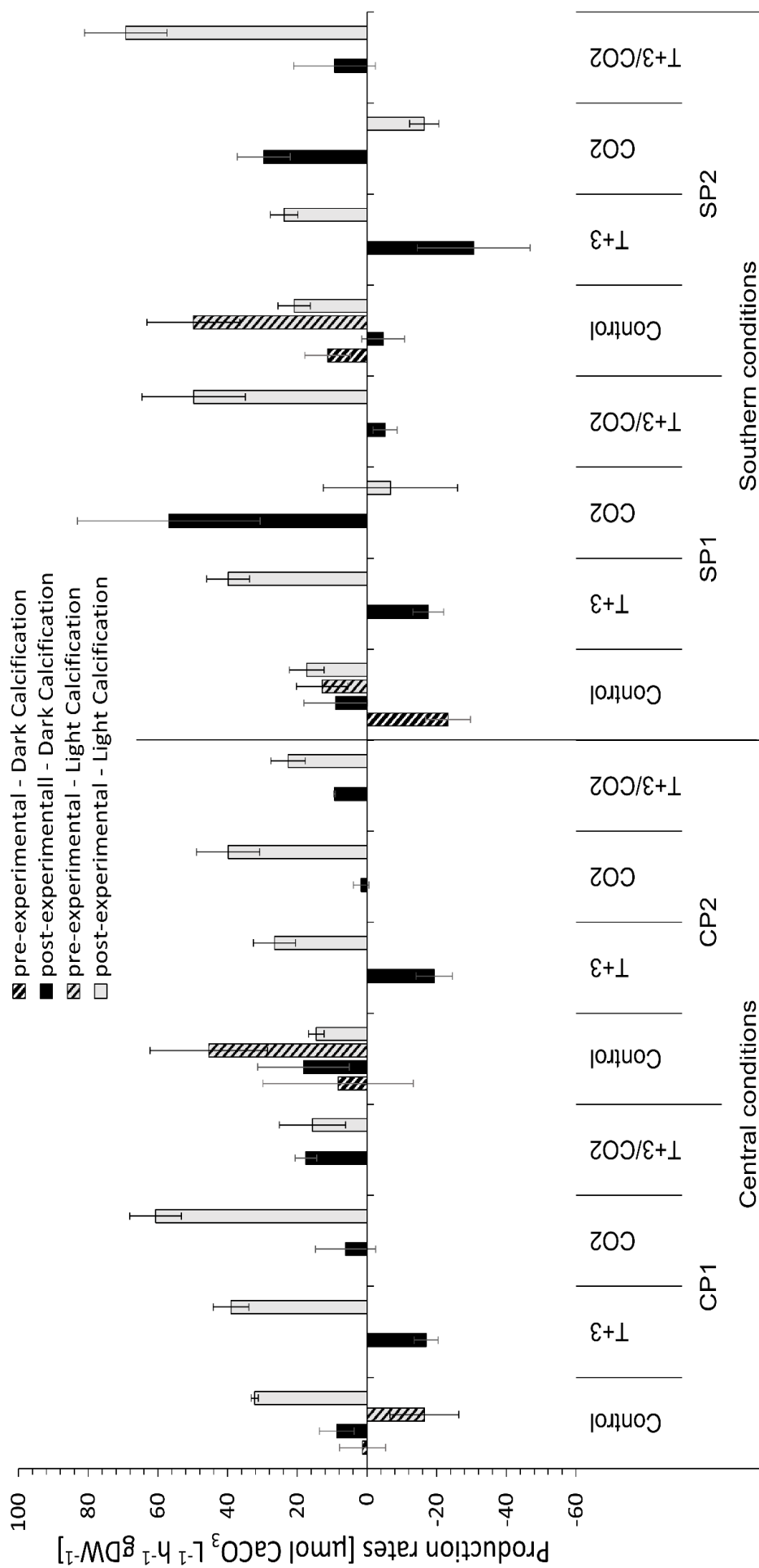


**Figure 5.7:** Light calcification and dark calcification rates [ $\mu\text{mol h}^{-1} \text{L}^{-1} \text{gDW}^{-1}$ ]  $\pm$ SE of *C. officinalis* before and after the Cross Experiment of each population under each treatment condition. Central and southern populations are abbreviated as CP and SP, respectively.

## 5.4.2 Structural Integrity in Temperature and pCO<sub>2</sub> Elevated Conditions along a Latitudinal Gradient

### 5.4.2.1 Linear Growth Rates

Monthly growth rates of NP in the Climate Change Experiment increased in all treatments compared to the Control (Figure 5.8, Table 5.6). Highest increases in NP were observed under elevated temperatures, followed by CO<sub>2</sub> treatments (NP1: T+3 > T+3/CO<sub>2</sub> > CO<sub>2</sub> > Control; NP2: T+3/CO<sub>2</sub> > CO<sub>2</sub> > T+3 > Control). Comparing NP between each other, NP1 showed lower monthly growth rates than NP2 in the Control, CO<sub>2</sub> and T+3/CO<sub>2</sub> treatment, but higher rates in the T+3 treatment (Table 5.6(A)). Only in NP, growth rates in the treatments T+3 and T+3/CO<sub>2</sub> were higher than in control treatments. Compared between location, NP showed the highest growth rates out of all populations and locations. NP1 showed significant different rates in Control compared to T+3 and T+3/CO<sub>2</sub> rates (Table 5.6(B)).

In CP, growth reduced and showed the lowest rates in the elevated temperature treatment contrary to expectations (CP1: T+3/CO<sub>2</sub> > CO<sub>2</sub> ≈ Control > T+3; CP2: CO<sub>2</sub> > T+3/CO<sub>2</sub> ≈ Control > T+3, Figure 5.8, Table 5.6(A)). Comparing CP between each other, CP1 showed lower monthly growth rates than CP2 in the Control, T+3 and CO<sub>2</sub> treatment, but higher rates in the T+3/CO<sub>2</sub> treatment (Table 5.6(A)). Contrary to populations from both marginal locations, CP show no clear pattern of increased or decreased growth rates with treatment. CP2 showed significant different rates in the CO<sub>2</sub> compared to the Control and T+3/CO<sub>2</sub> rates (Table 5.6(B)).

In SP, highest growth rates were found in control treatments, followed by high CO<sub>2</sub> treatments (Table 5.6(A), Figure 5.8). The lowest growth rates were observed in the climate change treatment (Table 5.6(A); SP1: Control > CO<sub>2</sub> > T+3/CO<sub>2</sub> > T+3; SP2: Control > CO<sub>2</sub> > T+3 > T+3/CO<sub>2</sub>). Comparing SP between each other, SP1 showed

higher monthly growth in all treatments compared to SP2. Only in SP, growth rates in CO<sub>2</sub> treatments are lower than in the Control. Marginally lower values with a more pronounced pattern were found in SP than in CP. SP2 showed significant different rates in the Control compared to the CO<sub>2</sub>, T+3 and T+3/CO<sub>2</sub> rates (Table 5.6(B)).

Comparing populations within treatment, the following significant differences were found: Control: CP2 vs. both NP, SP2; CO<sub>2</sub>: both SP vs. NP1, SP2 vs. CP2, NP1; T+3: both NP vs. both SP and both CP; T+3/CO<sub>2</sub>: both NP vs. both CP and both SP (Table 5.6(B), Figure 5.8).

Staining success always exceeded 65% in all populations and treatments (Figure 5.8). No clear pattern was found associating the staining success with the experimental treatments. The only trend observed was a greater staining success in marginal populations in CO<sub>2</sub> compared to T+3/CO<sub>2</sub> treatments, compared to a lower staining success in CP in CO<sub>2</sub> compared to T+3/CO<sub>2</sub> treatments.

(A)	Region	Population	Treatment	Growth rate [mm month <sup>-1</sup> ]		(B) Growth rates															
				Mean	±SE	North				Central				South							
						1	2	1	2	1	2	1	2	1	2						
			Control	0.51	0.065	Control	T+3	CO <sub>2</sub>	T+3/CO <sub>2</sub>	Control	T+3	CO <sub>2</sub>	T+3/CO <sub>2</sub>	Control	T+3	CO <sub>2</sub>	T+3/CO <sub>2</sub>	Control	T+3	CO <sub>2</sub>	T+3/CO <sub>2</sub>
			T+3	1.21	0.096	NS	NS	NS	NS	NS	NS	NS	NS	NS	NS	NS	NS	NS	NS	NS	NS
			CO <sub>2</sub>	0.63	0.074	NS	NS	NS	NS	NS	NS	NS	NS	NS	NS	NS	NS	NS	NS	NS	NS
			T+3/CO <sub>2</sub>	0.86	0.126	NS	NS	NS	NS	NS	NS	NS	NS	NS	NS	NS	NS	NS	NS	NS	NS
	North		Control	0.61	0.131	NS	NS	NS	NS	NS	NS	NS	NS	NS	NS	NS	NS	NS	NS	NS	NS
			T+3	0.76	0.102	NS	NS	NS	NS	NS	NS	NS	NS	NS	NS	NS	NS	NS	NS	NS	NS
			CO <sub>2</sub>	0.77	0.125	NS	NS	NS	NS	NS	NS	NS	NS	NS	NS	NS	NS	NS	NS	NS	NS
			T+3/CO <sub>2</sub>	0.79	0.122	NS	NS	NS	NS	NS	NS	NS	NS	NS	NS	NS	NS	NS	NS	NS	NS
	Central		Control	0.38	0.065	NS	NS	NS	NS	NS	NS	NS	NS	NS	NS	NS	NS	NS	NS	NS	NS
			T+3	0.26	0.037	NS	NS	NS	NS	NS	NS	NS	NS	NS	NS	NS	NS	NS	NS	NS	NS
			CO <sub>2</sub>	0.38	0.083	NS	NS	NS	NS	NS	NS	NS	NS	NS	NS	NS	NS	NS	NS	NS	NS
			T+3/CO <sub>2</sub>	0.41	0.064	NS	NS	NS	NS	NS	NS	NS	NS	NS	NS	NS	NS	NS	NS	NS	NS
	Central		Control	0.39	0.067	NS	NS	NS	NS	NS	NS	NS	NS	NS	NS	NS	NS	NS	NS	NS	NS
			T+3	0.35	0.066	NS	NS	NS	NS	NS	NS	NS	NS	NS	NS	NS	NS	NS	NS	NS	NS
			CO <sub>2</sub>	0.48	0.073	NS	NS	NS	NS	NS	NS	NS	NS	NS	NS	NS	NS	NS	NS	NS	NS
			T+3/CO <sub>2</sub>	0.39	0.068	NS	NS	NS	NS	NS	NS	NS	NS	NS	NS	NS	NS	NS	NS	NS	NS
	South		Control	0.54	0.067	NS	NS	NS	NS	NS	NS	NS	NS	NS	NS	NS	NS	NS	NS	NS	NS
			T+3	0.28	0.033	NS	NS	NS	NS	NS	NS	NS	NS	NS	NS	NS	NS	NS	NS	NS	NS
			CO <sub>2</sub>	0.42	0.056	NS	NS	NS	NS	NS	NS	NS	NS	NS	NS	NS	NS	NS	NS	NS	NS
			T+3/CO <sub>2</sub>	0.30	0.046	NS	NS	NS	NS	NS	NS	NS	NS	NS	NS	NS	NS	NS	NS	NS	NS
	South		Control	0.38	0.063	NS	NS	NS	NS	NS	NS	NS	NS	NS	NS	NS	NS	NS	NS	NS	NS
			T+3	0.26	0.061	NS	NS	NS	NS	NS	NS	NS	NS	NS	NS	NS	NS	NS	NS	NS	NS
			CO <sub>2</sub>	0.30	0.054	NS	NS	NS	NS	NS	NS	NS	NS	NS	NS	NS	NS	NS	NS	NS	NS
			T+3/CO <sub>2</sub>	0.16	0.027	NS	NS	NS	NS	NS	NS	NS	NS	NS	NS	NS	NS	NS	NS	NS	NS

**Table 5.6:** (A) Mean ±SE for monthly linear growth rates of the northern margin (n = 2), central (n = 2) and southern margin populations (n = 2) of *C. officinalis* in the NE Atlantic under Control (n = 3), elevated temperature (T+3, n = 3), elevated pCO<sub>2</sub> (n = 3) and Climate Change (T+3/CO<sub>2</sub>, n = 3) treatments in the Climate Change Experiment. (B) Statistical comparison between populations within treatments and treatments within populations.

Significance levels: NS = not significant \* = P < 0.05 \*\* = P < 0.01 \*\*\* = P < 0.005

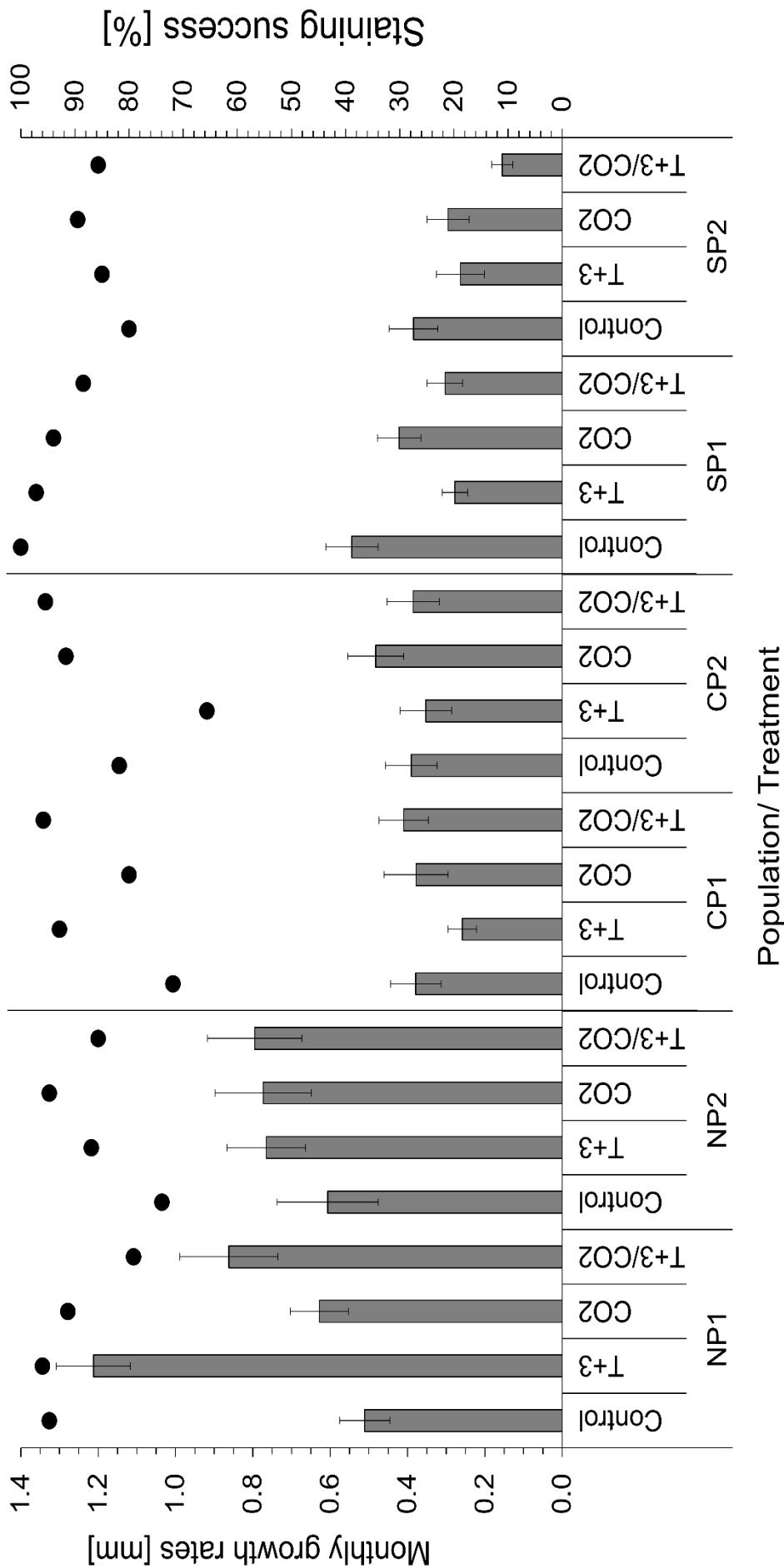


**Figure 5.8:** Monthly linear growth rates [mm month<sup>-1</sup>] (AV ±SE) of *C. officinalis* in the Climate Change Experiment for northern (n = 42, 48, 48 and 45 for Control, T+3, CO<sub>2</sub> and T+3/CO<sub>2</sub>, respectively), central (n = 65, 60, 44 and 46 for Control, T+3, CO<sub>2</sub> and T+3/CO<sub>2</sub>, respectively) and southern (n = 50, 55, 52 and 40 for Control, T+3, CO<sub>2</sub> and T+3/CO<sub>2</sub>, respectively) populations 1 and 2. Staining success is represented as closed circles (AV ±SE, n = see above).

Monthly linear growth rates in the Cross Experiment (Figure 5.9, Table 5.7) of CP (CP1 and CP2) were highest in T+3/CO<sub>2</sub> treatments, followed by T+3 treatments and lowest in CO<sub>2</sub> treatments (Table 5.7(A)). Both populations followed the same pattern (T+2/CO<sub>2</sub> > T+3 > Control > CO<sub>2</sub>). When compared within location, CP1 showed higher rates in all treatments compared to CP2. Treatments including elevated temperatures were higher than their respective Control. Both CP showed higher growth compared to both SP. Elevated temperature generally provided conditions that are more favourable for CP but increased pCO<sub>2</sub> showed a negative influence. Treatment T+3/CO<sub>2</sub> not only resembled a combination of treatments but also showed a combination of the effects observed for the individual treatments (Figure 5.9, Table 5.7(A)). Comparing both experiments, CP showed an opposing pattern in the Cross Experiment (clear pattern between treatments) compared to the Climate Change Experiment (no clear pattern between treatments). CP2 showed significant differences between CO<sub>2</sub> and T+3/CO<sub>2</sub> treatments (Table 5.7(B)).

Southern population 1 showed highest growth rates in the climate change treatment (T+3/CO<sub>2</sub>), whereas SP2 showed the highest growth rates in the CO<sub>2</sub> treatment (Table 5.7(A); SP1: T+3/CO<sub>2</sub> > T+3 > CO<sub>2</sub> > Control; SP2: CO<sub>2</sub> > T+3/CO<sub>2</sub> > Control > T+3, Figure 5.9). Comparing both populations, SP1 showed less growth in Control, CO<sub>2</sub> and T+2/CO<sub>2</sub> treatments and higher growth in the T+3 treatment (Table 5.7(A)). There is no clear pattern between treatments and growth is significantly less in SP compared to CP (Table 5.7(B)). Elevated temperature had no significant effects on the growth of SP. SP2 showed significant differences between T+3/CO<sub>2</sub> and T+3 or Control treatments (Table 5.7(B)).

All populations showed increased growth in the climate change treatment. Almost all populations, except SP2, showed at least marginally increased growth in T+3



treatments and CP showed a decrease compared to SP which showed an increase in CO<sub>2</sub> treatments, Figure 5.9, Table 5.7(A). Comparing populations within treatments, the following significant differences were found: Control and T+3 and T+3/CO<sub>2</sub>: both CP vs. both SP; CO<sub>2</sub>: SP1 vs. CP1 (Table 5.7(B)).

Staining success in this experiment always exceeded 70% and is similar in both experiments.

(A)

Temperature condition	Population	Treatment	Growth rates [mm month <sup>-1</sup> ]	
			Mean	±SE
Central	Central 1	Control	0.65	0.02
		T+3	0.74	0.09
		CO <sub>2</sub>	0.53	0.02
		T+3/CO <sub>2</sub>	0.81	0.01
	Central 2	Control	0.54	0.05
		T+3	0.65	0.04
		CO <sub>2</sub>	0.48	0.02
		T+3/CO <sub>2</sub>	0.62	0.09
South	Souther n 1	Control	0.35	0.10
		T+3	0.38	0.05
		CO <sub>2</sub>	0.38	0.09
		T+3/CO <sub>2</sub>	0.41	0.06
	Souther n 2	Control	0.36	0.03
		T+3	0.34	0.05
		CO <sub>2</sub>	0.44	0.07
		T+3/CO <sub>2</sub>	0.42	0.05

(B)

Growth rates	Southern condition											
	Southern population 1						Southern population 2					
	Control	T+3	CO <sub>2</sub>	T+3/CO <sub>2</sub>	Control	T+3	CO <sub>2</sub>	T+3/CO <sub>2</sub>	Control	T+3	CO <sub>2</sub>	T+3/CO <sub>2</sub>
Kruskal-Wallis H Test	***	***	***	***	***	***	***	***	***	***	***	***
Central condition	Central population 1						Central population 2					
	Control	T+3	CO <sub>2</sub>	T+3/CO <sub>2</sub>	Control	T+3	CO <sub>2</sub>	T+3/CO <sub>2</sub>	Control	T+3	CO <sub>2</sub>	T+3/CO <sub>2</sub>
	NS	NS	NS	NS	NS	NS	NS	NS	NS	NS	NS	NS
	*	**	***	*	NS	NS	NS	NS	NS	NS	NS	NS
Southern condition	Southern population 1						Southern population 2					
	Control	T+3	CO <sub>2</sub>	T+3/CO <sub>2</sub>	Control	T+3	CO <sub>2</sub>	T+3/CO <sub>2</sub>	Control	T+3	CO <sub>2</sub>	T+3/CO <sub>2</sub>
	NS	NS	NS	NS	NS	NS	NS	NS	NS	NS	NS	NS
	NS	NS	NS	NS	NS	NS	NS	NS	NS	NS	NS	NS

Significance levels: NS = not significant \* = P < 0.05 \*\* = P < 0.01 \*\*\* = P < 0.005

**Table 5.7:** (A) Mean ±SE for monthly linear growth rates of the central (n = 2) and southern margin populations (n = 2) of *C. officinalis* in the NE Atlantic under Control (n = 3), elevated temperature (T+3, n = 3), elevated pCO<sub>2</sub> (n = 3) and Climate Change (T+3/CO<sub>2</sub>, n = 3) treatments in the Cross Experiment. (B) Statistical comparison between populations within treatments and treatments within populations.

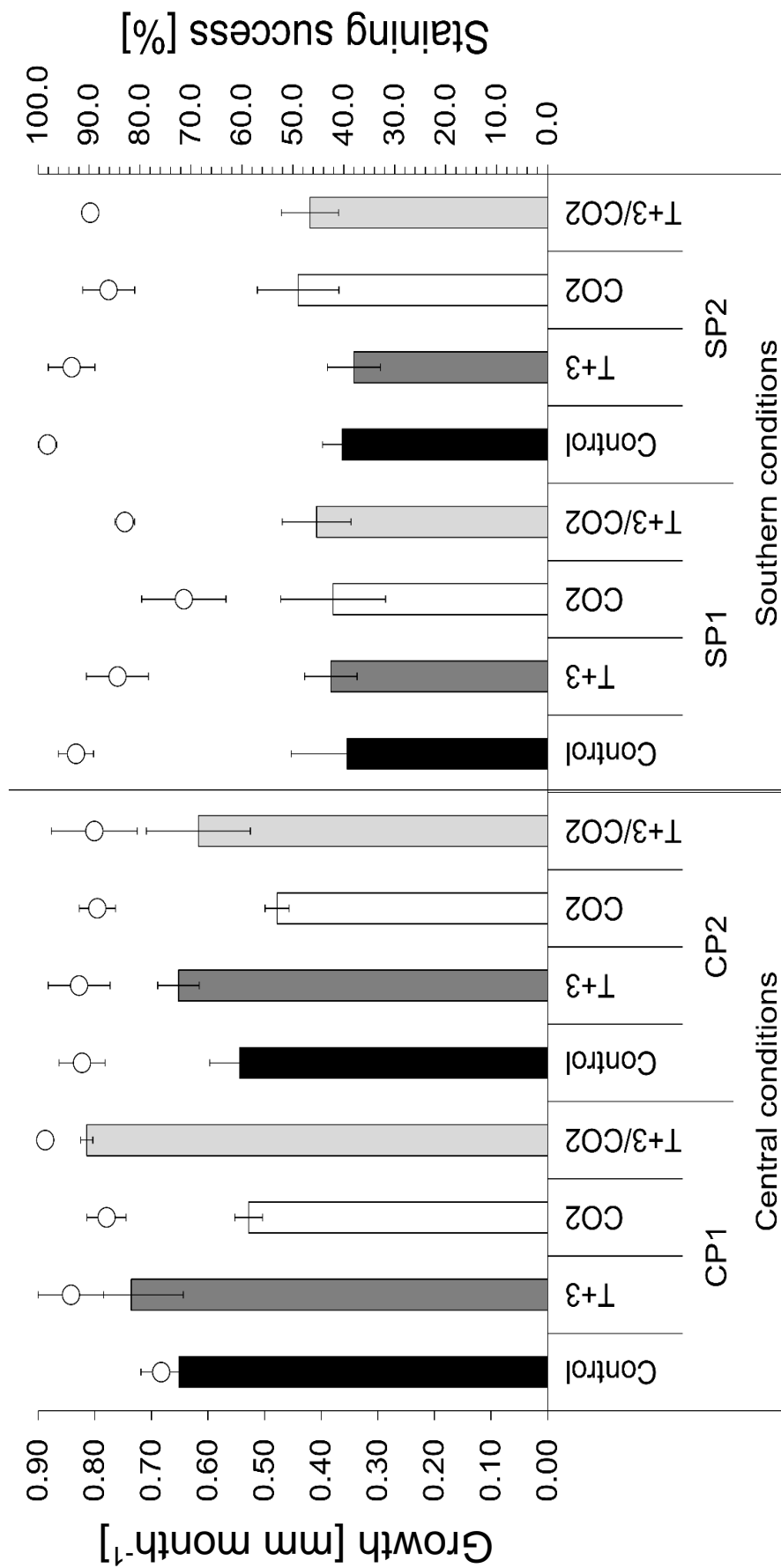


**Figure 5.9:** Monthly linear growth rates [mm month<sup>-1</sup>] (AV ±SE) of *C. officinalis* in the Cross Experiment for central (n = 193, 156, 175 and 145 for Control, T+3, CO<sub>2</sub> and T+3/CO<sub>2</sub>, respectively) and southern (n = 129, 121, 161 and 116 for Control, T+3, CO<sub>2</sub> and T+3/CO<sub>2</sub>, respectively) populations 1 and 2 under central and southern conditions, respectively. Staining success is represented as open circles (AV ±SE, n = see above).

#### 5.4.2.2 Elemental Composition of the Skeleton

For trace element raw data, a link to the online repository is given in Appendix D.

Magnesium/Calcium (Mg/Ca) ratios of NP in the Climate Change Experiment (Figure 5.10) showed a decrease in CO<sub>2</sub> and T+3 treatments and a slight increase in the T+3/CO<sub>2</sub> treatment in NP2, however NP1 showed a decline within T+3/CO<sub>2</sub> treatments. In control conditions, both populations showed an opposing trend with an increase in ratio values in NP2 and a decrease in NP1. In both NP in all treatments, Mg/Ca ratios declines from pre to post-experimental measurements. Both CP (Figure 5.10) showed an increase in the control and T+3/CO<sub>2</sub> treatments, however, not in the T+3 and CO<sub>2</sub> treatments. The most stable Mg/Ca ratios in CP were found in the T+3/CO<sub>2</sub> treatment, compared to a relatively steep decline in the individual treatments of elevated temperature and pCO<sub>2</sub>. In SP (Figure 5.12), Mg/Ca ratios decreased in all treatment except for the T+3/CO<sub>2</sub> treatment in SP2. A great decline in ratios was found in the control treatment in SP2 together with an initially much higher value compared to all other treatments in both SP. When comparing all three locations, much lower ratios were found in NP compared to CP and SP. The variability was highest in SP, followed by CP and it was shown to be lowest in NP. In all six populations showed highest values in the T+3/CO<sub>2</sub> treatment.

Vanadium/Calcium (V/Ca) ratios showed an increase in all NP in all treatments from prior to after the experiment (Figure 5.10). In NP1, all treatments showed similar increases, however, in T+3 a drastically steeper increase was observed compared to the other treatments. In NP2, The steepness of increase between pre and post-experimental measurements decreased with treatment, with the highest increase under control conditions and the lowest under T+3/CO<sub>2</sub> conditions. In CP (Figure 5.10), V/Ca ratios increased in all treatments in both populations from pre to post-

experimental measurements. The highest increase was found in T+3/CO<sub>2</sub> in CP1 (Figure 5.10). In SP (Figure 5.12), both populations showed an opposing trend with mostly decreasing ratios in SP2, except for in T+3, and increasing ratios in SP1, except for the Control. Lowest values in SP were found in the T+3/CO<sub>2</sub> treatment in SP2, however highest values were found in the same treatment in SP1. When comparing all three locations, much lower ratios were found in NP and CP compared to SP. The variability was highest in SP, followed by CP and it was shown to be lowest in NP. Four out of six populations (not for SP1 and CP1) showed lowest values in the T+3/CO<sub>2</sub> treatment.

Chromium/Calcium (Cr/Ca) ratios showed an increase in all NP and treatments from prior to post-experimental measurements (Figure 5.10). The least increase was found in the CO<sub>2</sub> treatments. NP2 showed little and NP1 average increased ratio values in T+3/CO<sub>2</sub> treatments. Ratio values increased in all treatments for both CP, except for T+3 in CP2 (Figure 5.10). In T+3 treatments, increase was found to be the least compared to control treatments. In SP1 (Figure 5.12), all ratios increased from prior to post-experimental measurements, except for an unnoticeable decrease in T+3. In SP2, a decrease in ratios was observed for the control and T+3/CO<sub>2</sub> treatments whereas the CO<sub>2</sub> and T+3 treatments showed a steep increase in values. SP2 showed the same pattern of decrease as in the control treatment however, values are much lower. When comparing all three locations, much lower ratios were found in marginal than in CP. The variability was highest in SP and lowest in CP and NP. Marginal populations showed lowest or intermediate values in the T+3/CO<sub>2</sub> treatment whereas CP showed highest values in both CO<sub>2</sub> including treatments.

Iron/Calcium (Fe/Ca) ratios showed an increase in all populations and treatments from pre to post-experimental measurements (Figure 5.10). In NP2, all treatment

showed a less steep increase compared to the control treatment. In NP2, all treatments but CO<sub>2</sub> showed comparable increases. In CP (Figure 5.10), ratios were relatively stable and did not show a drastic increase in all treatments, except for T+3/CO<sub>2</sub> in CP2 and T+3 in CP1. In the climate change treatment, CP showed similar values in CP1 than in the CO<sub>2</sub> treatment but not the T+3 treatment. Fe/Ca ratios showed an increase in all treatments in both SP (Figure 5.12). It was observed, that SP2 showed the highest increase in the T+3 treatment where a slight increase was found in SP1 in T+3/CO<sub>2</sub>. When comparing all three locations, highest ratios were found in SP followed by CP followed by NP. The variability was highest in NP and lowest in SP. CP and SP showed more constant levels of Fe/Ca ratios compared to NP. NP showed steep changes in ratios whereas CP and SP showed little increase. Marginal populations showed lowest or intermediate values in the T+3/CO<sub>2</sub> treatment whereas CP showed high or highest values.

Zinc/Calcium (Zn/Ca) ratios showed an increase in all treatments (Figure 5.10). However, NP2 showed little increase elevated temperature included treatments. In NP2, in all treatments a great increase in ratios was observed, except for T+3/CO<sub>2</sub>, where a less steep increase was found. Ratios of CP showed an overall increase in all conditions except for the treatments T+3 and T+3/CO<sub>2</sub> in CP2 (Figure 5.10). Highest ratios were found in T+3/CO<sub>2</sub> treatments in both CP. A drastic increase was found in the CO<sub>2</sub> treatment in CP2. In SP (Figure 5.12), ratios decreased in both populations in all treatments, except for in the T+3/CO<sub>2</sub> treatment in SP2 and the T+3 treatment in SP1. In SP2, highest values were found in the T+3/CO<sub>2</sub> treatment with pre-values being higher than post values of the other treatments. Additionally, SP2 showed the highest increase in the T+3/CO<sub>2</sub> treatment. SP1 showed a higher decrease than SP2. Higher values were found in the CO<sub>2</sub> included treatments in

both populations compared to the control and T+3 treatments. When comparing all three locations, highest ratios were found in SP followed by CP followed by NP. The steepest increase of ratios was found in NP (Figure 5.10). The variability was highest in SP and lowest in NP. SP showed a more constant level of ratios compared to CP and NP. NP showed steep changes in ratios whereas SP showed the smallest increase. All populations showed highest values in the T+3/CO<sub>2</sub> treatment.

Strontium/Calcium (Sr/Ca) ratios showed an increase in all treatments, but T+3 in NP1 (Figure 5.10). Ratios in the T+3/CO<sub>2</sub> treatment are always higher compared to the other treatments. In CP1 (Figure 5.10), elevated temperature included treatments showed lower ratios than in the control and CO<sub>2</sub> treatments. In CP2, control and climate change treatments show comparable values before and after the experiment whereas in individual treatments ratios decreased with the highest decline in T+3. In SP (Figure 5.12), ratios decreased in the majority of treatments, except for T+3/CO<sub>2</sub> in SP2 and control in SP1. All treatments showed comparable values between populations. CO<sub>2</sub> included treatments showed higher values compared to control and T+3 treatments in SP1 and partly in SP2. Ratio values follow the same pattern as the Mg/Ca ratios for SP. When comparing all three locations, 1.5-times higher ratios were found in SP compared to CP and NP. The steepest increase of ratios was found in SP. The variability was highest in marginal populations and lowest in CP (Figure 5.10). CP showed a more constant level of ratios compared to marginal populations. NP showed the steepest changes in ratios followed by SP followed by CP. All populations showed intermediate or highest values in the T+3/CO<sub>2</sub> treatment.

Cadmium/Calcium (Cd/Ca) ratios showed a decrease in all treatments from pre to post-experimental conditions, except for T+3 in NP1 which showed a slight increase

and a large error bar (Figure 5.10). Comparable values of ratios were observed in post-experimental data, except for T+3 in NP1 where the ratio increased. In CP (Figure 5.10), CO<sub>2</sub> included treatments were higher compared to the control and T+3 treatments in both populations. Compared to measurements before the experiment, ratios decreased in CP in all treatments, except for the Control. In SP (Figure 5.12), Cd/Ca ratios decreased in all treatments in both populations with the highest decline in SP1 CO<sub>2</sub>, as well as SP2 Control and CO<sub>2</sub>. Ratios in the T+3/CO<sub>2</sub> treatment were higher compared to all other treatments in both populations and showed a similar steep decrease than in the T+3 treatment. The greatest impact on the ratio was found by CO<sub>2</sub> increased treatments. When comparing all three locations, highest ratios were found in all marginal populations and up to 8-times lower values were found in CP. The steepest increase of ratios was found in SP. The variability was highest in NP and lowest in CP. CP showed a more constant level of ratios compared to marginal populations. SP showed the steepest changes in ratios followed by NP followed by CP. All populations showed some of their highest values in the T+3/CO<sub>2</sub> treatment.

Barium/Calcium (Ba/Ca) ratios showed an increase in all treatments, except for T+3/CO<sub>2</sub> in NP2 (Figure 5.10). No difference between treatments was found in NP2. In NP1, however a lower increase was observed in T+3 compared to the other treatments. In both CP (Figure 5.10), CO<sub>2</sub> included treatments increased surpassingly, whereas control and T+3 treatments only showed low negative and positive changes for CP2 and CP1, respectively. In SP (Figure 5.12), ratios increased in all treatments with an exceptionally high increase in the CO<sub>2</sub> treatment in SP1. When leaving out this exception, the highest values were found in the T+3/CO<sub>2</sub> treatment. When comparing all three locations, highest ratios were found

in SP and up to 2-times lower values were found in CP and NP. The steepest increase of ratios was found in some treatments of the SP (Figure 5.12), however, NP showed an overall steeper increase in all treatments. The variability was similar across all populations. Changes in ratios were more consistent in SP compared to CP and NP. NP showed the steepest changes in ratios followed by SP followed by CP. All populations showed highest values in the CO<sub>2</sub> including treatments.

In NP, the least change in all treatments was found in the climate change treatment (Figure 5.10). In control treatments, both NP showed a relatively high variability as well as a great change of ratio values. In CP, rates of all elements in the control treatments were relatively stable throughout the experiment. The most influence was found by CO<sub>2</sub> in the treatments CO<sub>2</sub> and T+3/CO<sub>2</sub>. Comparing the pattern of changes between elements, it was observed, that in CP, Ba, V and Cr showed an identical pattern of a low increase in control and T+3 treatments as well as, more importantly, a steep increase in both CO<sub>2</sub> included treatments (CO<sub>2</sub> and T+3/CO<sub>2</sub>) in CP but not in both marginal populations.

For figure comparison, note: In SP, V and Cr were presented on a y-axis of half the values compared to NP and CP. Fe/Ca ratios were presented on y-axis double the value of those of NP and CP. Zn/Ca ratios of SP were presented of y-axis 3-times higher compared to NP and CP. Sr/Ca ratios of SP were presented on y-axis which values started where those of NP and CP finished. Cd/Ca ratios of SP were presented on a y-axis 3-times higher than the one of CP and CP were presented on y-axis 3-times higher than the one of NP. Ba/Ca ratios were presented on a y-axis 4-time higher in SP than in NP and CP.

PERMANOVA and SIMPER analysis (Figure 5.13 - Figure 5.16) for the Climate Change Experiment investigating if *C. officinalis* was taking up the chemical



signature of the experimental treatments showed significant differences between pre and post-experimental measurements for all locations ( $P < 0.01$ , PERMANOVA in all cases). Additionally, a significant difference between both populations of the central regions were found during pairwise comparisons ( $P < 0.05$ , PERMANOVA). Pairwise comparisons also showed the following significant difference between time point nested in treatment nested in population: pre vs. post: NP1 Control, NP1 T+3, NP2 CO<sub>2</sub>, SP1 CO<sub>2</sub> ( $P < 0.001$ ), NP2 T+3/CP2, CP1 T+3/CO<sub>2</sub>, SP2 Control ( $P < 0.05$ , PERMANOVA for all 3 cases). Further significant difference were found when comparing treatments of one population with the source of treatment nested in population nested in condition ( $P < 0.01$ , PERMANOVA). Pairwise tests performed with PERMANOVA analysis revealed the following significances: NP1: CO<sub>2</sub> vs. T+3/CO<sub>2</sub> ( $P < 0.05$ ); CP2: Control vs. T+3 ( $P < 0.05$ ), T+3 vs. CO<sub>2</sub> ( $P < 0.05$ ), T+3 vs. T+3/CO<sub>2</sub> ( $P < 0.01$ ); SP1: Control vs. CO<sub>2</sub> ( $P < 0.01$ ), T+3 vs. CO<sub>2</sub> ( $P < 0.05$ ); SP2: Control vs. T+3/CO<sub>2</sub> ( $P < 0.01$ ), T+3 vs. T+3/CO<sub>2</sub> ( $P < 0.01$ ), CO<sub>2</sub> vs. T+3/CO<sub>2</sub> ( $P < 0.001$ ).

Further statistical analysis with PERMANOVA and treatment and population as fixed and random factors, respectively, revealed significant differences between populations nested in treatment ( $P < 0.001$ , PERMANOVA). Within the Control treatment, the following significant differences between populations were found (all tests: PERMANOVA pairwise comparison): NP1 vs. CP1 ( $P < 0.05$ ), NP1 vs. CP1 ( $P < 0.001$ ), NP1 vs. SP1 ( $P < 0.05$ ), NP1 vs. SP2 ( $P < 0.001$ ), NP2 vs. CP2 ( $P < 0.05$ ), NP2 vs. SP2 ( $P < 0.05$ ), CP1 vs. SP2 ( $P < 0.01$ ), CP2 vs. SP1 ( $P < 0.05$ ), CP2 vs. SP2 ( $P < 0.001$ ). Within the T+3 treatment, the following significant differences between populations were found (all tests: PERMANOVA pairwise comparison): NP1 vs. NP2 ( $P < 0.05$ ), NP1 vs. CP1 ( $P < 0.05$ ), NP1 vs. CP2 ( $P <$

0.01), NP2 vs. CP2 ( $P < 0.05$ ), NP2 vs. SP2 ( $P < 0.05$ ), CP1 vs. CP2 ( $P < 0.05$ ), CP2 vs. SP1 ( $P < 0.05$ ), CP2 vs. SP2 ( $P < 0.01$ ). Within the CO<sub>2</sub> treatment, the following significant differences between populations were found (all tests: PERMANOVA pairwise comparison): NP1 vs. SP1 ( $P < 0.001$ ), NP1 vs. SP2 ( $P < 0.05$ ), NP2 vs. CP1 ( $P < 0.05$ ), NP2 vs. CP2 ( $P < 0.05$ ), NP2 vs. SP1 ( $P < 0.01$ ), NP2 vs. SP2 ( $P < 0.05$ ), CP1 vs. SP1 ( $P < 0.001$ ), CP2 vs. SP1 ( $P < 0.001$ ), SP1 vs. SP2 ( $P < 0.05$ ). Within the T+3/CO<sub>2</sub> treatment, the following significant differences between populations were found (all tests: PERMANOVA pairwise comparison): NP1 vs. NP2 ( $P < 0.05$ ), NP1 vs. SP1 ( $P < 0.001$ ), NP1 vs. SP2 ( $P < 0.05$ ), NP2 vs. CP2 ( $P < 0.05$ ), NP2 vs. SP1 ( $P < 0.01$ ), NP2 vs. SP2 ( $P < 0.001$ ), CP1 vs. SP1 ( $P < 0.05$ ), CP1 vs. SP2 ( $P < 0.001$ ), CP2 vs. SP1 ( $P < 0.01$ ), CP2 vs. SP2 ( $P < 0.001$ ), SP1 vs. SP2 ( $P < 0.01$ ).

Additionally, SIMPER analysis presented the main composition of elements for each country in each treatment. Overall, 87.3%, 86.9%, 86.0% and 80.6% of the data are represented in PERMANOVA and SIMPER for NP, CP, SP and comparison analysis, respectively. Comparing pre and post-experimental compositions, for all populations in all treatments, more than 90% of the data are channelled in Ca, Mg, Sr and Zn, in this order. NP revealed Cr as an additional element to the major composition, however, only in the post-experimental measurements and in all treatments. CP showed no inclusion of Cr into 90% of the major elemental composition of the skeleton. SP revealed Cr as an additional element to the major composition, however, in random occurrences without clear pattern between pre and post-experimental measurements. Comparing the post-experimental measurements between locations, Cr was included into 90% of the skeletal trace elemental composition in all four marginal populations. It was discovered, that Fe,

Mg and Sr were the major elements determining NP; additional, less influential elements for these populations were discovered to be Cr, Zn, Ba and V. Major elements influencing CP were discovered to be Fe, Mg and Sr; furthermore, minor influential elements were revealed to be Cr, Ba, Zn and Cd. Major elements influencing SP were Fe and Mg; additional less influences were found to be caused by Sr, Cr, Cd and Zn. When comparing treatments, elements influencing these the most were Fe, Mg and Sr with fewer influences caused by Cr and Ba (Figure 5.13 - Figure 5.15 (E) and Figure 5.16 (D)).

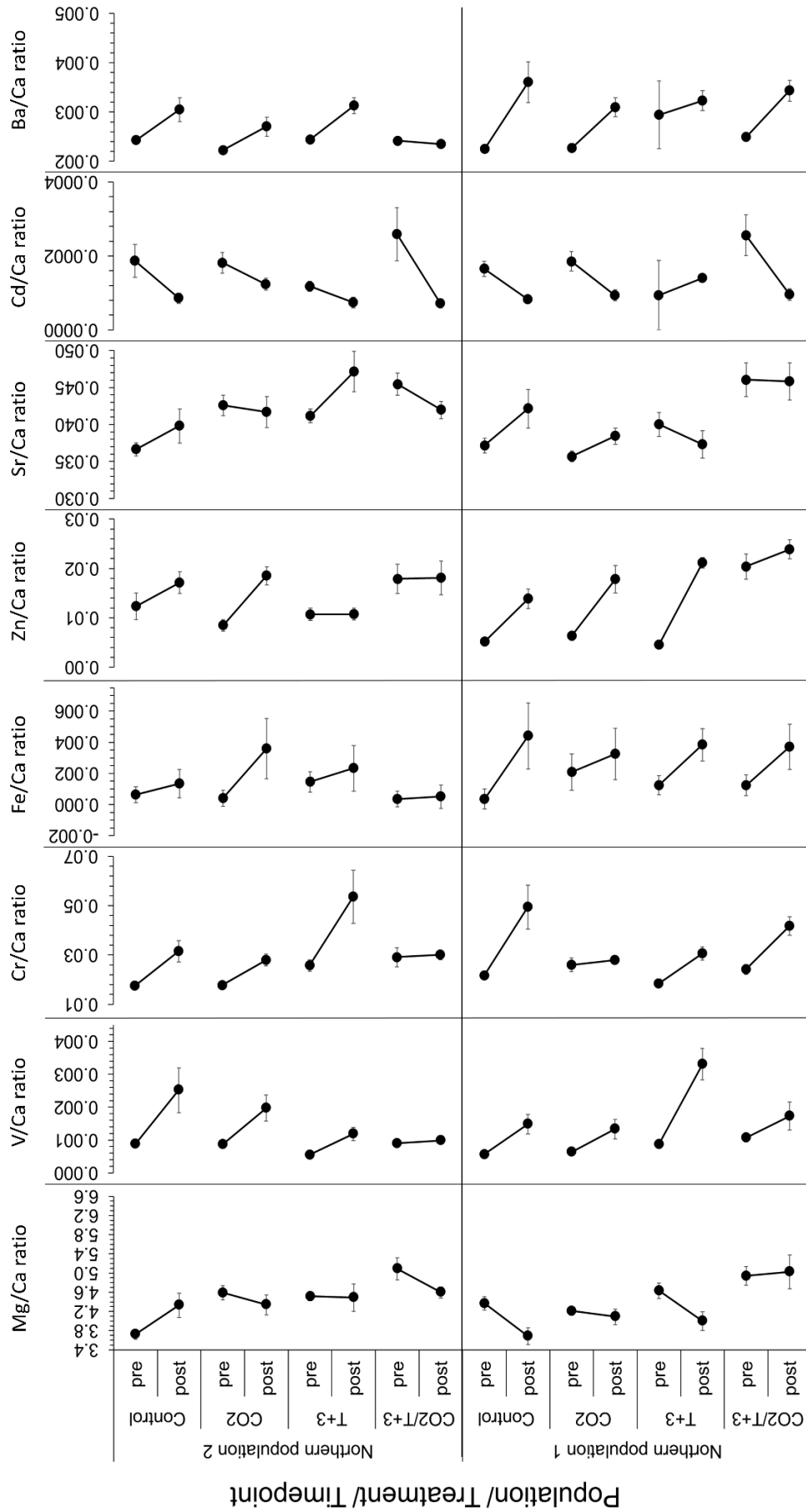


**Figure 5.10:** Element/Ca ratios for all elements in the Climate Change Experiment. Data points (AV  $\pm$ SE, n = 15) represent northern populations (NP1 and NP2) of *C. officinalis*, in pre and post-experimental conditions: Control, high pCO<sub>2</sub> (CO<sub>2</sub>), high temperature (T+3) and high pCO<sub>2</sub> and high temperature (CO<sub>2</sub>/T+3).

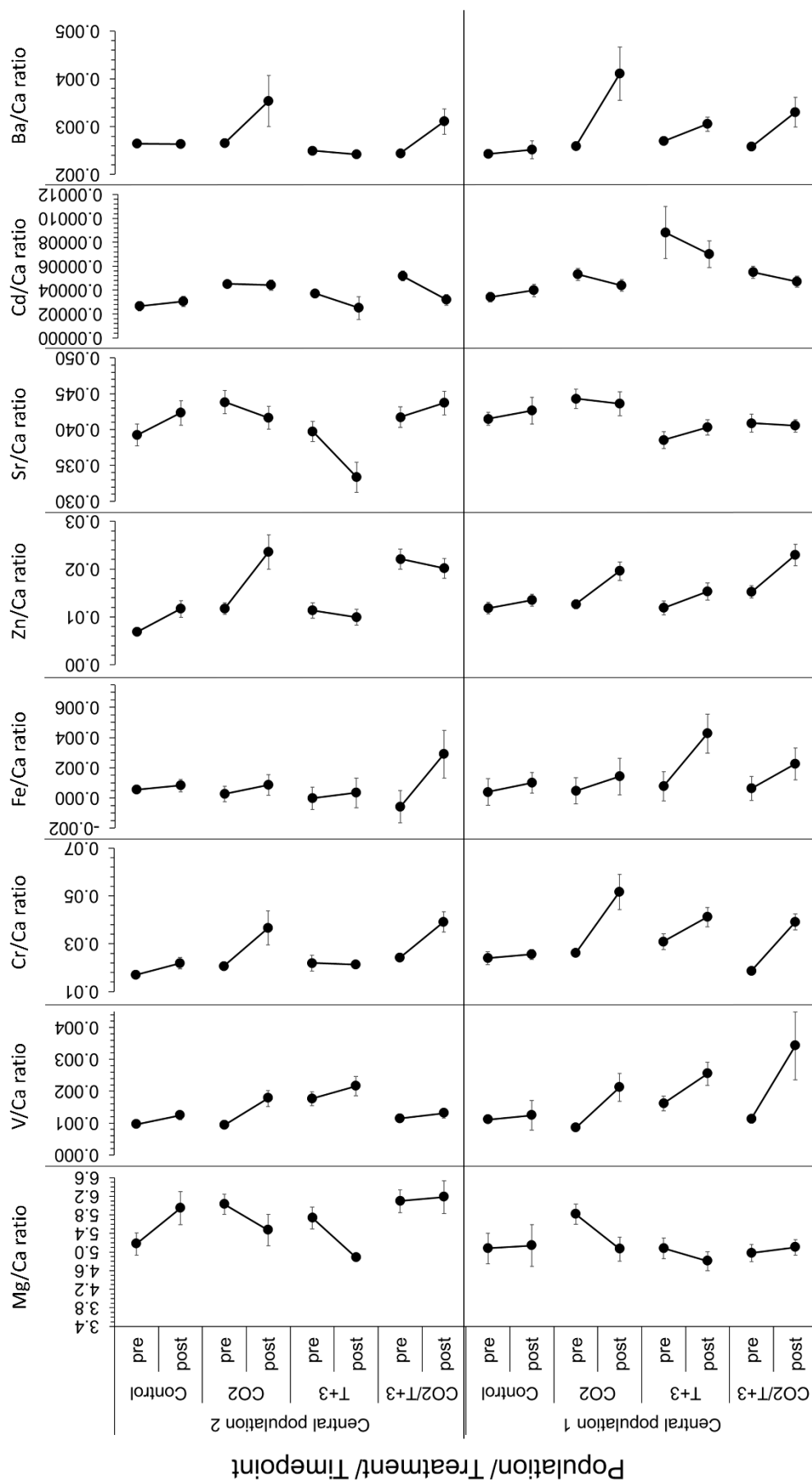


**Figure 5.11:** Element/Ca ratios for all elements in the Climate Change Experiment. Data points (AV ±SE, n = 15) represent central populations (CP1 and CP2) of *C. officinalis*, in pre and post-experimental conditions: Control, high pCO<sub>2</sub> (CO<sub>2</sub>), high temperature (T+3) and high pCO<sub>2</sub> and high temperature (CO<sub>2</sub>/T+3).

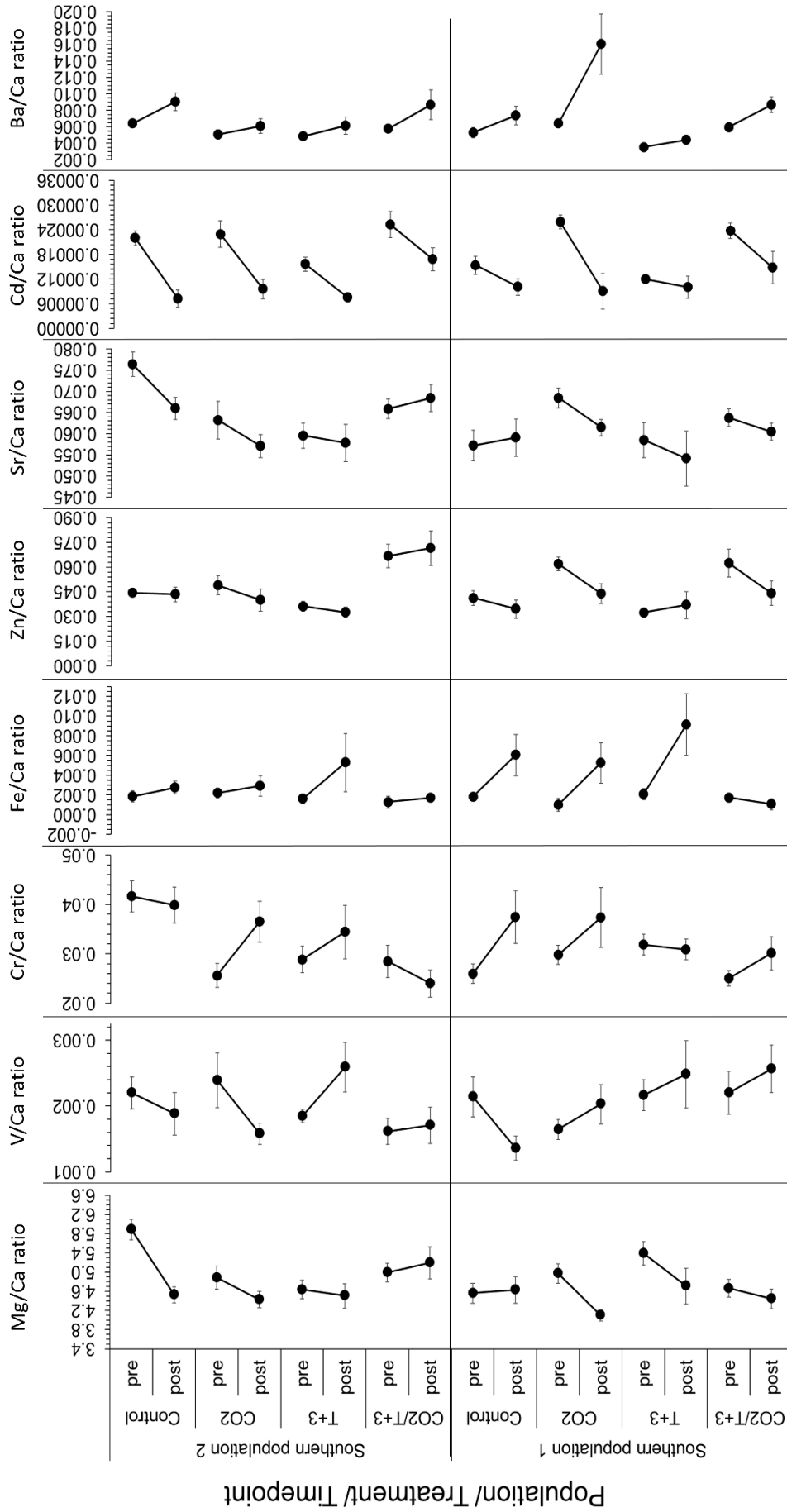


**Figure 5.12:** Element/Ca ratios for all elements in the Climate Change Experiment. Data points (AV ±SE, n = 15) represent southern populations (SP1 and SP2) of *C. officinalis*, in pre and post-experimental conditions: Control, high pCO<sub>2</sub> (CO<sub>2</sub>), high temperature (T+3) and high pCO<sub>2</sub> and high temperature (CO<sub>2</sub>/T+3).

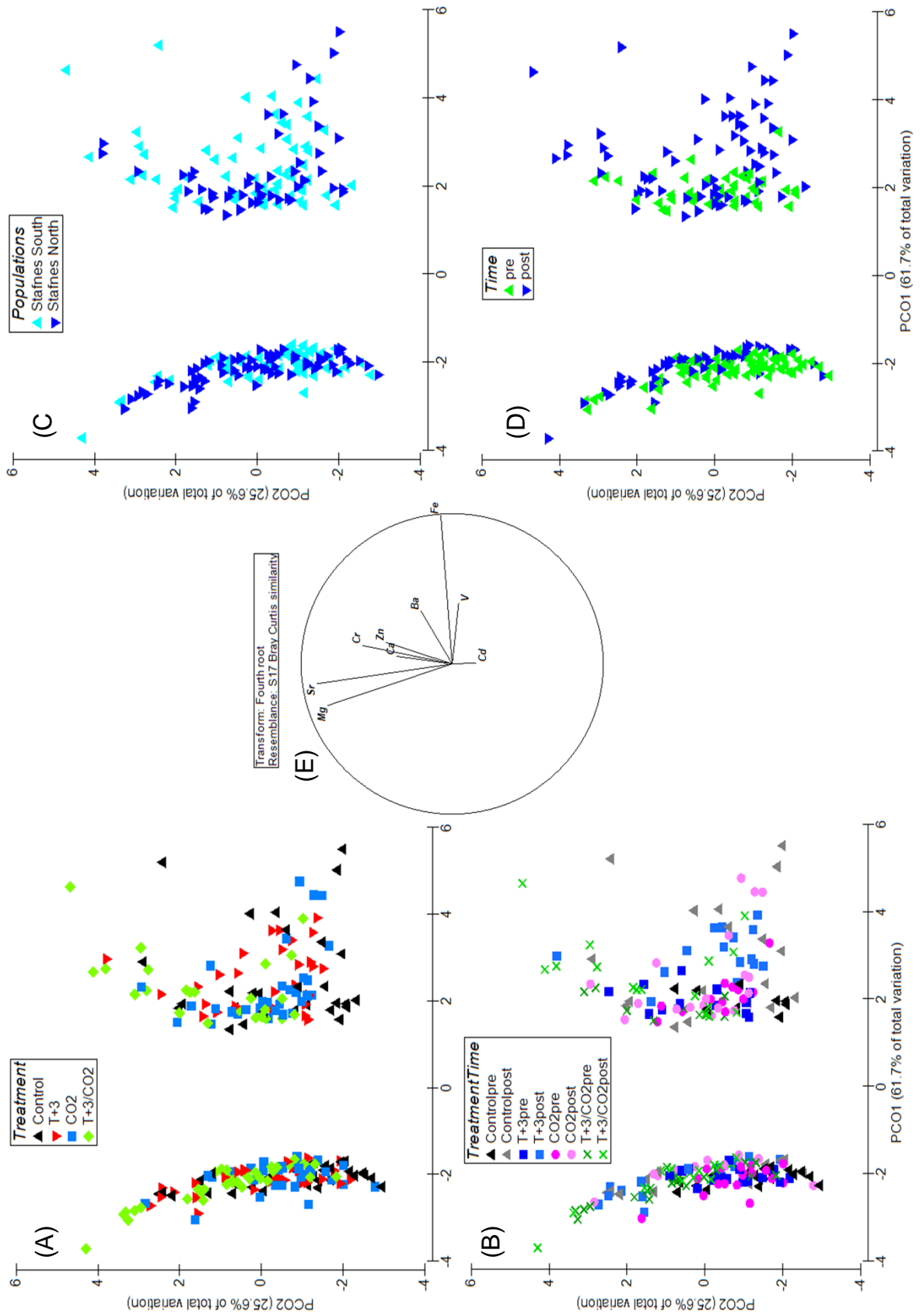


**Figure 5.13:** PERMANOVA (A-D) and SIMPER (E) results for northern populations of *C. officinalis* of the Climate Change Experiment.

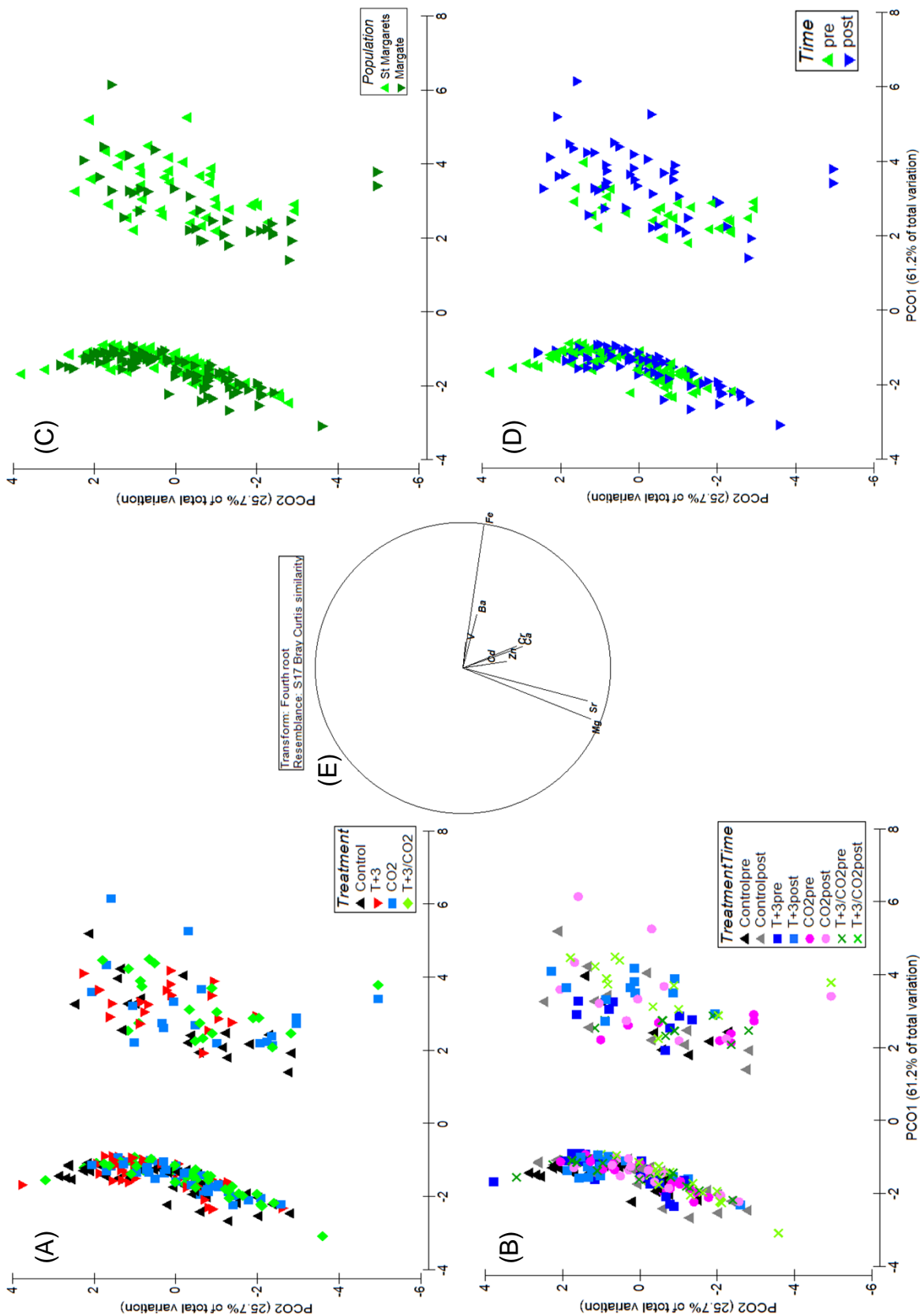


**Figure 5.14:** PERMANOVA (A-D) and SIMPER (E) results for central populations of *C. officinalis* of the Climate Change Experiment



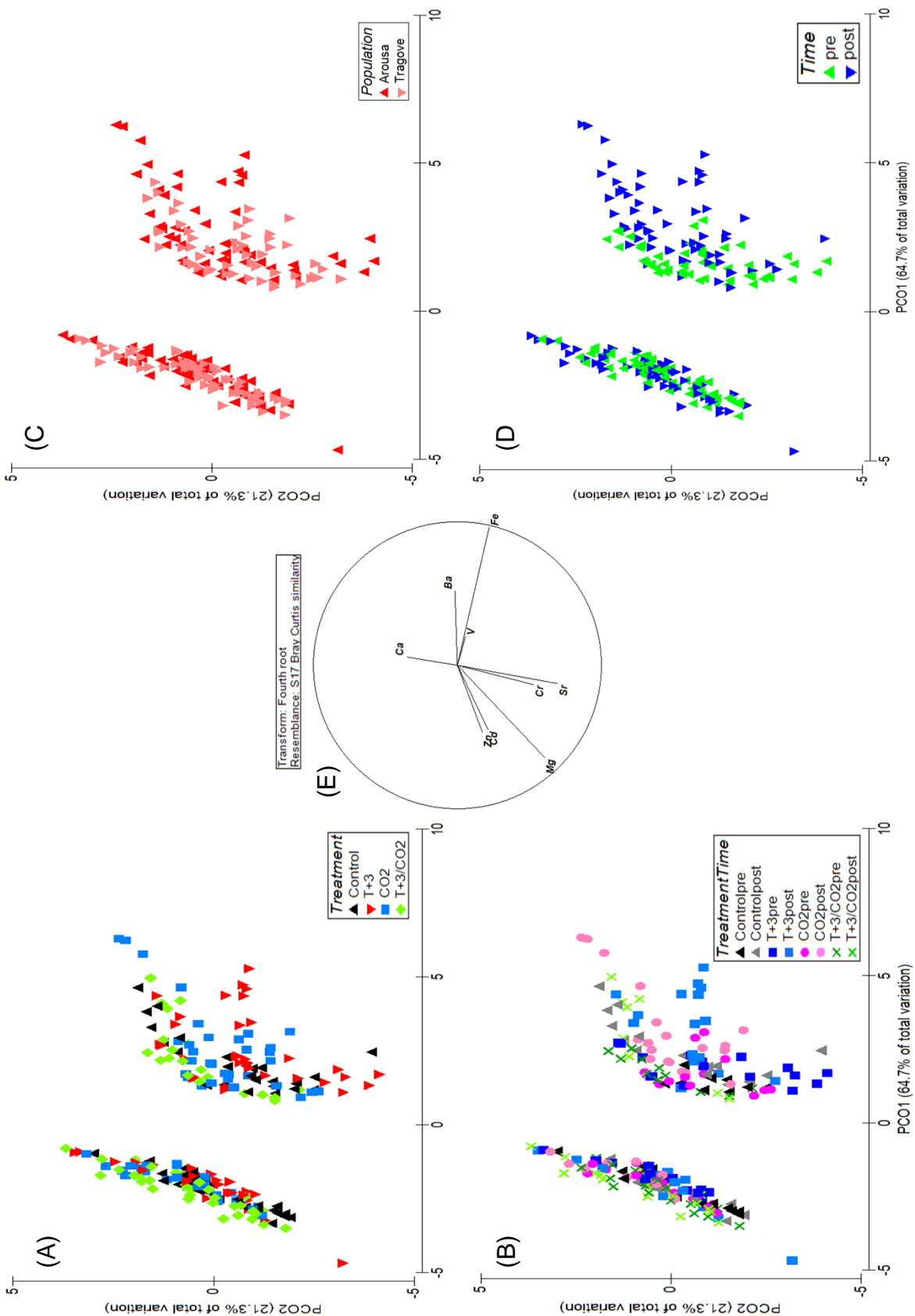


**Figure 5.15:** PERMANOVA (A-D) and SIMPER (E) results for southern populations of *C. officinalis* of the Climate Change Experiment.

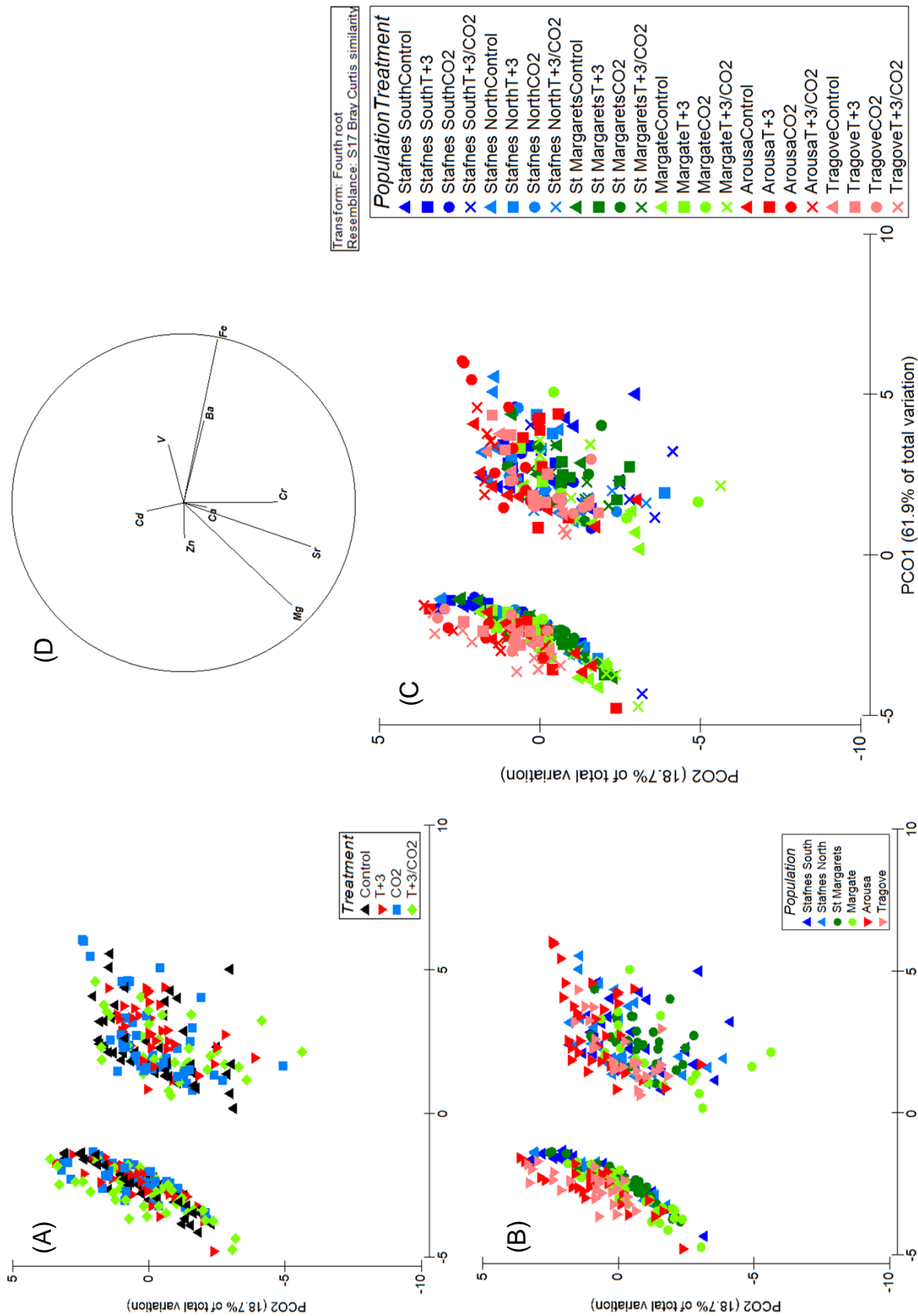


**Figure 5.16:** PERMANOVA (A-C) and SIMPER (D) results for all populations of *C. officinalis* of the Climate Change Experiment.

Magnesium/Calcium (Mg/Ca) ratios in the Cross Experiment showed a decrease in both CP in most treatments (Figure 5.17), except for temperature included treatments in CP1. Those two treatments of CP1 showed an increase that was more pronounced in T+3/CO<sub>2</sub> than in T+3. In SP (Figure 5.18), ratios decreased in all treatments and, except for SP2 CO<sub>2</sub>, all declines showed to be of a comparable magnitude. All ratios were comparable with control ratios prior and after the experiment. When comparing both locations, SP showed less variable and more stable results. SP showed marginally higher ratios compared to CP.

Vanadium/Calcium (V/Ca) ratios showed an increase in all treatments and CP with the highest increase in CP1 Control (Figure 5.17). In CP1, lowest rates were found in the T+3/CO<sub>2</sub> treatment whereas in CP2, a trend towards higher increases in CO<sub>2</sub> including treatments was observed. In SP (Figure 5.18), ratios decreased in all treatments. However, rates were marginally higher in T+3/CO<sub>2</sub> treatment in SP1, but were found to be the lowest in this treatment in addition to the CO<sub>2</sub> treatment in SP2. This shows an opposite trend when compared to CP (Figure 5.17). When comparing both locations, CP showed less variable and more stable results. Additionally, CP showed lower ratios compared to SP.

Chromium/Calcium (Cr/Ca) ratios showed an increase in all CP in all treatments (Figure 5.17). Higher increases were found in CP1 compared to CP2. The least steep increase was found in T+3/CO<sub>2</sub> in both populations. In SP (Figure 5.18), ratios declined in all treatments and mirror the pattern of Mg/Ca and Sr/Ca ratios. The highest values were found in treatment T+3/CO<sub>2</sub> in SP1 and lowest values were found in the same treatment in SP2. In SP2, temperature elevated treatments showed less change in ratios compared to the other treatments. When comparing

both locations, CP showed more stable results, however, SP showed less variability. Additionally, SP showed lower ratios compared to CP.

Iron/Calcium (Fe/Ca) ratios showed increased in both populations in all treatments, except for CP2 Control in which it decreased and CP2 T+3/CO<sub>2</sub> in which stable values were found (Figure 5.17). The highest increase in both CP was found in the T+3 treatment. In SP1 (Figure 5.18), ratios decreased in all but the control treatment with the highest decline in treatment T+3/CO<sub>2</sub> and no noticeable change in values in the remaining treatments. In SP2, an increase was only observed in the CO<sub>2</sub> exposed treatments that were higher compared to the control and T+3 treatments. When comparing locations, all populations showed comparable results and no great difference between variation, stability and value of the ratios.

Zinc/Calcium (Zn/Ca) ratios showed an increase in all populations in all treatments, except for CP2 T+3 and CO<sub>2</sub> (Figure 5.17). The most influential factor was found to be elevated temperature. The lowest rates were found in CP1 T+3/CO<sub>2</sub>. In SP (Figure 5.18), all ratios decrease during the experiment, except for SP1 Control, that increased drastically but also showed the greatest error bar. The lowest values were found in the temperature-exposed treatments with the overall lowest values in T+3/CO<sub>2</sub>. When comparing both locations, CP showed 3-times lower ratio values compared to CP. More stable and less variable results were found in SP. CP showed steeper declines in ratios compared to SP in the same treatments.

Strontium/Calcium (Sr/Ca) ratios showed opposing trend between CP (Figure 5.17). CP1 showed a decrease in the Control and an increase in all treatments, whereas CP2 showed an increase in the Control and a decrease in all treatments. The most pronounced changes were observed in the treatments including elevated temperatures in CP1. Whereas in CP2, most pronounced changes were observed

in CO<sub>2</sub> including treatments. In SP (Figure 5.18), ratios decreased in all treatments in both populations. The greatest decrease was observed in the CO<sub>2</sub> treatment, the least change was found in the T+3/CO<sub>2</sub> treatment. The pattern of changes in ratios was similar to this of Mg and Cr. When comparing both locations, SP showed less change and similar variability than CP. CP1 is the only population to show steeper increases in ratios compared to all other populations.

Cadmium/Calcium (Cd/Ca) ratios showed an increase in the T+3/CO<sub>2</sub> treatment in both CP (Figure 5.17), however, compared to all other treatments, it showed the lowest ratios. In CP1 and CP2, highest values were found in the control and T+3 treatment, respectively, highest variability was found in T+3. Values within the control treatment were similar in both CP, however a steady decline in rates were found from T+3 to CO<sub>2</sub> to T+3/CO<sub>2</sub>. Both SP (Figure 5.18) showed a decrease in their Cd/Ca values throughout the experiment. Nevertheless, the steepness of the decline is greater in SP1 and within SP1; it is highest in T+3/CO<sub>2</sub> and lowest in the control treatment. In SP2, the decline in all treatments were comparable. The lowest values were found in the control and T+3/CO<sub>2</sub> treatment for SP1 and SP2, respectively. When comparing both locations, SP showed less variability but greater increases than CP. Populations of both locations showed steep decreases in ratios in CO<sub>2</sub> exposed treatments. Ratios of CP were approximately half of those of SP and showed less pronounced changes.

Barium/Calcium (Ba/Ca) ratios showed an increase or stable values in both CP in all treatments (Figure 5.17). Lowest values were found in both treatments including elevated temperatures, in both CP. The steepest increase, however, was found in treatment not exposed to elevated temperatures. In SP (Figure 5.18), Ba ratios follow the reverse pattern of Sr and Mg. Ratio values increased in all treatments in

both populations, except for SP2 CO<sub>2</sub>. The highest values were found in T+3/CO<sub>2</sub> and CO<sub>2</sub> treatments, for SP1 and SP2, respectively. When comparing both locations, SP showed less variability and less increases than CP. CP showed steep increases in ratios in all but temperature exposed treatments. Rates were generally higher in CP compared to SP.

PERMANOVA and SIMPER analysis (Figure 5.19 - Figure 5.21) for the Cross Experiment investigating if *C. officinalis* was taking up the chemical signature of the experimental treatments showed significant differences between pre and post-experimental for all locations as well as regional comparison measurements ( $P < 0.01$ , PERMANOVA in all cases). Additionally, a significant difference between both populations of the southern regions as well as between central and southern conditions of the experiment were found during pairwise comparisons ( $P < 0.05$ , PERMANOVA in both cases). Pairwise comparisons also showed the following significant difference between time point nested in treatment nested in population (all tests: PERMANOVA pairwise comparison): pre vs. post: CP1 Control and T+3/CO<sub>2</sub> ( $P < 0.01$  in both cases), CP1 T+3 and CO<sub>2</sub> ( $P < 0.05$ ), CP2 CO<sub>2</sub> and T+3/CO<sub>2</sub> ( $P < 0.05$  in both cases), SP1 all treatments ( $P < 0.01$  in all cases), SP2 CO<sub>2</sub> ( $P < 0.001$ ). Further significant difference were found when comparing treatments of one population with the source of treatment nested in population nested in condition ( $P < 0.01$ , PERMANOVA). Pairwise tests performed with PERMANOVA analysis revealed the following significances: CP1: Control vs. T+3 ( $P < 0.001$ ), Control vs. T+3/CO<sub>2</sub> ( $P < 0.01$ ), T+3 vs. CO<sub>2</sub> ( $P < 0.05$ ), CO<sub>2</sub> vs. T+3/CO<sub>2</sub> ( $P < 0.05$ ); SP1: Control vs. CO<sub>2</sub> ( $P < 0.05$ ), Control vs. T+3/CO<sub>2</sub> ( $P < 0.01$ ); SP2: Control vs. CO<sub>2</sub> ( $P < 0.05$ ).

Further statistical analysis with PERMANOVA and treatment and population as fixed and random factors, respectively, revealed significant differences between populations nested in treatment ( $P < 0.001$ , PERMANOVA). Within the Control treatment, the following significant differences between populations were found (all tests: PERMANOVA pairwise comparison): CP1 vs. both SP ( $P < 0.01$ ), CP2 vs. both SP ( $P < 0.05$ ), SP1 vs. SP2 ( $P < 0.05$ ). Within the T+3 treatment, the following significant differences between populations were found (all tests: PERMANOVA pairwise comparison): CP1 vs. CP2 ( $P < 0.001$ ), CP1 vs. both SP ( $P < 0.001$ ), CP2 vs. both SP ( $P < 0.05$ ). Within the CO<sub>2</sub> treatment, the following significant differences between populations were found (all tests: PERMANOVA pairwise comparison): CP1 vs. both SP ( $P < 0.05$ ), CP2 vs. SP1 ( $P < 0.001$ ). Within the T+3/CO<sub>2</sub> treatment, the following significant differences between populations were found (all tests: PERMANOVA pairwise comparison): CP1 vs. CP2 ( $P < 0.01$ ), CP1 vs. both SP ( $P < 0.01$ ), CP2 vs. SP1 ( $P < 0.05$ ).

Additionally, SIMPER analysis presented the main composition of elements for each country in each treatment. Overall, 89.3%, 92.4% and 85.4% of the data are represented in PERMANOVA and SIMPER for CP, SP and comparison analysis, respectively. Comparing pre and post-experimental compositions, for all populations in all treatments, more than 90% of the data are channelled in the five major contributing elements: Ca, Mg, Sr, Zn and Cr, in this order. SP1 showed an inclusion of Fe into 90% of the major elemental composition of the skeleton in post-Control measurements. Comparing the post-experimental measurements between locations, Fe was included in the 90% limit of the skeletal trace elemental composition in SP1 Control and SP2 CO<sub>2</sub> treatments. Major elements influencing CP were discovered to be Fe, Mg and Sr; furthermore, minor influential elements

were Cr, Ba and V. Major elements influencing SP were Fe, Mg, Sr and Cr; additional fewer influences were caused by Zn and Cd. When comparing treatments, elements influencing these the most were Fe, Mg and Sr with fewer influences caused by Cr and Ba (Figure 5.19 and Figure 5.20 (E) and Figure 5.21 (D)).

Note for comparison of Figure 5.10 - Figure 5.12: 3-times higher y-axis values were chosen to present the Zn/Ca ratios of SP. Additionally, note that the y-axis of Cd/Ca ratios of SP starts roughly where the one of CP finishes.



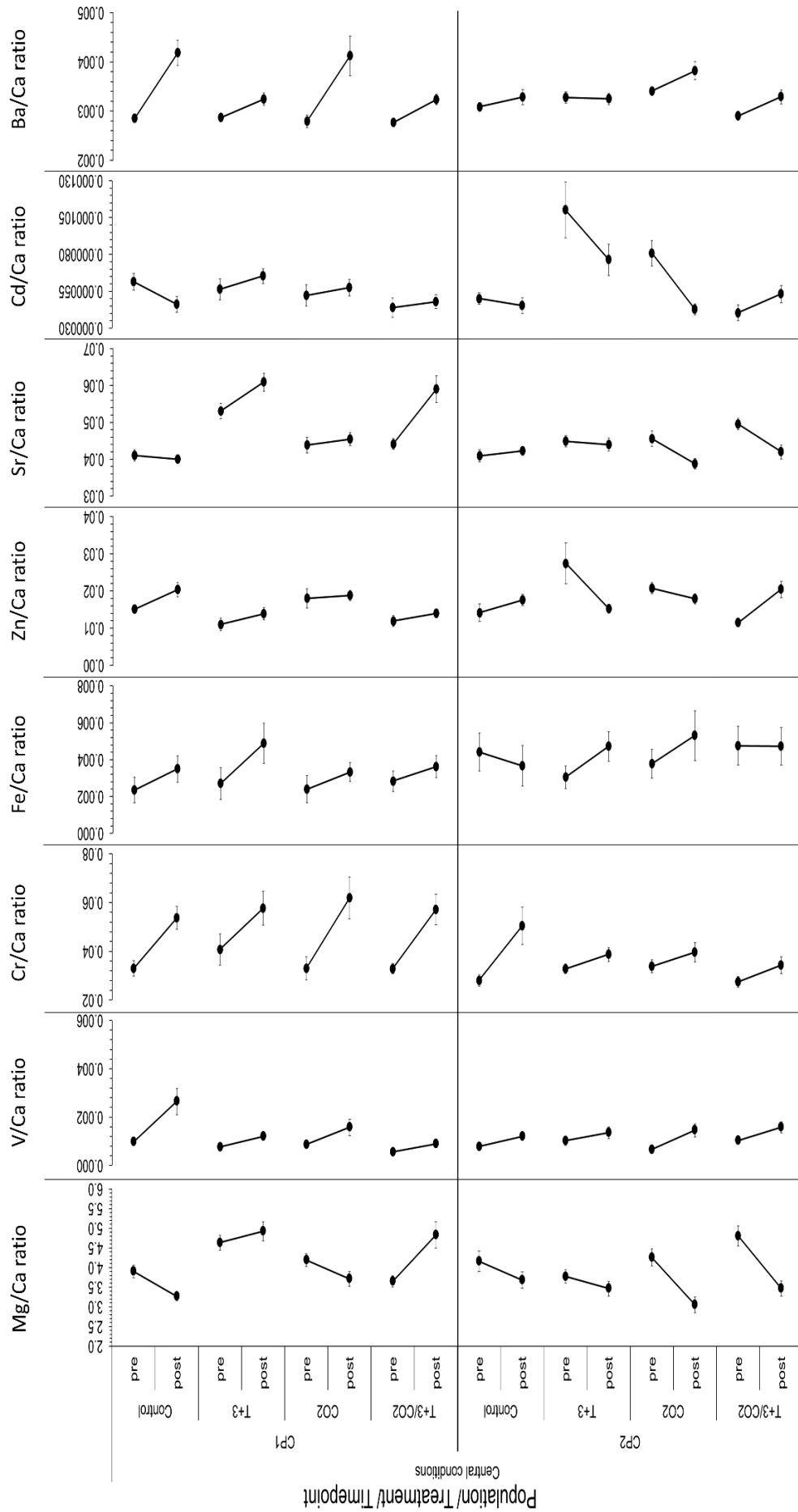


**Figure 5.17:** Element/Ca ratios for all elements in the Cross Experiment. Data points (AV  $\pm$ SE, n = 15) represent central populations (CP1 and CP2) of *C. officinalis*, in pre and post-experimental conditions: Control, high pCO<sub>2</sub> (CO<sub>2</sub>), high temperature (T+3) and high pCO<sub>2</sub> and high temperature (CO<sub>2</sub>/T+3).

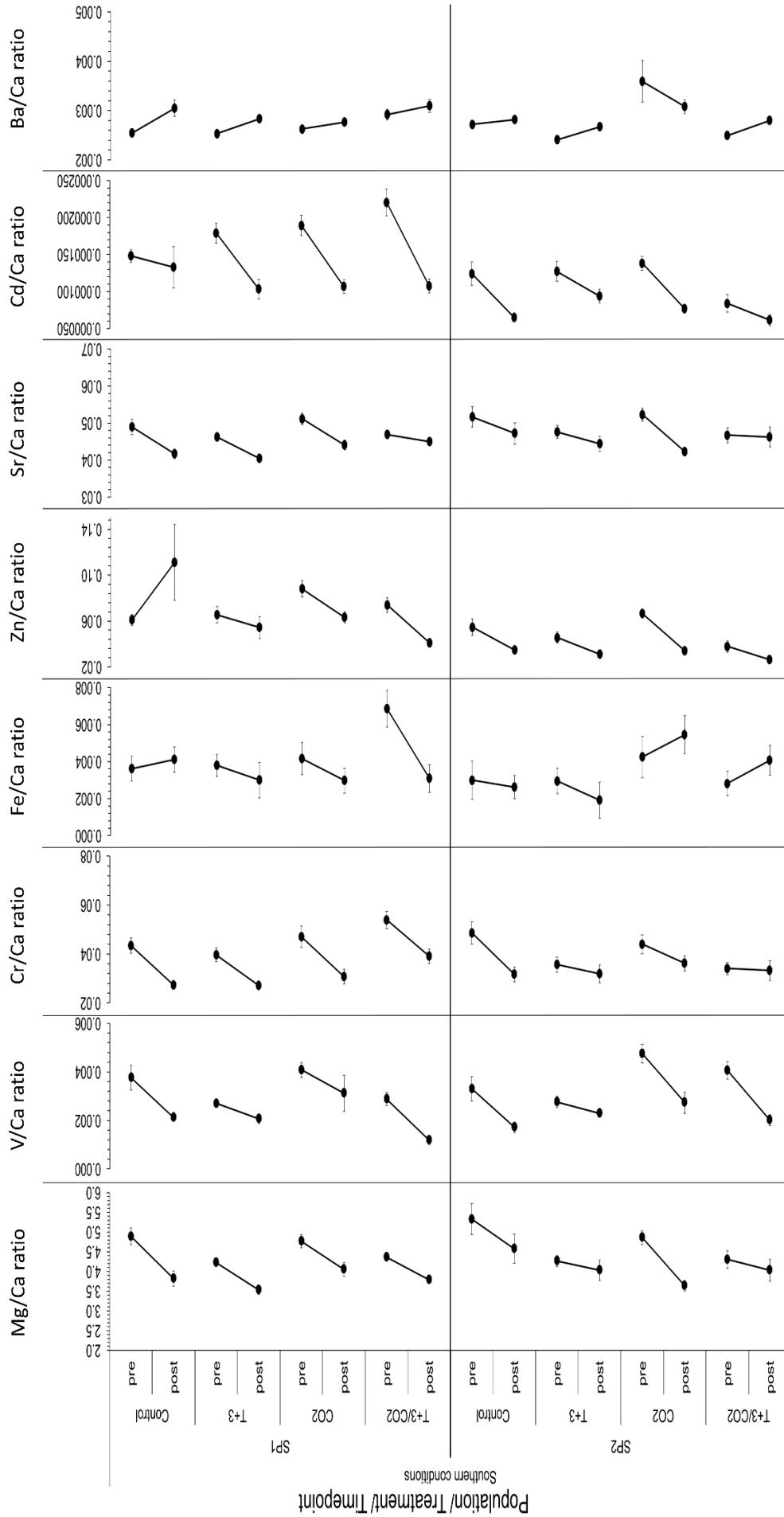


**Figure 5.18:** Element/Ca ratios for all elements in the Cross Experiment. Data points (AV  $\pm$ SE, n = 15) represent southern populations (SP1 and SP2) of *C. officinalis*, in pre and post-experimental conditions: Control, high pCO<sub>2</sub> (CO<sub>2</sub>), high temperature (T+3) and high pCO<sub>2</sub> and high temperature (CO<sub>2</sub>/T+3).

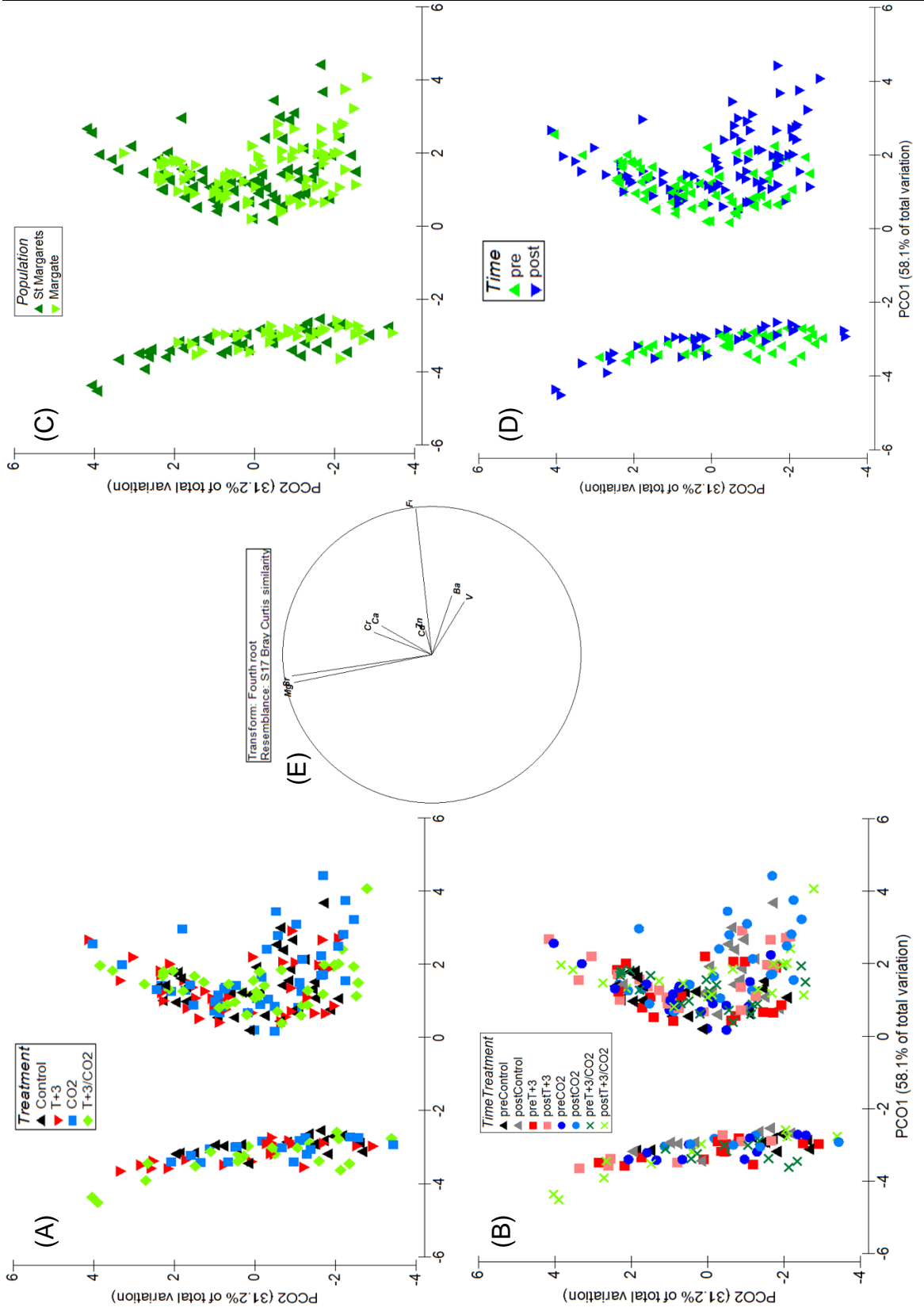


**Figure 5.19:** PERMANOVA (A-D) and SIMPER (E) results for central populations of *C. officinalis* of the Cross Experiment.

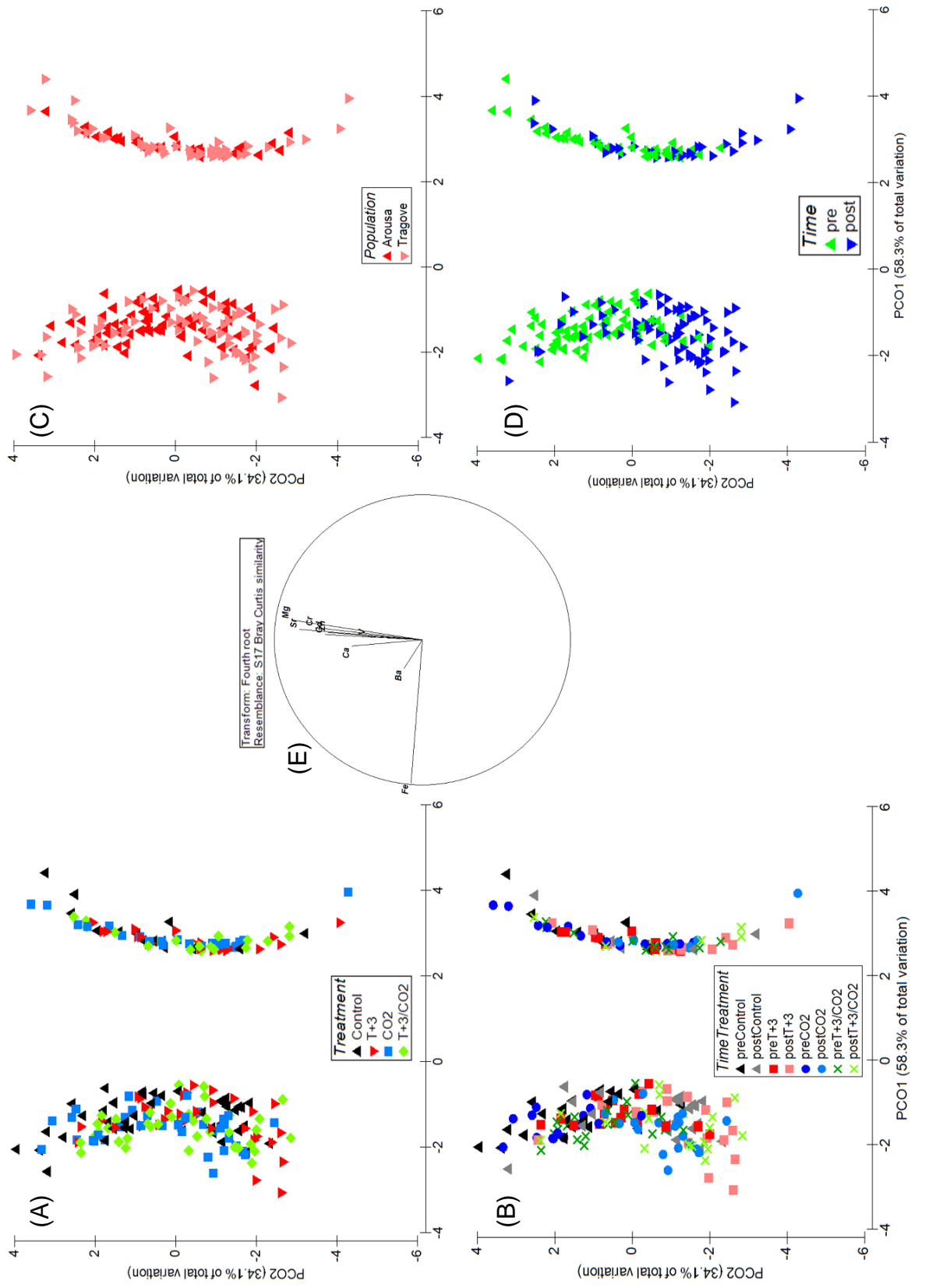


**Figure 5.20:** PERMANOVA (A-D) and SIMPER (E) results for southern populations of *C. officinalis* of the Cross Experiment.

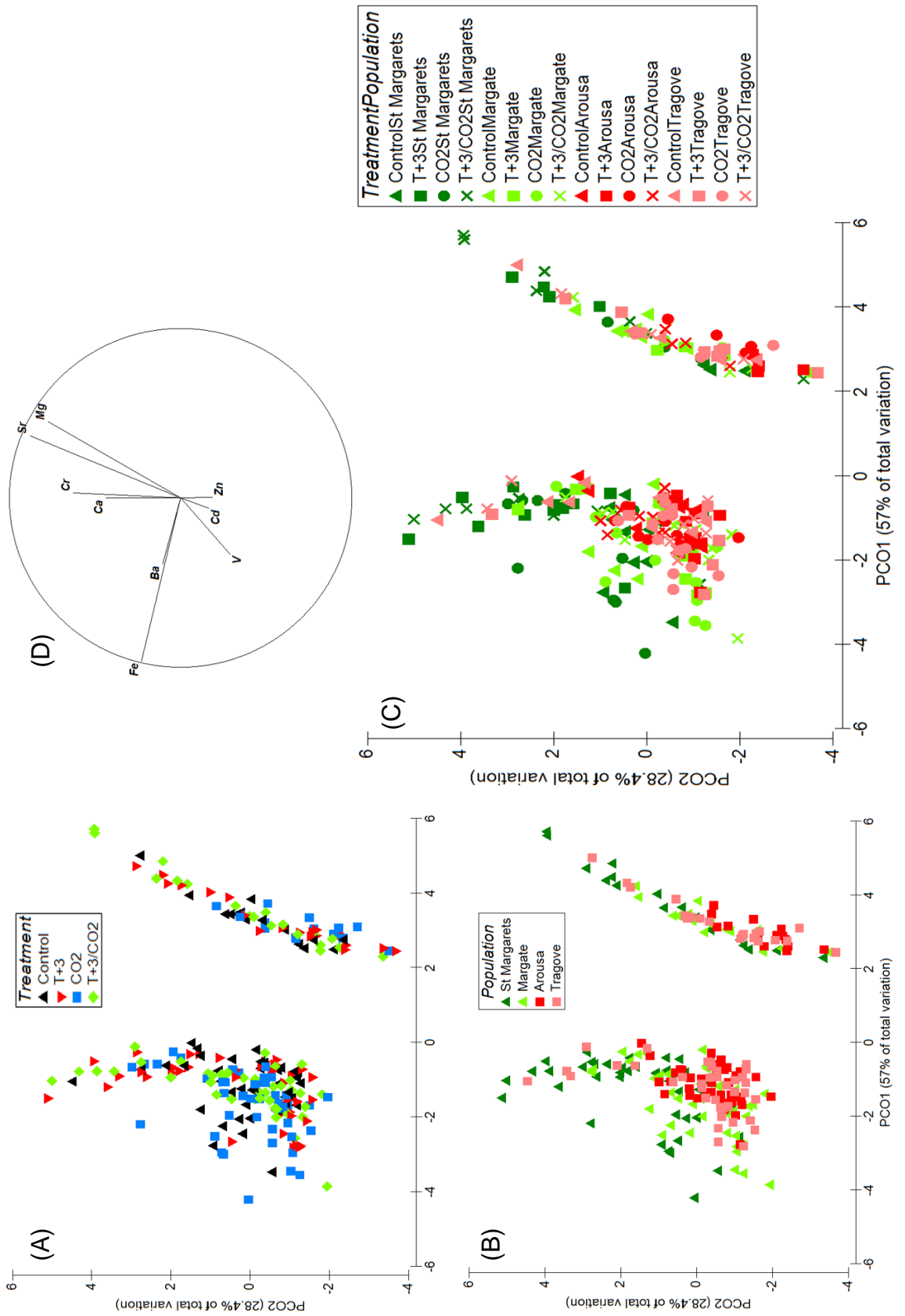


**Figure 5.21:** PERMANOVA (A-C) and SIMPER (D) results for all populations of *C. officinalis* of the Cross Experiment.

### 5.4.2.3 Cell wall thickness and condition

Cell wall thickness was measured inter- (lateral to growth direction) and intra-cell walls (horizontal to growth direction, Figure 2.13) of specimens originating from both experiments, the Climate Change and the Cross Experiment prior and after the experiments. Due to difficulties in separating cell walls of individual cells, the combined cell wall of two neighbouring cells was measured. Inter-cell walls were thicker than intra cell walls in all populations but 3 occasions of a population in a T+3 treatment. In both experiments, inter-cell wall thickness reduced or stayed equal during the experiment, in all populations and treatments, except for NP1 Control. Results of statistical tests (Kruskal-Wallis H tests for all) can be found in tables D3 and D4 in Appedix D, for the Cross Experiment and the Climate Change Experiment, respectively.

In the Climate Change Experiment (Table 5.10, Figure 5.22 - Figure 5.24, Table 5.8(A)), NP showed the most stable and thickest cell walls throughout all treatments (Figure 5.22, Table 5.8(A)). Whereas SP showed the least differences in thickness between intra and inter-cell walls (Figure 5.24) compared to NP and CP. In SP, all intra-cell wall thickness from prior to after the experiment increased in T+3 and decreased in all CO<sub>2</sub> treatments. In the T+3 treatment, NP showed an opposing trend between populations, however, both CP (Figure 5.23, Table 5.8(A)) decreased and both SP increased their intra cell wall thickness in this treatment from prior to after the experiment. Under elevated pCO<sub>2</sub>, NP and CP showed an opposing trend whereas SP showed decreased thickness in both types of cell walls after the experiment. In the climate change treatment, only NP showed increased post-intra-cell wall thickness compared to the respective pre-experimental thickness.

When comparing treatments in relation to the respective control of a population, a decrease was observed in inter-cell walls T+3 and inter-cell walls T+3/CO<sub>2</sub> in NP1 and in inter-cell walls T+3 and both cell walls CO<sub>2</sub> in NP2 (Table 5.8 (A), Figure 5.22). Central populations showed a decrease in all treatments in both types of cell wall (Figure 5.23, Table 5.8(A)). Southern populations stayed stable in their control condition from prior to after the experiment and showed a decline in almost all treatments in relation to the Control after the experiment, with the exception of intra cell wall T+3 and inter-cell wall T+3/CO<sub>2</sub> (Table 5.8 (A), Figure 5.24).

When ranking the treatments by thickness, it was observed that thickest cell walls were observed in either the CO<sub>2</sub> treatment (NP1) or the T+3/CO<sub>2</sub> treatment (NP2). In CP, thickest cell walls were observed in the control treatment and thinnest cell walls were observed in the T+3 and CO<sub>2</sub> treatment, for CP1 and CP2, respectively (Table 5.8 (A)). Southern population 1 showed least thick cell walls in the CO<sub>2</sub> and T+3/CO<sub>2</sub> treatments equally. No clear trend was observed in SP2. When comparing the populations with each other, NP1 showed higher intra cell walls than NP2 in both pCO<sub>2</sub> elevated treatments as well as lower inter-cell wall thickness in the T+3/CO<sub>2</sub> treatment. In all treatments, CP1 showed thinner cell walls compared to CP2. Intra cell walls of SP1 were observed to be thinner in the CO<sub>2</sub> treatment and inter-cell walls were observed to be thinner in the T+3/CO<sub>2</sub> treatment compared to SP2 (Table 5.8 (A)).

**Table 5.8:** (A) Mean  $\pm$ SE (n = 15) for inter- and intra-cell wall thickness (CWT) of *C. officinalis* (n = 2 populations for Northern, Central and Southern origin) under Control (n = 3), elevated temperature (T+3, n = 3), elevated pCO<sub>2</sub> (n = 3) and Climate Change (T+3/CO<sub>2</sub>, n = 3) treatments in the Climate Change Experiment. (B) Pre- and post-experimental statistical differences in populations within treatment and between treatments within population.

(A) Region	Population	Treatment	Time point	Inter-cell wall thickness [mm month <sup>-1</sup> ]		Intra-cell wall thickness [mm month <sup>-1</sup> ]	
				Mean	±SE	Mean	±SE
North	1	Control	pre	1.62	0.054	1.30	0.043
			post	1.70	0.060	1.42	0.056
		T+3	pre	2.20	0.086	1.49	0.043
			post	1.65	0.062	1.42	0.040
		CO <sub>2</sub>	pre	1.86	0.071	1.46	0.053
			post	1.71	0.074	1.53	0.051
	2	T+3/CO <sub>2</sub>	pre	2.30	0.086	1.44	0.050
			post	1.50	0.063	1.45	0.062
		Control	pre	1.86	0.067	1.47	0.055
			post	1.71	0.066	1.47	0.047
		T+3	pre	1.75	0.056	1.50	0.056
			post	1.62	0.055	1.55	0.058
Central	1	Control	pre	1.85	0.078	1.33	0.037
			post	1.82	0.059	1.36	0.041
		T+3	pre	1.79	0.048	1.49	0.049
			post	1.31	0.051	1.13	0.044
		CO <sub>2</sub>	pre	2.20	0.084	1.38	0.039
			post	1.72	0.072	1.33	0.057
T+3/CO <sub>2</sub>	pre	1.92	0.073	1.45	0.056		
	post	1.60	0.051	1.25	0.056		
South	1	Control	pre	2.19	0.080	1.63	0.058
			post	1.86	0.062	1.79	0.061
		T+3	pre	1.73	0.055	1.84	0.070
			post	1.72	0.066	1.67	0.041
		CO <sub>2</sub>	pre	1.88	0.067	1.49	0.055
			post	1.60	0.052	1.49	0.058
T+3/CO <sub>2</sub>	pre	1.96	0.051	1.50	0.048		
	post	1.77	0.067	1.60	0.056		
North	1	Control	pre	1.81	0.054	1.43	0.052
			post	1.81	0.060	1.41	0.061
		T+3	pre	1.82	0.058	1.41	0.053
			post	1.79	0.065	1.49	0.055
		CO <sub>2</sub>	pre	1.58	0.052	1.58	0.054
			post	1.53	0.050	1.40	0.047
	T+3/CO <sub>2</sub>	pre	1.70	0.050	1.28	0.048	
		post	1.53	0.053	1.39	0.050	
	2	Control	pre	1.95	0.066	1.43	0.050
			post	1.65	0.042	1.55	0.048
		T+3	pre	1.74	0.050	1.22	0.046
			post	1.64	0.059	1.30	0.044
CO <sub>2</sub>		pre	1.63	0.064	1.35	0.060	
		post	1.54	0.056	1.32	0.063	
T+3/CO <sub>2</sub>	pre	1.85	0.066	1.51	0.066		
	post	1.74	0.056	1.32	0.049		

(B) Population	Treatment	Time point	North		Central		South					
			pre	post	pre	post	pre	post				
North	1	Control	T+3/CO <sub>2</sub>	NS	NS	NS	NS	NS	NS	NS	NS	
			CO <sub>2</sub>	NS	NS	NS	NS	NS	NS	NS	NS	NS
		T+3	pre	NS	NS	NS	NS	NS	NS	NS	NS	NS
			post	NS	NS	NS	NS	NS	NS	NS	NS	NS
		CO <sub>2</sub>	pre	NS	NS	NS	NS	NS	NS	NS	NS	NS
			post	NS	NS	NS	NS	NS	NS	NS	NS	NS
	2	Control	T+3/CO <sub>2</sub>	NS	NS	NS	NS	NS	NS	NS	NS	NS
			CO <sub>2</sub>	NS	NS	NS	NS	NS	NS	NS	NS	NS
		T+3	pre	NS	NS	NS	NS	NS	NS	NS	NS	NS
			post	NS	NS	NS	NS	NS	NS	NS	NS	NS
		CO <sub>2</sub>	pre	NS	NS	NS	NS	NS	NS	NS	NS	NS
			post	NS	NS	NS	NS	NS	NS	NS	NS	NS
Central	1	Control	T+3/CO <sub>2</sub>	NS	NS	NS	NS	NS	NS	NS	NS	
			CO <sub>2</sub>	NS	NS	NS	NS	NS	NS	NS	NS	NS
		T+3	pre	NS	NS	NS	NS	NS	NS	NS	NS	NS
			post	NS	NS	NS	NS	NS	NS	NS	NS	NS
		CO <sub>2</sub>	pre	NS	NS	NS	NS	NS	NS	NS	NS	NS
			post	NS	NS	NS	NS	NS	NS	NS	NS	NS
	2	Control	T+3/CO <sub>2</sub>	NS	NS	NS	NS	NS	NS	NS	NS	NS
			CO <sub>2</sub>	NS	NS	NS	NS	NS	NS	NS	NS	NS
		T+3	pre	NS	NS	NS	NS	NS	NS	NS	NS	NS
			post	NS	NS	NS	NS	NS	NS	NS	NS	NS
		CO <sub>2</sub>	pre	NS	NS	NS	NS	NS	NS	NS	NS	NS
			post	NS	NS	NS	NS	NS	NS	NS	NS	NS
South	1	Control	T+3/CO <sub>2</sub>	NS	NS	NS	NS	NS	NS	NS	NS	
			CO <sub>2</sub>	NS	NS	NS	NS	NS	NS	NS	NS	NS
		T+3	pre	NS	NS	NS	NS	NS	NS	NS	NS	NS
			post	NS	NS	NS	NS	NS	NS	NS	NS	NS
		CO <sub>2</sub>	pre	NS	NS	NS	NS	NS	NS	NS	NS	NS
			post	NS	NS	NS	NS	NS	NS	NS	NS	NS
	2	Control	T+3/CO <sub>2</sub>	NS	NS	NS	NS	NS	NS	NS	NS	NS
			CO <sub>2</sub>	NS	NS	NS	NS	NS	NS	NS	NS	NS
		T+3	pre	NS	NS	NS	NS	NS	NS	NS	NS	NS
			post	NS	NS	NS	NS	NS	NS	NS	NS	NS
		CO <sub>2</sub>	pre	NS	NS	NS	NS	NS	NS	NS	NS	NS
			post	NS	NS	NS	NS	NS	NS	NS	NS	NS

Significance levels: NS = not significant; \* = p < 0.05; \*\* = p < 0.01; \*\*\* = p < 0.005.



In the Cross Experiment (Table 5.9, Table 5.10, Figure 5.25), inter-cell walls were always and intra-cell walls were mostly thicker prior compared to post-experimental measurements. Inter-cell walls are mostly thicker than inter-cell walls, except for 2 occasions (CP2 post T+3, SP2 post T+3, Table 5.9(A)).

In comparison with measurements prior to experimental exposure, cell wall thickness of CP did only increase in intra-cell walls in treatment CO<sub>2</sub> of CP1 (Table 5.9(A), Figure 5.25). All other cell walls of both CP decreased in thickness throughout the experiment (Table 5.9(A)). In both SP, a pronounced thickening of intra-cell walls was observed in the climate change treatment contrary to thinner walls in the control treatment (Table 5.9(A), Figure 5.25). The inter-cell walls of all populations in all treatments thinned. Comparing the treatments with their respective control treatment for each populations, it was observed, that in CP only intra cell walls thinned equally in the climate change treatments and inter-cell walls thickened equally in both CO<sub>2</sub>-included treatments. In SP, all types of cell walls thickened, except for 1 occasion (inter-cell wall of SP2 in T+3/CO<sub>2</sub>). In CP1, thickest intra- and inter-cell walls were observed in the CO<sub>2</sub> and T+3 treatments, whereas in CP2 thinnest inter- and intra-cell walls were observed in the T+3 treatment (Table 5.9(A)). The ranking of thickness in both SP showed the same pattern for intra- and inter-cell wall thickness of SP1, however, inter-cell wall thickness in SP2 showed a different pattern (Figure 5.25). All SP showed thickest cell walls in treatment T+3. CP2 showed lower values of inter-cell wall thickness in the T+3 condition, whereas in all other treatments, population 2 showed higher values throughout (Table 5.9(A)). In both experiments degraded cell walls were observed in post-experimental specimens in both CO<sub>2</sub>-included treatments (personal observation).

Statistical results are summarised in Table 5.9(B), Appendix D, Tables D1 and D2.

Temperature condition	Population	Treatment	Time point	Inter-cell wall thickness [mm month <sup>-1</sup> ]		Intra-cell wall thickness [mm month <sup>-1</sup> ]	
				Mean	±SE	Mean	±SE
				Central 1	Control	pre	1.90
		post	1.33	0.052	1.28	0.049	
	T+3	pre	2.03	0.070	1.79	0.066	
		post	1.61	0.046	1.39	0.060	
	CO <sub>2</sub>	pre	1.94	0.075	1.41	0.047	
		post	1.68	0.057	1.60	0.043	
	T+3/CO <sub>2</sub>	pre	2.10	0.059	1.92	0.068	
		post	1.34	0.058	1.21	0.048	
Central 2	Control	pre	1.87	0.056	1.61	0.063	
		post	1.68	0.055	1.74	0.065	
	T+3	pre	1.81	0.054	1.79	0.065	
		post	1.50	0.053	1.50	0.056	
	CO <sub>2</sub>	pre	1.96	0.072	1.62	0.052	
		post	1.76	0.050	1.61	0.052	
	T+3/CO <sub>2</sub>	pre	2.09	0.062	1.73	0.051	
		post	1.86	0.089	1.52	0.074	
Southern 1	Control	pre	1.73	0.058	1.20	0.050	
		post	1.20	0.033	1.11	0.045	
	T+3	pre	1.55	0.053	1.15	0.050	
		post	1.55	0.051	1.35	0.051	
	CO <sub>2</sub>	pre	1.81	0.064	1.55	0.053	
		post	1.29	0.042	1.19	0.046	
	T+3/CO <sub>2</sub>	pre	1.50	0.043	1.19	0.050	
		post	1.46	0.042	1.34	0.055	
Southern 2	Control	pre	1.78	0.056	1.39	0.047	
		post	1.58	0.052	1.14	0.027	
	T+3	pre	1.96	0.091	1.72	0.054	
		post	1.64	0.064	1.66	0.073	
	CO <sub>2</sub>	pre	1.64	0.054	1.38	0.037	
		post	1.59	0.059	1.47	0.057	
	T+3/CO <sub>2</sub>	pre	1.71	0.055	1.31	0.057	
		post	1.56	0.053	1.48	0.047	

**Table 5.9:** (A) Mean ±SE (n = 15) for inter- and intra-cell wall thickness (CWT) of *C. officinalis* (n = 2 populations for Central and Southern origin) under Control (n = 3), elevated temperature (T+3, n = 3), elevated pCO<sub>2</sub> (n = 3) and Climate Change (T+3/CO<sub>2</sub>, n = 3) treatments in the Cross Experiment. (B) Pre- and post-experimental statistical differences in populations within treatment and between treatments within population.

Inter-cell wall thickness Intra-cell wall thickness Kruskal Wallis H Test	Central condition															
	Central population 1				Central population 2				Southern population 1				Southern population 2			
	Control	T+3	CO <sub>2</sub>	T+3/CO <sub>2</sub>	Control	T+3	CO <sub>2</sub>	T+3/CO <sub>2</sub>	Control	T+3	CO <sub>2</sub>	T+3/CO <sub>2</sub>	Control	T+3	CO <sub>2</sub>	T+3/CO <sub>2</sub>
Time point	pre	post	pre	post	pre	post	pre	post	pre	post	pre	post	pre	post	pre	post
Central populatio n 1	Control	pre	***	NS	NS	NS	NS	NS	NS	NS	NS	NS	NS	NS	NS	NS
	T+3	pre	***	NS	NS	NS	NS	NS	NS	NS	NS	NS	NS	NS	NS	NS
	CO <sub>2</sub>	pre	NS	NS	NS	NS	NS	NS	NS	NS	NS	NS	NS	NS	NS	NS
	post	***	NS	NS	NS	NS	NS	NS	NS	NS	NS	NS	NS	NS	NS	NS
Central condition	T+3/CO <sub>2</sub>	pre	NS	*	NS	NS	NS	NS	NS	NS	NS	NS	NS	NS	NS	NS
	post	***	NS	NS	NS	NS	NS	NS	NS	NS	NS	NS	NS	NS	NS	NS
Central populatio n 2	Control	pre	NS	NS	NS	NS	NS	NS	NS	NS	NS	NS	NS	NS	NS	NS
	post	***	NS	NS	NS	NS	NS	NS	NS	NS	NS	NS	NS	NS	NS	NS
	T+3	pre	NS	NS	NS	NS	NS	NS	NS	NS	NS	NS	NS	NS	NS	NS
	post	NS	NS	NS	NS	NS	NS	NS	NS	NS	NS	NS	NS	NS	NS	NS
	CO <sub>2</sub>	pre	NS	NS	NS	NS	NS	NS	NS	NS	NS	NS	NS	NS	NS	NS
	post	NS	NS	NS	NS	NS	NS	NS	NS	NS	NS	NS	NS	NS	NS	NS
	T+3/CO <sub>2</sub>	pre	NS	NS	NS	NS	NS	NS	NS	NS	NS	NS	NS	NS	NS	NS
	post	***	NS	NS	NS	NS	NS	NS	NS	NS	NS	NS	NS	NS	NS	NS
Southern populatio n 1	Control	pre	NS	NS	NS	NS	NS	NS	NS	NS	NS	NS	NS	NS	NS	NS
	post	NS	NS	NS	NS	NS	NS	NS	NS	NS	NS	NS	NS	NS	NS	NS
	T+3	pre	NS	NS	NS	NS	NS	NS	NS	NS	NS	NS	NS	NS	NS	NS
	post	NS	NS	NS	NS	NS	NS	NS	NS	NS	NS	NS	NS	NS	NS	NS
	CO <sub>2</sub>	pre	NS	NS	NS	NS	NS	NS	NS	NS	NS	NS	NS	NS	NS	NS
	post	NS	NS	NS	NS	NS	NS	NS	NS	NS	NS	NS	NS	NS	NS	NS
	T+3/CO <sub>2</sub>	pre	NS	NS	NS	NS	NS	NS	NS	NS	NS	NS	NS	NS	NS	NS
	post	NS	NS	NS	NS	NS	NS	NS	NS	NS	NS	NS	NS	NS	NS	NS
Southern condition	Control	pre	NS	NS	NS	NS	NS	NS	NS	NS	NS	NS	NS	NS	NS	NS
	post	NS	NS	NS	NS	NS	NS	NS	NS	NS	NS	NS	NS	NS	NS	NS
	T+3	pre	NS	NS	NS	NS	NS	NS	NS	NS	NS	NS	NS	NS	NS	NS
	post	NS	NS	NS	NS	NS	NS	NS	NS	NS	NS	NS	NS	NS	NS	NS
	CO <sub>2</sub>	pre	NS	NS	NS	NS	NS	NS	NS	NS	NS	NS	NS	NS	NS	NS
	post	NS	NS	NS	NS	NS	NS	NS	NS	NS	NS	NS	NS	NS	NS	NS
	T+3/CO <sub>2</sub>	pre	NS	NS	NS	NS	NS	NS	NS	NS	NS	NS	NS	NS	NS	NS
	post	NS	NS	NS	NS	NS	NS	NS	NS	NS	NS	NS	NS	NS	NS	NS

Significance levels: NS = not significant. \* = P < 0.05. \*\* = P < 0.01. \*\*\* = P < 0.005.

**Table 5.10:** Overview of cell wall thickness results divided into experiment: pre vs. post-experimental measurements (anomalies: red arrowheads, similarities: yellow background), comparison of treatments to the control (differences: blue arrowheads), ranking of the treatments from highest to lowest (similarities: pink) and a comparison between both populations in each treatment (anomalies: green).

Climate Change Experiment		pre vs. post experiment		post Control vs. post treatment		Ranking by treatment		Population 1 vs. Population 2	
Population	Treatment	Intra	Inter	Intra	Inter	Intra	Inter	Intra	Inter
Northern population 1	Control	▲	▲			$CO_2 > T+3/CO_2 > C > T+3$	$CO_2 > C > T+3 > T+3/CO_2$	<	≈
	T+3	▼	▼	▲	▼			<	>
	CO <sub>2</sub>	▲	▼	▲	▲			>	>
	T+3/CO <sub>2</sub>	▲	▼	▼	▲			>	<
Northern population 2	Control	▼	▼			$T+3 \approx T+3/CO_2 > C > CO_2$	$T+3/CO_2 > C > T+3 > CO_2$		
	T+3	▲	▼	▲	▼				
	CO <sub>2</sub>	▼	▼	▼	▼				
	T+3/CO <sub>2</sub>	▲	▼	▲	▲				
Centre population 1	Control	▲	▼			$C > CO_2 > T+3/CO_2 > T+3$	$C > CO_2 > T+3/CO_2 > T+3$	<	<
	T+3	▼	▼	▼	▼			<	<
	CO <sub>2</sub>	▼	▼	▼	▼			<	<
	T+3/CO <sub>2</sub>	▼	▼	▼	▼			<	<
Centre population 2	Control	▲	▼			$C > T+3 > T+3/CO_2 > CO_2$	$C > T+3/CO_2 > T+3 > CO_2$		
	T+3	▼	≈	▼	▼				
	CO <sub>2</sub>	▲	▼	▼	▼				
	T+3/CO <sub>2</sub>	▲	▼	▼	▼				
Southern population 1	Control	≈	≈			$T+3 > C > CO_2 \approx T+3/CO_2$	$C > T+3 > CO_2 \approx T+3/CO_2$	>	>
	T+3	▲	▼	▲	▼			>	>
	CO <sub>2</sub>	▼	▼	▼	▼			<	≈
	T+3/CO <sub>2</sub>	▲	▼	▼	▼			>	<
Southern population 2	Control	▲	▼			$C > CO_2 \approx T+3/CO_2 > T+3$	$T+3/CO_2 > C \approx T+3 > CO_2$		
	T+3	▲	▼	▼	▼				
	CO <sub>2</sub>	▼	▼	▼	▼				
	T+3/CO <sub>2</sub>	▼	▼	▼	▲				
<b>Cross Experiment</b>									
Centre population 1	Control	▼	▼			$CO_2 > T+3 > C > T+3/CO_2$	$CO_2 > T+3 > T+3/CO_2 > C$	<	<
	T+3	▼	▼	▲	▲			<	>
	CO <sub>2</sub>	▲	▼	▲	▲			<	<
	T+3/CO <sub>2</sub>	▼	▼	▼	▲			<	<
Centre population 2	Control	▼	▼			$C > CO_2 > T+3/CO_2 > T+3$	$T+3/CO_2 > CO_2 > C > T+3$		
	T+3	▼	▼	▼	▼				
	CO <sub>2</sub>	▼	▼	▼	▲				
	T+3/CO <sub>2</sub>	▼	▼	▼	▲				
Southern population 1	Control	▼	▼			$T+3 \approx T+3/CO_2 > CO_2 > C$	$T+3 > T+3/CO_2 > CO_2 > C$	<	<
	T+3	▲	≈	▲	▲			<	<
	CO <sub>2</sub>	▼	▼	▲	▲			<	<
	T+3/CO <sub>2</sub>	▲	▼	▲	▲			<	<
Southern population 2	Control	▼	▼			$T+3 > T+3/CO_2 > CO_2 > C$	$T+3 > C \approx CO_2 > T+3/CO_2$		
	T+3	▼	▼	▲	▲				
	CO <sub>2</sub>	▲	▼	▲	▲				
	T+3/CO <sub>2</sub>	▲	▼	▲	▲				

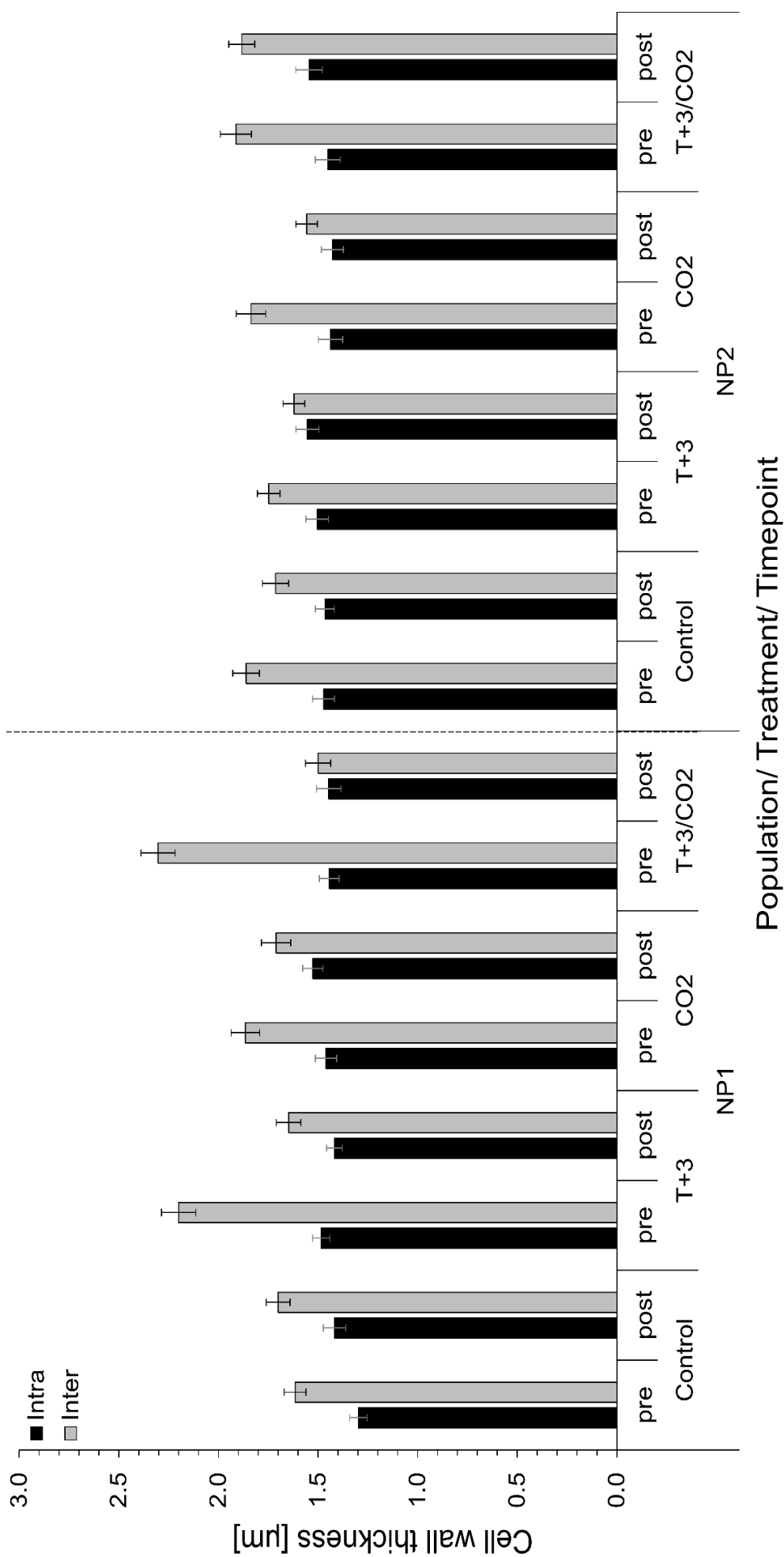


**Figure 5.22:** Inter- (grey bars) and intra-cell wall thickness (black bars) [ $\mu\text{m}$ ] of *C. officinalis* in the Climate Change Experiment. Black and grey bars ( $\text{AV} \pm \text{SE}$ ,  $n = 45$ ) represent northern populations (NP1 and NP2) pre and post-experimental, in each treatment, respectively.

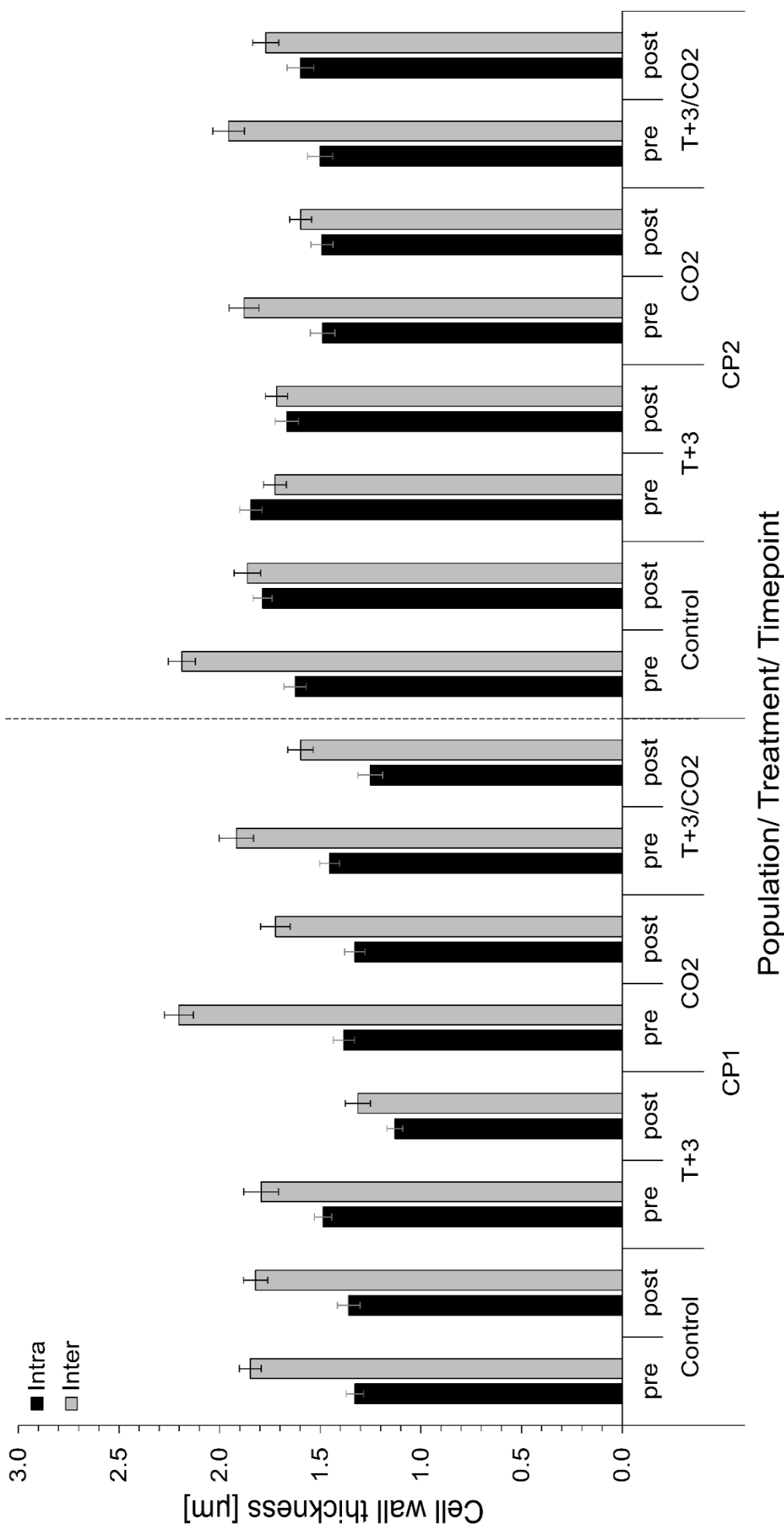
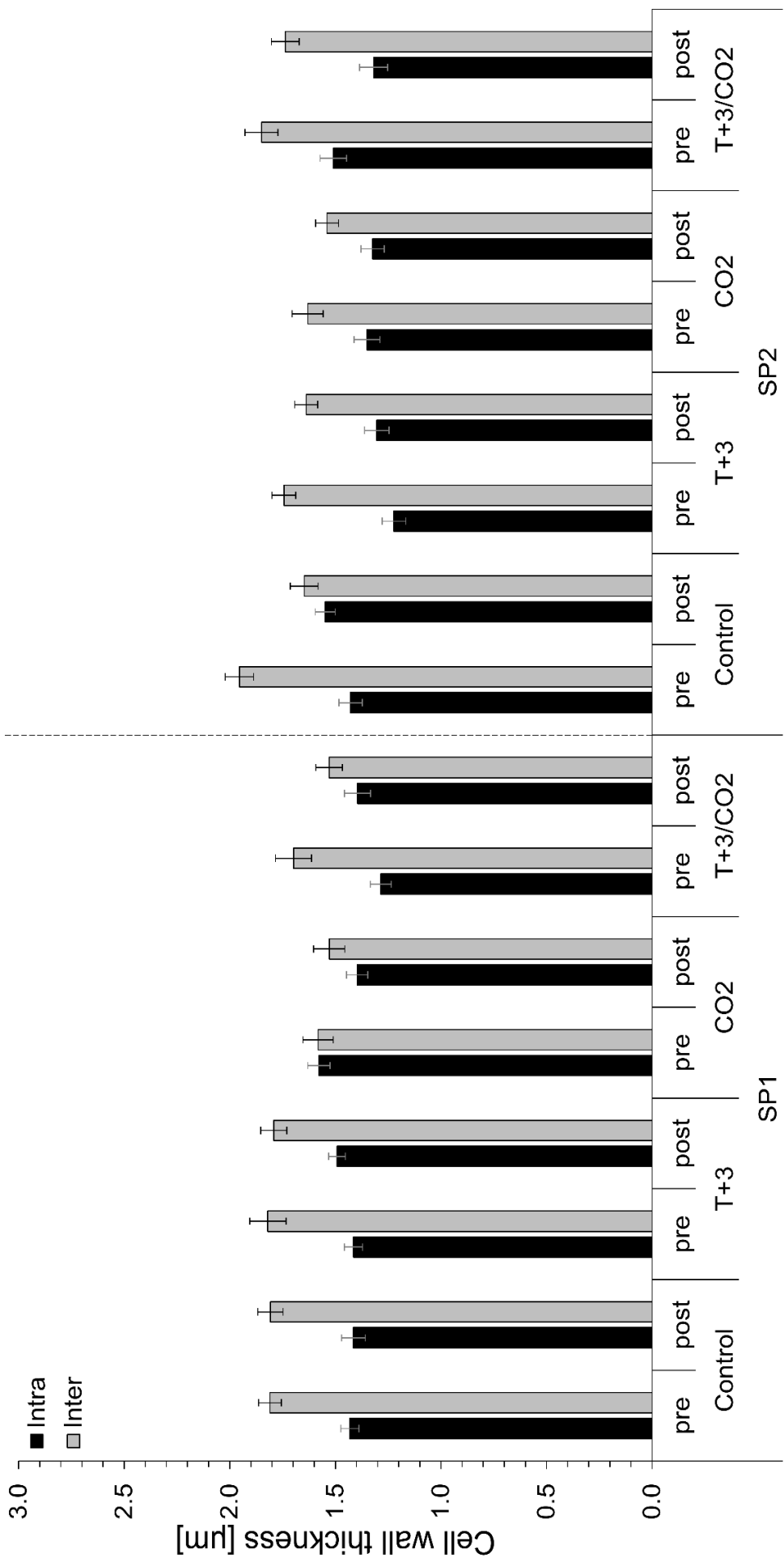


**Figure 5.23:** Inter- (grey bars) and intra-cell wall thickness (black bars) [ $\mu\text{m}$ ] of *C. officinalis* in the Climate Change Experiment. Black and grey bars ( $\text{AV} \pm \text{SE}$ ,  $n = 45$ ) represent central populations (CP1 and CP2) pre and post-experimental, in each treatment, respectively.



Population/ Treatment/ Timepoint

**Figure 5.24:** Inter- (grey bars) and intra-cell wall thickness (black bars) [ $\mu\text{m}$ ] of *C. officinalis* in the Climate Change Experiment. Black and grey bars (AV  $\pm$ SE, n = 45) represent southern populations (SP1 and SP2) pre and post-experimental, in each treatment, respectively.

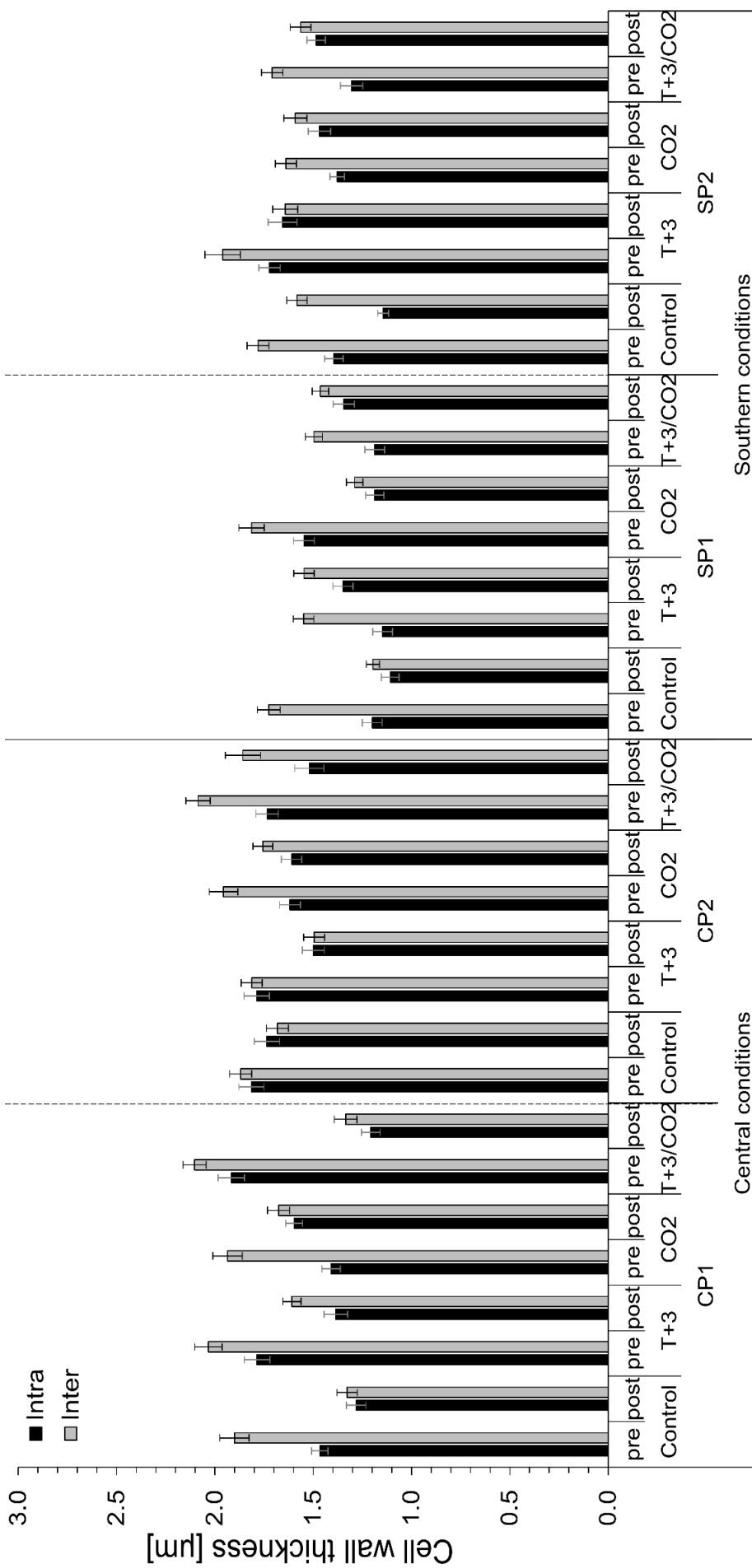


**Figure 5.25:** Inter- (grey bars) and intra-cell wall thickness (black bars) [ $\mu\text{m}$ ] of *C. officinalis* in the Cross Experiment. Black and grey bars ( $\text{AV} \pm \text{SE}$ ,  $n = 45$ ) represent central and southern populations under central and southern conditions, pre and post-experimental, in each treatment, respectively.

## 5.5 Discussion

This study investigated how physiological and structural traits of *C. officinalis* from across its geographical distribution in the NE Atlantic, differ when exposed to elevated temperatures and pCO<sub>2</sub>. For this, various physiological and structural parameters were determined and are discussed in the following paragraphs. Due to the exposure to a wide range of temperatures, *C. officinalis* shows different, including local and seasonal adaptation depending on their location.

### 5.5.1 Resilience to future thermal conditions

Understanding the impact of future climatic changes on *C. officinalis* and its interactions with the environment is crucial to predict how different divisions of the species distribution may be affected in their physiology and structural integrity. We present evidence for distinct vulnerability of central and peripheral populations of *C. officinalis*, a key marine ecosystem engineer (Kelaher *et al.*, 2003, Daleo *et al.*, 2006), to stress caused by thermal and carbonate chemistry changes.

To the authors' knowledge, no oxygen evolution curves (P-I curves) and calcification evolution curves (C-I curves) of marginal populations of *C. officinalis* were performed under climate change conditions, only one study reporting P-I curves on one central population of *C. officinalis* under decreased pH conditions was found (Hofmann *et al.*, 2012b). This study is to be interpreted with caution due to the lack of a combined treatment of decreased pH and increased temperature with a high probability of false interpretation of data when not in combination with elevated temperatures, as proven in this study where both individual and the combined treatments showed very different responses. P-I curves and C-I curves in this present study show clear regional responses between the central and southern locations. This first physiological response as well as the successful reduction of



pCO<sub>2</sub> levels in the experiments suggests that data obtained in this study could be interpreted as representative data for most populations of these and surrounding regions (Egilsdottir *et al.*, 2016, Williamson *et al.*, 2017), excluding those in extreme environments. However, there is added complexity when considering the maximum level of oxygen produced ( $P_{\max}$ ), indicating its dependency with the initial environment of the population. Therefore, values obtained for  $P_{\max}$  and  $C_{\max}$  in the winter experiment may be higher in summer as well as sunny conditions. Central and southern populations showed a decrease in all P-I parameters under climate change conditions which leads to the prediction of decreasing rates of primary production. An additional increase in CP and SP of Cr/Ca ratios functioning as growth and photosynthesis inhibitor as well as a decrease of Zn/Ca ratios acting as photosynthesis enhancement and favours CO<sub>2</sub>-assimilation (Kitano and Hood, 1962, Rout and Das 2003, Raven *et al.*, 1999), supports this assumption. However, this decrease in primary production was only observed in CP and not in SP in the Cross Experiment. Southern populations might therefore be more acclimatised to higher light levels and temperatures (e.g. experienced in summer) than those they were exposed to during the experiment (winter conditions) compared to CP which experience less light and temperature variations.

An increased level of  $C_{\max}$  in CP correlates with increased or stable light and dark calcification rates. Higher rates of  $C_{\max}$  in CP compared to SP may also originate in increasing light harvesting efficiency in CP compared to decreasing efficiency in SP under climate change conditions. Increased  $C_{\max}$  in all populations is mirrored with increasing light calcification rates of all populations in their respective environmental conditions. Uppermost decreases of maximum photosynthetic and calcification levels as well as light harvesting efficiency for both in SP, decreased highest under

elevated temperatures, without additional exposure to elevated acidification. This indicates that the main driver for stress in SP is temperature. This was already found for the southernmost populations of another species of intertidal macroalgae, *Fucus serratus* (Pearson *et al.*, 2009). The highly variable response in dark calcification rates in both locations highlights the importance of including, ideally, more than two populations into future climate change studies to fully understand the response of a region. Respiration rates are consistently higher in SP than in CP, which may be explained by decreased stress tolerance due to their location close to the species thermal, acidification and stress limit. The increase of respiration rates in SP combined with low production rates and increased heat stress could be a result of decreased  $P_{max}$ , light harvesting efficiency and a decrease in saturating light levels. Due to lower photosynthetic rates in high CO<sub>2</sub> treatments compared to the Control in all NP, CP and SP, it can be concluded that CO<sub>2</sub> does not provide a fertilising effect in *C. officinalis* under a climate change scenario. Including all 4 treatments, (1) Control, (2) elevated temperature, (3) elevated pCO<sub>2</sub> levels and (4) climate change: elevated temperature and pCO<sub>2</sub>, is highly recommended for future climate changes studies as it allows for thorough investigation of individual and combined effects on species physiology and structure. Additionally, in the two studies presented here, it was shown that conclusions drawn from the results of individual treatments may be highly misleading when trying to predict effects of future climatic changes, as it was already shown for the fleshy encrusting rhodophyte *Hildenbrandia* sp. (Schoenrock *et al.*, 2016). In this study, Schoenrock *et al.* showed a negative effect of individual temperature and pH treatments on this species but reveal a positive effect in the combined treatment.

Growth of CP stayed stable mirroring a simultaneous decrease in light calcification which cannot be compensated for by an increase in dark calcification. The reduction the thickness of both cell wall types confirm this finding and shows dissolution which leads to the hypothesis that light calcification can directly affect the structure of *C. officinalis*. Additionally, with values of light calcification surpassing those of dark calcification, it is shown to be the most valuable mechanism with the highest values. From these discoveries, together with the observed stable growth but decreasing cell wall thickness, it can be concluded, that CP favour spending more energy on linear growth instead of maintenance and build-up of cell walls, making them more porous. This change in structural integrity was already found for crustose coralline algae (McCoy and Ragazzola, 2014), identifying it as a strategy to cope with low pH across multiple genera. Cell wall thickness of inter-cell walls was found to be greater than intra cell walls in all populations at all times, supporting the hypothesis that inter-cell walls are more important regarding stability and protection against exposure to external mechanical forces. This also confirms the assumption that more energy is used to maintain or build up inter-cell walls instead of intra cell walls, which were seen to decrease in all but NP. Both cell wall thickness and linear growth are greater and greatest in NP compared to CP and SP. Central and southern populations show a reduction of growth and thickness in all populations exposed to climate change conditions, this may be explained by the lack of resilience and acclimatisation capacity to stressful future climatic conditions independently of seasons. Primary production increased in all but SP under climate change conditions, whereas only NP1 showed a decrease in respiration rates compared to an increase in all other populations. Elevated temperature and a potential fertilising effect of increased pCO<sub>2</sub> levels in NP might be the reason leading to these positive results. An additional reason might be that NP might already experience acidified

conditions and potential acclimatisation due to the elevated solubility of CO<sub>2</sub> in colder waters (Zeebe and Wolf-Gladrow, 2009). Temperature-initiated stress was observed in both temperature-elevated treatments in SP expressed by a reduction in photosynthetic rates, an increase in respiration, stable calcification rates and a decrease in growth as well as cell wall thicknesses. These results underline the fact that SP are already experiencing their thermal limit at current conditions and might not survive an additional, rapid increase in temperature until the end of this century. In addition, it was observed that elevated pCO<sub>2</sub> levels caused further strain in these populations.

The impact of climatic changes is also observed in reduced light calcification rates yielding in dissolution – exceedingly great in SP –, reduced or stable growth and reduced thickness in both types of cell wall in all but NP. This lets NP emerge as the most resilient populations and region compared to the other tested geographical locations. Elevated temperatures show a dominating influence on populations over elevated pCO<sub>2</sub>, contrary to literature which found corrosive effects on NP of coralline algae but only under high CO<sub>2</sub> conditions, not including elevated temperatures (Kamenos *et al.*, 2013). Dark calcification in marginal populations is larger in the climate change treatment compared to the Control, nevertheless, all marginal populations (NP and SP) decalcify in the dark whereas CP showed positive calcification leading to the assumption that CP are more robust towards changes in temperature and carbonate chemistry. Both CP and SP show stable or decreasing growth, as well as a decrease in cell wall thickness and light calcification, but an increase in dark calcification, showing that even though these populations are trying to compensate the dissolution effect in the light by calcification in the dark, the dissolution effect is too high to be compensated by dark calcification, ultimately

weakening the structural integrity of CP and SP. Compared to CP and SP, NP demonstrated the lowest photosynthetic and respiration rates as well as light and dark calcification rates. This is most likely due to the temperature effects on the metabolism and its evolution to be slower than in CP or SP which may have either a delayed negative effect on northern marginal populations or, more likely, provides them with sufficient time to allow full adaptation to changing conditions.

Trace elemental ratios are in line with most of the physiological responses to future climatic changes and their uptake is mostly favoured by increased  $p\text{CO}_2$ . Mg/Ca ratios, indicating changes in temperature (Milliman *et al.*, 1971, Kolesar, 1978), increased in all treatments including elevated temperatures, which coincide with expectations and literature. Comparable findings were described by Caragnano *et al.* (2014), here the authors found higher mol%  $\text{MgCO}_3$  within genus in specimens exposed to higher temperatures. Those changes are mostly observed indirectly through changes in growth and therefore Mg incorporation into the skeleton, and are enhanced in increasing light levels (Caragnano *et al.*, 2017, Andersson *et al.*, 2008). The development of Mg/Ca ratios follow those of the growth rate, confirming literature assumptions of a correlation between both. Greater V/Ca rates in CP and variable rates in marginal populations lead to a greater formation of chlorophyll a (Wilhelm and Wild, 1984a,b, Meisch and Benzschawel, 1978) in CP and less production of that pigment in marginal populations. This can especially be seen in SP where P-I parameters decrease potentially due to the lack of pigments through formation inhibition, in combination with a decline in growth which is also associated with an elevated V/Ca ratio. A decrease of Cr/Ca and Fe/Ca rates was observed in marginal populations compared to an increase in CP. Such a decrease may cause inhibition of photosynthetic processes or growth, which was initially favoured by

elevated Fe concentrations (Raven *et al.*, 1999 and references therein, Sari and Tuzen, 2008). This can be observed in SP, however, not in NP. This implies a good strategy for NP to cope with increasing concentrations of potentially damaging trace elements. The absorption of both, Cr and Fe into the skeleton is controlled thermodynamically and, in the case of Cr, additionally controlled by pH, which is a further sign, that NP may have evolved a mechanism to counteract the accumulation of these and potentially more harmful elements. An increase in Zn concentration is leading, according to literature, to a reduced viability of cell walls and an increased photosynthetic rate and CO<sub>2</sub> assimilation (Kitano and Hood, 1962, Rout and Das, 2003, Raven *et al.*, 1999). The reduction of cell wall viability was observed in CP and SP, however, not in NP, even though Zn/Ca ratios increased in all populations. An increased CO<sub>2</sub> assimilation is expressed in increased calcification rates, which corresponds with elevated light and dark calcification rates, except for light calcification rates in CP. Central populations might therefore be incapable of compensating the intake of potentially damaging elements with a physiological response. Sr/Ca ratios indicate the salinity in the organisms' environment (Schöne *et al.*, 2010, de Villiers, 1999). For that reason, as expected, Sr/Ca ratios increased during the experiments due to increased salinity in the local waters compared to the location of origin. However, when comparing individual treatments of elevated temperature and pCO<sub>2</sub>, it can be observed that high pCO<sub>2</sub> inhibits the uptake of Sr, however, higher temperatures showed the highest inhibition of uptake for this trace element. This indicates pollution and therefore reduced productivity and growth in algae and higher plants (Kangwe *et al.*, 2001, Vymazal, 1987 and references therein, Nazar *et al.*, 2012), yet surprisingly, Cd/Ca ratios increased in all, including NP. The northern sites used during this study are accredited as "organically certified" locations (Chapter 3) and it was expected for these sites to show the lowest

values in Cd/Ca ratios. However, only CP and SP were found to be highly influenced and inhibited by increased Cd concentrations, which is reflected in the reduction of growth and calcification. The associated reduction in productivity can only be found in reduced primary production rates in SP but not in CP or NP. This gives rise to the hypothesis that SP, already thermally stressed, fail to react appropriately to elemental concentrations leading to lower productivity. Literature describes Ba/Ca ratios as indicators for freshwater influx (Gillikin *et al.*, 2006) and being negatively correlated with salinity (Caragnano *et al.* 2014, Hanor and Chan, 1977, Nelson *et al.*, 2018, McCoy and Kamenos 2015 and references therein), therefore showing an opposing trend to Sr/Ca ratios (Schöne *et al.*, 2010, de Villiers, 1999). In the studies conducted here, no clear trend of Ba/Ca relating to future climate change conditions was found and Ba/Ca ratios are therefore unsuitable to act as an indicator in *C. officinalis*. This is confirming what was already shown for other genera where Ba/Ca ratios presented very little changes (Caragnano *et al.*, 2014).

When comparing both experiments, general species reactions to climatic changes can be observed in the Climate Change Experiment, whereas in the Cross Experiment, conclusions can be drawn for how *C. officinalis* would react in their own environment and which environmental influences effect the physiology of this species. Under climate change conditions, all populations showed the most stable rates and least changes in all trace elements compared to the other three treatments. Additionally, marginal populations showed even more stable rates under climate change conditions than CP, which showed greater magnitudes of change. Southern populations showed a different trend than CP when the climate change treatment was added under field temperature conditions, which leads to the discovery that *in situ* light, rather than temperature, influences the behaviour of the

algae under climate change conditions. In CP, Ba, V, Cr and Fe show an identical or very similar pattern between populations, which may also have a combined effect on Mg concentrations in the skeleton. A potential change in redox states under elevated CO<sub>2</sub> conditions and a subsequent reaction of Ba<sup>2+</sup>, CO<sub>3</sub><sup>2-</sup> and Ca<sup>2+</sup> with other compounds of the alga skeleton is thought to influence the above named elements. In accordance with literature, it was observed that Mg and Sr ratios show similar patterns which are thought to develop from a correlation between both elements due to the Mg lattice and the ability of Sr to bind and accumulate within this lattice. Questions arising from these studies include the unknown effect of elements on the fitness of the algae as well as how population variability might affect the uptake of trace elements with some locations showing opposite results.

### 5.5.1 Methodological Limitations

Due to some limitations in preparation of samples or implementation of analysis, some aspects were carefully considered. It was made sure that none of the limited sample sections were analysed, however, whilst measuring cell wall thickness it was noticed, that some parts were not polished horizontally but at an angle due to the nature of the branch and the positioning during the embedding process. Therefore, during data discussion, this was taken into consideration.

Additionally, a relatively high variability in trace elemental data sets can be observed. This may be due to the positioning of the ablation spot on the branch, which may not include the same amount of material in the top of the branch compared to the lower parts of the branch due to age and therefore thickness of the



cell walls and the lower amount of material associated with younger age as cell walls are still under construction.

The Climate Change Experiment was conducted as a summer experiment in a flow-through aquaria system with constant water supply, therefore high rates were expected compared to the Cross Experiment, which was designed as a winter experiment in a closed system with aquaria being placed in water baths to keep the respective temperatures constant. The two different experimental designs urge for caution when comparing populations.

Additional care was taken when interpreting results of the Climate Change Experiment as samples were potentially mixed during the bagging process due to human error – this is unlikely, but it cannot be ruled out. As a consequence, the Cross Experiment was planned and conducted, however, due to the lack of labour force and time, only two, the central and southern, locations were chosen for this experiment.

Samples used to determine calcification rates through titration of the Cross Experiment were sterile filtrated and stored prior to processing (Chapter 2). Even though samples were all treated the same way, due to time-restrictions some were processed up to two days past other samples which may have led to changes in alkalinity and subsequently calcification values. Additionally, manual titration was performed in the Climate Change Experiment whereas in the Cross Experiment an automated titrator was used for analysis. This manual titration, lacking filtration of samples prior to the procedure, may have had a great impact on the results of the total alkalinity due to the potential presence of organic matter and carbonates.

Due to stressful conditions during the Climate Change Experiment, some specimens of SP2 died, therefore, only population SP1 was incubated for physiological measurements. The remaining specimens of SP2 were kept for structural analysis at the end of the experiment.

In NP, Cr was revealed as an additional element to the major composition; however, this only occurred in the post-experimental measurements and could indicate a potential contamination of the supplied water and the algae through the system. This is supported by the extraordinary Fe influence revealed during the SIMPER statistical analysis. This potential contamination may cause a shift in elemental ratios towards the highly abundant elements; therefore, water samples for additional determination of trace elemental compositions of the experimental water are advised to be taken in future experiments.

Additionally, the number of populations per country of origin ( $n = 2$ ) might have been a limiting factor to interpret results. In some cases populations of the same country of origin showed variable or opposing results impeding clear interpretations.

## 5.6 Conclusion

To conclude, northern populations may be adapting better to warmer temperature conditions and elevated  $p\text{CO}_2$  in future oceans. At the same time, central and southern populations may experience a loss in percentage cover in intertidal, rocky, coastal zones. Central and southern populations' calcification, growth and cell wall thickness is negatively impacted by elevated sea surface temperatures and ocean acidification, potentially resulting in reduced resilience and subsequently disappearance from within their current habitats and ecosystems. Out of all regions,

southern populations are most negatively affected in physiological processes, as well as in their structural under climate change conditions, implying a major deficit of resilience in these populations. With sea surface temperatures warming in northern regions of the species distribution, southern populations may be able to shift their distribution north wards and therefore potentially disappear entirely in their original environment due to even warmer conditions in future ocean environments. However, increased dissolution of atmospheric CO<sub>2</sub> in colder waters in the north of the species distribution results in more acidic conditions forcing species to shift their distribution south wards. This opposing trend diminishes the species northern most and southern most range forcing the species into a narrow band of prevailing viable conditions. Resulting in a distribution squeeze in the NE Atlantic.

This study showed adaptation potentials of sample populations of *C. officinalis* to predicted future temperatures and pH across its geographic distribution in the NE Atlantic. It clarified significant differences between populations of different countries and presented an unequivocal North-to-South gradient in their physiology as well as their structural integrity and the ability to adapt to changing temperature. Northern populations proofed to be more resilient to and benefit from climate change conditions compared to central or southern populations. Similar findings arose from a study of a central populations of another coralline algae species, *Ellisolandia elongata*, which showed tolerance to widely fluctuating levels of CO<sub>2</sub> (Egilsdottir *et al.*, 2013). The severe effects on *C. officinalis* caused by changing temperatures and carbonate chemistry could also lead to changes within their respective ecosystems, due to the important functions these algae would no longer perform resulting in a dramatic drop in biodiversity associated with *C. officinalis*.

# Chapter 6

General Discussion

*Corallina officinalis* inhabits temperate intertidal rocky shores around the world and perform indispensable ecosystem functions (Jones *et al.*, 1994, 1997, Kelaher *et al.*, 2001, 2003, Liuzzi and Gappa, 2008). On a species, population and individual level, it can acclimatise to broad ranges of environmental conditions, including high temperature, salinity, desiccation and pH fluctuations (Williamson *et al.*, 2004, Viejo *et al.*, 2011). Most of the time, population-specific adaptation in physiology and morphology are not distinguishable. For this reason laboratory based analysis and experiments are inevitable to determine the species physiology, structure and response to changing parameters. This study investigated *C. officinalis* across its latitudinal geographic gradient in the NE Atlantic and its potential resilience in physiology and structural integrity to future climatic changes.

Previous studies have shown that this calcifying macroalgae may be severely impacted by future climatic changes due to dissolution of their calcareous skeleton as well as the temperature-induced impacts on their physiological processes (Ries, *et al.*, 2009, Ries, 2011, Ragazzola *et al.*, 2012, Egilsdottir *et al.*, 2013, Kamenos *et al.*, 2013). Changes in structure, but mostly physiology, such as primary production, respiration and calcification rates, under either increased temperature or decreased pH conditions were the focus of physiological research over more than a decade (Ries, *et al.*, 2009, Ries, 2011, Ragazzola *et al.*, 2012, Egilsdottir *et al.*, 2013, Kamenos *et al.*, 2013). Only a few studies were performed with the combined treatment of elevated temperature and decreased pH levels (Sinutok *et al.*, 2011, Martin *et al.*, 2013), none of which on central or marginal populations of articulated coralline algae. This is the first study investigating the physiological and structural responses of multiple marginal populations of *C. officinalis* to future climatic changes (IPCC, 2014a-c) and a comparison between those and central populations.

The first aim was to identify existing differences in physiology and structure between populations across their geographical distribution, comparing central and peripheral populations in their natural environment (Chapter 3).

A Common Garden Experimental approach was chosen to further elucidate the likelihood of adaptation of populations to existing thermal conditions across its geographic range and to determine whether each chosen population, with a focus on marginal populations, is able to flourish in all of these conditions (Chapter 4).

Further, it was aimed to ascertain how the concatenated effects of ocean acidification and sea surface water warming influences the physiology and structure of these important and potentially vulnerable calcareous macroalgae (Chapter 5).

Throughout this chapter, the results from this thesis will be explored and connected. It will be assessed to what extent populations of *C. officinalis* across the latitudinal distribution of the NE Atlantic differ in their physiology and structure and to what extent they show or develop resilience to future climatic conditions.

## 6.1 Are Laboratory Climate Change Studies Applicable to the Natural Environment?

Relating findings resulting from laboratory experiments to the natural environments is challenging. Consequently, a combined approach of identical field and laboratory studies was carried out during this project to assess the physiological and structural characteristics of northern edge (Iceland), central (UK) and southern edge (Spain) populations.

Experimental parameters were set as measured in the natural environment during sampling and oxygen supply, water movement and light settings were adjusted to

recreate natural conditions as accurately as possible. However, no tidal effect could be introduced due to the lack of equipment and space. Two similar, but fundamentally different climate change-recreating experiments were conducted. The Climate Change Experiment was conducted as an open, flow-through system with constant fresh water supply and average temperature and light condition of what is expected in the natural environment across the latitudinal gradient. In this way, general species reactions to climatic changes can be observed. The Cross Experiment aimed to show how populations would react in their natural environment and which environmental factors might play a crucial role in evolving physiological and structural resilience to future environmental conditions. Through the combination of the results of both of these experiments, it was determined that physiological processes (primary production, respiration, light and dark calcification) of all populations were comparable with those in the field during the same season including accounting differences in light intensities using the P-I and C-I curves. Therefore, data obtained during this project are representative of natural populations, to the largest extent.

Most of the available literature is focussing on the effect of an individual treatment on single populations of *C. officinalis* (Hofmann *et al.*, 2012b, Yildiz *et al.*, 2013, Padilla-Gamiño *et al.*, 2016). In Hofmann *et al.* (2012a) for instance, authors investigated effects of different CO<sub>2</sub> levels on two species of red algae. They found elevated protein and carbohydrate levels in both species. However, after long exposure and unintentionally including summer temperatures, one of the studied species, *Chondrus crispus*, showed a decline in these components and the authors suggest that elevated temperatures might be the reason. This example shows clearly how experiments focussing on an individual but not the combined climate

change treatment create misleading results. For best practice, when aiming to investigate the species response to potential future changes, all 4 treatments: (1) control; (2) elevated temperature; (3) elevated CO<sub>2</sub> levels; as well as their (4) combination, should be included in future experiments. For this reason, for the first time, this present study focusses on multiple populations and all individual and combined treatments to avoid such misinterpretations.

Synergetic effects were not only found in this project for *C. officinalis*, but also for other macroalgae species. Sinutok *et al.* (2011) showed that elevated temperatures intensified the negative impact of CO<sub>2</sub>-induced effects in *Halimeda* spp. and Diaz-Pulido *et al.* (2014) found a shift in main components of the skeleton of calcifying crustose algae to dolomite under high pCO<sub>2</sub> and temperatures. All of these studies present evidence that for a reliable transfer of results from laboratory experiments to natural populations and communities, a combined treatment of both key factors are inevitable.

This study emphasises the need to conduct identical field experiments alongside the planned laboratory experiments with multiple populations of one species to be able to connect results of both and to fully understand climatic impacts on the study species. The present studies provide a first insight into the expected responses of *C. officinalis* under changing climate.

## 6.2 Rapid Changes in Temperature and Carbonate Chemistry in the Oceans May Significantly Affect the Physiology of *Corallina officinalis*

Northern populations are regularly exposed to long dark periods and cold temperatures in the winter. Local adaptation to dark and cold periods was also found



during studies in the field as well as when transplanted within the species distribution range and under climate change conditions during this present project. A specific survival mechanism for long dark periods was not yet found. Potential explanations include dormancy and downregulation of metabolic processes including literature suggestions of seasonal photoacclimation (Williamson *et al.*, 2018). According to data obtained herein, northernmost populations prove to be resilient to a wide range of temperatures and have not yet reached their thermal limit. Reduced net production rates in northern populations under climate change conditions support the finding that energy is channelled to maintain the structural integrity to withstand the harshest environmental conditions found across the studied area. Herein, they are also shown to be able to compensate for the lack of production under climate change and low light conditions through highly increased production when light availability increases. These populations showed the lowest stress response and are therefore the most resilient populations across the studied area.

A high variability of the responses within each parameter in central populations over all treatments under climate change conditions and in the field presents local adaptation to their original ecosystem conditions. It may also make central populations relatively robust towards temperature and carbonate chemistry changes and shows environmental rather than genetic adaptation. Central populations experience their thermal optimum and may be able to withstand warmer temperatures; however, central populations already showed signs of stress reactions during this study. Conditions in the centre of the species distribution are more favourable compared to conditions in the south of their distribution (Lesica and Allendorf, 1995). A downregulation of calcification and upkeep of production rates observed in this study is likely to be driven by temperature and presents the

decoupling of these processes that were thought to be tightly coupled. Centre populations are more robust than southern populations.

Southern populations show the same decoupling of photosynthetic and calcification processes as centre populations, however, they downregulate photosynthetic processes before calcification, the opposite order to centre populations. No southern populations coped well under climate change conditions and both already showed light and temperature inhibition during the field studies in the summer. This leads to the assumption that southern populations already are at their thermal limit. For that reason, further elevation of temperatures, proven to be the main driver of stress responses, and additional stress due to changing carbonate chemistry may have a detrimental effect on the southern populations. During this study, southern populations showed low adaptation and resilience potential for future climatic conditions, which may lead to the southern range contraction, which is already observed in other species (Lima *et al.*, 2007). The little amount of energy southern populations are producing is seemingly invested in maintaining cell wall thickness but not growth, in this way, specimens are becoming shorter.

Marginal populations under climate change conditions show more stable rates with lower variability compared to centre populations. This implies more resilience of edge populations towards future changes. However, the increased thermal stress dictating southern marginal populations leads to the development of a North-to-South gradient of resilience instead of the generally assumed Centre-to-Margin gradient of resilience.

All populations examined in this study, show complex relationships instead of direct dependencies between environmental factors and physiological parameters. It was found that light calcification might be able to affect the structure of *C. officinalis* and

might also have a strong impact on its physiology. A reduction in percentage cover is predicted for southern and centre populations and was already observed in tropical and subtropical ecosystems (Doney *et al.*, 2009). Under climate change conditions, elevated CO<sub>2</sub> did not show the expected fertilizing effect whereas elevated temperatures demonstrated to be the major driver for changes in physiological parameters. This was also found in a quantitative physiological model on the effect of climate change and its components on coralline algae (Vásquez-Elizondo and Enríquez, 2016). This also presents southern conditions to be the least favourable for all populations.

### 6.3 Structural Resilience as a Mechanism to Withstand Changes in Carbonate Chemistry and Elevated Temperatures

Studies conducted as part of this thesis have demonstrated that northern populations of *C. officinalis* showed reduced hardness and increased elasticity during winter periods in the field in order to withstand stiffness and stress induced by colder winter temperatures and increased external mechanical impacts through storms or other environmental conditions. This is confirmed by a higher resistance of higher forces in higher temperatures in the summer, which leads to more pliable organic tissues. Northern populations showed the greatest ability out of all populations to withstand deformation. Under climate change conditions, northernmost populations seem to be less affected compared to the other populations, most likely due to the fact that they are already experiencing slightly more acidic conditions than other populations due to colder temperatures and an increased solubility of gases in colder waters. This fact might make these populations more resilient to future climatic changes. In addition, this study observed

thickest cell walls in northern populations leading to the assumption that low Mg/Ca contents are needed to allow softening of the branches to aid robustness against harsh environmental conditions. Under climate change conditions, however, Mg/Ca ratios were highest in northern populations resulting in relatively harder branches and an overall stronger structural integrity compared to all other populations. Northern populations might have found a mechanism to actively control the intake of trace elements, including those potentially damaging. A slower response to climatic changes might be observed in northern populations as these might show a delayed negative effect due to colder environmental conditions and a slower metabolism. However, a second possible hypothesis could entail that due to slower metabolic processes and more time compared to centre and southern populations for the changes to influence the organism, northern populations might be able to evolve resilience and adapt to future conditions.

Central populations in winter in the field showed a reduced hardness and an increased elasticity in the present studies, in order to withstand external mechanical impact, as seen for northern populations. However, central populations are not able to withstand the same forces compared to northern populations. Under climate change conditions, they spend more energy on growth rather than on cell wall maintenance and are, therefore, more porous opposite to what was found for northern populations of *C. officinalis* and in accordance to literature findings in a crustose coralline alga (McCoy and Ragazzola, 2014). This is leading to the assumption that this strategy is adapted across genera to cope in low pH environments. Mg/Ca rates of *C. officinalis* showed a softening of branches and a dissolution in the light, too high for compensated by dark calcification, under climate change conditions. This, and a reduced productivity due to increased cadmium

concentrations, may lead to a reduction in percentage cover in intertidal rocky shore ecosystems in the centre of the species distribution. This was already shown for one other population under high CO<sub>2</sub> conditions (Hofmann *et al.*, 2012b).

Southern populations in the field showed softer branches in winter compared to summer and a predominant reinforcement of cell walls in winter potentially to recover from high dissolution rates in the summer due to heat-induced inhibition. Cell wall thickness seems to be the lowest out of all populations leading to a chronic susceptibility to breakage making southern conditions less favourable for *C. officinalis*. On the contrary and as a result of these findings, southern populations showed the highest tensile strength out of all populations but also the highest deformation rate together with a temperature-induced structural flexibility in summer. Cadmium was noticed to have a negative impact on southern populations reducing their productivity and initiating a reduction of percentage cover, which is accelerated under climate change conditions, as observed in centre populations.

Results obtained during this project indicate that marginal populations are channelling their energy on the construction of their skeleton compared to centre populations, which are found to focus on increasing physiological processes. This could lead to a disadvantage for central populations under acidified conditions. The structural development in marginal populations might be favourable for survival under stressful conditions, independent of the origin of stress. This is supported by the finding of the highest Mg/Ca ratios in marginal populations in the summer supplying additional hardness and strength.

In all studied populations in the field, the intra-cell wall thickness was more important than the inter-cell wall thickness suggesting a high importance of the intra-cell walls in relation to absorption of external mechanical impacts and shocks leading to their

function to increase protection and resistance and performing a minor role in potential acidification buffering. However, this finding is the opposite in all experimental studies where inter-cell walls seem to play a more important role than intra-cell walls. This effect can be understood as induced by climatic changes and shows a shift within the structure of the algae towards a differentiation in defence strategies. Independent of their overall importance, cell walls are thicker in winter compared to summer making up an essential part of their stability, providing enhanced protection from autumn, winter and early spring storms. At the same time, a decrease in Mg/Ca content under colder conditions increased the branches elasticity, contributing to this protection. Central and southern populations showed reduced structural parameters under elevated temperature and climate change conditions independent of season leading to a lack of resilience and adaptation capacity in these populations. However, all populations in the studies increase their Mg content resulting in higher Mg/Ca ratios in order to strengthen their skeleton and take precaution for increased dissolution due to ocean acidification. A change in skeletal composition was already observed in other species (Diaz-Pulido *et al.*, 2014) and might therefore be very likely to occur in *C. officinalis*. However, the cost to maintain or change skeletal compositions under southern and climate change conditions might have an effect on the competitive success of *C. officinalis*. If populations are not able to maintain their cell wall thickness and skeletal content, literature has shown that *C. officinalis* might show reduced ability to absorb light (Yildiz *et al.*, 2013) which is also observed in this study. All of the above named effects in *C. officinalis* could ultimately lead to increased susceptibility to grazing as already found for crustose coralline algae (Johnson and Carpenter, 2012).

#### 6.4 How does the Centre-to-Margin Hypothesis develop for *Corallina officinalis* in Future Oceans?

Previously, it was assumed that the most robust populations are primarily located in the centre of a species distribution (Mayr, 1963, Whittaker, 1956, Brussard, 1984, Brown, 1984, Sagarin and Gaines, 2002). In case of this project, this would be within the UK. However, the data and findings described in this thesis and interpreted above elucidate a different kind of hypothesis or gradient. According to my findings, instead of a Centre-to-Margin, a conspicuous North-to-South gradient is predominant in *C. officinalis* along its latitudinal distribution in the NE Atlantic.

Northern populations proved to be different from centre and southern populations and centre populations are not always distinctively different from southern populations in all measured parameters. This was proven for the field populations, during and after the exposure to existing temperature conditions as well as for predicted future temperature and pH conditions across the geographic gradient. This finding is supported by a study investigating the genetics of *C. officinalis* across the same gradient, where Yesson *et al.* (2018) found a distinct difference between northern and centre as well as southern populations, and a much less pronounced genetic difference between centre and southern populations.

#### 6.5 Future Perspectives, Recommendations & Open Questions

Understanding the impact of climate change on important ecosystem engineers is important not only to understand the species itself, but also in the aspect of conservation of the particular species as well as all flora and fauna that is associated with it. To further elucidate the impact of future climatic changes on *C. officinalis* across a broad range like the NE Atlantic and in other areas of its distribution, nanoindentation analysis would prove valuable to determine hardness and the

elastic modulus and to be able to link and confirm results found in Mg/Ca ratios and cell wall thickness. In addition to these confirmations, future work should include the modelling of the distribution change and potential range shift. This work was started alongside this thesis and will further be explored and worked on. In addition to these points, it is also important to investigate how associated fauna and flora might be negatively affected under climate change conditions. When combining these two last points, the question arises, how biodiversity in intertidal rocky shore ecosystems around the world might change due to future climatic changes. Future experiments should consider tidal motion and effects on *C. officinalis*, which unfortunately this project was not able to investigate.

Many more factors may influence the physiology and structure of *C. officinalis* that were not investigated in this study. Some of these factors are sedimentation, turbidity, nutrient availability, age of algae, the use of algae of similar morphology and the use of F2 generations cultured under climate change conditions. Additionally, the introduction of grazers or epibionts would give insight on how external grazing pressure as well as inter- and intra-species competition around shading would influence the results obtained in this study.

During this study, additional questions emerged. For instance, how do trace elements affect the fitness of algae? How does the population's variability and local adaptation affect trace element uptake? Having a slower metabolism, do northern populations evolve to have faster metabolisms with increasing temperatures and if so, how would northern populations ultimately perform under changed carbonate chemistry conditions?



## 6.6 Novelties and Conclusions

This study presents results of the first investigation of the impact of future climatic changes on multiple populations of *C. officinalis*. Additionally, this is the first study conducted focussing on and comparing marginal with central populations of *C. officinalis* as well as including the climate change scenario in these investigations. It was found that northern populations from the NE Atlantic are most resilient to future climatic changes, potentially also making them more robust when facing other future climatic impacts such as, for instance, sea level rise, increasing numbers of storm and increasing amounts of heatwaves. In this study, it is presented in detail, that all examined populations focus their energy on the protection of the high-Mg calcite skeleton during winter periods. Southern populations were found to show multiple “emergency stress responses” such as using their little energy to produce conceptacles for reproduction, showing a change from thriving in their natural environment to a survival strategy under unfavourable southern and climate change conditions. An additional stress response is the decoupling of photosynthetic and calcification processes, which were previously assumed to be tightly coupled (Borowitzka and Larkum, 1976, Johansen, 1981, Koch *et al.*, 2013) but are shown to decouple under temperature stress and climate change conditions.

Effects on the physiology of *C. officinalis* were observed prior to effects on the structure under climate change conditions and were more pronounced in southern marginal populations compared to central populations. Even though first impacts were observed in physiological processes, structural integrity is more severely impacted after long-term exposure. This emphasises again that *C. officinalis* is concentrating on stabilizing its structure and, to a certain extent, is neglecting their physiological processes.

This study presents the first investigations into structural integrity of marginal populations of *C. officinalis* including comparisons between marginal populations as well as to central populations.

A pronounced North-to-South gradient rather than a confirmation of the Centre-to-Margin hypothesis was found in the field and under transplant as well as climate change conditions.

This study also showed for the first time that zinc has direct impacts on the calcification and therefore structure of these algae due to enhanced CO<sub>2</sub> assimilation. It is suggested to introduce zinc as an indicator for calcification in future analysis. On the other hand, it was observed that barium did not reflect literature suggestions to indicate freshwater influx. Therefore, in *C. officinalis*, barium is suggested unsuitable as indicator.

To conclude, the distribution of *C. officinalis* is expected to shift with changing climate and with a high probability, a margin squeeze will occur. This squeeze is caused by increasing sea surface temperatures in the southern range of the species distribution, whereas colder waters on the northern edge of the species distribution show an increase in dissolved CO<sub>2</sub> in the seawater causing more acidified conditions. Both of these unfavourable conditions ultimately force the populations to shift towards the middle of their range narrowing their distribution. Consequently, original environments might lose the important ecosystem functions this species is providing and may experience an impoverishment in biodiversity in the affected regions.

# References

- Abeli, T., Gentili, R., Mondoni, A., Orsenigo, S. and Rossi, G., 2014. Effects of marginality on plant population performance. *Journal of Biogeography*, 41(2), pp.239-249.
- Adey, W.H., and MacIntyre, I.G., 1973. Crustose Coralline Algae: A Re-evaluation in the Geological Sciences. *GSA Bulletin*, 84(3), 883–904.
- Adey, W.H., 1998. Coral reefs: algal structured and mediated ecosystems in shallow, turbulent, alkaline waters. *Journal of Phycology*, 34(3), pp.393-406.
- Aguirre, J., Perfectti, F. and Braga, J.C., 2010. Integrating phylogeny, molecular clocks, and the fossil record in the evolution of coralline algae (*Corallinales* and *Sporolithales*, Rhodophyta). *Paleobiology*, 36(4), pp.519-533.
- Aitken, S.N., Yeaman, S., Holliday, J.A., Wang, T. and Curtis-McLane, S., 2008. Adaptation, migration or extirpation: climate change outcomes for tree populations. *Evolutionary Applications* 1(1), 95–111.
- Altamirano, M., Flores-Moya, A. and Figueroa, F.L., 2003. Effects of UV radiation and temperature on growth of germlings of three species of *Fucus* (Phaeophyceae). *Aquatic Botany*, 75(1), pp.9-20.
- Amado-Filho, G.M., Moura, R.L., Bastos, A.C., Salgado, L.T., Sumida, P.Y., Guth, A.Z., Francini-Filho, R.B., Pereira-Filho, G.H., Abrantes, D.P., Brasileiro, P.S. and Bahia, R.G., 2012. Rhodolith beds are major CaCO<sub>3</sub> bio-factories in the tropical South West Atlantic. *PloS One*, 7(4), p.e35171.
- Anderson, M.J., Gorley, R.N. and Clark, K.L., 2009. PRIMER 6 & PERMANOVA+. 6.1. 13 & 1.0.
- Andersson, A.J., Mackenzie, F.T. and Bates, N.R., 2008. Life on the margin: implications of ocean acidification on Mg-calcite, high latitude and cold-water marine calcifiers. *Marine Ecology Progress Series*, 373, pp.265-273.

- Andrake, W., and Johansen, H.W., 1980. Alizarin red dye as a marker for measuring growth in *Corallina officinalis* L. (Corallinaceae, Rhodophyta). *Journal of Phycology* 16(4), 620–622.
- Araújo, R., Serrão, E.A., Sousa-Pinto, I. and Åberg, P., 2011. Phenotypic Differentiation at Southern Limit Borders: The Case Study of Two Furoid Macroalgal Species with Different Life-history Traits 1. *Journal of Phycology*, 47(3), pp.451-462.
- Araújo, R., Serrão, E.A., Sousa-Pinto, I. and Åberg, P., 2014. Spatial and temporal dynamics of furoid populations (*Ascophyllum nodosum* and *Fucus serratus*): a comparison between central and range edge populations. *PloS One*, 9(3), p.e92177.
- Araújo, R., Serrão, E.A., Sousa-Pinto, I., Arenas, F., Monteiro, C.A., Toth, G., Pavia, H. and Åberg, P., 2015. Trade-offs between life-history traits at range-edge and central locations. *Journal of Phycology*, 51(4), pp.808-818.
- Araújo, R., Vaselli, S., Almeida, M., Serrão, E. and Sousa-Pinto, I., 2009. Effects of disturbance on marginal populations: human trampling on *Ascophyllum nodosum* assemblages at its southern distribution limit. *Marine Ecology Progress Series*, 378, pp.81-92.
- Benedetti-Cecchi, L., 2006. Understanding the consequences of changing biodiversity on rocky shores: how much have we learned from past experiments? *Journal of Experimental Marine Biology and Ecology* 338, 193–204.
- Bennett, S., Wernberg, T., Arackal Joy, B., de Bettignies, T. and Campbell, A.H., 2015. Central and rear-edge populations can be equally vulnerable to warming. *Nature Communications* 6, 10280.
- Bentz, B.J., Régnière, J., Fettig, C.J., Hansen, E.M. and Hayes, J.L. *et al.*, 2010. Climate Change and Bark Beetles of the Western United States and Canada: Direct and Indirect Effects. *BioScience*, 60(8), 602–613.

- Berelson, W.M., Balch, W.M., Najjar, R., Feely, R.A., Sabine, C. and Lee, K., 2007. Relating estimates of CaCO<sub>3</sub> production, export, and dissolution in the water column to measurements of CaCO<sub>3</sub> rain into sediment traps and dissolution on the sea floor: A revised global carbonate budget. *Global Biogeochemical Cycles*, 21(1).
- Bertocci, I., Araújo, R., Vaselli, S. and Sousa-Pinto, I., 2011. Marginal populations under pressure: spatial and temporal heterogeneity of *Ascophyllum nodosum* and associated assemblages affected by human trampling in Portugal. *Marine Ecology Progress Series*, 439, pp.73-82.
- Blake, C. and Maggs, C.A., 2003. Comparative growth rates and internal banding periodicity of maerl species (Corallinales, Rhodophyta) from northern Europe. *Phycologia*, 42(6), pp.606-612.
- Borowitzka, M.A., 1982. Morphological and cytological aspects of algal calcification. In *International Review of Cytology* (Vol. 74, pp. 127-162). Academic Press.
- Borowitzka, M.A. and Larkum, A.W., 1976. Calcification in the green alga *Halimeda*: III. The sources of inorganic carbon for photosynthesis and calcification and a model of the mechanism of calcification. *Journal of Experimental Botany*, 27(5), pp.879-893.
- Breeman, A.M., 1988. Relative importance of temperature and other factors in determining geographic boundaries of seaweeds – experimental and phenological evidence, *Helgolander Meeresuntersuchungen* 42, 199–241.
- Bridle, J.R. and Vines, T.H., 2007. Limits to evolution at range margins: when and why does adaptation fail?. *Trends in Ecology and Evolution*, 22(3), pp.140-147.
- Brierley, A.S. and Kingsford, M.J., 2009. Impacts of climate change on marine organisms and ecosystems. *Current biology*, 19(14), pp.R602-R614.

- Brodie, J., Walker, R.H., Williamson, C.J. and Irvine, L.M., 2013. Epitypification and Redescription of *Corallina officinalis* L., the Type of the Genus, and *C. elongata* Ellis et Solander (Corallinales, Rhodophyta). *Cryptogamie Algologie* 34(1), 49–56.
- Brodie, J., Williamson, C.J., Smale, D.A., Kamenos, N.A., Mieszkowska, N. and Santos, R., *et al.*, 2014. The future of the north-east Atlantic benthic flora in a high CO<sub>2</sub> world, *Ecology and Evolution*, 4, 2787–2798.
- Brody, H. M., 2004. P. 247 in *Phenotypic plasticity: functional and conceptual approaches*. Oxford University Press, Oxford, U.K.
- Broecker, W.S. and Takahashi, T., 1977. The solubility of calcite in sea water. In *Thermodynamics in Geology* (pp. 365-379). Springer, Dordrecht.
- Brown, J.H., 1984. On the relationship between abundance and distribution of species. *The American Naturalist*, 124(2), pp.255-279.
- Brussard, P.F., 1984. Geographic patterns and environmental gradients: the central-marginal models in *Drosophila* revisited. *Annual Review of Ecology and Systematics* 15: 25\_ /64.
- Bozinovic, F., Calosi, P. and Spicer, J.I., 2011. Physiological correlates of geographic range in animals. *Annual Review of Ecology, Evolution and Systematics* 42, 155–179.
- Calosi, P., Melatunan, S., Turner, L.M., Artioli, Y., Davidson, R.L. and Byrne, J.J., *et al.*, 2017. Regional adaptation defines sensitivity to future ocean acidification. *Nature Communications*, 8, 13994.
- Caragnano, A., Basso, D., Jacob, D.E., Storz, D., Rodondi, G., Benzoni, F. and Dutrieux, E., 2014. The coralline red alga *Lithophyllum kotschyenum* f. affine as proxy of climate variability in the Yemen coast, Gulf of Aden (NW Indian Ocean). *Geochimica et Cosmochimica Acta*, 124, pp.1-17.

- Caragnano, A., Basso, D., Storz, D., Jacob, D.E., Ragazzola, F., Benzoni, F. and Dutrieux, E., 2017. Elemental variability in the coralline alga *Lithophyllum yemenense* as an archive of past climate in the Gulf of Aden (NW Indian Ocean). *Journal of Phycology*, 53(2), pp.381-395.
- Case, T.J., and Taper, M.L., 2000. Interspecific Competition, Environmental Gradients, Gene Flow, and the Coevolution of Species' Borders. *The American Naturalist* 155(5), 583–605.
- Chave, K.E., 1954a. Aspects of the biogeochemistry of magnesium 1. Calcareous marine organisms. *The Journal of Geology*, 62(3), pp.266-283.
- Chave, K.E., 1954b. Aspects of the biogeochemistry of magnesium 2. Calcareous sediments and rocks. *The Journal of Geology*, 62(6), pp.587-599.
- Chave, K.E. and Wheeler, B.D., 1965. Mineralogic changes during growth in the red alga, *Clathromorphum compactum*. *Science*, 147(3658), pp.621-621.
- Chenelot, H., Jewett, S.C. and Hoberg, M.K., 2011. Macrobenthos of the nearshore Aleutian Archipelago, with emphasis on invertebrates associated with *Clathromorphum nereostratum* (Rhodophyta, Corallinaceae). *Marine Biodiversity*, 41(3), pp.413-424.
- Chisholm, J.R., 2000. Calcification by crustose coralline algae on the northern Great Barrier Reef, Australia. *Limnology and Oceanography*, 45(7), pp.1476-1484.
- Chisholm, J.R.M. and Gattuso, J., 1991. Validation of the alkalinity anomaly technique for investigating calcification of photosynthesis in coral reef communities. *Limnology and Oceanography*, 36(6), 1232–1239.
- Clark, J.S., Poore, A.G. and Doblin, M.A., 2018. Shaping up for stress: Physiological flexibility is key to survivorship in a habitat-forming macroalga. *Journal of Plant Physiology*, 231, pp.346-355.



- Clarke, S.A., Walsh, P., Maggs, C.A. and Buchanan, F., 2011. Designs from the deep: marine organisms for bone tissue engineering. *Biotechnology advances*, 29(6), pp.610-617.
- Collevatti, R.G., Nabout, J.C. and Diniz-Filho, J.A.F., 2011. Range shift and loss of genetic diversity under climate change in *Caryocar brasiliense*, a Neotropical tree species. *Tree Genetics and Genomes*, 7(6), 1237–1247.
- Colthart, B.J., and Johansen, H.W., 1973. Growth rates of *Corallina officinalis* (Rhodophyta) at different temperatures. *Marine Biology* 18(1), 46–49.
- Cornwall, C.E., Hepburn, C.D., Pritchard, D., Currie, K.I., McGraw, C.M., Hunter, K.A. and Hurd, C.L., 2012. Carbon-use Strategies in Macroalgae: Differential Responses to Lowered pH and Implications for Ocean Acidification 1. *Journal of Phycology*, 48(1), pp.137-144.
- Cornwall, C.E. and Hurd, C.L., 2015. Experimental design in ocean acidification research: problems and solutions. *ICES Journal of Marine Science*, 73(3), pp.572-581.
- Coull, B.C. and Wells, J.B.J., 1983. Refuges from fish predation – experiments with phytal meiofauna from the New Zealand rocky intertidal. *Ecology*, 64, 1599–1609.
- Couto, R.P., Neto, A.I. and Rodrigues, A.S., 2010. Metal concentration and structural changes in *Corallina elongata* (Corallinales, Rhodophyta) from hydrothermal vents. *Marine Pollution Bulletin*, 60(4), pp.509-514.
- Daleo, P., Escapa, M., Alberti, J. and Iribarne, O., 2006. Negative effects of an autogenic ecosystem engineer: interactions between coralline turf and an ephemeral green alga. *Marine Ecology Progress Series* 315, 67–73.
- Dam, H.G., 2013. Evolutionary adaptation of marine zooplankton to global change. *Annual Review of Marine Science* 5(1), 349-370.

- Daume, S., Brand-Gardner, S. and Woelkerling, W.J., 1999. Preferential settlement of abalone larvae: diatom films vs. non-geniculate coralline red algae. *Aquaculture*, 174(3-4), pp.243-254.
- Davenport, J., Butler, A. and Cheshire, A., 1999. Epifaunal composition and fractal dimensions of marine plants in relation to emersion. *Journal of the Marine Biological Association of the UK*. 79(2), 351–355.
- Davison, I.R., 1991. Environmental effects on algal photosynthesis: temperature. *Journal of Phycology* 27(1), 2–8.
- Dayton, P.K., 1972. *Toward an understanding of community resilience and the potential effects of enrichments to the benthos at McMurdo Sound, Antarctica*. Proceedings of the Colloquium on Conservation Problems in Antarctica, ed. B.C. Parker (Allen Press, Lawrence, KS), 81–96.
- De Bettignies, T., Thomsen, M.S. and Wernberg, T., 2012. Wounded kelps: patterns and susceptibility to breakage. *Aquatic Biology*, 17(3), pp.223-233.
- Denny, M. W., 1988. *Biology and the Mechanics of the Wave-Swept Environment*. Princeton, New Jersey: Princeton University Press.
- Denny, M.W. and King, F.A., 2016a. The extraordinary joint material of an articulated coralline alga. I. Mechanical characterization of a key adaptation. *Journal of Experimental Biology*, 219(12), pp.1833-1842.
- Denny, M.W. and King, F.A., 2016b. The extraordinary joint material of an articulated coralline alga. II. Modeling the structural basis of its mechanical properties. *Journal of Experimental Biology*, 219(12), pp.1843-1850.
- De Villiers, S., 1999. Seawater strontium and Sr/Ca variability in the Atlantic and Pacific oceans. *Earth and Planetary Science Letters*, 171(4), pp.623-634.

Diaz-Pulido, G., Anthony, K.R.N., Kline, D.I., Dove, S. and Hoegh-Guldberg, O., 2012. Interactions between ocean acidification and warming on the mortality and dissolution of coralline algae. *Journal of Phycology* 48(1), 32–39.

Diaz-Pulido, G., Nash, M.C., Anthony, K.R., Bender, D., Opdyke, B.N., Reyes-Nivia, C. and Troitzsch, U., 2014. Greenhouse conditions induce mineralogical changes and dolomite accumulation in coralline algae on tropical reefs. *Nature Communications*, 5, p.3310.

Díez, I., Mugerza, N., Santolaria, A., Ganzedo, U., and Gorostiaga, J. M., 2012. Seaweed assemblage changes in the eastern Cantabrian Sea and their potential relationship to climate change. *Estuarine, Coastal and Shelf Science*, 99, 108–120.

Digby, P.S.B., 1977. Growth and calcification in the coralline algae, *Clathromorphum circumscriptum* and *Corallina officinalis*, and the significance of pH in relation to precipitation. *Journal of the Marine Biological Association of the UK*. 57(4), 1095-1109.

Dickson, A.G., 1981. An exact definition of total alkalinity and a procedure for the estimation of alkalinity and total inorganic carbon from titration data. *Deep Sea Research Part A. Oceanographic Research Papers*, 28(6), pp.609-623.

Dickson, A.G. and Millero, F.J., 1987. A comparison of the equilibrium constants for the dissociation of carbonic acid in seawater media, *Deep Sea Research Part A. Oceanographic Research Papers*, 34(10), 1733–1743.

Dickson, A.G.; Sabine, C.L. and Christian, J.R. (eds), 2007. *Guide to best practices for ocean CO<sub>2</sub> measurement*. Sidney, British Columbia, North Pacific Marine Science Organization, 191pp. (PICES Special Publication 3)

Doney, S.C., Fabry, V.J., Feely, R.A. and Kleypas, J.A., 2009. Ocean acidification: the other CO<sub>2</sub> problem. *Annual Review of Marine Science*, 1, pp.169-192.

- Eckert, C.G., Samis, K.E. and Loughheed, S.C., 2008. Genetic variation across species' geographical ranges: the central–marginal hypothesis and beyond. *Molecular Ecology*, 17(5), pp.1170-1188.
- Eggert, A., 2012. Seaweed responses to temperature. In *Seaweed biology* (pp. 47-66). Springer, Berlin, Heidelberg.
- Egilsdottir, H., Noisette, F., Noel, L.M.-L.J., Olafsson, J. and Martin, S., 2013. Effects of pCO<sub>2</sub> on physiology and skeletal mineralogy in a tidal pool coralline alga *Corallina elongata*, *Marine Biology*, 160, 2103–2112.
- Egilsdottir, H., Olafsson, J. and Martin, S., 2016. Photosynthesis and calcification in the articulated coralline alga *Ellisolandia elongata* (Corallinales, Rhodophyta) from intertidal rock pools, *European Journal of Phycology*, 51, 59–70.
- El Haïkali, B., Bensoussan, N., Romano, J.C. and Bousquet, V., 2004. Estimation of photosynthesis and calcification rates of *Corallina elongata* Ellis and Solander, 1786, by measurements of dissolved oxygen, pH and total alkalinity. *Science Marina*. 68(1), 45–56.
- Etterson, J.R. and Shaw, R.G., 2001. Constraint to adaptive evolution in response to global warming. *Science*, 294(5540), pp.151-154.
- Fabry, V.J., Seibel, B.A., Feely, R.A. and Orr, J.C., 2008. Impacts of ocean acidification on marine fauna and ecosystem processes. *ICES Journal of Marine Science*, 65(3), pp.414-432.
- Faxafloahafnir sf. (2019). Associated Icelandic Ports. Available at: <https://www.faxafloahafnir.is/> (Accessed: 13 September 2019).
- Ferreira, J.G., Arenas, F., Martínez, B., Hawkins, S.J. and Jenkins, S.R., 2014. Physiological response of fucoid algae to environmental stress: comparing range centre and southern populations. *New Phytologist*, 202(4), pp.1157-1172.

- Foster, M.S., 2001. Rhodoliths: between rocks and soft places. *Journal of Phycology* 37, 659–667.
- Franco, A.M., Hill, J.K., Kitschke, C., Collingham, Y.C., Roy, D.B., Fox, R., Huntley, B. and Thomas, C.D., 2006. Impacts of climate warming and habitat loss on extinctions at species' low-latitude range boundaries. *Global Change Biology*, 12(8), 1545–1553.
- Ganning, B., 1971. Studies on chemical, physical and biological conditions in Swedish rockpool ecosystems. *Ophelia*, 9(1), pp.51-105.
- Gaston, K.J., 2009. Geographic range limits: achieving synthesis. *Proceedings of the Royal Society London B: Biological Sciences*, 276, 1395–1406.
- Galbraith, H., Jones, R., Park, R., Clough, J., Herrod-Julius, S., Harrington, B. and Page, G., 2002. Global climate change and sea level rise: potential losses of intertidal habitat for shorebirds. *Waterbirds*, 25(2), pp.173-184.
- Gao, K., Aruga, Y., Asada, K., Ishihara, T., Akano, T. and Kiyohara, M., 1993. Calcification in the articulated coralline alga *Corallina pilulifera*, with special reference to the effect of elevated CO<sub>2</sub> concentration. *Marine Biology*, 117(1), pp.129-132.
- Gattuso, J.P., Allemand, D. and Frankignoulle, M., 1999. Photosynthesis and calcification at cellular, organismal and community levels in coral reefs: a review on interactions and control by carbonate chemistry. *American Zoologist*, 39(1), pp.160-183.
- GBIF Secretariat, *Corallina officinalis* Linnaeus, 1758, 2017. GBIF Backbone Taxonomy. Checklist dataset <https://doi.org/10.15468/39omei> accessed via GBIF.org on 2019-09-13. Link: [GBIF.org/species/5276013](https://www.gbif.org/species/5276013)

Gherardi, D.F. and Bosence, D.W., 1999. Modeling of the ecological succession of encrusting organisms in recent coralline-algal frameworks from Atol das Rocas, Brazil. *Palaios*, pp.145-158.

Gillikin, D.P., Dehairs, F., Lorrain, A., Steenmans, D., Baeyens, W. and André, L., 2006. Barium uptake into the shells of the common mussel (*Mytilus edulis*) and the potential for estuarine paleo-chemistry reconstruction. *Geochimica et Cosmochimica Acta*, 70(2), pp.395-407.

Grahame, J. and Hanna, F.S., 1989. Factors affecting the distribution of the epiphytic fauna of *Corallina officinalis* (L.) on an exposed rocky shore. *Ophelia*, 30(2), pp.113-129.

Gran, G., 1952. Determination of the equivalence point in potentiometric titrations. Part II. *Analyst*, 77(920), pp.661-671.

Guillong, M., Meier, D.L., Allan, M.M., Heinrich, C.A. and Yardley, B.W., 2008. Appendix A6: SILLS: A MATLAB-based program for the reduction of laser ablation ICP-MS data of homogeneous materials and inclusions. *Mineralogical Association of Canada Short Course*, 40, pp.328-333.

M.D. Guiry in Guiry, M.D. & Guiry, G.M. 2020. AlgaeBase. World-wide electronic publication, National University of Ireland, Galway. <http://www.algaebase.org>; searched on 17 February 2020.

Guo, Q., 2014. Central-marginal population dynamics in species invasions. *Frontiers in Ecology and Evolution*, 2, p.23.

Guo, Q., Taper, M., Schoenberger, M. and Brandle, J., 2005. Spatial-temporal population dynamics across species range: from centre to margin. *Oikos*, 108(1), 47–57.

- Hain, M.P., Foster, G.L. and Chalk, T., 2018. Robust constraints on past CO<sub>2</sub> climate forcing from the boron isotope proxy. *Paleoceanography and Paleoclimatology*, 33(10), pp.1099-1115.
- Halfar, J., Zack, T., Kronz, A. and Zachos, J.C., 2000. Growth and high-resolution paleoenvironmental signals of rhodoliths (coralline red algae): a new biogenic archive. *Journal of Geophysical Research: Oceans*, 105(C9), pp.22107-22116.
- Hall-Spencer, J.M., Rodolfo-Metalpa, R., Martin, S., Ransome, E., Fine, M., Turner, S.M., Rowley, S.J., Tedesco, D. and Buia, M.C., 2008. Volcanic carbon dioxide vents show ecosystem effects of ocean acidification. *Nature*, 454(7200), p.96.
- Hampe, A. and Jump, A.S., 2011. Climate relicts: past, present, future. *Annual Review of Ecology, Evolution, and Systematics*, 42, pp.313-333.
- Hampe, A. and Petit, R.J., 2005. Conserving biodiversity under climate change: the rear edge matters. *Ecology letters*, 8(5), pp.461-467.
- Hanor, J.S. and Chan, L.H., 1977. Non-conservative behavior of barium during mixing of Mississippi River and Gulf of Mexico waters. *Earth and Planetary Science Letters*, 37(2), pp.242-250.
- Helmuth, B., Harley, C.D., Halpin, P.M., O'Donnell, M., Hofmann, G.E. and Blanchette, C.A., 2002. Climate change and latitudinal patterns of intertidal thermal stress. *Science*, 298(5595), pp.1015-1017.
- Helmuth, B., Mieszkowska, N., Moore, P. and Hawkins, S.J., 2006. Living on the edge of two changing worlds: forecasting the responses of rocky intertidal ecosystems to climate change. *Annual Review of Ecology, Evolution and Systematics*, 37, 373–404.
- Henrich, L., Holz, R. and Knepe, G., 1996. Physically based cooling line model to meet growing demands in temperature and flexibility. *Ironmaking and Steelmaking (UK)*, 23(1), pp.79-81.

- Hepburn, C.D., Pritchard, D.W., Cornwall, C.E., McLeod, R.J., Beardall, J., Raven, J.A. and Hurd, C.L., 2011. Diversity of carbon use strategies in a kelp forest community: implications for a high CO<sub>2</sub> ocean. *Global Change Biology*, 17(7), pp.2488-2497.
- Hind, K.R., Gabrielson, P.W., Lindstrom, S.C. and Martone, P.T., 2014. Misleading morphologies and the importance of sequencing type specimens for resolving coralline taxonomy (Corallinales, Rhodophyta): *Pachyarthron cretaceum* is *Corallina officinalis*. *Journal of Phycology*, 50(4), pp.760-764.
- Hofmann, L., Straub, S. and Bischof, K., 2012a. Competition between calcifying and noncalcifying temperate marine macroalgae under elevated CO<sub>2</sub> levels, *Marine Ecology Progress Series*, 464, 89–105.
- Hofmann, L., Yildiz, G., Hanelt, D. and Bischof, K., 2012b. Physiological responses of the calcifying rhodophyte, *Corallina officinalis* (L.), to future CO<sub>2</sub> levels, *Marine Biology* 159, 783–792.
- Hofmann, G.E., Evans, T.G., Kelly, M.W., Padilla-Gamiño, J.L., Blanchette, C.A. and Washburn, L., *et al.*, 2014. Exploring local adaptation and the ocean acidification seascape-studies in the California Current Large Marine Ecosystem. *Biogeosciences*, 11, 1053–1064.
- IBM Corp. Released (2016). *IBM SPSS Statistics for Windows*, Version 24.0. (software) Armonk, NY: IBM Corp.
- IPCC, 2014a: *Climate Change 2014: Synthesis Report. Contribution of Working Groups I, II and III to the Fifth Assessment Report of the Intergovernmental Panel on Climate Change* [Core Writing Team, R.K. Pachauri and L.A. Meyer (eds.)]. IPCC, Geneva, Switzerland, 151 pp.
- IPCC, 2014b: Summary for policymakers. In: *Climate Change 2014: Impacts, Adaptation, and Vulnerability. Part A: Global and Sectoral Aspects. Contribution of*



*Working Group II to the Fifth Assessment Report of the Intergovernmental Panel on Climate Change* [Field, C.B., V.R. Barros, D.J. Dokken, K.J. Mach, M.D. Mastrandrea, T.E. Bilir, M. Chatterjee, K.L. Ebi, Y.O. Estrada, R.C. Genova, B. Girma, E.S. Kissel, A.N. Levy, S. MacCracken, P.R. Mastrandrea, and L.L. White (eds.)]. Cambridge University Press, Cambridge, United Kingdom and New York, NY, USA, pp. 1-32.

IPCC, 2014c: *Climate Change 2014: Mitigation of Climate Change. Contribution of Working Group III to the Fifth Assessment Report of the Intergovernmental Panel on Climate Change* [Edenhofer, O., R. Pichs-Madruga, Y. Sokona, E. Farahani, S. Kadner, K. Seyboth, A. Adler, I. Baum, S. Brunner, P. Eickemeier, B. Kriemann, J. Savolainen, S. Schlömer, C. von Stechow, T. Zwickel and J.C. Minx (eds.)]. Cambridge University Press, Cambridge, United Kingdom and New York, NY, USA.

IPCC, 2013: *Climate Change 2013: The Physical Science Basis. Contribution of Working Group I to the Fifth Assessment Report of the Intergovernmental Panel on Climate Change* [Stocker, T.F., D. Qin, G.-K. Plattner, M. Tignor, S.K. Allen, J. Boschung, A. Nauels, Y. Xia, V. Bex and P.M. Midgley (eds.)]. Cambridge University Press, Cambridge, United Kingdom and New York, NY, USA, 1535 pp.

Irvine, L. M. and Chamberlain, Y. M. C., 1994 *Seaweeds of the British Isles, Vol 1, Part 2B*, British Museum (Natural History), London.

Jochum, K.P., Nohl, U., Herwig, K., Lammel, E., Stoll, B. and Hofmann, A.W., 2005. GeoReM: a new geochemical database for reference materials and isotopic standards. *Geostandards and Geoanalytical Research*, 29(3), pp.333-338.

Johansen, H.W., 1981. *Coralline Algae, A First Synthesis*, CRC Press, Boca Raton, Florida, USA, p. 239.

Johansen, H.W., 1975. Variability in articulated coralline algae (Rhodophyta). *Nova Hedwigia*, 26, pp.135-149.

Johnson, M.D. and Carpenter, R.C., 2012. Ocean acidification and warming decrease calcification in the crustose coralline alga *Hydrolithon onkodes* and increase susceptibility to grazing. *Journal of Experimental Marine Biology and Ecology*, 434, pp.94-101.

Jones, C.G., Lawton, J.H. and Shachak, M., 1994. Organisms as ecosystem engineers, *Oikos*, 69, 373–386.

Jones, C.G., Lawton, J.H. and Shachak, M., 1997. Positive and negative effects of organism as physical ecosystem engineers. *Ecology*. 78 (7), 1946-1957.

Jueterbock, A., Kollias, S., Smolina, I., Fernandes, J.M., Coyer, J.A., Olsen, J.L. and Hoarau, G., 2014. Thermal stress resistance of the brown alga *Fucus serratus* along the North-Atlantic coast: acclimatization potential to climate change. *Marine Genomics*, 13, pp.27-36.

Kamenos, N.A., Burdett, H.L., Aloisio, E., Findlay, H.S., Martin, S., Longbone, C., Dunn, J., Widdicombe, S. and Calosi, P., 2013. Coralline algal structure is more sensitive to rate, rather than the magnitude, of ocean acidification. *Global Change Biology*, 19(12), pp.3621-3628.

Kamenos, N.A., Cusack, M. and Moore, P.G., 2008. Coralline algae are global palaeothermometers with bi-weekly resolution. *Geochimica et Cosmochimica Acta*, 72(3), pp.771-779.

Kangwe, J.W., Hellblom, F., Semesi, A.K., Mtolera, M.S.P. and Bjork, M., 2001. Heavy metal inhibition of calcification and photosynthetic rates of the geniculate calcareous algae *Amphiroa tribulus*. *WIOMSA Book Series*, (1), pp.147-157.

Kelaher, B.P., Chapman, M.G. and Underwood, A.J., 2001. Spatial patterns of diverse macrofaunal assemblages in coralline turf and their associations with environmental variables. *Journal of the Marine Biological Association of the UK*. 81, 917–930.

- Kelaher, B.P., Underwood, A.J. and Chapman, M.G., 2003. Experimental transplantations of coralline algal turf to demonstrate causes of differences in macrofauna at different tidal heights. *Journal of Experimental Marine Biology and Ecology* 282(1–2), 23–41.
- Kelly, M.W. and Hofmann, G.E., 2013. Adaptation and the physiology of ocean acidification. *Functional Ecology* 27, 980–990.
- Kerr, R.A., 2011. Humans are driving extreme weather; time to prepare.
- Kiessling, W. and Simpson, C., 2011. On the potential for ocean acidification to be a general cause of ancient reef crises. *Global Change Biology*, 17(1), pp.56-67.
- Kiessling, W., Simpson, C., Beck, B., Mewis, H. and Pandolfi, J.M., 2012. Equatorial decline of reef corals during the last Pleistocene interglacial. *Proceedings of the National Academy of Sciences*, 109(52), pp.21378-21383.
- Kim, J.H., Lam, S.M.N. and Kim, K.Y., 2013. Photoacclimation strategies of the temperate coralline alga *Corallina officinalis*: a perspective on photosynthesis, calcification, photosynthetic pigment contents and growth. *Algae*, 28(4), pp.355-363.
- Kim, J.H., Nemson, J.A. and Melis, A., 1993. Photosystem II reaction center damage and repair in *Dunaliella salina* (green alga) (analysis under physiological and irradiance-stress conditions). *Plant Physiology*, 103(1), pp.181-189.
- Kitano, Y. and Hood, D.W., 1962. Calcium carbonate crystal forms formed from sea water by inorganic processes. *Journal of the Oceanographical Society of Japan*, 18(3), pp.141-145.
- Koch, M., Bowes, G., Ross, C. and Zhang, X.H., 2013. Climate change and ocean acidification effects on seagrasses and marine macroalgae. *Global Change Biology*, 19(1), pp.103-132.

Kleypas, J.A., Feely, R.A., Fabry, V.J., Langdon, C., Sabine, C.L. and Robbins, L.L., 2006. Impacts of Ocean Acidification on Coral Reefs and Other Marine Calcifiers: A Guide for Future Research, Report of a workshop held 18-20 April 2005, St. Petersburg, FL, sponsored by NSF, NOAA, and the U.S. Geological Survey, 88 pp.

Kolesar, P.T., 1978. Magnesium in calcite from a coralline alga. *Journal of Sedimentary Research*, 48(3), pp.815-819.

Kolzenburg, R., Nicasastro, K.R., McCoy, S.J., Ford, A.T., Zardi, G.I. and Ragazzola, F., 2019. Understanding the margin squeeze: Differentiation in fitness-related traits between central and trailing edge populations of *Corallina officinalis*. *Ecology and Evolution*, 9(10), pp.5787-5801.

Kordas, R.L., Harley, C.D. and O'Connor, M.I., 2011. Community ecology in a warming world: the influence of temperature on interspecific interactions in marine systems. *Journal of Experimental Marine Biology and Ecology*, 400(1-2), pp.218-226.

Kroeker, K.J., Micheli, F. and Gambi, M.C., 2013a. Ocean acidification causes ecosystem shifts via altered competitive interactions. *Nature Climate Change*, 3(2), p.156.

Kroeker, K.J., Kordas, R.L., Crim, R., Hendriks, I.E., Ramajo, L. and Singh, G.S., *et al.*, 2013b. Impacts of ocean acidification on marine organisms: quantifying sensitivities and interaction with warming. *Global Change Biology* 19, 1884–1896.

Kuffner, I.B., Andersson, A.J., Jokiel, P.L., Rodgers, K.S. and Mackenzie, F.T., 2008. Decreased abundance of crustose coralline algae due to ocean acidification. *Nature Geoscience* 1(2), 114–117.

Kübler, J.E., Johnston, A.M. and Raven, J.A., 1999. The effects of reduced and elevated CO<sub>2</sub> and O<sub>2</sub> on the seaweed *Lomentaria articulata*. *Plant, Cell & Environment*, 22(10), pp.1303-1310.

Laffoley, D.D.A. and Baxter, J.M. eds., 2016. *Explaining ocean warming: Causes, scale, effects and consequences*. Gland, Switzerland: IUCN.

Lepais, O., Muller, S.D., Saad-Limam, S.B., Benslama, M., Rhazi, L., Belouahem-Abed, D., Daoud-Bouattour, A., Gammar, A.M., Ghrabi-Gammar, Z. and Bacles, C.F.E., 2013. High genetic diversity and distinctiveness of rear-edge climate relicts maintained by ancient tetraploidisation for *Alnus glutinosa*. *PLoS One*, 8(9), p.e75029.

Lesica, P. and Allendorf, F.W., 1995. When are peripheral populations valuable for conservation? *Conservation biology*, 9(4), pp.753-760.

Lesica, P. and McCune, B., 2004. Decline of arctic-alpine plants at the southern margin of their range following a decade of climatic warming. *Journal of Vegetation Science*, 15(5), 679–690.

Levin, D.A., 1970. Developmental instability and evolution in peripheral isolates. *The American Naturalist*, 104(938), pp.343-353.

Levitus, S., Antonov, J.I., Boyer, T.P., Locarnini, R.A., Garcia, H.E. and Mishonov, A.V., 2009. Global ocean heat content 1955–2008 in light of recently revealed instrumentation problems. *Geophysical Research Letters*, 36(7).

Lewis, E. and Wallace, D.W.R., 1998. CO2SYS - Program developed for the CO2 system calculations. Technical report Oak Ridge, Tenn., USA: Report ORNL/CDIAC-105, Oak Ridge, Tenn., USA.

Lima, F.P., Ribeiro, P.A., Queiroz, N., Hawkins, S.J. and Santos, A.M., 2007. Do distributional shifts of northern and southern species of algae match the warming pattern? *Glob Change Biology* 13(12), 2592–2604.

Lindström, S., 2016. Palynofloral patterns of terrestrial ecosystem change during the end-Triassic event—a review. *Geological Magazine*, 153(2), pp.223-251.

Lobban, C.S., Harrison, P.J., 1994. *Seaweed ecology and physiology*. Cambridge University Press.

Longerich, H.P., Jackson, S.E. and Günther, D., 1996. Inter-laboratory note. Laser ablation inductively coupled plasma mass spectrometric transient signal data acquisition and analyte concentration calculation. *Journal of Analytical Atomic Spectrometry*, 11(9), pp.899-904.

Loxton, J., Najorka, J., Humphreys-Williams, E., Kuklinski, P., Smith, A.M., Porter, J.S. and Jones, M.S., 2017. The forgotten variable: Impact of cleaning on the skeletal composition of a marine invertebrate. *Chemical Geology*, 474, pp.45-57.

Lucassen, M., Koschnick, N., Eckerle, L.G. and Pörtner, H.-O., 2006. Mitochondrial mechanisms of cold adaptation in cod (*Gadus morhua* L.) populations from different climatic zones. *Journal of Experimental Biology*, 209(13), 2462–2471.

Linnaeus, C.V., 1758. *Systema Naturae, edition X, vol. 1* (Systema naturae per regna tria naturae, secundum classes, ordines, genera, species, cum characteribus, differentiis, synonymis, locis. Tomus I. Editio decima, reformata).

Liuzzi, M.G. and Gappa, J.L., 2008. Macrofaunal assemblages associated with coralline turf: species turnover and changes in structure at different spatial scales. *Marine Ecology Progress Series*, 363, pp.147-156.

Lüning, K., 1990. *Seaweeds: Their Environment, Biogeography and Ecophysiology*, John Wiley and Sons, New York, NY, USA.

Mackenzie, F.T., Lerman, A. and Andersson, A.J., 2004. Past and present of sediment and carbon biogeochemical cycling models. *Biogeosciences Discussions* 1(1), 27–85.

Magill, C.L., Maggs, C.A., Johnson, M.P. and O'Connor, N., 2019. Sustainable Harvesting of the Ecosystem Engineer *Corallina officinalis* for Biomaterials. *Frontiers in Marine Science*, 6, p. 285.

- Martin, S., Clavier, J., Chauvaud, L. and Thouzeau, G., 2007. Community metabolism in temperate maerl beds. I. Carbon and carbonate fluxes. *Marine Ecology Progress Series*, 335, 19–29.
- Martin, S., Cohu, S., Vignot, C., Zimmerman, G. and Gattuso, J.P., 2013. One-year experiment on the physiological response of the Mediterranean crustose coralline alga, *Lithophyllum cabiochae*, to elevated p CO<sub>2</sub> and temperature. *Ecology and Evolution*, 3(3), pp.676-693.
- Martin, S. and Gattuso, J.-P., 2009. Response of Mediterranean coralline algae to ocean acidification and elevated temperature, *Global Change Biology*, 15, 2089–2100.
- Martínez, B., Arenas, F., Rubal, M., Burgués, S., Esteban, R., García-Plazaola, I., Figueroa, F.L., Pereira, R., Saldaña, L., Sousa-Pinto, I. and Trilla, A., 2012. Physical factors driving intertidal macroalgae distribution: physiological stress of a dominant furoid at its southern limit. *Oecologia*, 170(2), pp.341-353.
- Martone, P.T. and Denny, M.W., 2008a. To bend a coralline: effect of joint morphology on flexibility and stress amplification in an articulated calcified seaweed. *Journal of Experimental Biology* 211: 3421–3432.
- Martone, P.T. and Denny, M.W., 2008b. To break a coralline: mechanical constraints on the size and survival of a wave-swept seaweed. *Journal of Experimental Biology*, 211(21), pp.3433-3441.
- Martone, P.T., Alyono, M., and Stites, S., 2010. Bleaching of an intertidal coralline alga: untangling the effects of light, temperature, and desiccation. *Marine Ecology Progress Series* 416, 57–67.
- Mayr, E., 1963. Animal species and evolution. *Animal species and evolution*.

- Mehrbach, C., Culberson, C.H., Hawley, J.E. and Pytkowicz, R.M., 1973. Measurement of the apparent dissociation constants of carbonic acid in seawater at atmospheric pressure. *Limnology and Oceanography* 18(6), 897–907.
- Meisch, H.U. and Benzschawel, H., 1978. The role of vanadium in green plants. *Archives of Microbiology*, 116(1), pp.91-95.
- Melbourne, L.A., Griffin, J., Schmidt, D.N. and Rayfield, E.J., 2015. Potential and limitations of finite element modelling in assessing structural integrity of coralline algae under future global change. *Biogeosciences*, 12(19), pp.5871-5883.
- McConnaughey, T.A. and Falk, R.H., 1991. Calcium-proton exchange during algal calcification. *The Biological Bulletin*, 180(1), pp.185-195.
- McConnaughey, T.A., LaBaugh, J.W., Rosenberry, D.O., Striegl, R.G., Reddy, M.M., Schuster, P.F. and Carter, V., 1994. Carbon budget for a groundwater-fed lake: Calcification supports summer photosynthesis. *Limnology and Oceanography*, 39(6), pp.1319-1332.
- McCoy, S.J. and Kamenos, N.A., 2015. Coralline algae (Rhodophyta) in a changing world: integrating ecological, physiological, and geochemical responses to global change, *Journal of Phycology*, 51, 6–24.
- McCoy, S.J., Pfister, C.A., Olack, G. and Colman, A.S., 2016. Diurnal and tidal patterns of carbon uptake and calcification in geniculate inter-tidal coralline algae. *Marine Ecology* 37, 553–564.
- McCoy, S.J. and Ragazzola, F., 2014. Skeletal trade-offs in coralline algae in response to ocean acidification. *Nature Climate Change*, 4(8), p.719.
- Milliman, J.D., Gastner, M. and Müller, J., 1971. Utilization of magnesium in coralline algae. *Geological Society of America Bulletin*, 82(3), pp.573-580.



- Moberly Jr, R., 1968. Composition of Magnesian Calcites of Algae and Pelecypods by Electron Microprobe Analysis. *Sedimentology*, 11(1-2), pp.61-82.
- Morley, S.A., Hirse, T., Pörtner, H.-O. and Peck, L.S., 2009. Geographical variation in thermal tolerance within Southern Ocean marine ectotherms. *Comparative Biochemistry and Physiology, Part A Molecular and Integrative Physiology* 153(2), 154–161.
- Mota, C.F., Engelen, A.H., Serrao, E.A., Coelho, M.A., Marbà, N., Krause-Jensen, D. and Pearson, G.A., 2018. Differentiation in fitness-related traits in response to elevated temperatures between leading and trailing edge populations of marine macrophytes. *PloS One*, 13(9), p.e0203666.
- Morris, S. and Taylor, A.C., 1983. Diurnal and seasonal-variation in physicochemical conditions within intertidal rock pools, *Estuarine, Coastal and Shelf Science*, 17, 339–355.
- Nazar, R., Iqbal, N., Masood, A., Khan, M.I.R., Syeed, S. and Khan, N.A., 2012. Cadmium toxicity in plants and role of mineral nutrients in its alleviation. *American Journal of Plant Sciences*, 3(10), p.1476.
- Nelson, W.A., 2009. Calcified macroalgae – critical to coastal ecosystems and vulnerable to change: a review. *Marine and Freshwater Research* 60, 787–801.
- Nelson, T.R., DeVries, D.R. and Wright, R.A., 2018. Salinity and temperature effects on element incorporation of gulf killifish *Fundulus grandis* otoliths. *Estuaries and Coasts*, 41(4), pp.1164-1177.
- Nicastro, K.R., Zardi, G.I., Teixeira, S., Neiva, J., Serrão, E.A. and Pearson, G.A., 2013. Shift happens: trailing edge contraction associated with recent warming trends threatens a distinct genetic lineage in the marine macroalga *Fucus vesiculosus*. *BMC Biology*. 11(1), 6.

- Noël, L.M.L.J., Hawkins, S.J., Jenkins, S.R. and Thompson, R.C., 2009. Grazing dynamics in intertidal rockpools: connectivity of microhabitats. *Journal of Experimental Marine Biology and Ecology* 370, 9–17.
- Noisette, F., Duong, G., Six, C., Davoult, D. and Martin, S., 2013. Effects of elevated pCO<sub>2</sub> on the metabolism of a temperate rhodolith *Lithothamnion corallioides* grown under different temperatures. *Journal of Phycology*, 49(4), pp.746-757.
- O'Connor, M.I., 2009. Warming strengthens an herbivore–plant interaction. *Ecology*, 90(2), pp.388-398.
- Oomori, T., Kaneshima, H., Maezato, Y. and Kitano, Y., 1987. Distribution coefficient of Mg<sup>2+</sup> ions between calcite and solution at 10–50 C. *Marine Chemistry*, 20(4), pp.327-336.
- Orr, J.C., Fabry, V.J., Aumont, O., Bopp, L., Doney, S.C., Feely, R.A., Gnanadesikan, A., Gruber, N., Ishida, A., Joos, F. and Key, R.M., 2005. Anthropogenic ocean acidification over the twenty-first century and its impact on calcifying organisms. *Nature*, 437(7059), p.681.
- Padilla-Gamiño, J.L., Gaitán-Espitia, J.D., Kelly, M.W. and Hofmann, G.E., 2016. Physiological plasticity and local adaptation to elevated pCO<sub>2</sub> in calcareous algae: an ontogenetic and geographic approach. *Evolutionary Applications*, 9(9), pp.1043-1053.
- Pandolfi, J.M., Connolly, S.R., Marshall, D.J. and Cohen, A.L., 2011. Projecting coral reef futures under global warming and ocean acidification. *Science*, 333(6041), pp.418-422.
- Pandolfi, J.M. and Kiessling, W., 2014. Gaining insights from past reefs to inform understanding of coral reef response to global climate change. *Current Opinion in Environmental Sustainability*, 7, pp.52-58.

- Pardo, C., Peña, V., Berreiro, R. and Bárbara, I., 2015. A molecular and morphological study of *Corallina sensu lato* (Corallinales, Rhodophyta) in the Atlantic Iberian Peninsula. *Cryptogamie Algologie* 36(1), 31-54.
- Parmesan, C., 2006. Ecological and Evolutionary Responses to Recent Climate Change. *Annual Review of Ecology, Evolution and Systematics*, 37(2006), 637–669.
- Parmesan, C., Ryrholm, N., Stefanescu, C., Hill, J.K., Thomas, C.D., Descimon, H., Huntley, B., Kaila, L., Kullberg, J., Tammaru, T. and Tennent, W.J., 1999. Poleward shifts in geographical ranges of butterfly species associated with regional warming. *Nature*, 399(6736), p.579.
- Parmesan, C. and Yohe, G., 2003. A globally coherent fingerprint of climate change impacts across natural systems. *Nature*, 421(6918), p.37.
- Paton, C., Hellstrom, J., Paul, B., Woodhead, J. and Hergt, J., 2011. Lolite: Freeware for the visualisation and processing of mass spectrometric data. *Journal of Analytical Atomic Spectrometry*, 26(12), pp.2508-2518.
- Pearson, G.A., Lago-Leston, A. and Mota, C., 2009. Frayed at the edges: selective pressure and adaptive response to abiotic stressors are mismatched in low diversity edge populations. *Journal of Ecology*, 97(3), pp.450-462.
- Pelini, S.L., Diamond, S.E., MacLean, H., Ellison, A.M., Gotelli, N.J., Sanders, N.J. and Dunn, R.R., 2012. Common garden experiments reveal uncommon responses across temperatures, locations, and species of ants. *Ecology and Evolution*, 2(12), 3009–3015.
- Pentecost, A., 1978. Calcification and photosynthesis in *Corallina officinalis* L. using the  $^{14}\text{CO}_2$  method. *British Phycological Journal*, 13(4), pp.383-390.

Pinsky, M.L., Eikeset, A.M., McCauley, D.J., Payne, J.L. and Sunday, J.M., 2019. Greater vulnerability to warming of marine versus terrestrial ectotherms. *Nature*, 569(7754), pp.108-111.

Pörtner, H.-O., D.M. Karl, P.W. Boyd, W.W.L. Cheung, S.E. Lluch-Cota, Y. Nojiri, D.N. Schmidt, and P.O. Zavialov, 2014: Ocean systems. In: *Climate Change 2014: Impacts, Adaptation, and Vulnerability. Part A: Global and Sectoral Aspects. Contribution of Working Group II to the Fifth Assessment Report of the Intergovernmental Panel on Climate Change* [Field, C.B., V.R. Barros, D.J. Dokken, K.J. Mach, M.D. Mastrandrea, T.E. Bilir, M. Chatterjee, K.L. Ebi, Y.O. Estrada, R.C. Genova, B. Girma, E.S. Kissel, A.N. Levy, S. MacCracken, P.R. Mastrandrea, and L.L. White (eds.)]. Cambridge University Press, Cambridge, United Kingdom and New York, NY, USA, pp. 411-484.

Putra, A.D., (2019). Reconstruction of pH and Temperature of Historical and Recent Environmental Changes Using *Corallina officinalis* (Master of Philosophy Dissertation), University of Portsmouth.

Ragazzola, F., 2008. Carbon Acquisition Mechanisms in *Corallina Elongata* Ellis & Solander and *Corallina officinalis* L. (Doctoral dissertation)

Ragazzola, F., Foster, L., Form, A., Anderson, P.S.L., Hansteen, T.H. and Fietzke, J., 2012. Ocean acidification weakens the structural integrity of coralline algae, *Global Change Biology* 18(9), 2804–2812.

Ragazzola, F., Foster, L.C., Form, A.U., Büscher, J., Hansteen, T.H. and Fietzke, J., 2013. Phenotypic plasticity of coralline algae in a high CO<sub>2</sub> world. *Ecology and Evolution*, 3(10), pp.3436-3446.

Ragazzola, F., Foster, L.C., Jones, C.J., Scott, T.B., Fietzke, J., Kilburn, M.R. and Schmidt, D.N., 2016. Impact of high CO<sub>2</sub> on the geochemistry of the coralline algae *Lithothamnion glaciale*. *Scientific Reports*, 6, p.20572.

Ragazzola, F., Raiteri, G., Fabbri, P., Scafè, M., Florio, M., Nannini, M. and Lombardi, C., 2017. Structural integrity of *Ellisolandia elongata* reefs: A mechanical approach to compare tensile strengths in natural and controlled environments. *Marine Ecology*, 38(5), p.e12455.

Rasband, W.S., 2016. 'ImageJ' (software). Bethesda, Maryland, USA: U.S. National Institute of Health. Available at: <https://imagej.nih.gov/ij/>.

Raven, J.A. and Beardall, J., 2003. Carbon acquisition mechanisms of algae: carbon dioxide diffusion and carbon dioxide concentrating mechanisms. In *Photosynthesis in Algae* (pp. 225-244). Springer, Dordrecht.

Raven, J.A., Evans, M.C. and Korb, R.E., 1999. The role of trace metals in photosynthetic electron transport in O<sub>2</sub>-evolving organisms. *Photosynthesis Research*, 60(2-3), pp.111-150.

Raven, J.A., Giordano, M., Beardall, J. and Maberly, S.C., 2012. Algal evolution in relation to atmospheric CO<sub>2</sub>: carboxylases, carbon-concentrating mechanisms and carbon oxidation cycles. *Philosophical Transactions of the Royal Society B: Biological Sciences*, 367(1588), pp.493-507.

Reid, P.C. and Hill, C., 2016. Ocean warming: setting the scene. *Explaining ocean warming: Causes, Scale, Effects and Consequences*, p.17.

Reddin, C.J., Nätscher, P.S., Kocsis, Á.T., Pörtner, H.O. and Kiessling, W., 2020. Marine clade sensitivities to climate change conform across timescales. *Nature Climate Change*, pp.1-5.

Riebesell, U., Fabry, V.J., Hansson, L. and Gattuso, J.P., 2011. *Guide to best practices for ocean acidification research and data reporting*. Office for Official Publications of the European Communities.

Ries, J.B., 2011. Skeletal mineralogy in a high-CO<sub>2</sub> world. *Journal of Experimental Marine Biology and Ecology* 403, 54–64.

Ries, J.B., Cohen, A.L. and McCorkle, D.C., 2009. Marine calcifiers exhibit mixed responses to CO<sub>2</sub>-induced ocean acidification. *Geology*, 37(12), pp.1131-1134.

Ritson-Williams, R., Arnold, S.N., Fogarty, N.D., Steneck, R.S., Vermeij, M.J. and Paul, V.J., 2009. New perspectives on ecological mechanisms affecting coral recruitment on reefs. *Smithsonian Contributions to the Marine Sciences*, 38, p.437.

Rodolfo-Metalpa, R., Houlbrèque, F., Tambutté, É., Boisson, F., Baggini, C., Patti, F.P., Jeffree, R., Fine, M., Foggo, A., Gattuso, J.P. and Hall-Spencer, J.M., 2011. Coral and mollusc resistance to ocean acidification adversely affected by warming. *Nature Climate Change*, 1(6), p.308.

Rosenthal, Y., Boyle, E.A. and Slowey, N., 1997. Temperature control on the incorporation of Mg, Sr, F and Cd into benthic foraminiferal shells from Little Bahama Bank: prospects for thermocline paleoceanography. *Geochimica et Cosmochimica Acta*, 61(17), pp.3633-3643.

Rothäusler, E., Rugiu, L. and Jormalainen, V., 2018. Forecast climate change conditions sustain growth and physiology but hamper reproduction in range-margin populations of a foundation rockweed species. *Marine Environmental Research*, 141, pp.205-213.

Rout G. and Das P., 2003. Effect of metal toxicity on plant growth and metabolism: I. Zinc. *Agronomie* 23(1):3–11

Saada, G., Nicastro, K.R., Jacinto, R., McQuaid, C.D., Serrão, E.A., Pearson, G.A. and Zardi, G.I., 2016. Taking the heat: distinct vulnerability to thermal stress of central and threatened peripheral lineages of a marine macroalga. *Diversity and Distributions*, 22(10), pp.1060-1068.

Sagarin, R.D. and Gaines, S.D., 2002. The 'abundant centre' distribution: to what extent is it a biogeographical rule?. *Ecology Letters*, 5(1), pp.137-147.

Sagarin, R.D. and Gaines, S.D., 2006. Recent studies improve understanding of population dynamics across species ranges. *Oikos*, 115(2), pp.386-388.

Sagarin, R.D., Gaines, S.D. and Gaylord, B., 2006. Moving beyond assumptions to understand abundance distributions across the ranges of species. *Trends in Ecology and Evolution*, 21(9), pp.524-530.

Sanford, E., Holzman, S.B., Haney, R.A., Rand, D.M. and Bertness, M.D., 2006. Larval tolerance, gene flow, and the northern geographic range limit of fiddler crabs. *Ecology*, 87(11), 2882–2894.

Sarı, A. and Tuzen, M., 2008. Biosorption of total chromium from aqueous solution by red algae (*Ceramium virgatum*): Equilibrium, kinetic and thermodynamic studies. *Journal of Hazardous Materials*, 160(2-3), pp.349-355.

Schöne, B.R., Zhang, Z., Jacob, D., Gillikin, D.P., Tütken, T., Garbe-Schönberg, D., McConnaughey, T. and Soldati, A., 2010. Effect of organic matrices on the determination of the trace element chemistry (Mg, Sr, Mg/Ca, Sr/Ca) of aragonitic bivalve shells (*Arctica islandica*)—Comparison of ICP-OES and LA-ICP-MS data. *Geochemical Journal*, 44(1), pp.23-37.

Schoenrock, K.M., Schram, J.B., Amsler, C.D., McClintock, J.B., Angus, R.A. and Vohra, Y.K., 2016. Climate change confers a potential advantage to fleshy Antarctic crustose macroalgae over calcified species. *Journal of Experimental Marine Biology and Ecology*, 474, pp.58-66.

Sexton, J.P., McIntyre, P.J., Angert, A.L. and Rice, K.J., 2009. Evolution and ecology of species range limits. *Annual Review of Ecology, Evolution and Systematics*, 40, pp.415-436.

Sinutok, S., Hill, R., Doblin, M.A., Wuhrer, R. and Ralph, P.J., 2011. Warmer more acidic conditions cause decreased productivity and calcification in subtropical coral reef sediment-dwelling calcifiers. *Limnology and Oceanography*, 56(4), pp.1200-1212.

Slater, S.M., Twitchett, R.J., Danise, S. and Vajda, V., 2019. Substantial vegetation response to Early Jurassic global warming with impacts on oceanic anoxia. *Nature Geoscience*, 12(6), pp.462-467.

Smale, D.A., and Wernberg, T., 2013. Extreme climatic event drives range contraction of a habitat-forming species. *Proceedings of the Royal Society B: Biological Sciences*, 280: 20122829 .

Smith, S.V and Key, G.S., 1975. Carbon dioxide and metabolism in marine environments, *Limnology and Oceanography*, 20(3), 493–495.

Smith, A.D. and Roth, A.A., 1979. Effect of carbon dioxide concentration on calcification in the red coralline alga *Bossiella orbigniana*. *Marine Biology*, 52(3), pp.217-225.

Smith, A.M., Sutherland, J.E., Kregting, L., Farr, T.J. and Winter, D.J., 2012. Phylomineralogy of the coralline red algae: correlation of skeletal mineralogy with molecular phylogeny. *Phytochemistry*, 81, pp.97-108.

Somero, G.N., 2010. The physiology of climate change: how potentials for acclimatization and genetic adaptation will determine 'winners' and 'losers'. *Journal of Experimental Biology*, 213(6), pp.912-920.

Sosdian, S.M., Greenop, R., Hain, M.P., Foster, G.L., Pearson, P.N. and Lear, C.H., 2018. Constraining the evolution of Neogene ocean carbonate chemistry using the boron isotope pH proxy. *Earth and Planetary Science Letters*, 498, pp.362-376.

Stefánsson, U. and Ólafsson, J., 1991. *Nutrients and fertility of Icelandic waters*. Marine Research Institute.

Steller, D.L., Riosmena-Rodríguez, R., Foster, M.S. and Roberts, C.A., 2003. Rhodolith bed diversity in the Gulf of California: the importance of rhodolith structure and consequences of disturbance. *Aquatic conservation: Marine and Freshwater*



---

*Ecosystems*, 13(S1), pp.S5-S20.

Steneck, R. S., 1986. The ecology of coralline algal crusts: convergent patterns and adaptative strategies. *Annual Reviews in Ecology, Evolution and Systematics* 17(1), 273–303.

Stanley, S.M., Ries, J.B. and Hardie, L.A., 2002. Low-magnesium calcite produced by coralline algae in seawater of Late Cretaceous composition. *Proceedings of the National Academy of Sciences*, 99(24), pp.15323-15326.

Stanley, S.M., 2016. Estimates of the magnitudes of major marine mass extinctions in earth history. *Proceedings of the National Academy of Sciences*, 113(42), pp.E6325-E6334.

Tavares, A.I., Nicastro, K.R., Kolzenburg, R., Ragazzola, F., Jacinto, R. and Zardi, G.I., 2018. Isolation and characterization of nine microsatellite markers for the red alga *Corallina officinalis*. *Molecular Biology Reports*, 45(6), pp.2791-2794.

Teske, P.R., Sandoval-Castillo, J., Golla, T.R., Emami-Khoyi, A., Tine, M., von der Heyden, S. and Beheregaray, L.B., 2019. Thermal selection as a driver of marine ecological speciation. *Proceedings of the Royal Society B*, 286(1896), p.20182023.

Thomas, C.D., Cameron, A., Green, R.E., Bakkenes, M., Beaumont, L.J., Collingham, Y.C., Erasmus, B.F., De Siqueira, M.F., Grainger, A., Hannah, L. and Hughes, L., 2004. Extinction risk from climate change. *Nature*, 427(6970), pp.145-148.

Tomanek, L., 2010. Variation in the heat shock response and its implication for predicting the effect of global climate change on species' biogeographical distribution ranges and metabolic costs. *Journal of Experimental Biology*, 213(6), pp.971-979.

van der Heijden, L.H. and Kamenos, N.A., 2015. Reviews and syntheses: Calculating the global contribution of coralline algae to total carbon burial, *Biogeosciences* 12, 6429–6441.

Vásquez-Elizondo, R.M. and Enríquez, S., 2016. Coralline algal physiology is more adversely affected by elevated temperature than reduced pH. *Scientific Reports*, 6, p.19030.

Viejo, R.M., Martínez, B., Arrontes, J., Astudillo, C. and Hernández, L., 2011. Reproductive patterns in central and marginal populations of a large brown seaweed: drastic changes at the southern range limit. *Ecography*, 34(1), pp.75-84.

Vinogradov, A., 1953. The elementary composition of marine organisms. *Sears Foundation for Marine Research*, Mem, 2.

Vymazal, J., 1987. Toxicity and accumulation of cadmium with respect to algae and cyanobacteria: a review. *Toxicity Assessment*, 2(4), pp.387-415.

Walker, R.H., Brodie, J., Russell, S., Irvine, L.M. and Orfanidis, S., 2009. Biodiversity of Coralline Algae in the Northeastern Atlantic Including *Corallina caespitosa* sp. nov. (Corallinoideae, Rhodophyta) 1. *Journal of Phycology*, 45(1), pp.287-297.

Walsh, P.J., Buchanan, F.J., Dring, M., Maggs, C., Bell, S. and Walker, G.M., 2008. Low-pressure synthesis and characterisation of hydroxyapatite derived from mineralise red algae. *Chemical Engineering Journal*, 137(1), pp.173-179.

Walther, G.R., Post, E., Convey, P., Menzel, A., Parmesan, C., Beebee, T.J., Fromentin, J.M., Hoegh-Guldberg, O. and Bairlein, F., 2002. Ecological responses to recent climate change. *Nature*, 416(6879), p.389.

Watkinson, A.R., and Sutherland, W.J., 1995. Sources, sinks and pseudo-sinks. *Journal of Animal Ecology* 126–130.

Wernberg, T., Russell, B.D., Thomsen, M.S., Gurgel, C.F.D. and Bradshaw, C.J.A., et al., 2011. Seaweed communities in retreat from ocean warming. *Current Biology* 21, 1828–1832.

Whittaker, R.H., 1956. Vegetation of the Great Smoky Mountains. *Ecological Monographs*, 26: 1\_/80.

Wilhelm, C. and Wild, A., 1984a. The variability of the photosynthetic unit in *Chlorella* I. The effect of vanadium on photosynthesis, productivity, P-700 and cytochrome f in undiluted and homocontinuous cultures of chlorella. *Journal of plant physiology*, 115(2), pp.115-124.

Wilhelm, C. and Wild, A., 1984b. The variability of the photosynthetic unit in *Chlorella* II. The effect of light intensity and cell development on photosynthesis, P-700 and cytochrome f in homocontinuous and synchronous cultures of *Chlorella*. *Journal of plant physiology*, 115(2), pp.125-135.

Williamson, C.J., Brodie, J., Goss, B., Yallop, M., Lee, S. and Perkins, R., 2014. *Corallina* and *Ellisolandia* (Corallinales, Rhodophyta) photophysiology over daylight tidal emersion: interactions with irradiance, temperature and carbonate chemistry, *Marine Biology*, 161, 2051–2068.

Williamson, C.J., Walker, R.H., Robba, L., Russell, S., Irvine, L.M. and Brodie, J., 2015. Towards resolution of species diversity and distribution in the calcified red algal genera *Corallina* and *Ellisolandia* (Corallinales, Rhodophyta), *Phycologia*, 54, 2– 11.

Williamson, C.J., Perkins, R., Voller, M., Yallop, M.L. and Brodie, J., 2017. The regulation of coralline algal physiology, an in situ study of *Corallina officinalis* (Corallinales, Rhodophyta). *Biogeosciences*, 14, 4485-4498.

Williamson, C.J., Perkins, R., Yallop, M.L., Peteiro, C., Sanches, N., Gunnarsson, K., Gamble, M. and Brodie, J., 2018. Photoacclimation and photoregulation

strategies of *Corallina* (Corallinales, Rhodophyta) across the NE Atlantic. *Journal of Phycology* 53:3, 290-306.

Woelkering, W.J., 1988. *The coralline red algae: an analysis of the genera and subfamilies of nongeniculate Corallinaceae*. Oxford University Press.

Wolf-Gladrow, D.A., Riebesell, U.L.F., Burkhardt, S. and Bijma, J., 1999. Direct effects of CO<sub>2</sub> concentration on growth and isotopic composition of marine plankton. *Tellus B*, 51(2), pp.461-476.

Yang, A., Dick, C.W., Yao, X. and Huang, H., 2016. Impacts of biogeographic history and marginal population genetics on species range limits: a case study of *Liriodendron chinense*. *Scientific Reports*, 6, p.25632.

Yesson, C., Jackson, A., Russell, S., Williamson, C.J. and Brodie, J., 2018. SNPs reveal geographical population structure of *Corallina officinalis* (Corallinaceae, Rhodophyta). *European Journal of Phycology*, 53(2), pp.180-188.

Yildiz, G., Hofmann, L.C., Bischof, K. and Dere, Ş., 2013. Ultraviolet radiation modulates the physiological responses of the calcified rhodophyte *Corallina officinalis* to elevated CO<sub>2</sub>. *Botanica Marina*, 56(2), pp.161-168.

Zardi, G.I., Nicastro, K.R., Serrão, E.A., Jacinto, R., Monteiro, C.A. and Pearson, G.A., 2015. Closer to the rear edge: Ecology and genetic diversity down the core-edge gradient of a marine macroalga. *Ecosphere*, 6(2), pp.1-25.

Zeebe, R.E. and Wolf-Gladrow, D., 2001. *CO<sub>2</sub> in seawater: equilibrium, kinetics, isotopes* (No. 65). Gulf Professional Publishing.

Zeebe, R.E. and Wolf-Gladrow, D.A., 2009. Carbon dioxide, dissolved (ocean). *Encyclopedia of Paleoclimatology and Ancient Environments*, pp.123-127.

Zhang, Y.G., Pagani, M., Liu, Z., Bohaty, S.M. and DeConto, R., 2013. A 40-million-year history of atmospheric CO<sub>2</sub>. *Philosophical Transactions of the Royal*

*Society A: Mathematical, Physical and Engineering Sciences*, 371(2001), p.20130096.

Žuljević, A., Kaleb, S., Peña, V., Despalatović, M., Cvitković, I., De Clerck, O., Le Gall, L., Falace, A., Vita, F., Braga, J.C. and Antolić, B., 2016. First freshwater coralline alga and the role of local features in a major biome transition. *Scientific reports*, 6, p.19642.

# Appendix A

Research Ethics Review Checklist  
UPR16 and Certificate of Ethics Review

## FORM UPR16

### Research Ethics Review Checklist



Please include this completed form as an appendix to your thesis (see the Research Degrees Operational Handbook for more information)

<b>Postgraduate Research Student (PGRS) Information</b>		<b>Student ID:</b>	795203
<b>PGRS Name:</b>	Regina Kolzenburg		
<b>Department:</b>	School of Biological Sciences	<b>First Supervisor:</b>	Dr. Federica Ragazzola
<b>Start Date:</b> (or progression date for Prof Doc students)	01.10.2015		
<b>Study Mode and Route:</b>	Part-time <input type="checkbox"/>	MPhil <input type="checkbox"/>	MD <input type="checkbox"/>
	Full-time <input checked="" type="checkbox"/>	PhD <input checked="" type="checkbox"/>	Professional Doctorate <input type="checkbox"/>
<b>Title of Thesis:</b>	The Resilience of Marginal Populations of the Red Alga <i>Corallina officinalis</i> to Climate Change		
<b>Thesis Word Count:</b> (excluding ancillary data)	69,692		
<p>If you are unsure about any of the following, please contact the local representative on your Faculty Ethics Committee for advice. Please note that it is your responsibility to follow the University's Ethics Policy and any relevant University, academic or professional guidelines in the conduct of your study</p> <p>Although the Ethics Committee may have given your study a favourable opinion, the final responsibility for the ethical conduct of this work lies with the researcher(s).</p>			
<b>UKRIO Finished Research Checklist:</b>			
(If you would like to know more about the checklist, please see your Faculty or Departmental Ethics Committee rep or see the online version of the full checklist at: <a href="http://www.ukrio.org/what-we-do/code-of-practice-for-research/">http://www.ukrio.org/what-we-do/code-of-practice-for-research/</a> )			
a) Have all of your research and findings been reported accurately, honestly and within a reasonable time frame?	YES	<input checked="" type="checkbox"/>	
	NO	<input type="checkbox"/>	
b) Have all contributions to knowledge been acknowledged?	YES	<input checked="" type="checkbox"/>	
	NO	<input type="checkbox"/>	
c) Have you complied with all agreements relating to intellectual property, publication and authorship?	YES	<input checked="" type="checkbox"/>	
	NO	<input type="checkbox"/>	
d) Has your research data been retained in a secure and accessible form and will it remain so for the required duration?	YES	<input checked="" type="checkbox"/>	
	NO	<input type="checkbox"/>	
e) Does your research comply with all legal, ethical, and contractual requirements?	YES	<input checked="" type="checkbox"/>	
	NO	<input type="checkbox"/>	
<b>Candidate Statement:</b>			
I have considered the ethical dimensions of the above named research project, and have successfully obtained the necessary ethical approval(s)			
<b>Ethical review number(s) from Faculty Ethics Committee (or from NRES/SCREC):</b>	FC10-C40B-9F1B-14BA-BDD3-9860-37E0-BAFC		
If you have <i>not</i> submitted your work for ethical review, and/or you have answered 'No' to one or more of questions a) to e), please explain below why this is so:			
<b>Signed (PGRS):</b>	See next page	<b>Date:</b>	28.09.2019

UPR16 – April 2018

--	--	--



## Certificate of Ethics Review

<b>Project Title:</b>	Resilience of Marginal Populations of the macroalgae <i>Corallina officinalis</i> (Rhodophyta, Corallinales) to Climate Change
<b>User ID:</b>	795203
<b>Name:</b>	Regina Kolzenburg
<b>Application Date:</b>	31/07/2017 15:05:05

You must download your certificate, print a copy and keep it as a record of this review.

It is your responsibility to adhere to the University Ethics Policy and any Department/School or professional guidelines in the conduct of your study including relevant guidelines regarding health and safety of researchers and University Health and Safety Policy.

It is also your responsibility to follow University guidance on Data Protection Policy:

- General guidance for all data protection issues
- University Data Protection Policy

You are reminded that as a University of Portsmouth Researcher you are bound by the UKRIO Code of Practice for Research; any breach of this code could lead to action being taken following the University's Procedure for the Investigation of Allegations of Misconduct in Research.

Any changes in the answers to the questions reflecting the design, management or conduct of the research over the course of the project must be notified to the Faculty Ethics Committee. **Any changes that affect the answers given in the questionnaire, not reported to the Faculty Ethics Committee, will invalidate this certificate.**

This ethical review should not be used to infer any comment on the academic merits or methodology of the project. If you have not already done so, you are advised to develop a clear protocol/proposal and ensure that it is independently reviewed by peers or others of appropriate standing. A favourable ethical opinion should not be perceived as permission to proceed with the research; there might be other matters of governance which require further consideration including the agreement of any organisation hosting the research.

### Governance Checklist

**A1-BriefDescriptionOfProject:** I will compare marginal and central populations of the not endangered or endemic macroalgae *Corallina officinalis* to climate change. I will be sampling for specimen in the UK, Iceland and Spain and then incubate these specimen in different conditions to measure photosynthesis, respiration, calcification as well as structural integrity of the algae.

**A2-Faculty:** PBS

**A3-VoluntarilyReferToFEC:** No

**Certificate Code:** FC10-C40B-9F1B-14BA-BDD3-9860-37E0-BAFC Page 1

**A5-AlreadyExternallyReviewed:** No

**B1-HumanParticipants:** No

**HumanParticipantsDefinition**

**B2-HumanParticipantsConfirmation:** Yes

**C6-SafetyRisksBeyondAssessment:** No

**D2-PhysicalEcologicalDamage:** No

**D4-HistoricalOrCulturalDamage:** No

**E1-ContentiousOrIllegal:** No

**E2-SociallySensitiveIssues:** No

**F1-InvolvesAnimals:** No

**F2-HarmfulToThirdParties:** No

**G1-ConfirmReadEthicsPolicy:** Confirmed

**G2-ConfirmReadUKRIOCodeOfPractice:** Confirmed

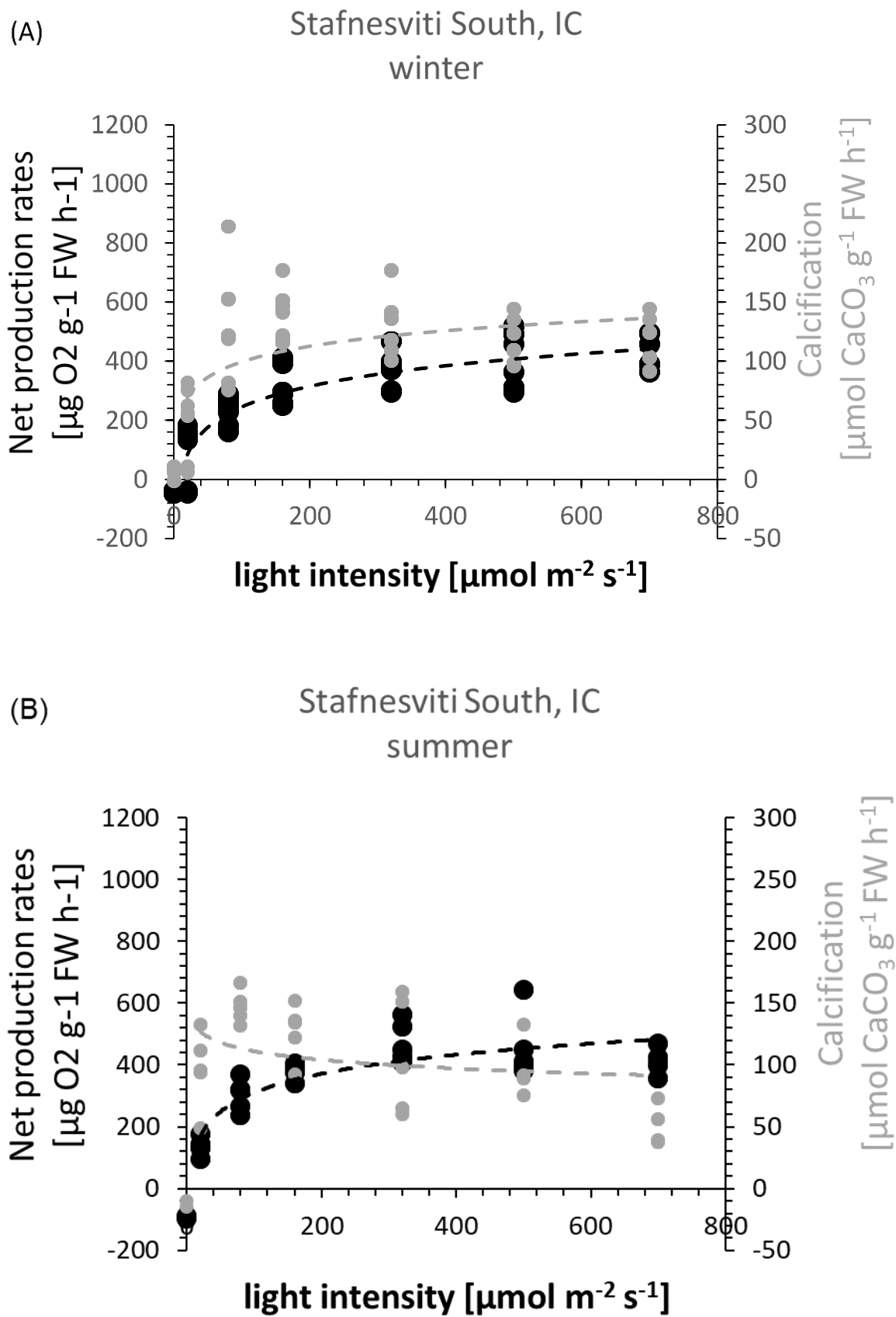
**G3-ConfirmReadConcordatToSupportResearchIntegrity:** Confirmed

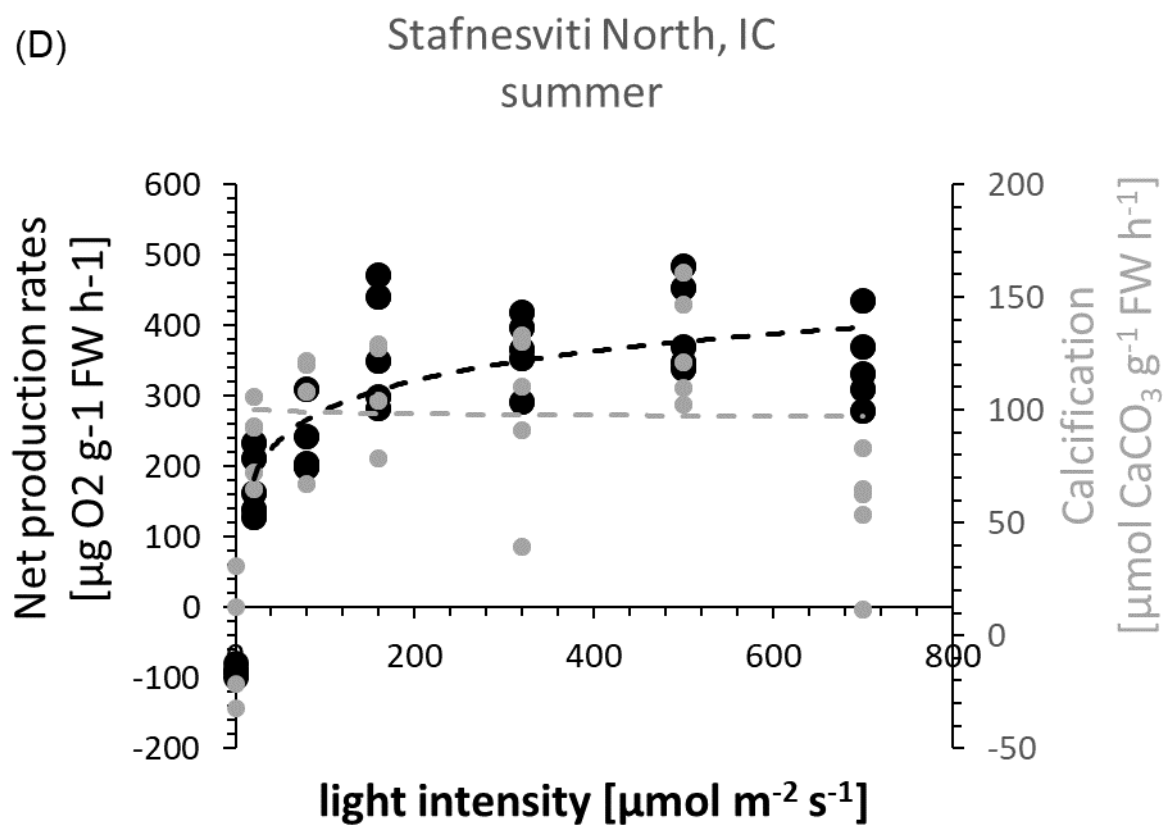
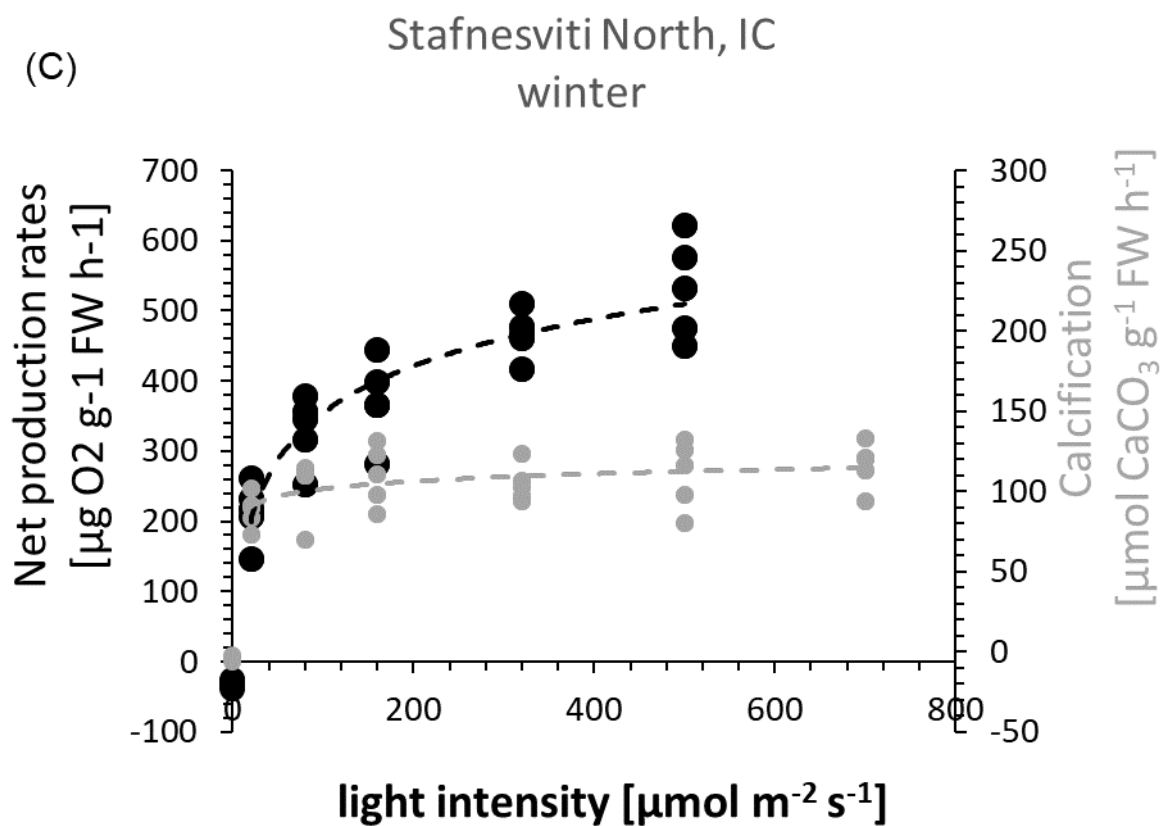
**G4-ConfirmedCorrectInformation:** Confirmed

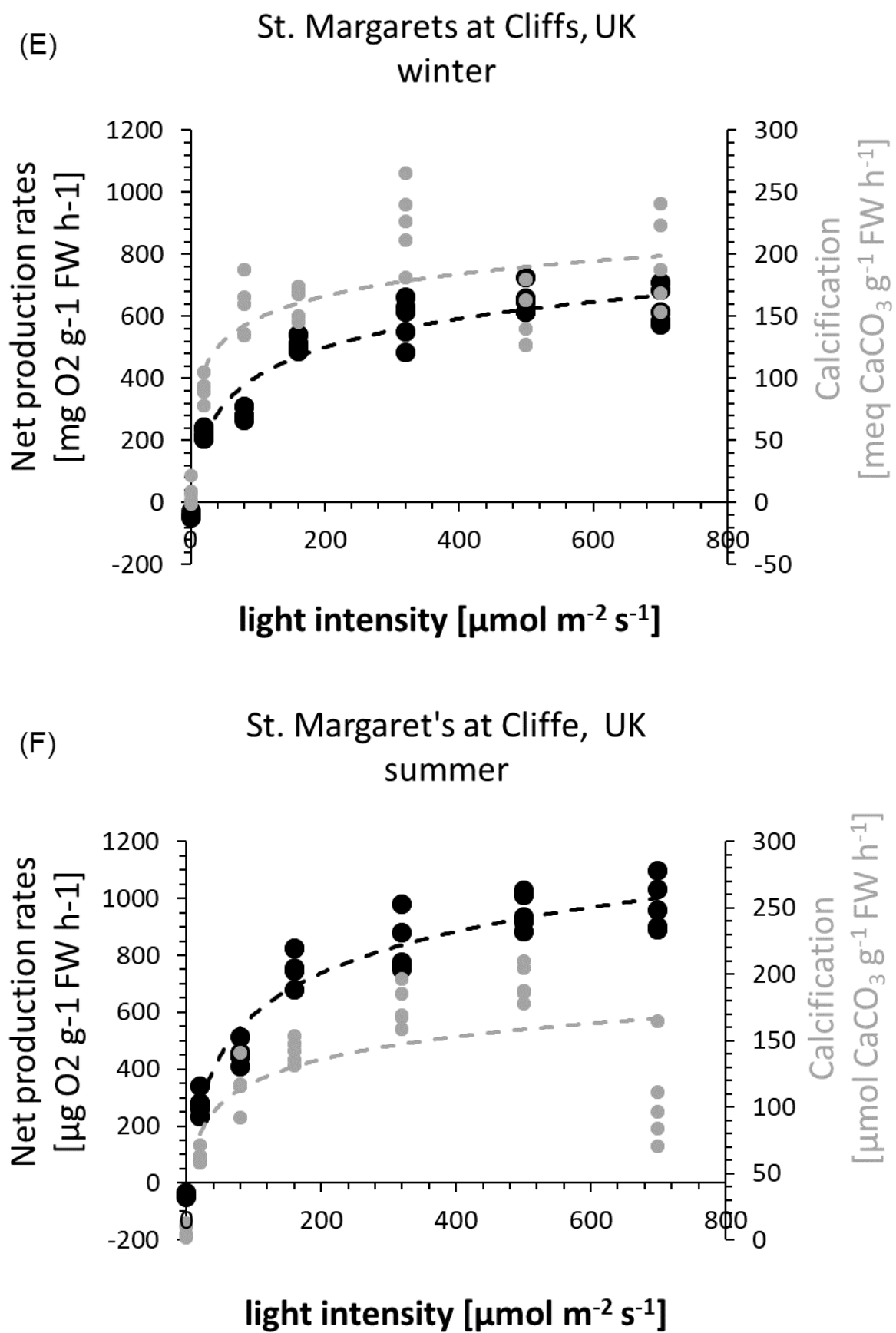


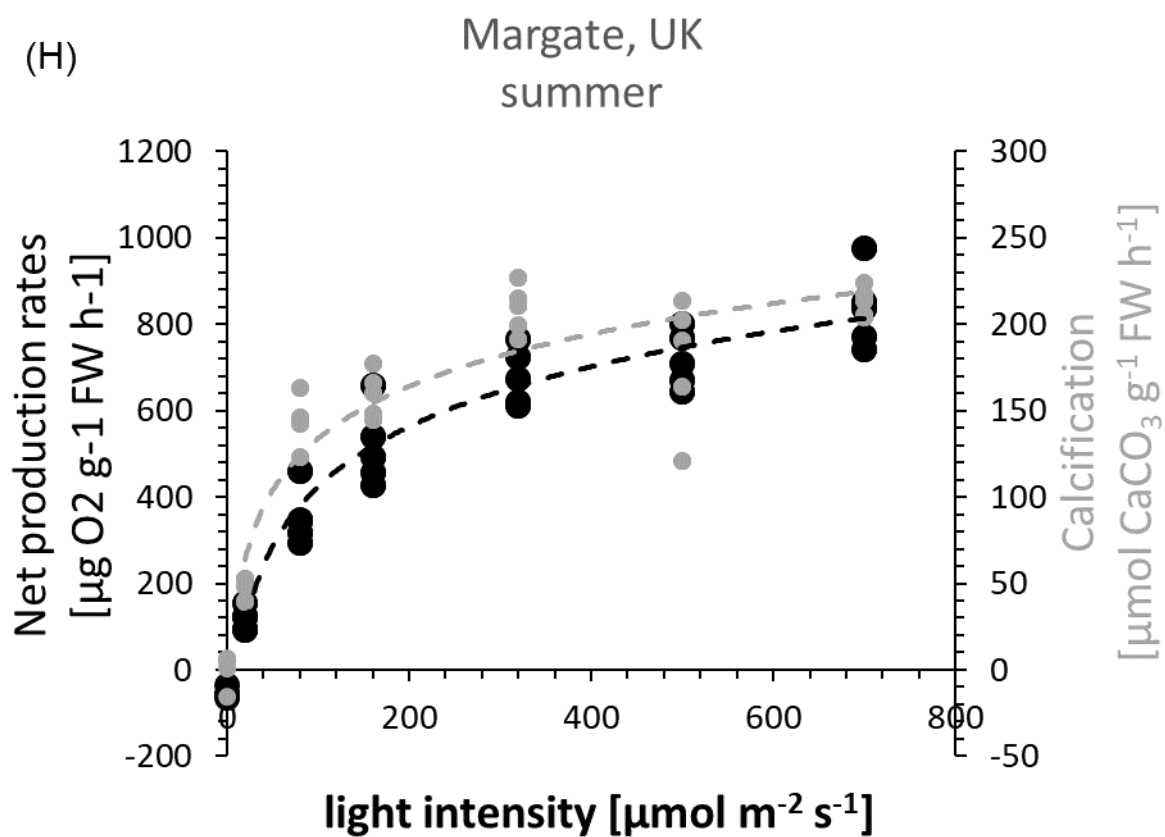
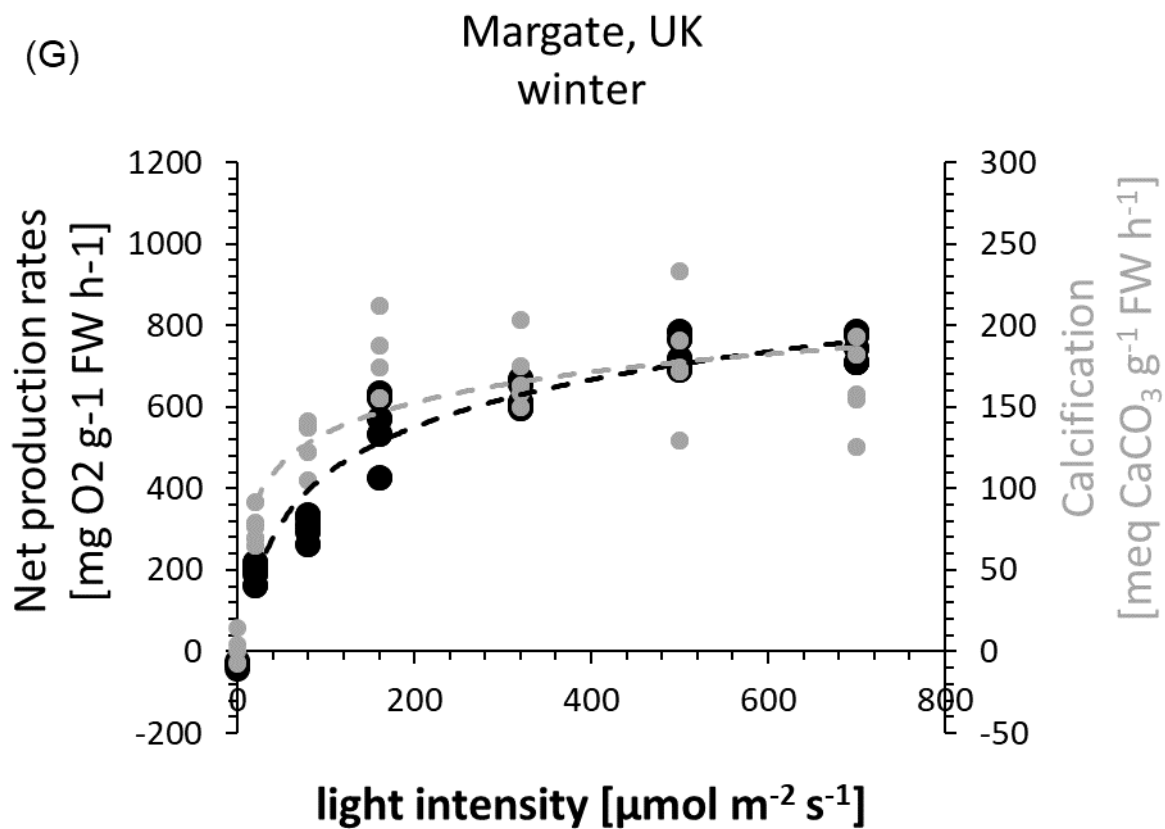
# Appendix B

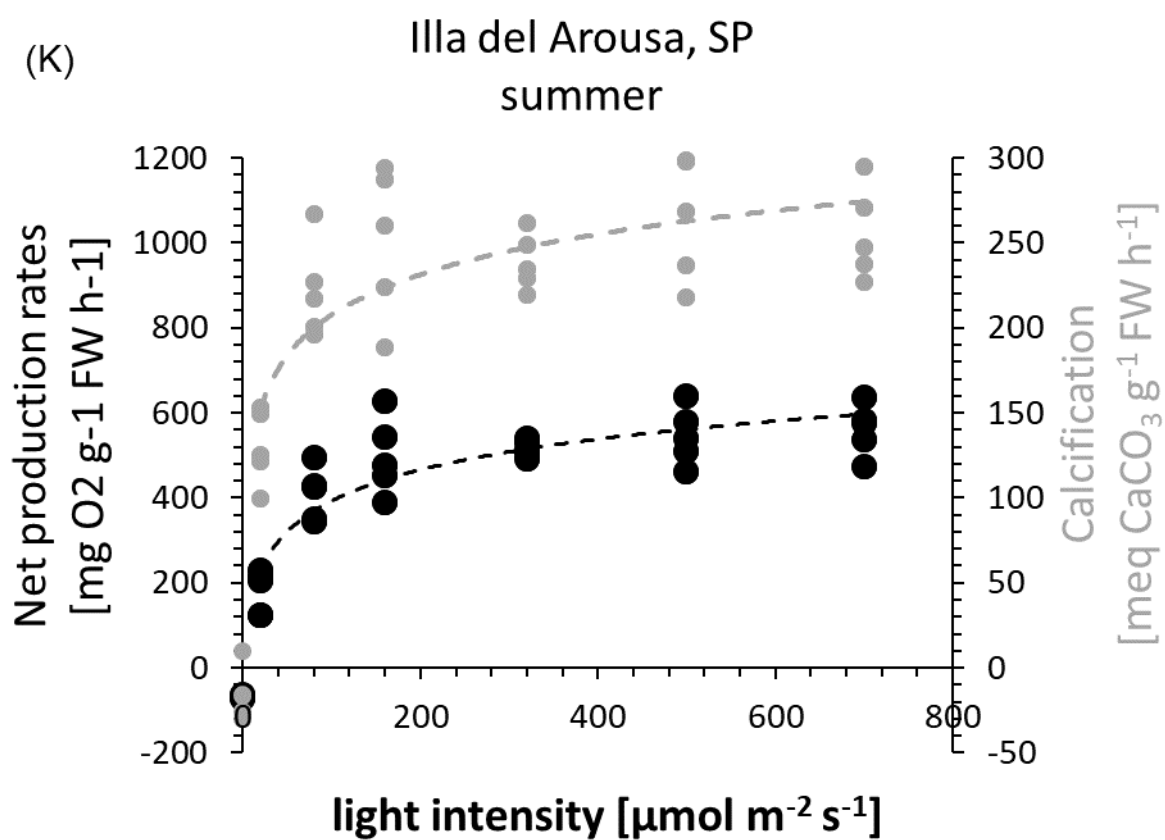
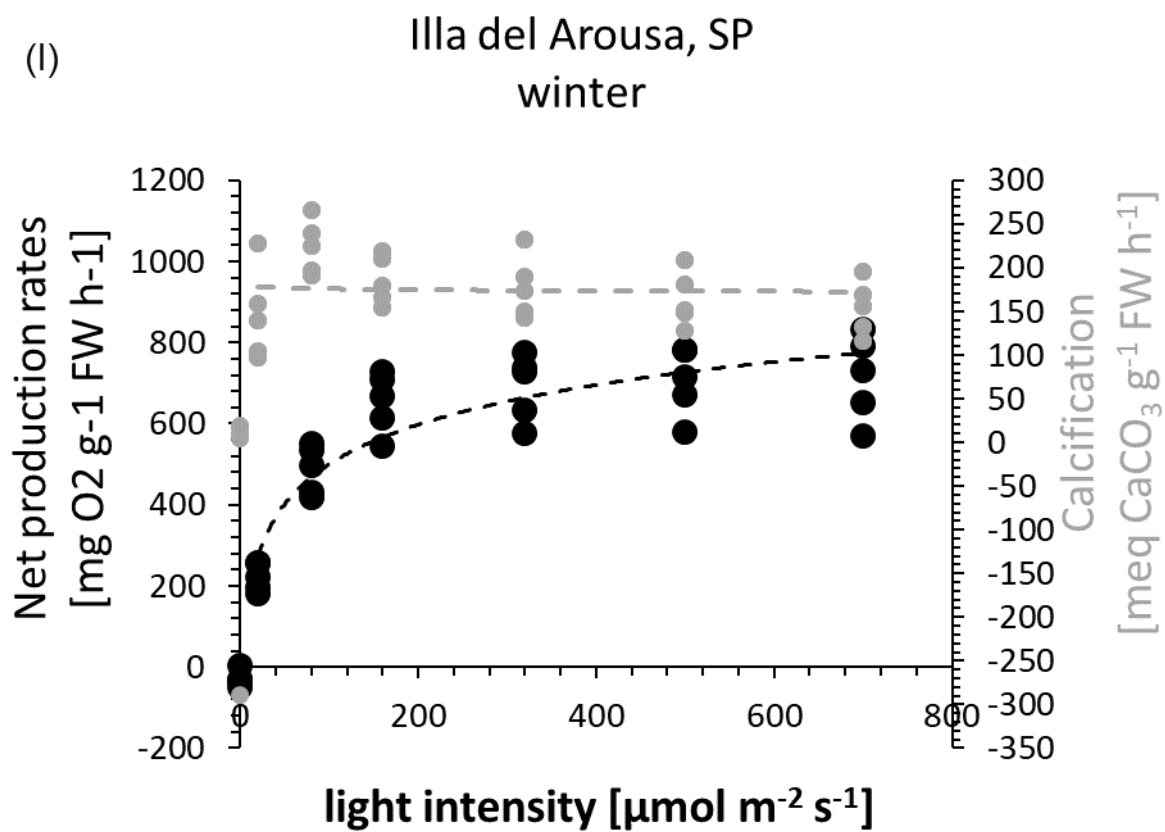
Chapter 3 – Characterisation of  
*Corallina officinalis* across its  
geographical distribution in the NE  
Atlantic











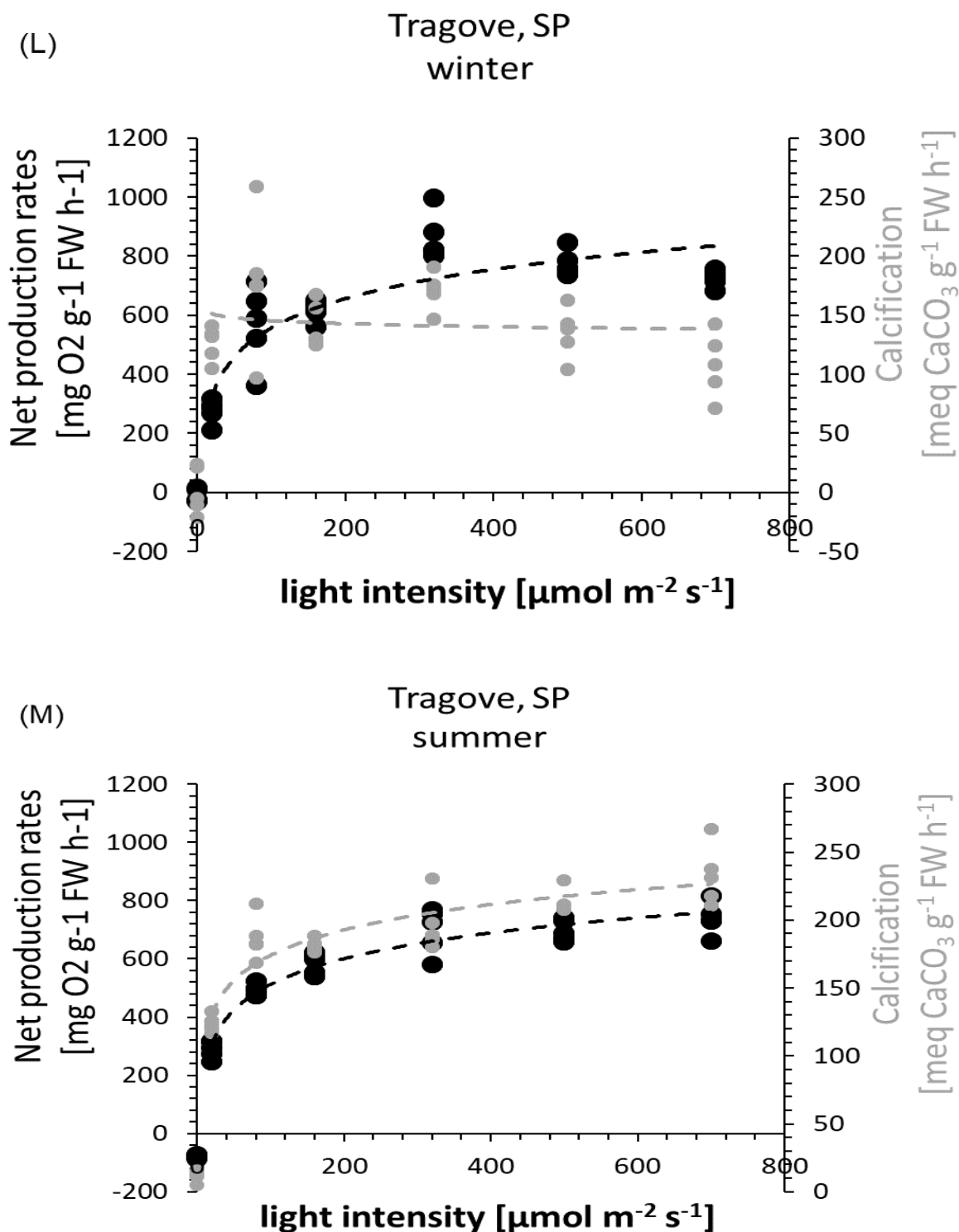


**Figure B1:** P-I and C-I curves of all populations across the geographic distribution of *C. officinalis* in the NE Atlantic and season. A-D, E-H and I-M represent northern, centre and southern populations, respectively. Countries of origin are abbreviated as Iceland (IC), United Kingdom (UK) and Spain (SP). Grey closed circles represent calcification rates, black closed circles represent net production rates. Trend lines are shown as dashed lines of the respective colour.

(A)

# Certificate



Vottunarstofan Tún ehf.  
(EN45011 – ISAC Accreditation No. 11)  
certifies that:

## ALKEMISTINN EHF. Reykjanes, Iceland

has satisfied the requirements for inspection, operating procedures and production methods as specified in the **Tún Standards for Organic Production** for the following:

<b>TYPE OF OPERATION:</b>	<b>Agriculture:</b> Collection of Wild Terrestrial and Marine Plants
<b>CERTIFIED LAND:</b>	<b>Organic:</b> 39.5 ha
<b>CERTIFIED PRODUCTS:</b>	Wild Collected Herbs and Marine Plants
<b>CERTIFICATE RENEWAL DATE</b>	31.12.2015
<b>LICENCE NUMBER:</b>	IS-1 TUN-104

Signed on behalf of Vottunarstofan Tún ehf.

Vottunarstofan Tún ehf. • Tharabakki 3 • IS-109 Reykjavík • Iceland  
Tel: +354 511 1330 • Fax: +354 511 1331 • tun@tun.is • www.tun.is



(B)

# Certificate



Vottunarstofan Tún ehf.  
(EN45011 – ISAC Accreditation No. 11)  
certifies that:

## **ALKEMISTINN EHF.** **Reykjanes, Iceland**

has satisfied the requirements for inspection, operating procedures and production methods as specified in the Tún Standards for Organic Production for the following:

<b>TYPE OF OPERATION:</b>	<b>Agriculture:</b> Collection of Wild Terrestrial and Marine Plants
<b>CERTIFIED LAND:</b>	<b>Organic:</b> 39.5 ha
<b>CERTIFIED PRODUCTS:</b>	Wild Collected Herbs and Marine Plants
<b>CERTIFICATE RENEWAL DATE</b>	31.12.2016
<b>LICENCE NUMBER:</b>	IS-1 TUN-104



Signed on behalf of Vottunarstofan Tún ehf.

Vottunarstofan Tún ehf. • Tharabakki 3 • IS-109 Reykjavík • Iceland  
Tel: +354 511 1330 • Fax: +354 511 1331 • tun@tun.is • www.tun.is

(C)



# Certificate

**Vottunarstofan Tún ehf.**  
 (EN45011 – ISAC Accreditation No. 11)  
 certifies that:

**ALKEMISTINN EHF.**  
**Reykjanes, Iceland**

has satisfied the requirements for inspection, operating procedures and production methods as specified in the **Tún Standards for Organic Production** for the following:

<b>TYPE OF OPERATION:</b>	<b>Agriculture:</b> Collection of Wild Terrestrial and Marine Plants
<b>CERTIFIED LAND:</b>	<b>Organic:</b> 39.5 ha
<b>CERTIFIED PRODUCTS:</b>	Wild Collected Herbs and Marine Plants
<b>CERTIFICATE RENEWAL DATE</b>	31.12.2017
<b>LICENCE NUMBER:</b>	IS-1    TUN-104

  
 \_\_\_\_\_  
 Signed on behalf of Vottunarstofan Tún ehf.

Vottunarstofan Tún ehf. • Tharabakki 3 • IS-109 Reykjavík • Iceland  
 Tel: +354 511 1330 • Fax: +354 511 1331 • tun@tun.is • www.tun.is  
 This certificate is the property of Vottunarstofan Tún ehf. and must be returned immediately on request. Reproduction is prohibited except by written approval of Tún. Its use is subject to compliance with the relevant standards of Vottunarstofan Tún ehf.

**Figure B2:** Certificates of organic certification of northern sampling sites in Iceland from 2015 (A), 2016 (B) and 2017 (C), obtained and kindly provided by Daniel Coaten at the University of Iceland.

For raw data, please follow the link:

<https://figshare.com/s/rk55724d31ebe56b13bf13>

By following the link, you agree not to share the link or any of the content with a third person.

# Appendix C

Chapter 4 – Adaptation of *Corallina officinalis* to temperature regimes across its geographical distribution in the NE Atlantic: A Common Garden Approach

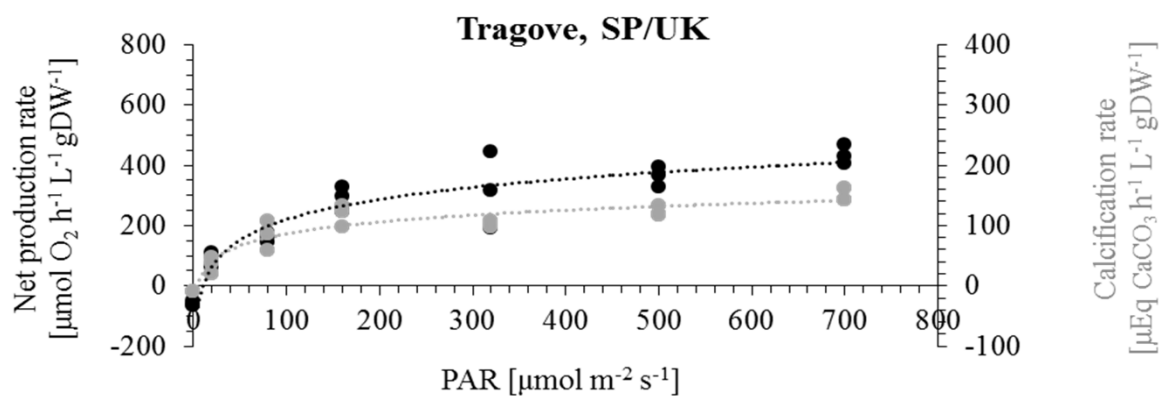


**Figure C1:** Oxygen and calcification evolution curve of the Tragove (southern) population under central conditions. Black plot refers to net production data. Grey plot refers to calcification rates. Trend lines are shown as dashed lines in their respective colour.

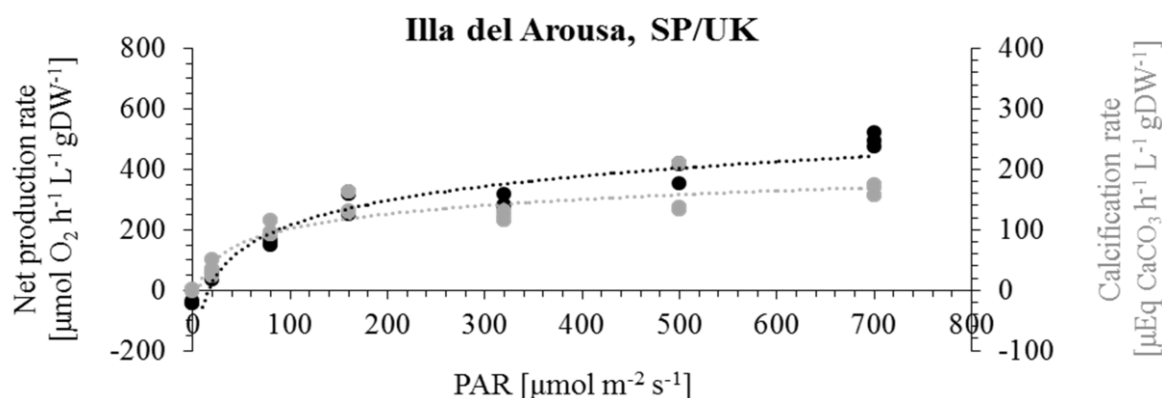


**Figure C2:** Oxygen and calcification evolution curve of the Illa del Arousa (southern) population under central conditions. Black plot refers to net production data. Grey plot refers to calcification rates. Trend lines are shown as dashed lines in their respective colour.

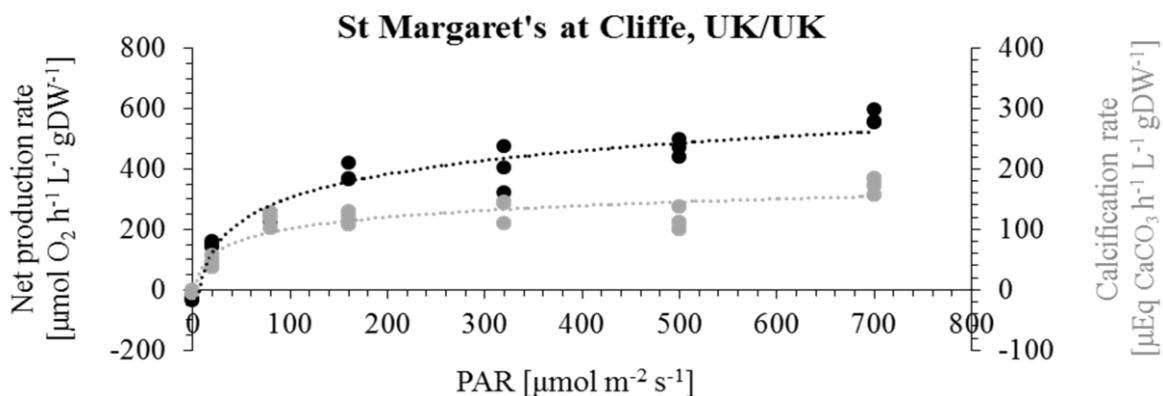


**Figure C3:** Oxygen and calcification evolution curve of the St Margaret's at Cliffe (centre) population under central conditions. Black plot refers to net production data. Grey plot refers to calcification rates. Trend lines are shown as dashed lines in their respective colour.

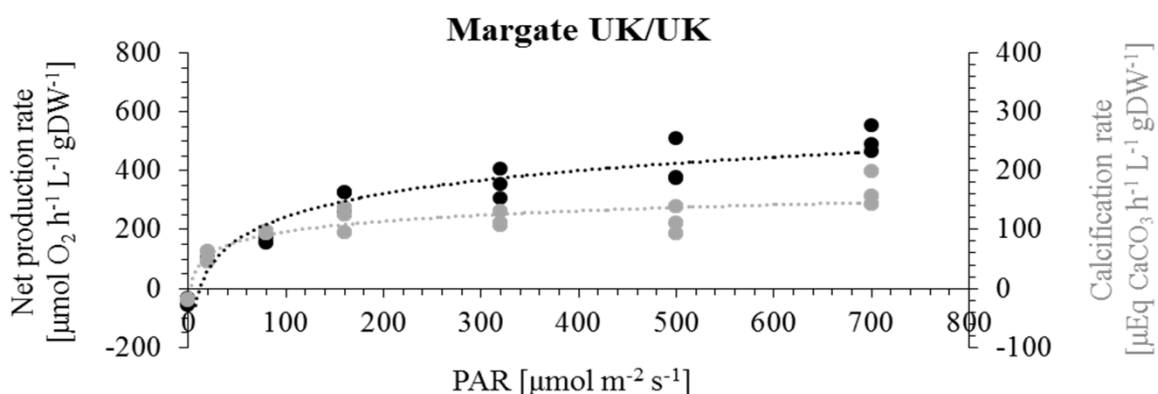


**Figure C4:** Oxygen and calcification evolution curve of the Margate (centre) population under central conditions. Black plot refers to net production data. Grey plot refers to calcification rates. Trend lines are shown as dashed lines in their respective colour.

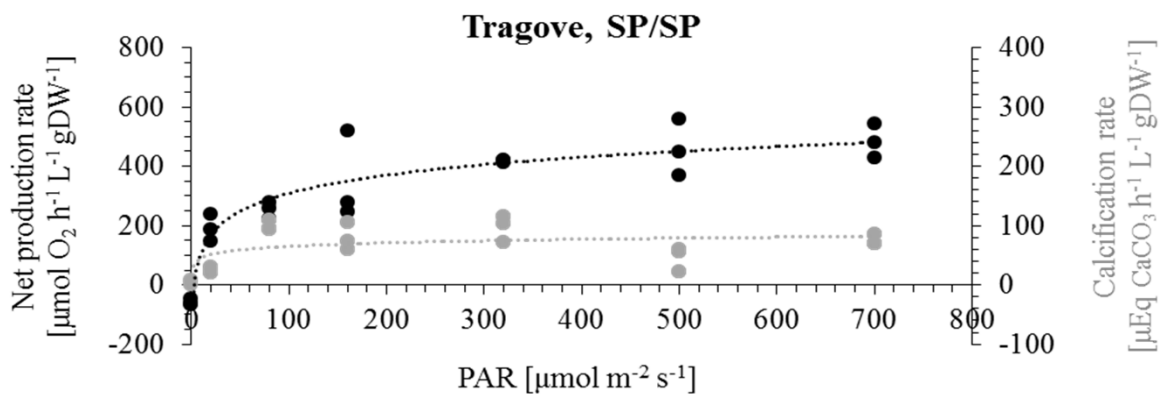


**Figure C5:** Oxygen and calcification evolution curve of the Tragove (southern) population under southern conditions. Black plot refers to net production data. Grey plot refers to calcification rates. Trend lines are shown as dashed lines in their respective colour.

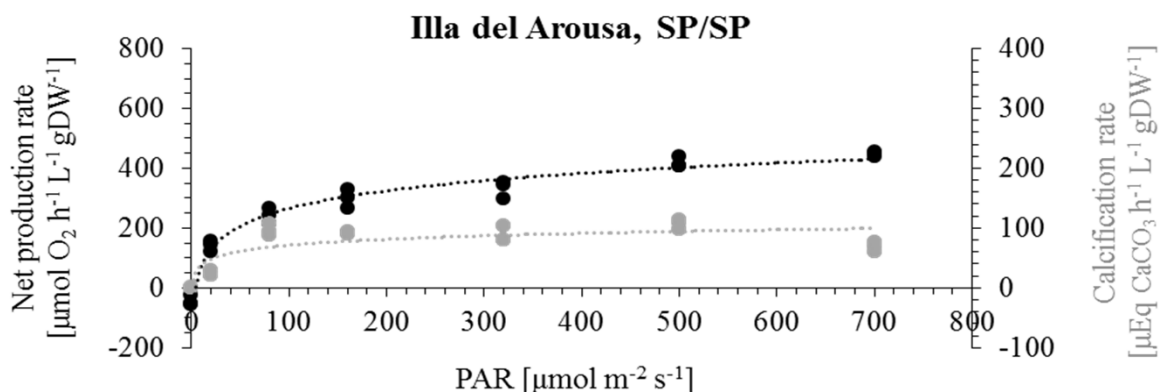


**Figure C6:** Oxygen and calcification evolution curve of the Illa del Arousa (southern) population under southern conditions. Black plot refers to net production data. Grey plot refers to calcification rates. Trend lines are shown as dashed lines in their respective colour.

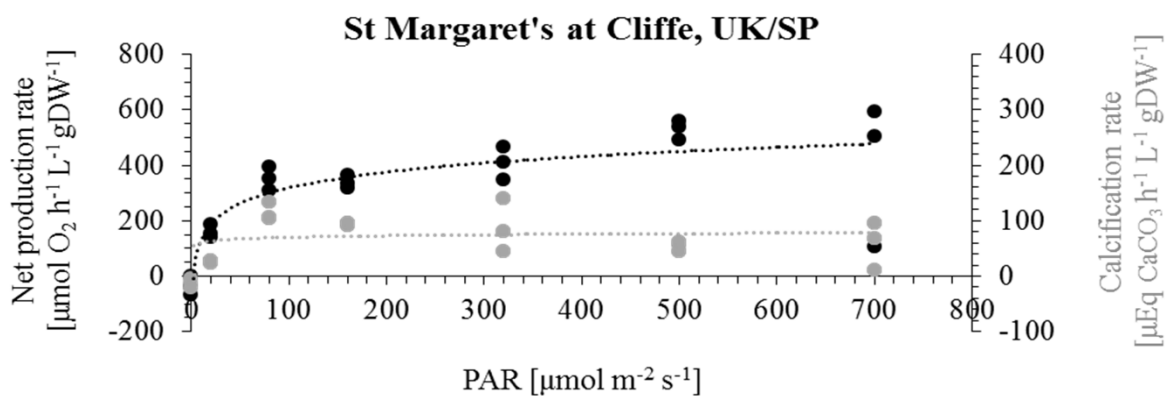


**Figure C7:** Oxygen and calcification evolution curve of the St Margaret's at Cliffe (centre) population under southern conditions. Black plot refers to net production data. Grey plot refers to calcification rates. Trend lines are shown as dashed lines in their respective colour.

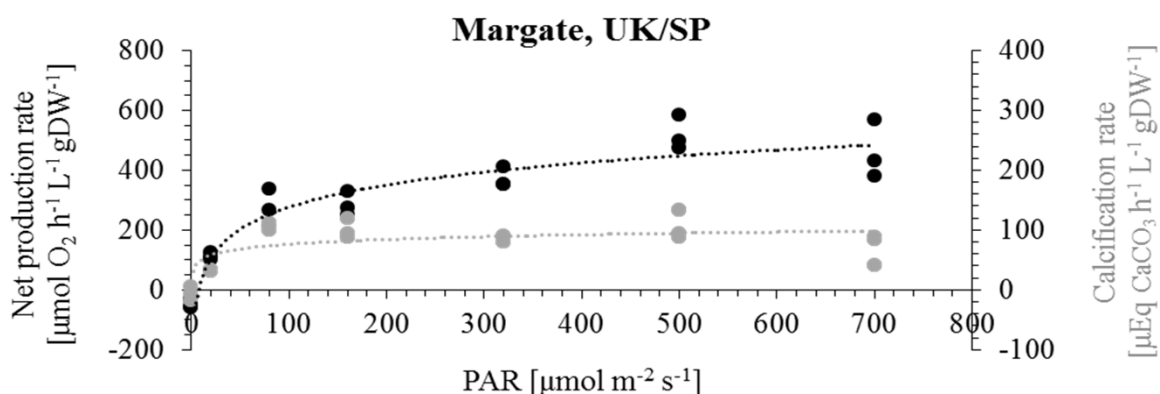


**Figure C8:** Oxygen and calcification evolution curve of the Margate (centre) population under southern conditions. Black plot refers to net production data. Grey plot refers to calcification rates. Trend lines are shown as dashed lines in their respective colour.



See the following publication below:

Kolzenburg, R., Nicastro, K.R., McCoy, S.J., Ford, A.T., Zardi, G.I. and Ragazzola, F., 2019. Understanding the margin squeeze: Differentiation in fitness-related traits between central and trailing edge populations of *Corallina officinalis*. *Ecology and evolution*, 9(10), pp.5787-5801.


Received: 25 January 2019 | Revised: 18 March 2019 | Accepted: 19 March 2019

DOI: 10.1002/ece3.5162

ORIGINAL RESEARCH

Ecology and Evolution  WILEY

## Understanding the margin squeeze: Differentiation in fitness-related traits between central and trailing edge populations of *Corallina officinalis*

Regina Kolzenburg<sup>1</sup>  | Katy R. Nicastro<sup>2</sup> | Sophie J. McCoy<sup>3</sup> | Alex T. Ford<sup>1</sup> | Gerardo I. Zardi<sup>4</sup> | Federica Ragazzola<sup>1</sup>

<sup>1</sup>Institute of Marine Sciences, University of Portsmouth, Portsmouth, UK

<sup>2</sup>Centre of Marine Sciences (CCMAR), University of Algarve, Faro, Portugal

<sup>3</sup>Department of Biological Sciences, Florida State University, Tallahassee, Florida

<sup>4</sup>Department of Zoology and Entomology, Rhodes University, Grahamstown, South Africa

### Correspondence

Regina Kolzenburg and Federica Ragazzola, Institute of Marine Sciences, University of Portsmouth, Portsmouth, UK.  
Emails: regina.kolzenburg@port.ac.uk; federica.ragazzola@port.ac.uk

### Funding information

National Research Foundation; South African Research Chairs Initiative (SARChI), Grant/Award Number: IF/01413/2014/CP1217/CT0004; University of Portsmouth, Grant/Award Number: research development fund (RDF); Fundação para a Ciência e Tecnologia (FCT-MEC), Grant/Award Number: UID/Multi/04326/2013

**Abstract:** Assessing population responses to climate-related environmental change is key to understanding the adaptive potential of the species as a whole. Coralline algae are critical components of marine shallow water ecosystems where they function as important ecosystem engineers. Populations of the calcifying algae *Corallina officinalis* from the center (southern UK) and periphery (northern Spain) of the North Atlantic species natural distribution were selected to test for functional differentiation in thermal stress response. Physiological measurements of calcification, photosynthesis, respiration, growth rates, oxygen, and calcification evolution curves were performed using closed cell respirometry methods. Species identity was genetically confirmed via DNA barcoding. Through a common garden approach, we identified distinct vulnerability to thermal stress of central and peripheral populations. Southern populations showed a decrease in photosynthetic rate under environmental conditions of central locations, and central populations showed a decline in calcification rates under southern conditions. This shows that the two processes of calcification and photosynthesis are not as tightly coupled as previously assumed. How the species as whole will react to future climatic changes will be determined by the interplay of local environmental conditions and these distinct population adaptive traits.

### KEYWORDS

calcification, climate change, common garden experiment, coralline algae, intertidal, photosynthesis, P-I curve, uncoupling

## 1 | INTRODUCTION

Anthropogenic input of carbon dioxide in the atmosphere resulted in a changing climate over the past decades and might further fuel global climate change in future centuries (IPCC, 2013). Key components of climate change in the ocean are ocean acidification (OA; decreasing pH and  $\Omega\text{CO}_3^-$ ) and rising sea surface temperatures.

Living organisms already experience effects of climatic changes and will continue to be critically affected by these changes (Bentz et al., 2010; Lesica & McCune, 2004; Sanford, Holzman, Haney, Rand, & Bertness, 2006). Investigating and monitoring organism physiology provides important information to predict their acclimatization and resilience to future environmental conditions and potential changes in their distribution (Kelly & Hofmann, 2013).

This is an open access article under the terms of the Creative Commons Attribution License, which permits use, distribution and reproduction in any medium, provided the original work is properly cited.

© 2019 The Authors. *Ecology and Evolution* published by John Wiley & Sons Ltd.

*Ecology and Evolution*, 2019, 1–15.

www.ecolevol.org | 1

It is suggested that the geographic center of a species distribution holds the most favorable conditions and therefore holds the highest population density (Brussard, 1984; Whittaker, 1956). When moving away from the center toward the margins of the distribution, environmental variables are thought to become less favorable due to greater abiotic stress and increased interspecific competition (Aitken, Yeaman, Holliday, Wang, & Curtis-McLane, 2008), initiating a decrease in population densities and lower relative fertility (Case & Taper, 2000). Further, Watkinson and Sutherland (1995) described a higher mortality than recruitment rate for local marginal populations, also called sink populations, whose survival depends on influx of zygotes or spores from source populations. Species react differently to environmental changes. In terrestrial studies, Franco et al. (2006) showed that three out of four butterfly species are reported extinct or showed drastic distributional changes due to climate change along with habitat degradation and loss. Another study by Lesica and McCune (2004) showed that the southern margin of arctic-alpine indicator plants species declined in their abundance within 13 years which is caused by increasing average summer temperatures. Previous research has also found that different populations of the same species respond differently to altered environmental conditions (Bozinovic, Calosi, & Spicer, 2011; Calosi et al., 2017; Gaston, 2009). In the marine environment, a number of studies across several taxonomic groups, for example, fish, molluscs, zooplankton, or seaweed, have focused on the diversification of populations along a thermal-latitude gradient (Bennett, Wernberg, Arackal Joy, Bettignies, & Campbell, 2015; Dam, 2013; Lucassen, 2013; Morley, Hirse, Pörtner, & Peck, 2009).

Calcifying organisms are at the forefront of those affected by climatic changes and can therefore act as indicator species for induced impacts on marine organisms. One of the major groups affected by climate change is calcifying benthic macroalgae (Kroeker et al., 2013). Amongst those are coralline red algae (Corallinales, Rhodophyta) which are critical components of marine shallow water ecosystems from polar regions to the tropics (Adey & MacIntyre, 1973; Steneck, 1986). They function as important ecosystem engineers and play a crucial role as an essential structural element in the majority of rocky coastal zones (Benedetti-Cecchi, 2006; Dayton, 1972; van der Heijden & Kamenos, 2015; Johansen, 1981; Jones, Lawton, & Shachak, 1994; Kelaher, Chapman, & Underwood, 2001; Nelson, 2009; Noël, Hawkins, Jenkins, & Thompson, 2009). They often form complex, extremely dense, and highly branched turfs which are considered the extreme end of algal structural complexity (Coull & Wells, 1983; Davenport, Butler, & Cheshire, 1999). Branches consist of calcified segments (intergenicula), which are produced through high-magnesium (Mg) calcite precipitation in the cell walls, and noncalcified segments (genicula); this structure provides flexibility and elasticity for every individual branch (Martone & Denny, 2008). Coralline turf is highly variable, with frond length and density differing at small spatial scales; they can host abundant and diverse macrofaunal assemblages with up to 250,000 individuals per m<sup>2</sup> (Kelaher et al., 2001). In addition, macroalgal physiological processes such as photosynthesis and respiration alter CO<sub>2</sub> and HCO<sub>3</sub><sup>-</sup>

in the water in the intertidal environment. This causes changes in pH across diurnal as well as spatial scales related to species distributions (Morris & Taylor, 1983; Williamson et al., 2014; Williamson, Perkins, Voller, Yallop, & Brodie, 2017). Depending on the extent of these changes in the carbonate chemistry and especially in combination with the climatic changes named above, calcification of coralline algae can be severely affected.

Geniculated coralline algae (also known as articulated coralline algae), like *Corallina officinalis*, form turfs across large areas on hard substratum in the intertidal ecosystems of the Northeast Atlantic. *C. officinalis* is commonly found in sheltered, low intertidal zones, where it primarily inhabits the lower part of rock pools and channels that remain damp or filled during extreme tides or conditions, and at the edge of the intertidal to subtidal zones (Digby, 1977; Egilsdottir, Noisette, Noel, Olafsson, & Martin, 2013; Williamson et al., 2014). In order to maintain their abundance in temperate intertidal ecosystems, coralline algae are suggested to have a good ability to adapt to great and fast changes in environmental conditions, such as solar irradiance, physical stress, water temperature, or carbonate chemistry (e.g., large pH variations) which fluctuate tidally, diurnal, monthly, and seasonally (Egilsdottir et al., 2013; Hofmann et al., 2014; Martone, Alyono, & Stites, 2010; Williamson et al., 2014).

In particular, temperature is one of the main factors governing the small-scale vertical distribution of macroalgae on a shore (Lüning, 1990) and the large-scale geographical distribution of macroalgal species (Ganning 1971). At the organism level, temperature regulates major chemical reactions, which in turn affect metabolic pathways (Lobban & Harrison, 1994). For example, carbonic anhydrase (CA) is affected by temperature altering the carbon fixation pathways in photosynthesis (Lobban & Harrison, 1994). Water temperature affects recruitment, survival, growth as well as reproduction of macroalgae (Breeman, 1988) and thus drives the species' distribution (Breeman, 1988; Lüning, 1990). Most importantly, current increase in global temperature, and therefore a possible exceeding of the species' temperature threshold, is causing species-level responses in macroalgae, such as species range shifts (reviewed by Helmuth, Mieszkowska, Moore, & Hawkins, 2006; Nicasro et al., 2013; Smale & Wernberg, 2013; Parmesan, 2006; Wernberg et al., 2011). This ongoing temperature increase, and what is predicted for future scenarios, is causing a chronic, due to gradual warming, or an acute stress, due to extreme temperature events (Brodie et al., 2014). Adaptations will need to include facilitation of all metabolic processes at elevated temperatures, especially those for photosynthesis, respiration, calcification, and therefore growth. Hofmann, Straub and Bischof (2012), Hofmann, Yildiz, Hanelt, and Bischof (2012), Egilsdottir et al. (2013), and Noisette et al. (2013) found that with ongoing climate change, and therefore worsening OA and rising water temperatures, interactions between coralline algal physiology and variable environmental parameters are likely to be significantly negatively affected.

It remains unclear how and whether the wider distributed, turf-forming algae *C. officinalis* will be able to withstand such changes. It is likely that the species as a whole will show some resilience

when exposed to predicted climate change conditions. However, it is uncertain which areas or portions of the species distribution will be affected the most by the changes. At present, there are very few studies regarding the physiological responses of intertidal benthic organisms to current climate conditions across its distribution (reviewed by Helmuth et al., 2006; Diez, Muguerza, Santolaria, Ganzedo, & Gorostiaga, 2012). This gap in knowledge complicates the establishment of detailed predictions for this species future (Brodie et al., 2014; Nelson, 2009; Williamson et al., 2017). In this study, physiological responses (photosynthesis, respiration, calcification, photosynthesis-irradiance curves, and calcification-irradiance curves) of *C. officinalis* across its natural distribution in the eastern North Atlantic were investigated using the approach of common garden experiments. England was chosen as central population for this study, referring to confirmed genetic data by Brodie, Walker, Williamson, and Irvine (2013). Spain was studied representing the southern margin of the species distribution (Williamson et al., 2015).

We hypothesized that central populations are more robust to elevated temperatures and therefore are able to adapt to the temperature conditions already experienced by southern populations. In contrast, we predicted that southern populations will be able to adapt to the most favorable central conditions.

## 2 | MATERIAL AND METHODS

### 2.1 | Species collection

Specimens ( $n = 72$ ) of *Corallina officinalis* Linnaeus populations ( $n = 2$ ) were collected intertidally, during low tide in an average depth of 0.31 m from the water surface at sites in the South East Coast of the UK (central population 1: St Margarets Bay: N 51.148056, E 1.385056; population 2: Westbrook Bay: N 51.388840, E 1.367170; beeline distance between populations: 26.85 km) and the North West Coast of Spain (southern margin population 1: Illa del Arousa: N 42.56870, W 8.89171; population 2: Tragove: N 42.52444, W 8.82772; beeline distance between populations: 7.19 km) in February 2017. Specimens were transported into the laboratory at the Institute of Marine Sciences of the University of Portsmouth, UK, using temperature-insulating containers. Only healthy specimens without epiphytes and indication of bleaching or damage were selected for this study.

### 2.2 | Species identification

To verify species identification, genomic DNA was extracted from three replicates of each population using PowerSoil DNA Isolation Kit (MoBio Laboratories, Carlsbad, CA) in accordance with the manufacturer's instructions. Partial amplification of around 664-bp fragment of standard DNA barcode region (COI-5P) was performed using primers GazF1 and GazR with polymerase chain reaction conditions described in Pardo, Peña, Berreiro, and Bárbara (2015). Amplified fragments were run in an ABI PRISM 3130xl automated

capillary sequencer (Applied Biosystems, CCMAR Portugal). MtDNA sequences were aligned, proofread, and edited in GENEIOUS 3.8 (Drummond et al., 2011). Determination of taxonomic status was made by comparing the sequences obtained in our study to published sequences retrieved from GenBank. For *Corallina officinalis*: BM000806013, BM000804477, BM000804459, BM000804370, BM000804472 (Williamson et al., 2015). For *Ellisolandia elongata*: JQ615843, BM000806006 (Williamson et al., 2015), KF461004, KF461018, KF461017 (Pardo et al., 2015). For *Corallina caespitosa*: BM000806012, BM000804521, BM000804492, BM000804378, BM000806003 (Williamson et al., 2015). Following an alignment and trimming of GenBank sequences and the ones from this study, pairwise sequence similarity scores were calculated using CLUSTALW multiple sequence alignment program (Thompson, Higgins, & Gibson, 1994; Table 1).

### 2.3 | Experimental setup

In the laboratory, specimens were carefully placed upright onto a rock in the water, held in place with a net (2 mm mesh size) in order to simulate natural conditions and each population was color coded for future identification. Aquaria of 11.1 L ( $n = 3$ ) for each of the two countries and temperature conditions (total  $n = 12$ ) were set up in a water bath (for detailed setup see Figure 1). 75% of the water in the replicate aquaria was changed every second day and treated with UV light (P2-110W Commercial UV Steriliser, max. flow rate: 65 L/min. Tropic Marine Centre (TMC), London, UK) prior to the disposal. Temperature conditions were kept constant using TK-2000 chillers (cooling capacity of 870 W, 800 L/hr. TECO, Ravenna, Italy). Each aquarium was equipped with a water pump (V<sup>2</sup>PowerPump 800, Flow rate: 700 L/hr. TMC, London, UK) and an air stone to simulate tidal water movements and ensure oxygen supply with ambient air. Specimens were kept at their respective local in situ temperatures measured during sampling (central conditions: temperature: 5.7°C, light: 57  $\mu\text{mol m}^{-2} \text{s}^{-1}$ ; southern conditions: temperature: 11.3°C, light: 184  $\mu\text{mol m}^{-2} \text{s}^{-1}$ ). Both treatments were subject to a light:dark cycle of 10:14 hr (taken from the average of natural conditions of center and southern locations) produced and controlled by AQUABEAM 600 Ultima Reef White lights with cloud function (TMC, London, UK). Additionally, sunset and sunrise were mimicked through a slow increase and decrease of light intensities over a period of 1 hr. All specimens were kept in their corresponding conditions for a minimum of 1 week to acclimate to aquaria conditions. Following the initial acclimatization,

**TABLE 1** Pairwise sequence similarity scores (%)

	<i>Corallina officinalis</i> —this study
<i>Corallina officinalis</i> —Williamson et al. (2015)	99.59–100
<i>Corallina caespitosa</i> —Williamson et al. (2015)	89.79–92.24
<i>Ellisolandia elongata</i> —Williamson et al. (2015) & Pardo et al. (2015)	83.67–84.89

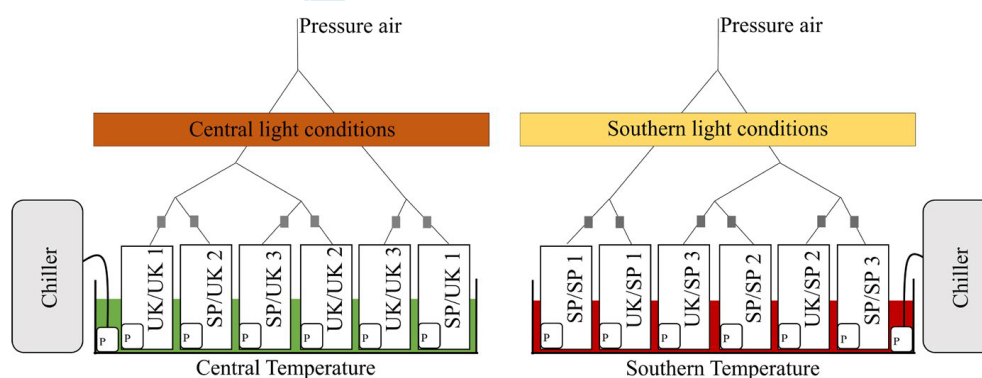


**FIGURE 1** Detailed schematic of the common garden experiment setup. Representing central (UK) conditions on the left in green and dark orange and southern (Spanish, SP) conditions on the right in red and light orange. Squares with "P" represent installed pumps for water movement. Gray squares represent pressure air adjustment valves

half of the central and southern populations were gradually acclimatized (increase/decrease of  $1.5^{\circ}\text{C}/\text{week}$  and  $40 \mu\text{mol m}^{-2} \text{s}^{-1}/\text{week}$ , respectively) to the opposite temperature and light conditions over a period of 3.5 weeks. After acclimatization, specimens were randomly and equally distributed within the corresponding replicate aquaria and kept for three months (Figure 1).

#### 2.4 | Monitoring of water parameters

Temperature, salinity, dissolved oxygen, pH, and total alkalinity ( $A_T$ ) were monitored daily. Irradiance was measured once a month to monitor the decrease in light intensity using a HOBO UA-002-64 Pendant Temp/Light data logger (accuracy:  $0.47^{\circ}\text{C}$ , resolution:  $0.1^{\circ}\text{C}$ . Tempcon, Arundel, UK). Temperature and salinity were measured with a CO310-1 portable salinity and temperature probe (accuracy: 0.2% for salinity,  $\pm 0.2^{\circ}\text{C}$  for temperature; resolution: 0.1 for salinity,  $0.1^{\circ}\text{C}$  for temperature. VWR, Leicestershire, UK). Dissolved oxygen and pH were measured with an HQ30d portable multi-parameter meter and a luminescent dissolved oxygen (LDO101, accuracy:  $\pm 0.1 \text{ mg/L}$ . HACH, Manchester, UK) and pH probe (PHC301, accuracy:  $\pm 0.02 \text{ pH}$ , HACH, Manchester, UK. Calibrated on the National Bureau of Standards (NBS) scale and converted into total scale values using Tris/HCl and 2-aminopyridine/HCl buffer solutions after Dickson, Sabine, and Christian (2007)).  $A_T$  was monitored daily in one randomly chosen replicate for each treatment, using the alkalinity anomaly technique after Smith and Key (1975), Chisholm and Gattuso (1991), and Dickson et al. (2007), (SOP 3b).  $A_T$  titrations were carried out with an automatic titrator TitroLine 7000 (measurement accuracy:  $0.002 \pm 1$  digit, dosing accuracy: 0.15%, dosing precision: 0.05%–0.07%. Schott SI Analytics, Mainz, Germany) to ensure minimal variation. As titrant, 0.1N hydrochloric acid (HCl) was used, which was validated against Certified Reference Material provided by Andrew G. Dickson (Batch 154, Scripps Institution of Oceanography).

#### 2.5 | Physiological incubation procedures and measurements

To determine saturating light levels of *C. officinalis* populations before and after the experiment, the oxygen production (P-I curve) and calcification (C-I curve) evolution under increasing light conditions were measured. For this,  $0.97 \pm 0.07 \text{ g}$  fresh weight of algal fronds was transferred into a clear closed cell 58 ml incubation chamber and incubated successively for 1 hr at each of the seven different light intensities (0, 20, 80, 160, 320, 500, and  $700 \mu\text{mol m}^{-2} \text{s}^{-1}$ ; AQUARAY Nature Perfect, TMC, London, UK), starting from the lowest to the highest to minimize stress. Three replicates per light intensity were incubated simultaneously and bubble-free. To account and correct for metabolism effects by other organisms, reference incubations without algae were performed alongside the above-described incubations for all light intensities. Aluminum foil was used to coat the chambers to determine calcification and respiration rates in the dark. Irradiance was measured with a Quantitherm PAR/Temperature Sensor with a QTP1 probe (resolution:  $1 \mu\text{mol m}^{-2} \text{s}^{-1}$ ,  $0.02^{\circ}\text{C}$ , respectively. Hansatech, Norfolk, UK).

Differences in oxygen concentration, pH, and  $A_T$  were determined in order to calculate photosynthesis, respiration, and calcification rates by measuring oxygen, pH, and  $A_T$ , respectively, before and after the incubations. Prior to the  $A_T$  measurements, seawater samples were filtered through a syringe filter (hydrophilic 25 mm,  $0.2 \mu\text{m}$  PTFE. Fisherbrand, Loughborough, UK) into sterile 50 ml tubes (Plastic Centrifuge Tubes. Fisherbrand, Loughborough, UK). Immediately after, potentiometric titrations were performed using an automatic titrator (details: see above) calibrated on the NBS scale. Results were calculated based on a Gran function after Dickson et al. (2007). The carbonate system of the seawater was calculated from pH,  $A_T$ , salinity, and temperature using the Excel Macro CO2Sys (Version 2.1, Lewis & Wallace, 1998) with K1 and K2 according to Mehrbach, Culberson, Hawley, and Pytkowicz (1973) and refit by Dickson and

**TABLE 2** Carbonate system parameters of the whole setup during the 3-month culturing of *Corallina officinalis*. All numbers are mean values ( $n = 81 \pm SD$ ). pH, salinity, temperature, and total alkalinity ( $A_T$ ) were measured while the other parameters were calculated

Treatment	pH (total scale)	Sal	T [°C]	$A_T$ [ $\mu\text{mol/kg}$ ]	DIC [ $\mu\text{mol/kg}$ ]	$\text{HCO}_3^-$ [ $\mu\text{mol/kg}$ ]	$\Omega_{\text{Ca}}$	$\Omega_{\text{Ar}}$	$\text{pCO}_2$ [ $\mu\text{atm}$ ]
Center	$8.19 \pm 0.07$	$32.9 \pm 0.6$	$5.70 \pm 0.73$	$2,344 \pm 43$	$2,185.9 \pm 46.6$	$2049.1 \pm 50.6$	$2.32 \pm 0.27$	$1.48 \pm 0.17$	$377 \pm 61$
South	$8.22 \pm 0.08$	$33.2 \pm 0.5$	$11.33 \pm 0.39$	$2,326 \pm 37$	$2,100.0 \pm 46.4$	$1925.6 \pm 54.3$	$3.23 \pm 0.30$	$2.08 \pm 0.19$	$319 \pm 45$

Millero (1987) (Table 2). Measurement ranges of pH values represent in situ values and are highly dependent on temperature.

To determine changes in photosynthesis, respiration, and calcification rates most likely to be found in the field, additional incubations ( $n = 3$ ) of all treatments at ambient light conditions ( $57 \mu\text{mol m}^{-2} \text{s}^{-1}$  for center and  $184 \mu\text{mol m}^{-2} \text{s}^{-1}$  for southern populations) were performed before and after the study following the protocol above. Calculations were performed following the methodology described above.

The weight of algae fronds used in the incubations was transformed from FW into dry weight (DW) by multiplying FW measurements with the factor 0.62286. This factor was determined from FW and DW weight measurements of thirty 1 g frond bundles from all populations before and after algae were left to dry for 48 hr in an oven at  $60^\circ\text{C}$ .

## 2.6 | Data and statistical analysis

The maximum potential photosynthetic rate per individual ( $P_{\text{max}}$  [ $\text{mg O}_2 \text{g}^{-1} \text{FW hr}^{-1}$ ]) was directly determined from the oxygen evolution curves, whereas the slope of the light-limited region of the P-I curve stating the efficiency of the algae to harvest light ( $\alpha$ ) was calculated using Excel. The irradiance at which photosynthesis is saturated ( $I_k$  [ $\mu\text{mol m}^{-2} \text{s}^{-1}$ ]) was calculated using the following relationship:

$$I_k = \frac{P_{\text{max}}}{\alpha} \quad (1)$$

Primary production was measured using oxygen fluxes such as photosynthesis ( $P_N$  [ $\text{mg O}_2 \text{g}^{-1} \text{FW hr}^{-1}$ ]) and respiration ( $R$  [ $\text{mg O}_2 \text{g}^{-1} \text{FW hr}^{-1}$ ]) and was calculated as follows:

$$P_N \text{ or } R (\text{O}_2) = \left( \frac{\Delta \text{O}_2 \times V}{\Delta t \times \text{FW}} \right) \quad (2)$$

with  $\Delta \text{O}_2$  as the change in dissolved oxygen concentration [ $\text{mg/L}$ ],  $V$  as the volume of the incubation chamber [ $\text{L}$ ],  $\Delta t$  as the incubation time [ $\text{hr}$ ], and FW as the fresh weight of the algae.

Calcification ( $G$  [ $\text{meq CaCO}_3 \text{g}^{-1} \text{FW hr}^{-1}$ ]) rates were estimated using the following equation:

$$G (\text{CaCO}_3) = - \left( \frac{\Delta A_T \times V}{2 \times \Delta t \times \text{FW}} \right) \quad (3)$$

with  $\Delta A_T$  as the change in total alkalinity [ $\text{meq/L}$ ].

All analyses were run in SPSS Statistics 24 (IBM Corp, 2016), and data were tested for normality and homogeneity prior analyses (Shapiro-Wilk and Levene's test, for  $p$  values, Table S1, see Data Repository). Data for net production ( $n = 3$ ) were not normally distributed, resulting in statistical analysis using the nonparametric Kruskal-Wallis  $H$  test. Data for respiration ( $n = 3$ ) as well as dark calcification ( $n = 3$ ) measurements showed a significant Levene's test with raw as well as transformed data due to high variance. Therefore, data were analyzed using multiple single comparisons of one-way analysis of variance (ANOVA). Normally distributed data of the dependent variable light calcification ( $n = 3$ ) were analyzed using two-way ANOVAs for individuals from each country of origin (UK (center) or

SP (southern margin)) with treatment (three levels: pre-experiment, central conditions, and southern conditions) as the fixed factor. When significant effects were found, data were further explored by running a post hoc Tukey's HSD test. Tests were performed for central and southern populations under each temperature condition comparing measurements before and after the experiment.

Additional two-way ANOVAs and Tukey's HSD post hoc tests of central and southern populations were performed to identify significant differences in their maximum oxygen production and calcification level of all populations in all temperature treatments.

### 3 | RESULTS

The experimental setup allowed for very stable parameters under all conditions and was not unexpectedly influential toward physiological behavior of specimens. All samples were identified as *C. officinalis*. Sequences have been submitted to Gene Bank (accession numbers central populations: Bankit2159662 COUK1 MK072600 - Bankit2159662 COUK6 MK072605 and southern populations: Bankit2159662 COSP1 MK072606 - Bankit2159662 COSP6 MK072611).

#### 3.1 | P-I and C-I curves

The average saturating light levels ( $P_{max}$ ) for all populations of one country did not differ between central or southern temperature conditions after 3 months of culturing (Figure 1; Figures A1–A8 in Appendix A).  $P_{max}$  of central populations was ~1.8 and ~1.2 times higher than of southern populations under southern and central conditions, respectively. Central population 1 showed a significant difference versus southern populations under central conditions ( $p < 0.05$ , Tukey HSD  $p < 0.05$ , 2-way ANOVA in both cases). Southern population 1 showed a significant difference versus central populations under southern conditions ( $p < 0.05$ , Tukey HSD  $p < 0.05$ , 2-way ANOVA in both cases). The photosynthetic efficiency,  $\alpha$ , of central populations did not differ in both treatments. However, all southern populations under central conditions showed up to 50% less light harvesting efficiency than under southern conditions. The saturating light intensity  $I_k$  of all populations was noticeably higher in central than in southern populations, under southern conditions, but very similar under central conditions. Southern populations developed a ~50% higher saturating light intensity in central (~85  $\mu\text{mol m}^{-2} \text{s}^{-1}$ ) than under southern conditions (~44  $\mu\text{mol m}^{-2} \text{s}^{-1}$ ).

The average saturating calcification levels ( $C_{max}$ ) were ~1.54 times significantly higher under central compared to southern conditions in all four populations ( $p < 0.005$ , Tukey HSD  $p < 0.005$ , 2-way ANOVA for all four cases) (Figure 2; Figures A1–A8 in Appendix A). The calcification efficiency  $\alpha$  was higher under central than under southern conditions. Central populations showed a slightly higher efficiency than southern populations under both temperature conditions (Figure 2). Central populations showed a decrease in efficiency under southern conditions by a factor of 1.6 compared to central

conditions. Southern populations showed an increasing trend by a factor of ~1.68 in light harvesting efficiency in central compared to southern populations. The saturating light intensity  $I_k$  did not change drastically in southern populations when acclimatized to southern or central conditions. In central populations, however,  $I_k$  increased by 132.5% (~19  $\mu\text{mol m}^{-2} \text{s}^{-1}$ ) under southern conditions in comparison to central conditions.

Photoinhibition of photosynthesis rates was not observed in any of the populations;  $P_{max}$  was reached in all populations and treatments. Inhibition of calcification was observed in all populations under southern conditions.

#### 3.2 | Photosynthesis and respiration

*Corallina officinalis* net production rates (Figure 3) in central populations did not change significantly in the different conditions over the course of the experiment. Contrary to central population 1, central population 2, however, showed significantly lower primary production rates under southern compared to central conditions after the experiment ( $p < 0.05$ , Kruskal–Wallis  $H$  test). Southern populations showed a similar oxygen production rate before and after the experiment under southern conditions. Central populations showed lower oxygen production rates under southern conditions but higher rates under central conditions compared to pre-experiment measurements (Figure 3). Only southern population 2 showed a significant negative change in production rates, actually resulting in respiration rates, under central experimental conditions compared to starting conditions ( $p < 0.05$ , Kruskal–Wallis  $H$  test). When comparing populations within regions, none of the central or southern populations were significantly different within each other before the experiment. However, central populations were significantly different from southern population 1 prior to the experiment ( $p < 0.05$ , Kruskal–Wallis  $H$  test).

Respiration rates of central populations (Figure 3) did not change significantly throughout the experiment despite a positive trend under central conditions and were stable under southern conditions. Respiration rates of southern populations were stable under southern conditions, whereas they increased significantly under central compared to southern conditions ( $F_{1,5} = 25.346$  and  $F_{1,5} = 21.848$  for southern populations 1 and 2, respectively,  $p < 0.01$ , 1-way ANOVA for both southern populations). Central populations showed a significant difference between each other after the experiment under both temperature treatments ( $F_{1,5} = 36.975$  and  $F_{1,5} = 26.769$  for central populations 1 and 2, respectively,  $p < 0.01$ , 1-way ANOVA in both cases). Comparing populations, none of the populations within a region were significantly different from each other before the experiment. Under central as well as southern conditions, all central populations were significantly different from all southern populations (Under central conditions:  $F_{1,5} = 19.119$  for UK1 vs. SP1,  $F_{1,5} = 18.837$  for UK1 vs. SP2,  $F_{1,5} = 16.455$  for UK2 vs. SP1,  $F_{1,5} = 16.431$  for UK2 vs. SP2,  $p < 0.05$ , 1-way ANOVA for all cases; under southern conditions:  $F_{1,5} = 130.367$  for UK1 vs. SP1,  $F_{1,5} = 125.643$  for UK1 vs.



SP2,  $F_{1,5} = 61.485$  for UK2 vs. SP1,  $F_{1,5} = 60.270$  for UK2 vs. SP2,  $p < 0.01$ , 1-way ANOVA for all cases) but not significantly different from each other.

### 3.3 | Calcification

Calcification rates in light (Figure 4) were significantly different before and after the experiment under southern conditions for southern

population 1 ( $p < 0.05$ , Tukey HSD  $p < 0.05$ , 2-way ANOVA), but not for southern population 2. Under central conditions, southern populations showed a nonsignificant decrease of calcification rates. In contrast to central population 2, central population 1 showed a significant increase in calcification rates in the light under central conditions ( $p < 0.05$ , Tukey HSD  $p < 0.01$ , 2-way ANOVA) and both showed a highly significant lower rate under southern conditions ( $p < 0.01$ , Tukey HSD  $p < 0.01$ , 2-way ANOVA in both cases) compared to

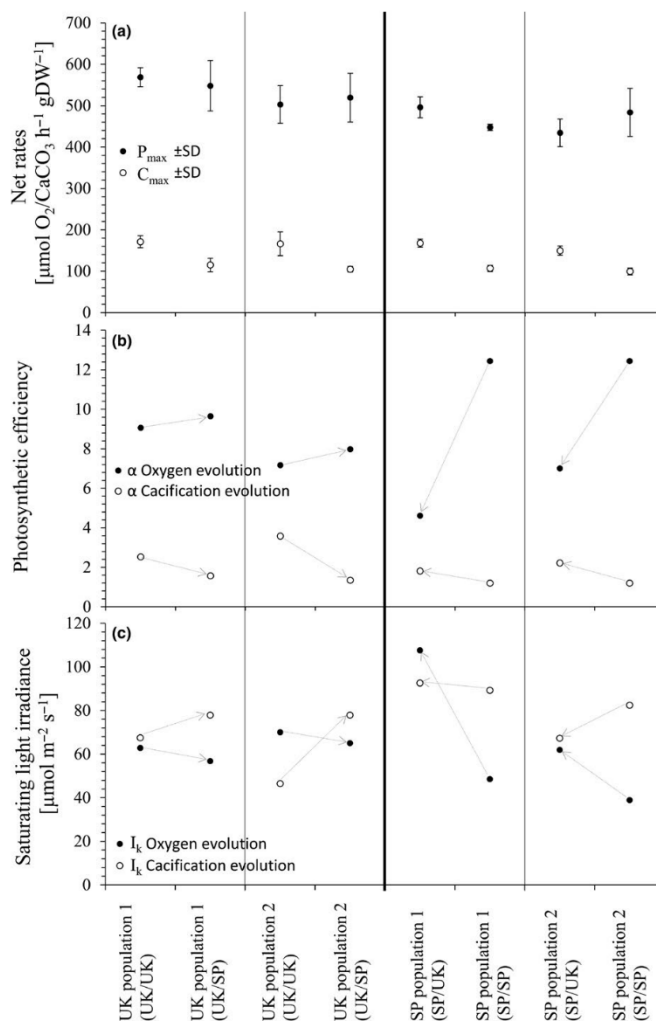


**FIGURE 2** Evolution curve characteristics for net production and calcification ( $AV \pm SD$ ,  $n = 3$ ) of the central (UK) and southern (SP) populations ( $n = 2$ ) under both southern (SP) and central (UK) conditions. (a)  $P_{max}/C_{max}$  = maximum production, (b)  $\alpha$  = initial slope as indicator for photosynthetic efficiency, (c)  $I_k$  = saturating irradiance. Arrows indicate direction of change from original to altered conditions. For detailed graphs, see Figures A1–A8 in Appendix A. Statistical differences are summarized in Table S1 of the supplementary document

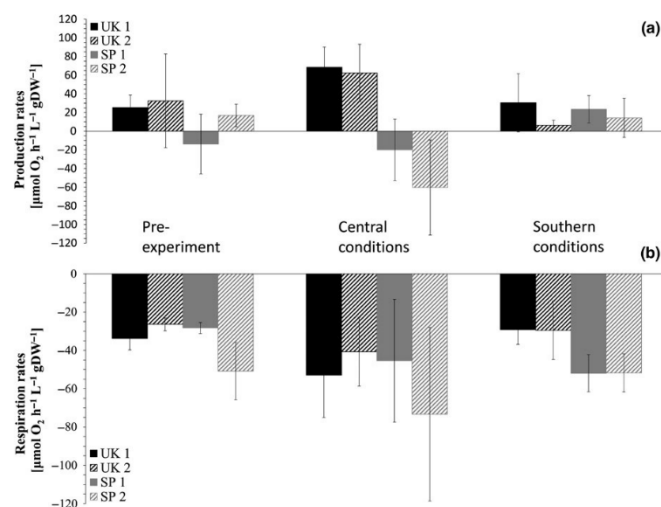


**FIGURE 3** (a) Primary production and (b) respiration rates [ $\mu\text{mol hr}^{-1} \text{ L}^{-1} \text{ gDW}^{-1}$ ]  $\pm$  SD of *Corallina officinalis* before and after the common garden experiment of each population under each geographic treatment condition. Southern populations (SP1 and SP2) are represented in gray, central populations (UK1 and UK2) are represented in black. Statistical differences are summarized in Supporting Information Table S1

pre-experiment as well as the central conditions ( $p < 0.05$ , Tukey HSD  $p < 0.05$ , 2-way ANOVA in both cases). In contrast to the second population, southern population 1 is significantly different to both central populations under central conditions ( $p < 0.05$ , Tukey HSD  $p < 0.05$ , 2-way ANOVA in both cases). Comparing populations within a region, populations were found not to be significantly different from each other throughout the experiment.

Calcification rates in the dark (Figure 4) increased under central conditions but decreased under southern conditions for central

populations. The development of dark calcification rates for southern populations showed a significant increase for population 1 under southern conditions compared to the beginning of the experiment ( $F_{2,6} = 5.013$ ,  $p < 0.05$ , Tukey HSD  $p < 0.05$ , 2-way ANOVA) but no significant change for southern population 2. Under central conditions, southern populations showed an increasing trend. Comparing populations within a region, only the southern populations were significantly different from each other before the experiment ( $F_{1,4} = 11.016$ ,  $p < 0.05$ , 1-way ANOVA).

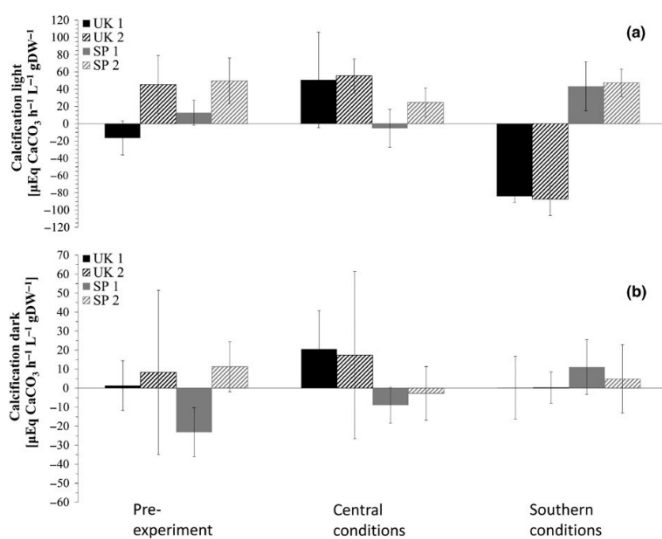


**FIGURE 4** (a) Calcification rates in the light and (b) dark [ $\mu\text{mol hr}^{-1} \text{ L}^{-1} \text{ gDW}^{-1}$ ]  $\pm$  SD of *Corallina officinalis* before and after the common garden experiment of each population under each geographic treatment condition. Southern populations (SP1 and 2) are represented in gray, central populations (UK1 and 2) are represented in black. Statistical differences are summarized in Supporting Information Table S1



## 4 | DISCUSSION

Understanding the physiology of *C. officinalis* and its interactions with the environment is crucial to predict how different portions of the species distribution may be affected by current and future warming rates. We present evidence for distinct vulnerability to thermal stress of central and peripheral populations of *C. officinalis*, a key marine ecosystem engineer (Daleo, Escapa, Alberti, & Iribarne, 2006; Kelaher, Underwood, & Chapman, 2003).

This study also provides genetic evidence that *C. officinalis* is found farther south than reported by earlier studies of *C. officinalis* distribution (Williamson et al., 2015). We present Illa de Arousa (SP1) and Tragove (SP2) as the most southern, genetically confirmed populations of *C. officinalis* distribution in the Eastern North Atlantic.

Oxygen evolution curves (P-I curves) and calcification evolution curves (C-I curves) show clear regional responses. This suggests that data obtained in this study could be interpreted as representative data for most populations of these and surrounding regions (Egilsdottir, Olafsson, & Martin, 2015; Williamson et al., 2017), excluding those in extreme environments. However, there is added complexity when we consider the maximum level of oxygen produced ( $P_{max}$ ), indicating its dependency with the initial environment of the population. Central populations may get more stressed under higher temperature conditions, as already published for crustose coralline algae (Diaz-Pulido, Anthony, Kline, Dove, & Hoegh-Guldberg, 2012).  $C_{max}$  confirms that central conditions are more favorable than southern conditions for all four populations. In P-I curves, southern populations show a steeper  $\alpha$  than central populations, demonstrating a more efficient light harvesting capability. The steeply decreasing  $\alpha$  in oxygen evolution curves of southern populations under central conditions can be explained either by increased physiological stress and a lower capacity for photosynthesis or by a geographic effect causing different responses depending on latitudinal origin of populations (Williamson et al., 2018). For the same populations and conditions however,  $\alpha$  of the calcification evolution curves increases slightly which outline an opposite trend compared to  $\alpha$  of oxygen evolution curves described above. This coincides with the observed, significant reduction of net production but not calcification rates for southern populations. A minimal increase of  $\alpha$  in oxygen evolution curves of central populations under southern conditions correlates with Williamson et al. (2018) who also found that central populations do not differ significantly in winter and summer conditions, which are similar to southern conditions in this study. In warmer temperatures, the tested populations also show an increase in their saturating light irradiance ( $I_k$ ) for C-I curves; however, even higher  $I_k$  values for calcification evolution have been reported in France and the UK (Egilsdottir et al., 2015; Williamson et al., 2017). This indicates that *C. officinalis* might be able to withstand future central conditions regarding  $I_k$  for its calcification, up to a certain extent.  $I_k$  values for P-I curves are lower under southern compared to central conditions for all populations in this study. This indicates that all specimens maintained under southern conditions reach their maximum photosynthetic level at lower irradiance and could therefore experience

damage of photosynthetic systems sooner compared to same populations living under central conditions. Additionally, maximum photosynthetic levels at low irradiance together with the lower light harvesting efficiency may result in exhaustion of photosynthetic systems due to very fast reactions within the metabolic pathways and the energy consumption for photon harvesting. Southern temperature conditions, therefore, present a less favorable environment for all populations.

This study highlights a significant change in primary production of southern margin and central populations when subjected to temperature conditions of the opposite distributional region. Central populations show reduced respiration rates under southern conditions. Similar behavior was found by Davison (1991) for the brown alga *Saccharina latissima*. Central populations show reduced net production under southern conditions indicating stress. However, they are still able to withstand warmer temperatures, in contrast to southern populations which may not be able to survive changing conditions over prolonged periods in their current habitat and may experience a southern range contraction (Lima, Ribeiro, Queiroz, Hawkins, & Santos, 2007). Net production rates of southern populations drop drastically under central conditions, resulting in oxygen uptake instead of production. These rates are similar to rates found under southern conditions, indicating these populations are unable or may take a longer time to adapt to central conditions. It has been shown that photosynthesis can stimulate calcification and that its increase could offset the  $CaCO_3$  dissolution in different calcifying algae in response to increased  $CO_2$  (Borowitzka, 1989; Gattuso, Allemand, & Frankignoulle, 1999; Hofmann et al. 2012; Johnson, & Carpenter, 2012; McCoy, Pfister, Olack, & Colman, 2016). Therefore, it can be expected and findings indicate that central populations downregulate calcification before photosynthesis and respiration in warmer temperature conditions.

Calcification in the light and in the dark showed drastic negative changes for central populations under southern conditions, confirming the uncoupling of photosynthesis and calcification. Central populations are shutting down light calcification metabolism resulting in dissolution. Central and southern populations have similar light calcification before and after the experiment under central control conditions demonstrating that there was no tank/experiment effect on the populations. Light calcification and dark calcification found in the literature are lower than these found in this study (Egilsdottir et al., 2013; El Haikali, Bensoussan, Romano, & Bousquet, 2004; Williamson et al., 2017). This coincides with the elevated photosynthesis and respiration rates. Southern populations reduce light calcification only by a small amount under central conditions (McCoy et al., 2016) but show increased respiration and decreased net production, suggesting downregulation of photosynthetic activity before calcification mechanisms. This is also supported by  $C_{max}$  values obtained in this study which are higher under central conditions than under the control southern conditions. High variability in dark calcification was observed in all populations in all treatment, reflecting findings of McCoy et al. (2016), and indicating that the already small amount of dark calcification is easily influenced by environmental

parameters such as temperature. Dark calcification rates of central populations decreased to close to zero under southern conditions, confirming downregulation of dark calcification. This, in addition to the decline in light calcification rates, results in a higher dissolution rate of central populations under southern conditions than under control conditions. A decrease of dark calcification of southern populations under central conditions indicated slow or no ability of southern populations to adapt to colder temperature regimes. At the same time, central populations show similar behavior in warmer temperatures. All of this shows that the two processes of calcification and photosynthesis are not as tightly coupled as previously assumed.

While oxygen evolution and calcification evolution data perfectly mirror the net production and respiration, calcification results show the high in situ variability between central populations which is due to environmental adaptations rather than genetic adaptations. This is supported by the very similar calcification rates in the light after the incubation of central populations in southern conditions compared to the pre-experimental measurements. This also means that we are unable to determine the timing of when central populations kept under southern conditions began to reduce light calcification rates.

A high variability in both  $\alpha$  and  $I_K$  of P-I and C-I curves, also found by Egilsdottir et al. (2015), in southern populations shows that adaptation ability can strongly depend on region of origin and the stress already experienced in their natural environment. Combining the knowledge gained from this study, central populations seem to be more robust, resilient, and adaptable to future climatic changes as predicted by the IPCC (2013) than southern populations. According to Williamson et al. (2017), *C. officinalis* populations in South England are adapted to variability in environmental stressors both in short (tidal) and long (seasonal) timescales. This is consistent with the findings of primary production, respiration as well as light and dark calcification, leaving the central populations better adapted to changes than southern populations in this study and others. This supports the center-to-margin hypothesis (Guo, Taper, Schoenberger, & Brandle, 2005) for *C. officinalis*. Additionally, this study also demonstrates that *C. officinalis* needs a minimum amount of 4 weeks, but preferably longer, to fully acclimatize to altered conditions such as changes in temperature or  $pCO_2$ .

Even though relatively static conditions were kept in this experiment and no tidal movement was simulated due to facility restrictions, parameters were chosen to be at the predominant existing light and temperature conditions of the season in which the algae were sampled in and which they would experience when submerged during intertidal periods. This ensured the measurement of the optimum and most realistic physiological responses of *C. officinalis* to the opposite populations conditions by being in their predominant state of being submerged and not stressed by abiotic factors during low tide conditions.

The speed in which climatic changes are observed today may be too rapid for this species to be able to adapt fully to them. This may result in loss of genetic diversity in *C. officinalis*, and species ranges

may shift and become confined. This was previously also found by Collevatti, Nabout, and Diniz-Filho (2011) in a common garden experiment with the neotropical tree species *Caryocar brasiliense*, which experiences a climate change induced restriction of ideal habitat for their southern margin populations. According to the authors, this leads to a drastic decrease of genetic diversity and numbers of alleles due to the survival and reproduction success of only the most adapted genotypes under future climatic conditions. Additionally, it leads to the reduction in individual fitness and therefore population evolutionary potential. Another study performed a common garden experiment on multiple species of ants and found an elevated temperature induced decrease in survival and brood production (Pelini et al., 2012). The authors of this study indicate that the decline in these two factors will lead to a loss of genetic diversity. A potential change in genetic diversity and percentage cover due to a potential decrease in growth rates of *C. officinalis* in rocky shore intertidal ecosystems has been suggested to lead to loss of diversity of this macroalgae genus as well as associated flora and fauna. It is unclear, however, how flora and fauna would adapt to gradual changes in hosts.

To conclude, central populations may be adapting better to warmer temperature conditions in future oceans but at the same time may experience a loss in percentage cover in intertidal, rocky, coastal zones. Central populations' calcification is negatively impacted by elevated sea surface temperatures, potentially resulting in reduced resilience. Southern populations' most negatively affected physiological process in central conditions was production rates, implying a reduced resilience in these populations as well. With sea surface temperatures warming up in northern regions of the species distribution, southern populations may be able to shift their distribution northern wards and therefore potentially disappear entirely in their original environment due to even warmer conditions in future ocean environments.

#### ACKNOWLEDGMENTS

The authors would like to thank the volunteers for their help with sampling and field incubations, Aditya Putra and Patricia Easterby for their help during the experimental phase of the experiment and the technicians at CCMAR helping with the genetic species identification. We would also like to thank the two anonymous reviewers for their critical feedback and therefore valuable improvement of the manuscript. This study was funded by the research development fund (RDF) of the University of Portsmouth and further supported by UID/Multi/04326/2013, IF/01413/2014/CP1217/CT0004 from the Fundação para a Ciência e Tecnologia (FCT-MEC, Portugal) and the South African Research Chairs Initiative (SARChI) of the Department of Science and Technology and the National Research Foundation.

#### CONFLICT OF INTEREST

The authors declare that they have no conflict of interest.

## AUTHOR CONTRIBUTIONS

RK and FR designed the research. RK performed the research. KN and GZ performed the genetic analysis. RK led the writing of the manuscript with contribution from FR, AF, KN, SM, and GZ. FR provided critical feedback and helped shape the research and analysis. All authors contributed substantially to revisions of the manuscript.

## DATA ACCESSIBILITY

Statistical data supporting the results are available under: <https://doi.pangaea.de/10.1594/PANGAEA.899568>.

## ORCID

Regina Kolzenburg  <https://orcid.org/0000-0002-2139-960X>

## OPEN RESEARCH BADGES



This article has earned an Open Materials Badge for making publicly available the components of the research methodology needed to reproduce the reported procedure and analysis. All materials are available at <https://doi.pangaea.de/10.1594/PANGAEA.899568>.

## REFERENCES

- Adey, W. H., & MacIntyre, I. G. (1973). Crustose coralline algae: A re-evaluation in the geological sciences. *Geological Society of America Bulletin*, 84(3), 883–904. [https://doi.org/10.1130/0016-7606\(1973\)84<883:CCAARI>2.0.CO;2](https://doi.org/10.1130/0016-7606(1973)84<883:CCAARI>2.0.CO;2)
- Aitken, S. N., Yeaman, S., Holliday, J. A., Wang, T., & Curtis-McLane, S. (2008). Adaptation, migration or extirpation: Climate change outcomes for tree populations. *Evolutionary Applications*, 1(1), 95–111. <https://doi.org/10.1111/j.1752-4571.2007.00013.x>
- Benedetti-Cecchi, L. (2006). Understanding the consequences of changing biodiversity on rocky shores: How much have we learned from past experiments? *Journal of Experimental Marine Biology and Ecology*, 338, 193–204. <https://doi.org/10.1016/j.jembe.2006.06.020>
- Bennett, S., Wernberg, T., Arackal Joy, B., de Bettignies, T., & Campbell, A. H. (2015). Central and rear-edge populations can be equally vulnerable to warming. *Nature Communications*, 6, 10280. <https://doi.org/10.1038/ncomms10280>
- Bentz, B. J., Régnière, J., Fettig, C. J., Hansen, E. M., Hayes, J. L., Hicke, J. A., ... Seybold, S. J. (2010). Climate Change and Bark Beetles of the Western United States and Canada: Direct and Indirect Effects. *BioScience*, 60(8), 602–613. <https://doi.org/10.1525/bio.2010.60.8.6>
- Borowitzka, M. A. (1989). Carbonate calcification in algae – Inhibition and control. In S. Mann, J. M. Webb, & R. J. P. Williams (Eds.), *Biomining: Chemical and biochemical perspectives* (pp. 65–94). Weinheim, Germany: John Wiley & Sons.
- Bozinovic, F., Calosi, P., & Spicer, J. I. (2011). Physiological correlates of geographic range in animals. *Annual Review of Ecology, Evolution, and Systematics*, 42, 155–179.
- Breeman, A. M. (1988). Relative importance of temperature and other factors in determining geographic boundaries of seaweeds – experimental and phenological evidence. *Helgolander Meeresunters*, 42, 199–241.
- Brodie, J., Walker, R. H., Williamson, C. J., & Irvine, L. M. (2013). Epitypification and redescription of *Corallina officinalis* L., the type of the genus, and *C. elongata* Ellis et Solander (Corallinales, Rhodophyta). *Cryptogamie, Algologie*, 34(1), 49–56.
- Brodie, J., Williamson, C. J., Smale, D. A., Kamenos, N. A., Mieszkowska, N., Santos, R., et al. (2014). The future of the north-east Atlantic benthic flora in a high CO<sub>2</sub> world. *Ecology and Evolution*, 4, 2787–2798.
- Brussard, P. F. (1984). Geographic patterns and environmental gradients: The central-marginal models in *Drosophila* revisited. *Annual Review of Ecology and Systematics*, 15, 25–64.
- Calosi, P., Melatunan, S., Turner, L. M., Artioli, Y., Davidson, R. L., Byrne, J. J., ... Rundle, S. D. (2017). Regional adaptation defines sensitivity to future ocean acidification. *Nature Communications*, 8, 13994. <https://doi.org/10.1038/ncomms13994>
- Case, T. J., & Taper, M. L. (2000). Interspecific Competition, environmental gradients, gene flow, and the coevolution of species' borders. *The American Naturalist*, 155(5), 583–605. <https://doi.org/10.1086/303351>
- Chisholm, J. R. M., & Gattuso, J. (1991). Validation of the alkalinity anomaly technique for investigating calcification of photosynthesis in coral reef communities. *Limnology and Oceanography*, 36(6), 1232–1239. <https://doi.org/10.4319/lo.1991.36.6.1232>
- Collevatti, R. G., Nabout, J. C., & Diniz-Filho, J. A. F. (2011). Range shift and loss of genetic diversity under climate change in *Caryocar brasiliense*, a Neotropical tree species. *Tree Genetics & Genomes*, 7(6), 1237–1247. <https://doi.org/10.1007/s11295-011-0409-z>
- Coull, B. C., & Wells, J. B. J. (1983). Refuges from fish predation – Experiments with phytal meiofauna from the New Zealand rocky intertidal. *Ecology*, 64, 1599–1609. <https://doi.org/10.2307/1937513>
- Daleo, P., Escapa, M., Alberti, J., & Iribarne, O. (2006). Negative effects of an autogenic ecosystem engineer: Interactions between coralline turf and an ephemeral green alga. *Marine Ecology Progress Series*, 315, 67–73. <https://doi.org/10.3354/meps315067>
- Dam, H. G. (2013). Evolutionary adaptation of marine zooplankton to global change. *Annual Review of Marine Science*, 5(1), 349–370. <https://doi.org/10.1146/annurev-marine-121211-172229>
- Davenport, J., Butler, A., & Cheshire, A. (1999). Epifaunal composition and fractal dimensions of marine plants in relation to emersion. *Journal of the Marine Biological Association of the UK*, 79(2), 351–355. <https://doi.org/10.1017/S0025315498000393>
- Davison, I. R. (1991). Environmental effects on algal photosynthesis: temperature. *Journal of Phycology*, 27(1), 2–8. <https://doi.org/10.1111/j.0022-3646.1991.00002.x>
- Dayton, P. K. (1972). Toward an understanding of community resilience and the potential effects of enrichments to the benthos at McMurdo Sound, Antarctica. In B. C. Parker (Ed.), *Proceedings of the colloquium on conservation problems in Antarctica* (pp. 81–96). Lawrence, KS: Allen Press.
- Diaz-Pulido, G., Anthony, K. R. N., Kline, D. I., Dove, S., & Hoegh-Guldberg, O. (2012). Interactions between ocean acidification and warming on the mortality and dissolution of coralline algae. *Journal of Phycology*, 48(1), 32–39.
- Dickson, A. G., & Millero, F. J. (1987). A comparison of the equilibrium constants for the dissociation of carbonic acid in seawater media. *Deep-Sea Research A*, 34(10), 1733–1743.
- Dickson, A. G., Sabine, C. L., & Christian, J. R. (eds) (2007). *Guide to best practices for ocean CO<sub>2</sub> measurement*. Sidney, BC, Canada: North Pacific Marine Science Organization, 191 pp. (PICES Special Publication 3).
- Diez, I., Mugerza, N., Santolaria, A., Ganzedo, U., & Gorostiaga, J. M. (2012). Seaweed assemblage changes in the eastern Cantabrian Sea and their potential relationship to climate change. *Estuarine*

- Coastal and Shelf Science*, 99, 108–120. <https://doi.org/10.1016/j.cscs.2011.12.027>
- Digby, P. S. B. (1977). Growth and calcification in the coralline algae, *Clathromorphum circumscriptum* and *Corallina officinalis*, and the significance of pH in relation to precipitation. *Journal of the Marine Biological Association of the United Kingdom*, 57(4), 1095–1109. <https://doi.org/10.1017/S0025315400026151>
- Drummond, A. J., Ashton, B., Buxton, S., Cheung, M., Cooper, A., & Duran, C. et al. (2011). Geneious v5.4. (software). Retrieved from <http://www.geneious.com>
- Egilsdottir, H., Noiset, F., Noel, L.-M.-L.-J., Olafsson, J., & Martin, S. (2013). Effects of pCO<sub>2</sub> on physiology and skeletal mineralogy in a tidal pool coralline alga *Corallina elongata*. *Marine Biology*, 160, 2103–2112.
- Egilsdottir, H., Olafsson, J., & Martin, S. (2015). Photosynthesis and calcification in the articulated coralline alga *Ellisolandia elongata* (Corallinales, Rhodophyta) from intertidal rock pools. *European Journal of Phycology*, 51, 59–70.
- El Haikali, B., Bensoussan, N., Romano, J. C., & Bousquet, V. (2004). Estimation of photosynthesis and calcification rates of *Corallina elongata* Ellis and Solander, 1786, by measurements of dissolved oxygen, pH and total alkalinity. *Scientia Marina*, 68(1), 45–56.
- Franco, A. M., Hill, J. K., Kitschke, C., Collingham, Y. C., Roy, D. B., Fox, R., ... Thomas, C. D. (2006). Impacts of climate warming and habitat loss on extinctions at species' low-latitude range boundaries. *Global Change Biology*, 12(8), 1545–1553. <https://doi.org/10.1111/j.1365-2486.2006.01180.x>
- Ganning, B. (1971). Studies on chemical, physical and biological conditions in Swedish rockpool ecosystems. *Ophelia*, 9, 51–105.
- Gaston, K. J. (2009). Geographic range limits: Achieving synthesis. *Proceedings of the Royal Society B: Biological Sciences*, 276, 1395–1406. <https://doi.org/10.1098/rspb.2008.1480>
- Gattuso, J. P., Allemand, D., & Frankignoulle, M. (1999). Photosynthesis and calcification at cellular, organismal and community levels in coral reefs: A review on interactions and control by carbonate chemistry. *American Zoologist*, 39(1), 160–183.
- Guo, Q., Taper, M., Schoenberger, M., & Brandie, J. (2005). Spatial-temporal population dynamics across species range: From centre to margin. *Oikos*, 108(1), 47–57. <https://doi.org/10.1111/j.0030-1299.2005.13149.x>
- Helmuth, B., Mieszkowska, N., Moore, P., & Hawkins, S. J. (2006). Living on the edge of two changing worlds: Forecasting the responses of rocky intertidal ecosystems to climate change. *Annual Review of Ecology, Evolution, and Systematics*, 37, 373–404. <https://doi.org/10.1146/annurev.ecolsys.37.091305.110149>
- Hofmann, G. E., Evans, T. G., Kelly, M. W., Padilla-Gamiño, J. L., Blanchette, C. A., Washburn, L., et al. (2014). Exploring local adaptation and the ocean acidification seascape—studies in the California Current Large Marine Ecosystem. *Biogeosciences*, 11, 1053–1064.
- Hofmann, L., Straub, S., & Bischof, K. (2012). Competition between calcifying and noncalcifying temperate marine macroalgae under elevated CO<sub>2</sub> levels. *Marine Ecology Progress Series*, 464, 89–105. <https://doi.org/10.3354/meps09892>
- Hofmann, L., Yildiz, G., Hanelt, D., & Bischof, K. (2012). Physiological responses of the calcifying rhodophyte, *Corallina officinalis* (L.), to future CO<sub>2</sub> levels. *Marine Biology*, 159, 783–792.
- IBM Corp. (2016). *IBM SPSS statistics for Windows, Version 24.0. (software)*. Armonk, NY: IBM Corp.
- IPCC (2013). *Climate change 2013: The physical science basis. Contribution of Working Group I to the Fifth Assessment Report of the Intergovernmental Panel on Climate Change* (Stocker, T.F., D. Qin, G.-K. Plattner, M. Tignor, S.K. Allen, J. Boschung, A. Nauels, Y. Xia, V. Bex and P.M. Midgley [eds.]). Cambridge, UK and New York, NY: Cambridge University Press, 1535 pp.
- Johansen, H. W. (1981). *Coralline algae, a first synthesis* (p. 239). Boca Raton, FL: CRC Press.
- Johnson, M. D., & Carpenter, R. C. (2012). Ocean acidification and warming decrease calcification in the crustose coralline alga *Hydrolithon onkodes* and increase susceptibility to grazing. *Journal of Experimental Marine Biology and Ecology*, 434, 94–101.
- Jones, C. G., Lawton, J. H., & Shachak, M. (1994). Organisms as ecosystem engineers. *Oikos*, 69, 373–386.
- Kelaker, B. P., Chapman, M. G., & Underwood, A. J. (2001). Spatial patterns of diverse macrofaunal assemblages in coralline turf and their associations with environmental variables. *Journal of the Marine Biological Association of the UK*, 81, 917–930. <https://doi.org/10.1017/S0025315401004842>
- Kelaker, B. P., Underwood, A. J., & Chapman, M. G. (2003). Experimental transplantations of coralline algal turf to demonstrate causes of differences in macrofauna at different tidal heights. *Journal of Experimental Marine Biology and Ecology*, 282(1–2), 23–41. [https://doi.org/10.1016/S0022-0981\(02\)00443-4](https://doi.org/10.1016/S0022-0981(02)00443-4)
- Kelly, M. W., & Hofmann, G. E. (2013). Adaptation and the physiology of ocean acidification. *Functional Ecology*, 27, 980–990. <https://doi.org/10.1111/j.1365-2435.2012.02061.x>
- Kroeker, K. J., Kordas, R. L., Crim, R., Hendriks, I. E., Ramajo, L., Singh, G. S., ... Gattuso, J.-P. (2013). Impacts of ocean acidification on marine organisms: Quantifying sensitivities and interaction with warming. *Global Change Biology*, 19, 1884–1896. <https://doi.org/10.1111/gcb.12179>
- Lesica, P., & McCune, B. (2004). Decline of arctic-alpine plants at the southern margin of their range following a decade of climatic warming. *Journal of Vegetation Science*, 15(5), 679–690. <https://doi.org/10.1111/j.1654-1103.2004.tb02310.x>
- Lewis, E., & Wallace, D. W. R. (1998). *CO2SYS - Program developed for the CO2 system calculations*. Technical report Oak Ridge, Tenn., USA: Report ORNL/CDIAC-105, Oak Ridge, Tenn., USA.
- Lima, F. P., Ribeiro, P. A., Queiroz, N., Hawkins, S. J., & Santos, A. M. (2007). Do distributional shifts of northern and southern species of algae match the warming pattern? *Global Change Biology*, 13(12), 2592–2604.
- Lobban, C. S., & Harrison, P. J. (1994). 'Pollution', *Seaweed ecology and physiology* (1st ed., pp. 255–282). Cambridge, UK: Cambridge University Press.
- Lüning, K. (1990). *Seaweeds: Their environment, biogeography and ecophysiology*. New York, NY: John Wiley and Sons.
- Martone, P. T., Alyono, M., & Stites, S. (2010). Bleaching of an intertidal coralline alga: Untangling the effects of light, temperature, and desiccation. *Marine Ecology Progress Series*, 416, 57–67. <https://doi.org/10.3354/meps08782>
- Martone, P. T., & Denny, M. W. (2008). To bend a coralline: Effect of joint morphology on flexibility and stress amplification in an articulated calcified seaweed. *Journal of Experimental Biology*, 211, 3421–3432.
- McCoy, S. J., Pfister, C. A., Olack, G., & Colman, A. S. (2016). Diurnal and tidal patterns of carbon uptake and calcification in geniculate intertidal coralline algae. *Marine Ecology*, 37, 553–564. <https://doi.org/10.1111/maec.12295>
- Mehrbach, C., Culbertson, C. H., Hawley, J. E., & Pytkowicz, R. M. (1973). Measurement of the apparent dissociation constants of carbonic acid in seawater at atmospheric pressure. *Limnology and Oceanography*, 18(6), 897–907.
- Morley, S. A., Hirse, T., Pörtner, H.-O., & Peck, L. S. (2009). Geographical variation in thermal tolerance within Southern Ocean marine ectotherms. *Comparative Biochemistry and Physiology Part A: Molecular & Integrative Physiology*, 153(2), 154–161. <https://doi.org/10.1016/j.cbpa.2009.02.001>
- Morris, S., & Taylor, A. C. (1983). Diurnal and seasonal variation in physicochemical conditions within intertidal rock pools.

- Estuarine, Coastal and Shelf Science*, 17, 339–355. [https://doi.org/10.1016/0272-7714\(83\)90026-4](https://doi.org/10.1016/0272-7714(83)90026-4)
- Nelson, W. A. (2009). Calcified macroalgae – Critical to coastal ecosystems and vulnerable to change: A review. *Marine and Freshwater Research*, 60, 787–801. <https://doi.org/10.1071/MF08335>
- Nicastro, K. R., Zardi, G. I., Teixeira, S., Neiva, J., Serrão, E. A., & Pearson, G. A. (2013). Shift happens: Trailing edge contraction associated with recent warming trends threatens a distinct genetic lineage in the marine macroalga *Fucus vesiculosus*. *BMC Biology*, 11(1), 6. <https://doi.org/10.1186/1741-7007-11-6>
- Noël, L. M. L. J., Hawkins, S. J., Jenkins, S. R., & Thompson, R. C. (2009). Grazing dynamics in intertidal rockpools: Connectivity of microhabitats. *Journal of Experimental Marine Biology and Ecology*, 370, 9–17. <https://doi.org/10.1016/j.jembe.2008.11.005>
- Pardo, C., Peña, V., Berreiro, R., & Bárbara, I. (2015). A molecular and morphological study of *Corallina sensu lato* (Corallinales, Rhodophyta) in the Atlantic Iberian Peninsula. *Cryptogamie, Algologie*, 36(1), 31–54.
- Parmesan, C. (2006). Ecological and evolutionary responses to recent climate change. *Annual Review of Ecology, Evolution, and Systematics*, 37(2006), 637–669.
- Pelini, S. L., Diamond, S. E., MacLean, H., Ellison, A. M., Gotelli, N. J., Sanders, N. J., & Dunn, R. R. (2012). Common garden experiments reveal uncommon responses across temperatures, locations, and species of ants. *Ecology and Evolution*, 2(12), 3009–3015. <https://doi.org/10.1002/ece3.407>
- Sanford, E., Holzman, S. B., Haney, R. A., Rand, D. M., & Bertness, M. D. (2006). Larval tolerance, gene flow, and the northern geographic range limit of fiddler crabs. *Ecology*, 87(11), 2882–2894. [https://doi.org/10.1890/0012-9658\(2006\)87\[2882:LTGFAT\]2.0.CO;2](https://doi.org/10.1890/0012-9658(2006)87[2882:LTGFAT]2.0.CO;2)
- Smale, D. A., & Wernberg, T. (2013). Extreme climatic event drives range contraction of a habitat-forming species. *Proceedings of the Royal Society B: Biological Sciences*, 280, 20122829.
- Smith, S. V., & Key, G. S. (1975). Carbon dioxide and metabolism in marine environments. *Limnology and Oceanography*, 20(3), 493–495.
- Steneck, R. S. (1986). The ecology of coralline algal crusts: Convergent patterns and adaptive strategies. *Annual Review of Ecology and Systematics*, 17(1), 273–303. <https://doi.org/10.1146/annurev.es.17.110186.001421>
- Thompson, J. D., Higgins, D. G., & Gibson, T. J. (1994). CLUSTAL W: Improving the sensitivity of progressive multiple sequence alignment through sequence weighting, position-specific gap penalties and weight matrix choice. *Nucleic Acids Research*, 22(22), 4673–4680.
- van der Heijden, L. H., & Kamenos, N. A. (2015). Reviews and syntheses: Calculating the global contribution of coralline algae to total carbon burial. *Biogeosciences*, 12, 6429–6441. <https://doi.org/10.5194/bg-12-6429-2015>
- Watkinson, A. R., & Sutherland, W. J. (1995). Sources, sinks and pseudo-sinks. *The Journal of Animal Ecology*, 64, 126–130.
- Wernberg, T., Russell, B. D., Thomsen, M. S., Gurgel, C. F. D., Bradshaw, C. J. A., Poloczanska, E. S., & Connell, S. D. (2011). Seaweed communities in retreat from ocean warming. *Current Biology*, 21, 1828–1832. <https://doi.org/10.1016/j.cub.2011.09.028>
- Whittaker, R. H. (1956). Vegetation of the Great Smoky Mountains. *Ecological Monographs*, 26, 1–80.
- Williamson, C. J., Brodie, J., Goss, B., Yallop, M., Lee, S., & Perkins, R. (2014). *Corallina* and *Ellisolandia* (Corallinales, Rhodophyta) photo-physiology over daylight tidal emersion: Interactions with irradiance, temperature and carbonate chemistry. *Marine Biology*, 161, 2051–2068. <https://doi.org/10.1007/s00227-014-2485-8>
- Williamson, C. J., Perkins, R., Voller, M., Yallop, M. L., & Brodie, J. (2017). The regulation of coralline algal physiology, an in situ study of *Corallina officinalis* (Corallinales, Rhodophyta). *Biogeosciences*, 14, 4485–4498.
- Williamson, C. J., Perkins, R., Yallop, M. L., Peteiro, C., Sanches, N., Gunnarsson, K., ... Brodie, J. (2018). Photoacclimation and photoregulation strategies of *Corallina* (Corallinales, Rhodophyta) across the NE Atlantic. *Journal of Phycology*, 53(3), 290–306.
- Williamson, C. J., Walker, R. H., Robba, L., Russell, S., Irvine, L. M., & Brodie, J. (2015). Towards resolution of species diversity and distribution in the calcified red algal genera *Corallina* and *Ellisolandia* (Corallinales, Rhodophyta). *Phycologia*, 54, 2–11.

**How to cite this article:** Kolzenburg R, Nicastro KR, McCoy SJ, Ford AT, Zardi GI, Ragazzola F. Understanding the margin squeeze: Differentiation in fitness-related traits between central and trailing edge populations of *Corallina officinalis*. *Ecol Evol*. 2019;00:1–15. <https://doi.org/10.1002/ece3.5162>

## APPENDIX A

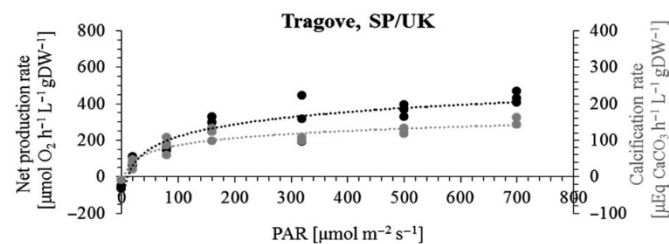


**FIGURE A1** Oxygen and calcification evolution curve of the Tragove (southern) population under central conditions. Black plot refers to net production data. Gray plot refers to calcification rates

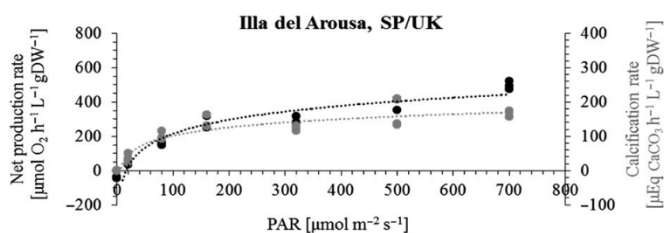


**FIGURE A2** Oxygen and calcification evolution curve of the Illa del Arousa (southern) population under central conditions. Black plot refers to net production data. Gray plot refers to calcification rates

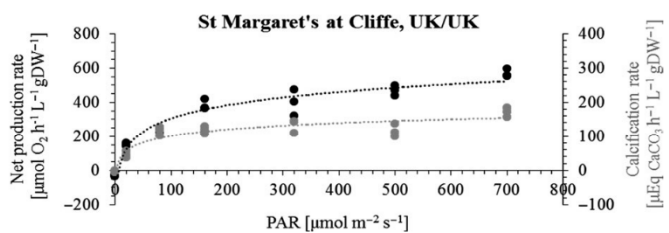


**FIGURE A3** Oxygen and calcification evolution curve of the St Margaret's at Cliffe (center) population under central conditions. Black plot refers to net production data. Gray plot refers to calcification rates

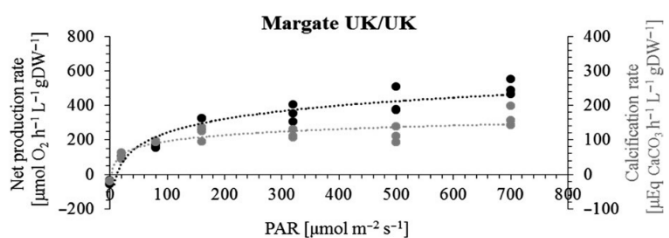


**FIGURE A4** Oxygen and calcification evolution curve of the Margate (center) population under central conditions. Black plot refers to net production data. Gray plot refers to calcification rates



**FIGURE A5** Oxygen and calcification evolution curve of the Tragove (southern) population under southern conditions. Black plot refers to net production data. Gray plot refers to calcification rates

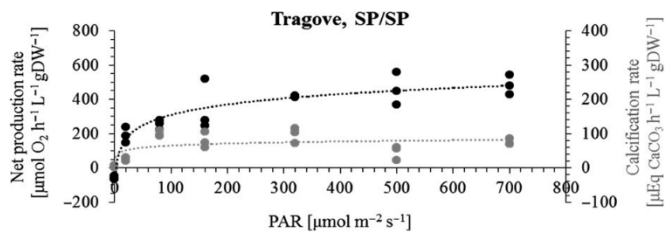


**FIGURE A6** Oxygen and calcification evolution curve of the Illa del Arousa (southern) population under southern conditions. Black plot refers to net production data. Gray plot refers to calcification rates

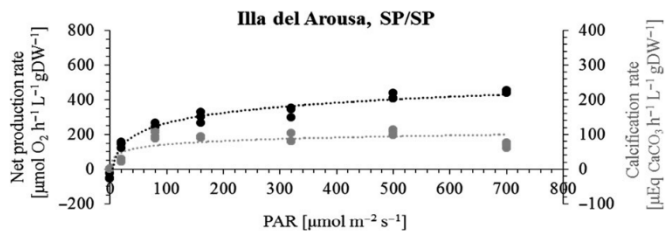


**FIGURE A7** Oxygen and calcification evolution curve of the St Margaret's at Cliffe (center) population under southern conditions. Black plot refers to net production data. Gray plot refers to calcification rates

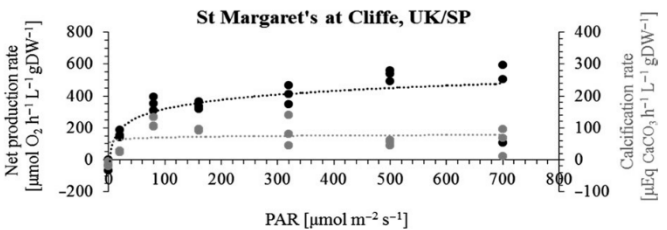
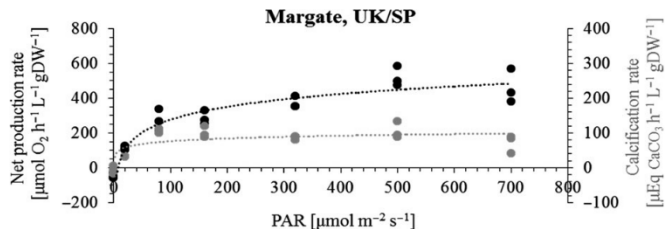


**FIGURE A8** Oxygen and calcification evolution curve of the Margate (center) population under southern conditions. Black plot refers to net production data. Gray plot refers to calcification rates



For raw data, please follow the link:

<https://figshare.com/s/rk55724d31ebe56b13bf13>

By following the link, you agree not to share the link or any of the content with a third person.



# Appendix D

Chapter 5 – Adaptation of *Corallina officinalis* to future climatic changes across its geographical distribution in the NE Atlantic

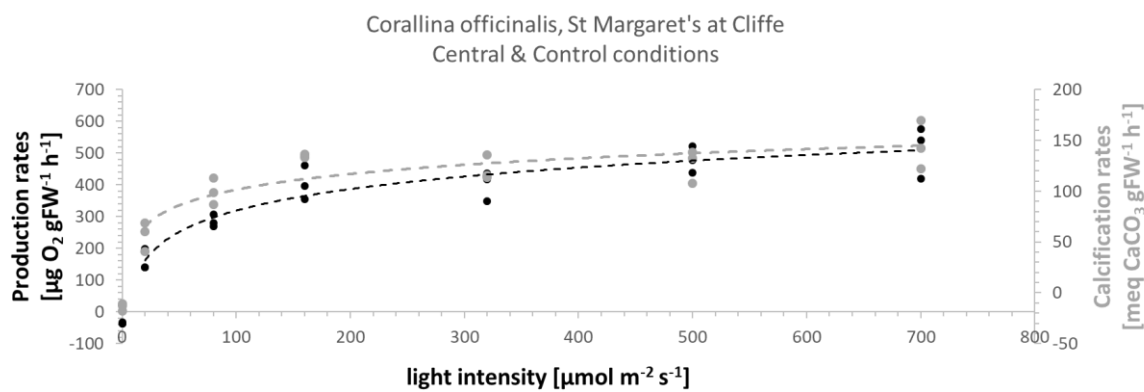


**Figure D1:** Oxygen and calcification evolution curve of the St Margaret's at Cliffe (centre) population under central control conditions. Black closed circles refer to gross production, grey closed circles refer to calcification rates. Trend lines are displayed as dashed line in their respective colour.

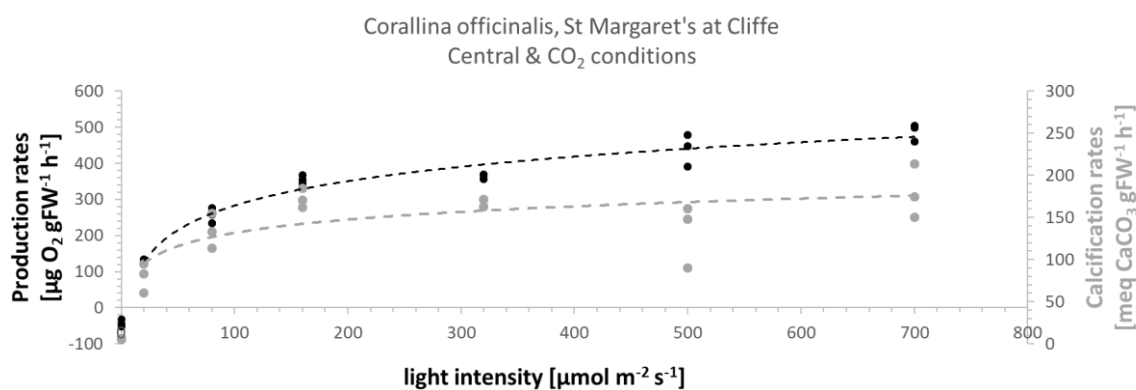


**Figure D2:** Oxygen and calcification evolution curve of the St Margaret's at Cliffe (centre) population under central, high CO<sub>2</sub> conditions. Black closed circles refer to gross production, grey closed circles refer to calcification rates. Trend lines are displayed as dashed line in their respective colour.

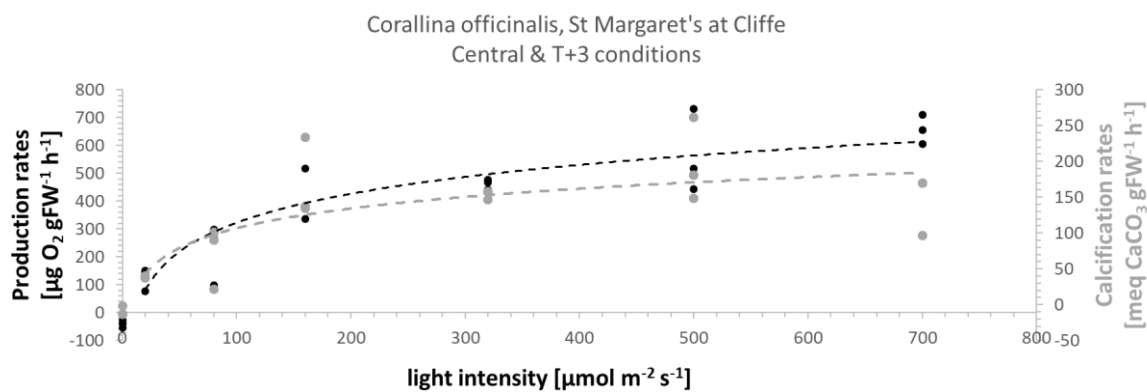


**Figure D3:** Oxygen and calcification evolution curve of the St Margaret's at Cliffe (centre) population under central, high temperature (T+3) conditions. Black closed circles refer to gross production, grey closed circles refer to calcification rates. Trend lines are displayed as dashed line in their respective colour.

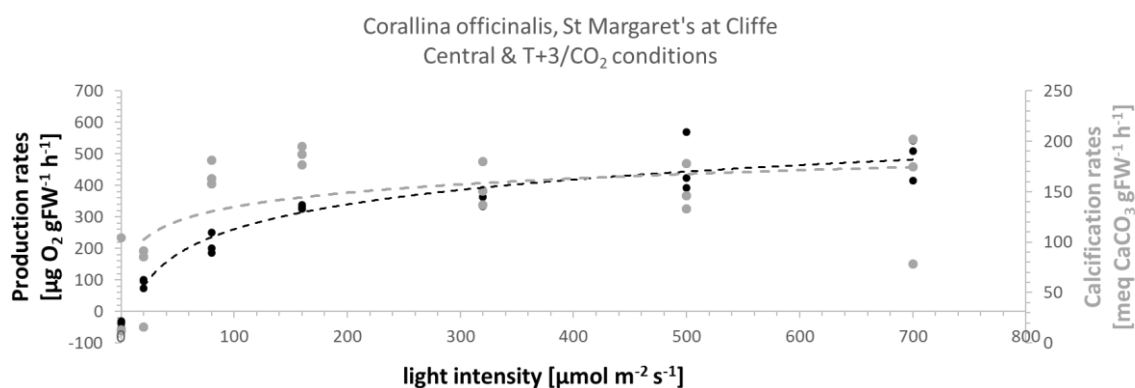


**Figure D4:** Oxygen and calcification evolution curve of the St Margaret's at Cliffe (centre) population under central, climate change (T+3/CO<sub>2</sub>) conditions. Black closed circles refer to gross production, grey closed circles refer to calcification rates. Trend lines are displayed as dashed line in their respective colour.

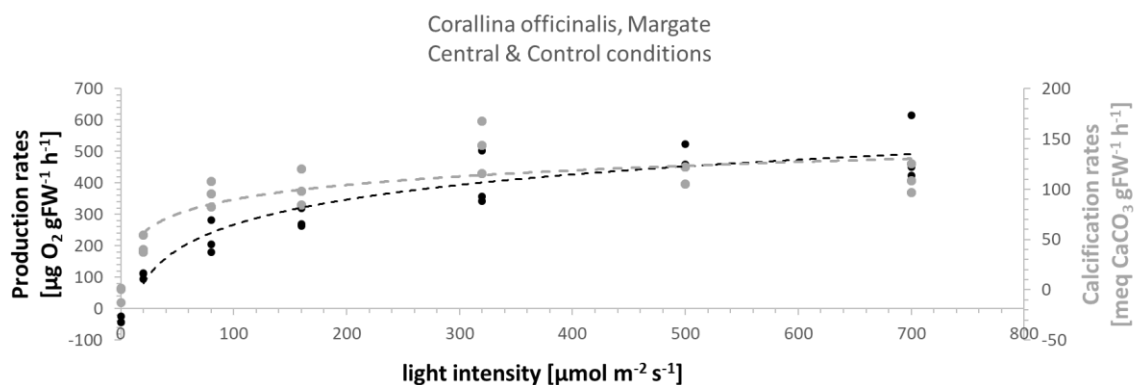


**Figure D5:** Oxygen and calcification evolution curve of the Margate (centre) population under centre, control conditions. Black closed circles refer to gross production, grey closed circles refer to calcification rates. Trend lines are displayed as dashed line in their respective colour.

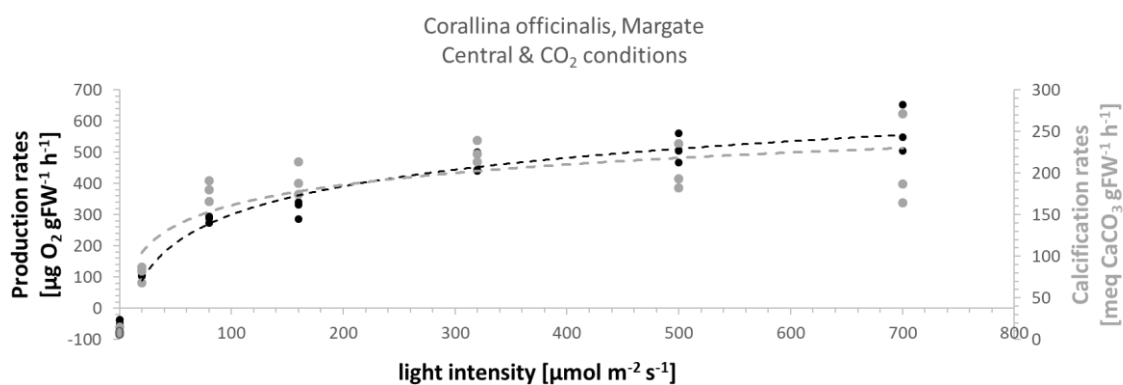


**Figure D6:** Oxygen and calcification evolution curve of the Margate (centre) population under centre, high CO<sub>2</sub> conditions. Black closed circles refer to gross production, grey closed circles refer to calcification rates. Trend lines are displayed as dashed line in their respective colour.

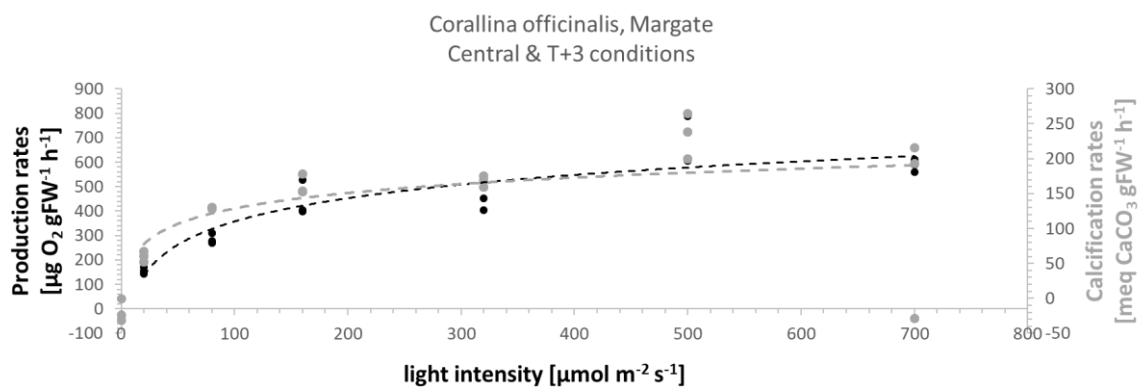


**Figure D7:** Oxygen and calcification evolution curve of the Margate (centre) population under centre, high temperature (T+3) conditions. Black closed circles refer to gross production, grey closed circles refer to calcification rates. Trend lines are displayed as dashed line in their respective colour.

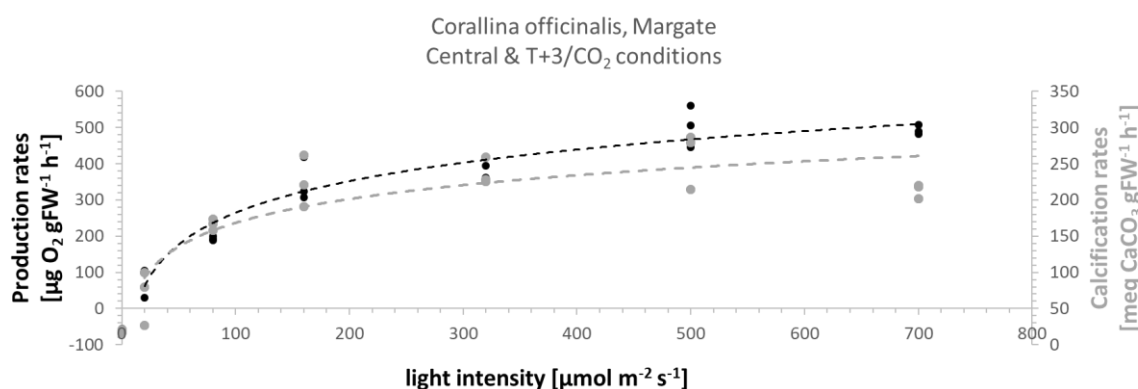


**Figure D8:** Oxygen and calcification evolution curve of the Margate (centre) population under centre, climate change (T+3/CO<sub>2</sub>) conditions. Black closed circles refer to gross production, grey closed circles refer to calcification rates. Trend lines are displayed as dashed line in their respective colour.

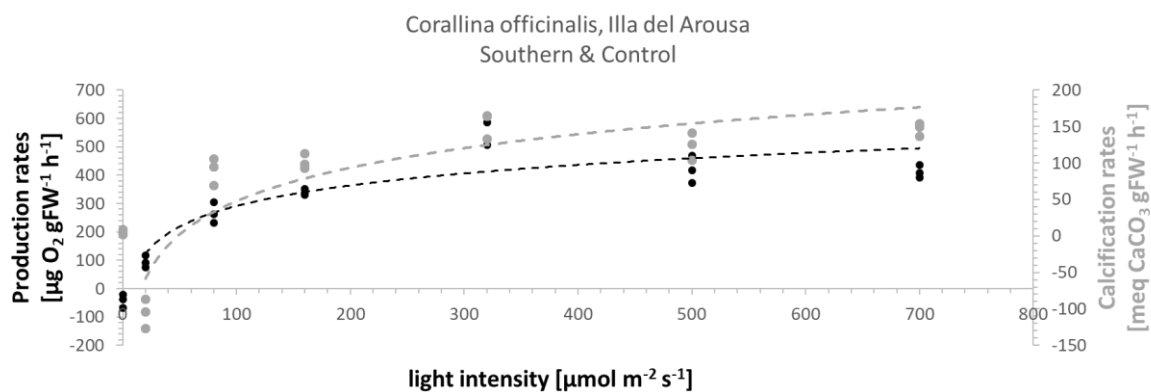


**Figure D9:** Oxygen and calcification evolution curve of the Illa del Arousa (southern) population under southern, control conditions. Black closed circles refer to gross production, grey closed circles refer to calcification rates. Trend lines are displayed as dashed line in their respective colour.

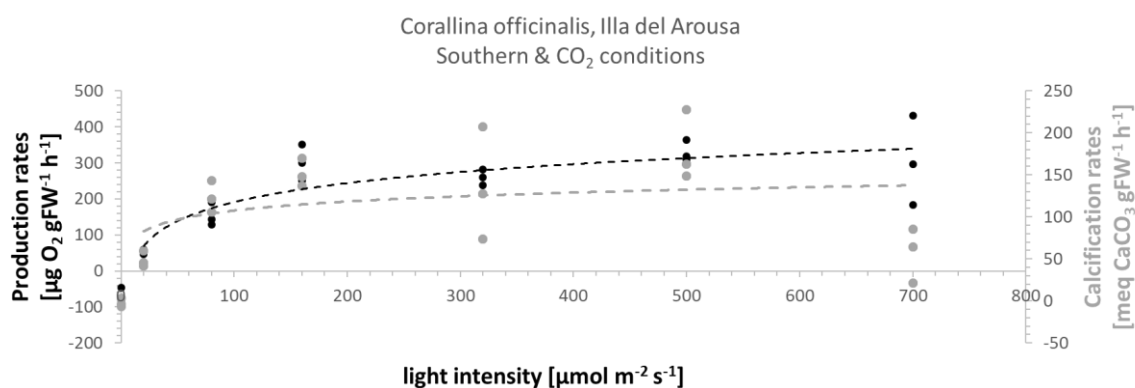


**Figure D10:** Oxygen and calcification evolution curve of the Illa del Arousa (southern) population under southern, high CO<sub>2</sub> conditions. Black closed circles refer to gross production, grey closed circles refer to calcification rates. Trend lines are displayed as dashed line in their respective colour.

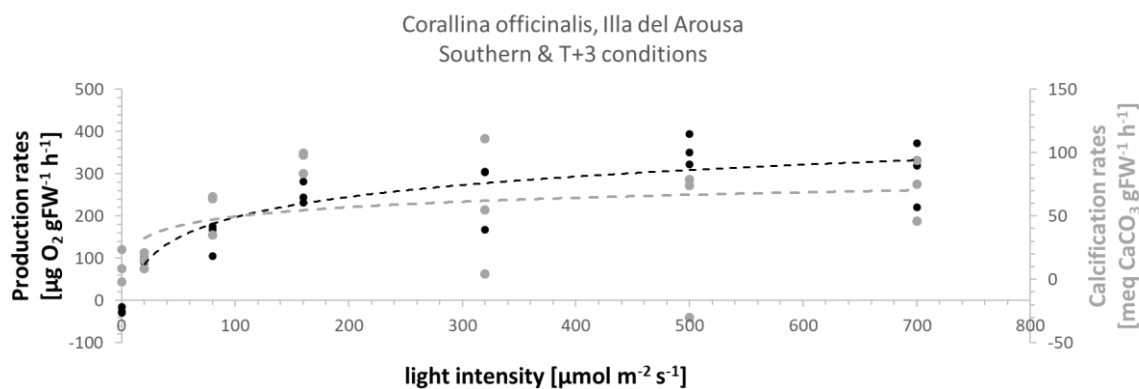


**Figure D11:** Oxygen and calcification evolution curve of the Illa del Arousa (southern) population under southern, high temperature (T+3) conditions. Black closed circles refer to gross production, grey closed circles refer to calcification rates. Trend lines are displayed as dashed line in their respective colour.

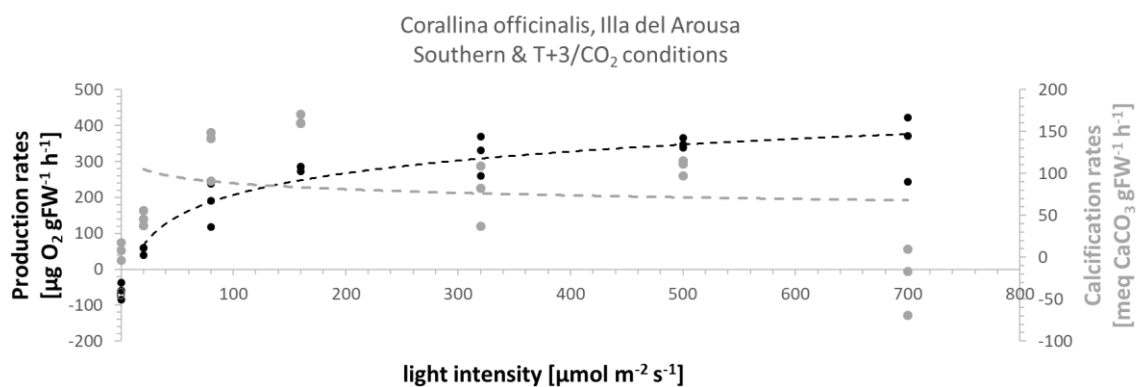


**Figure D12:** Oxygen and calcification evolution curve of the Illa del Arousa (southern) population under southern, climate change (T+3/CO<sub>2</sub>) conditions. Black closed circles refer to gross production, grey closed circles refer to calcification rates. Trend lines are displayed as dashed line in their respective colour.

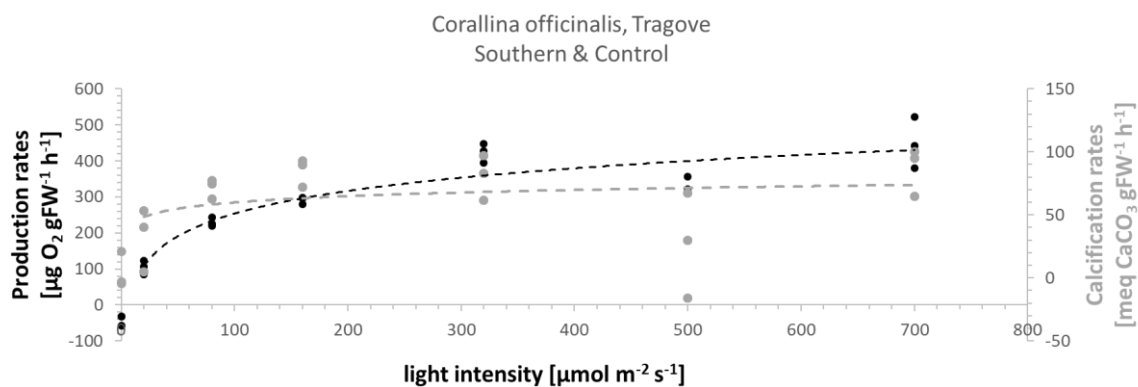


**Figure D13:** Oxygen and calcification evolution curve of the Tragove (southern) population under southern, control conditions. Black closed circles refer to gross production, grey closed circles refer to calcification rates. Trend lines are displayed as dashed line in their respective colour.

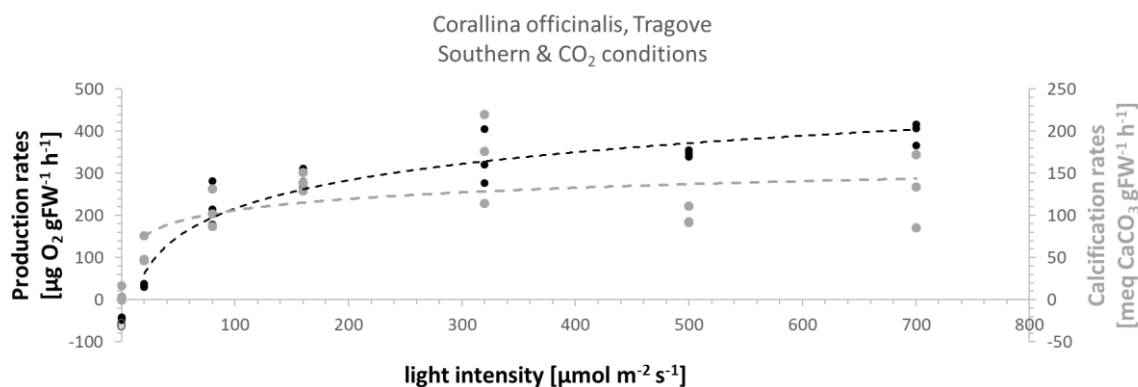


**Figure D14:** Oxygen and calcification evolution curve of the Tragove (southern) population under southern, high CO<sub>2</sub> conditions. Black closed circles refer to gross production, grey closed circles refer to calcification rates. Trend lines are displayed as dashed line in their respective colour.



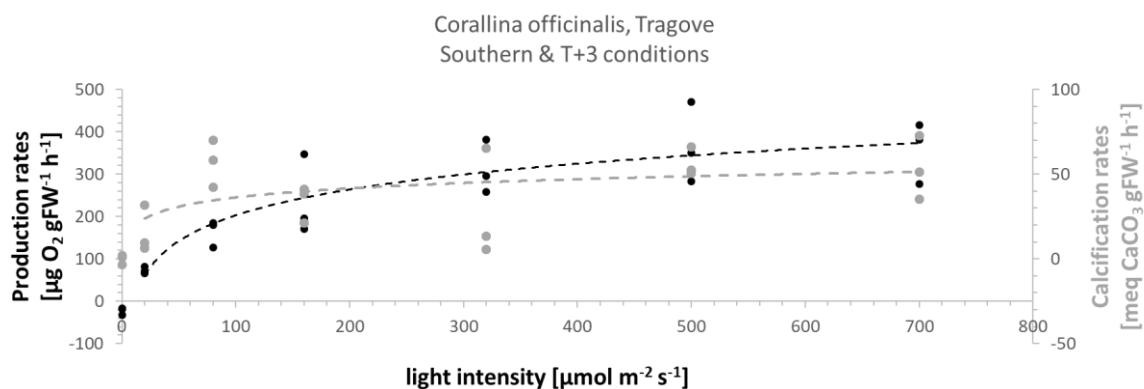


**Figure D15:** Oxygen and calcification evolution curve of the Tragove (southern) population under southern, high temperature (T+3) conditions. Black closed circles refer to gross production, grey closed circles refer to calcification rates. Trend lines are displayed as dashed line in their respective colour.

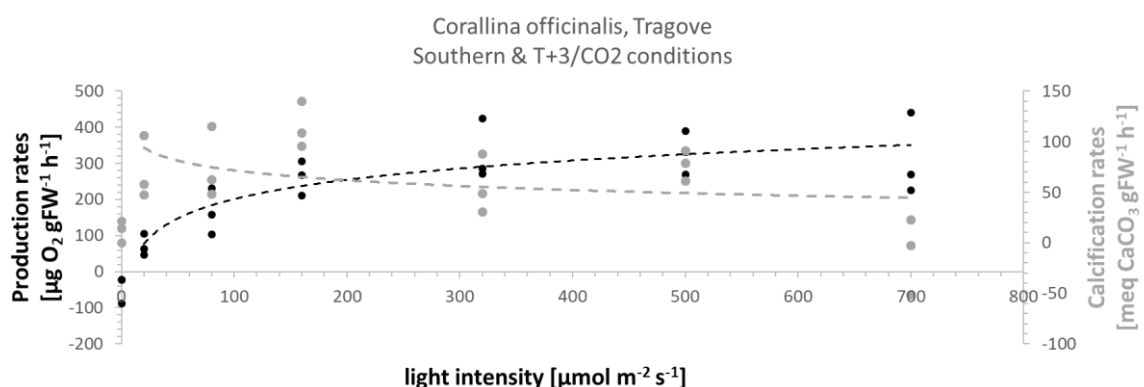


**Figure D16:** Oxygen and calcification evolution curve of the Tragove (southern) population under southern, climate change (T+3/CO<sub>2</sub>) conditions. Black closed circles refer to gross production, grey closed circles refer to calcification rates. Trend lines are displayed as dashed line in their respective colour.

For raw data, please follow the link:

<https://figshare.com/s/rk55724d31ebe56b13bf13>

By following the link, you agree not to share the link or any of the content with a third person.

**Table D1:** Significant statistical results of cell wall thickness analysis of the Climate Change Experiment comparing pre and post-experimental, within populations and within treatment measurements.

Relevant significances											
	Time	Treatment/ Pop	Pop vs Pop/ Treat vs. Treat		p-value		Time	Treatment/ Pop	Pop vs Pop/ Treat vs. Treat		p-value
Vertical (inter)	post	NP2	CO2	T+3/CO2	0.001	Horizontal (intra)	post	Control	SP1	CP2	0.000
	post	NP2	T+3	T+3/CO2	0.004		post	Control	SP1	SP2	0.027
	post	NP1	T+3/CO2	CO2	0.023		post	Control	CP1	CP2	0.000
	post	NP1	T+3/CO2	Control	0.022		post	Control	CP1	SP2	0.009
	post	CP2	CO2	Control	0.003		post	Control	NP2	CP2	0.001
	post	CP1	T+3	CO2	0.000		post	Control	NP1	CP2	0.000
	post	CP1	T+3	Control	0.000		post	Control	SP2	CP2	0.016
	post	CP1	T+3	T+3/CO2	0.002		post	T+3	SP1	CP2	0.012
	post	CP1	T+3/CO2	Control	0.012		post	T+3	SP1	SP2	0.018
	post	SP1	CO2	Control	0.002		post	T+3	CP1	SP1	0.000
	post	SP1	CO2	T+3	0.005		post	T+3	CP1	CP2	0.000
	post	SP1	T+3/CO2	Control	0.003		post	T+3	CP1	NP2	0.000
	post	SP1	T+3/CO2	T+3	0.010		post	T+3	CP1	NP1	0.000
	post	SP2	CO2	Control	0.012		post	T+3	CP1	SP2	0.025
	post	SP2	CO2	T+3/CO2	0.018		post	T+3	NP2	CP2	0.044
	post	T+3	CP1	SP1	0.000		post	T+3	NP1	CP2	0.002
	post	T+3	CP1	CP2	0.000		post	T+3	NP1	CP2	0.001
	post	T+3	CP1	NP2	0.001		post	T+3	SP2	CP2	0.000
	post	T+3	CP1	NP1	0.001		post	T+3	SP2	NP2	0.004
	post	T+3	CP1	SP2	0.001		post	CO2	CP1	CP2	0.031
	post	CO2	SP1	NP1	0.045		post	CO2	CP1	NP1	0.015
	post	T+3/CO2	SP1	CP2	0.010		post	CO2	SP2	CP2	0.040
	post	T+3/CO2	SP1	NP2	0.000		post	CO2	SP2	NP1	0.020
	post	T+3/CO2	SP1	SP2	0.018		post	T+3/CO2	SP1	CP2	0.005
	post	T+3/CO2	CP1	NP2	0.002		post	T+3/CO2	CP1	SP1	0.036
	post	T+3/CO2	NP1	CP2	0.002		post	T+3/CO2	CP1	CP2	0.000
	post	T+3/CO2	NP1	NP2	0.000		post	T+3/CO2	CP1	NP2	0.000
	post	T+3/CO2	NP1	SP2	0.004		post	T+3/CO2	CP1	NP1	0.010
	pre	NP1	CO2	T+3	0.006		post	T+3/CO2	NP1	CP2	0.020
	pre	NP1	CO2	T+3/CO2	0.001		post	T+3/CO2	SP2	CP2	0.000
	pre	NP1	Control	CO2	0.011		post	T+3/CO2	SP2	NP2	0.007
	pre	NP1	Control	T+3	0.000		post	CP2	CO2	T+3	0.016
	pre	NP1	Control	T+3/CO2	0.000		post	CP2	Control	CO2	0.001
	pre	CP2	CO2	Control	0.015		post	CP1	Control	T+3	0.004
	pre	CP2	T+3	Control	0.000		post	CP1	T+3	CO2	0.011
	pre	CP2	T+3	T+3/CO2	0.008		post	SP2	Control	CO2	0.005
	pre	CP1	Control	CO2	0.001		post	SP2	Control	T+3	0.001
	pre	CP1	T+3	CO2	0.002		post	SP2	Control	T+3/CO2	0.002
	pre	CP1	T+3/CO2	CO2	0.027		pre	Control	CP1	CP2	0.000
	pre	SP1	CO2	Control	0.006		pre	Control	NP2	CP2	0.000
	pre	SP1	CO2	T+3	0.007		pre	Control	NP1	SP1	0.035
	pre	SP2	CO2	Control	0.000		pre	Control	NP1	CP2	0.000
pre	SP2	CO2	T+3/CO2	0.016	pre	Control	NP1	NP2	0.025		
pre	SP2	T+3	Control	0.039	pre	Control	SP2	CP2	0.022		
pre	Control	SP1	CP2	0.005	pre	T+3	SP1	CP2	0.000		
pre	Control	CP1	CP2	0.002	pre	T+3	CP2	NP2	0.000		
pre	Control	NP2	CP2	0.009	pre	T+3	CP1	CP2	0.000		
pre	Control	NP1	SP1	0.019	pre	T+3	SP2	SP1	0.010		
pre	Control	NP1	CP2	0.000	pre	T+3	SP2	CP2	0.000		
pre	Control	NP1	CP1	0.042	pre	T+3	SP2	CP1	0.001		
pre	Control	NP1	NP2	0.011	pre	T+3	SP2	NP2	0.001		
pre	Control	NP1	SP2	0.001	pre	T+3	SP2	NP1	0.000		
pre	T+3	SP1	NP1	0.002	pre	CO2	CP1	SP1	0.012		
pre	T+3	CP2	NP1	0.000	pre	CO2	SP2	SP1	0.011		
pre	T+3	CP1	NP1	0.002	pre	T+3/CO2	SP1	CP2	0.010		
pre	T+3	NP2	NP1	0.000	pre	T+3/CO2	SP1	CP1	0.047		
pre	T+3	SP2	NP1	0.000	pre	T+3/CO2	SP1	NP2	0.033		
pre	CO2	SP1	CP2	0.002	pre	T+3/CO2	SP1	SP2	0.019		
pre	CO2	SP1	CP1	0.000	pre	NP1	Control	CO2	0.034		
pre	CO2	SP1	NP2	0.008	pre	NP1	Control	T+3	0.004		
pre	CO2	SP1	NP1	0.003	pre	NP1	Control	T+3/CO2	0.047		
pre	CO2	CP2	CP1	0.008	pre	CP1	Control	T+3	0.046		
pre	CO2	NP2	CP1	0.002	pre	CP2	CO2	T+3	0.000		
pre	CO2	NP1	CP1	0.005	pre	CP2	T+3/CO2	T+3	0.001		
pre	CO2	SP2	CP2	0.006	pre	SP1	Control	T+3/CO2	0.044		
pre	CO2	SP2	CP1	0.000	pre	SP2	Control	T+3	0.010		
pre	CO2	SP2	NP2	0.021	pre	SP2	T+3	T+3/CO2	0.001		
pre	CO2	SP2	NP1	0.009	pre	SP2	T+3	CO2	0.049		
pre	T+3/CO2	SP1	CP2	0.004	CP1	T+3	pre	post	0.000		
pre	T+3/CO2	SP1	CP1	0.032	CP1	T+3/CO2	pre	post	0.004		
pre	T+3/CO2	SP1	NP1	0.000	SP1	CO2	pre	post	0.034		
pre	T+3/CO2	CP1	NP1	0.007	SP2	T+3/CO2	pre	post	0.031		
pre	T+3/CO2	NP2	NP1	0.004							
pre	T+3/CO2	SP2	NP1	0.000							
NP2	CO2	pre	post	0.005							
NP1	T+3	pre	post	0.000							
NP1	T+3/CO2	pre	post	0.000							
CP1	CO2	pre	post	0.000							
CP1	T+3	pre	post	0.000							
CP1	T+3/CO2	pre	post	0.001							
CP2	CO2	pre	post	0.003							
CP2	Control	pre	post	0.017							
CP2	T+3/CO2	pre	post	0.027							

**Table D2:** Significant statistical results of cell wall thickness analysis of the Cross Experiment comparing pre and post-experimental, within populations and within treatment measurements.

Relevant significances											
	Time	Treatment/ Pop	Pop vs Pop/ Treat vs. Treat		p-value		Time	Treatment/ Pop	Pop vs Pop/ Treat vs. Treat		p-value
Vertical (Inter)	post	Control	CP1	CP2	0.000	Horizontal (Intra)	post	Control	CP1	CP2	0.000
	post	Control	CP1	SP2	0.001		post	Control	SP1	CP2	0.000
	post	Control	SP1	CP2	0.000		post	Control	SP2	CP2	0.000
	post	Control	SP1	SP2	0.000		post	Control	SP2	CP1	0.046
	post	CO2	SP1	CP2	0.000		post	T+3	SP1	SP2	0.002
	post	CO2	SP1	CP1	0.000		post	T+3	CP1	SP2	0.009
	post	CO2	SP1	SP2	0.000		post	CO2	SP1	CP2	0.000
	post	CO2	SP2	CP2	0.047		post	CO2	SP1	CP1	0.000
	post	T+3/CO2	SP1	CP2	0.000		post	CO2	SP1	SP2	0.001
	post	T+3/CO2	CP1	CP2	0.000		post	CO2	SP2	CP1	0.049
	post	T+3/CO2	CP1	SP2	0.010		post	T+3/CO2	SP1	CP2	0.044
	post	T+3/CO2	SP2	CP2	0.006		post	T+3/CO2	CP1	CP2	0.000
	post	CP1	Control	CO2	0.000		post	T+3/CO2	CP1	SP2	0.000
	post	CP1	Control	T+3	0.001		post	CP1	Control	CO2	0.000
	post	CP1	T+3	T+3/CO2	0.002		post	CP1	T+3	CO2	0.006
	post	CP1	T+3/CO2	CO2	0.000		post	CP1	T+3/CO2	CO2	0.000
	post	CP2	T+3	Control	0.023		post	CP1	T+3/CO2	T+3	0.022
	post	CP2	T+3	T+3/CO2	0.000		post	CP2	T+3/CO2	Control	0.034
	post	CP2	T+3	CO2	0.001		post	SP1	CO2	T+3	0.035
	post	SP1	Control	T+3	0.000		post	SP1	CO2	T+3/CO2	0.035
	post	SP1	Control	T+3/CO2	0.001		post	SP1	Control	T+3	0.005
	post	SP1	CO2	T+3	0.005		post	SP1	Control	T+3/CO2	0.005
	post	SP1	CO2	T+3/CO2	0.038		post	SP2	Control	CO2	0.000
	pre	CO2	SP2	CP2	0.003		post	SP2	Control	T+3	0.000
	pre	CO2	SP2	CP1	0.008		post	SP2	Control	T+3/CO2	0.000
	pre	T+3	SP1	CP2	0.001		pre	Control	SP1	CP2	0.000
	pre	T+3	SP1	CP1	0.000		pre	Control	SP1	CP1	0.001
	pre	T+3	SP1	SP2	0.000		pre	Control	SP1	SP2	0.024
	pre	T+3/CO2	SP1	CP2	0.000		pre	Control	CP1	CP2	0.000
	pre	T+3/CO2	SP1	CP1	0.000		pre	Control	SP2	CP2	0.000
	pre	T+3/CO2	SP1	SP2	0.006		pre	T+3	SP1	CP2	0.000
	pre	T+3/CO2	SP2	CP2	0.000		pre	T+3	SP1	CP1	0.000
pre	T+3/CO2	SP2	CP1	0.000	pre	T+3	SP1	SP2	0.000		
pre	CP1	CO2	T+3/CO2	0.040	pre	CO2	CP1	CP2	0.010		
pre	CP1	Control	T+3/CO2	0.028	pre	CO2	SP2	CP2	0.005		
pre	CP2	T+3	T+3/CO2	0.032	pre	CP1	CO2	T+3	0.000		
pre	SP1	T+3/CO2	Control	0.006	pre	CP1	CO2	T+3/CO2	0.000		
pre	SP1	T+3	CO2	0.009	pre	CP1	Control	T+3	0.002		
pre	SP1	T+3/CO2	CO2	0.000	pre	CP1	Control	T+3/CO2	0.000		
pre	SP2	CO2	T+3	0.009	pre	SP1	Control	CO2	0.000		
CP1	CO2	pre	post	0.018	pre	SP1	T+3	CO2	0.000		
CP1	Control	pre	post	0.000	pre	SP1	T+3/CO2	CO2	0.000		
CP1	T+3	pre	post	0.000	pre	SP2	CO2	T+3	0.000		
CP1	T+3/CO2	pre	post	0.000	pre	SP2	Control	T+3	0.000		
CP2	Control	pre	post	0.031	pre	SP2	T+3/CO2	T+3	0.000		
CP2	T+3	pre	post	0.000	pre	T+3/CO2	SP1	CP2	0.000		
CP2	T+3/CO2	pre	post	0.008	pre	T+3/CO2	SP1	CP1	0.000		
SP1	CO2	pre	post	0.000	pre	T+3/CO2	SP2	CP2	0.000		
SP1	Control	pre	post	0.000	pre	T+3/CO2	SP2	CP1	0.000		
SP2	T+3	pre	post	0.006	CP1	CO2	pre	post	0.013		
					CP1	Control	pre	post	0.014		
					CP1	T+3	pre	post	0.000		
					CP1	T+3/CO2	pre	post	0.000		
					CP2	T+3	pre	post	0.006		
					CP2	T+3/CO2	pre	post	0.018		
					SP1	CO2	pre	post	0.000		
					SP1	T+3	pre	post	0.013		
					SP1	T+3/CO2	pre	post	0.043		
					SP2	Control	pre	post	0.001		
					SP2	T+3/CO2	pre	post	0.028		